

Thomas D. Rossing *Editor*

The Science of String Instruments

 Springer

The Science of String Instruments

Thomas D. Rossing
Editor

The Science of String Instruments



Editor

Thomas D. Rossing
Stanford University
Center for Computer Research in Music and Acoustics (CCRMA)
Stanford, CA 94302-8180, USA
rossing@ccrma.stanford.edu

ISBN 978-1-4419-7109-8 e-ISBN 978-1-4419-7110-4

DOI 10.1007/978-1-4419-7110-4

Springer New York Dordrecht Heidelberg London

© Springer Science+Business Media, LLC 2010

All rights reserved. This work may not be translated or copied in whole or in part without the written permission of the publisher (Springer Science+Business Media, LLC, 233 Spring Street, New York, NY 10013, USA), except for brief excerpts in connection with reviews or scholarly analysis. Use in connection with any form of information storage and retrieval, electronic adaptation, computer software, or by similar or dissimilar methodology now known or hereafter developed is forbidden.

The use in this publication of trade names, trademarks, service marks, and similar terms, even if they are not identified as such, is not to be taken as an expression of opinion as to whether or not they are subject to proprietary rights.

Printed on acid-free paper

Springer is part of Springer Science+Business Media (www.springer.com)

Contents

1	Introduction.....	1
	Thomas D. Rossing	
2	Plucked Strings	11
	Thomas D. Rossing	
3	Guitars and Lutes	19
	Thomas D. Rossing and Graham Caldersmith	
4	Portuguese Guitar	47
	Octavio Inacio	
5	Banjo	59
	James Rae	
6	Mandolin Family Instruments.....	77
	David J. Cohen and Thomas D. Rossing	
7	Psalteries and Zithers	99
	Andres Peekna and Thomas D. Rossing	
8	Harpsichord and Clavichord	123
	Neville H. Fletcher and Carey Beebe	
9	Harp	145
	Chris Waltham	
10	Burmese Arched Harp	167
	Robert M. Williamson	

11	Plucked String Instruments in Asia.....	173
	Shigeru Yoshikawa	
12	Bowed Strings.....	197
	Thomas D. Rossing and Roger J. Hanson	
13	Violin	209
	Joseph Curtin and Thomas D. Rossing	
14	Cello	245
	Eric Bynum and Thomas D. Rossing	
15	Double Bass	259
	Anders Askenfelt	
16	Bows, Strings, and Bowing.....	279
	Knut Guettler	
17	Viols and Other Historic Bowed String Instruments	301
	Murray Campbell and Patsy Campbell	
18	The Hutchins–Schelleng Violin Octet After 50 Years	317
	George Bissinger	
19	Hammered Strings	347
	Thomas D. Rossing	
20	Some Remarks on the Acoustics of the Piano	353
	Nicholas Giordano	
21	Hammered Dulcimer	371
	David Peterson	
22	Electric Guitar and Violin	393
	Colin Gough	
23	Virtual String Synthesis.....	417
	Nelson Lee and Julius O. Smith III	
Index.....		457

Contributors

Anders Askenfelt

Royal Institute of Technology (KTH), Department of Speech, Music, and Hearing, Stockholm, Sweden

Carey Beebe

Carey Beebe Harpsichords Australia, Factory 35/17 Lorraine Street, Peakhurst, NSW 2210, Australia

George Bissinger

Acoustics Laboratory, East Carolina University, Howell Science Complex, Room E208, Greenville, NC 27858, USA

Eric Bynum

214 Macoy Ave, Culpeper, VA 22701, USA

Graham Caldersmith

12 Main Street, Comboyne, NSW 2429, Australia

Murray Campbell

School of Arts, Culture and Environment, University of Edinburgh, Edinburgh EH1 1JZ, UK

Patsy Campbell

School of Arts, Culture and Environment, University of Edinburgh, Edinburgh EH1 1JZ, UK

David J. Cohen

9402 Belfort Rd, Henrico, VA 23229, USA

Joseph Curtin

Joseph Curtin Studios, 3493 W. Delhi Road, Ann Arbor, MI 48103, USA

Neville H. Fletcher

Research School of Physics and Engineering, Australian and National University, Canberra, ACT 0200, Australia

Nicholas Giordano

Department of Physics, Purdue University, 525 Northwestern Avenue,
West Lafayette, IN 47907-2036, USA

Colin Gough

44 School Road, Birmingham B13 9SN, UK

Knut Guettler

The Norwegian Academy of Music, Eilins vei 20, Jar 1358, Norway

Roger J. Hanson

2806 Edgewood Drive, Cedar Falls, IA 50613-5658, USA

Octavio Inacio

ESMAE, Rua da Alegria, 503, Porto 4000-045, Portugal

Nelson Lee

Stanford University, Center for Computer Research in Music
and Acoustics (CCRMA), Stanford, CA 94302-8180, USA

Andres Peekna

5908 North River Bay Road, Waterford, WI 53185-3035, USA

David Peterson

University of Central Arkansas, 56 Ridge Drive, Greenbrier, AR, USA

James Rae

827 Valkyrie Lane NW, Rochester, MN 55901, USA

Thomas D. Rossing

Stanford University, Center for Computer Research in Music
and Acoustics (CCRMA), Stanford, CA 94302-8180, USA

Julius O. Smith III

Stanford University, Center for Computer Research in Music
and Acoustics (CCRMA), Stanford, CA 94302-8180, USA

Chris Waltham

Department of Physics & Astronomy, University of British Columbia,
6242 Agricultural Road, Vancouver, BC V6T 1Z1, Canada

Robert M. Williamson

Department of Physics, Oakland University, Rochester, MI 48309-4401, USA

Shigeru Yoshikawa

Graduate School of Kyushu University, 4-9-1 Shiobaru, Minami-ku,
Fukuoka 815-8540, Japan

Chapter 1

Introduction

Thomas D. Rossing

String instruments are found in almost all musical cultures. Bowed string instruments form the backbone of symphony orchestras, and they are used widely as solo instruments and in chamber music as well. Guitars are used universally in pop music as well as in classical music. The piano is probably the most versatile of all musical instruments, used widely not only in ensemble with other musical instruments but also as a solo instrument and to accompany solo instruments and the human voice.

In this book, various authors will discuss the science of plucked, bowed, and hammered string instruments as well as their electronic counterparts. We have tried to tell the fascinating story of scientific research with a minimum of mathematics to maximize the usefulness of the book to performers and instrument builders as well as to students and researchers in musical acoustics. Sometimes, however, it is difficult to “translate” ideas from the exact mathematical language of science into words alone, so we include some basic mathematical equations to express these ideas.

It is impossible to discuss all families of string instruments. Some instruments have been researched much more than others. Hopefully, the discussions in this book will help to encourage further scientific research by both musicians and scientists alike.

1.1 A Brief History of the Science of String Instruments

Quite a number of good histories of acoustics have been written (Lindsay 1966, 1973; Hunt 1992; Beyer 1999), and these histories include musical acoustics. Carleen Hutchins has written about the history of violin research (Hutchins 2000). Relatively less has been written about scientific research on other string instruments.

Pythagoras, who established mathematics in Greek culture during the sixth century BC, studied vibrating strings and musical sounds. He reportedly discovered

T.D. Rossing (✉)
Center for Computer Research in Music and Acoustics (CCRMA),
Stanford University, Stanford, CA 94302-8180, USA
e-mail: rossing@ccrma.stanford.edu

that dividing the length of a vibrating string into simple ratios produced consonant musical intervals. According to legend, he also observed how the pitch of the string changed with tension and the tones generated by striking musical glasses, but these are probably just legends (Hunt 1992).

Most early acoustical investigations were closely tied to musical acoustics. Galileo reviewed the relationship of the pitch of a string to its vibrating length, and he related the number of vibrations per unit time to pitch. The English mathematician Brook Taylor provided a dynamical solution for the frequency of a vibrating string based on the assumed curve for the shape of the string when vibrating in its fundamental mode. Daniel Bernoulli set up a partial differential equation for the vibrating string and obtained solutions which d'Alembert interpreted as waves traveling in both directions along the string (Beyer 1999).

1.1.1 Bowed String Instruments

During the sixteenth century, two families of viols developed: the *viola da gamba*, or “leg viol,” and the *viola da braccio*, or “arm viol.” These instruments, which normally had six strings tuned in fourths (except for a major third separating the third and fourth strings), developed in different sizes from treble to bass. They have remained popular to this day, especially for playing music from their period and accompanying singing.

The instruments in the violin family were developed in Italy during the sixteenth and seventeenth centuries and reached a peak in the eighteenth century in the hands of masters such as Antonio Stradivari and Giuseppe Guarneri del Gesù of Cremona. The viola, tuned a perfect fifth below the violin, is the alto member of the violin family. It is a distinctly different instrument, however, as is the violoncello or cello, the baritone member of the family. The double bass or contrabass, which is tuned in fourths, has mainly developed from the bass viol.

The all-important bow was given its present form by Francois Tourte (1747–1835). Two important characteristics of his bows are the inward curving stick of pernambuco wood and the “frog” with a metal ferrule to keep the bow hair evenly spread.

In his *Harmonie Universelle*, Marin Mersenne (1488–1648) discussed string instruments and indicated that he could hear at least four overtones in the sound of a vibrating string. The stick and slip action of the bow on the string appears to have been first recognized by Jean-Marie Duhamel (1797–1872).

Hutchins (2000) calls Felix Savart (1791–1841) the “grandfather” of violin research. He developed a cog-wheel machine to measure frequency, and he made many tests of the vibrational characteristics of the violin and its component parts. Working with the famous violinmaker Jean Baptiste Vuillaume (1798–1875), Savart was able to measure the so-called “tap gone” frequencies in a dozen or so violins made by Antonio Stradivari and Joseph Guarneri.

Herman von Helmholtz (1821–1894), who was trained as a physician, contributed much to our understanding of violin science as well as to the science of hearing and perception. His book *On Sensations of Tone* (1862) combines his knowledge of both physiology and physics and of music as well. He worked with little more than a stringed instrument, tuning forks, and his famous resonators to show that pitch is due to the fundamental frequency but that the quality of a musical sound is due to the presence of upper partials.

In order to study vibrations of violin strings and speech sounds, von Helmholtz invented a vibration microscope, which displayed Lissajous patterns of vibration. One lens of the microscope is attached to the prong of a tuning fork, so a fixed spot appears to move up and down. A spot of luminous paint is then applied to the string, and a bow is drawn horizontally across the vertical string. The point on the horizontally vibrating violin string forms a Lissajous pattern as it moves. By viewing patterns for a bowed violin string, von Helmholtz was able to determine the actual motion of the string, and such motion is still referred to as Helmholtz motion.

John William Strutt, who was to become the third Baron Rayleigh, was born at the family estate in Terling England, in 1842. He enrolled at Eton, but illness caused him to drop out, and he completed his schooling at a small academy in Torquay before entering Trinity College, Cambridge. His ill health may have been a blessing for the rest of the world. After nearly dying of rheumatic fever, he took a long cruise up the Nile River, during which he concentrated on writing *Science of Sound*. The first volume of this book develops the theory of vibrations and its applications to strings, bars, membranes, and plates, while the second volume begins with aerial vibrations and the propagation of waves in fluids.

Bowed string instruments have frequently attracted the attention of scientific researchers. Outstanding contributions to our understanding of violin acoustics have been made by Felix Savart, Hermann von Helmholtz, Lord Rayleigh, C.V. Raman, Frederick Saunders, and Lothar Cremer, all of whom also distinguished themselves in fields other than violin acoustics. In more recent times, the work of Professor Saunders has been continued by members of the Catgut Acoustical Society, led by Carleen Hutchins. This work has made good use of modern tools such as computers, holographic interferometers, and FFT analyzers. One noteworthy product of modern violin research has been the development of an octet of scaled violins, covering the full range of musical performance (Hutchins 1967).

1.1.2 Lutes and Guitars

The lute, which probably originated in the Near East, became the most popular instrument throughout much of Europe in the sixteenth and seventeenth centuries. The European lute derives both in name and form from the Arab instrument known as al ‘Ud, which in Arabic means literally “the wood.” The Arab ‘Ud was introduced into Europe by the Moors during their conquest and occupation of Spain (711–1492).

Many different designs have existed through the ages. The long lute, the neck of which is longer than its body, dates back to at least 2000 BC and has modern descendants in several different countries (e.g., the *tar* of Turkey and Iran, the *sitar* and *vina* of India, the *bouzouki* of Greece, the *tambura* of India and Yugoslavia, and the *ruan* of China). The short lute is the ancestor of the European lute as well as many other plucked string instruments.

The middle Renaissance (1500–1580) lute had six courses, the top string often being single. The use of a plectrum facilitated the playing of single highly ornamented lines of melody. This style can still be heard in modern ud music.

The late Renaissance (1580–1620) is a particularly interesting time for the lute. It was well established as an instrument of the court and was studied by many prosperous citizens. The student of the lute needed to be sufficiently affluent to afford the instrument, music, strings, and tuition. Its main uses were as a solo instrument or to accompany voice, but it was also used in ensembles, known as consorts. John Dowland, perhaps the finest lute virtuoso ever, played and published his music in England and on the continent during this time. Many cities supported lute-making workshops, and some lute makers were, to judge by their tax records, comfortably well off. Most lutes built at the present time are replicas or near copies of surviving instruments found in museums or private collections.

There are basically two types of modern guitars: acoustic and electric. The acoustic guitar family includes classical guitars, flamenco guitars, Portuguese or *fado* guitars, flat-top guitars, archtop guitars, resonator (Dobro) guitars, 12-string guitars, acoustic bass guitars (including the *guitarrón* or *chitarrone* used in Mariachi music).

The modern six-string guitar is a descendant of the sixteenth-century Spanish *vihuela*, which has its roots in antiquity. The modern word, *guitar*, was adopted into English from the Spanish *guitarra*, derived from the earlier Greek word *kithara*. The Renaissance guitar, which was not taken too seriously, had four courses of double strings. During the Baroque period, a fifth course was added. At the end of the Baroque period, the double strings gave way to single strings, and a sixth string was added. Although Boccherini and other composers of the eighteenth century included the guitar in some of their chamber music, the establishment of the guitar as a concert instrument took place largely in the nineteenth century. Fernando Sor (1778–1839) was the first in a long line of Spanish virtuosos and composers for the guitar.

The Spanish luthier Antonio de Torres (1817–1892) contributed much to the development of the modern classical guitar when he enlarged the body and introduced a fan-shaped pattern of braces to the top plate. Francisco Tarrega (1852–1909), perhaps the greatest of all nineteenth-century players, introduced the apoyando stroke and generally extended the expressive capabilities of the guitar. Excellent accounts of the historical development of the guitar are given by Jahnel (1981) and Turnbull (1974).

Unlike the lute, toward which very little scientific research has been directed, the guitar has been studied rather extensively in recent years. In addition to papers in acoustical journals such as *Journal of the Acoustical Society of America*, *Acustica/Acta Acustica*, *Applied Acoustics*, and *Acoustics Technology*, a number of papers have

appeared in more specialized journals such as *Catgut Acoustical Journal*, *American Lutherie*, *Journal of Guitar Acoustics*, and *Frets*. Pioneer researchers include Graham Caldersmith, Ove Christensen, Erik Jansson, Juergen Meyer, and Bernard Richardson. Nearly every international symposium on musical acoustics (ISMA) has included several papers on the acoustics of guitars, and most of the papers given at a special session on guitars at a meeting of the Acoustical Society of America were published in the September 1982 issue of *Journal of Guitar Acoustics*.

Guitar researchers have paid considerable attention to the resonances of the guitar body, and how the low-frequency resonances can be regarded as being due to the coupled vibrations of the top plate, back plate, and enclosed air. Luthiers have experimented with different bracing patterns, especially in the top plate. Unlike the violin, which has changed very little for many decades, the guitar is still evolving.

Electric guitars have become one of the most popular musical instruments in the musical world. Adolph Rickenbacher is often given credit for inventing the electric guitar in the 1930s. In the early 1940s, Les Paul designed and built a solid-body electric guitar at the Gibson Guitar factory, which became very popular. In the 1950s, Clarence Leonidas (Leo) Fender developed a solid-body guitar, which came to be known as the Telecaster. Fender also developed a popular electric bass (the Precision Bass) in the 1950s. Surprisingly little scientific research was done (or at least published) on electric guitars until the 1990s. Fleischer and Zwicker (1998) carefully studied mechanical vibrations of electric guitar bodies and their effect on the sound and playing characteristics. Later, Fleischer applied similar studies to the electric bass (Fleischer 2000).

1.1.3 Harpsichords, Clavichords, and Dulcimers

The harpsichord, which produces sound by plucking the strings, dates from the Middle Ages, although the oldest preserved harpsichords come from Italy and date from the 1500s. Hans Ruckers and other Flemish harpsichord makers took the lead around 1580 by using longer strings and a heavier case. In eighteenth-century France, Paul Taskin and the Blancher family extended the range to about five octaves. Harpsichord building became important in England during the Renaissance.

At the peak of its development, the harpsichord lost out to the piano with its much wider dynamic range. The twentieth century, however, saw a revival of interest in harpsichord building and the use of modern materials such as Delrin for the jacks. Today, harpsichords are widely used for playing early music.

The clavichord produces sound by striking brass or iron strings with small metal blades called tangents. Because the string vibrates from the bridge only as far as the tangent, multiple keys with multiple tangents can be assigned to the same string – a practice called *fretting*. The clavichord was invented early in the fourteenth century, and it was popular in the sixteenth to eighteenth centuries. It had fallen out of use by the middle of the nineteenth century, but was revived by Arnold Dolmetsch late in the century.

The name *dulcimer* is used to describe two different types of instrument, one plucked and one hammered. The term comes from the Latin and Greek words *dulce* and *melos*, which combine to mean “sweet tune.” This name applies more aptly to the plucked dulcimer, which is probably no more than 200 years old and is a popular instrument in the Appalachian mountains.

The ancient origins of the hammered dulcimer, on the other hand, are undoubtedly in the Near East, where instruments of this type have been made and played for perhaps 5,000 years. *Santir* and *psanterim* were names applied early to such instruments, and are probably derived from the Greek *psalterion*. Today, the dulcimer is known as the *santouri* in Greece and as the *santur* in India.

From the Near East the instrument traveled both east and west. Arabs took it to Spain where a dulcimer-like instrument is depicted on a cathedral relief from 1184. Introduction into the Orient came much later. The Chinese version is still known as the *yang ch'in*, or foreign zither. Though its use in China is reported to date from about the beginning of the nineteenth century, Korean tradition claims association with the hammer dulcimer from about 1725 (Rizzetta 1997).

1.1.4 Piano

The piano, invented by Bartolomeo Cristofori (1655–1731) around 1709, is one of the most versatile of all musical instruments. The oldest existing piano, built by Cristofori in 1721, is on display at the Metropolitan Museum of Art in New York (Conklin 1996a). Cristofori's key mechanism was adopted by other piano makers, including Gottfried Silbermann, who showed one of his pianos to Bach. Piano making, as practiced by Andreas and Nannette Stein, flourished in Vienna in the late eighteenth century. Viennese pianos, as used by Mozart, generally had wooden frames and two strings per note. In the early part of the nineteenth century, the piano continued to develop. The tonal range increased from 5 to $7\frac{1}{3}$ octaves. Broadwood in England and Erard in France became the foremost builders of pianos. The double escapement action (invented by Sébastien Erard), the use of three strings (for all but the lowest notes), and the iron frame were adopted. Over stringing was patented for use in grand pianos by Henry Steinway in 1859.

One of the foremost piano researchers of our time is Harold Conklin. After he retired from the Baldwin Piano Company, he published a series of three papers in the *Journal of the Acoustical Society of America* that could serve as a textbook for piano researchers (Conklin 1996a, b, c). Gabriel Weinreich explained the behavior of coupled piano strings and the aftersound that results from this coupling. Others who have contributed substantially to our understanding of piano acoustics are Anders Askenfelt, Eric Jansson, Juergen Meyer, Klaus Wogram, Ingolf Bork, Donald Hall, Isao Nakamura, and Hideo Suzuki. Many other string instruments have been studied scientifically, but space will not allow a discussion of their history here.

1.1.5 Electric and Virtual String Instruments

The best-known electric string instrument is the electric guitar (see Sect. 1.1.2; see also Chap. 3), but electric violins are quite common as well. The electric violin, like the electric guitar, uses pickups to sense the vibrations of the bowed strings, an electronic amplifier, and a loudspeaker. Pickups or microphones may be attached to conventional violins, but more commonly an electric violin has a solid body to minimize vibration and feedback from body to strings. Mathews and Kohut (1972) pioneered the use of electronic filters to simulate the resonances of the violin and thus give the sound a violin-like quality. The electric violin with filters has served as a research tool as well as a musical instrument.

The term *virtual string instrument* is used to describe a variety of experimental systems, the most usual being systems for synthesizing guitar and violin sounds. Successful methods for achieving this have included physical modeling synthesis (*Computer Music Journal* 1992) and digital waveguide synthesis (see Chap. 23). The term is also used to refer to virtual (usually digital) means for playing a violin.

1.2 Modal Analysis of String Instruments

In most string instruments, the vibrating string transfers its vibrational energy to a solid structure or sounding board that radiates much more efficiently than the string itself. The vibrational behavior of the structure is often quite complicated, but fortunately it can often be described in terms of normal modes of vibration. An important aspect of the science of string instruments is analyzing the normal modes of vibration.

Modal analysis is widely used to describe the dynamic properties of a structure in terms of the modal parameters: natural frequency, damping factor, modal mass, and mode shape. The analysis may be done either experimentally or mathematically. In mathematical modal analysis, one attempts to uncouple the structural equations of motion so that each uncoupled equation can be solved separately. When exact solutions are not possible, numerical approximations such as finite-element and boundary-element methods are used (Rossing 2007).

1.2.1 Experimental Modal Testing

In experimental modal testing, a measured force at one or more points excites the structure, and the response is measured at one or more points to construct frequency response functions. The modal parameters can be determined from these functions by curve fitting using a computer. Various curve-fitting methods are used. Several convenient ways have developed for representing these modes graphically, either

statically or dynamically. By substituting microphones or intensity probes for the accelerometers, modal analysis methods can be used to explore sound fields. In this chapter we mention some theoretical methods but we emphasize experimental modal testing applied to structural vibrations and also to acoustic fields.

Modal testing may use sinusoidal, random, pseudo random, or impulsive excitation. The response may be measured mechanically, optically, or indirectly (e.g., by observing the radiated sound field). The first step in experimental modal testing is generally to obtain a set of frequency response functions.

The frequency response function (FRF) is a fundamental measurement that isolates the inherent dynamic properties of a mechanical structure. The FRF describes the motion-per-force input-output relationship between two points on a structure as a function of frequency. Because both force and motion are vector quantities, they have directions associated with them. An FRF is actually defined between a single input point and direction and a single output point.

A roving hammer test is the most common type of impact test. An accelerometer is fixed at a single point, and the structure is impacted at as many points as desired to define the mode shapes of the structure. Using a 2-channel FFT analyzer, FRFs are computed, one at a time, between each impact DOF and the fixed response point. A suitable grid is usually marked on the structure to define the impact points.

Not all structures can be impact tested. Sometimes the surface is too delicate

Most experimental modal analysis relies on a modal parameter estimation (curve fitting) technique to obtain modal parameters from the FRFs. Curve fitting is a process of matching a mathematical expression to a set of experimental points by minimizing the squared error between the analytical function and the measured data.

Single-degree-of-freedom (SDOF) methods estimate modal parameters one mode at a time. Multiple-degrees-of-freedom (MDOF), global, and multi-reference methods can estimate modal parameters for two or more modes at a time. Local methods are applied to one FRF at a time. Global and multi-reference methods are applied to an entire set of FRFs at once.

1.2.2 Mathematical Modal Analysis

In mathematical modal analysis, one attempts to uncouple the structural equation of motion by means of some suitable transformation, so that the uncoupled equations can be solved. The frequency response of the structure can then be found by summing the respective modal responses in accordance with their degree of participation in the structural motion.

Sometimes it is not possible to obtain exact solutions to the equation of motion. Computers have popularized the use of numerical approximations such as finite-element and boundary-element methods.

1.2.3 Sound Field Analysis

Although modal analysis developed primarily as a way of analyzing mechanical vibrations – by substituting microphones or acoustic intensity probes for accelerometers – experimental modal testing techniques can be used to explore sound fields. Modal testing has been used to explore standing acoustic waves inside air columns and to explore radiated sound fields from a vibrating structure. It can also be used to explore acoustical modes in rooms.

1.2.4 Holographic Modal Analysis

Holographic interferometry offers the best spatial resolution of operating deflection shapes. In cases where the damping is small and the modes are well separated in frequency, the operating deflection shapes correspond closely to the normal mode shapes. Modal damping can be estimated with a fair degree of accuracy from half power points determined by counting fringes. Phase modulation allows analysis to be done at exceedingly small amplitudes and also offers a means to separate modes that overlap in frequency. TV holography allows the observation of vibrational motion in real time; it is a fast, convenient way to record deflection shapes.

References

- R. T. Beyer (1999) *Sounds of Our Times* (Springer, New York, 1999).
- Computer Music Journal* **16**, special issue on physical modeling (Winter 1992).
- H. A. Conklin (1996a) Design and tone in the mechanoacoustic piano. Part I. Piano hammers and tonal effects. *J. Acoust. Soc. Am.* **99**, 3286–3296.
- H. A. Conklin (1996b) Design and tone in the mechanoacoustic piano. Part II. Piano structure. *J. Acoust. Soc. Am.* **100**, 695–709.
- H. A. Conklin (1996c) Design and tone in the mechanoacoustic piano. Part III. Piano strings and scale design. *J. Acoust. Soc. Am.* **100**, 1286–1298.
- H. Fleischer (2000) *Dead Spots of Electric Basses* (Universität der Bundeswehr München, Neubiberg).
- H. Fleischer and T. Zwicker (1998) Mechanical vibrations of electric guitars. *Acustica/Acta Acustica* **84**, 758–765.
- H. L. F. Helmholtz, (1877) *On the Sensations of Tone*, 4th ed. Translated by A. J. Ellis, Dover, New York, 1954.
- F. V. Hunt (1992) *Origins in Acoustics* (Acoustical Society of America, Woodbury, NY, 1992).
- C. M. Hutchins (1967) Founding a new family of fiddles. *Phys. Today* **20**(3), 23–27.
- C. M. Hutchins (2000) A history of violin research. *Catgut Acoust. Soc. J.* **4**(1), 4–10.
- F. Jahnel (1981) *Manual of Guitar Technology*. Verlag Das Musikinstrument, Frankfurt am Main.
- R. B. Lindsay (1966) The story of acoustics. *J. Acoust. Soc. Am.* **39**, 629–644.
- R. B. Lindsay (1973) *Acoustics: Historical and Philosophical Development* (Dowden, Hutchinson & Ross, Stroudsburg, PA). Translation of Sauveur's paper, p. 88

- M. V. Mathews and J. Kohut (1972) Electronic simulation of violin resonances. *J. Acoust. Soc. Am.* **53**, 1620–1626.
- L. Rayleigh (J. W. Strutt) (1894) *The Theory of Sound*, Vols. 1 and 2, 2nd ed. (Macmillan, London); reprinted by Dover, 1945.
- S. Rizzetta (1997) *Hammer Dulcimer: History and Playing* (Smithsonian Institution, Washington, DC)
- T. D. Rossing (2007) “Modal analysis.” In *Springer Handbook of Acoustics*, ed. T. D. Rossing (Springer, Heidelberg).
- H. Turnbull (1974) *The Guitar from the Renaissance to the Present Day*. Batsford, London.
- H. von Helmholtz (1862) *Die Lehre von den Tonempfindungen* (Longmans, London). Translated by Alexander Ellis as *On the Sensations of Tone* and reprinted by Dover, 1954.

Chapter 2

Plucked Strings

Thomas D. Rossing

In the next ten chapters we will discuss the science of plucked string instruments. Acoustic guitars and lutes are discussed in Chap. 3. Portuguese guitars, used in *fado* music, are discussed in Chap. 4 and guitars in Chap. 5, while electric guitars are discussed in Chap. 22. Banjos are discussed in Chap. 5, while mandolins are the subject of Chap. 6. Zithers and psalteries, especially Baltic psalteries, are discussed in Chap. 7. Harpsichords are discussed in Chap. 8, while harps are discussed in Chap. 9 and 10. Finally, plucked string instruments from Asia, such as the *koto*, *shamisen*, *biwa*, *gayageum*, *geomungo*, *ch'in*, *p'In-p'a*, and *sitar* are discussed in Chap. 11. These instruments are very different in character and in their musical roles, but they all depend upon plucked strings vibrating and exciting one or more soundboards or radiating surfaces.

2.1 Transverse Waves on a String

The equation describing transverse waves on a uniform string is derived in many books (see e.g., Sect. 2.2 in Fletcher and Rossing 1998).

$$\frac{\partial^2 y}{\partial t^2} = \frac{T}{\mu} \frac{\partial^2 y}{\partial x^2} = c^2 \frac{\partial^2 y}{\partial x^2}. \quad (2.1)$$

If a string with linear density μ (kg/m) is stretched to a tension T , waves will propagate at a speed c given by $\sqrt{(T/\mu)}$.

The general solution to (2.1) can be written in a form credited to d'Alembert:

$$y = f_1(ct - x) + f_2(ct + x). \quad (2.2)$$

T.D. Rossing (✉)

Center for Computer Research in Music and Acoustics (CCRMA),
Stanford University, Stanford, CA 94302-8180, USA
e-mail: rossing@ccrma.stanford.edu

The function $f_1(ct - x)$ represents waves traveling to the right, whereas the function $f_2(ct + x)$ represents waves traveling to the left. The nature of functions f_1 and f_2 is arbitrary; for example, they can be sinusoidal or they can describe impulsive waves.

2.1.1 Impulsive Waves, Reflection, and Interference

Impulsive waves are discussed in Chap. 2 of *Science of Sound* (Rossing et al. 2002). If a rope is fixed at one end and is given a single impulse by quickly moving the other end up and down, an impulse will travel at speed c and will maintain its shape fairly well as it moves down the rope. When the impulse reaches the end of the rope, it will reflect back to the sender. The reflected pulse is very much like the original pulse except that it is upside-down, as shown in Fig. 2.1b. If the end of the rope were free to flop (instead of being fixed), the reflected pulse would be right-side-up, as shown in Fig. 2.1a.

An interesting feature of waves is that two of them, traveling in opposite directions, can pass right through each other and emerge with their original identities. The *principle of linear superposition* describes this behavior. For waves on a rope or string, the displacement at any point is the sum of the displacements of the two individual waves. When the pulses have the same sense, they add when they meet; when they have opposite sense, they subtract when they meet. These are examples of constructive and destructive interference, respectively. Superposition of wave pulses traveling in opposite directions is illustrated in Fig. 2.1.

2.1.2 Standing Waves

When the ends of a string are fixed, as in most string instruments, waves reflect back from the fixed ends and give rise to *standing waves*. In the case of two identical

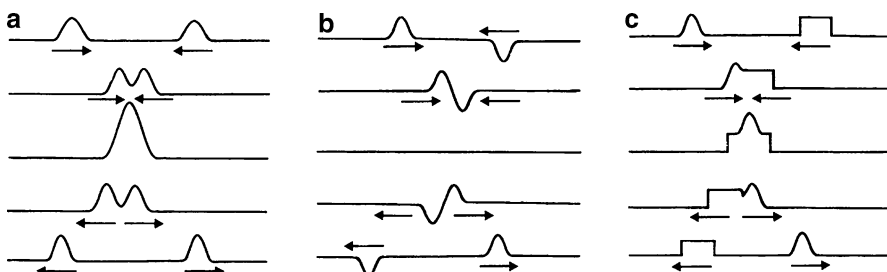


Fig. 2.1 The superposition of wave pulses that travel in opposite directions: (a) pulses in the same direction; (b) pulses in opposite directions; (c) pulses with different shapes

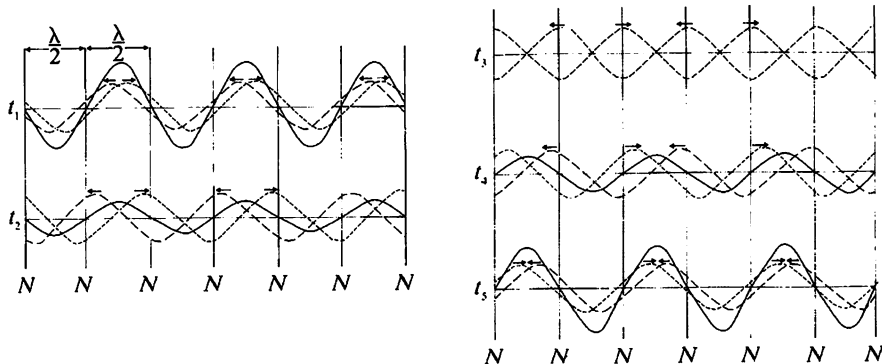


Fig. 2.2 Interference of two identical waves in a one-dimensional medium. At times t_1 and t_5 there is constructive interference, and at t_3 there is destructive interference. Note that at points marked N , the displacement is always zero

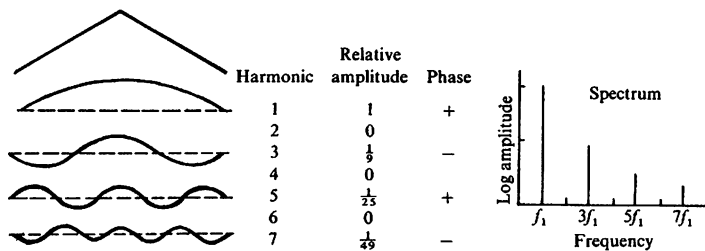


Fig. 2.3 Frequency analysis of a string plucked at its center. Odd-numbered modes of vibration add up in appropriate amplitude and phase to give the shape of the string

waves (i.e., same frequency and amplitude) traveling in opposite directions on a string, there will be alternate regions of constructive and destructive interference, as shown in Fig. 2.2. The points of destructive interference that always have zero displacement are called *nodes* and are denoted by N in Fig. 2.2. Between the nodes are points of constructive interference called *antinodes* where the displacement is maximum. At the antinodes the displacement oscillates at the same frequency as in the individual waves; the amplitude is the sum of the individual wave amplitudes. The nodes are one-half wavelength apart (as are the antinodes as well). Because they do not move on the string, the waves are called *standing waves*. If the amplitudes of the two waves are different, they will not cancel completely, and the nodes will represent points of minimum (but not zero) displacement.

Standing waves can be written as a sum of normal modes of the string, each of which represents vibration at a particular frequency. The general solution to the wave equation can be written as a sum of normal modes:

$$Y = \sum (C_n \sin \omega_n t + \varphi_n) \sin k_n x, \quad (2.3)$$

where C_n is the amplitude of the n th mode and φ_n is its phase.

2.2 Plucked String: Time and Frequency Analyses

When a string is plucked, pulse waves propagate in both directions from the pluck point. When these pulses reach the ends of the string, they reflect back and set up standing waves. The resulting vibration can be considered to be a combination of several modes of vibration. For example, if the string is plucked at its center, the resulting vibration will consist of the fundamental plus the odd-numbered harmonics. Figure 2.3 illustrates how the modes associated with the odd-numbered harmonics, when each is present in the correct proportion, add up at one instant in time to give the initial shape of the center-plucked string. Modes 3, 7, 11, etc., must be opposite in phase from modes 1, 5, and 9 in order to give maximum displacement at the center, as shown at the top. Finding the normal mode spectrum of a string, given its initial displacement, calls for *frequency analysis* or *Fourier analysis*.

Because the modes shown in Fig. 2.1 have different frequencies of vibration, they quickly get out of phase, and the shape of the string changes rapidly after plucking. The shape of the string at each moment can be obtained by adding the normal modes at that particular time, but it is more difficult to do so because each of the modes will be at a different point in its cycle. The resolution of the string motion into two pulses that propagate in opposite directions on the string, which we call *time analysis*, is illustrated in Fig. 2.4.

If the string is plucked at a point other than its center, the spectrum, or recipe, of the constituent modes is different, of course. For example, if the string is plucked one-fifth of the distance from one end, the spectrum of mode amplitudes shown in

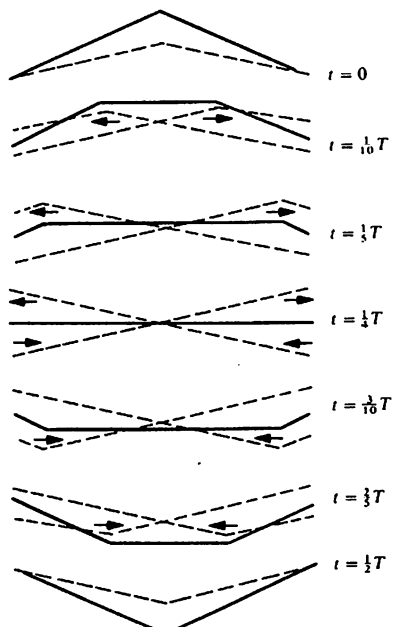


Fig. 2.4 Time analysis of the motion of a string plucked at its midpoint through one half-cycle. Motion can be thought of as due to two pulses traveling in opposite directions

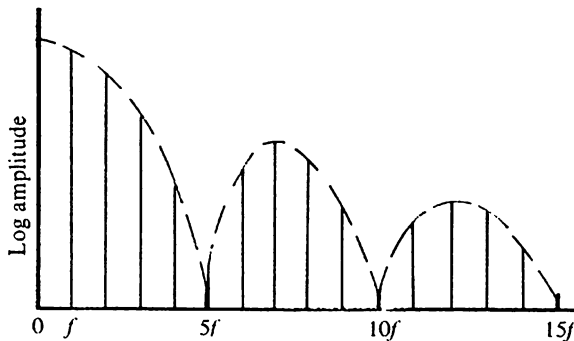


Fig. 2.5 Spectrum of a string plucked one-fifth of the distance from one end

Fig. 2.5 is obtained. Note that the fifth harmonic is missing. Plucking the string one-fourth of the distance from the end suppresses the fourth harmonic, and so on.

A time analysis of the string plucked at one-fifth of its length is shown in Fig. 2.6. A bird racing back and forth within a parallelogram boundary can be viewed as the resultant of two pulses (dashed lines) traveling in opposite directions. Each of these pulses can be described in terms of d'Alembert's solution to the wave equation (2.2).

2.3 Force Exerted by the String

The force exerted by a plucked string on the bridge can be estimated by reference to Fig. 2.6. To a first approximation, the force normal to the bridge or soundboard will be $T \sin \theta$, and the parallel to the soundboard will be $T \cos \theta$, where T is the tension and θ is the angle between the string and the plate or soundboard.

The tension T does change during the cycle, however, as the length of the string changes (see Fig. 2.6). If the string has a cross-sectional area A and an elastic (Young's) modulus E , the transverse and longitudinal forces can be written

$$F_T = (T_0 + \Delta T) \sin \theta,$$

$$F_L = (T_0 + \Delta T) \cos \theta T_0 + \frac{EA \Delta L}{L_0}. \quad (2.4)$$

The change in the transverse force during a cycle is primarily due to the change in the direction or slope. The change in the longitudinal force, on the other hand, is due mainly to the slight change in length of the string during the cycle.

In a typical guitar pluck the amplitude of the transverse force pulses is roughly 40 times greater than the amplitude of the longitudinal force pulses, and they couple more efficiently to the top plate. However, the longitudinal force pulses are

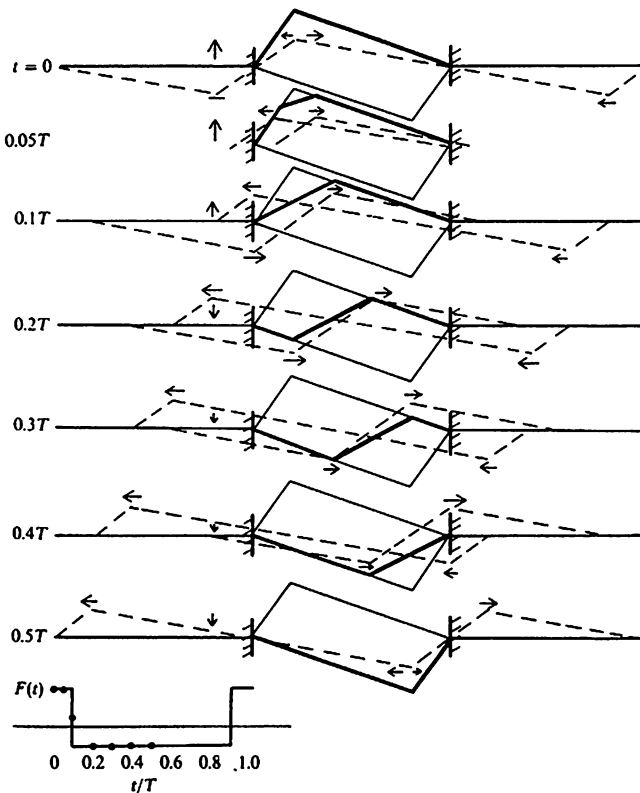


Fig. 2.6 Time analysis through one half-cycle of the motion of a string plucked one-fifth of the distance from one end. The motion can be thought of as due to two pulses [representing the two terms in (2.2)] moving in opposite directions. The resultant motion consists of two bends, one moving clockwise and the other moving counterclockwise around a parallelogram. The normal force on the end support, as a function of time, is shown at the bottom

proportional to the square of the plucking amplitude, so the difference diminishes with increasing amplitude (Fletcher and Rossing 1998).

2.4 Plucking

In a harpsichord the string is plucked by a plectrum attached to a jack which moves vertically (see Chap. 8). In other plucked string instruments, such as lutes, harps, guitars, mandolins, and psalteries, the string is plucked by the player's fingers or a hand-held plectrum. Not very much research has been done on the mechanics of either type of plucking.

Harpsichord jacks originally employed suitably shaped crow's quills to do the actual plucking, but modern instruments frequently substitute a thin strip of plastic (such as Delrin). The plectrum is generally mounted in a holder called the tongue, which is mounted in the jack. The tongue is able to rotate on an axle so the plectrum will easily slide past the string on its return journey. However, the tongue does not rotate when the plectrum is moving upwards.

The harpsichord player has relatively little control over the loudness of a note; the loudness is pretty much the same regardless of how fast a key is pressed. A mathematical model of the plucking action predicted that the loudness of a harpsichord note would depend upon the upward velocity of the jack (Griffel, 1994). However, Giordano and Winans (1999) found experimentally that the loudness is essentially independent of jack velocity.

The finger-string interaction in a concert harp has been described by Le Carrou et al. (2007). A model describing the trajectory of two masses, one modeling the finger and the other one modeling the string, was developed. The parameters of this model (equivalent mass, stiffness, and coupling parameter) were directly deduced from images of the finger and string displacements obtained with a high-speed camera. Three different phases of harp excitation were identified: sticking phase, slipping phase, and free oscillation phase. The initial amplitude and velocity distributions of the string were found to be quite different for different players.

The classical guitar is also plucked by the player's fingers. The sound of a classical guitar depends partly on the way in which the fingertip and fingernail interact with the string. Two different ways a guitar can be plucked are known as *apoyando* and *tirando* strokes (also called the *rest* and *free* strokes). Apoyando comes from a Spanish word meaning "resting." After plucking the finger rests on the next higher string on the guitar. Tirando, on the other hand, comes from a Spanish word meaning "pulling." After plucking, the finger does not touch the adjacent string. Although the apoyando stroke tends to induce slightly more vertical string motion, there is little difference between the two strokes in this regard (Taylor, 1978).

The string is in contact with the fingernail for about 100 ms. During this time, transverse and torsional waves are created on the string, which alter the local forces at the plucking point. Increasing the finger's mass or damping results in a longer contact time, while increasing the finger's stiffness results in a shorter contact (Pavlidou and Richardson 1995).

The folk guitar, which has steel strings, is often plucked with a plectrum (flat pick). Players wishing not to use a pick sometimes strum the guitar or employ finger strumming or finger picking. Finger picking is a technique of using the thumb and at least one other finger to pick or pluck notes using the fingernails or fingertips.

Further discussion of plucking appears in the chapters devoted to the various plucked string instruments.

References

- N. H. Fletcher (1976a) Plucked strings – a review, *Catgut Acoust. Soc. Newslett.* 26, 13–17.
- N. H. Fletcher (1976b) *Physics and Music* (Heinemann Educational Australia, Richmond, VIC).
- N. H. Fletcher and T. D. Rossing (1998) *Physics of Musical Instruments*, 2nd ed. (Springer, New York).
- N. Giordano and J. P. Winans II (1999) Plucked strings and the harpsichord, *J. Sound Vib.* 224, 455–473.
- D. H. Griffel (1994) The dynamics of plucking, *J. Sound Vib.* 175, 289–297.
- A. J. M. Houtsma, R. P. Boland, and N. Adler (1975) A force transformation model for the bridge of acoustic lute-type instruments, *J. Acoust. Soc. Am.* 58, S131 (abstract).
- J. -L. Le Carrou, F. Gautier, F. Kerjan, and J. Gilbert (2007) The finger-string interaction in the concert harp, Proc. ISMA 2007, Barcelona.
- M. Pavlidou and B. E. Richardson (1995) The string-finger interaction in the classical guitar, Proc. ISMA, Dourdan.
- T. D. Rossing, F. R. Moore, and P. A. Wheeler (2002) *Science of Sound*, 3rd ed. (Addison Wesley, San Francisco).
- J. Taylor (1978) *Tone Production on the Classical Guitar* (Musical New Services, Ltd., London).

Chapter 3

Guitars and Lutes

Thomas D. Rossing and Graham Calder Smith

Lute-type instruments have a long history. Various types of necked chordophones were in use in ancient Egyptian, Hittite, Greek, Roman, Turkish, Chinese, and other cultures. In the ninth century, Moors brought the *oud* (or *ud*) to Spain. In the fifteenth century, the *vihuela* became popular in Spain and Portugal. About the same time guitars with four double-strings became popular, and Italy became the center of the guitar world.

This chapter will focus mainly on acoustic guitars, with briefer discussion of electric guitars and lutes. Chapter 4 discusses the Portuguese guitar; Chap. 6 discusses the mandolin; and Chap. 11 discusses some plucked string instruments in Asia.

3.1 Acoustic Guitars

The earliest known six-string guitar was built in 1779 by Gaetano Vinaccia in Italy. Stradivarius is known to have built several guitars. Composers who played the guitar included Rossini, Verdi, von Weber, and Schubert. Fernando Sor (1778–1839) was the first of a long line of Spanish virtuosos and composers for the guitar.

The Spanish luthier Antonia de Torres Jurado (1817–1892) contributed much to the development of the modern classical guitar when he enlarged the body and introduced a fan-shaped pattern of braces to the top plate. Francisco Tarrega (1852–1909), perhaps the greatest of nineteenth-century players, introduced the apoyando stroke and generally extended the expressive capabilities of the guitar. Excellent accounts of the historical development of the guitar are given by Jahnel (1981) and Turnbull (1974).

T.D. Rossing (✉)
Center for Computer Research in Music and Acoustics (CCRMA),
Stanford University, Stanford, CA 94302-8180, USA
e-mail: rossing@ccrma.stanford.edu

Acoustic guitars generally fall into one of four families of design: classical, flamenco, flat top (or folk), and arch top. Classical and flamenco guitars have nylon strings; flat top and arch top guitars have steel strings. Steel string guitars usually have a steel rod embedded inside the neck, and their sound boards are provided with crossed bracing. The modern guitar generally has six strings tuned to E2, A2, D3, G3, B3, and E4 (82, 110, 147, 196, 247, and 330 Hz, respectively).

3.1.1 The Guitar as a System of Coupled Vibrators

The guitar can be considered to be a system of coupled vibrators, as shown in Fig. 3.1. The plucked strings store energy, but they radiate only a small amount of sound directly. They transmit vibrational energy to the top plate and bridge, which, in turn, share this energy with the back plate, the ribs, and the air cavity. Sound is radiated by the vibrating plates and through the sound hole.

At low frequencies, the top plate transmits energy to the back plate via both the ribs and the air cavity; the bridge essentially acts as part of the top plate, at high frequencies, however, most of the sound is radiated by the top plate, and the mechanical properties of the bridge may become significant.

3.1.2 Force Exerted by the Vibrating String

As the string vibrates, it exerts a force that has both transverse and longitudinal components, as discussed in Chap. 2. For a typical high-E nylon string, the maximum transverse force is roughly 40 times greater than the maximum longitudinal force amplitude. However the longitudinal force increases with the square of the pulse amplitude, so the differences diminish with increasing amplitude. The elastic

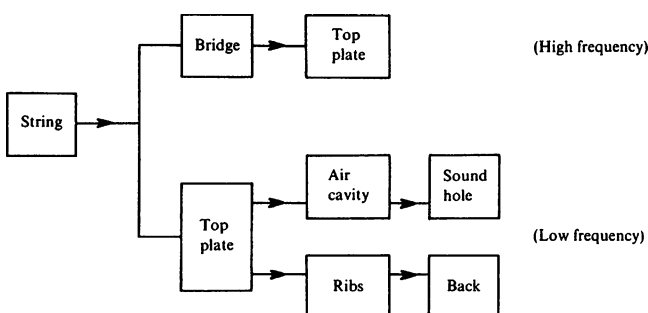


Fig. 3.1 Simple schematic of a guitar. At low frequencies, sound is radiated by the top and back plates and the sound hole. At high frequencies, most of the sound is radiated by the top plate

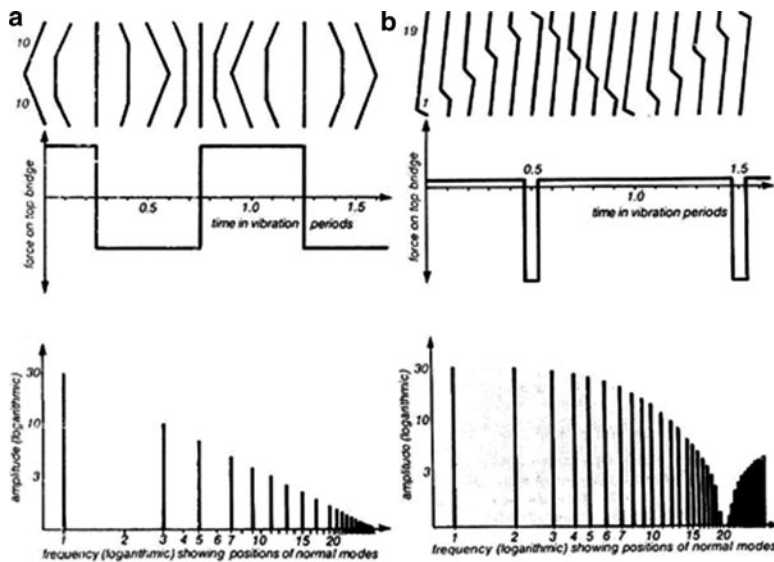


Fig. 3.2 Waveforms and spectra of the transverse bridge force for a string plucked (a) at its center and (b) at one-twentieth of its length from the bridge (Fletcher 1976)

(Young's) modulus for steel is about 40 times greater than for nylon, and string tensions are about 50% greater, so the longitudinal and transverse force amplitudes will be more nearly equal (Fletcher and Rossing 1998).

The longitudinal force pulses occur at twice the frequency of the vibrating string and they have essentially triangular waveforms as compared with the rectangular waveform of the transverse pulses (Fig. 3.2).

3.1.3 Frequency Response of Guitars

Guitar sound spectra obtained by several different researchers, including Richardson (1982), Meyer (1983), Jansson (1983), Ross and Rossing (1979), and Ross (1979) show individual differences, but all of them show strong peaks around 100 and 200 Hz, several peaks in the 400–700 Hz region, and a broad set of peaks above 1.5 kHz. (These sound spectra show the radiated sound level when a sinusoidal force of constant amplitude is applied perpendicular to the bridge). The strong peaks around 100, 200, and 400 Hz, which stem from resonances of the guitar body, do much to determine the low-frequency tonal characteristics of the guitar. Meyer found that the peak level of the resonance near 400 Hz correlates especially well with the quality rating of the guitar by listeners. See Fig. 3.3.

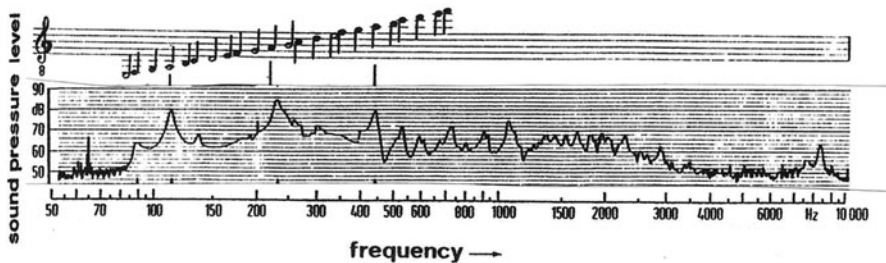


Fig. 3.3 Classical Guitar Sound spectrum for a sinusoidal force applied perpendicular to the bridge. Note the strong peaks around 100 and 200 Hz, several peaks around 400–700 Hz and the collection of peaks in the region 1,500–2,500 Hz (adapted from Meyer 1983)

3.2 Vibrations of the Guitar Body

3.2.1 Normal Modes of Vibration

The complex vibrations of the guitar body can be described in terms of *normal modes* of vibration. Normal modes are independent ways in which a structure vibrates. They are characterized by nodal lines (along which the motion is a minimum) and anti-nodes (along which the vibrational motion is maximum) as well as by modal frequency and damping. A normal mode can be excited by applying a force of the right frequency to any point on the structure that is not on a nodal line. Similarly, the motion can be detected at any point that is not on a nodal line. In practice, however, the instrumentation used for excitation and detection of the motion may modify the structure slightly, by adding mass or stiffness (or both).

Mode shapes are unique for a structure, whereas the deflection of a structure at a particular frequency, called an *operating deflection shape* (ODS), may result from the excitation of more than one normal mode. When exciting a structure at a resonance frequency, the ODS will be determined mainly by one mode, although if several modes have nearly the same frequency, special techniques may be required to determine their contributions to the observed ODS. Modes of a structure are functions of the entire structure. A mode shape describes how every point on the structure moves when it is excited at a point. The distinction between a normal mode, an operating deflection shape, and a resonance is an important one to make in order to avoid misunderstanding (see Richardson 1997; Rossing 2007).

Modal testing is a systematic method for identification of the modal parameters of a structure, such as natural frequencies, modal shapes, and modal damping. In guitar testing, the excitation is usually a sinusoidal force or an impulse. Detection methods include: measuring acceleration with an accelerometer; measuring surface velocity with a vibrometer; determining deflection by means of holographic interferometry; determining nodes with Chladni patterns.

3.2.2 Modes of Component Parts

Figure 3.4 shows the vibration modes of a guitar plate blank (without braces) with a free edge, and Fig. 3.5 shows the modes calculated for a plate with traditional fan bracing (also with a free edge). Mode shapes for the first five modes in a classical guitar plate glued to fixed ribs are shown in Fig. 3.6. These mode shapes are in reasonably good agreement with the modes calculated by Richardson

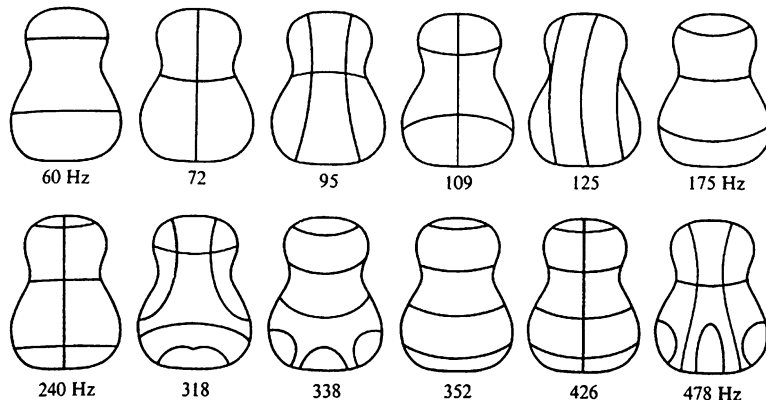


Fig. 3.4 Vibration modes of a guitar back plate blank (without braces) with a free edge (from Rossing 1982)

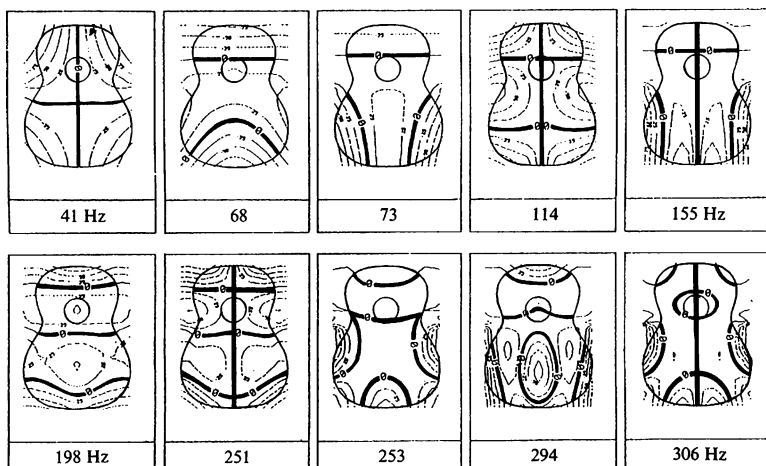


Fig. 3.5 Vibration modes of a classical guitar top plate with traditional fan bracing, free edges (adapted from Richardson and Roberts 1985)

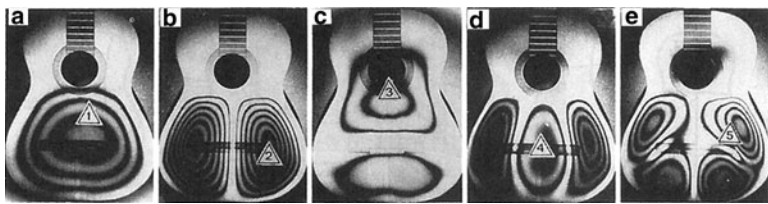


Fig. 3.6 Vibration modes of a classical guitar top plate glued to fixed ribs but without the back (Janson 1971)

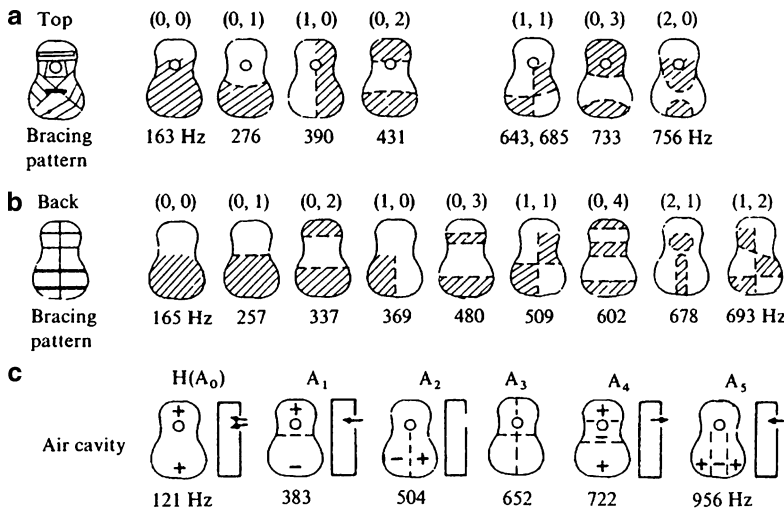


Fig. 3.7 (a) Modes of a folk guitar top (Martin D-28) with the back and ribs in sand. (b) Modes of the back with the top and ribs in sand. (c) Modes of the air cavity with the guitar body in sand. Mode designations are given above the figures and mode frequencies below

and Roberts (1985) for a clamped edge, although the actual boundary condition probably is somewhere between clamped and simply supported (hinged).

Obviously, the observed mode shapes and frequencies of the top plate depend upon the exact boundary conditions and acoustic environment during testing. A convenient and readily reproducible arrangement is to immobilize the back and ribs of the guitar (e.g., in sand) and to close the sound hole.

Figure 3.7a shows the modes of a steel-string dreadnaught guitar measured with the back and ribs in sand and sound hole closed with a lightweight sheet of balsa wood. The modes are quite similar to those of the classical guitar in Fig. 3.6 except that the (1,0) mode now occurs at a higher frequency than the (0,1) mode, and the (2,0) mode has moved up in frequency and changed its shape because of the crossed bracing.

Commonly, the back plate of a guitar is rather simply braced with a center strip and three (most classical guitars) or four (steel-string dreadnaught guitar) cross braces, as shown in Fig. 3.7b. Some vibrational modes of the back are shown in Fig. 3.7b.

Also shown in Fig. 3.7 are the modes of the air cavity of a folk guitar. These were measured with the top, back, and ribs immobilized in sand but with the sound hole open. The lowest mode is the Helmholtz resonance, the frequency of which is determined by the cavity volume and the sound hole diameter. There is also a small dependence on the cavity shape and the sound hole placement, but these are usually not variables in guitar design. The term *Helmholtz resonance* is sometimes applied to the lowest resonance of the guitar (around 100 Hz), but this resonance involves considerable motion of the top and back plates and so it is not a true Helmholtz cavity resonance. Higher air modes resemble the standing waves in a rectangular box.

Frequencies of the principal modes of the top plate, back plate, and air cavity in two folk guitars and two classical guitars are given in Table 3.1. The main difference is in the relative frequencies of the (1,0) and (0,1) modes in the top plates. In the fan-braced classical guitars, the (0,1) mode occurs at a higher frequency than the (1,0) mode, while in the cross-braced top plate of the folk guitars and in the back plates of both types, the reverse is generally true. In the Martin D-28 in Fig. 3.7 the fundamental modes of the top plate and back plate were tuned to almost the same frequency.

Table 3.1 Frequencies of the principal modes of the top plate, back plate, and air cavity in four guitars (Fletcher and Rossing, 1998).

Top plate	(0,0)	(0,1)	(1,0)	(0,2)	(1,1)	(0,3)	(2,0)	(1,2)
<i>Steel string</i>								
Martin D-28	163	326	390	431	643	733	756	
Martin D-35	135	219	313	397	576	626	648	777
<i>Classical</i>								
Kohno 30	183	388	296	466	558		616	660
Conrad	163	261	228	382	474		497	
Back plate	(0,0)	(0,1)	(0,2)	(1,0)	(0,3)	(1,1)	(2,0)	(1,2)
<i>Steel string</i>								
Martin D-28	165	257	337	369	480	509	678	693
Martin D-35	160	231	306	354	467	501	677	
<i>Classical</i>								
Kohno 30	204	285	368	417	537	566	646	856
Conrad	229	277	344	495	481	573	830	611
Air cavity	A ₀		A ₁	A ₂	A ₃	A ₄	A ₅	
		(Helmholtz)		(0,1)	(1,0)	(1,1)	(0,2)	(2,0)
<i>Steel string</i>								
Martin D-28	121		383	504	652	722		956
Martin D-35 118	392		512	666	730	975		
<i>Classical</i>								
Kohno 30	118		396	560	674	780		
Conrad	127		391	558	711	772		1033

3.2.3 Coupling of the Top Plate to the Air Cavity: Two-Oscillator Model

The coupling of the vibrating components at low frequency has been modeled by several investigators. If we fix the back plate and the ribs, the guitar can be viewed as a two-mass vibrating system as shown in Fig. 3.8(a). The vibrating strings apply a force $F(t)$ to the top plate, whose mass and stiffness are represented by m_p and K_p . A second piston of mass m_h represents the mass of air in the soundhole, and the volume V of enclosed air acts as the second spring. This model was proposed by Caldersmith (1980) and by Christensen and Vistasen (1980) and further developed by Richardson and Roberts (1985).

The two-mass model predicts two resonances with an anti-resonance between them. These correspond to f_1 , f_2 , and f_A in Fig. 3.8(b). The two resonances f_1 and f_2 span the lowest top plate mode f_p and the Helmholtz resonance f_A ; that is, f_A and f_p will lie between f_1 and f_2 . In fact, it can be shown that $f_1^2 + f_2^2 = f_A^2 + f_p^2$ (Ross and Rossing 1979; Ross 1979). If $f_p > f_A$ (as it is in most guitars), f_A will lie closer to f_1 than to f_2 , as shown in Fig. 3.8(b).

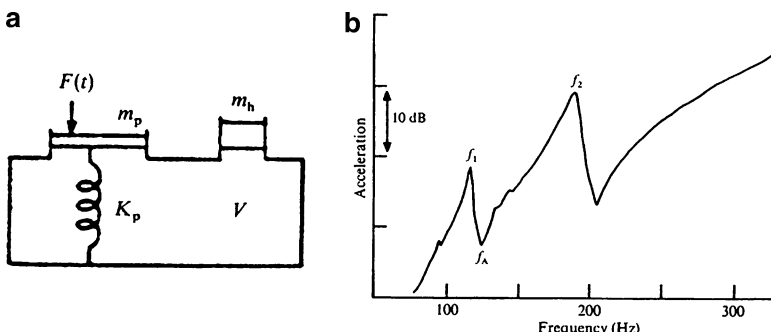


Fig. 3.8 (a) Two-mass model representing the motion of a guitar with a rigid back plate and ribs. (b) Low-frequency response curve for a Martin D-28 folk guitar with its back plate and ribs immobilized in sand. The bridge was driven on its treble side by a sinusoidal force of constant amplitude, and the acceleration was recorded at the driving point (Fletcher and Rossing 1998)

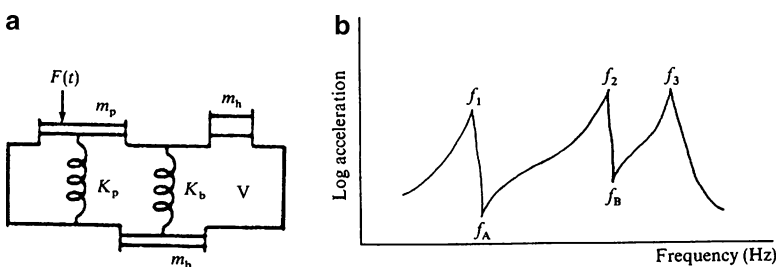


Fig. 3.9 (a) Three-dimensional model representing the motion of a guitar with ribs fixed. (b) Frequency response curve predicted by the three-mass model. A third resonance and a second anti-resonance have been added to the response curve of the two-mass model

3.2.4 Coupling to the Back Plate: Three-Oscillator Model

Coupling of the back plate, top plate, and the enclosed air can be modeled by a three-mass model, as shown in Fig. 3.9a. An additional mass m_b and an additional spring K_b represent the mass and stiffness of the back plate. The frequency response curve in Fig. 3.9b has three resonance peaks and two anti-resonances. The three-mass model predicts that $f_1^2 + f_2^2 + f_3^2 = f_A^2 + f_p^2 + f_b^2$. This relationship has been verified by experimental measurements in several guitars with the ribs immobilized (Rossing et al. 1985).

3.2.5 Low-Frequency Resonances of a Guitar Body

The frequency response of a guitar is characterized by a series of resonances and anti-resonances. In order to determine the vibration configuration at each of its major resonances, it can be driven sinusoidally at one or more points, and its motion observed optically, electrically, or mechanically. Optical sensing techniques include holographic interferometry (Stetson 1981) and laser velocimetry (Boullosa 1981). Acoustical detection techniques have included using an array of microphones (Strong et al. 1982) and scanning with a single microphone (Ross and Rossing 1979). A mechanical pickup consists of an accelerometer or a velocity transducer of very small mass (such as a phonograph cartridge).

Many guitars have three resonances in the range of 100 to 250 Hz due to coupling between the (0,0) top and back modes and the A_0 (Helmholtz) air mode. When the (0,0) modes in the top plate and back plate are close in frequency, the coupled modes may appear as in Fig. 3.10. At the lowest of the three resonances, the top and back plates move in opposite directions, so the guitar “breathes” in and out of the sound hole. In the second resonance, the top and back plates move in the same direction, as shown in Fig. 3.10. In the highest of the three resonances, the plates again move in opposite directions, but the air in the sound hole moves opposite to its motion in the lowest resonance.

Note that the resonance frequencies in Fig. 3.10 are for a guitar freely supported on rubber bands. Fixing the ribs lowers the second resonance from 193 to 169 Hz (because the center of mass must move), but the first and third resonances remain essentially unchanged in frequency because they involve very little motion of the



Fig. 3.10 Vibrational motion of a freely supported Martin D-28 folk guitar at three resonances in the low-frequency region (Fletcher and Rossing 1998)

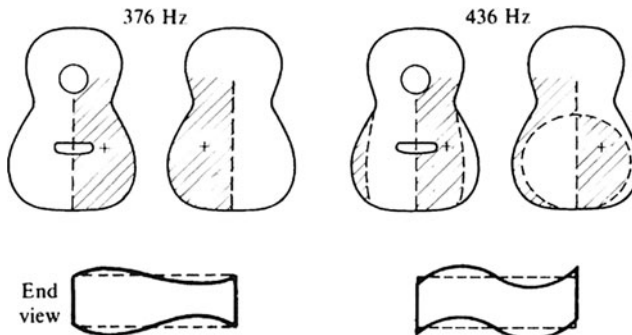


Fig. 3.11 Vibrational configurations of a Martin D-28 guitar at two resonances resulting from “seesaw” motion of the (1,0) type

ribs. This illustrates the dependence of the vibrational modes on the method of support and suggests that the timbre of the instrument depends upon the way it is held by the player.

The (1,0) modes in the top plate and back plate couple with the A2 air mode (see Fig. 3.7) to give at least one strong resonance between 250 and 300 Hz in a classical guitar, but closer to 400 Hz in a cross-braced guitar. Motion of the plates at two such resonances in a Martin D-28 folk guitar are shown in Fig. 3.11.

Above 400 Hz, the coupling between the top and back plates modes appears to be weaker, so the observed resonances are due mainly to resonances in one or the other of the plates (generally the top plate). A fairly prominent (2,0) top plate resonance is often observed around 550 Hz in classical guitars, but this mode is less prominent in folk guitars. Vibrational configurations of a classical guitar top plate at several resonances are illustrated by the holographic interferograms in Fig. 3.12. Q -values are a measure of the sharpness of each resonance.

In classical guitars the (0,1) top plate mode also couples with the A1 internal air mode which drives the air piston, so (0,1) occurs twice at around 360 and 440 Hz depending on guitar design. Even though the top plate does not radiate very efficiently in the (0,1) mode the sound hole can radiate strongly and can contribute to the low-frequency output depending on how close the saddle is to the (0,1) nodal line.

3.2.6 Modal Shapes

A modal shape represents the motion of the guitar in a normal mode of vibration. Optical methods give the best spatial resolution of a given operational deflection shape (ODS), which in many cases closely resembles a normal mode. Optical methods include holographic interferometry, speckle-pattern interferometry, and scanning laser vibrometry.

Another technique for obtaining modal shapes, called *experimental modal testing*, excites the guitar body with a force hammer and uses an accelerometer to

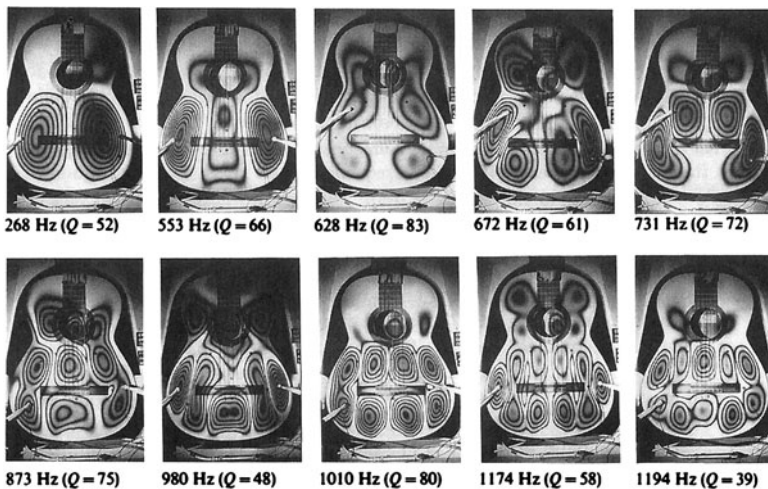


Fig. 3.12 Holographic interferograms of a classical guitar top plate at several resonances. Resonance frequencies and Q -values (a measure of the sharpness of the resonance) are given (Richardson and Roberts 1985)

sense its motion. The force hammer is moved from point to point in a grid, and a frequency response function (FRF) determined for each point of excitation. The resulting FRFs are processed by a computer and the modal shape is determined by use of a curve-fitting program.

3.3 String Forces

A player can alter the tone of a guitar by adjusting the angle through which the string is plucked. Not only do forces parallel and perpendicular to the bridge excite different sets of resonances, but they result in tones that have different decay rates, as shown in Fig. 3.13. When the string is plucked perpendicular to the top plate, a strong but rapidly decaying tone is obtained. When the string is plucked parallel to the plate, on the other hand, a weaker but longer tone results. Thus, a guitar tone can be regarded as having a compound decay rate, as shown in Fig. 3.13 (bottom). The spectra of the initial and final parts of the tone vary substantially, as do the decay rates.

Classical guitarists use primarily two strokes, called *apoyando* and *tirando* (sometimes called the *rest* and *free* strokes). The fingernail acts as sort of a ramp, converting some of the horizontal motion of the finger into vertical motion of the string, as shown in Fig. 3.14. Although the *apoyando* stroke tends to induce slightly more vertical string motion, there is little difference between the two strokes in this

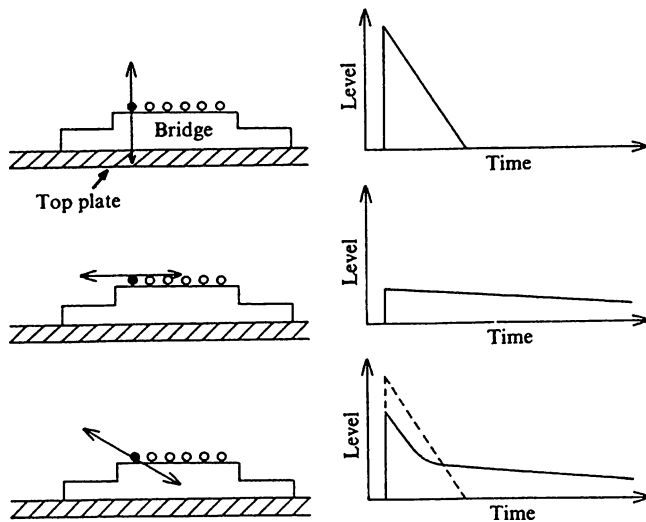


Fig. 3.13 Decay rates of guitar tone for different plucking directions (Jansson 1983)

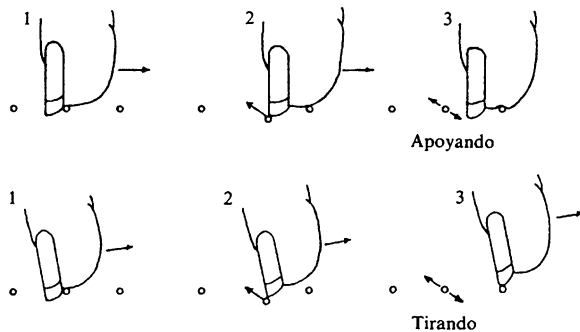


Fig. 3.14 Finger motion and resulting string motion of apoyando and tirando strokes. In the apoyando stroke, the finger comes to rest on an adjacent string; in the tirando stroke, it rises enough to clear it (Taylor 1978)

regard. However, the player can change the balance between horizontal and vertical string motion by varying the angle of the fingertip (Taylor 1978).

3.4 Sound Radiation

Sound radiation from a guitar, like most musical instruments, varies with direction and frequency. Even with sinusoidal excitation at a single point (such as the bridge), the radiated sound field is complicated because several different modes of vibration with different patterns of radiation may be excited at the same time. Figure 3.15

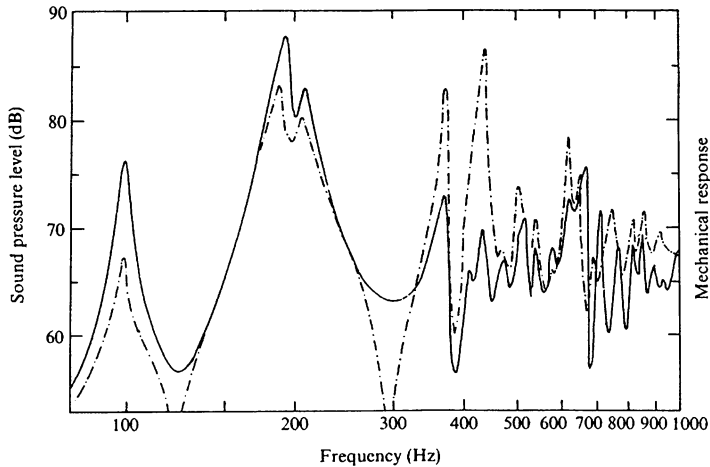


Fig. 3.15 Mechanical frequency response and sound spectrum one meter in front of a Martin D-28 steel-string guitar driven by a sinusoidal force of 0.15 N applied to the treble side of the bridge. The *solid curve* is the sound spectrum; the *dashed curve* is acceleration at the driving point

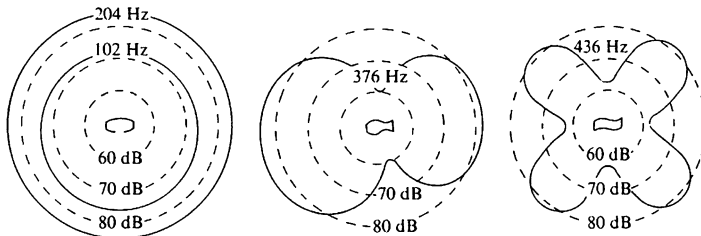


Fig. 3.16 Sound radiation patterns at four resonance frequencies in a Martin D-28 folk guitar (compare with Fig. 3.7 which show the corresponding modal shapes) (Popp and Rossing 1986)

shows the sound spectrum one meter in front of a Martin D-28 folk guitar in an anechoic room when a sinusoidal force of 0.15 N is applied to the treble side of the bridge. Also shown is the mechanical frequency response curve (acceleration level versus frequency). Note that most of the mechanical resonances result in peaks in the radiated sound, but that the strong resonances around 376 and 436 Hz (which represent “seesaw” motion; see Fig. 3.11) do not radiate strongly in this direction. The mode at 102 Hz radiates efficiently through the sound hole.

Figure 3.16 shows polar sound radiation patterns in an anechoic room for the modes at 102, 204, 376, and 436 Hz. The modes at 102 and 204 Hz radiate quite efficiently in all directions, as would be expected in view of the mode shapes (see Fig. 3.7). Radiation at 376 Hz, however, shows a dipole character, and at 436 Hz a strong quadrupole character is apparent, as expected from Fig. 3.7 (Popp and Rossing 1986).

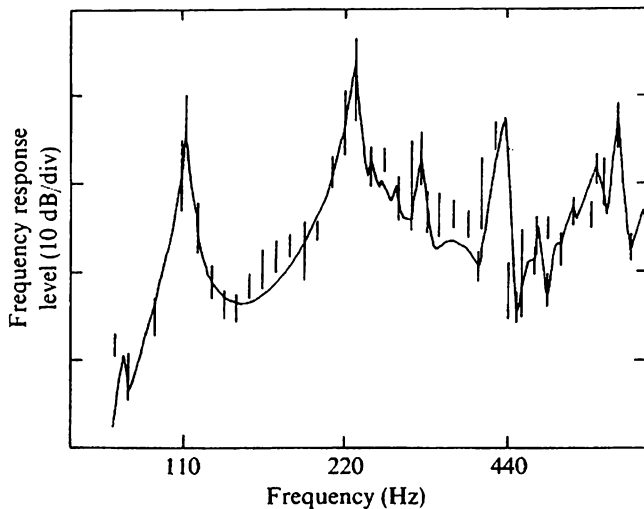


Fig. 3.17 Comparison of the sound level of the fundamentals of played notes (bars) to the guitar frequency response function (solid curve) with its level adjusted for a good fit. A graph of the rate of sound decay (dB/s) versus frequency similarly follows the frequency response curve (Caldersmith and Jansson 1980)

The output spectrum of a guitar may be calculated by multiplying the bridge force spectrum by the frequency response function of the guitar body. This is greatly complicated, however, by the rapid change in the force spectrum with the time after the pluck (see Fig. 3.13). Caldersmith and Jansson (1980) measured the initial sound level and the rate of sound decay for played notes on guitars of high and medium quality. They found that both the initial sound level and the rate of decay replicate the frequency response curve of a guitar, as shown in Fig. 3.17. At strong resonances, however, the initial levels are slightly lower, and the levels decay faster than predicted by the frequency response curves.

3.5 Quality

Rating the sound quality of classical guitars and how the quality depends on design and construction details have been studied by several investigators. According to Jansson (2002), most guitar players feel that *tonal strength* or *carrying power* is the most important single quality criterion, with tone length and timbre being the second most important. In the previous section, we mentioned how the initial sound level and rate of sound decay depends upon the resonances of a guitar body.

Tones from recorded music were analyzed in the form of long time average spectra (LTAS), and it was found that better guitars have a higher level up to 3,000 Hz. Comparing two guitars, it was found that the less good guitars tended to have a lower level below 2,000 Hz and above 400 Hz (Jansson 2002).

Some extensive listening tests were conducted at the Physikalisch-Technische Bundesanstalt in Germany to try to correlate quality in guitars to their measured frequency response (Meyer 1983). Some of the features that correlated best with high quality were:

1. The peak level of the third resonance (around 400 Hz);
2. The amount by which this resonance stands above the resonance curve level;
3. The sharpness (Q value) of this resonance;
4. The average level of one-third-octave bands in the range 80–125 Hz;
5. The average level of one-third-octave bands in the range 250–400 Hz;
6. The average level of one-third-octave bands in the range 315–5,005 Hz;
7. The average level of one-third-octave bands in the range 80–1,000 Hz;
8. The peak level of the second resonance (around 200 Hz).

3.5.1 Influence of Design and Construction

Meyer found that using fewer struts, varying their spacing, adding transverse bracing and reducing the size of the bridge, to have desirable effects (Meyer 1983). He experimented with several different bridge shapes and found that a bridge without “wings” gave the best result.

Jansson (2002) found the following order of importance for different parts in determining quality:

1. Bridge
2. Top plate thickness
3. Cross bars or struts.

So-called “frame” guitar designs have a rigid waist bar to inhibit leakage of vibrational energy from the lower bout to the upper bout and other parts of the guitar.

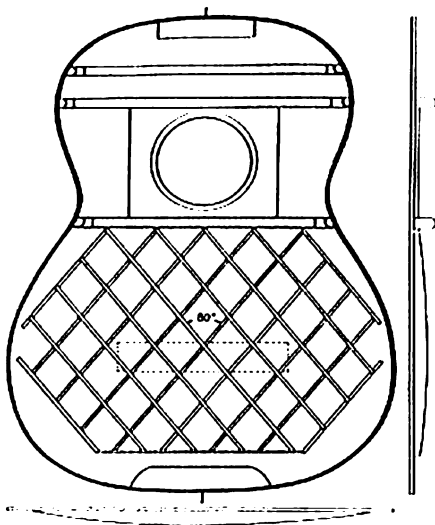
3.5.2 The Bridge

The bridge has a marked stiffening effect on the top plane, and thus affects the vibrations. For a heavy bridge the frequency of the first top plate resonance may decrease, the mass giving a larger contribution than the stiffness increase. Hand-made Spanish bridges tend to be considerably lighter and less rigid than factory-made bridges. For low frequencies the mass increase may dominate, but at higher frequencies the stiffening effect dominates (Jansson 2002).

3.5.3 Thickness of the Top Plate and Braces

Richardson and Roberts (1985) studied the influence of top plate and strut thickness with finite-element modeling using a computer. At the start, the plate thickness

Fig. 3.18 Lattice bracing of a guitar top plate used by Australian luthier Greg Smallman. Struts are typically of carbon-fiber-epoxy, thickest at the bridge and tapering away from the bridge in all directions (Caldersmith and Williams 1986)



was 2.9 mm, and the struts were 14 mm high and 5 mm wide. Their calculations showed that the cross struts gave a large influence at least for the low resonances. A reduction in strut height also results in a large influence on the resonance frequencies. Reduction in top plate thickness, especially thinning along the edge, has the greatest effect of all.

Richardson and his students have also found that reducing the *effective mass* has a great effect on radiation of high-frequency sound, even more than tuning the mode frequencies (Richardson 1998). The effective mass is difficult to control, however, after the choice of materials and general design has been made. Of primary importance is the effective mass of the fundamental sound board mode.

Australian luthier Greg Smallman, who builds guitars for John Williams, has enjoyed considerable success by using lightweight top plates supported by a lattice of braces, the heights of which are tapered away from the bridge in all directions, as shown in Fig. 3.18. Smallman generally uses struts of carbon-fiber-epoxy epoxied to balsa wood (typically 3 mm wide and 8 mm high at their tallest point) in order to achieve high stiffness-to-mass ratio and hence high-resonance frequencies or “lightness” (Caldersmith and Williams 1986).

3.5.4 Asymmetrical and Radial Bracing

Although many classical guitars are symmetrical around their center plane, a number of luthiers (e.g., Hauser in Germany and Ramirez in Spain, Schneider and Eban in the United States) have had considerable success by introducing varying degrees of asymmetry into their designs. Most asymmetric guitars have shorter but thicker struts on the treble side, thus making the plate stiffer. Three such top plate designs are shown in Fig. 3.19.

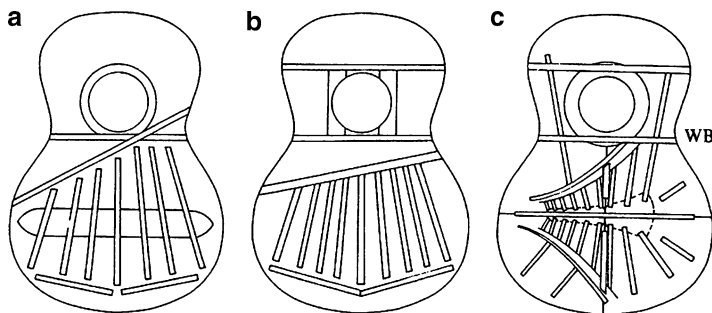


Fig. 3.19 Examples of asymmetric top plates: (a) Ramirez (Spain); (b) Fleta (Spain); (c) Eban (United States)

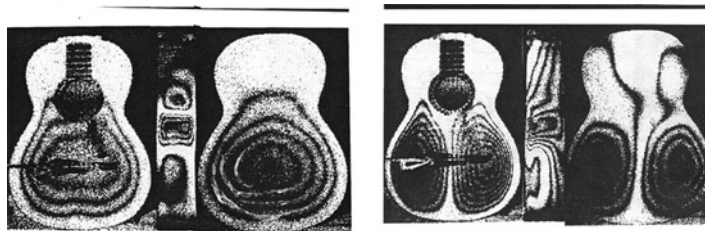


Fig. 3.20 Holographic interferograms showing modal shapes of two low-frequency modes at 101 and 304 Hz in a radially braced classical guitar (Rossing and Eban 1999)

The very asymmetric design in Fig. 3.19c was proposed by Kasha (1974) and developed by luthiers Richard Schneider, Gila Eban, and others. It has a split asymmetric bridge (outlined by the dashed line) and closely spaced struts of varying length. A waist bar (WB) bridges the two long struts and the sound hole liner.

Despite its asymmetry the vibrational modal shapes, at least at low frequency, are quite similar to other good classical guitars, as shown in the holographic interferograms in Fig. 3.20. The particular guitar in this modal study had a one-piece bridge and radial bracing in the back plate as well as the top plate. Other luthiers have had considerable success with radial bracing. Australian luthier Simon Marty uses a radial bracing of balsa or cedar reinforced with carbon fiber. Trevor Gore has had success using falcate bracing with curved braces of balsa and carbon fiber.

3.6 A Family of Scaled Guitars

Members of guitar ensembles (trios, quartets) generally play instruments of similar design, but Australian physicist/luthier Graham Caldersmith has created a new family of guitars especially designed for ensemble performance. (Actually, he has created two such families: one of classical guitars and one of steel-string folk guitars). His classical guitar family, including a treble guitar, a baritone guitar,

and a bass guitar in addition to the conventional guitar – which becomes the tenor of the family – has been played and recorded extensively by the Australian quartet Guitar Trek (Caldersmith 1995).

Caldersmith's guitar families include carefully scaled instruments, the tunings and resonances of which are translated up and down by musical fourths and fifths, in much the same way as the Hutchins–Schelleng violin octet (see Chap. 18). Caldersmith's bass guitar is a four-string instrument tuned the same as the string bass and the electric bass (E1, A1, D2, G2), an octave below the four lowest strings of the standard guitar. The baritone is a six-string instrument tuned a musical fifth below the standard, while the treble is tuned a musical fourth above the standard, being then an octave above the baritone. Caldersmith uses an internal frame, but a graded rectangular lattice instead of the diagonal lattice (see Fig. 3.21). The Australian Guitar Quartet is shown in Fig. 3.22.

Fig. 3.21 Caldersmith guitar with internal frame and *rectangular* lattice



Fig. 3.22 The Australian Guitar Quartet play on scaled guitars: bass and baritone by Graham Caldersmith, standard and treble by Greg Smallman and Eugene Philp

3.7 Synthetic Materials

Traditionally guitars have top plates of spruce or redwood with backs and ribs of rosewood or some comparable hardwood. Partly because traditional woods are sometimes in short supply, luthiers have experimented with a variety of other woods, such as cedar, pine, mahogany, ash, elder, and maple. Bowls of fiberglass, used to replace the wooden back and sides of guitars, were developed by the Kaman company in 1966; their Ovation guitars have become popular, partly because of their great durability.

One of the first successful attempts to build a guitar mostly of synthetic materials was described by Haines et al. (1975). The body of this instrument, built to the dimensions of a Martin folk guitar, used composite sandwich plates with graphite-epoxy facings around a cardboard core. In listening tests, the guitar of synthetic material was judged equal to the wood standard for playing scales, but inferior for playing chords. In France, Charles Besnainou and his colleagues have constructed lutes, violins, violas, cellos, double basses, and harpsichords, as well as guitars, using synthetic materials (Besnainou 1995).

3.8 Other Families of Guitars

Most of our discussion has been centered on classical guitars, with occasional comparison to the steel-string American folk (flat top) guitar. There are several other types of acoustic guitars in use throughout the world, including flamenco, archtop, 12-string, jazz, resonator, etc. Portuguese guitars will be discussed in Chap. 4. Some Asian plucked string instruments of the lute family will be discussed in Chap. 11.

The *gypsy guitar*, known in France as the *manouche* guitar, gained popularity in the late 1920s. Played by Django Reinhardt throughout his career, the instrument has seen a revival in interest. The community of gypsy jazz players today is a small, but growing one, and the original Selmer–Maccaferri guitars are highly valued and widely copied. Its low-gauge strings offer its player a brighter, more metallic tone, with an ease for creating a very distinct vibrato (Lee et al. 2007).

3.9 Electric Guitars

Although a contact microphone or other type of pickup can be attached to an acoustic guitar to provide an electrical output, the electric guitar has developed as a distinctly different instrument. Most electric guitars employ electromagnetic pickups, although piezoelectric and optical pickups are also used.

Electric guitars may have a solid body or a hollow body, the solid design being the more common. Vibrations of the body have much less influence on tone in the

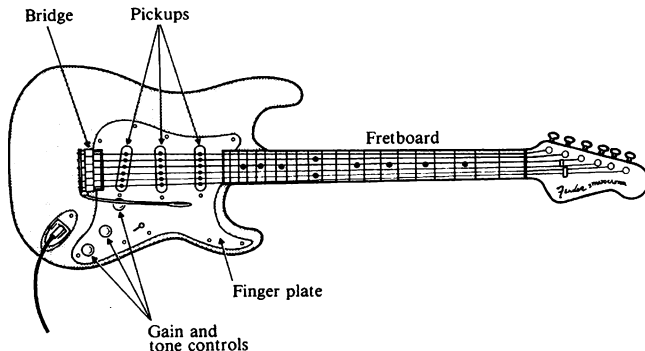


Fig. 3.23 An electric guitar

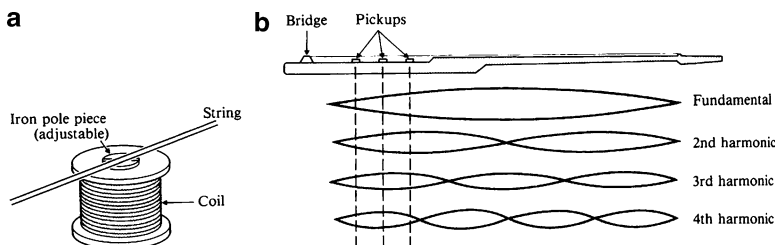


Fig. 3.24 Arrangement of multiple pickups to sample various harmonics of the string

electric guitar than in its acoustic cousin. The solid guitar, although heavier, is less susceptible to acoustic feedback (from the loudspeaker to the guitar), and it also allows the strings to continue vibrating for a longer time. Figure 3.23 shows the main features of an electric guitar.

The electromagnetic pickup consists of a coil with a magnetic core. The vibrating string causes changes in the magnetic flux through the core, thus inducing an electric signal in the coil. Most electric guitars have at least two pickups for each string; some have three. These pickups, located at different points along the string, sample different strengths of the various harmonics, as shown in Fig. 3.24. The front pickup (nearest the fretboard) generates the strongest signal at the fundamental frequency, whereas the rear pickup (nearest the bridge) is most sensitive to the higher harmonics (the resulting tones are sometimes characterized as “mellow” and “gutsy,” respectively). Switches or individual gain controls allow the guitarist to mix together the signals from the pickups as desired. Magnetic pickups are discussed in Chap. 22 as well as in a paper by Horton and Moore (2009).

Most magnetic pickups have a threaded pole piece that can be adjusted in height by screwing it in or out. Adjusting the pole piece closer to the string will usually increase the volume, but if it is too close to the string, distortion will result due to the force exerted on the string by the magnet. The distortion becomes especially

noticeable when fingering beyond the twelfth fret, which brings the string down close to the pickup. *Humbucking pickups* have two coils wound in such a way that stray magnetic fields (from power cords, lights, etc.) will induce opposing electrical signals in the two coils; thus the hum they produce will be minimized. Some electric guitars mix humbucking pickups and single-coil pickups.

Piezoelectric pickups are typically piezoelectric materials placed on the bridge which respond to the force of the vibrating strings on the bridge. They generate a sound different from magnetic pickups, which some musicians prefer. They do not pick up noise from stray magnetic fields.

Optical pickups, which use infrared LEDs and photodetectors to sense the string vibration, are now appearing on the scene. Since optical pickups are not magnetic, steel strings do not have to be used. Optical pickups sense string *displacement*, whereas magnetic pickups sense string *velocity*, and piezoelectric pickups sense string *force*. Clearly, some flexibility is gained by mixing outputs of all three sensors.

3.9.1 *Body Vibrations and Dead Spots*

The vibrations of strings are influenced by their end supports. As a result of nonrigid end supports, energy can flow from the strings to the body of an instrument, causing the string vibrations to decay faster than in the case of rigid supports. In an electric guitar, this mechanism can lead to *dead spots* at certain locations on the fretboard (Fleischer and Zwicker 1998).

Dead spots in a typical electric guitar with a symmetrical headstock (such as the Les Paul) occur around 200 and 450 Hz. In a typical guitar with an asymmetrical headstock (such as the Stratocaster), the dead spots occur at slightly higher frequencies, the difference being due to torsional motion of the neck.

3.9.2 *Electric Bass*

A special type of electric guitar is the *bass guitar* or *electric bass* widely used in rock and jazz bands. Tuning of a four-string electric bass is E-A-D-G, tuned in fourths with the lowest note being E1 at 41.2 Hz. This is the same tuning as the acoustic bass. The highest note produced is about G4 at 392 Hz. Tuning of the five string bass is B-E-A-D-G with lowest note B0 = 30.87 Hz. Six-string tuning is B-E-A-D-G-C. The fretboard is longer than that of the ordinary electric guitar (about 90 cm compared to about 65 cm). An electric bass also has dead spots at frequencies for which the neck conductance is a maximum. In a typical bass, these occur around 40, 110, and 150 Hz (Fleischer 2000).

Electric guitars are discussed in more detail in Chap. 22.

3.10 Lutes

Lutes are generally thought to have originated in Mesopotamia around 2000 BC, from which they traveled both west to Europe and east to Asia. Many different designs and variations on the basic design have existed through the ages. The long lute, having a neck longer than the body, which date back to around 2000 BC, has modern descendants in several countries (e.g., the *tar* of Turkey and Iran, the *sitar* and *vina* of India, the *bouzouki* of Greece, the *tambura* of India and Yugoslavia, and the *ruan* of China). The short lute, which dates from about 800 BC, is the ancestor of the European lute as well as many other plucked string instruments around the world.

The European lute first appeared in the thirteenth century, deriving its name from the Arabic phrase “*al-oud*,” which means “made of wood.” The lute is one of the most attractive and delicate of all Renaissance musical instruments. Its principal characteristics are an exceptional lightness of construction, a rounded back constructed from a number of ribs, and a peg-box set at an angle to the fingerboard, as shown in Fig. 3.25.

Instruments of the sixteenth century generally had eleven strings in six courses (all but the uppermost consisting of two unison strings), which might be tuned to A2, D3, G3, B3, E4, and A4, although the tuning was often changed to fit the music being played. Sometimes the lower three courses were tuned in octaves.

In the seventeenth century, an increasing number of bass courses were added. These usually ran alongside the fingerboard, so that they were unalterable in pitch during playing. Lundberg (1987) describes a family of Italian sixteenth/seventeenth-century lutes as follows:

Small octave: four courses, string length 30 cm;

Descant: seven courses, string length 44 cm;



Fig. 3.25 Examples of Renaissance lutes

Alto: seven courses, string length 58 cm;
Tenor: seven courses, string length 67 cm;
Bass: seven courses, string length 78 cm;
Octave bass: seven courses, string length 95 cm.

The pear-shaped body of the lute is fabricated by gluing together a number (from 9 up to as many as 37) of thin wooden ribs. The table or sound board is usually fabricated from spruce, 2.5–3.0 mm thick, although other woods, such as cedar and cypress, have also been used. The table is braced by transverse bars (typically seven) above, below, and at the sound hole (see Jahnel 1981).

3.10.1 Acoustics of the European Short Lute

Only a few studies on the acoustical behavior of lutes have been reported. Firth (1977) measured the input admittance (driving point mobility) at the treble end of the bridge and the radiated sound level 1 m away, which are shown in Fig. 3.26.

Firth associates the peak at 132 Hz with the Helmholtz air mode and the peaks at 304, 395, and 602 Hz with resonances in the top plate. Figure 3.27 illustrates five such resonances and also shows how the positions of the nodal lines are related to the locations of the bars. The resonances at 515 and 652 Hz are not excited to any extent by a force applied to the bridge because they have nodes very close to the bridge.

3.10.2 Acoustics of the Turkish Long-Necked Lute

The Turkish *tanbur* is a long-necked lute with a quasi-hemispherical body shell made of 17, 21, or 23 thin slices of thickness 2.5–3.00 mm. The slices are usually cut from ebony, rosewood, pearwood, walnut, or cherry. The sound board is made of a thin (1.5–2 mm) spruce panel. It has neither a sound hole or braces. The strings

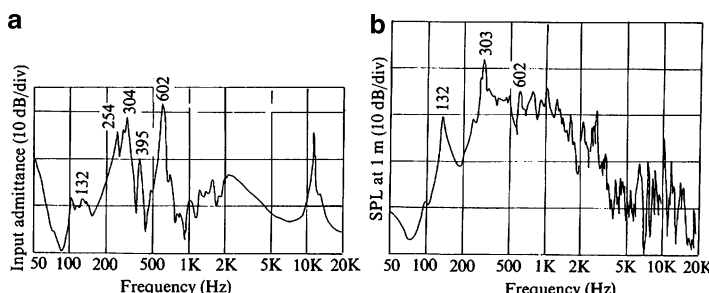


Fig. 3.26 (a) Mechanical input admittance (mobility) at the treble end of a lute bridge; (b) sound pressure level 1 m from the top plate (belly) (Firth 1977)

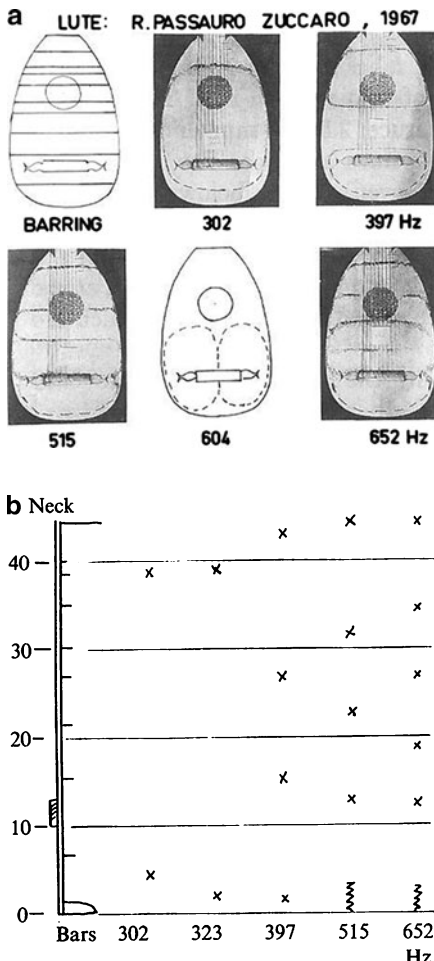


Fig. 3.27 (a) Barring pattern and nodal patterns in the top plate of a lute at five resonances; (b) locations of nodes compared to the bridge and the bars (Firth 1977)

are stretched between a raised nut and a violin-like bridge. The long neck (73.5–84 cm), which is typically made of ebony or juniper, hosts 5,258 movable frets of gut or nylon. The tanbur has seven strings, six of them grouped in pairs, and the lowest string, tuned to A1, is single. The pairs are tuned to A2, D2, and again A2 (or alternatively A2, E2, and A2). It is illustrated in Fig. 3.28.

The impulse response of the tanbur body for three orthogonal force impulses applied to bridge are shown in Fig. 3.29. These responses include the effects of driving point admittance of the bridge, the vibration of body and neck, and the directivity of the radiation pattern. These responses were recorded in an anechoic room (Erkut et al. 1999).

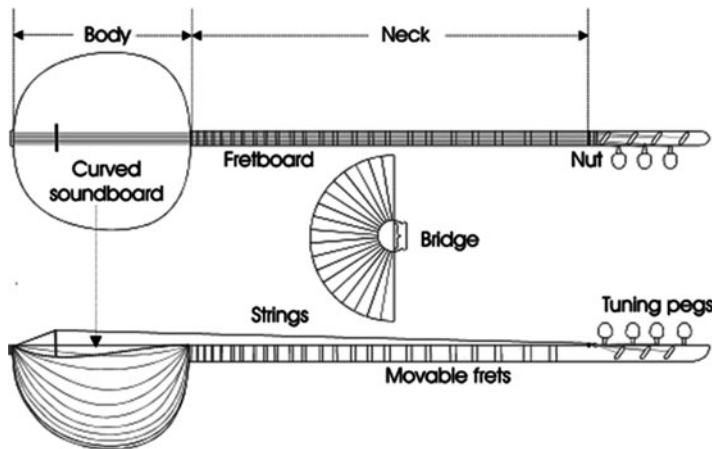


Fig. 3.28 Turkish *tanbur* (from Erkut et al. 1999)

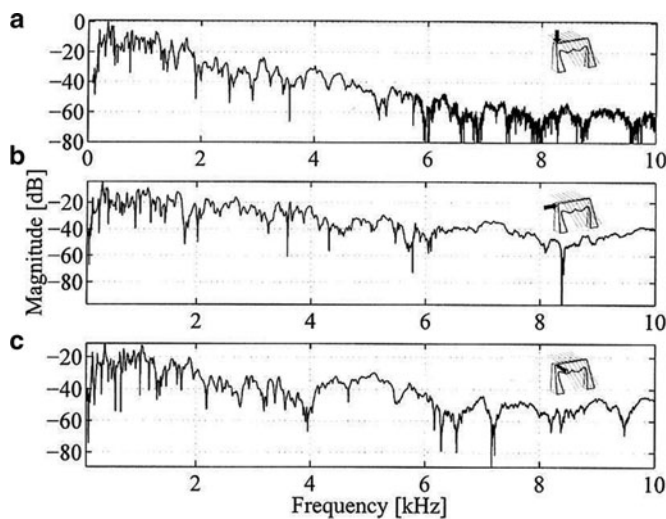


Fig. 3.29 Magnitude spectra of the tanbur body impulse responses: (a) The vertical impulse response spectrum; (b) the horizontal impulse response spectrum; (c) the longitudinal impulse response spectrum (Erkut et al. 1999)

The vertical impulse response is relatively stronger compared to the other directions. The pronounced low-pass characteristics of the body above 400 Hz are evident. Short-time Fourier transform of the vertical impulse response is shown in Fig. 3.30. The tanbur body vibrations decay considerably faster than those of a guitar body, and the peaks around 344 and 275 Hz decay faster than the peak around 191 Hz.

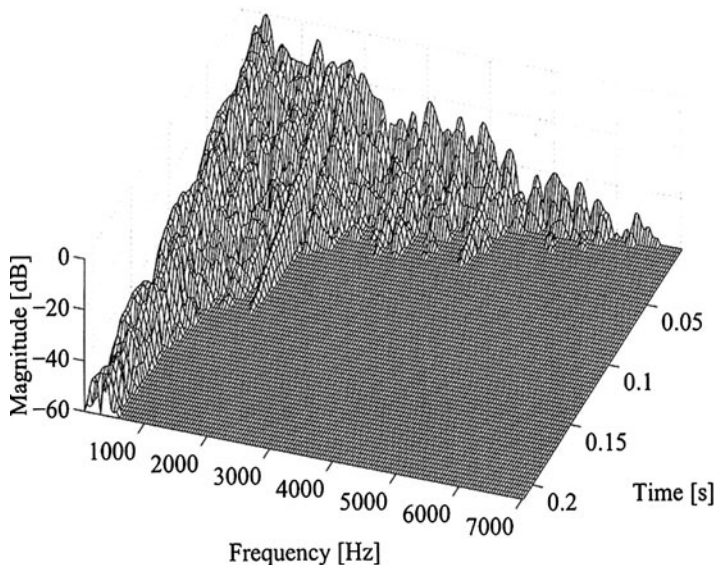


Fig. 3.30 Short-time Fourier transform of the vertical impulse response

3.11 Concluding Remarks

The lute family of string instruments includes many instruments found in many world cultures, past and present. In this chapter we have discussed guitars and lutes. Chapters 4–6, and 10 discuss other instruments in the lute family.

References

- C. Besnainou (1995). “From wood mechanical measurements to composite materials for musical instruments: New technology for instrument makers.” *MRS Bull.* **20**(3), 34–36.
- R. R. Boullosa (1981). “The use of transient excitation for guitar frequency response testing.” *Catgut Acoust. Soc. Newslett.* **36**, 17.
- G. Caldersmith (1995). “Designing a guitar family.” *Appl. Acoust.* **46**, 3–17.
- G. W. Caldersmith and E. V. Jansson (1980). “Frequency response and played tones of guitars.” Quarterly Report STL-QPSR 4/1980, Department of Speech Technology and Music Acoustics, Royal Institute of Technology (KTH), Stockholm, pp. 50–61.
- G. Caldersmith and J. Williams (1986). “Meet Greg Smallman.” *Am. Lutherie* **8**, 30–34.
- O. Christensen and R. B. Vistisen (1980) “ Simple model for low-frequency guitar function.” *J. Acoust. Soc. Am.* **68**, 758–766.
- C. Erkut, T. Tolonen, M. Karjalainen, and V. Välimäki (1999). “Acoustical analysis of tanbur, a Turkish long-necked lute.” *Proceedings 6th International Congress on Sound and Vibration*, Copenhagen.
- I. Firth (1977). “Some measurements on the lute.” *Catgut Acoust. Soc. Newslett.* **27**, 12.
- H. Fleischer (2000). *Dead Spots of Electric Basses*. Institut für Mechanik, Universität der Bundeswehr München.

- H. Fleischer and T. Zwicker (1998). "Mechanical vibrations of electric guitars." *Acustica* **84**, 758–765.
- N. H. Fletcher (1976). *Physics and Music*. Heinemann Educational Australia, Richmond, VIC.
- N. H. Fletcher and T. D. Rossing (1998). *The Physics of Musical Instruments*, 2nd ed. Springer, New York.
- D. W. Haines, C. M. Hutchins, and D. A. Thompson (1975). "A violin and a guitar with graphite-epoxy composite soundboards." *Catgut Acoust. Soc. Newslett.* **23**, 25–28.
- N. G. Horton and T. R. Moore (2009). "Modeling the magnetic pickup of an electric guitar." *Am. J. Phys.* **77**, 144–150.
- F. Jahnel (1981). *Manual of Guitar Technology*. Verlag Das Musikinstrument, Frankfurt am Main.
- E. V. Jansson (1971) "A study of acoustical and hologram interferometric measurements on the top plate vibrations of a guitar." *Acustica* **25**, 95–100.
- E. V. Jansson (1983) "Acoustics for the guitar player." In *Function, Construction, and Quality of the Guitar* (E. V. Jansson ed.) Royal Swedish Academy of Music, Stockholm, pp. 7–26.
- E. V. Jansson (2002). *Acoustics for Violin and Guitar Makers*, 4th ed. Royal Institute of Technology, Stockholm. Chapter VI.
- M. Kasha (1974). "Physics and the perfect sound." In *Brittanica Yearbook of Science and the Future*, Encyclopedia Britannica, Chicago.
- N. Lee, A. Chaigne, J. O. Smith III, K. Arcas (2007). "Measuring and understanding the gypsy guitar." *Proceedings of the International Symposium on Musical Acoustics*, Barcelona.
- R. Lundberg (1987). "Historical lute construction: The Erlangen lectures." *Am. Lutherie* **12**, 32–47.
- J. Meyer (1983). "Quality aspects of the guitar tone." In *Function, Construction, and Quality of the Guitar* (E. V. Jansson ed.) Royal Swedish Academy of Music, Stockholm, pp. 77–108.
- J. Popp and T. D. Rossing (1986). "Sound radiation from classical and folk guitars." *International Symposium on Musical Acoustics*, West Hartford, Connecticut, July 20–23.
- B. E. Richardson (1982). *A Physical Investigation Into Some Factors Affecting the Musical Performance of the Guitar*, PhD thesis, University of Wales.
- B. E. Richardson (1998). "The classical guitar: Tone by design." *Proceedings of the International Symposium on Musical Acoustics 1998* (D. Keefe, T. Rossing, C. Schmid eds.) Acoustical Society of America, Woodbury.
- M. H. Richardson (1997). "Is it a mode shape, or an operating deflection shape?" *Sound Vib.* **31**(1), 54.
- B. E. Richardson and G. W. Roberts (1985). "The adjustment of mode frequencies in guitar: A study by means of holographic interferometry and finite element analysis." *Proceedings of SMAC 83*. Royal Swedish Academy of Music, Stockholm, pp. 285–302.
- R. E. Ross (1979). "The acoustics of the guitar: An analysis of the effect of bracing stiffness on resonance placement." MS thesis, Northern Illinois University.
- R. E. Ross and T. D. Rossing (1979). Plate vibrations and resonances of classical and folk guitars. *J. Acoust. Soc. Am.* **65**, 72.
- T. D. Rossing (1982) "Plate vibrations and applications to guitars." *J. Guitar Acoust.* **3**, 23–41.
- T. D. Rossing, J. Popp, and D. Polstein (1985) "Acoustical response of guitars." *Proc. SMAC 83*. Royal Swedish Academy of Music, Stockholm, pp. 311–332.
- T. D. Rossing (2007) "Modal analysis." In *Springer Handbook of Acoustics* (T. D. Rossing ed.) Springer, Heidelberg.
- T. D. Rossing and G. Eban (1999). "Normal modes of a radially braced guitar determined by electronic TV holography." *J. Acoust. Soc. Am.* **106**, 2991–2996.
- K. A. Stetson (1981). "On modal coupling in string instrument bodies." *J. Guitar Acoust.* **3**, 23–31.
- J. Taylor (1978). *Tone Production on the Classical Guitar*. Musical New Services, Ltd., London.
- H. Turnbull (1974). *The Guitar from the Renaissance to the Present Day*. Batsford, London.
- W. Y. Strong, T. B. Beyer, D. J. Bowen, E. G. Williams, and J. D. Maynard (1982) "Studying a guitars radiation properties with nearfield holography." *J. Guitar Acoustics* **6**, 50–59.

Chapter 4

Portuguese Guitar

Octavio Inacio

When referring to Portuguese traditional music, *fado* inevitably comes to mind. In this particular style of Portuguese music a singer is accompanied by two instruments: a classical guitar (more commonly known as *viola*) and a pear-shaped plucked chordophone, with six courses of double strings – the Portuguese guitar. The characteristic sonority of this instrument is a great part of what makes *fado* so distinguishable from any other style of traditional music in Europe. While from an ethnological and a musical perspective this instrument has gained the attention of a handful of researchers (de Oliveira 2000; Cabral 1998), the scientific study of the vibroacoustic dynamics of these instruments is very recent. Fortunately, as with most other instruments, decades of refining craftsmanship have provided Portuguese guitars of excellent quality. Even if still unknown to the greater part of the musical world, the sonority, timbre and dynamical range of the Portuguese guitar continue to seduce many new listeners.

4.1 Origins

Directly descended from the Renaissance European *cittern*, the Portuguese guitar as we know it today underwent considerable technical modifications in the last century (dimensions, mechanical tuning system, etc.) although it has kept the same number of six double courses, the string tuning, and the finger plucking technique characteristic of this type of instrument which is named *dedilho*, meaning the use of the forefinger nail upward and downward, as a plectrum.

There is evidence of the guitar's use in Portugal since the thirteenth century (in its earlier form, the *cítola*) amongst troubadour and minstrel circles and in the Renaissance period, although initially it was restricted to noblemen in court circles. Later, its use became more popular, and references have been found to citterns

O. Inacio (✉)
ESMAE, Rua da Alegria, 503, Porto 4000-045, Portugal
e-mail: OctavioInacio@ESMAE-IPP.PT

being played in the theater as well as in taverns and barbershops, in the seventeenth and eighteenth centuries in particular.

In 1649, the catalog of the Royal Music Library of King John IV of Portugal was published, containing the best-known books of cittern music from foreign composers of the sixteenth and seventeenth centuries. The complexity and technical difficulty of the musical pieces leads to the belief that there were highly skilled players in Portugal during that period. Later in the eighteenth century (ca. 1750) the so-called English guitar made its appearance in Portugal. It was a type of cittern locally modified by German, English, Scottish, and Dutch makers, and it was enthusiastically greeted by the new mercantile bourgeoisie of the city of Porto who used it in the domestic context of *Hausmusik* practice. The use of this type of guitar never became widespread. It disappeared in the second half of the nineteenth century when the popular version of the cittern came into fashion again by its association with the Lisbon song (fado) accompaniment.

Nowadays, the Portuguese guitar has become fashionable for solo music as well as for accompaniment, and its wide repertoire is often presented in concert halls and at classical and world music festivals around the world (Cabral 1998).

4.2 Types and Characteristics

There are basically two models of this instrument: the Coimbra and the Lisbon guitars, named after the towns where the two different styles of fado were developed. However, a few guitars can still be found with slightly different characteristics which are known as Porto guitars (see Fig. 4.1).

The most distinguishable characteristics of the Portuguese guitar are the pear-shaped body and the head, which exhibits tear-shaped (Coimbra model) or spiral-shaped (Lisbon model) decorations. The top plate (sound board) can be slightly

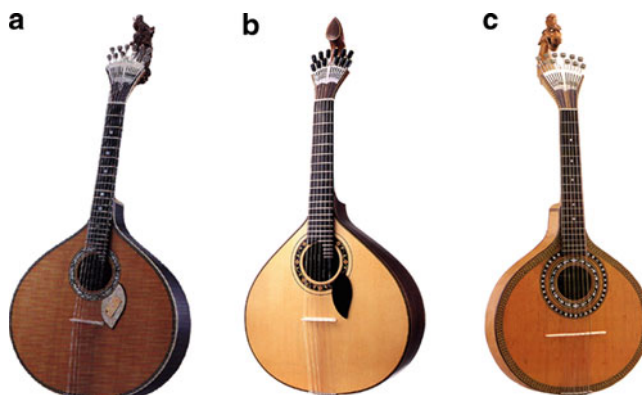


Fig. 4.1 Portuguese guitars: (a) Lisbon, (b) Coimbra, and (c) Porto models

curved while the back plate is usually flat; both parts are joined by ribs and run roughly parallel to each other. The soundhole is round and typically decorated with pearl-shell infills. The six courses of double strings are stretched from the nut to the *atadilho* (a small tailpiece at the end of the body of the instrument) passing over the bridge (usually made of bone) which is simply placed between the strings and the sound board. The main characteristics that distinguish the different types of guitars are mainly concerned with the sizes and tunings. Lisbon guitars have an effective string length of 440–445 mm, while in Coimbra and Porto guitars the length is usually 470 mm (Henrique 2003). In all these types of guitars, the lowest three orders of strings are doubled to the octave while the remaining three higher-pitched orders are composed of two unison strings.

4.3 Vibroacoustic Behavior

In an earlier study (Inácio et al. 2004), some of the vibroacoustic characteristics of this instrument were analyzed. In order to have a representative sample of the broad range of sound qualities that these instruments may exhibit, vibration and acoustical measurements were performed on ten different instruments. These instruments varied on the type (Lisbon, Coimbra, or Porto), builder, and year of construction, as well as on the materials of the top (sound board) and back plate. Table 4.1 describes the main characteristics of the instruments used in the experiments.

To allow a relevant comparison between the modal characteristics of the different instruments, accelerance frequency response functions, $H_v(\omega) = \ddot{Y}_r(\omega)/F_e(\omega)$, were measured using impact excitation, $F_e(\omega)$, applied perpendicularly to the sound board at four locations common to all the instruments. The acceleration response, $\ddot{Y}_r(\omega)$, was measured by a lightweight accelerometer placed on the sound board close to the lower string side of the bridge. Simultaneously, vibroacoustic transfer functions, $H_a(\omega) = p_r(\omega)/F_e(\omega)$ were measured using the same excitation signal, $F_e(\omega)$, while the response, $p_r(\omega)$, was measured by a microphone facing the instrument at approximately 0.5 m distance.

Table 4.1 Description of the guitars used in the experiments

Guitar	Construction year	Builder	Type	Top plate	Back plate
A	1998	Fernando Meireles	Coimbra	<i>Picea abies</i>	<i>Dalbergia latifolia</i>
B	1971	Gilberto Grácio	Coimbra	<i>Picea abies</i>	<i>Dalbergia nigra</i>
C	1969	Gilberto Grácio	Coimbra	<i>Picea abies</i>	<i>Juglans nigra</i>
D	1990	Gilberto Grácio	Coimbra	<i>Picea abies</i>	<i>Dalbergia latifolia</i>
E	1920	António Duarte	Porto	<i>Picea abies</i>	<i>Dalbergia nigra</i>
F	1964	João P. Grácio	Lisbon	<i>Picea abies</i>	<i>Dalbergia nigra</i>
G	1950	Francisco Silva	Lisbon	<i>Picea abies</i>	<i>Juglans regia</i>
H	1925	João Grácio Júnior	Lisbon	<i>Picea abies</i>	<i>Dalbergia nigra</i>
I	1903	Augusto Vieira	Lisbon	<i>Picea abies</i>	<i>Dalbergia nigra</i>
J	1966	Joaquim Grácio	Lisbon	<i>Picea abies</i>	<i>Dalbergia nigra</i>

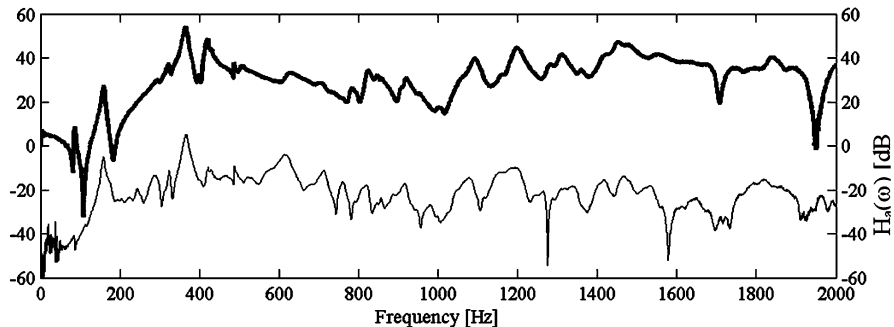


Fig. 4.2 Example of an accelerance (heavy line) and vibroacoustic (thin line) frequency response function of guitar E

The instrument was placed inside a highly sound-absorbing chamber and suspended from a rigid structure by means of rubber bands. The strings were properly tuned and damped by a textile or plastic material on each side of the bridge. A full experimental modal identification, based on impact testing, was also performed on one of the instruments. A mesh of 114 impact locations was defined, covering both the sound board and the fingerboard in order to identify possible coupled motions.

Figure 4.2 shows a typical accelerance frequency response function (FRF) and the corresponding vibroacoustic transfer function for guitar E, with impact location at the lower string end of the bridge. The acceleration response is measured at approximately the same location but on the guitar sound board. The sound pressure response is measured at 0.5 m from the front of the instrument as described before. The accelerance FRF shows a first peak below 100 Hz, which does not contribute considerably to the radiated sound, as can be seen from comparison with the vibroacoustic FRF. Up to 500 Hz the response of the guitar is dominated by modes with lower damping factors than in the higher frequency range where separate modes become much more difficult to distinguish.

Figures 4.3 and 4.4 depict the accelerance and vibroacoustic frequency response functions for the ten guitars for excitation and response locations. For the first five guitars ($A \neq E$) there are only two resonances below 200 Hz, where the first one (at approximately 100 Hz) does not radiate sound efficiently, and could be due to a coupled motion between the fingerboard and the body, a phenomena that is also found in classical guitars. Interestingly, this first structural resonance is not so apparent in Lisbon guitars (F–J). The second resonance, however, is present in all guitars and is responsible for an important part of the radiated sound spectrum. Due to its low frequency (ranging from 121 to 160 Hz) and its radiation efficiency it is clear that this resonance is due to the air cavity mode that occurs in most string instruments with a hollow resonator (Elejabarrieta 2002).

In order to identify this Helmholtz resonance, a piece of foam was placed over the soundhole, canceling any possible air oscillations through it. Figure 4.5 shows a comparison between the accelerance FRF measured with and without the foam for

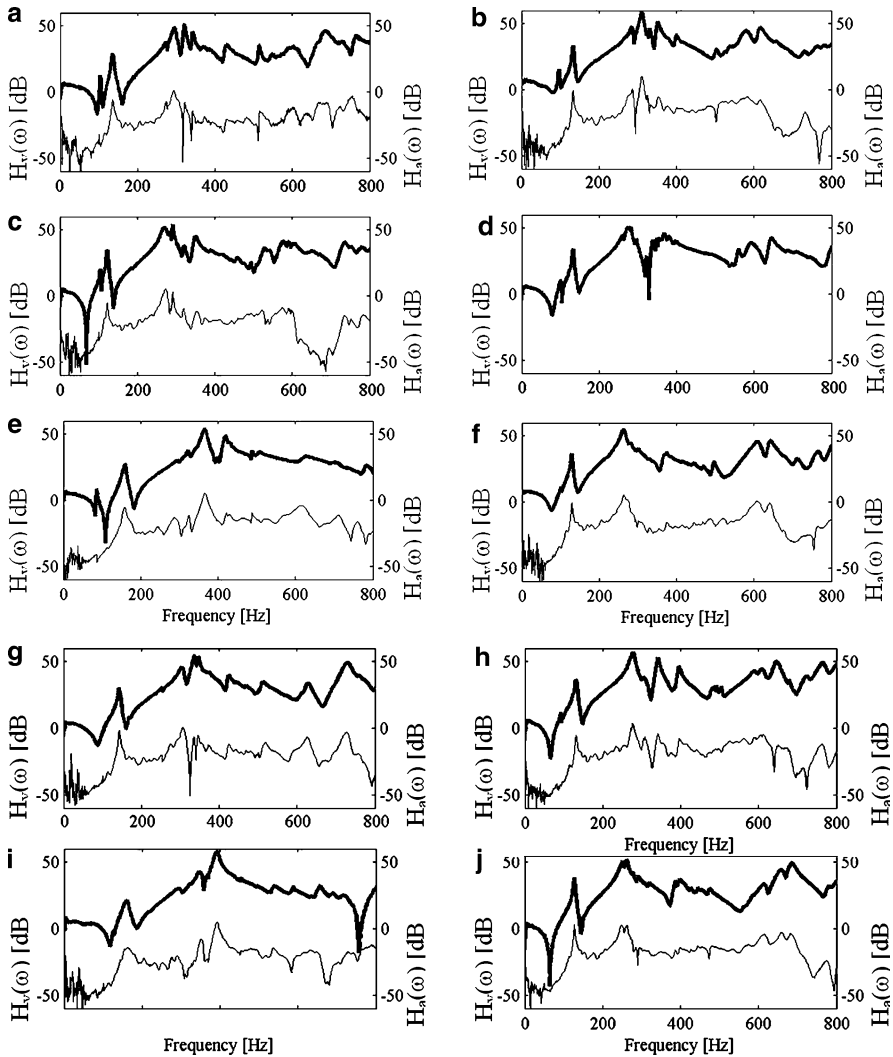


Fig. 4.3 Accelerance (heavy line) and vibroacoustic (thin line) frequency response function for guitars a–j in the frequency range of 0–800 Hz

the same points of excitation and response. The red line (with foam) shows the missing resonance at approximately 130 Hz in comparison with the black line (without foam). This is also apparent in the vibroacoustic FRF shown at the lower part of the plot, which proves that this acoustical resonance is coupled to a structural resonance of the body at the same frequency, as also verified in

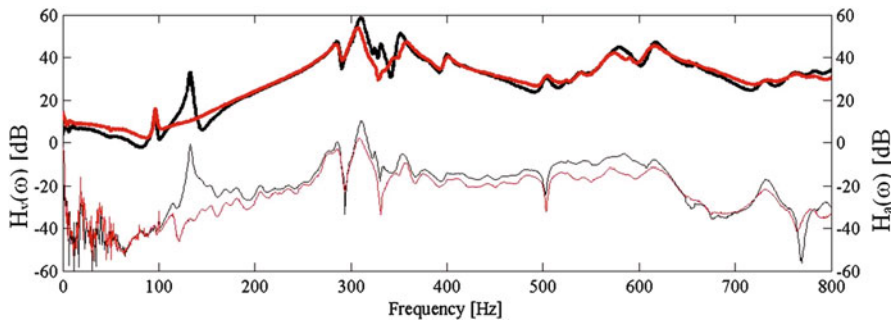


Fig. 4.4 Accelerance (*heavy lines*) and vibroacoustic (*thin lines*) frequency response function for guitars a–j in the frequency range of 0–800 Hz

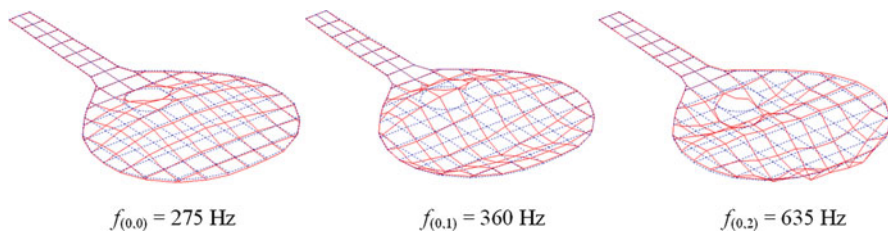


Fig. 4.5 Mode shapes of three resonances of the sound board of guitar D

classical guitars (Inácio et al. 2004; Caldersmith 1995). This phenomenon was found for all the guitars studied.

Between 250 and 450 Hz there is at least one major resonance, or group of resonances, responsible for a significant part of the radiated spectrum. The most important of these is the (0,0) monopole mode, shown in Fig. 4.6 for guitar D, which radiates sound more efficiently, in contrast with the (0,1) longitudinal dipole mode where adjacent antinodes move in anti-phase and eliminate any net volume flow (Meyer 1983). For guitar D, the (0,2) longitudinal tripole mode shows up only at 635 Hz.

4.4 Subjective Acoustical Quality Evaluation

Portuguese guitar builders have relied on the opinion of musicians and their own experience to form a judgment of this subjective characteristic, and tentatively improve the quality of their work. A more scientific approach (whether more efficient or not is still a matter of discussion) is to perform a statistical analysis of the opinions of a great number of listeners on the sound of such instruments and correlate them with measurable physical parameters. This last approach has been thoroughly developed by several authors in relation to the sound quality evaluation of classical guitars. Nonetheless, the measurable physical parameters

that serve as the basis to this correlation procedure can differ significantly for different authors.

Jansson (1983a, b) and Meyer (1983) established several different objective parameters for this purpose based on the characteristics of the sound decay of each partial for a particular note; the modal properties of the instrument body; or even the radiated sound pressure level for a specific range of one-third octave bands. Orduña-Bustamante (1992) followed a similar approach using the measurement of attack and decay times as well as sound pressure level in wider frequency bands, while Boullosa et al. (1999) based their research on the tuning characteristics and the radiation efficiency of the guitars. More recently, Hill et al. (2003) defined a set of acoustical parameters based on standard input impedance measurements at string positions on the bridge as well as sound radiation properties measured by spherically traveling microphones surrounding the instrument driven at different resonant frequencies. Following the study of the vibroacoustic characteristics of the Portuguese guitar (Inácio et al. 2004), a subjective quality evaluation was performed (Santiago et al. 2004) with the aim of establishing a correlation between the subjective preferences of a number of listeners and some objective physical measures.

4.4.1 Objective Parameters

From the vast quantity of objective parameters that are described in the literature (Jansson 1983a, b; Meyer 1983; Orduña-Bustamante 1992; Boullosa et al. 1981; Hill et al. 1983) to evaluate the quality of classical guitars, it was decided to make use of the low-frequency modal characteristics reported in Inácio et al. (2004) and calculate a set of objective parameters based on the research by Jansson (1983a, b) and Meyer (1983). The parameters chosen were the following:

f_i and L_i – the frequency and amplitude of the first three major resonances, where i stands for the resonance number (1, 2, or 3);

a_i^1 – the frequency interval between the first two major resonances and the frequency of the closest musical notes, in cents, where i stands for the resonance number (1, 2, or 3);

a_2 – the presence of a lower-amplitude resonance below the first major resonance;

a_3 – the difference from an octave of the frequency interval between the first and the second major resonances, in cents.

4.4.2 Listening Tests

Listening tests were performed by a set of 60 individuals, a random opportunistic sample, all with an academic or professional relationship with music: students and teachers of music technologies, classical music, jazz, or composition. All listened to a sound recording of a 20-s fragment of “*Estudo de Dedilho*” by Pedro Caldeira Cabral, played by the composer on each of the ten different guitars. The choice of

the piece of music to be reproduced was selected from a set of other possible alternatives, for its counterpoint character and the existence of several low- and high frequency-tones, which covered a considerably broad frequency spectrum. The musical piece was recorded in a small recital hall with a reverberation time (T_{30}) of approximately 0.9 s in the 500-Hz octave band, a natural environment for both the player and the listeners, close to their usual listening references. A sound level meter was also placed at 1 m from the instrument in order to measure the time-averaged sound pressure level for each guitar, which allowed the calibration of the reproduced sound level during the listening tests.

4.4.3 *Test Conditions*

The 60 subjects listened individually to the sound sample through a stereo loudspeaker set. The loudspeakers were placed inside a highly sound-absorbing chamber so that any influence for the listening room acoustics would be negligible. This arrangement allowed all the listeners to be in the same acoustical conditions for evaluating their subjective response to the instruments. This approach was preferred to a live performance done simultaneously for all the subjects, such as the one used in Elejabarrieta (2002). Furthermore, the fact that they could not see the instruments excluded the possibility of preference over different visual characteristics and also as suggested in Henrique (2003), the most relevant question to this work was a simple option of preference for one guitar among a choice of two. However, for the purpose of trying to unfold the reason for the choice of a particular instrument, other aspects, defined by subjective parameters, were taken into account.

4.4.3.1 *Subjective Parameters Used*

Apart from the most important question of which guitar was preferred, the subjects were also asked to choose one of the guitars in relation to three subjective parameters. These were clearly explained to the listeners as the following:

- *Timbre*: One of the subjective characteristics of sound that allows the listener to differentiate between two sounds of the same pitch and intensity. Timbre results from the subjective correlation of all the properties of sound that do not directly influence pitch and intensity, such as temporal envelopment, energy spectral distribution, and degree of partials inharmonicity. The attack transient is also fundamental to the characterization of the timbre of an instrument (Orduña-Bustamante 1992).
- *Volume*: Considered as the subjective correlate to sound pressure level at the point of listening, as a result of the direct sound and reflections inside a room.
- *Clarity*: Considered as a subjective measure of the degree of perception of each individual note produced by the instrument as clear and distinct from one another.

4.4.3.2 Conditions of the Guitars

Not all of the guitars were played regularly by the musician. Apart from the fact (or myth?) that instruments that are not played frequently cannot perform adequately, this can adversely affect the musician's ability to obtain the "best" sound, as he does on an instrument that he is used to playing on a daily basis.

Only three instruments were played and tuned regularly. The others were either played frequently in the past and were not at the present time, or they were never significantly played. Furthermore, not all the instruments had new strings, which were only placed on the ones with poorer string conditions. It can be concluded that it was not possible to have all the guitars under the same playing conditions.

4.4.4 Test Procedure

Following a similar procedure to the ones used in Henrique (2003) and Elejabarrieta (2002), the recorded music samples were reproduced in pairs. Each pair corresponds to two successive recordings made with two different guitars. However, control pairs with the same guitar were also used to give more reliability to the results. The two musical samples in each pair were separated by a 1-s interval and a 5- to 10-s interval was used between pairs, so that the listeners could erase the memory of the previous pair. The test procedure consisted of the following steps:

- (a) Each individual made a set of six comparisons of guitar pairs, in which five pairs were of different guitars and a sixth consisted of a pair of samples of the same guitar. The 12 ($10 + 2 \times 1$) samples were randomly combined to form ten different sets of comparisons to be attributed to different listeners. The extra pair of equal guitars was repeated the same number of times in all the comparison sets.
- (b) For each pair of music samples, the listener gave a preference about one of them. This resulted in a choice for six instruments, which in turn composed another set of three comparisons. Preferences according to the subjective parameters referred were also registered;
- (c) The next comparison gave rise to the choice of three guitars, which then were compared all together. The music samples were then played twice so as to minimize the possible *short memory effect*.¹
- (d) After the choice of one guitar was achieved, the following subject was called (without contact with the previous one) and a different set of comparisons was presented using the same procedure described.

¹ Effect in which the subject's memory unconsciously loses the hearing reference to the first music sample in the pair comparison. This effect is usually appreciable when the second music sample is frequently preferred to the first one, even after changes in the pair order are realized.

4.5 Results

4.5.1 Subjective Tests

Figure 4.6 presents the results of the overall votes for each guitar. Guitar D was the most voted for instrument, while guitar E was not voted for in any of the comparisons. The majority of the votes were for the first four guitars, which are of the Coimbra type.

Comparing these results with the number of choices on the individual subjective parameters, suggests that the *timbre* is the most relevant (of the three used in this study) to evaluate the preference over one instrument. Interestingly, guitar A has a higher number of votes in each subjective parameter than the most preferred guitar.

4.5.2 Objective Tests

Table 4.2 shows the results of the analysis carried to the frequency response measurements, according to the parameters defined in Sect. 4.4.1. This analysis was not straightforward because in some of the guitars a large number of modes were bundled together at certain frequencies. Nevertheless, a careful attempt was made to obtain relevant results.

It appears that the lower the frequency is of the three major resonances, the better is the subjective preference. A similar relation can be stated for the difference in levels between the first two resonances, which can be correlated to the balance in the lower register of the guitar sound. One of the objective parameters that can have a better correlation is a_2 . The presence of a resonance below the first major resonance appears for all the guitars (except for guitar E) that had more than 10% of the votes in the overall choice.

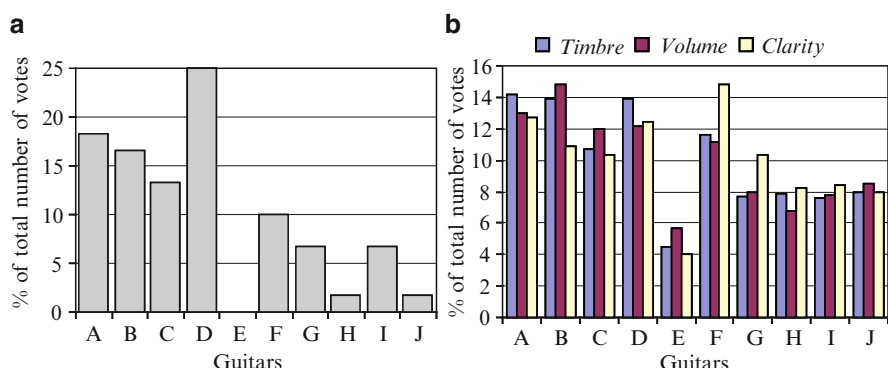


Fig. 4.6 Results of the (a) overall choice votes and (b) subjective parameters preferences

Table 4.2 Results on the objective parameters

Guitar	f_1 (Hz)	f_2 (Hz)	f_3 (Hz)	L_1 (dB)	L_2 (dB)	L_3 (dB)	$a_1^1(\varphi)$	$a_1^2(\varphi)$	a_2	$a_3(\varphi)$
A	135	295	322	31	51	55	45	8	Yes	153
B	132	285	310	33	47	59	16	48	Yes	132
C	121	270	291	35	52	54	35	45	Yes	189
D	132	274	370	34	51	46	16	20	Yes	64
E	159	365	420	27	54	49	38	24	Yes	239
F	129	263	355	36	55	38	24	9	No	33
G	142	305	336	30	46	54	42	34	No	123
H	131	279	341	37	57	53	3	11	No	109
I	160	348	391	21	43	58	51	6	No	145
J	127	255	386	38	52	37	49	44	No	7

References

- R. R. Boullosa, “The use of transient excitation for guitar frequency response testing.” *Catgut Acoust. Soc. Newslet.* **36**, 17, 1981.
- R. R. Boullosa, F. Orduña-Bustamante, and A. P. López, “Tuning characteristics, radiation efficiency, and subjective quality of a set of classical guitars,” *Applied Acoustics*, **56**, 183–197, 1999.
- P. C. Cabral, *A Guitarr Portuguesa*, ASA Editores, 1st edition, Lisbon, 1998.
- G. Calder Smith, “Designing a guitar family,” *Applied Acoustics* **46**, 3–17, 1995.
- E. V. de Oliveira, *Instrumentos Musicais Populares Portugueses*, Fundação Calouste Gulbenkian/ Museu Nacional de Etnologia, 3rd edition, Lisbon, 2000.
- M. J. Elejabarrieta, “Air cavity modes in the resonance box of the guitar: the effect of the sound hole,” *Journal of Sound and Vibration* **252**, 584–590, 2002.
- L. Henrique, *Acústica Musical*, Fundação Calouste Gulbenkian, 1st edition, Lisbon, 2003.
- T. J. W. Hill, B. E. Richardson, and S. J. Richardson, “Modal Radiation from Classical Guitars: Experimental Measurements and Theoretical Predictions,” in *Proceedings of the Stockholm Music Acoustics Conference (SMAC 03)*, **1**, pp. 129–132, Stockholm, Sweden, August 6–9, 2003.
- O. Inácio, F. Santiago, and P. C. Cabral, “The Portuguese Guitar Acoustics: Part 1 – Vibroacoustic Measurements,” in *Proceedings of the IV Iberoamerican Acoustics Congress*, Guimarães, Portugal, September 13–17, 2004.
- E. V. Jansson, “Acoustics for the guitar player,” in E. V. Jansson (ed.) *Function, Construction and Quality of the Guitar*. Royal Swedish Academy of Music, Stockholm, Publication no. 38, pp. 7–26, 1983a.
- E. V. Jansson, “Acoustics for the guitar maker,” in E. V. Jansson (ed.) *Function, Construction and Quality of the Guitar*. Royal Swedish Academy of Music, Stockholm, Publication no. 38, pp. 27–50, 1983b.
- J. Meyer, “Quality aspects of the guitar tone,” in E. V. Jansson (ed.) *Function, Construction and Quality of the Guitar*. Royal Swedish Academy of Music, Stockholm, Publication no. 38, pp. 51–76, 1983.
- F. Orduña-Bustamante, “Experiments on the relation between acoustical properties and the subjective quality of classical guitars,” *Catgut Acoust. Soc. J. (Series II)* **2(1)**, 20–23, 1992.
- F. Santiago, O. Inácio, and P. C. Cabral, “The Portuguese Guitar Acoustics: Part 2 – Subjective Acoustical Quality Evaluation,” in *Proceedings of the IV Iberoamerican Acoustics Congress*, Guimarães, Portugal, September 13–17, 2004.

Chapter 5

Banjo

James Rae

5.1 Introduction

The acoustic properties of the banjo have been subjected to very little scientific study. The few studies that exist have used the five-string banjo. Dickey (2003) used a structural dynamics model to simulate the effects of features such as loss factor, head tension, bridge mass, and string excitation location on qualities such as loudness, brightness, and sound decay. He showed that his model predictions agreed well with accepted banjo setup practices. Rae and Rossing (2004) published some of the first performance data obtained from sound and vibration measurements from real banjos. Stephay and Moore studied banjo bridge impedance and head motion using electronic speckle pattern interferometry (2008).

Banjos come in three different classifications. There is a four-string banjo, which usually has a resonator attached and is popular in ragtime and Dixieland jazz music. It is usually played with a flat pick in a strumming or flat picking style. There is an often resonator-less five-string banjo used in old-time music. It is often played in what is called *claw hammer* style where the strings are picked and brushed with the fingers, often without the aid of picks. The third style of banjo is also a five-string banjo, but it includes a resonator. It is generally played with finger picks and is popular in bluegrass music.

Much of the uniqueness of banjos stems from the fact that many of their important parts are not made from wood. Rather, they are made from various metals, which have acoustic impedances quite different from those of wood. At several key locations on the instrument, vibration transfer must occur across wood–metal or metal–wood interfaces where the mismatch of acoustic impedance is expected to be large. In addition, the major sound-radiating surface is not wood. Rather, it is a thin, tightly stretched membrane made of Mylar, which is more responsive than typical sound-radiating surfaces on other string instruments. On banjos used for playing bluegrass music, the back surface of the instrument is

J. Rae (✉)
827 Valkyrie Lane NW, Rochester, MN 55901, USA
e-mail: rae.james@mayo.edu

a curved resonator made of laminated wood secured to the upper part of the banjo by way of four metal bolts. With the resonator in place, the instrument has an enclosed air cavity, as found on many other string instruments.

Another unique feature of the banjo is that most of its parts are not glued together and are amenable to modification (tuning) after the instrument has been constructed. For example, the Mylar head is attached to the instrument by a hoop and 24 hook-bolt devices that can be used to change the tightness of the head over a rather wide range. The bridge is not attached so it can be changed with ease. There are many bridge designs constructed of many different kinds of material, and they offer increased flexibility for changing the banjo's sound with a minimum of effort. Many banjos have adjustable tailpieces that can alter the angles that the strings make over the bridge, thus allowing adjustment of the magnitude of the string tension force vector that is directed downward toward the head. It is also possible to use adjustable-height bolts (called Raejusters) to change the spacing between the resonator and the upper part of the banjo so that adjustments of the frequencies of the cavity resonances can be made in a matter of seconds.

Most of these adjustments have not yet been studied with good scientific methods, so the observations are anecdotal, without good theoretical models to predict what is measured. This chapter stems from the author's post-retirement hobby. While a few of the studies were done in the laboratory of Dr. Tom Rossing, most were done in the author's own basement. The results presented are part of a series of trials done on experimental banjos constructed by the author from a large number of quality parts. Many of the parts were custom-made to the author's specifications by well-known banjo parts makers. The findings were compared to those from six high-quality commercial banjos in the author's personal collection.

5.2 Banjo Anatomy

To understand many banjo acoustics issues, one must understand how a banjo is constructed. It has an assembly called the pot, which includes a bell metal tone ring resting on top of a wooden rim (Fig. 5.1). A Mylar head sits on the top of the tone ring and is held in place by a substantial group of hardware that includes a hoop which sits on an outer projection of the head, a flange that seats against a ridge in the rim, and a series of long bolts that bridge between the hoop and flange. The flange is not connected to the rim. Rather, it is held against the rim ridge by compression when the head bolts are tightened. Many banjos have a resonator attached, which is usually a laminate of a light wood such as poplar, with four internal lugs threaded into the resonator internal wall. Four thumb screws thread into the lugs to hold the resonator in place. The thumb screws go through either four metallic brackets attached to the flange or four angle brackets screwed into the outside of the rim. Raejusters are alternative thumb screws with an Allen wrench socket in their top. They take the place of normal thumb screws and allow the pot assembly to be raised quantitatively with respect to the resonator floor. The neck is long enough to

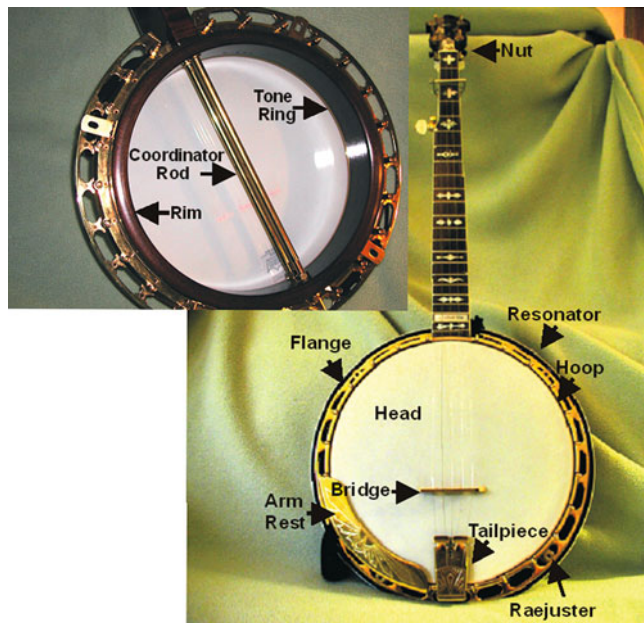


Fig. 5.1 Banjo with labeled parts

support the approximately 26.3-in. scale length. The end that abuts the pot has two metal bolts that attach it to the pot. One end of each is a lag screw that screws directly into the wood of the neck. The other end of the same bolt is threaded and screws into two structures called coordinator rods. Coordinator rods run from the inside of the neck side of the rim into two holes in the opposite side of the rim where they are attached by nuts. The neck also contains a truss rod that resides in a channel in the neck's interior. The tailpiece mounts on the hoop and on a bracket attached to the lower coordinator rod. Many tailpieces have a mechanism for adjusting their height and thus the angle the strings make with the head behind the bridge. Banjos also have an arm rest that keeps the picking arm from resting on the head and partially damping it. The strings terminate on a removable wooden bridge and a fixed nut often made of bone.

5.3 Banjo Sound

A five-string banjo is usually tuned to an open G or DBGDG for strings 1–5 (294, 248, 196, 147, and 393 Hz, respectively). This differs from most other string instruments where the fundamental frequencies fall monotonically with increasing string number. Banjos can be tuned many other ways, but for the studies done here, they were always tuned to an open G.

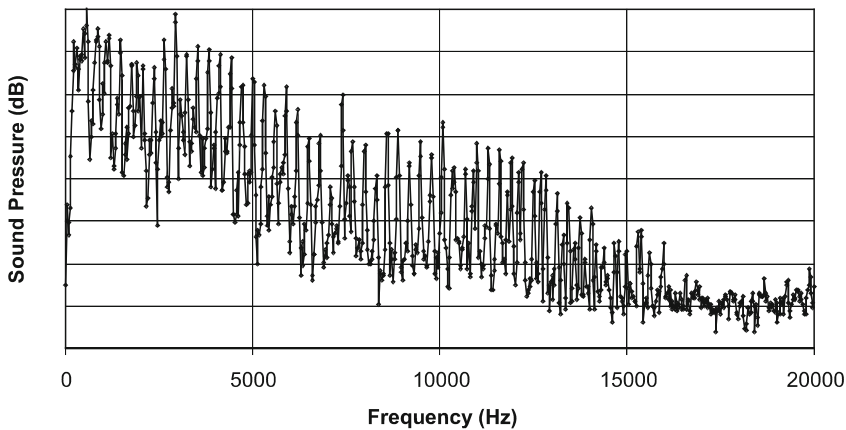


Fig. 5.2 Harmonics resulting from Fourier processing of banjo sound following a pluck of the open first string near the bridge

Figure 5.2 shows the power spectrum of the radiated sound when the first string is plucked at a precise location. This is obtained by applying Fourier analysis to the sound signal recorded by a microphone with a flat response to 20 kHz located about three feet from the center of the banjo's head. As expected, the discrete peak frequencies are multiples of a fundamental frequency. Like the string energy driving the banjo, the radiated energy is also essentially harmonic in nature. Of course, many of the peaks are small and completely outside the ability of human ears to hear, so it is useful to re-plot such spectra in another way.

Figure 5.3 is a plot of the fraction of sound power as a function of frequency. It is obtained by linearizing the power spectrum (i.e., converting from decibels to linear) and then summing the amplitude of every frequency point. Then a running sum is done as follows: Point 1 is divided by the total and then plotted. Then points 1 and 2 are added, divided by the total and plotted. Then points 1, 2, and 3 are added, divided by the total and plotted. This is continued for all points. These fraction of total sound versus frequency plots (as we call them) are very useful. They can be used to show frequency content from any power spectrum or frequency response function records whether they are sound levels or vibration levels.

The total sum of all of the frequency points can be used as a figure of merit for total sound or total vibration output, so this approach is used for comparing many banjo features after experimental measurements. From such plots, several important things can be determined. First, a banjo is capable of radiating sound to 15–20 kHz. However, about 99.9% of the sound power radiated occurs in a 6-kHz bandwidth. Second, over 80% of the sound power is due to the first six to seven harmonics. Observers with excellent hearing might detect *coloration* of the sound from frequency peaks above 6 kHz, but to most ears the banjo is about a 6-kHz instrument. Another interesting and initially surprising observation is that the banjo does not have very good low-frequency response. The fundamental frequencies of

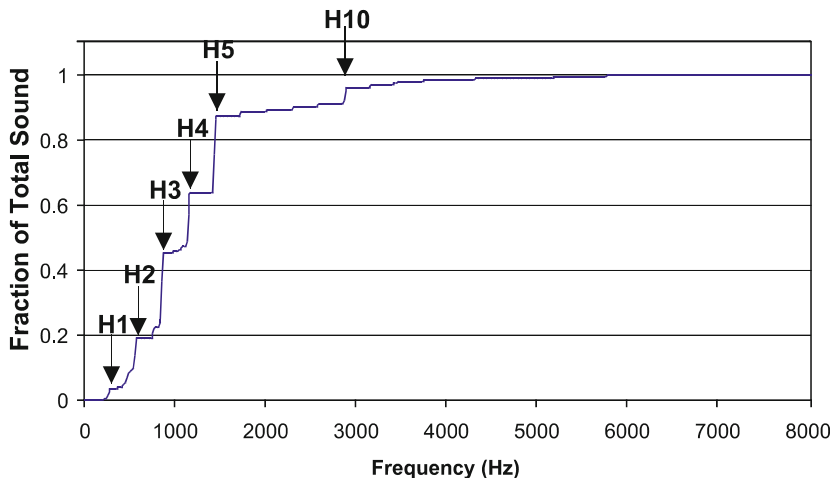


Fig. 5.3 Example of fraction of total sound vs. frequency plots

its open third and fourth strings are about 196 and 147 Hz, respectively, and yet those frequencies are poorly represented in the output sound.

One useful way of looking at banjo-radiated sound is to produce a highly averaged power spectrum of the sound recorded by a microphone placed about three feet from the banjo's head when the strings are brushed repeatedly at all possible locations between the bridge and the neck. This is done using a pick of the sort that would be used by many banjo players. Brushing is repeated until the power spectrum no longer changes from one brush to the next, and is then continued for another minute or so in order to accumulate a large number of averages. With attention to trying to brush the strings with the same force each time and with the large number of averages, the spectra become quite repeatable even in the absence of a constant force *plucker*. A radiated sound spectrum obtained from that procedure is plotted in Fig. 5.4. Again, as in Figs. 5.2 and 5.3, it is clear that the banjo response is poor below 200 Hz.

The major response is in a band from about 400 to 1,200 Hz and thereafter falls substantially at increasing frequency. An interesting bump in the frequency response occurs in the frequency range of 2–4 kHz. This bump would not be expected from power distribution in the strings. A similar transfer function can be determined by use of a white-noise-driven shaker attached to a driving point impedance head. The tip of the impedance head is placed on the banjo bridge near its center while recording from a microphone placed about one foot above the head.

The vibrations are delivered using the apparatus shown in Fig. 5.5. Using the force determined by the impedance head and the sound emitted from the head, a transfer function relating sound pressure and frequency can be obtained (data not shown). A similarly shaped transfer function can be determined by vibrating the bridge and directly measuring vibrations with an accelerometer placed on the head close to the bridge (data not shown). Playing the banjo and analyzing the sound also gives a similar

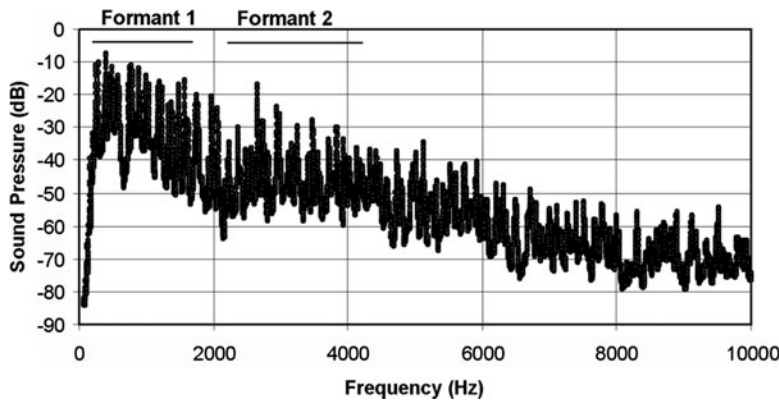


Fig. 5.4 Banjo frequency response determined by all position brushes and radiated sound. Lines show regions of major formants

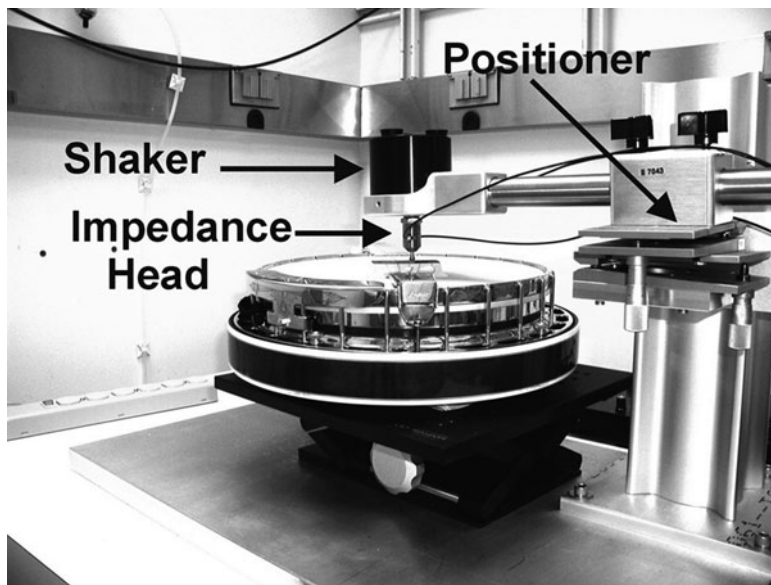


Fig. 5.5 Apparatus for vibrating the bridge

transfer function as does analyzing the sound from head taps or bridge taps when the strings are not damped. The important point is that the 400–1,200 Hz format and the 2,000–4,000 Hz formant are seen in results from all 12 banjos tested using all of the methods described above to produce sound output or measurable vibrations. The two consistently occurring formants do vary in detail based on which of the harmonics in the regions have the largest amplitudes. To understand how a banjo makes sound, one must know what gives rise to the formants.

5.4 Head Modes

Because the head is the main sound-radiating structure in the banjo, it is imperative to understand how it works. One useful and powerful technique is holographic interferometry. It allows one to visualize movements of the head as it radiates sound at specified frequencies. There are several books about the technique and several publications in the scientific literature detailing its use (Roberts and Rossing 1998; Fletcher and Rossing 1998; Kreis 2005; Jones and Wykes 1989). For the banjo measurements using this method to date, the banjo was rested on foam rubber on one edge of its resonator and then clamped with a foam rubber-lined clamp about halfway up the neck. The strings were damped. The bridge or the head was vibrated by securing a small magnet on the bridge or head with petro wax and then bringing an electric coil very close to the magnet. Sinusoidal electric current was passed through the coil, which generated a magnetic field that produced a force at a particular frequency as holographic images were produced via a small CCD video camera. The frequencies were slowly increased while keeping the coil current constant so as to generate interferograms showing head movements at all relevant frequencies. These studies were repeated at different head tensions and at different cavity resonance frequencies.

Figure 5.6 shows some composite results for selected head modes. As expected, the spatial vibration patterns on the head were those expected for drum head (membrane) modes, each of which has a name consistent with drum head nomenclature. The arrows on the figure show where discrete modes can be seen for a head stretched to “bluegrass tightness.” The tension was not actually measured but was recorded as torque wrench settings or as the dominant tone resulting from tapping the head with the strings damped. Tap tuning of the head is what banjo luthiers usually use to discern when the head is at its desired tension. Interesting features are that the spatial patterns are quite symmetrical even though the vibrated bridge does not sit in the center of the head. The first mode (0,1) occurs at around 208 Hz or so, well above the frequencies of the fundamentals of strings three and four in open G tuning. It is generally a wide mode encompassing a frequency range of 20–30 Hz. The last “strong” mode occurred at about 2,000 Hz. *Strong* here means visually strong since many of the higher-frequency, spatially complex modes are not very efficient sound radiators. Very weak modes can be seen at frequencies above 2,000 Hz, but usually cannot be seen well enough to be given a drum head mode name.

Similar images captured with the head at different tensions allowed the formulation of some very simple principles. As head tension was raised, the peak frequency of each mode shifted to higher frequencies. When the head was really tight, each mode was quite narrow and did not overlap any other mode. *Narrow* means that the mode appears and disappears over a very narrow band, sometimes as little as a few Hz in width. *Not overlapping* means each visualized mode is discrete. As you sweep up in frequency, one mode disappears before the next one appears. At low head tensions, but not outside those that might be used for some kinds of banjo playing, discrete modes were not seen. The mode width was large and so each

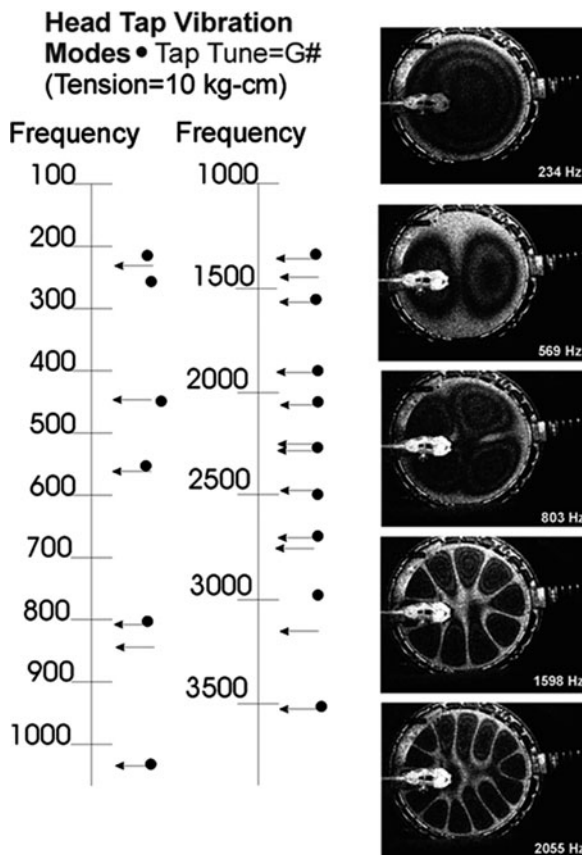


Fig. 5.6 Selected banjo head modes, $(0,1) = 234$ Hz, $(1,1) = 509$ Hz $(2,1) = 803$ Hz, $(5,1) = 1,593$ Hz, $(7,1) = 2,055$ Hz. Dots show positions of sound peaks determined from head tap experiments

mode overlapped its neighboring modes. So most of the head seemed to be in motion at all frequencies. At head tensions between low and high, the behavior was intermediate to the two extremes.

Thankfully, much can be learned about head modes without expensive instrumentation. With the strings damped, one can record sound coming from the banjo when the head is given a distinct rap a couple of inches or so from the edge of the head. With Fourier analysis, the radiated sound can be analyzed into the discrete frequencies that it contains. Figure 5.7 is a representative example of such an experiment. The sound peaks turn out to be at essentially the same peak frequencies as those of the head modes determined by holographic interferometry (Fig. 5.6). Head taps then give a strategy for setting the desired head tension. This can be repeated after head tension changes until the main peak occurs at the desired frequency. Many bluegrass banjo players prefer 418 Hz (G#). Rarely do bluegrass

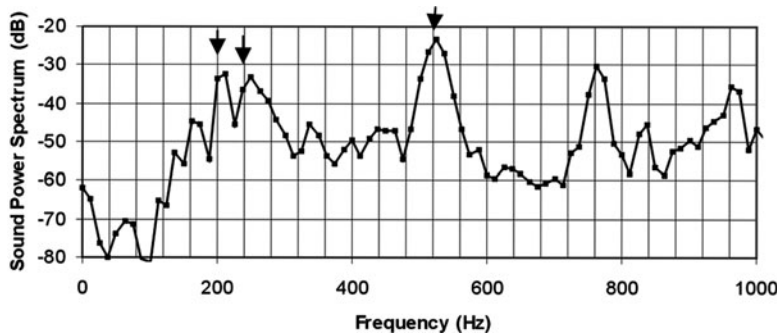


Fig. 5.7 Low-frequency head mode peaks from the spectrum of sound emitted following head taps. Arrow shows dominant peak

players like something outside the F to A# range. Figure 5.7 is data from a quite tight head. The highest amplitude sound peak (single arrow), the one likely identified by luthiers in head tap tuning, is at about 550 Hz (about C#). So this head is more taut than would be used by bluegrass musicians. It should be realized that while luthiers talk of tuning the head to a single frequency, heads cannot be tuned to one frequency by adjusting head tension. Head taps elicit many head mode frequencies simultaneously, essential all of which can be seen in the power spectrum of the sound resulting from a head tap.

With this background, we can compare Figs. 5.4 and 5.6. Maximum sound output is in the 400–1,200 Hz range. The major head modes with high sound radiation efficiency occur over that same frequency range. It is also true that the amplitudes of string resonances are relatively large in that frequency range. These factors undoubtedly contribute to the high sound output in that frequency range that contributes about 85–90% of banjo radiated-sound power.

5.5 Harmonics Analysis

Because five-string banjos are played by precisely picking strings at specified locations along the strings' length, the radiated sound is made up of frequency peaks associated with string harmonics. Picking a string at a precise location and then subjecting the radiated sound to Fourier analysis allows repeatable quantitation of the relative amplitude of each harmonic from each string at each place where it is fretted and picked. While this encompasses an enormous number of combinations, this approach can be standardized and used to determine a sound signature for use in comparing different banjos.

In studies here, individual strings were picked with a 1-mm stainless steel pick applied to each string at a position 1/25th of the string's length from the banjo's bridge. This resulted in failure to excite harmonics 25, 50, 75, etc., all of which are unimportant to banjo sound. Picking in this location, however, made the spectra less

complicated. The sound was recorded by a microphone placed the same distance from the banjo's head for each experiment. Measurements were done on all five open strings on 12 high-quality banjos. A table was generated for the fraction of the total sound generated by each harmonic. Several important fundamentals were discerned. To begin with, all 12 of the banjos were unique. The relative amplitudes of the first few harmonics were different in each banjo. All but two were similar in that most of the sound was associated with the first six to seven harmonics. In strings 1 and 5 (the highest-frequency strings) up to 20–30% of the sound was associated with the fundamental frequency of the strings. For strings 3 and 4, it was considerably less. In fact, the fundamental for string 4 was often about 0.01% of the total sound. The value was so low that it suggests that the 147-Hz fundamental is not heard at all but is surmised by the ears and brains from hearing higher-order harmonics. Each banjo also had harmonics in the 10th to 15th range that contributed substantially to the total sound. These undoubtedly are those associated with the 2,000–4,000 Hz formant. Two banjos were unique in that two harmonics in this frequency range accounted for nearly 50% of the total sound output. These results suggest that quantifying sound from single string plucks is a good way to characterize differences between banjos.

5.6 Resonators

Many banjos have resonators, but not all. Yet they all sound unmistakably like banjos. Obviously resonators are not required for the unique banjo sound. So, what purpose do resonators serve? Because they are generally highly laminated, their main surface is not flexible, so they are not an effective sound radiator. Add to this the ways that banjos are played mostly, where the resonator rests against the player's abdomen and so is continually highly damped. The large surface of the resonator has only small amplitude vibrations as shown by holographic interferometry or by analyzing the output from an attached accelerometer. In either case, when the bridge is vibrated by a white noise signal or a series of sine waves, only low-amplitude vibrations in the resonator can be detected.

Another possible role of the resonator is to reflect internal sound waves out through the flange holes. In fact, this is touted as the major role of the resonator by many banjo luthiers and players. While some of this may occur, the convex surface inside the resonator would largely reflect sound waves back toward the head rather than through the flange holes. Resonators are poorly shaped to be effective reflectors. However, their existence creates an internal cavity that is analogous to a Helmholtz resonator. A well-known example of a Helmholtz resonator is a bottle with a neck. In a banjo with a resonator (Fig. 5.8), the analogous bottle volume is that which occurs from the inside of the head to the internal top surface of the resonator in the space inside the rim. The analogous neck is the space between the bottom of the rim and the resonator, the space between the outside of the rim

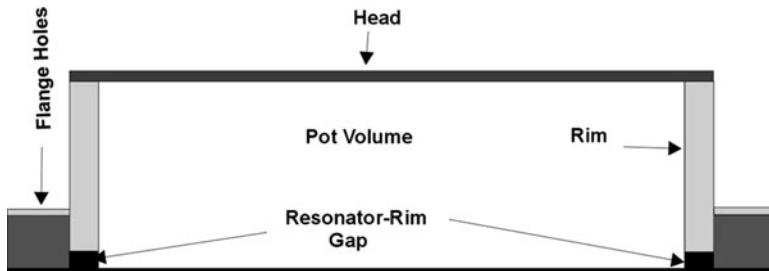


Fig. 5.8 Diagram of banjo parts that are part of the Helmholtz resonator analogy

and the lateral internal surface of the resonator, and also the combined volume of all the flange holes. While it is widely known that changing the bottle volume affects the pitch of the sound that comes when one blows across the lip, it is less well known that the cross-sectional area of the neck also has decided effects. Reducing the neck volume lowers the pitch of the sound whereas increasing the neck volume raises it.

In a banjo, adjustments that change the height of the pot with respect to the resonator have a proportionately larger effect on *neck* volume than *bottle* volume. So, raising the pot makes the cavity resonance frequency more treble, whereas lowering it makes it more bass. Obstructing some or all flange holes also makes the cavity resonance more bass. The resonance is easily measured by burying the banjo in sand and placing sand bags on the head and neck so as to damp all resonance modes except that due to the cavity. Then sinusoidal air of different frequencies is blown through a flange hole into the cavity while the sound is measured with a microphone also in the cavity. These measurements show that the cavity resonance can be tuned to be in the range 190–230 Hz while maintaining a reasonable-quality banjo sound.

Head tap measurements, as described earlier, also allow the cavity to be tuned to a particular desired setting. As background, with holographic interferometry, the (0,1) head mode of a banjo that has its head tuned to G# and a resonator attached occurs at about 209 Hz. If you remove the resonator, the apparent (0,1) mode is at about 254 Hz. The 209 and 254 Hz modes are really two different modes (see double arrows in Fig. 5.7). If one installs Raejusters, the banjo pot can be quantitatively raised above the resonator in small increments. What happens as the pot is raised is that both modes become visible. As the pot rises, the 209-Hz peak becomes smaller and the 254-Hz peak gets larger. At high enough pot heights, the 209-Hz peak disappears with the 254-Hz peak achieving maximum amplitude. So, a person setting up a banjo needs to raise the pot until a preferred sound is obtained. Then head taps and Fourier processing can be done to determine the relative amplitudes of the 209 and 254 Hz peaks. Thereafter, the relative amplitudes can always be set to the same ratio to get repeatable tuning of the cavity. The two peaks will be a little different in frequency from one banjo to another or from one head stiffness to another. However, the procedure of adjusting the relative amplitudes of the two peaks is a useful cavity-tuning procedure.

Some additional information can be learned about what resonators do by comparing banjo measurements with and without the resonator. Four small factors can be identified. The maximum sound volume that can be obtained is larger with a resonator than without. However, when a sound level meter is placed about three feet from the center of the head and the strings are repeatedly vigorously brushed, the maximum sound level recorded without the resonator is usually only 1–2 dB less in total sound level than the 105 dB or so level with the resonator in place. It should be realized that the measurement of maximum volume may be misleading. It would be far better to measure the output sound level as a function of the energy delivered to the string using some sort of adjustable constant force plucker. To date, no such experiments have been done.

The relationship of fraction of total sound vs. frequency is shifted to slightly higher frequencies when the resonator is present. This frequency shift is determined by comparing sound recordings with all position brushes with and without the resonator (Fig. 5.9). Clearly, in the absence of the resonator, a larger fraction of the banjo's total sound output occurs at lower frequencies. This was found in each of 12 banjos tested, although the extent of the frequency shift was a little different from one banjo to another. Also, the duration of sound transients is increased by as much as 20% when the resonator is present. That result was verified by recording power spectra of the sound from string plucks at various times after the pluck. By that approach, it was possible to determine the decay rate of individual harmonic frequencies. Many individual frequencies decayed at a slower rate when the resonator was present. This means that the resonator slightly increased the “sustain” of the banjo sound. Finally, the relative amplitudes of several head mode vibrations were altered when the resonator was attached. No studies have yet been done to determine the mechanism by which this occurs, but a change in certain sound peak heights (but not frequencies) was easily seen following head taps at different Raejuster heights.

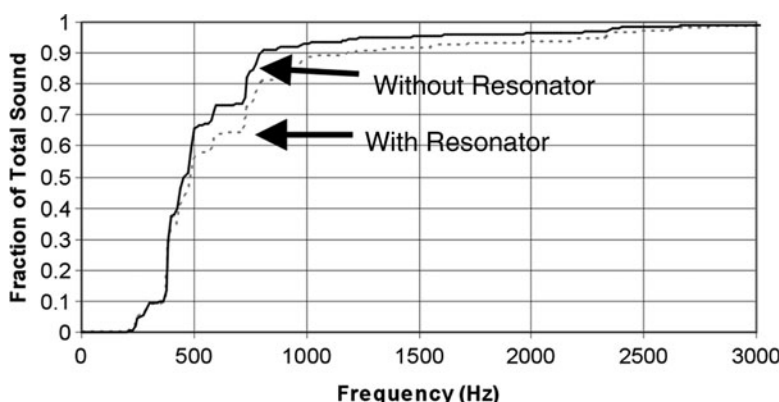


Fig. 5.9 Overplots of fraction of total sound power vs. frequency from all position brushes with and without a resonator

5.7 Bridges

The banjo bridge is the main conduit for passing string vibrations into the head of the banjo. Bridges are generally made of two different woods. A thin top wood is usually an extremely hard and dense wood. The body of the bridge is also usually a dense, hard wood but less so than the top wood. Most bridges are made with three legs, one at each end and one midway between the two in the center of the bridge.

To understand the frequency response of bridges, it is necessary to know something about the basic nature of wood. Wood is orthogonally anisotropic. It is stiffest along the long axis of the branch of a tree limb. That direction has the fastest sound velocity. Banjo bridges are made so that the long direction of the bridge is along the axis of the limb and therefore the fastest sound velocity is in that direction. If the growth ring lines seen at either end of the bridge are parallel to the head, then the direction from top to bottom is the second stiffest and has a lower sound velocity than that from end to end. The direction from bridge front to back is the least stiff and has the lowest sound velocity. This anisotropy can be quantified in cubes of wood by using the apparatus shown in Fig. 5.5, but with the bridge resting on a rigid support.

A shaker is driven by a signal generated in *Labview*, a well-known scientific instrumentation computer software and hardware package. The computer signal is often white noise that provides all frequencies in a given bandwidth at the same average power. It delivers all banjo-relevant frequencies at essentially the same time. Connected to the white noise-driven shaker is an impedance head that measures simultaneously force and acceleration at its tip. When it is pressed against a piece of wood it measures the ease with which the wood is micro-squashed. That depends upon the mass and stiffness of the wood. Figure 5.10 shows results from a cube of wood precisely cut along its orthogonal planes. The plot of accelerance vs. frequency quantifies the ease with which the wood is squashed at each frequency. It is related to the ease with which the wood is vibrated at each frequency. Most woods show orthogonal planes anisotropy but the actual frequencies of the peaks depend on the stiffness and density of the particular wood. In a small number of woods, the peak frequencies and amplitudes are the same in two planes, but it is rare.

It is therefore relatively easy to make bridges with widely different frequency responses. Soft woods with low stiffness and density have main resonance peaks that can be as low as 700–800 Hz, whereas the peaks for dense stiff woods can be as high as 3,500 Hz. It is possible to get results between these two extremes by choosing woods with intermediate density and stiffness. Alternatively, bridges can be made from grain-rotated stiff woods. If the grain lines seen at the ends of banjo bridges are vertical rather than horizontal, the resonance peaks will occur at up to several hundred Hz lower in frequency than when the end grain is horizontal. Another useful trick for banjo bridges is to drill holes through the outer legs and glue 1/32-in. to 1/64-in. aluminum rods into the holes. This stiffens the bridge in those local regions and increases the peak resonance frequencies.

Given that the highest pitch strings rest in those regions, the result is to “tune” the bridge to accept frequencies found in the strings nearest them. A bridge made of

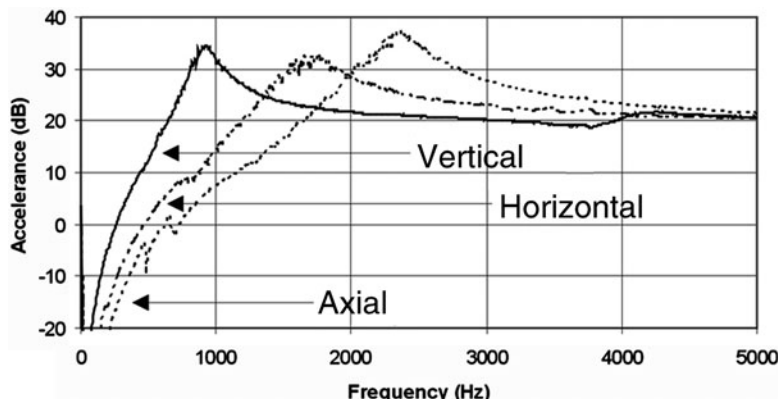


Fig. 5.10 Example of different resonances in different orthogonal planes in snakewood

lower-frequency wood with aluminum rods through the outer legs will have resonance peaks at lower frequency for the low-pitch strings and higher frequency for the high-pitch strings. Another trick is to make the center leg of the bridge offset toward the first string side of the bridge. This creates a less well supported region in the expanse where the lowest-frequency fourth string sits. The longer expanse shows more physical up-and-down movement and thus a lower-frequency peak response. In a sense, the bridge is tuned to accept the vibrations inherent to the individual strings it serves. However, the vibrations in most of the bridge do not show such frequency separations. That is because the sound velocity in any direction in the bridge is very fast by comparison to the time it takes for the strings to make a sine wave of any relevant banjo frequency. This same phenomenon explains why energy transfer from the bridge to the head is relatively independent of surface area of contact of the bridge with the head over a substantial range of surface areas. Bridges are generally made so that string vibrations in the range of 200–2,500 Hz are effectively transferred to the head. This also explains, in part, why banjos radiate sound at the frequencies they do. Bridges transfer 147 Hz (fourth string) poorly. That, along with the absence of a head mode at that frequency, explains why banjos do not radiate the lowest frequencies well.

Of course, measurements made on isolated bridges on rigid surfaces do not mimic what happens when the bridge is sitting on the head. It is necessary to be able to measure bridge function on an intact banjo. This is easily possible by using the apparatus shown in Fig. 5.5. The bridge is vibrated using a computer-generated white noise signal to a shaker while recording the sound from a microphone placed about a foot above the middle of the banjo head. A driving point impedance head is attached to the shaker. The force delivered to the bridge and resulting sound radiated are used to establish a frequency response function. This data was transformed into a fraction of total sound vs. frequency plot as described earlier. So while this procedure produces a transfer function with both of the main formants (as described earlier), it also proves to be a good way to quantify bridge contributions to the total sound (Fig. 5.11). It is a good way to fit bridges to particular banjos.

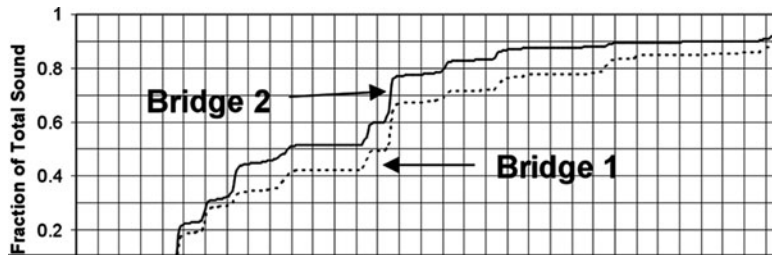


Fig. 5.11 Fraction of total sound pressure vs. frequency plots generated by the all-position brush procedure to demonstrate that bridges measured to have different main resonances on solid supports impart different frequency characteristics to the sound of an intact banjo

5.8 Tone Rings, Rims, and Neck

When a string is released after being picked, it contains energy. The energy is gone once the string stops vibrating. It is instructive to contemplate where the energy goes. Three general pathways are involved: energy radiated as sound; energy lost by friction between the moving string and the air surrounding it; and energy lost to friction or other loss mechanisms within the instrument. In many instruments, these three pathways dissipate energy nearly equally. Very little work has been done in banjos or other string instruments to precisely quantify these losses, but some general principles can be suggested for banjos. These come from experiments where isolated banjo necks, rims, and rings are vibrated with a white noise-driven shaker, and the vibrations in the parts are measured with an accelerometer placed at varying distances from the vibration site. Similar experiments were done with rings sitting on rims and with stringless banjos.

The majority of the experiments were done by vibrating the bridges of intact banjos using the white noise-driven shaker apparatus of Fig. 5.5 while recording from other banjo parts with accelerometers. An example of these results is shown in Fig. 5.12 which overplots fraction of total vibration vs. frequency from several banjo parts along with a figure of merit for the total vibrations in each part from a single banjo. While the actual frequency content varied a little from one banjo to another, simple principles were easily determined. By far the largest amplitude vibrations came from the head near the bridge, and these vibrations occurred in the frequency range where the banjo makes the majority of its sound (400–1,200 Hz).

The vibrations in the neck, ring, rim, and resonator were similar in size at most frequencies but very much less than those in the head in the 400–1,200 Hz frequency range. In the frequency range of 2,000–4,000 Hz (that of the second formant), head vibration amplitudes fell while those in all the other parts increased so as to become about the same in amplitude as those in the head. These vibrations likely play a role in the second formant. However, it must be realized that these tests were all done with steady-state vibrations, whereas a banjo is plucked. Therefore,

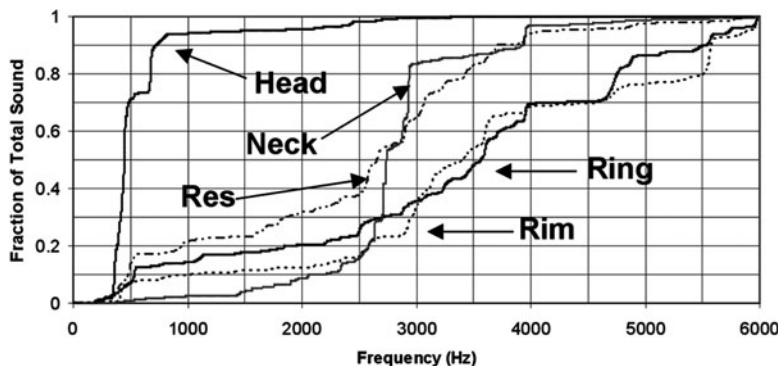


Fig. 5.12 Overplots of fraction of total sound pressure vs. frequency for head, ring, rim, neck, and resonator. Figures of total sound merit are head = 981.851; ring = 426; rim = 440; neck = 736; resonator = 1,753

its sound is made largely from decaying transients. It is very important to measure the time course and frequency content of those transients at various times into the decay. By doing so in every major banjo part, it should be possible to quantify many aspects of internal loss mechanisms.

5.9 Summary

Banjo sound is determined by many factors. However, the most important two are undoubtedly the bridge and the head. As in most string instruments, the impedance match between the strings and bridge is by design decidedly poor. Such a mismatch ensures that string vibrations will largely be reflected back into the strings rather than traversing the bridge to the head. This allows string energy to be transferred through the bridge to the head in a slow and orderly fashion. Better impedance matching would result in more string energy transferred to the head per unit time and in its ultimate limit would produce sound radiated from the head that sounded rather like a rifle shot – a huge volume with essentially no sustain. So, banjo sound is largely about what string energy actually gets into the banjo from the bridge and nut and how it is dissipated.

There are few banjo sound or vibration measurements to date that attempt to characterize banjos from this perspective. In some other string instruments, it is believed that about one-third of steel string energy is dissipated by friction of the moving string with the air surrounding it. Another third or so is dissipated by sound largely radiated from whatever effective soundboards exist. The final third is lost in the internal structure of the instrument largely due to heat generated as vibrations produce friction between adjacent regions of the wood or other materials moving past each other. Therefore, in the banjo and other string instruments, the sound is determined about as much by vibrations that do not reach the soundboard as those that do.

Banjos have many sites of acoustic impedance mismatches: strings and bridge, head and tone ring, tone ring and rim, string and nut, nut and neck, neck and tone ring, and neck and rim. Of these, only the neck–rim interface is expected to exhibit a reasonable impedance match. In other string instruments, most of the parts are made of similar materials and are connected through solid glue joints. In banjos, many of the parts interfaces involve compression fits from parts bolted together.

Banjos also have many more tunable parts than most other string instruments. Most prominent of these is the head, the tension of which can be changed over a wide range. This allows one to dictate to some extent the amplitude, frequency, and width of the vibration modes of the main soundboard. In addition, by raising or lowering the pot with respect to the resonator, the frequency of the main cavity resonance can be adjusted. Parts exist that allow this to be done repeatedly, requiring only a few seconds to accomplish. As pointed out earlier, this adjustment also has some minor effects on head modes. An adjustable tailpiece height is common for many types of banjo tailpieces. There are easily more than a dozen different tailpieces that can be used to replace a banjo's tailpiece in just a matter of minutes. As with other string instruments, string gauges make a major difference in sound as does the choice of woods used for making the neck and rim. Banjo bridges are also easily replaced and can be made to have widely different resonances from one bridge to another and even from one position on the bridge to another. Main parts such as neck, ring, rim, and head are rather easily changed. So, a banjo is more like an instrument you assemble and reassemble rather than one that once made is difficult to alter.

Not much of this comes as a surprise to banjo luthiers. Over more than 150 years they have used their ears and brains to fine-tune the sound of banjos. Banjo science, which might provide physical mechanisms to explain the luthiers' choices or even suggest some new approaches, is simply in its infancy. The science that exists is rife with assumptions and observations often without good scientific models to support them. There is much yet to be done.

References

- J. Dickey, "The structural dynamics of the American five-string banjo," *J. Acoust. Soc. Am.* **114**, 2958–2966, 2003.
- N. H. Fletcher and T. D. Rossing, *Physics of Musical Instruments*, 2nd ed., Springer, New York, 1998.
- R. Jones and C. Wykes, *Holographic and Speckle Interferometry*, Cambridge University Press, Cambridge, UK, 1989.
- T. Kreis, *Handbook of Holographic Interferometry*, Wiley-VCH, Weinheim, 2005.
- J. Rae and T.D. Rossing, The Acoustics of the Banjo. In: Proceedings of ISMA 2004, Nara, Japan (Acoustical Soc. Japan, 2004), Paper 2-S1-1.
- M. Roberts and T. D. Rossing, "Normal modes of vibration in violins," *Catgut Acoust. Soc. J.* **3**(5), 9–15, 1998.
- L. A. Stephey and T. R. Moore, "Experimental investigation of an American five-string banjo," *J. Acoust. Soc. Am.* **124**(5), 3276–3283, 2008.

Chapter 6

Mandolin Family Instruments

David J. Cohen and Thomas D. Rossing

6.1 Introduction

The mandolin family of instruments consists of plucked chordophones, each having eight strings in four double courses. With the exception of the mandobass, the courses are tuned in intervals of fifths, as are the strings in violin family instruments. The soprano member of the family is the mandolin, tuned G3-D4-A4-E5. The alto member of the family is the mandola, tuned C3-G3-D4-A4. The mandola is usually referred to simply as the mandola in the USA, but is called the tenor mandola in Europe. The tenor member of the family is the octave mandolin, tuned G2-D3-A3-E4. It is referred to as the octave mandolin in the USA, and as the octave mandola in Europe. The baritone member of the family is the mandocello, or mandoloncello, tuned C2-G2-D3-A3. A variant of the mandocello not common in the USA is the five-course *liuto moderno*, or simply *liuto*, designed for solo repertoire. Its courses are tuned C2-G2-D3-A3-E4. A mandobass was also made by more than one manufacturer during the early twentieth century, though none are manufactured today. They were fretted instruments with single string courses tuned E1-A1-D2-G2. There are currently a few luthiers making piccolo mandolins, tuned C4-G4-D5-A5.

The mandolin appears to have descended from the medieval *gittern* in Italy, where it took two forms. One was the Milanese or Lombardian mandolin, called the *mandola* or *mandolino*, with six double courses of strings tuned in thirds and fourths. The other was the Neapolitan mandolin, called the *mandoline*, with four double courses tuned in fifths as in the modern mandolin. The Milanese mandolin fell into disuse in the late nineteenth century, and the Neapolitan mandolin ultimately prevailed. The early history of the mandolin was discussed by Sparks (1995); Tyler and Sparks (1989); and Gill and Campbell (1984).

T.D. Rossing (✉)
Center for Computer Research in Music and Acoustics (CCRMA),
Stanford University, Stanford, CA 94302-8180, USA
e-mail: rossing@ccrma.stanford.edu

The mandolin became a concert instrument in nineteenth-century Europe. Vivaldi, Mozart, Beethoven, Mascagni, Leoncavallo, Puccini, and other opera composers wrote music specifically for the mandolin. The Neapolitan mandolin was brought to America during the nineteenth century by Italian immigrants. With the formation of mandolin clubs and mandolin orchestras during the period from about 1880 to 1900, the mandolin became very popular. American manufacturers such as C.F. Martin, Lyon & Healy, and others manufactured mandolins to meet the demand.

In 1895, violinist and woodcarver Orville Gibson applied for a patent for a new type of mandolin. He dispensed with the bowl back and instead carved the arched top and the back plates from either single or book matched pieces of wood, as in the violin. In 1902, a group of businessmen in Kalamazoo, MI, bought the rights to Gibson's ideas and his name. They formed the Gibson Mandolin-Guitar Mfg. Co., Ltd., and began manufacturing Orville Gibson's designs. They advertised vigorously, attacking the bowl-back mandolin as a dinosaur in a scientific age and calling it a "tater bug" for the similarity of the appearance of the mandolin bowl to the striped carapace of the potato beetle. The Gibson mandolins, along with similar instruments from other American manufacturers, were to become the dominant type of mandolin in America.

Despite the decreasing popularity of the mandolin in 1920s America, the Gibson Company did not want to give up on the mandolin. They put employee Lloyd Loar in charge of designing and producing a superior mandolin. In 1922, he introduced the Style 5 family of instruments, including the F5 mandolin. The F5 borrowed some additional elements of violin morphology, including f-holes, primarily longitudinal *tone bar* bracing similar to the violin bass bar, and a fingerboard end suspended above the top plate of the instrument. The longer Gibson scale (13.88", or 352 mm) was also displaced toward the head of the instrument. The F5 mandolin was not a marketing success, but folk musicians, and especially bluegrass music founder Bill Monroe, would later come to appreciate the characteristics of the F5 mandolin. The Loar-era F5s would eventually become the most highly sought after and most frequently imitated mandolins in America. Eventually, the mandolin found its way into many different types of folk music, including Appalachian string band music and its descendants, as well as blues, jug band music, Celtic music, and Klezmer music. The history of mandolin orchestras and mandolin family instruments in America has been discussed by Johnson (1989, 1990).

6.2 Types of Mandolins

At first glance, it would appear that a mandolin is simply a mandolin, and is defined by its tuning. But as seen above, mandolins had two major forms distinguished by different tunings in nineteenth-century Europe, and they took a significantly different form in twentieth-century America. While archtop mandolins share

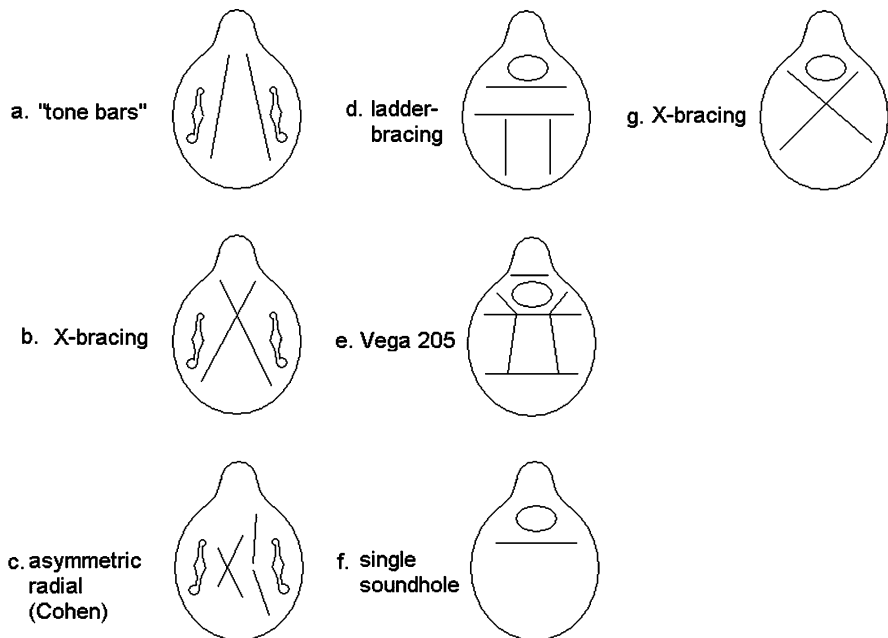


Fig. 6.1 Common bracing patterns in f-hole and oval soundhole mandolins: (a) tone bars/f-holes, (b) X-bracing/f-holes, (c) asymmetric radial/f-holes, (d) ladder bracing (Neapolitan), (e) ladder bracing (Vega 205), (f) single soundhole brace, (g) X-bracing/oval hole

the traditional stringing and tuning of the Neapolitan mandolin, they have a recognizably different sound. Neapolitan mandolins and archtop mandolins comprise a majority of the mandolins currently being played, but there are other types, each with their own following. Each type of mandolin has a characteristic sound hole configuration and bracing pattern. Figure 6.1 contains drawings of the bracing pattern/sound hole combinations common in the various types of mandolin family instruments. Following are descriptions of the major types of mandolin family instruments currently being made and/or played.

6.2.1 Neapolitan Mandolins

Also known as *bowlback* mandolins, these instruments have a body comprised of a top, or *table* with a *cant*, or *pliage*, under the bridge and a deep bowl-shaped body made from strips of hardwood assembled over a mold. The bowl is usually not braced, but may be lined with paper. The top is usually ladder-braced with two longitudinal extensions (Fig. 6.1d), and these mandolins have a single oval or round sound hole. The scale length typically varies from the violin scale length, approx.



Fig. 6.2 Types of mandolins: (a) front view of 1920 Calace (Neapolitan) mandolin (courtesy of Jonathan Rudie), (b) rear view of 1920 Calace, (c) Washburn model 1915 flatback mandolin, (d) front view of 1920 Vega model 205 “cylinderback” mandolin (courtesy of Maxwell McCullough), (e) view from the heel of the back of the 1920 Vega 205, (f) 1924 Gibson F4 mandolin (courtesy of Maxwell McCullough)

12.87" (327 mm), to as long as 13.25" (337 mm). Figure 6.2a shows the front, and Fig. 6.2b shows the back view of a 1920 Calace mandolin (courtesy of Jonathan Rudie).

6.2.2 Flatback Mandolins

These mandolins are sometimes referred to as *pancake* mandolins. The backs are made from flat plates of hardwood, and the tops are made from flat plates of a softwood. In some cases, the tops and backs are truly flat, while others have a modest arch induced by precurved bracing. Both top and back plates are usually ladder-braced (Fig. 6.1d), though in some examples the top plate may have only a single transverse brace between the bridge and the single oval or round sound hole

(Fig. 6.1f). The scale length varies from that of the shortest Neapolitan scale lengths to as long as 13.88" (353 mm). Figure 6.2c shows a model 1915 Washburn mandolin of this type.

6.2.3 Cylinderback Mandolins and Other Unique Designs

The early twentieth century saw a number of unique designs intended to improve the volume and/or tone quality of the mandolin. One such design was the Vega *cylinderback* mandolin. Its top plate was flat except for a slight pliage at the bridge location, and had modified ladder-bracing and an oval sound hole (Fig. 6.1e). The back plate was made from a flat hardwood plate fitted to precurved ladder braces with an exaggerated cycloid-like shape. Figure 6.2d shows a front view and Fig. 6.2e shows a view of the back from the heel of a 1920 Vega 205 cylinderback mandolin (courtesy of Maxwell McCullough).

6.2.4 Archtop Mandolins, Oval Sound Hole

Top and back plates in these mandolins are carved into an arch similar but not identical to violin arches. Back plates are not braced. Top plates traditionally had a single transverse brace between the bridge and the sound hole (Fig. 6.1f), though some modern luthiers use X-bracing in this type of instrument (Fig. 6.1g). Scale lengths are most commonly 13.88" (353 mm), though custom makers offer scale lengths as short as 13" (330 mm). Figure 6.2f shows a front view of a 1924 Gibson F4 mandolin (courtesy of Maxwell McCullough).

6.2.5 Archtop Mandolins, f-Holes

Top and back plates are also carved to arches in this type of instrument. The f-holes are positioned similarly to violin f-holes. Backs are not braced. Top plates are most commonly braced either with (roughly) parallel longitudinal tone bars (Fig. 6.1a) or with X-bracing (Fig. 6.1b). The most common scale length for this type of instrument is 13.88" (353 mm), though custom makers offer shorter and longer scales. Both the oval hole and the f-hole archtop mandolins have been made in both the F-body style and the A-body style. The former has a teardrop body shape embellished with an upper bout ionic volute or scroll and two points on the side of the body opposite the scroll. The latter has a simple teardrop body shape. The leftmost instrument in Fig. 6.3 is a 2005 Cohen F-style mandolin.

6.2.6 *Mandolas, Octave Mandolins, and Mandocecellos*

The larger mandolin family instruments are found in all of the above varieties. Mandola scale lengths vary from the original Gibson scale length of 15.75" (400 mm) to 17" (432 mm) and occasionally longer. The most common scale length on manufactured mandolas is currently 17". Octave mandolin scale lengths vary from about 19" (483 mm) to about 24" (610 mm), and occasionally longer. The shorter scale lengths are preferred by players using the octave mandolin primarily for melody lines, while the longer scale lengths are preferred by players using the instrument primarily for rhythm playing. The most common scale length for mandocecellos is the original Gibson scale length, 24.75" (629 mm), though some are made with longer scale lengths. For visual comparison of the relative sizes of mandolin family instruments, Fig. 6.3 shows a mandolin family quartet consisting, from left to right, of a 2005 Cohen F mandolin, a 2004 Cohen A mandola, a 2007 Cohen C# octave mandolin, and a 2006 Cohen A mandocecello.

Determining whether or not mandolin family instruments will evolve in the future, and to what they might evolve into, is facilitated by a physical understanding of what they currently are, as well as a general understanding of the physics of plucked stringed instruments. Investigations into the physics of mandolin family instruments have begun only recently (see Cohen and Rossing 2000, 2003; Taguti and Yamanaka 2006). Since mandolin family instruments *are* plucked stringed instruments, some understanding of them can be gained from what is currently known about guitars. It is most efficient to list only a few sources containing important references. The short-lived *Journal of Guitar Acoustics* may still be



Fig. 6.3 Front views of a mandolin quartet. *Left to right:* 2005 Cohen F mandolin, 2004 Cohen A mandola, 2006 Cohen C# model octave mandolin, 2006 Cohen A mandocecello. Body size ratios are mandolin:mandola:octave mandolin:mandocecello = 1.00:1.15:1.31:1.46

purchased from its editor (White 1980–1983). A good starting place is the series of three introductory articles on guitar acoustics written for the Guild of American Luthiers by Rossing (1983–1984, 1988), as well as Chap. 3 of this work and references therein.

6.3 Normal Modes of Vibration and Holographic Interferometry

String players recognize that an open string does not vibrate at just any frequency, but instead vibrates at particular frequencies determined by its length, mass, and tension. Those frequencies are its modal frequencies or *eigen* frequencies. Each of those frequencies is associated with a specific normal mode of vibration for the string. Similarly, the instrument body has its own normal modes of motion and associated modal frequencies, as does the mass of air in the sound hole(s). Normal modes of motion are covered in Sect. 3.2, and normal modes of the component parts of guitars are covered in Sect. 3.2.1. For a mandolin family instrument, a given normal mode of motion of the assembled instrument will be determined by the coupled motion of its strings, bridge, top and back plates, ribs or sides, air in the body cavity and in the sound hole(s), and the neck/headstock/fingerboard assembly.

The deflection of an object at a particular frequency is called an operating deflection shape (ODS). An ODS may result from the excitation of more than one normal mode. A curve-fitting program may be employed to determine the individual normal modes from the ODS. If two or more normal modes do not overlap significantly at a given frequency, the ODS at that frequency may be a good representation of the normal mode shape.

Experimental modal testing may be accomplished using any transducer capable of detecting motion. Multiple transducers can be used to increase the spatial resolution of an ODS. Holographic interferometry offers by far the best spatial resolution of ODSs, effectively detecting motion at an unlimited number of points (Jansson et al. 1970). The form of holographic interferometry known as electronic TV holography allows the observation of vibrational motion in real time, and is a fast and convenient way to record ODSs (Jansson et al. 1994).

Figure 6.4 is a diagram of an electronic TV holography system. Light from a laser passes through a beam splitter, which splits the beam into a reference beam and an object beam. The reference beam is fed through an optical fiber to illuminate a CCD camera. The object beam is expanded and rotated in small steps to reduce laser speckle noise. The object beam then reflects off the object (i.e., the instrument body) through a video lens into the CCD camera, where it interferes with the reference beam to produce a holographic image of the object.

In order for the TV holography system to image the ODSs of an object, the object must be set in motion with a sinusoidal excitation. One way to do that is to affix a small magnet to the object and drive the magnet with the sinusoidal field

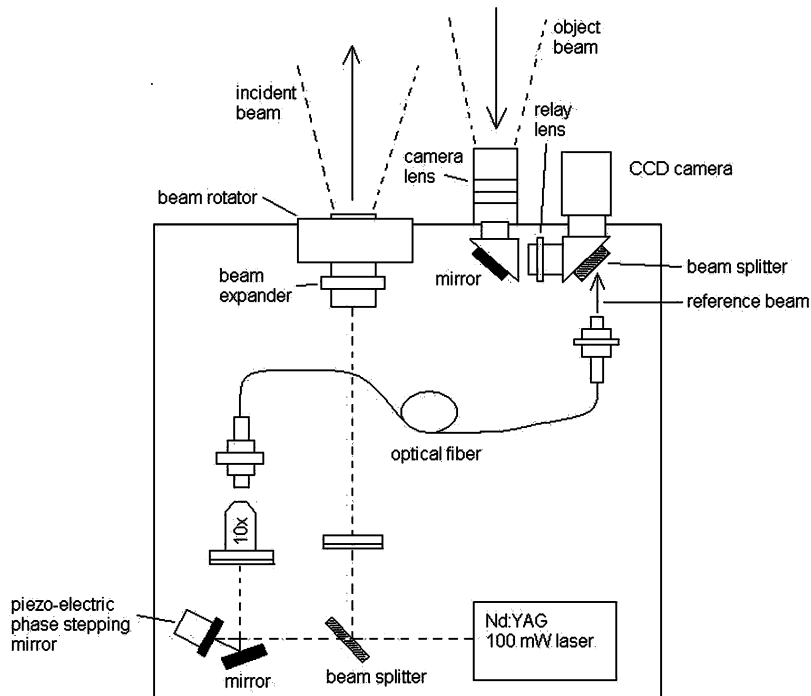


Fig. 6.4 Drawing of the TV holography system. The incident beam is reflected by the object (e.g., a mandolin) to become the object beam

from a small coil driven by an audio signal generator. The frequency is scanned until the object comes into resonance, then the frequency is maintained at the resonance frequency until the image of the ODS is recorded. In practice, a small (approx. 0.2 g) NdFeB magnet can be attached to the bridge of an instrument temporarily with wax. In order to image those ODSs which have nodes directly under the bridge or nearby, the magnet and coil may have to be moved to another location on the instrument body which is closer to an *antinode*, or point of maximum amplitude, for that particular ODS. The shapes and frequencies of the ODSs may also be affected by the way the object is supported. Modal frequencies obtained from holography done on an instrument suspended by large rubber bands will be different from those done on a rigidly clamped instrument. Rigid clamping is usually done at the endpin and at the juncture of the neck and the headstock.

6.4 Normal Mode Shapes in Mandolins

The shapes of mandolin normal modes vary with body shape, sound hole position (s), and to a smaller extent, bracing pattern. Figure 6.5 shows ODSs from TV holography that approximate the first five normal mode shapes of the body of an

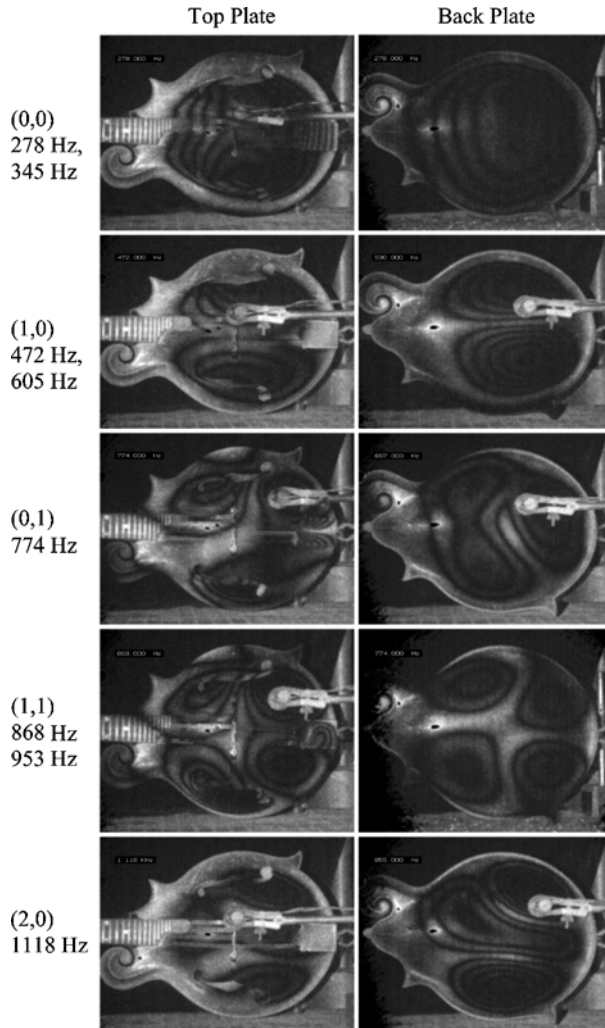


Fig. 6.5 Operating deflection shapes approximating the first five body normal modes of a 1924 Gibson F5 mandolin. The top plate ODSs are in the *left column* of photos, and the back plate ODSs are in the *right column* of photos. (Mandolin courtesy of Drew Carson)

f-hole type mandolin, in this case a 1924 Gibson F5. The ODSs are shown for the top plates on the left and for the back plates on the right. Each dark line or *fringe* in the images represents an amplitude change of one-fourth of the wavelength of the laser light used. For a frequency-doubled Nd:YAG laser, each fringe represents an amplitude difference of approximately 133 nm. Light areas between closed patterns of fringes are associated with nodal lines in the ODSs.

Other than whole-body bending modes of motion, the lowest body mode is the (0,0) mode, seen in the top frames of Fig. 6.5. The (0,0) mode is a trampoline-like

motion of each plate, in which all areas of the plate move in phase. The antinode is near the center of the plate, and there are no nodes save at the periphery of the plate. This mode shape occurs at two different frequencies in some mandolins, in which case it is called a *doublet*. It occasionally occurs at three different frequencies in some other mandolins, in which case it is called a *triplet*. In guitars, the (0,0) mode may be either a doublet or a triplet.

With mandolin as with guitars, the simplest models applied to the (0,0) mode are the *two-oscillator model* and the *three oscillator model*. The former is discussed in Sect. 3.2.3, and the latter is discussed in Sect. 3.2.4. In early experiments, mandolins with relatively stiff back plates deviated from the two-oscillator model by 5% or less, while one mandolin with a less stiff back plate deviated by 22% (Cohen and Rossing 2003).

The remainder of Fig. 6.5 shows the modes typically seen in mandolins up to around 1 kHz. The next higher soundbox mode of motion after the (0,0) modes is the (1,0) mode of the top and back plates, seen in the second frames down from the top. This is a sideways rocking motion of the plates, with a nodal line approximately along the center seam of each plate. The third frames down show the (0,1) mode, which is a longitudinal rocking motion. The nodal line in the (0,1) mode is approximately under the bridge, although as seen in Fig. 6.5, it can be quite distorted. The fourth frames down show the (1,1) mode, a twisting motion of the plates vibrating in four segments. The (1,1) mode has one node approximately along the center seam of the plate, and a second node perpendicular to the first approximately under the bridge. The bottom frames show the (2,0) mode, in which the plate vibrates in three segments and has two nodal lines roughly parallel to the center seam. In the (2,0) mode, the region between the two nodes and along the center of the plate is antiphase to the regions outside the two nodes.

If two modes overlap in frequency, the observed ODS in the frequency region where the overlap occurs will look like a mixture of the two modes. This may appear as a change in orientation of nodes, or as a different ODS shape. On occasion the nodes of the (2,0) mode will be oriented diagonally to the center seam of the body (Fig. 6.5, back plate). Due to mixing with other modes, the node of the (0,1) mode in back plates sometimes appears as three vibrating segments.

As with other stringed instruments, the main air resonance of a mandolin is the Helmholtz resonance, with its frequency denoted by f_0 or f_H . The lowest air resonance frequency measured when the instrument body is not immobilized is *not* the Helmholtz resonance, though it is related to it. It is usually denoted A_0 . Higher air resonance frequencies are usually denoted f_1, f_2, \dots , when measured with the instrument body immobilized, and A_1, A_2, \dots , when the instrument body is not immobilized.

Figure 6.6 contains drawings of the first three air resonances in f-hole and oval hole mandolins. It is difficult to find descriptions of the Helmholtz air resonance related to instrument body shapes. The air in the body cavity is a spring of air shaped like the body cavity of the instrument. The higher air modes are analogous to those observed in guitars, and have been described as being analogous to standing wave shapes (Rossing 1983–1984, 1988). The second air resonance, f_1 ,

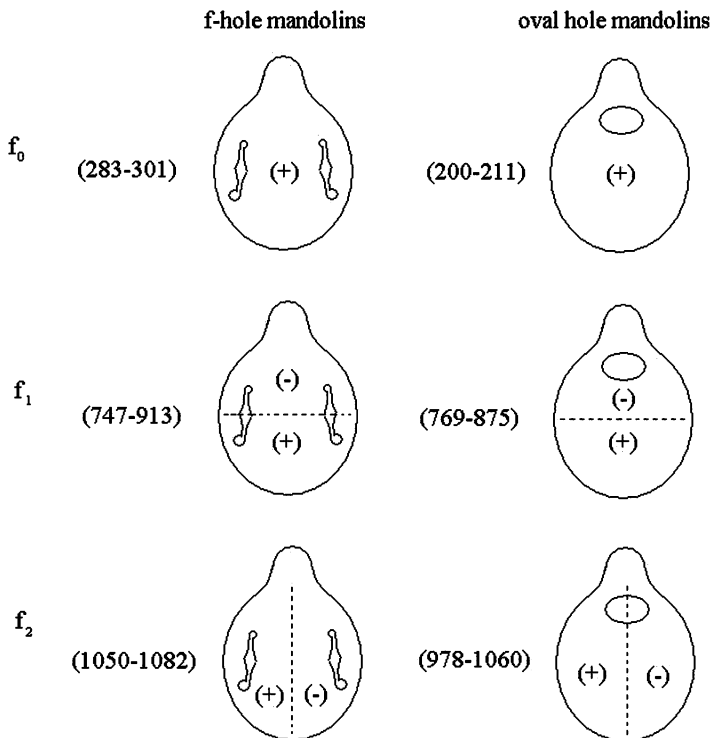


Fig. 6.6 Drawing of the first three air resonances for f-hole type mandolins (left) and oval hole mandolins (right). The Helmholtz resonance is at the *top*, with its' frequency denoted by f_0 . The longitudinal sloshing air mode is in the *middle*, with its' frequency denoted by f_1 . The sideways sloshing air mode is at the *bottom*, with its' frequency denoted by f_2

has a node perpendicular to the center seam of the plates, and can be thought of as a longitudinal sloshing of the air in the cavity. The third air resonance, f_2 , has a node along the center seams of the plates, and can be thought of as a sideways sloshing of the air in the instrument body cavity. Accounts of one method used to measure air resonance frequencies can be found in Cohen and Rossing (2000, 2003).

6.5 Normal Mode Frequencies in Different Types of Mandolins

Inasmuch as mandolins are made primarily from wood, and every piece of wood is unique, the normal mode frequencies for each mandolin are also unique. Modal analysis of examples of the different types of mandolins reveals that some generalizations can be made about the modal frequencies of each type of mandolin. The overall body shape, sound hole position(s), and associated bracing patterns

all exert some influence on modal frequencies. Even within types of mandolins, however, a range of frequencies will be observed for any given mode.

The second column in Table 6.1 lists the body mode frequency ranges for two Neapolitans, and the third column lists the modal frequencies for a Vega cylinder-back mandolin. Beginning with the Neapolitans, it can be seen that the (0,0) mode is a doublet occurring at 500 Hz or higher. The ladder bracing combined with the narrow width (approx. 8", or 20 cm) of the top plate results in high body mode frequencies. The cross-grain stiffness from the ladder bracing also tends to raise the frequencies of modes involving cross-grain bending. Consequently, the (1,0) mode occurs at a higher frequency than does the (0,1) mode and the (2,0) mode occurs at a higher frequency than does the (0,2) mode. The bowls, though unbraced, are very stiff. No normal modes of motion were found in the bowls below about 1.2 kHz. The f_0 frequency is low, approx. 180–200 Hz, and higher air resonances are difficult to observe. The relatively large frequency separation between f_0 and the (0,0) modes suggests weak coupling between the two modes. Recent transfer mobility measurements on Neapolitan mandolins by Taguti and Yamanaka (2006) also placed the lowest or (0,0) resonance at 500 Hz or higher.

The top plate of the Vega 205 is not as stiff overall as Neapolitan mandolin top plates, in part due to the wider body (approx. 10" or 25 cm). The (0,0) mode in this example occurred as a triplet well below the (0,0) mode frequencies observed for Neapolitans. As with the Neapolitans, the (1,0) mode occurs at a higher frequency than does the (0,1) mode, again a consequence of the cross-grain stiffness from the ladder bracing. The cross-grain stiffness, combined with the longitudinal stiffness due to the unusual shape of the back plate, result in a truncated set of modes. No (0,1) mode was observed, nor was a (2,0) mode, though (1,0) and (1,1) modes were observed. The first three air resonance frequencies were positioned similarly to those of the oval hole archtop mandolins, as will be seen. This mandolin sounded more like an oval hole archtop mandolin rather than a Neapolitan.

The fourth column in Table 6.1 lists the five lowest body mode frequency ranges for several archtop oval sound hole mandolins from the period 1917 to 1924. Because all of these mandolins have a single transverse brace located near the sound hole, the top plates of these mandolins are not as stiff overall as the top plates of Neapolitan mandolins. The (0,0) mode occurs as a doublet in some examples, and as a triplet in others, at similar frequencies to those of the Vega 205. The phase relationships between top plate, back plate, and air in the sound holes for the (0,0) modes were explained as follows by Cohen and Rossing (2000): In the lowest (0,0) mode, occurring at approx. 200–210 Hz, air is pumped into the sound hole as the plates move outward from each other. For those oval hole mandolins having a triplet (0,0) mode, the highest frequency member of the triplet has air moving out of the sound hole as the plates move outward. For the middle member of the triplet, the plates are moving in the same direction and consequently little sound is radiated. Figure 6.7 is a diagram showing the plate/air phase relationships for the (0,0) triplet.

The cross-grain stiffness of the top plate is lower in the archtop oval hole mandolins than in the Vega 205, and the (1,0) mode occurs at lower frequencies than the (0,1) mode. It is interesting that in some of these mandolins, the (1,1) and

Table 6.1 Ranges of modal frequencies in mandolins and mandolas

Instruments	Neapolitan mandolins ^{a,b}	Vega 205 cylinderback mandolin ^c	Archtop ^{d-h}	Archtop ^{i-k}	Archtop mandola ^l	Archtop mandola ^m
Soundhole Bracing	Round or oval Ladder	Oval Modified ladder	Oval Single soundhole	f-Holes or c-holes Tone bars or asymmetric radial	Oval Single soundhole (has Virzi)	c-holes Asymmetric radial
Mode						
(0,0) (a)	496–549	202	200–210	237–318	173	234
(b)	529–618	403	358–441	345–452	346	368
(0)	792–1012	439	465–491			
(1,0) (a)	792–1012	876	46–603	472–482	439	402
(b)				605	540	
(0,1) (a)	658–769	599	717–819	620–774	485	558
(b)			902	767–824	568	666
(1,1) (a)	1357	730	746–876	821–896	771	728
(b)	1471		873–1033	933–953		
(2,0)	1092–1380		Not observed	1005–1089	837–1118	Not observed
<i>f</i> ₀	183–200	209		205–211	283–301	185
<i>f</i> ₁	815	795		725–875	747–913	629
<i>f</i> ₂	Not observed	1050		978–1060	1050–1082	1157
				1280–1300 (with Virzi)		

^a1920 Calace mandolin courtesy of Michael Schoeder and Jonathan Rudie

^b1908 Martin mandolin courtesy of Eugene Braig

^c1920 Vega 205 cylinderback mandolin courtesy of Maxwell McCullough

^d1917 Lyon & Healy "A" mandolin courtesy of Maxwell McCullough

^e1917 Gibson F4 mandolin courtesy of Gary Silverstein

^f1923 Gibson A3 mandolin courtesy of Gary Silverstein

^g1924 Gibson A4 mandolin courtesy of Maxwell McCullough

^h1924 Gibson F4 mandolin courtesy of Maxwell McCullough

ⁱ1924 Gibson F5 mandolin courtesy of Drew Carson

^j2000 Cohen C# mandolin

^k2001 Cohen "A" mandolin

^l1919 Gibson H1 mandola courtesy of Gary Silverstein

^m2000 Cohen "A" mandola

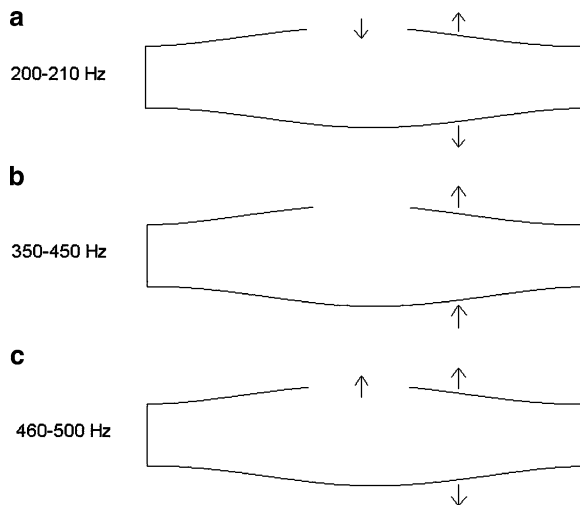


Fig. 6.7 Drawing of plate/air phase relationships for oval hole mandolins. (a) lowest mode, air is moving into the soundhole as the plates are moving away from each other; (b) middle mode; (c) highest frequency mode, air is moving out of the soundhole as the plates are moving away from each other

occasionally the (0,1) modes occur as doublets, while they occur as singlets in others. For the higher modes, as for the (0,0) mode, it is possible to have the top and back plates vibrating either in phase or antiphase. That might account for the observed doublets in some modes in these mandolins, but it does not account for all of them. A possible explanation for the occurrence of some, but not all, of the observed doublets is that different modes overlap in frequency enough to split each other. The proximity of the (0,1) mode and the f_1 air mode frequencies suggest that oval hole mandolins may radiate in the 700–900 Hz region. However, sound spectra for the mandolins did not show particularly strong output in that frequency range. For all mandolins with the exception of the Neapolitans, the (0,0) modes and often the (1,0) mode(s) occur at similar frequencies for the top and back plates, as expected from the two-oscillator and three-oscillator models. For higher-frequency modes, however, the motion of the back plate may show little correlation with that of the top plate. A similar situation has been found for guitars (Rossing et al. 1985).

The mandolins in the fourth column of Table 6.1 all have f_0 frequencies in the neighborhood of 210 Hz. The f_1 frequency seems to be more variable, ranging from 725 to 875 Hz. The f_2 frequency varies by <100 Hz for three of these mandolins, but is higher by 200–300 Hz for the remaining two. The body and sound hole dimensions for those mandolins are much the same as for the first three, but they have a device called a Virzi tone producer, which is a disc of spruce hung from the inside of the top plate with spruce supports. A detailed drawing of the device as installed in mandolins can be seen in an article by Davis (1989). It is possible that

the Virzi device is responsible for the approx. 200–300 Hz increase in the f_2 frequency observed in the latter instruments, though more observations in several examples of the instruments would be needed to confirm that. There do not appear to be any significant differences in the body mode frequencies due to the presence of the device.

The fifth column of Table 6.1 lists body mode frequencies for three f-hole type mandolins, including one vintage Gibson F5 mandolin and two mandolins constructed by the first author. The *c-holes* in the latter mandolins have approximately the same areas as the f-holes in the Gibson mandolin and are positioned similarly. The 1924 Gibson F5 and the 2001 Cohen A have the tone bars bracing, while the 2000 Cohen 402 C# model has an asymmetric radial bracing pattern (see Fig. 6.1c). None of these instruments has a Virzi tone producer, though some of the early Gibson F5 mandolins were fitted with them.

The (0,0) mode in these mandolins most commonly occurs as a doublet, and only occasionally as a triplet. The f_0 frequency is considerably higher for the f-hole type than for other types of mandolins, usually occurring between 270 and 300 Hz. The total area of the f-holes or c-holes is about 4.0 in.² (26 cm²), compared to about 2.7 in.² (17 cm²) for the oval hole in each of the mandolins in the fourth column. The larger total sound hole area combined with the same or similar body volume is responsible for the higher f_0 frequency in the f-hole type mandolins. In the lower frequency member of the (0,0) doublet, there is considerable air flow through the sound holes as the top and back plates move outward from each other. In the higher frequency (0,0) mode, the air motion in the sound holes is opposite in phase to that in the lowest mode. As seen in the fifth column, the lowest (0,0) mode frequency can be 20 Hz or more below the f_0 frequency. The implication is that the coupling between the (0,0) plate modes and the Helmholtz resonance is strongest in f-hole type mandolins. There are some examples of these instruments, however, for which the coupling is not as strong. In some examples, the lowest (0,0) mode frequency may be above the f_0 frequency (Cohen and Rossing 2000, 2003). Even in those instruments, the interaction between the (0,0) mode and the Helmholtz resonance is strong enough for coupling to occur and give rise to doublets having (0,0) shape. By way of comparison of mandolin types, Neapolitans have the weakest coupling of the (0,0) body mode to the Helmholtz air resonance; oval hole archtops and cylinderback mandolins exhibit stronger coupling; and strong coupling is also observed in some examples of the f-hole type archtop mandolins.

It is tempting to conclude that more coupling is better, since it should result in a firmer bass response. In fact, each type of mandolin has its adherents. In Europe, the Neapolitan mandolin predominates among classical players and groups, and is not without its adherents in America. Oval sound hole archtops, cylinderback mandolins, and flattop mandolins are preferred by players of Celtic music and by some classical players, while f-hole type mandolins are overwhelmingly preferred by bluegrass players. Even within musical genres, however, exceptions can be found. The f-hole type mandolins are often described by players as having *focus* and strong midrange response, while oval hole archtops are described as having a *tubby* low end.

The (1,0) mode in f-hole type mandolins sometimes occurs as a doublet, similar to what is observed in most guitars. Using small accelerometers, it was determined that the top and back plates move in opposite directions in the lower (1,0) mode, presumably giving rise to radiation with a dipole component (Cohen and Rossing 2000). The (2,0) mode is thought of as a fairly strong monopole radiator in classical guitars (Caldersmith 1985). It is possible that the (2,0) mode could give rise to monopole radiation in some mandolins, but there is not yet conclusive evidence for it. The (0,1) mode, also considered important for classical guitars, is not expected to be important for f-hole type mandolins, because little net movement of air in the f-holes is expected.

The comparisons between different types of mandolins raise questions about the effect of different bracing patterns on the modal properties of a single mandolin. Experiments to that end were performed by the first author on a mandolin with a removable back plate (a 2001 Cohen A, part of the data in the fifth column of Table 6.1). The different bracing patterns had little if any effect on the mode shapes, and only modest effects on the modal frequencies. Similar results have been found for guitars. Rossing (1982) compared guitar plate modes with those of plates having a variety of shapes and physical properties, and concluded that overall stiffness is more important than specific bracing patterns. Richardson (2002) used holographic interferometry to observe mode shapes and frequencies for a single classical guitar with several different bracing patterns, and also found that mode shapes were affected little by bracing patterns, while modest differences were observed for the modal frequencies. Meyer (1983a, b) compared guitarists' impressions of several classical guitars with modal frequencies and other physical properties of the instruments. He also noted that the exact positions of the braces were not as important as the overall stiffness of the plates.

6.6 Sustain in Mandolins

The sustain of a plucked note is of concern to mandolinists just as it is to guitarists. Different musical genres dictate different preferences for the amount of sustain desirable in a mandolin. The sustain of a plucked instrument string is related to losses caused by damping, which causes exponential decay of the amplitude of the string vibration. One measure of damping losses is the amount of time required for the amplitude to decrease to $1/e$ of its initial value, that is, to just under 37%. That time interval is variously called the *characteristic time*, *decay time*, *lifetime*, or *relaxation time*, and is usually assigned the symbol τ . The use of the characteristic time offers the advantage that a consistent value of the maximum or initial amplitude is not necessary for every trial.

The three loss mechanisms for vibrating strings are air damping, internal damping, and transfer of energy to other vibrating systems. The air damping or viscous damping depends on frequency and density of the string, and is more important in metal strings. The internal damping is a material property and is independent of

string length, radius, and tension. It is most important in gut or nylon strings. Of the three mechanisms, the third, losses to motion of the rest of the instrument, is most dependent on constructional details of the instrument. As such, it is the only loss mechanism that the luthier can address. It would seem that an understanding of that loss mechanism would lead to finding ways to build sustain, or lack of it, into an instrument according to the needs of the player. In practice, that may not be a simple task. String losses to motion of the instrument body depend in a complex way on frequency.

Figure 6.8 contains plots of characteristic time vs. frequency for two mandolins, one a Neapolitan (the Calace mandolin from Table 6.1) and the other an archtop f-hole type (the Cohen A from the fifth column of Table 6.1). To determine the characteristic times, notes were plucked parallel to the top plate surface approximately 1 m from a microphone; the amplitudes were recorded vs. time; the maximum amplitudes were determined graphically; and the time intervals for the amplitudes to decrease to 37% of their maximum values were determined graphically from the amplitude vs. time plots. It should be noted here that the actual amplitude vs. time curves are not simple exponentials, but instead may exhibit compound decay. Consequently, the characteristic times in Fig. 6.8 are deliberate simplifications.

Starting with the Calace Neapolitan mandolin plot in Fig. 6.8a, it can be seen that the characteristic times decrease by an order of magnitude in the frequency region from approximately 400 to 500 Hz, then remain low at higher frequencies. Referring to Table 6.1 offers some explanation. There are no body motions in this mandolin below the lower (0,0) mode peaking at 496 Hz. At approximately 400 Hz and below, the body is not stealing energy from the strings and the characteristic times are relatively long, reflecting primarily the contributions of air damping and internal damping. For comparison, a decay time of 0.4 s is fairly short for a steel string guitar. At frequencies of about 440 Hz and above, the Neapolitan mandolin body becomes active and the strings lose energy to it, resulting in the much shorter observed characteristic times.

While the plot in Fig. 6.8b looks very different, a related situation exists for the archtop f-hole type mandolin. In this case, the characteristic times from 196 to 440 Hz are relatively short, reflecting losses to the (0,0) doublet and the lower (1,0) mode in that frequency region. The longer characteristic times from about 500 to 650 Hz reflect the absence of modal peaks in that frequency region, while the shorter characteristic times above 650 Hz reflect losses to the upper (1,0), and the (0,1), (2,0), and (1,1) modes in the frequency region from 670 to 900 Hz and above. Referring to Table 6.1, it can be seen that while there are some variations in the frequencies of these lower modes in archtop f-hole type mandolins, the overall pattern seen in Fig. 6.8b would be expected to remain. It is difficult to see how changes could be made in such things as bracing patterns, graduations, arching, etc., in such a way as to predictably even out the characteristic times over the useful playing range of this type of mandolin. As is also true for Neapolitan mandolins, it appears that players have accepted and even embraced the irregularities characteristic of the instrument.

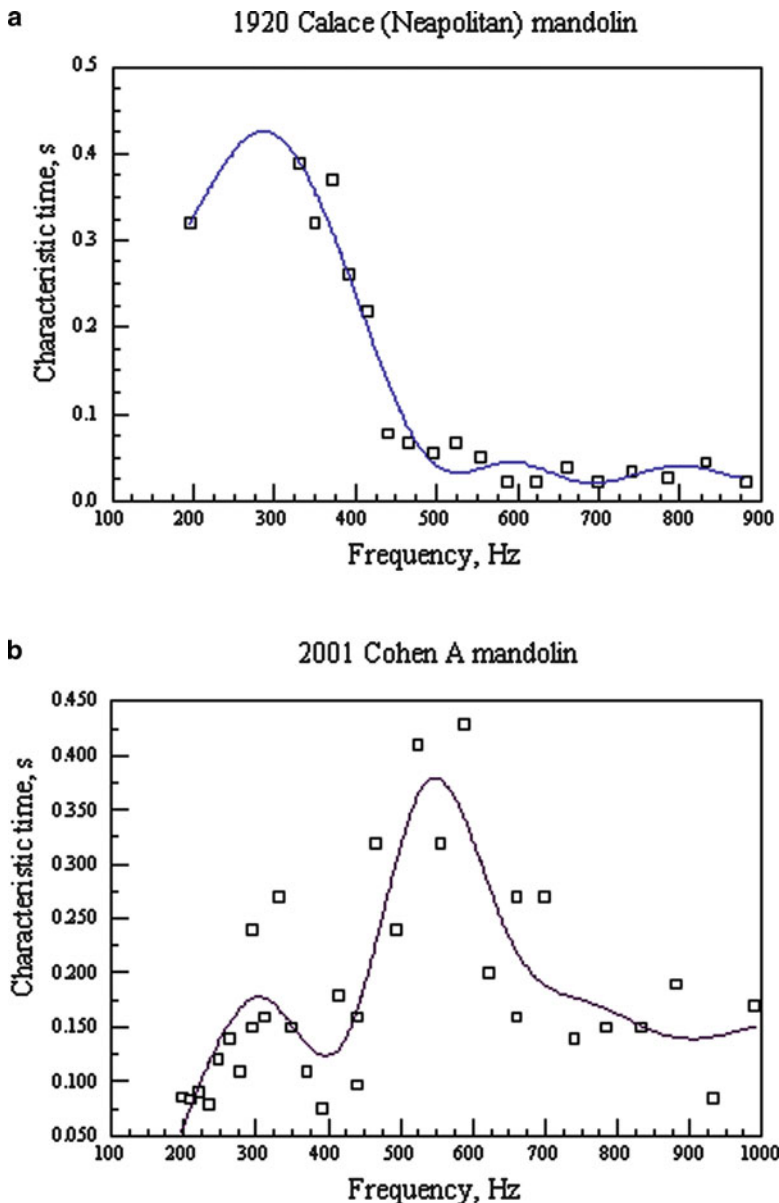


Fig. 6.8 Characteristic times vs. frequency for two mandolins; (a) a 1920 Calace Neapolitan mandolin and (b) a 2001 Cohen A archtop f-hole type mandolin

6.7 Other Mandolin Family Instruments: Normal Modes in Two Mandolas

The basic shapes of archtop mandola modes are similar to those of mandolins (Cohen and Rossing 2003). The lower modal frequencies for a 1919 Gibson H1 with an oval sound hole, a single sound hole brace, and a Virzi tone producer (apparently retrofitted) are listed in the sixth column of Table 6.1. The lower modal frequencies for a 2001 Cohen A mandola with c-holes and asymmetric radial bracing are listed in the seventh column. The mandola modal frequencies are predictably lower than the corresponding mandolin modal frequencies, roughly following the law of general similarity (Fletcher and Rossing 1998). The law states that if all linear dimensions of an instrument are increased by a factor K , and all else is assumed equal, the normal modes of the instrument body will decrease in frequency by a factor $1/K$, i.e.,

$$K = L_1/L_2 = f_2/f_1. \quad (6.1)$$

The relation can be applied to a comparison of the c-hole Cohen A mandola with c-hole or f-hole mandolins. Mandola dimensions are about 15% larger than mandolin dimensions. A lowest (0,0) mandolin mode frequency of 270 Hz is well within the range of observed lowest (0,0) mode frequencies. Assigning the subscript 1 to mandolins and the subscript 2 to mandolas, assuming that a mandola is 15% larger, and other things are equal, one has

$$1.00/1.15 = f_2/270 \text{ Hz}$$

or

$$f_2 = 270 \text{ Hz}/1.15 = 235 \text{ Hz}.$$

The estimated value of 235 Hz is in fortuitously good agreement with the observed value of 234 Hz for the Cohen A mandola, because the similarity relation is only approximately correct. This mandola, however, is another example of an f-hole type instrument for which the lowest (0,0) mode frequency is higher than the Helmholtz resonance frequency (Cohen and Rossing 2000, 2003). In this instrument, as in previous examples, the coupling is still strong enough to result in a doublet with (0,0) mode shape. Because the lowest (0,0) mode frequency is about where it is to be expected on the basis of similarity, stronger coupling in this instrument can be achieved by raising the Helmholtz air resonance frequency. This can be accomplished either by making the sound holes larger or by decreasing the body depth, or by doing both.

The lowest (0,0) mode frequency of the oval sound hole 1919 Gibson H1 is slightly below the Helmholtz resonance frequency for that instrument, following a pattern similar to that for oval sound hole mandolins. Application of the general law

of similarity starting with a lowest (0,0) mode frequency of 210 Hz for oval sound hole mandolins gives an expected value of 183 Hz for an oval sound hole mandola, in reasonable agreement with the observed value of 173 Hz. In both f-hole type and oval sound hole mandolas, the two (0,0) modes and the Helmholtz air resonance follow the phase relationships of Fig. 6.7a, c. The relatively high f_2 (sideways sloshing air resonance) frequency for the Gibson mandola with the Virzi device appears to add another data point for the effect of the device seen in Table 6.1. Comparison of some of the other body mode frequencies of the oval sound hole vs. c-hole or f-hole type mandolas is probably best deferred until more data is available.

6.8 Mandocellos

Although most mandocellists play oval sound hole instruments such as vintage Gibson K1, K2, or K4 models, there have been some mandocellos made using a 16" archtop guitar body with f-holes. Some modern luthiers have also built mandolin-shaped mandocellos with f-holes. While no modal data is yet available for mandocellos, application of the general law of similarity can be instructive. Mandocello bodies are typically about 46% larger than mandolins. Using the oval sound hole mandolin for comparison to the oval-sound hole mandocello, one has for the lowest (0,0) mode for a mandocello

$$f_{MC} = 210 \text{ Hz} (1.00/1.46) = 144 \text{ Hz}.$$

The Helmholtz air resonance frequency for a 2000 Cohen oval sound hole mandocello having body dimensions similar to those of a Gibson K4 was measured to be 145 Hz. A lowest (0,0) body mode at 144 Hz would be expected to result in weaker than desirable coupling for an instrument intended to be the baritone member of a quartet. The (0,0) body mode/Helmholtz resonance coupling can be strengthened by either raising the Helmholtz resonance frequency or lowering the lowest (0,0) mode frequency, or by doing both. As the sound hole in the 2000 Cohen mandocello is already quite a bit larger than that of a Gibson K4, and further thinning of the top plate would not be a good option for reasons of structural integrity, other ways of lowering the (0,0) mode frequency and/or raising the Helmholtz resonance frequency must be found. The most obvious way to do this is to increase the plate size while simultaneously decreasing the body depth. This can be accomplished either by changing the dimensions of a mandolin-shaped mandocello, or by using an archtop guitar body shape. Archtop guitar bodies typically utilize larger plate dimensions and thinner body depths than the traditional mandolin-shaped mandocello. For the working luthier, application of the general law of similarity as in the examples above can provide initial guidance in developing a family of instruments. Because the law is approximate, refinements beyond the initial estimates will depend on systematic variations, observations, and corrections by luthiers.

6.9 Summary and Conclusions

While the mechanical vibrations of mandolin bodies show some similarities to those of guitars, the diversity of body types and sound hole configurations in mandolins makes for some interesting variations in the distributions of modal frequencies. Those variations are in turn accompanied by interesting variations in the tonal attributes of the various types of mandolins. Flat top steel string guitars are much less diverse in both their constructional details and in the frequency distribution of body vibrational modes and air resonances. The fact that fingerstyle guitarists prefer smaller-bodied guitars while plectrum or flatpick style guitarists prefer larger bodied guitars mainly reflects a preference for guitars with a modestly different bass/treble balance.

Modal analysis is certainly not all there is to understanding the acoustics of stringed instruments, but in the case of the different types of mandolins, it has helped greatly in understanding the differences between them. Neapolitan mandolins are characterized by a wide frequency separation between f_0 at approx. 180 Hz and the (0,0) doublet in the top plate at approx. 500 Hz or above. The tendency for these instruments to have treble response to the exclusion of bass response and a transition from moderate sustain below 400 Hz to quick decay above 500 Hz is directly attributable to the positions of modal frequencies. Similarly, the positions of modal frequencies in other types of mandolins are integral parts of their respective tonal characters. Oval hole archtop mandolins are characterized by a relatively low f_0 , approx. 210 Hz, and a (0,0) mode that is often split into a triplet with the lowest member at approx. 200–210 Hz, the middle member at approx. 350–400 Hz, and the highest member at approx. 400–500 Hz. Archtop f-hole type mandolins are characterized by a higher f_0 , approx. 270–300 Hz, and a (0,0) mode that is often split into a doublet with the lower member occurring at approx. 250–320 Hz and the higher member occurring at approx. 350–465 Hz. For both f-hole type and oval hole archtop mandolins, strongest sound radiation is expected to occur from the interaction of the (0,0) mode and the Helmholtz air resonance.

Larger members of the mandolin family of instruments are gaining exposure as exposure to the mandolin itself increases. Preliminary applications of the general law of similarity to these instruments suggest that their sonic attributes may be improved by some optimization of their physical dimensions.

References

- Caldersmith, G.: Radiation from lower guitar modes. In: *The Big Red Book of American Lutherie*, Vol. 1, pp. 68–72. Guild of American Luthiers, Tacoma, WA (2000). Originally published in *American Lutherie*, #2 (1985).
- Cohen, D., Rossing, T.D.: Normal modes of vibration in two mandolins. *J. Catgut. Acoust. Soc.* **4**(2), Series II, 48–54 (2000).
- Cohen, D., Rossing, T.D.: The acoustics of mandolins. *Acoust. Sci. Tech.* **24**, 1–6 (2003).

- Davis, T.: An interview with Darryl Wolfe, F5 expert. In: *The Big Red Book of American Lutherie*, Vol. 2, pp. 228–235. Guild of American Luthiers, Tacoma, WA (2001). Originally published in *American Lutherie*, #18 (1989).
- Fletcher, N., Rossing, T.D.: Bowed stringed instruments. In: *The Physics of Musical Instruments*, 2nd ed., Springer-Verlag, New York, pp. 323–326 (1998).
- Gill, D., Campbell, R.: Mandolin. In: *The New Grove Dictionary of Musical Instruments*. S. Sadie, ed., MacMillan, London (1984).
- Jansson, E., Molin, N-E., Saldner, H.O.: On eigenmodes of the violin – electronic holography and admittance measurements. *J. Acoust. Soc. Am.* **95**, 1100 (1994).
- Jansson, E., Molin, N-E., Sundin, H.: The resonances of a violin body studied by hologram interferometry and acoustical methods. *Phys. Scripta* **2**, 243 (1970).
- Johnson, J.R.: The mandolin orchestra in America. In: *The Big Red Book of American Lutherie*, Vol. 2, pp. 262–279. Guild of American Luthiers, Tacoma, WA (2001). Originally published in *American Lutherie*, #s 19, 20, 21 (1989–1990).
- Meyer, J.: Quality aspects of the guitar tone. In: *Function, Construction, and Quality of the Guitar*. E.V. Jansson, ed., Royal Swedish Academy of Music, Stockholm, pp. 51–76 (1983a).
- Meyer, J.: The function of the guitar body and its dependence on constructional details. In: *Function, Construction, and Quality of the Guitar*. E.V. Jansson, ed., Royal Swedish Academy of Music, Stockholm, pp. 77–108 (1983b).
- Richardson, B.E.: Simple models as a basis for guitar design. *J. Catgut Acoust. Soc.* **4**(5), Series II, 30–36 (2002).
- Rossing, T.D.: Plate vibrations and applications to guitars. *J. Guitar Acoustics* No. 6, 65–73 (1982).
- Rossing, T.D.: An introduction to guitar acoustics. In: *The Big Red Book of American Lutherie*, Vol. 2, pp. 124–134. Guild of American Luthiers, Tacoma, WA (2001). Originally published in *American Lutherie*, #11 and #12 (1983/1984).
- Rossing, T.D.: Sound radiation in guitars. In: *The Big Red Book of American Lutherie*, Vol. 2, pp. 144–152. Guild of American Luthiers, Tacoma, WA (2001). Originally published in *American Lutherie*, #16 (1988).
- Rossing, T.D., Popp, J., Polstein, D.: Acoustical Response of Guitars. *SMAC* 83. Royal Swedish Academy of Music, Stockholm, pp. 311–332 (1985).
- Sparks, P.: *The Classical Mandolin*. Clarendon Press, Oxford (1995).
- Taguti, T., Yamanaka K.: Measurement of the bridge-to-table transfer mobility of two mandolins. *9th Western Pacific Acoustics Conference, Seoul, Korea, June 26–28* (2006).
- Tyler, J., Sparks, P.: *The Early Mandolin*. Clarendon Press, Oxford (1989).
- White, T., ed. *Journal of Guitar Acoustics*. The complete seven issues plus an introduction, tutorial, and appendix can be purchased from Tim White, Editor, *Journal of Guitar Acoustics*, 146 Lull Road, New Boston, NH USA 03070; e-mail: tpwhiteco@aol.com

Chapter 7

Psalteries and Zithers

Andres Peekna and Thomas D. Rossing

7.1 Introduction

The terms *psaltery* and *zither* are somewhat interchangeable. Both denote string instruments with strings that span the length of the sound box and sound board. From a musicological classification viewpoint, *psalteries* belong in the *zither* family of instruments, which also includes Appalachian dulcimers, autoharps, and hammered dulcimers.

Historically, on the other hand, psalteries came before zithers. Psalteries from medieval and Renaissance Europe have been described in historical sources. These psalteries were often played with two goose-quills, one in each hand.

In popular usage these days, the term *zither* typically refers to folk instruments popular in Northern and Alpine Europe. Many consider them to be descendants of psalteries. They in turn branch into *zithers without fretboard* and *fretted (Alpine) zithers*.

Psalteries are usually thought of as plucked-string instruments. Yet there are some exceptions. One is the *bowed psaltery*, a triangular-shaped instrument in which each string is accessible for bowing close to its tuning-peg.

The *hammered dulcimer* (see Chap. 21), or its larger variant, the *cimbalom*, can also be considered a subset, or branch, of zithers or psalteries. One reason we mention it in this chapter is because it had significant influence on some modernized Baltic psalteries.

T.D. Rossing (✉)
Center for Computer Research in Music and Acoustics (CCRMA),
Stanford University, Stanford, CA 94302-8180, USA
e-mail: rossing@ccrma.stanford.edu

7.2 Influence of Stresses in Strings on the Instrument's Shape

The general formula for tensile force in a flexible string vibrating at its fundamental frequency is four times the lineal density (mass per unit length) times frequency squared, times vibrating length squared. An important special case arises when the strings are made of a homogeneous material. In this case, the tensile stress (force per unit cross-sectional area) is given by four times the density (mass per unit volume) times frequency squared times length squared. Consistent units must be used. For example, in the case of steel strings, the formula for stress in megapascals (1 MPa = 145 psi) becomes 0.031332 times frequency squared times length squared, with length expressed in meters. For strings of the strongest modern copper-alloy, beryllium copper C17200, this becomes 0.032996 times frequency squared times length squared. (Values of mass density are from *Materials Selector* 1993.)

The important thing to note here is that for the string tensile stress to remain constant, the product of frequency times length must remain constant. That is, for each factor of two increase in frequency, going an octave higher, the string length has to decrease by a factor of two. This brings about the concave outward curvilinear shape of many psalteries, as well as harps, in the range of their melody-strings. One type of medieval psaltery was symmetrical side-to-side, which gave it a pig-snout appearance. In Italy, it was known as *strumento di porco*, in Germany, as *Schweinekopf*.

Bass strings required a different solution. Instead of going beyond practical boundaries in length, their lineal density was increased by wrapping, usually with copper-alloy wire, around a core. At the ends of wrapped bass strings, flexibility was maintained by the relatively thin diameter of the core. The penalties of insufficient flexibility at the string ends (when the string begins to act as a stiff flexural rod) can be heard on the highest strings of the piano, which some do not consider particularly pleasant in sound quality. (Flexular stiffness of vibrating strings is treated at depth in Fletcher and Rossing (1998) and applied to the hammered dulcimer in Chap. 21.)

7.3 Plucking Stiffness, and Strength of a Plucked String

When the instrument is properly designed, all its strings feel about the same to its player. Resistance to plucking a string a given lateral distance before release can be described in units such as newtons per millimeter or pounds per inch of lateral deflection. When a string is plucked at its center, the plucking stiffness is given by four times the string tensile force (stress times stress-bearing cross-sectional area), divided by its length. Plucking the string away from its center brings in a slight modification. Some instrument makers use the plucking stiffness formula as a guideline, to be overruled by actual trials. This is one reason why the higher-tuned strings tend to be thinner.

In plucked-string instruments, strings tend to break at an end while plucked. Thus, in attempting to predict string strength, bending stresses that occur at the

string ends also need to be taken into account. In the plucking process, it is commonly assumed that the string is laterally displaced at a given point, initially with zero velocity, then suddenly released. This suggests using a static analysis for calculating stresses just before release.

Formulas for beams loaded statically in both tension and under lateral forces are presented in *Roark's Formulas for Stress and Strain* (Young 1989). When applied to a string with diameter very small compared to its length, they reduce to a very simple formula. For a string plucked at its center, the ratio of bending stress to tensile stress averaged over the string cross section is given by the ratio of the string-plucking lateral force to the total tensile force in the string, multiplied by the square root of the ratio of Young's modulus to average tensile stress in the string. Plucking the string away from its center brings in a slight modification (Peekna 2009). The total stress at a string end is the average tensile stress plus the bending stress.

7.4 String Materials

Traditional string materials include various wires, as well as gut, horsehair from a horse's tail, and legendary references to long maiden's hair. The specific reference to maiden's hair suggests avoidance of weak points brought about by pregnancy (von Wunder 1999).

Contrary to popular belief, drawing metal wire is an old art. One clue to its age is provided by the fact that mail-armor was invented by the Celts ca. 400 bce. Iron or steel wire served as raw material for the rings of mail.

Metal wires tend to deliver a higher-volume sound than the other materials. Thus, they were preferred early on. There are historical references and surviving examples of instruments with copper alloy (usually bronze) and steel strings. Because of their lower breaking strength, strings of copper-alloy cannot be tuned as high as can steel strings. In our experience with carved Baltic psalteries, steel strings provide a brighter, cheerful sound, while copper alloy strings yield a more mellow, more somber sound quality, which can be more appropriate for some tunes (Peekna 1998, 2008).

In the archaeology of old Novgorod, metal strings were found in association with Baltic psalteries, a.k.a. *guslis*. The spectral analysis of one such wire from the middle of the eleventh century showed <10% copper, >10% iron, 10% silver, and the remaining material, gold. According to the experiments conducted by the Glinka Museum of Music (Moscow), this wire showed sufficient strength for use as a string for musical instruments (Povetkin 1989a). Legends from Estonia also mention golden strings.

Improved strength of modern wires makes it possible to tune strings to higher tensions than before. For example, the absolute tuning is known for a carved Baltic psaltery with strings of copper-alloy (*Kaarma kannel*, Estonian National Museum, cat. A292:2, made in 1890); from its tuning and dimensions, the tensile stresses in

its strings (excluding the bourdon) were in the range 250–310 MPa. By contrast, optimum tensile stresses in strings of beryllium copper C17200 (Cu 98.1%, Be 1.9%, the strongest modern copper alloy) on a Baltic psaltery reproduction came out to be in the range 400–600 MPa (Peekna 1998). Similarly, the absolute tuning for a steel-stringed carved Baltic psaltery together with its dimensions (*Ungavitsa kannel*, Estonian National Museum, cat. 18573, donated 1914) implies string tensile stresses in the range 535–900 MPa, while experience with modern wire suggests that 800–1,200 MPa is more ideal.

7.5 Acoustical Study of Carved Baltic Psalteries

One of the authors (Andres Peekna) is a research engineer and physicist originally from Estonia who became a performing and recording amateur musician of folk instrumental music from that country, and he made his own carved Baltic psalteries, patterned after museum specimens in Estonia. The primary objective of our acoustical studies was to learn how to make better carved Baltic psalteries.

The carved Baltic psaltery is a plucked string instrument, without frets. Six examples are shown in Fig. 7.1, along with a violin and a Swedish *nyckelharpa* for size comparison. Three others are shown in Fig. 7.2. To eliminate ambiguities, we denote each instrument specimen by the maker's initials followed by the sequence number.

The Baltic psaltery is at least 1,000 years old. The sound boxes of its archaic forms were carved from a single block of wood, hence its name: the *carved* Baltic psaltery. (A similar case of carving/hollowing is the Dutch wooden shoe.) The sound board was separate, in most cases. Some are also known to be hollowed from below (without a bottom), and others were hollowed out from a side, leaving both



Fig. 7.1 Six carved Baltic psalteries along with a violin and a Swedish *nyckelharpa*

Fig. 7.2 Three carved Baltic psalteries included in our study. From left: AP1, AH19, and KD9



sound board and bottom intact but leaving the side open. Sometimes, the side was covered with a plank.

The Baltic psaltery is a folk instrument found throughout the East Baltic area, encompassing Finland, Estonia, Latvia, Lithuania, and northwestern Russia. For a long time, people in each country considered it their very own, though it is really a *regional instrument*. Local names are *kantele* in Finland, *kannel* in Estonia, *kokle* in Latvia, *kankles* in Lithuania, and *gusli* in northwestern Russia. The sound quality of a good carved Baltic psaltery can be described as a cross between a guitar and a harpsichord, or like a harp, except with a longer ring (sustain).

An important feature of antique carved Baltic psalteries is that no two specimens have ever been found that are exactly alike. This individualized tradition leaves the field wide open for experimentation. The instrument can be modified without violating tradition. (This is very exciting for those of us with a scientific bent.)

7.5.1 *History of the Carved Baltic Psaltery*

The hypothesis that the Baltic psaltery may have evolved from the lyre has been around since the 1970s. Persuasive arguments in favor were given by the Russian scholar, artist, and restorer of ancient instruments, (Povetkin 1989b). While not fully aware of the total extent of Povetkin's work, the Estonian-American sociologist Ain Haas independently presented arguments that the Baltic psaltery evolved from the lyre, and that its evolution was accelerated by contacts between ethnically different groups (Haas 2001; this paper received the Vilis Vitols prize from the Association for the Advancement of Baltic Studies in 2003).

A more recent comprehensive overview of the instrument's history was given by the Russian-American evolutionary biologist Ilya T  mkin. In his innovative paper, he applies cladistic analysis from evolutionary biology in reconstructing the possible evolution of this family of instruments (T  mkin 2004). The phylogenetic approach is extended in a more recent paper together with Niles Eldredge (T  mkin and Eldredge 2007).

7.5.2 Playing Techniques

There are several playing techniques, each emphasizing harmony. There is no one "correct" technique. One technique can best be described as playing a prehistoric autoharp. The fingers of the left hand are used to mute unwanted notes, while the right hand strums across with a wood or stiff leather plectrum, or with fingers. Unlike playing an autoharp, the fingers of the left hand also pick out intermediate notes. Thus fast, intricate melodies are easy to play. The hand positions are shown in Fig. 7.3. The same technique also appears in Fig. 7.7.

Another technique is the *intertwined plucking technique*, in which each finger has a definite position on its respective string, and always returns to it. In this technique too, harmony is essential. It is described in several instruction manuals, including the English-language *A Guide to Five-String Kantele Playing* (Laitinen and Saha 1988) and *My Kantele Is My Teacher* (Thompson 2004). Because of its emphasis on harmony, it has often been said that "this instrument needs no accompaniment." Indeed, it has been primarily a solo instrument. Yet, historically



Fig. 7.3 Playing on a 12-string carved kannel

it has also been played together with other instruments, in Estonia most notably with violin and bagpipe. In Russia, two guslis were sometimes played together, or a gusli with an accordion.

7.5.3 *Body Resonances of Some Carved Baltic Psalteries*

For our acoustical studies, we chose a total of six instruments based on (1) high sound quality and volume as discerned by a consensus of performing and recording musicians familiar with the music and the instruments, (2) representation of different geographic styles, and (3) availability. We make no claim of including the best carved Baltic psalteries on a worldwide basis in this limited study. The most important results were published in greater detail in an earlier paper (Peekna and Rossing 2005a).

The primary investigative technique we employed was electronic TV holography. This enables recording of what are in effect contour maps of the vibrational modes of the instrument's sound board (or the back, as the case may be).

A sinusoidal exciting force was generally applied by attaching a small iron-neodymium-boron magnet to the body of the psaltery and applying a sinusoidally varying magnetic field by means of a coil driven by an audio-frequency amplifier. In several cases, prior experience in choosing the location of minimal distortion for a contact microphone served as a guideline for choosing the driving point. This was either on the frame or on the sound board at or near the edge of the frame. Locating a contact microphone inward on the sound board produced distortion, probably due to maximizing or missing some body-resonances depending on whether it was at a maximum or at a node line between maxima.

Experimentally, all modal testing was done by measuring operating deflection shapes (OSDs) and then interpreting them in specific ways to define mode shapes. Strictly speaking, some type of curve-fitting program should be used to determine the normal modes from the observed OSDs, even when an instrument is excited at a single frequency. In practice, however, if the mode overlap is small, the single-frequency OSDs provide a good approximation to the normal modes.

Operational deflection shapes (mode shapes) for the six-string *kannel* AP1 (next to the violin in Fig. 7.1, and at left in Fig. 7.2) are shown in Fig. 7.4. Based on the experience of the authors and others, this is an outstanding instrument, with excellent sound quality and volume. Its soundboard is made of Sitka spruce, and its sound box is made of American basswood.

In Fig. 7.4, each arrowhead points to the location of a peak response. The vertical bars at the arrowheads are rough measures of the width of each peak at half the power level of each peak. These peaks were located by counting fringes while keeping the excitation current constant and varying the frequency. The *Q*-values of each body resonance, which express the ratio of spring force to damping force at each peak, are determined from the widths at half the power level of the peaks.

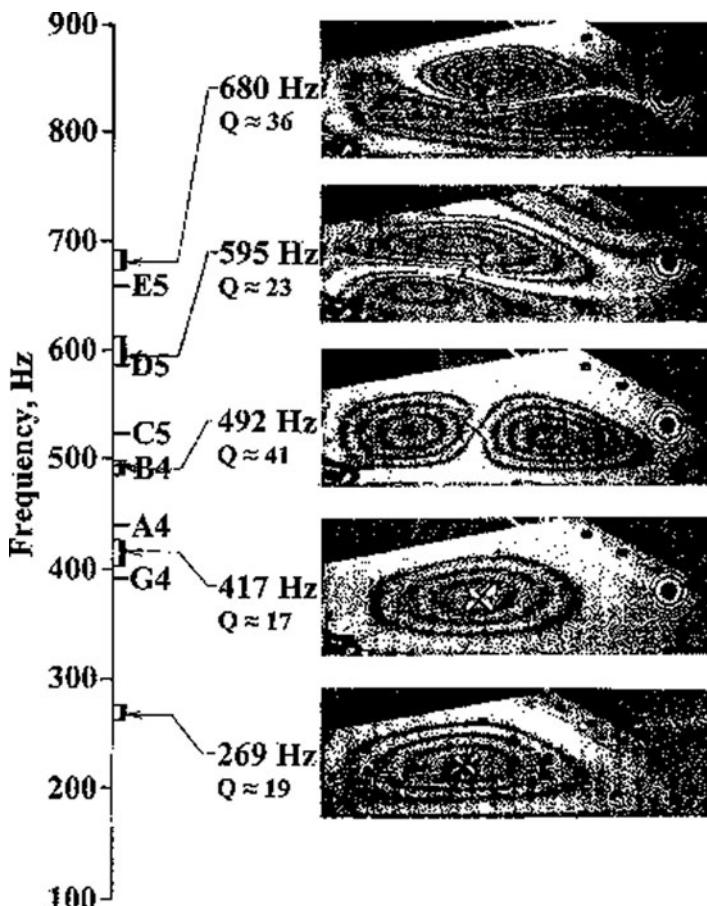


Fig. 7.4 Holographic interferograms showing sound board operational deflection shapes in the kannel AP1, along with the tuning of its six strings

Although the numerical data in Fig. 7.4 were taken with adhesive tape across the strings (in order to make sure the strings did not affect the body resonances), the mode shape pictures in Fig. 7.4 were taken with the tape removed, for clarity. Differences in mode *shapes* with and without tape across the strings were not significant.

The lowest mode at 269 Hz is well below the playing range and therefore of little significance in a steady state or nearly steady state, though it may affect the attack sound. The mode at 417 Hz involves air motion in-and-out of the sound holes in the same direction as the sound board motion, and it radiates sound efficiently. The location of the body resonance with the greatest radiating efficiency between the G4 and A4 strings is optimal from the standpoints of typical melodic structure and playing techniques. Four body resonances are available to support the fundamentals of its six strings.

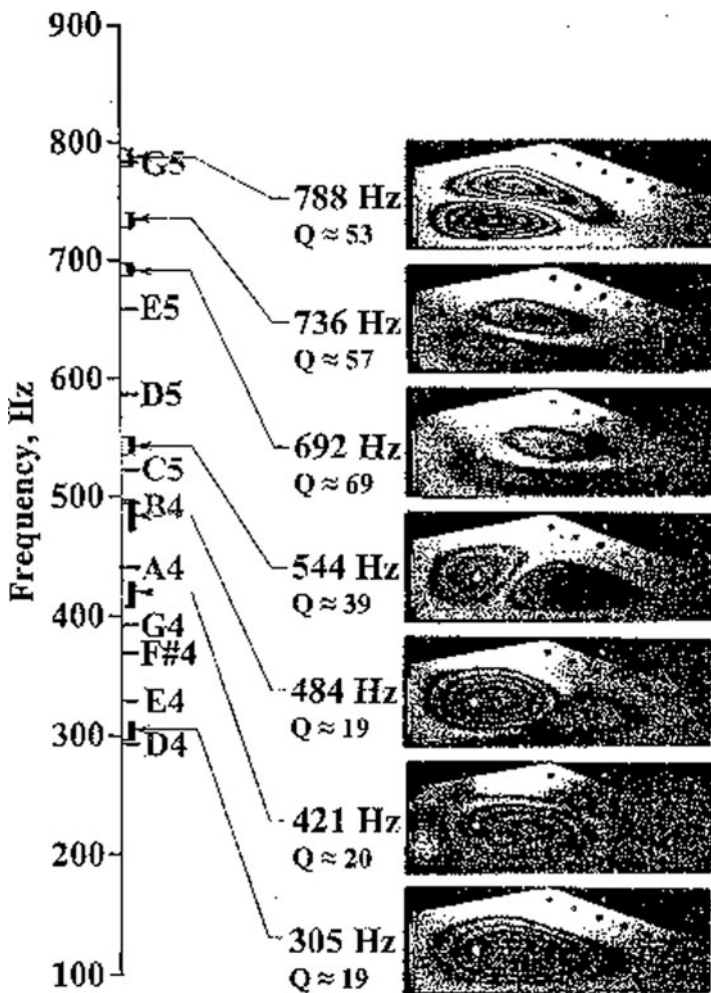


Fig. 7.5 Holographic interferograms showing operational deflection shapes in the kannel AH19, along with the tuning of its ten strings

Operational deflection shapes (mode shapes) for the outstanding ten-string kannel AH19 are shown in Fig. 7.5. This kannel is shown at the center of Fig. 7.2. The tuning shown in Fig. 7.5, with the F#5 missing from the diatonic scale, is traditional relative tuning on Finnish ten-string kanteles. Materials are Sitka spruce for the soundboard, and American basswood for the soundbox. Here again, the mode with the strongest radiating efficiency reinforces the G4 and A4 strings, while the lowest body-resonance reinforces the low dominant, which is another desirable feature in view of the typical repertoire plus the playing techniques employed. Seven body resonances are available to support the fundamentals of its ten strings.

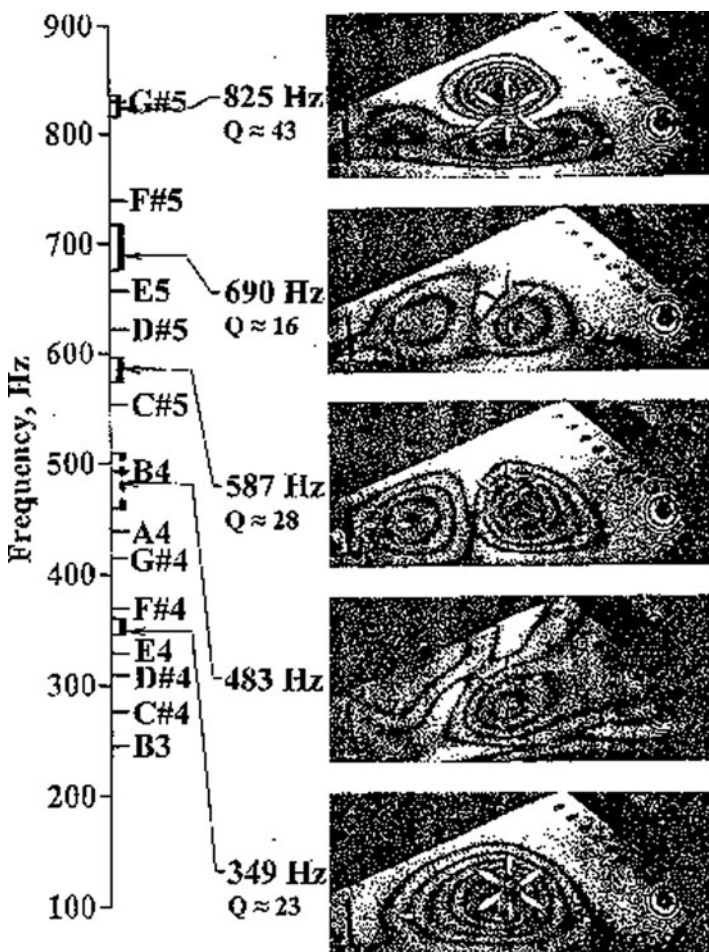


Fig. 7.6 Holographic interferograms showing soundboard operational deflection shapes in the kokle KD9, along with the tuning of its 13 strings

The modes and tuning of the outstanding 13-string Latvian *kokle* KD9 are shown in Fig. 7.6. This *kokle* is shown at right in Fig. 7.2. It has a sound board of very tight-grained Alpine spruce and a soundbox of American basswood. This instrument is also of relatively light construction, with a bottom thickness of 6 mm (compared with 7 mm in other instruments in this study). The instrument is tuned diatonically to the key of E, extending from B3 (low dominant) to G#5. The dashed vertical line near the B4 indicates complex and changing operational deflection shapes involving frame motion, over a broad range. Five body resonances are available to support its 13-string range. Relative to its number of strings, this is fewer than in AP1 and AH19, but better than two others in our study.

Results on the other three, less outstanding instruments, are not presented here. Two of these had more symmetrical soundboxes. There are also other reasons to believe that the complex asymmetric shape of the soundboard and soundbox of Baltic psalteries help increase the number of body resonances within the tuning range of the instrument.

7.5.4 *Coupling of Strings to Body Resonances*

An interesting question is: How far can a body resonance be from a given string and still be excited by that string? An opportunity for investigating string-to-body resonance coupling was brought up by the TV holography system's ability to scan at 0.1-Hz intervals. This brought about the ability to resolve narrow resonances at the string frequencies, while the body was driven externally. This was done by scanning for narrow peaks within the tuning range of a string left free to vibrate, while driving a point on the body by coil and magnet. Such a scan has to be done at intervals as fine as 0.1 Hz, as the peaks at the string frequencies are very narrow. With Baltic psalteries, two narrow peaks separated by only a few 2–5 Hz are often seen. This is probably due to the influence of the knot in the end of the string opposite the tuning pegs, which creates a slightly higher string frequency for motion perpendicular to the soundboard than for motion parallel to the soundboard (Välimäki et al. 2002; Erkut et al. 2002). Researchers in Finland also demonstrated convincingly that due to the resulting amplitude modulation, the knot has a beneficial effect on the timbre of the instrument.

The amplitude of a narrow peak relative to its neighboring (much broader) body resonance can be determined by counting fringes while keeping all test conditions except driving frequency the same. This means using the same excitation current, and no changes in the test setup, for each amplitude ratio comparison. It has been suggested that this amplitude ratio can serve as an approximate measure of coupling the string vibrations to the body resonances (Peekna and Rossing 2005a). Such data were taken on the instruments AP1, AH19, and KD9; these instruments are shown in Fig. 7.2. The data are shown in Table 7.1.

In generating the data for the higher strings of the ten-string kannel AH19 and the 13-string kokle KD9, masking tape was applied across strings that were an octave lower in order to rule out confusion between the fundamental of a high string with the second harmonic of a string tuned an octave lower. A general trend noticeable in Table 7.1 is that (with only three exceptions) the higher-frequency peak has a higher relative amplitude than the lower-frequency peak. Better coupling of the higher-frequency string mode is indeed expected as it involves string motion in the same direction as the soundboard motion.

Note that a feature common to all three of these instruments is a symmetric resonance (therefore with high radiating efficiency) between the keynote and the tone above. The results in Table 7.1 also imply that in each instrument, there is reasonably

Table 7.1. Amplitude ratios of narrow peaks at strings to neighboring body resonances at their peaks

Kannel AP1		G4	A4	B4	C5	D5	E5
String tuning		1.2 1.0	1.5 0.7	1.2 1.1	—	0.75	0.3
Amplitude ratios, higher string freq.							
Amplitude ratios, lower string freq.							
Kannel AH19		D4	E4	F#4	G4	A4	B4
String tuning		0.45	0.1	0.45	0.6	0.9	0.5
Amplitude ratios, higher string freq.	0.95			0.4	0.7	0.95	
Amplitude ratios, lower string freq.	0.5						
Kokle KD9		B3	C#4	D#4	E4	F#4	G#4
String tuning		0.3	0.4	0.8	0.9	0.2	—
Amplitude ratios, higher string freq.	0.4			0.35	1.0		
Amplitude ratios, lower string freq.					0.7		
Amplitude ratio, third string freq.							

good coupling between these strings and the resonance between them. This is important from the point of view of the melodic structures and playing techniques.

When comparing the population of body resonances within the tuning range with the number of strings, the kannels AP1 (six strings, four body resonances) and AH19 (ten strings, seven body resonances) fare slightly better than the kokle KD9 (13 strings, five body resonances, although one of these is likely to involve more than one normal mode). Yet on the basis of sound quality and volume, KD9 is superior in the range from its low keynote on up. This is partly explained by improved results on coupling the strings and body resonances, for the kokle KD9, as is evident in Table 7.1. This may arise from its relatively light construction.

Another method for investigating coupling of strings to the body is by exciting each string directly. With steel strings, excitation can be provided by a magnetic coil close to each string. This was tried with the kannel AP1. For several reasons, the results were not useful. The affecting factors involved the inability to precisely reproduce exciting positions at various strings plus variations in ferromagnetic properties among batches of steel string materials. For these reasons, this approach was not pursued further.

7.5.5 Experiments with Distribution of Sound Holes

For a long time, we wondered why the Baltic psalteries that were reasonably accurate reproductions of museum specimens, with distributed sound holes, performed better than modernized mass-produced versions that had a single sound hole, instead of the old-style, more distributed pattern. This suggested that the old masters had it right to begin with.

Perhaps the oldest example of a plucked string instrument with distributed sound holes is the lyre found near Trossingen, in southwestern Germany, and dated to approximately AD 580 (Theune-Grosskopf 2006). Its soundboard had eight small holes in two rows of four, placed so the bridge might fit between the two rows, plus two more holes located near the tips of the arms. (See Sect. 7.5.1 regarding possible evolution of the Baltic psaltery from the lyre.) Our experiments with distribution of sound holes involved the kannel AP1. This Saaremaa-style kannel has a central rosette and 11 small (4.6-mm-diam) holes closer to its ends. It is shown at left in Fig. 7.2.

The Helmholtz resonance is the lowest mode of the air cavity when the bottom, sides, and sound board are immobilized, as can be achieved by burying the instrument in sand, except at the sound holes. In turn, the Helmholtz resonance influences the lower body resonances. The method of calculating the Helmholtz resonance was extended to include several sound holes of unequal diameters, and also sound hole diameters close to the sound board thickness (Peekna and Rossing 2005a). For the kannel AP1, eliminating three-fourths of the central rosette was predicted to produce the same downward frequency shift as eliminating the 11 small holes.

The sound of the instrument was observed when (a) three-fourths of the central rosette was covered by light and sufficiently stiff material, and (b) the 11

4.6-mm-diam holes were covered and the central rosette was left open. In both cases, the most noticeable feature was that the G4 string still sounded good, but the A4 string no longer did, which is an expected result of the downward shift of the body resonance that is between the G4 and A4 strings when all the holes are open.

However, a significant difference between cases (a) and (b) was noticed in the sound of the higher strings. This difference was more noticeable to a listener free to move around than it was to the player. This difference in perception was probably due to the fact that the higher three resonances in the tuning range have a node line traversing the sound board (see Fig. 7.4). Such modes tend to radiate more in directions parallel to the sound board and perpendicular to the node line, rather than perpendicular to the sound board. In case (a) with three-fourths of the central rosette covered, there was not much difference in the sound of the higher four strings, but in case (b), with the 11 small holes covered, there was a definite deterioration of sound quality and volume in the range of the higher strings.

Subsequent observation of vibrational modes by electronic TV holography revealed no significant shift of the higher three resonances (see Fig. 7.4) in case (a). In case (b), with the 11 small holes covered, the two highest body resonances likewise did not shift significantly, but the resonance shown near B4 in Fig. 7.4 now shifted close to the A4. This shift is probably due to the mass of the air inside the cavity as it moves longitudinally (analogous to water sloshing in a bathtub). On the other hand, distributed sound holes largely neutralize the effect of the air mass moving in this way, thus raising the lowest mode with a node line crossing the sound board to near the B4 string, where it does best.

7.5.6 Some Conclusions and Applications

It is beneficial to have a high population of body resonances within the tuning range of the instrument. The complex asymmetric shape of the carved Baltic psaltery may help. Designers and makers of other instruments, please note that too much symmetry, though pleasing to the eye, does not always benefit the sound. Violins break symmetry by the eccentric sound post and the bass bar (Chap. 13). Almost all guitars have asymmetric internal bracing of the soundboard (Chap. 3).

Coupling of the strings to the body resonances was also found to be important. Light construction, which minimizes mass especially around the main sound box, was found to facilitate this, as was indicated by the results on the outstanding kokle KD9 and confirmed by investigating another outstanding kokle IJ1, made by Ieva Sijats Johnson, Zionsville, Indiana, USA. In particular, this Baltic psaltery is the first we have investigated that shows some degree of coupling of *all* its strings to its body resonances (Peekna and Rossing 2005c).

Wood materials are notorious for their irreproducibility. Therefore, how can we locate the lower body resonances at their optimum locations in a reliable manner? Adjustment of the sound hole areas provides an opportunity to customize each

instrument, regardless of the variability inherent in wood properties. The higher is the total sound hole area, the higher is the lowest body resonances.

In one case, we started with a 12-string kannel designed and built by Ain Haas, AH25. We started with no sound holes, and gradually included them toward increased total sound hole area. Results were evaluated mostly by listening tests, but also filled in by TV holography at strategic points. The drilling/enlarging technique involved high rotational speed combined with slow axial feed; it worked well. In contrast to previous findings, the Q -values also helped in interpreting the results from these trials. An optimum in both sound quality and volume was attained.

In another case, we started with an instrument having excessive sound hole area, instrument AH31. Working downward, by covering sound holes by light and sufficiently stiff material, a perceived optimum in sound quality and volume was likewise reached. (Both findings are documented in Peekna and Rossing 2005b). The beneficial effect of distributed sound holes suggests possible extension to other string instruments. This has yet to be tested.

Further approaches would attempt to combine all positive aspects, also including light construction of the sound box. An antique carved kannel specimen in the Museum of Theatre and Music in Tallinn, Estonia (*Soelaane kannel*, 8121, TMM Mi2, dated 1830) was made available for detailed inspection. This instrument had undergone an accident that had broken its bottom. The resulting hole in its bottom gave the opportunity to reach inside to examine thickness variations.

The results were interesting. The thickness of the sides of the sound box at its very top was considerable, about 7–8 mm, and tapered progressively downward, until it reached no more than 2 mm at parts of the bottom (part of which broke and is lost). It is as if this instrument were designed by a modern engineer who set out to retain the most wood in regions of highest stress, while minimizing total weight.

7.5.7 *Features of Proposed New Traditional-Style Designs*

An ideal instrument would have nearly constant stress in its strings. This means that, for an octave increase, the string length should be cut in half. Such was very nearly the case in the kannels AP1, AP2, and AH19, and the kokle IJ1 (plus several others). Experience has suggested that absolute levels of string stress would be in the range 800–1,200 MPa for steel strings, and in the range 400–600 MPa for strings of beryllium copper.

To minimize mass, the sound box of this instrument would have downward-tapering sides and a thin bottom. Hollowing the inside with modern power tools suggests keeping the inside of the sides vertical (i.e., perpendicular to the bottom). Their outside surfaces can easily be cut down near the bottom by planing.

The Saaremaa Island (Estonia) style of sound hole distribution appears optimal for Baltic psalteries of similar design. This involves a single larger hole or rosette at the center of the sound board, plus smaller holes scattered elsewhere. Centering the main sound hole (or rosette) maximizes the radiating efficiency of the symmetric mode in

which the air in the sound holes moves in the same direction as the sound board. The scattered smaller holes affect the higher modes of the air cavity in a beneficial way.

The sound hole areas would be customized (for each individual instrument) by starting with low estimates, and gradually enlarging until the symmetric mode in which the air moves in the same direction as the sound board is between the keynote and the note above. This can be done by listening tests.

7.5.8 *A More Radical Design from Finland*

A more radical approach, proposed by some Finnish researchers, retained some traditional features (Penttinen et al. 2005). It introduced a sound board with edges not fixed to the sound box, somewhat similar to floating sound boards in hammered dulcimers (see Chap. 21). The sound board was attached to the bottom at but three points, by three screws. A further evolved instrument of similar design, though no longer of carved construction, made by Jyrkki Pölkki, was demonstrated at the sixth International Baltic Psaltery Conference, Kaustinen, Finland, November 2008. The instrument shown in Fig. 7.7 is played by Pauliina Syrjälä. The construction



Fig. 7.7 A new family of Baltic psalteries

scheme of the instrument can be described as what you would get upon joining two large turtle carapaces, with their inner sides facing toward each other, fastened together at three points by pillars and screws. The sound holes get replaced by an annular space between the two halves, much as in a banjo.

Andres Peekna had the opportunity to try out this instrument, and was impressed by its volume and pleasant timbre, though it fell off somewhat at the highest strings. This may be the beginning of a new, promising family of instruments.

7.6 Zithers

7.6.1 *Zithers Without Fretboard*

A picture is shown in Fig. 7.8 taken from a cover of a recording. The instrument consists of two or more octaves of melody strings, plus grouped bass chords. Each hand of the player had its thumb-plectrum. While the other fingers may have damped out dissonant notes, such was not always the case. Note that in the playing position, the strings are parallel to the player's line of sight.

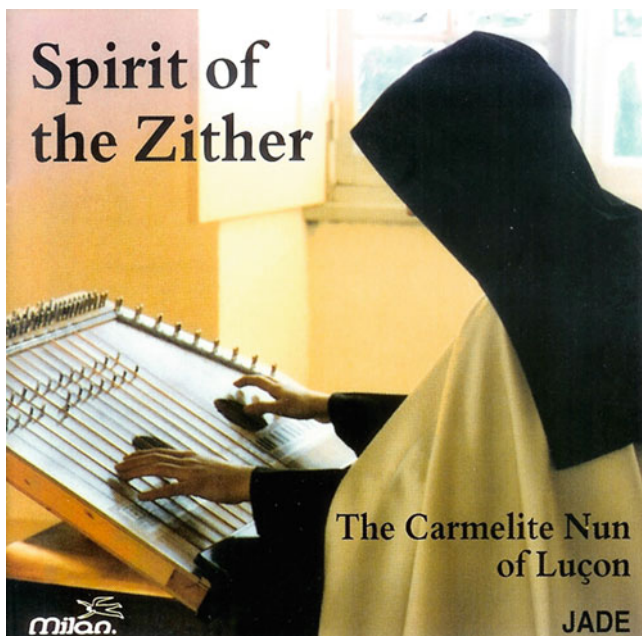


Fig. 7.8 The unfretted zither

7.6.2 Fretted (Alpine) Zithers

A picture is shown in Fig. 7.8 also taken from the cover of a recording. The strings are perpendicular to the player's line of sight. The fretboard is closest to the player, who uses fingers of the left hand on the frets, while a metal thumb-pick on the right thumb plucks the fretted melody strings. The bass strings are plucked with the remaining fingers of the right hand. It takes considerable skill and training to play this instrument, but in the hands of its master, it produces a full sound that fits not only folk melodies but also Renaissance and Baroque compositions very well.



Fig. 7.9 The fretted (Alpine) zither

7.7 Hammered Dulcimers

Hammered dulcimers, discussed in Chap. 21, appear to have descended from the Persian *santur*. In various countries they are known as *cimbalom*, *hackbrett*, *yang-qin*, *khim*, *antouri*, *santoor*, *salterio*, *yanggeum*, etc. In Hungary, the large concert cimbalom, comparable in range (and weight) to a small piano, is used in classical orchestral music as well as in folk music. The hammered dulcimer, while a versatile and fine-sounding instrument, generally has the disadvantage of no provision for damping. Thus, its designers cannot afford to build in a long ring (sustain).

7.8 Modernized Baltic Psalteries

7.8.1 Diatonically Tuned Versions

In Estonia, the transition to box-like construction began ca. 1,800. This had the advantage of permitting many more strings than was possible with the old carved style. It was influenced by many instruments from Southern and Central Europe. The earliest box kannels in Estonia differed from their carved predecessors in having more melodic range and wrapped bass strings.

Around 1900 in Estonia, grouped bass-accompaniment chords, such as on unfretted zithers, also became widespread. Such an instrument is shown in Fig. 7.10. In some

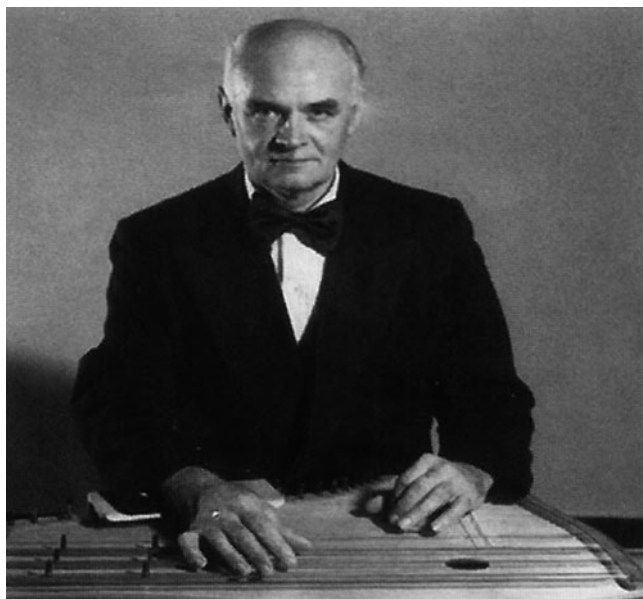


Fig. 7.10 Alfred Kuus, from Southern Estonia, playing the Estonian zither-like kannel

ways, it is almost identical to the unfretted zither. Both have several octaves of melody strings, plus grouped bass-accompaniment chords. A minor difference is that the order of strings in the bass-accompaniment chords is the reverse on these two instruments.

The major differences between these instruments, however, are in playing position and playing technique. Referring back to the unfretted zither (Fig. 7.8), its strings are parallel to the player's line of sight. In Fig. 7.10, they are perpendicular, with the highest strings closest to the player. Also, note that the player, Alfred Kuus (1922–2008) from southern Estonia, is playing the melody strings with his *left* hand, as do many other players from southern Estonia. Kuus attributed this to carryover from playing the old-style carved kannel, in which the right hand controlled the rhythm while the left hand picked many of the melody notes. (See Figs. 7.3 and 7.7)

Another carryover from the old style involves using anchor-fingers on the melody strings. The anchor-fingers are either the little finger, the fourth finger, or the thumb, as the situation may require. During a musical passage, at least one finger maintains contact with its string. This eliminates the need for looking at the strings and fingers, and frees the eyes for looking at and reacting to the dancers, or sheet music.

A newer version of the Estonian zither-like kannel is shown in Fig. 7.11. Note the second line of tuning pegs among the lower octaves of the melody strings. Thus, each note on the lower octaves is actually a double note, not tuned in unison but an octave apart. The effect is a very rich sound, as if two players were playing the same melody an octave apart, in perfect unison. (This kannel was made by its player, Ilmar Tiideberg, who lives in the same village in southern Estonia that Alfred Kuus is from; they were good friends.) In northern Estonia, the modernized kannel is often called *simbel*, which is simply the translation into Estonian of *cimbalom*. More on the influence of the hammered dulcimer is given in the next subsection.

7.8.2 Chromatic Baltic Psalteries

The old diatonic tuning was seen as a serious limitation. Approaches toward chromatic tuning differed widely. In Latvia and Lithuania, *kokles* and *kankles*, respectively, were made with tuning mechanisms at the end of each string, which, by flipping a lever, would induce a sharp or flat. This made it possible to play diatonically in any key, although changes of key in the middle of a tune would become problematic. A picture of such a Latvian kokle is shown in Fig. 7.12. Another problem was relatively short ring (sustain). This may relate to the excess metal mass, which was added at the end of each string.

Current Finnish concert kanteles have tuning-change levers that affect the corresponding note in all octaves at the same time. This makes it possible for a skilled player to switch keys in the middle of a tune. A 39-string concert grand kantele, made by Lovikka Ky, in Ylitornio, Finland, is shown in Fig. 7.13. Each



Fig. 7.11 Ilmar Tiideberg, Southern Estonia, playing his variant of the Estonian zither-like kannel



Fig. 7.12 A chromatic Latvian kokle. Each string has at its tuning-peg end a metal mechanism for half-tone changes



Fig. 7.13 A Finnish concert kantele. Levers for half-tone changes, at lower right, affect all octaves



Fig. 7.14 Chromatic Estonian kannel, with crossed-string construction

string end at the right in the figure is close to its corresponding lever-actuated rod. An abrupt shift in longitudinal position occurs as the next octave is reached. This is reflected in a corresponding shift in the tuning peg locations toward the left in the figure, which otherwise would lie along a smooth curve.

Meanwhile, Väino Maala in Estonia followed a different approach. He borrowed the concept of crossed strings from the hammered dulcimer. For a time, the Tallinn piano factory made such instruments, now discontinued. The instrument shown in Fig. 7.14, played by Kristi Mühling, who teaches at the Estonian Academy of Music and Theatre, was made according to her specifications in Finland. The strings corresponding to the white keys on the piano are positioned high on the player's

right, while the strings corresponding to the black keys on the piano are positioned high on the player's left. This kind of instrument has great versatility and it has proven successful in playing both folk music and classical music. Its disadvantage is that mastering this instrument takes considerable skill and training, which do not automatically carry over from the older instruments in the same line.

Acknowledgments We would like to thank Ain Haas (Indianapolis, IN, USA), Andrejs Jansons (Leonia, NJ, USA), and Ieva Sijats Johnson (Zionsville, IN, USA) for loaning their instruments for this study as well as other comments and contributions. We thank the evolutionary biologist who also makes and plays his own instruments (guslis), Ilya Témkin (New York, NY, USA), for sharing his latest papers with us, plus significant contributions on especially the early history, including string materials. We also thank Henri Penttinen (Helsinki, Finland) for stimulating comments.

References

- Erkut, C., Karjalainen, M., Huang, P., and Välimäki, V. (2002) Acoustical analysis and model-based sound synthesis of the kantele, *Journal of the Acoustical Society of America* **112**, 1681–1691.
- Fletcher, N.H. and Rossing, T.D. (1998) *The Physics of Musical Instruments*. 2nd ed. Springer-Verlag, New York.
- Haas, A. (2001) Intercultural contact and the evolution of the Baltic psaltery, *Journal of Baltic Studies* **32**, 209–250.
- Laitinen, H. and Saha, H. (1988) *A Guide to Five-String Kantele Playing*. Kansanmuusiiikki-instituutti, Kaustinen, Finland.
- Materials Selector 1993. *Materials Engineering*, December 1992. Penton Publishing, Cleveland.
- Peekna, A. (1998) An experiment with beryllium copper strings on a carved kannel, presented at the Second Festival of Traditional Arts, "Jalkala 98," Jalkala Museum (near Zelenogorsk), Russia.
- Peekna, A. (2009) Comparing beryllium copper strings to steel strings on a carved kannel, *Musiikin suunta* (U. of Helsinki, Finland), 3/2009: 54–61.
- Peekna, A. and Rossing, T.D. (March/April 2005a) The acoustics of carved Baltic psalteries, *Acta Acustica/Acoustica* **91**, 269–276.
- Peekna, A. and Rossing, T.D. (August 2005c) Acoustics of Baltic psaltery, another outstanding Latvian kokle, *Proceedings of Forum Acusticum 2005* Budapest (available on CD-ROM): 391–394, Paper No. 442-0.
- Peekna, A. and Rossing, T.D. (May 2005b) Tuning the lower resonances of carved Baltic psalteries by adjusting the areas of the sound holes, presented at the joint meeting of the American Acoustical Society and the Canadian Acoustics Association, Vancouver, BC.
- Penttinen, H., Erkut, C., Pölkki, J., Välimäki, V., and Karjalainen, M. (2005) Design and analysis of a modified kantele with increased loudness, *Acta Acustica/Acoustica* **91**, 261–268.
- Povetkin, V.I. (1989a) Zvonkie struny drevnikh novgorodskikh guslej. *Novgorodsky Istorichesky Sbornik* **3**(13), 51–62.
- Povetkin, V.I. (1989b) O proiskhodzenii guslej s igrovym oknom, v G.A. Fedorov-Davidov, E.A. Rybina, A.S. Khoroshev, *Istoria I kultura drevnerusskogo goroda*. Izd-vo Moskovskogo universiteta: Moskva, pp. 116–127. (English translation: V.I. Povetkin, On the origin of the gusli with the hand-hole. In: G.A. Fedorov-Davidov, E.A. Rybina, and A.S. Khoroshev, eds., *History and Culture of the Ancient Russian City*, Moscow University Press, Moscow.)
- Témkin, I. (2004) Evolution of the Baltic psaltery, a case for phyloorganology, *The Galpin Society Journal* **57**, 219–230.
- Témkin, I. and Eldredge, N. (2007) Phylogenetics and material cultural evolution, *Current Anthropology* **48**(1), 146–153.

- Theune-Grosskopf, B. (2006) Die vollständig erhaltene Leier des 6. Jahrhunderts aus Grab 58 von Trossingen Lkdr. Tuttlingen, Baden-Württemberg, *Germania* **84**, 93–142.
- Thompson, L.K. (2004) *My Kantele Is My Teacher: Basic Info and Instruction for 5/10 String Kanteles*. Brass Window, Stoneham, ME.
- Välimäki, V., Huopaniemi, J., Karjalainen, M., and Jánosy, Z. (2002) Physical modeling of plucked string instruments with application to real-time sound synthesis, *Journal of the Audio Engineering Society* **44**, 331–353.
- von Wunder, C. (1999) Private communication. (Christina von Wunder was a nyckelharpa player in the Estonian instrumental folk music ensemble of Chicago, called Tuuletargad, led by Andres Peekna.)
- Young, W.C. (1989) *Roark's Formulas for Stress and Strain*. 6th ed. McGraw-Hill, New York.

Chapter 8

Harpsichord and Clavichord

Neville H. Fletcher and Carey Beebe

8.1 Introduction

While plucked string instruments such as harps are known to have been used in many parts of the world for several thousand years, the idea of using a keyboard to control the plucking action does not seem to have developed until the late fourteenth century, with an instrument similar to what we now know as the harpsichord. These early keyboard instruments were represented in paintings, carvings, and written descriptions from the time. Most of the development of the harpsichord, however, took place in the sixteenth and seventeenth centuries in Italy, Flanders, Germany, and England.

Italian harpsichords generally had the functional instrument enclosed in a decorative case and had a rather different string scaling from the others, giving them a longer and narrower shape. The harpsichords developed a little later in Flanders, particularly by the Ruckers family, had a single, more solid case and, because of different string scaling, were a little broader in shape. These instruments soon became popular and were exported all over the world. Excellent accounts of this history and of the distinctions between instruments from different countries have been given by Hubbard (1965), Russell (1973), and Kottick (1987, 2003), while both Kottick and Zuckermann (1969) relate these traditions to the harpsichord revival in the second half of the twentieth century.

The clavichord, which is a more personal instrument, has received much less attention, but good historical and practical descriptions are given by Russell (1973), Neupert (1965), Brauchli (1998), and Vermeij (2004). A general technical discussion of harpsichords and clavichords has been given by Fletcher and Rossing (1998) based upon detailed separate studies of the two modern instruments by Fletcher (1977) and Thwaites and Fletcher (1981), and more recently by Kottick et al. (1985, 1991).

N.H. Fletcher (✉)

Research School of Physics and Engineering, Australian
and National University, Canberra, ACT 0200, Australia
e-mail: neville.fletcher@anu.edu.au

In this chapter, we shall be concerned with the design, construction, and acoustic performance of harpsichords and clavichords, rather than their historical development, though the instruments on which we report measurements and design details are modern instruments based upon classic models from the seventeenth and eighteenth centuries. Because there is an important distinction between the sound production mechanisms of harpsichords and clavichords, they will be considered separately.

8.2 The Harpsichord

8.2.1 General Design

A typical harpsichord by a modern maker is shown in Fig. 8.1. As will be discussed later, it may have either one or two keyboards. In many earlier harpsichords, as with other keyboard instruments, the naturals were often covered with dark wood and the chromatic keys with light-colored material such as bone or ivory. Many instrument makers, however, used the current configuration with white naturals and black chromatic keys. As in a modern grand piano, the lid serves the dual purpose of keeping dust out when closed and directing the sound towards the audience when open. The whole case is of wood, and the string tension is supported by a set of wooden braces running between the sides. The pattern of these braces varies according to different national traditions (Kottick 2003). There are also ribs glued to the underside of the thin soundboard to stiffen it, and the bottom of the case is closed with a wooden panel.

In addition to the standard harpsichord where the strings run straight away from the player, there are two smaller versions using the same plucking action. One, known as the virginal, generally had a rectangular case with the strings running nearly parallel to the keyboard, with the bass strings toward the front, but other shapes were also made. Another, known as the spinet, has a triangular case with the strings running obliquely to the keyboard, which is on one of the longer sides, and with the bass strings at the back. Many variants of these instruments were also made, such as a so-called “mother and child” virginal with an inset smaller, or even a rectangular double harpsichord with the two instruments in a single rectangular case and the players facing each other (Kottick 2003).

The basis of harpsichord operation is simply a mechanization of the plucking action of the harp, or perhaps the psaltery, in which there is a set of taut strings, each tuned to the pitch of a different note, clamped rigidly at one end and coupled to a light soundboard at the other, as in almost all string instruments. The function of the soundboard is crucial, since a vibrating string by itself radiates hardly any sound. The questions of importance are thus the material and mounting of the strings, their support and coupling to the soundboard, the mechanics of the keyboard and the plucking action, and the overall design. It is also important to understand what



Fig. 8.1 A modern Flemish harpsichord by Carey Beebe based on classical instruments by the seventeenth-century Antwerp maker Andreas Ruckers. The keyboard compass has been extended down to G_1 in the bass and up to D_6 in the treble. Note the traditional painted decoration on the soundboard, and printed papers lining the case and lid. The small protrusions on the right-hand side (cheek) enable the player to reach around and engage or disengage either of the two sets of jacks by sliding the appropriate register on or off

controls the sound quality and how this can be modified for particular musical purposes (Fletcher 1977).

Figure 8.2 gives more details of the construction of a harpsichord such as that shown in Fig. 8.1. Each metal string is wound around a tuning pin, which is secured in a solid wooden block, the *wrestplank*. The string then runs at an angle past a thin brass pin on a wooden bridge (the *nut*). Before reaching its other end, it passes over a bridge mounted on the soundboard, being held in place by passing at an angle

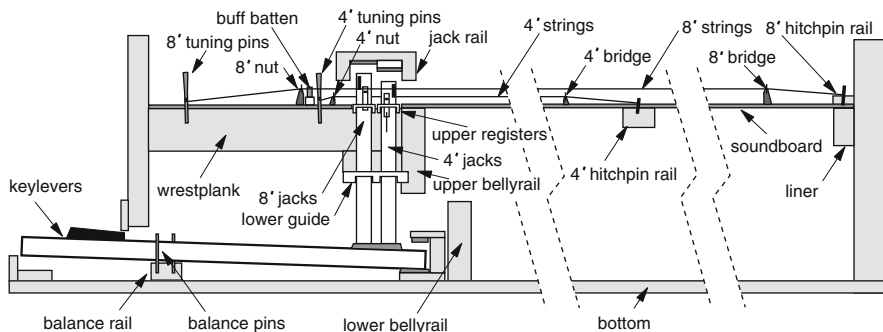


Fig. 8.2 Cross-section of the harpsichord action. Each jack passes through a slotted upper register and a lower guide, and the player can manipulate the upper register to move the whole set of jacks so the quills are just out of range of normal plucking contact with the strings and they do not sound

around another small brass pin. The bridge serves to transfer the force of the vibrating string to the soundboard and cause it to vibrate in sympathy. The *choir* of full-length unison-pitch strings (also called *8-foot* or *8'* strings by analogy with the 8-foot stops of an organ, this being the length of the longest pipe C_2) are then secured to *hitchpins* in the *hitchpin rail* at the inside perimeter of the heavy case, while half-length (*4'*) octave strings are anchored through the soundboard into a curved wooden support on its underside.

As shown in Figs. 8.2 and 8.3, each key has resting upon it a *jack* for each choir. The jack body contains a tongue, so arranged that it can be pivoted backward against a thin spring – originally a hog bristle but these days often a thin wire or plastic monofilament – but cannot pass forward through the jack. Protruding from the tongue is a thin flexible quill, originally made from the spine of a crow or raven feather but now more usually of Delrin or Celcon, which are hard but flexible industrial polymers. Each jack also has a protruding felt damper that normally rests in contact with the wire and so inhibits its vibration. When the key is depressed, this raises the jack so that the damper is lifted off the string and the quill displaces the string until it bends sufficiently for the string to slip off, after which the string vibrates freely. When the player's finger is removed from the key, the jack returns by gravity, the tongue is deflected backward so that the quill flips easily under the string, and the felt damper stifles the vibration so that the sound ceases in a fraction of a second.

The “feel” of the keyboard action depends upon the mass, length, and pivot position of the key, the stiffness of the plucking quill, and the distance of the plucked string from the face of the jack. A short distance here will give a relatively stiff action but strong string excitation, while a greater distance with a longer quill gives a lighter action and a softer sound. Careful adjustments are therefore very important. The jacks for a whole choir of strings are positioned accurately by passing through slots in a narrow wooden register just below the strings and a lower guide running across the instrument above the rear of the keys, as shown in Figs. 8.2 and 8.3. A harpsichord usually has more than one choir of strings, and

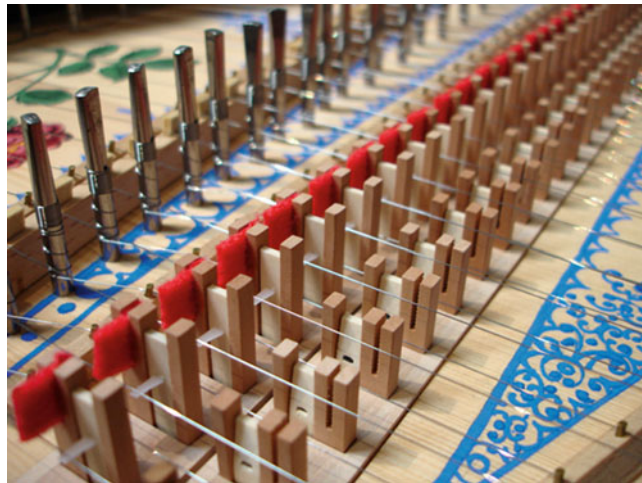


Fig. 8.3 Close-up of the action of the Flemish-style harpsichord shown in Fig. 8.1. In this instrument there are the traditional two choirs of strings, the shorter 4' choir, for which the tuning pins can be seen, being tuned an octave above the other 8' choir, for which the tuning pins are out of sight to the left. Both sets of jacks are visible because the jackrail has been removed. The set of leather pads of the buff stop that can be moved into contact with the 8' strings just beside their nut is visible behind the 4' tuning pins

separate choirs can be activated at will by moving the appropriate upper register a little along its length so that the quills of that set either pluck or pass by the strings. Some modern instruments have a pedal mechanism to accomplish this so that changes can be made rapidly while playing.

8.2.2 *Plucked Strings*

As was discussed in Chap. 2, the fundamental vibration frequency f , and thus the musical pitch of a string, depends upon its length, diameter, and tension, as well as the material from which it is made, the relation being

$$f = \frac{1}{2L} \left(\frac{T}{m} \right)^{1/2} \quad (8.1)$$

where L is the string length, T its tension, and m its mass per unit length. Harpsichord strings differ from those of most other plucked string instruments in being made of metal, usually iron or brass. Because these materials are much heavier than gut or nylon, metal strings must be held at a higher tension for a given length, but because of this greater tension they can be made thinner and still produce the same sound output. Metal strings can sustain this higher tension stress and also retain their

tension more stably than do the softer materials. The other difference is that, while soft materials such as gut or nylon tend to absorb internally the higher frequencies of the string vibration so as to give a “mellow” sound, this does not happen nearly as much for metals, so that the sound can be much “brighter.”

If all the strings were the same diameter and brought to the same tension, then it would be necessary to double their length for each octave decrease of pitch. For the five-octave range of a large harpsichord this would give a length change of a factor of 32, which is not practical, so the strings of the lower octaves are made more nearly of equal length, their diameter increased, and their material changed to make them even heavier. The upper strings are normally made of mild steel, generally referred to as *iron*, and the lower ones of brass, which is more dense but cannot support as much tension. Many instruments use two different brass alloys – red brass, which is 90% copper and 10% zinc for the extreme bass, and yellow brass, which is 70% copper and 30% zinc up into the tenor region. Typical scaling parameters for a modern version of a classical Ruckers harpsichord are shown in Fig. 8.4, while the string composition and diameter variation are shown in Fig. 8.5.

Another major design feature to be considered before we examine mechanical design is the position at which each string is plucked. What is important is not so much the vibration of the string itself, because it radiates only a very small amount of sound directly, but rather the force that the vibrating string applies through the bridge to the soundboard, and this depends greatly on the position of the plucking

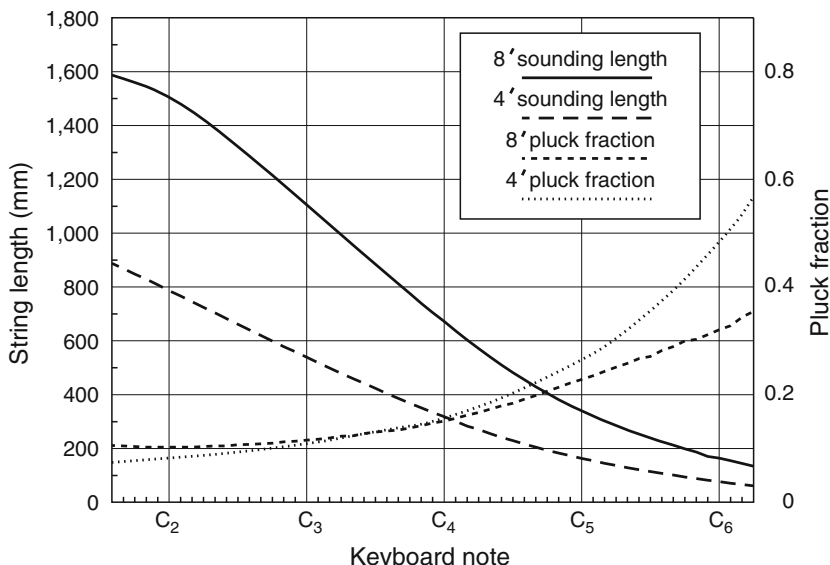


Fig. 8.4 Scaling of (a) string sounding length, (b) plucking position, and (c) string diameter for the 8' and 4' string choirs of the modern-reproduction Ruckers harpsichord of Fig. 8.1. The pluck fraction gives the position of the plucking point from the nut relative to the total sounding length of the string involved

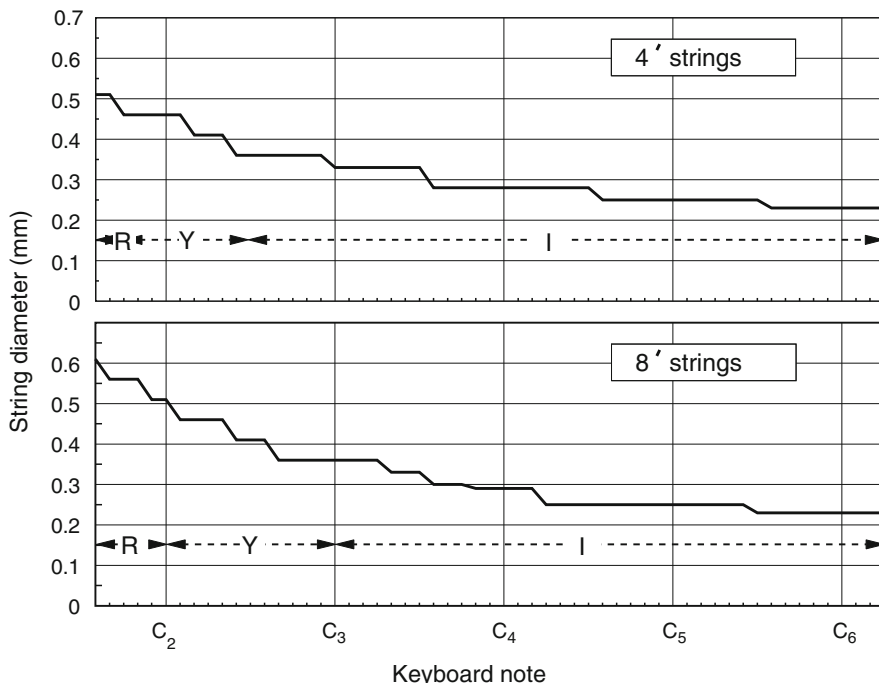


Fig. 8.5 Scaling of string diameter and composition for the 8' and 4' string choirs of the modern-reproduction Ruckers harpsichord of Fig. 8.1. The symbols *R*, *Y*, and *I* denote red brass, yellow brass, and iron, respectively

point. If a string is plucked at a position $1/n$ of its length from one end, the shape with time of this repetitive force on the bridge, which is near the remote end of the string, is a strong downward force for a fraction $1/n$ of a period followed by a much weaker upward force for the remainder of the period, as shown in Fig. 8.6. Harmonics below the n th are all strong; the n th harmonic is missing; and harmonics above the n th decrease in amplitude with increasing frequency, as shown in the lower panels of Fig. 8.6.

The perceived tone quality of the radiated sound depends on the relative amplitudes of the lower harmonics, perhaps up to the eighth, which is three octaves above the fundamental. A string plucked at a moderate fraction of its length from the end, as in (a) and (b) of Fig. 8.6, will sound *mellow* because the amplitudes of its harmonics fall rapidly with increasing frequency, but quite loud because of the high amplitude of the fundamental. A string plucked at a very small fraction of its length from one end, as in (c) and (d), will have a relatively *bright* sound because many harmonics are as prominent as the fundamental, though it will not be as loud because all these amplitudes are lower.

Most harpsichords have more than one choir of strings and these are plucked at different points to take advantage of this effect and give tonal variety to the sound.

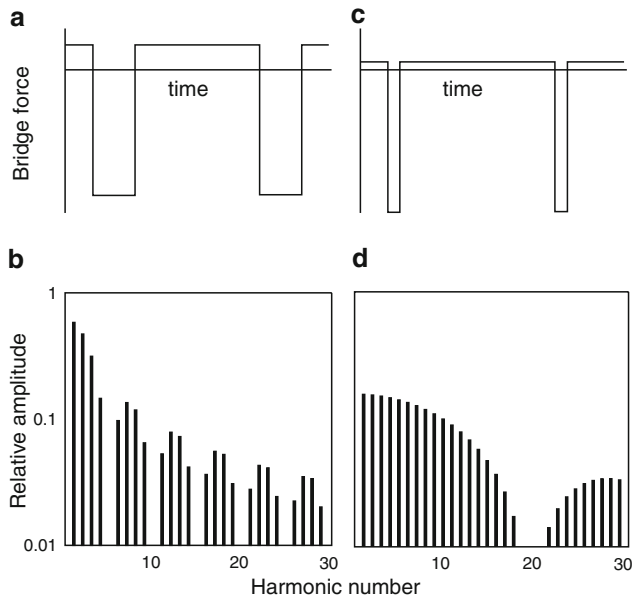


Fig. 8.6 (a) Time evolution of the force acting on the bridge for a string plucked at one-fifth of its length from the nut end. (b) Spectrum of the force exerted on the bridge for this plucking position. (c) Time evolution of the force acting on the bridge for a string plucked one-twentieth of the distance from the nut. (d) Spectrum of the force exerted on the bridge for this plucking position

A choir plucked very close to the nut constitutes a *lute stop* and has a bright and nasal but generally softer sound, because the quill is unable to displace the string by more than a small distance at this point. In a well-designed harpsichord, however, the strings of even a single choir are not all plucked at the same fraction of their length, but over a designed range, as shown in Fig. 8.4, so as to give an appropriate balance to the sound throughout its compass.

8.2.3 Soundboard and Radiation

When a string vibrates, it exerts a force through the bridge on the soundboard causing it to vibrate as well, though with much smaller amplitude than that of the string. It is this vibration of the soundboard that transfers the sound to the air, because it is able to actually displace the air, in contrast to the string which simply moves through it. The exact shape and amplitude of the vibrations of the soundboard are therefore very important in determining the overall sound quality of the instrument, just as they are for the body of a violin. The soundboard itself is usually made from spruce, of which popular varieties for musical instruments are Norway spruce (*Picea abies*) or Engelmann spruce (*Picea engelmannii*).

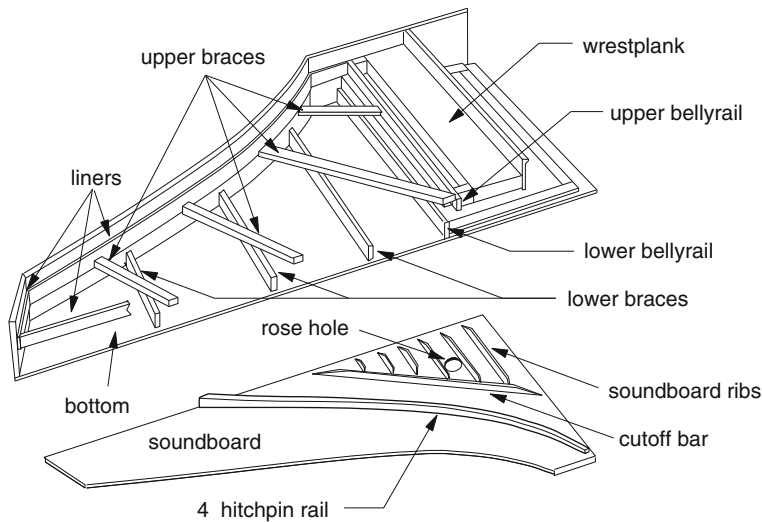


Fig. 8.7 Exploded view of the structure of a typical Flemish harpsichord such as the one studied here. The soundboard is stiffened by wooden ribs glued to its under surface, while the whole case is strengthened by frames at its *top* and *bottom* to support the string tension (from an original by The Paris Workshop)

The soundboard is assembled so that the wood grain runs in the long direction at right angles to the keyboard. It is typically only about 3 mm thick and is thinned slightly in some areas, particularly in the treble corner. The acoustic and vibrational properties of these wood species have been discussed in detail by Bucur (1995), their main advantages relating to low density, high stiffness, and low internal damping. Glued to its underside in a particular pattern are light ribs, as shown in Fig. 8.7, which stiffen the soundboard and raise the frequencies of some of its resonances. The rib positions also influence the shapes of the vibrational modes of the soundboard and thus affect its radiation efficiency. Mounted in a hole cut in the soundboard near its bass end is a small decorated emblem or *rose*. Its main function is an identification of the maker, but it also combines with the larger spaces above the keys to provide an acoustic vent to the air cavity under the soundboard, with effects to be described below.

The shapes of the vibrational modes of the soundboard are determined by its overall shape and by its stiffness distribution, which is strongly influenced by grain direction, wood being 10–20 times as stiff along the grain as it is across, as well as by the ribs and bridges attached to it. In its lowest mode, the soundboard simply vibrates in and out like the lowest mode of a drumhead, while at higher frequencies the mode shapes divide it into progressively smaller areas, each one of which vibrates in anti-phase to its neighbors. Sketches of some of these mode shapes have been given by Savage et al. (1992).

The impedance of the air between the soundboard and the bottom of the case is also important. At low frequencies it is simply compressed and flows to some extent out

through the rose hole and the spaces above the keys, either in-phase or out-of-phase with the overall motion of the soundboard, thus modifying the resonance frequencies and splitting the low-frequency drumhead resonance into two. The lower of these two resonances, with the enclosed air flowing out through the apertures while the soundboard moves inwards, is the lowest resonance of the whole instrument, typically near 30 Hz, and determines the *fullness* of its bass response, while the upper resonance is important at a slightly higher frequency. At higher frequencies, where the largest dimension of the cavity is comparable to or greater than the sound wavelength, there can be resonances within the air itself and these will couple to the higher modes of the soundboard. Of course, all these resonances overlap to some extent because of vibrational and acoustic losses. The whole situation is very complicated, and a detailed study by Savage et al. (1992) identifies 36 vibrational modes below 600 Hz. There will be many more above this frequency.

If the design of the soundboard and case has been well developed, then these resonances will be fairly evenly distributed over the audible frequency range, so that there are no very pronounced maxima or minima in the sound output. The resonant response of the soundboard does, however, influence the overall sound quality of the harpsichord and varies from one maker to another. As a general rule, a large harpsichord can be expected to have a fuller bass sound than a small one, simply because large structures generally have resonances of lower frequency and radiate them more efficiently than do smaller structures. Finally, the nature of the wood used to make the soundboard is also important, since its internal damping influences both the general shape of the response at high frequencies and also the prominence of the resonances (Kottick et al. 1991).

8.2.4 Acoustic Balance

Sound balance is an important feature of the sound of a musical instrument. This has three major components: initial loudness, decay time, and tonal quality. Because music written specially for an available instrument of the period is likely to explore its full compass and resources, it is desirable that the initial loudness of all the notes should be nearly the same. On instruments such as the pianoforte the performer can adjust the relative loudness of individual notes, but this is not possible on the harpsichord, so uniform loudness should be built into the instrument design. This is a matter of case and soundboard design, string length and diameter, and pluck mechanics as discussed above. Long experience allowed instrument makers to develop appropriate designs for all these things well before the advent of acoustic analysis, and the result is that their harpsichords, along with good modern instruments, have nearly constant initial loudness across the whole four and a half octave compass from G₁ to D₆. For the Ruckers instrument of Fig. 8.1, the measured sound pressure level at a distance of 2 m for a rapidly repeated short scale

passage was 70 ± 5 dB(A) over the whole compass for the 8' string choir and 68 ± 3 dB(A) for the 4' choir. When combined, the level was 72 ± 5 dB(A).

To evaluate these figures we should note that the “A” means the reference level has been adjusted over the whole frequency range to approximately match the sensitivity of human hearing. For comparison, we should also note that measurements of similar scale-patterns played *mezzoforte* on a piano give a level of about 80 dB(A), but the pianist has control over at least the range from 70 to 90 dB(A). These figures will be compared with those for the clavichord later on.

The second important feature of sound quality is the decay time of the sound when a note is played and the key is held down. This time depends on the amount of energy stored in the string by its initial displacement and the rate at which this energy is dissipated. A set of measurements on the modern-reproduction Ruckers harpsichord is shown in Fig. 8.8. The decay time decreases steadily with rising pitch, the total variation being more than a factor of two over the keyboard compass in the case of the 8' choir and nearly a factor of four in the case of the 4' choir. The slope is very close to $(1/\text{frequency})^{0.25}$ for the 8' choir and has the much steeper slope $(1/\text{frequency})^{0.45}$ for the 4' choir. Such a result is appropriate, because low notes in music are generally played more slowly than high notes, and a longer decay time is generally desirable to give “fullness” to the sound.

A note on the harpsichord, or any other *acoustic* musical instrument, is, however, not simply a copy of a lower note transformed to a higher frequency. This is because

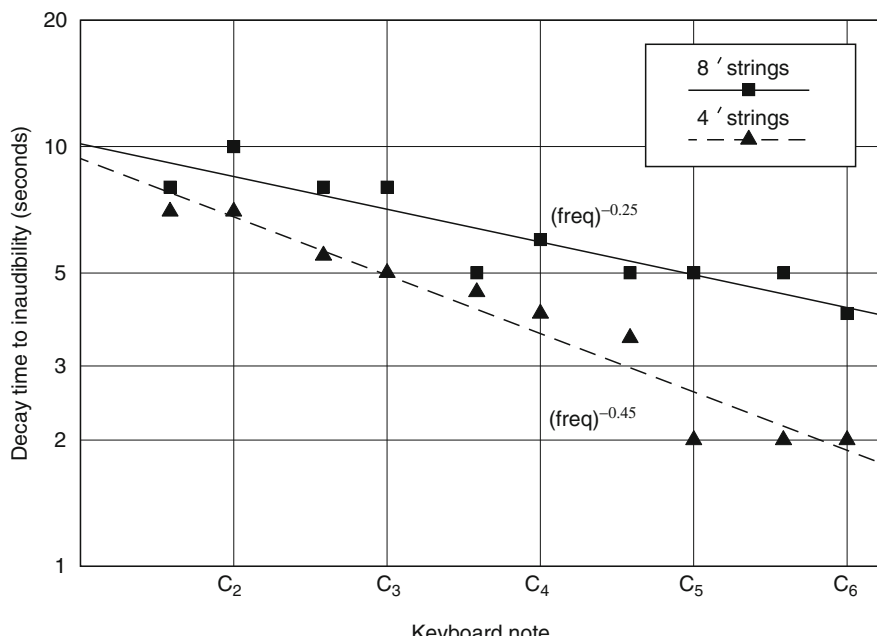


Fig. 8.8 Measured decay time to inaudibility as a function of pitch for a selection of notes played on the reproduction Ruckers instrument of Fig. 8.1

of the difference in string diameter, plucking point, soundboard response, and radiation efficiency. These features contribute to the complex musical nature of the sound compared with the *synthetic* sound of many simple electronic imitations.

In considering the design of harpsichords and other string instruments, it is important to realize that only a few percent of the energy stored in the vibrating string is radiated as sound. Most of it is dissipated in viscous losses from the motion of the string through the air and in losses to the material of the soundboard. To maximize the radiated sound level, it is important to have a soundboard that is as large as possible and to ensure that it is made of a material and in a way that minimizes internal losses. Most aspects of the design and construction are now a matter of tradition, but modern studies of the acoustics of wood (Bucur 1995) can reveal why the decisions that were made in the past are essentially correct.

The third aspect of tone quality is the tonal balance over the entire compass of the instrument. In a four and a half octave harpsichord such as the one examined here, the fundamental frequency of the 8' choir ranges from about 46 Hz in the bass to about 1.1 kHz in the treble if the instrument is tuned to standard *Baroque* pitch $A_4 = 415$ Hz. Remembering that human hearing sensitivity decreases below about 500 Hz, the bass notes might be expected to sound very weak. This is corrected by the fact that the lower strings have a much shorter fractional plucking length than the higher strings, as shown in Fig. 8.4, and thus have much greater harmonic development up to about the tenth harmonic than do the higher strings. At the other end of the range, the extreme treble strings are plucked proportionally much further from the end and so have much less harmonic development. This tends to equalize the subjective loudness of the sound and to give a balanced quality over the whole compass.

8.2.5 *Design Extensions*

The discussion above has been concerned with basic aspects of harpsichord design and operation, but there are several extensions to the basic instrument that are important. Most of these aim to give the performer greater influence over the nature of the sound and to provide subtle variants of the basic tone quality. Some of these have been mentioned before, but it is helpful to consider them together.

A simple addition found on many instruments consists of a batten with a set of small felt or leather pads glued to its upper surface, which is able to slide against the 8' nut as shown in Figs. 8.2 and 8.3. This is known as the *buff stop*. The effect of the pads is to damp dramatically the upper harmonics of the string vibration, and thus of the radiated sound, to produce a very mellow quality such as can be expected from the gut strings of an early lute or guitar. This addition is rare in Italian harpsichords, but is found in most other instruments.

A development that has already been displayed in Fig. 8.3 and discussed above is the incorporation of a second (4') choir of strings tuned an octave above the main unison or 8' choir. Some very large modern harpsichords have gone even further in

this direction and incorporate a sub-octave 16' string choir, something few original instruments had. Again, because it is not practical to double the string length, the solution is to use nearly the same lengths and tensions as the standard 8' strings, but to double the string diameter so as to increase the mass per unit string length m by a factor of four, thus halving the frequency, as given by (8.1). Because of limits to the size of the soundboard, the bass strings of this set do not have a strong fundamental, but provide extra harmonics in between all those of the 8' choir. This gives an overall rich and almost “orchestral” sound that can be impressive in appropriate musical compositions. Incorporation of a 16' string set, however, causes other problems and it is unusual now even on modern instruments.

Considerable emphasis has been placed in the discussion upon the importance of choice of plucking point in determining the harmonic development and thus the subjective brightness of the sound. The first and simplest way to accomplish this is to have a second choir of strings, also at unison pitch but plucked closer to the nut so as to give a sound that is not so loud but has much more harmonic development, as illustrated in Fig. 8.6. The choirs would then be described according to their plucking position, for example, “front 8-foot” plucking closest to the player and “back 8-foot” closer to the middle of the instrument. An additional set plucking very close to the nut would be called the lute stop, as already discussed.

While it is possible to have the additional string choirs in these examples plucked by a set of jacks operated from the same keyboard as the standard set and to turn each set on or off by moving the appropriate register, this creates difficulties for the performer if it is desired, as it often is, to have short interpolated phrases with different sound quality. The solution is to have a second keyboard, located just above and behind the first as in an organ, which plucks the second set of strings. It is then easy for the performer to shift hands from one keyboard to the other to produce tonal contrast effects. The builder is not, however, limited to one set of strings for each keyboard but can have several sets in much the same way as is done for the stops of a pipe organ. The instrument then becomes very versatile and tonally flexible. Some quite early Flemish instruments were made with two keyboards, but surprisingly in those days the aim was not to produce different tone colors but rather to transpose the notes upward by a perfect fourth.

If an additional keyboard can be considered, then why not a pedalboard as well? Indeed, some classical harpsichords show signs of having had this feature, probably largely because it then made them good substitutes for a pipe organ, as far as practice was concerned, and of a size and cost that organists could reasonably manage for their homes. The pedalboard could operate either with a *pull-down* mechanism for the keyboard notes, or with its own set of strings. This addition does not appear to have carried over to the present day, with few makers interested in such complexities, but such instruments were built in the middle of the twentieth century.

In addition to these relatively minor but important additions to the standard simple harpsichord, there have been some much more adventurous developments. Some of these simply involved changing the overall shape of the instrument. The spinet has already been mentioned and also the virginal. These were, for the most part, simply adaptations to make the instrument fit more easily into a small living room, but some

were much more adventurous. Chief among these were a combination of a harpsichord and a fortepiano, often with separate keyboards, and the claviorganum, which was a combination of a harpsichord and a pipe organ. This latter instrument was probably never really popular because of the tuning problems when combining strings with pipes: as the temperature rises, the organ goes sharp but the harpsichord strings go flat. Detailed specifications of some of these instruments from the 1500s and 1700s are given by Hubbard (1965) and by Kottick (2003).

8.3 The Clavichord

8.3.1 General Design

The clavichord is sometimes seen as a very close relation of the harpsichord, partly because they developed over the same period and by the late eighteenth century most musicians probably had at least one of each instrument in their homes, but the basic acoustics of the two instruments is really very different. General descriptions of the clavichord have been given by Russell (1973), Neupert (1965), and Brauchli (1998), while the first technical study of which we are aware is that by Thwaites and Fletcher (1981). The surviving instruments of the Bavarian clavichord maker Christian Hubert have been the subject of a detailed study by Vermeij (2004).

Figure 8.9 shows a typical double-fretted clavichord, the meaning of the term *fretted* to be explained presently. It is a quite small instrument, only about a meter long, and is designed to be placed on a table for playing. The best modern versions



Fig. 8.9 Modern version of a typical double-fretted clavichord made in the eighteenth century by the Bavarian maker Christian Hubert. An unfretted instrument looks very similar but is usually larger, while a triple-fretted instrument is usually smaller

are all essentially copies of instruments built more than 200 years ago. The keyboard compass is typically just over four octaves from C₂ to D₆. The reason the clavichord has not developed into a concert instrument is that the sound it produces is very quiet – typically less than about 50 dB(A) at 2 m – so that it is best used for personal performances or, at most, with a solo instrument such as the recorder.

The brass strings of this clavichord, of which there are 74 arranged as 37 pairs, run at a small angle to the long spine side of the case where they are fixed to rigid hitchpins. The strings run over a wooden bridge mounted on a thin soundboard, as shown in Fig. 8.10, to their termination at individual tuning pins. The soundboard itself, as shown in Fig. 8.9, covers less than one-third of the area of the instrument and is vented through one or more small apertures, called the *mouseholes*, cut in the bellyrail. The combination of enclosed volume and aperture dimensions influences the frequency of the lowest or Helmholtz resonance of the cavity, which is typically around 150 Hz. The effect of this resonance is to enhance the lower frequencies produced by the string vibrations in the same way as does the body cavity of a cello, vented through the f-holes, or the vented box of a bass loudspeaker. As with the harpsichord soundboard discussed before, there are complex resonances of even the simple clavichord soundboard and these are coupled to sound waves in the air enclosed in the cavity. More details are given in the references listed (Brauchli 1998; Fletcher and Rossing 1998; Thwaites and Fletcher 1981). The fact that each note is produced by a pair of strings tuned to the same pitch obviously increases the loudness, but has another effect that will be discussed presently.

We come now to the meaning of the term fretted in describing the clavichord. Because the vibrating length of the string is determined by the distance between the



Fig. 8.10 Detail of action of the reproduction Hubert clavichord. Each key is pivoted on the balance rail and, when it is depressed, the brass tangent at its distal end strikes the pair of strings corresponding to that note. The listing cloth is clearly visible

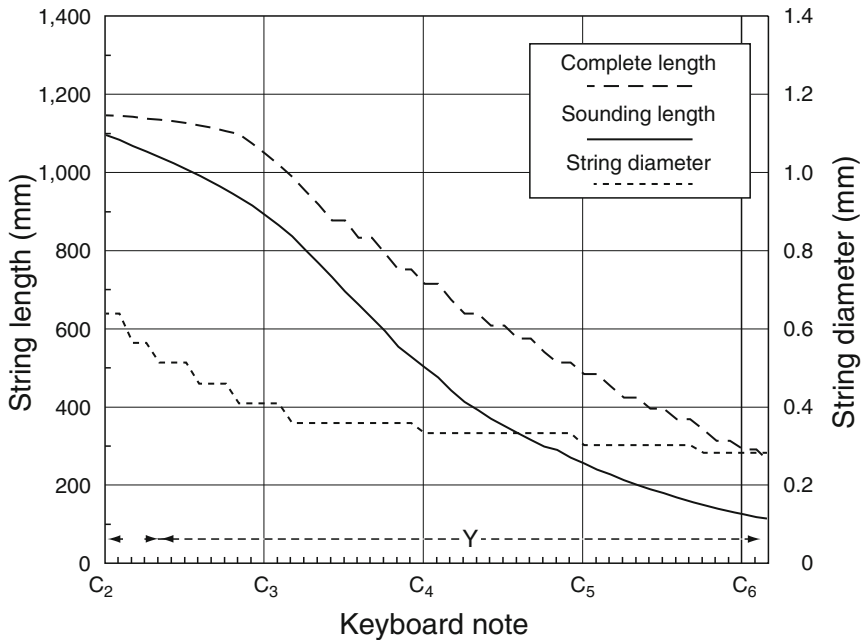


Fig. 8.11 Measured string lengths and diameters for the reproduction classical double-fretted clavichord of Fig. 8.9. Strings from C₂ to F#₂ are of red brass (R) and all other strings are of yellow brass (Y)

tangent impact point and the bridge, it is clearly possible to play more than one note on a given pair of strings, provided this is not attempted simultaneously. This multiple use of strings is termed fretting; it has essentially no effect on performance provided that note pairs that are never used simultaneously, such as C and C#, are combined on the same string pair. This results in a small and economical instrument, which can be made even smaller by triple-fretting the strings. Not all clavichords use this design technique, however, and many larger unfretted instruments were made with independent string pairs for each note. Such instruments have a larger soundboard, thus often leading to a stronger bass sound.

Figure 8.11 gives details of string lengths and diameters for a modern version designed by D. Jacques Way and Marc Ducornet after an original double-fretted clavichord by the Bavarian maker Christian Gottlob Hubert. The lowest seven pairs of strings, covering the range from C₂ to F#₂, are unfretted and made from red brass, though the original probably used over-wrapped strings, while the higher strings are yellow brass and fretted from about an octave above this for the remainder of the compass. The *overall length* is the total length between the hitchpin at the left end of the instrument, including the damped length between the pin and the impact point of the tangent, and the bridge, while the “sounding length” is just that from the impact point of the tangent to the bridge.

8.3.2 String Excitation in the Clavichord

The action of a clavichord is very different from that of a harpsichord, although the key lever is mounted on a pinned balance rail just as shown in Fig. 8.2. Each key lever has near its distal end a “tangent” made from a thin brass plate and so arranged that it strikes a pair of strings towards one end, as shown in Fig. 8.10. Importantly, the tangent then remains in contact with the string, holding it in a slightly displaced position, until the key is released. The tangent impact sets the string into vibration, but only the longer section of the string continues to vibrate because the shorter section is damped by the *listing cloth* twined between the strings. This is very different from the fortepiano or pianoforte action, in which a relatively heavy felt-covered hammer strikes and then quickly rebounds from the string which is firmly mounted at both its ends. The excitation of the clavichord string is much less than that of a string hit by a sharp hammer because the excitation consists simply of displacing one end of the string over a time of about 10 ms and holding it in the displaced position. Relatively little energy is transferred to the string during this process compared with that in a strike and rebound of the piano, or the pluck of the harpsichord.

Unlike the harpsichord, this action gives the clavichord player direct dynamic control over the sound by varying the speed at which the key strikes the string and the force exerted while the sound is sustained. Because of these variables, the actual string excitation in a clavichord is more difficult to analyze than the vibration of a harpsichord string. The displacement of 1–2 mm caused by the key action typically takes about 10 ms, during which time a displacement wave has been able to travel some distance along the string. The displacement of the tangent then becomes steady and the string vibrates under the influence of its initial displacement and velocity distribution. Analysis shows that the force on the bridge typically has a spectrum that falls fairly smoothly at about 8 dB/octave (Thwaites and Fletcher 1981). Because the displacement of the string by the tangent increases its tension by a small amount, the player can even create a slight pitch vibrato effect, called *Bebung* in German, by varying the finger force exerted on the key.

The loudness and tone quality of the clavichord sound depends greatly on soundboard material and thickness, as well as on its size and the dimensions of the mousehole(s). The sound level at a 2-m distance for the reproduction Hubert instrument is a very quiet 50 dB(A), fairly uniformly across the compass. The decay time to inaudibility, which is also important for sound quality, is around 4 s over most of the compass, but decreases to less than 3 s in the top octave, measured at the same 2-m distance in a fairly quiet environment. Very similar measurements were earlier reported for a modern version of a triple-fretted instrument (Thwaites and Fletcher 1981).

The fact that each note is produced by two strings tuned to the same pitch has a very subtle effect that was carried on to the pianoforte. Vibration of the two strings is not independent, because they both run over the bridge that is not completely rigid. While the strings are nominally tuned to the same frequency and struck in the

same way, there are always slight differences, and the slight bridge motion tends to couple the vibrations of the two strings, adding further complications (Weinreich 1977). When the strings are moving in the same direction, the force on the bridge is large and the radiated sound is greatest, but it decays quickly. When the strings vibrate in opposite directions, the force on the bridge is small and the sound is quiet, but it decays slowly, taking as long as 4 s to reach inaudibility. The total sound of the instrument therefore has a relatively loud onset, which decays quickly to a more sustained quieter sound, the total effect to a listener at close range being of clarity combined with mellowness.

8.4 Keyboard Tuning

There are two important features of keyboard tuning. The first is the overall pitch, which is generally specified by giving the frequency of A₄, and the frequencies of the individual notes within an octave span. Most modern musical instruments are tuned to standard pitch of A₄ = 440 Hz, though there are minor variations such as 442 Hz for the Boston Symphony Orchestra. In earlier times, however, there was no such standardization, and today we regard A392 as French Baroque pitch, A415 as Baroque pitch, A430 as the Classical pitch used by Mozart, and A466 as Renaissance pitch. (These nominal frequencies have, however, with the exception of A430, been adjusted slightly to conform to notes of the normal A440 scale so that they can be reached by simple transposition.) Changes in overall pitch can also have the effect of changing the perceived tone quality of a performance because of the slightly different prominence of harmonics and also the slightly different decay times. Both the instruments examined in detail above were tuned to A415.

The second feature concerns the exact tuning of notes within the octave. Most musical instruments allow the performer at least some control over the pitch of the individual note being played, but this is not true of keyboard instruments. It is therefore important that the strings of the instrument be tuned to exactly the desired frequencies, and this raises important problems. Each note produced by a musical instrument has a fundamental accompanied by a whole set of overtones of higher frequencies. In a stringed instrument, provided the strings are very thin and tightened to a high tension and that the supports at each end of the string are very nearly rigid, the overtone frequencies will be almost exact integer multiples of the frequency of the fundamental, and are then called *harmonics* – the *n*th harmonic having frequency *n* times that of the fundamental. (It should be noted that scientific and musical terminologies are in disagreement here, since musicians often confusingly refer to the first overtone, which has frequency twice that of the fundamental, as the *first harmonic*, whereas it is scientifically the second. In this chapter we adhere to the scientific terminology.)

The tuning of the keyboard is required to produce combinations of notes that sound pleasant, rather than rough. If one of the harmonics of the first note has a frequency very close to that of some harmonic of the second note, then this will

produce fluctuating *beats* in the sound. A very slow beat is not unpleasant, but rapid beats make the interval sound rough. The aim therefore is to tune the notes of the keyboard to eliminate fast beats as much as possible. This initially resulted in the classic “Pythagorean” tuning, in which octaves were tuned to the frequency ratio 2:1 and perfect fifths to the similarly acoustically pure ratio 3:2. It might appear to be possible to tune the whole keyboard by following the “cycle of fifths” C, G, D, . . . , F, C, but unfortunately the final C (really B \sharp) is substantially sharper than would be found by stepping up pure octaves from the initial C, which is a discrepancy known as the *Pythagorean comma*. This is clear from arithmetic, because $3/2$ raised to the power of 12 to complete the cycle of fifths is certainly not an integer, which it needs to be to match 2 raised to the power of 7, which brings one to the same note reached by octave intervals. The error, allowing for octave transpositions, is $(3/2)^{19} - 1$, which is about 1.4%, or about a quarter of a semitone, because one semitone is a frequency change of about 5.9%.

There is, however, another problem that arose when musicians began to use major thirds in their compositions several centuries ago. A *just* major third has a frequency ratio 5/4, which is smooth and pleasant. A Pythagorean major third, however, tuned for example by the sequence of four perfectly tuned fifths CGDAE and a two-octave jump downward, has a frequency ratio 81:64, which is far from being simple, so that the Pythagorean major third has a rather different and somewhat “sharp” sound. This discrepancy between a Pythagorean major third and the just ratio of 5/4 is called the *syntonic comma* and is a frequency difference of about 1.25%, or about a fifth of a semitone.

Is it possible to tune a keyboard exactly? Unfortunately arithmetic defeats us once again, and it is not possible to devise a tuning with both exact fifths and thirds in all keys when there are only 12 distinct pitches available in the keyboard octave. A once-popular tuning called *quarter-comma meantone* tunes all the fifths flat by a quarter of the syntonic comma, which is not very much. This gives perfectly in-tune thirds in several useful keys, but several keys are completely unusable and there are no enharmonic equivalents available – each note has only one name, G-sharp or A-flat, for example, and must be tuned as such (Kottick 1987; Haynes 2002; Barbour 1951; Lubenow and Meyn 2007; Sethares 1998).

While meantone tunings were commonly used from the beginning of the sixteenth through to the middle of the nineteenth century, some innovative musicians or theoreticians devised better compromises, sometimes known now as *well temperaments*, which allowed music to be played in any key (Barbour 1951; Lubenow and Meyn 2007; Sethares 1998). Two of the most successful of these were Werckmeister III from the early 1700s and the later Kirnberger III of 1771, Kirnberger having studied under Bach. Bach probably used a slightly different temperament of his own for his famous “48 Preludes and Fugues” of *Das wohltemperirte Clavier* and perhaps encoded details on the title page (Lubenow and Meyn 2007), but in each of these temperaments all keys sound pleasant but subtly different.

The modern solution to all these dilemmas is the total compromise known as equal temperament (Sethares 1998) in which all keys sound equally out of tune. In this temperament all the fifths are tuned flat by about 0.1% to eliminate the

Pythagorean comma, so that all semitone intervals are exactly equal, with frequency ratio $2^{1/12}$ or about 1.0595. The major thirds are still considerably sharp, with a ratio about 1.26 instead of 1.25, which is about one-sixth of a semitone mistuning, but all keys are now exactly equivalent, which is a great advantage for more modern music. Equal temperament might be tolerable with the mellow tone of the modern piano, but it sounds very harsh with the high harmonic content of the plucked strings of the harpsichord. Some harpsichordists use equal temperament for simplicity or because of familiarity, but classical music sounds better and more authentic in an appropriate tuning, and these are enjoying a revival.

There is one further thing related to tuning that should be mentioned. The requirement that the strings of a musical instrument be thin and under high tension ensures that the prime restoring force on a displaced string is that of tension, rather than that of string stiffness. This is true for the harpsichord and clavichord, but not for the piano, which uses much thicker strings. This leads to *inharmonicity*, where the overtone frequencies are all stretched a little bit above those of true harmonics. The octaves on a piano must be tuned to a frequency ratio a little greater than two, so that there are no prominent beats and the interval sounds “in tune.” The result is that the tuning of a grand piano is stretched by about half a semitone across the whole keyboard range, though not quite uniformly because of the variation in string length and diameter, so that this does not help with reconciling the Pythagorean comma. This problem does not occur to any significant extent with the harpsichord or clavichord because of their relatively very thin strings. As well as covering possible tunings for standard harmonic sounds, an excellent and interesting analysis of possible tunings for sounds with extremely inharmonic overtones has been given in a book by Sethares (1998), though this extension fortunately has no real relevance to harpsichords!

8.5 Conclusion

The harpsichord and the clavichord were, between them, responsible for the development of nearly all “Western” keyboard music before the advent of the piano. (The exception is music written for the organ, which has a very different background.) As musical tastes changed, these two instruments were largely superseded by the piano in the late eighteenth and early nineteenth centuries, and it seemed that they might disappear forever. Things changed dramatically, however, by the first half of the twentieth century when there was a revival of interest in performing music in traditional style on original instruments, and there is no doubt that performances of great works such as Bach’s *Brandenburg Concerto No. 5* sound entirely different and less appropriate when the harpsichord is replaced by a piano. Modern makers of traditional keyboard instruments are active in many areas of the world, and the changes that they have made, such as the substitution of Delrin or Celcon for the natural crow feather quills, have been with the aim of making the instrument more reliable rather than of introducing any fundamental changes to the success of the historic instrument. Long may this revival continue!

References

- J.M. Barbour *Tuning and Temperament: A Historical Survey* (Michigan State College Press, East Lansing, MI, 1951; reprinted Dover, New York, NY, 2004)
- B. Brauchli *The Clavichord* (Cambridge University Press, Cambridge, 1998)
- V. Bucur *Acoustics of Wood* (CRC Press, New York, NY, 1995)
- N.H. Fletcher “Analysis of the design and performance of harpsichords” *Acustica* **37**, 139–147 (1977)
- N.H. Fletcher and T.D. Rossing *The Physics of Musical Instruments*, 2nd ed. (Springer, New York, NY, 1998) chapter 11
- B. Haynes *A History of Performing Pitch: The Story of “A”* (The Scarecrow Press, Lanham, MD, 2002)
- F. Hubbard *Three Centuries of Harpsichord Making* (Harvard University Press, Cambridge, MA, 1965)
- E.L. Kottick “The acoustics of the harpsichord: response curves and modes of vibration” *Galpin Society Journal* **38**, 55–71 (1985)
- E.L. Kottick *The Harpsichord Owner’s Guide* (University of North Carolina Press, Chapel Hill and London, 1987)
- E.L. Kottick *A History of the Harpsichord* (Indiana University Press, Bloomington, IN, 2003)
- E.L. Kottick, L. Marshall, and T.J. Hendrickson “The acoustics of the harpsichord” *Scientific American* **264**(2), 110–115 (1991)
- M. Lubenow and J-P. Meyn “Musician’s and physicist’s view on tuning keyboard instruments” *European Journal of Physics* **28**, 23–35 (2007)
- H. Neupert *The Clavichord* trans. A.P.P. Feldberg (Bärenreiter-Verlag, Kassel, 1965)
- R. Russell *The Harpsichord and Clavichord*, 2nd ed. (Faber and Faber, London, 1973)
- W.R. Savage, E.L. Kottick, T.J. Henderson, and K.D. Marshall “Air and structural modes of a harpsichord” *Journal of the Acoustical Society of America* **91**, 2180–2189 (1992)
- W.A. Sethares *Tuning, Timbre, Spectrum, Scale* (Springer, London, 1998)
- S. Thwaites and N.H. Fletcher “Some notes on the clavichord” *Journal of the Acoustical Society of America* **69**, 1476–1483 (1981)
- K. Vermeij *The Hubert Clavichord Data Book – A Description of All Extant Clavichords by Christian Gottlob Hubert* (Clavichord International Press, Bennebroek, the Netherlands, 2004)
- G. Weinreich “Coupled piano strings” *Journal of the Acoustical Society of America* **62**, 1474–1485 (1977)
- W.J. Zuckermann *The Modern Harpsichord* (October House, New York, NY, 1969)

Chapter 9

Harp

Chris Waltham

9.1 Introduction

The aim of this chapter is to describe the Western harp from the points of view of mechanical engineering and acoustics, and how it has evolved into its current form. Section 9.2 notes the earliest recorded beginnings, and sketches the route by which we have arrived at the modern instrument. The structure is explained, including how the instrument is played. The two major acoustical components of the harp, the strings and the soundboard/soundbox system, their contributions to the sound of the harp, and how they have evolved into their present state, are considered in more detail in Sects. 9.3 and 9.4. Section 9.5 looks at the whole instrument and the sound it produces.

9.2 Overview

9.2.1 *Origins and Development*

The classification system of Hornbostel and Sachs defines a harp to be a many-stringed chordophone whose soundboard is oriented perpendicular to the plane of the strings (von Hornbostel and Sachs 1914). There is no bridge connecting the strings to the soundboard, a feature that distinguishes it from the lyre. The earliest harps appeared in Mesopotamia in the third millennium BCE, and were of the arched variety, that is to say, the frame was an open L-shape with the strings joining the two parts. Harps of this form continue to be played in various parts of the world, notably Southeast Asia. The first harps with a complete triangular frame – *frame*

C. Waltham (✉)

Department of Physics & Astronomy, University of British Columbia,
6242 Agricultural Road, Vancouver, BC V6T 1Z1, Canada
e-mail: cew@phas.ubc.ca

harps – appeared briefly in classical Greece and Italy, but this form was then forgotten until it re-emerged in northwest Europe around AD 800 (Rensch 1972, 1998). This chapter will concentrate on the line of development from these early frame harps to today's Western concert harps.

There are severe technical challenges in building a harp. They need a large number of strings to obtain a useable pitch range, and this inevitably puts the soundboard under great stress. To complicate matters, they frequently require complex sharpening mechanisms in order to play chromatic music. In addition, as with any plucked stringed instrument, the harp tends to be quiet, and one has to work hard to raise the sound output without thinning the soundboard beyond its capacity to anchor the strings.

There have been three distinct areas of technological development in European harps aimed at balancing these issues. Firstly, strings have become much stronger and therefore capable of withstanding a greater tension – thus producing a more harmonic sound – and of storing more potential energy for the production of greater sound. Secondly, improved techniques in cutting and bonding wood have produced soundboards that are stronger and thinner, again producing a greater volume of sound. Better construction techniques have also produced much larger harps, with more strings. Thirdly and most recently, mechanisms have been devised by which strings can be raised and lowered in pitch by a semitone, avoiding the need to have a string for every chromatic pitch.

9.2.2 Structure

A Western harp is basically a triangular structure, formed of the post or (fore)pillar, the neck, and a soundboard mounted on a soundbox. The strings are attached at one end to tuning pegs and bridge-pins mounted in the neck, and at the other end to the soundboard. The basic geometry is shown in Fig. 9.1. The structure has to be made strong enough to withstand a total string tension of up to 20 kN for a full-size concert harp.

The following specifications are taken from instruments produced by the world's leading manufacturers of concert harps: Salvi Harps of Italy (Firth and Bell 1985), Lyon and Healy Harps of Chicago, Les Harpes Camac of France (Le Carrou 2006) and the Aoyama Harp Company of Japan (Otake and Aoyama 2007). The soundboard is approximately trapezoidal in shape, as shown in Fig. 9.2, and is typically around 1.4 m in length, 0.5 m wide at the base, 0.1 m at the top, and of thickness varying 11–12 mm at the bottom (bass) end to 2–2.5 mm at the top (treble). It is made of strips of spruce (Sitka or Engelmann) between 3 and 8 cm wide bonded together, and covered with a thin veneer, typically also of spruce. Sometimes, as in the case of the Salvi Aurora (Fig. 9.3), the soundboard has flared *wings* at the bass end, which protrude beyond the width of the soundbox. The strings are connected through two strong bars of hardwood mounted along the centerline of the soundboard, one on the outside (the cover bar is visible on the front), and one heavier reinforcing bar inside.

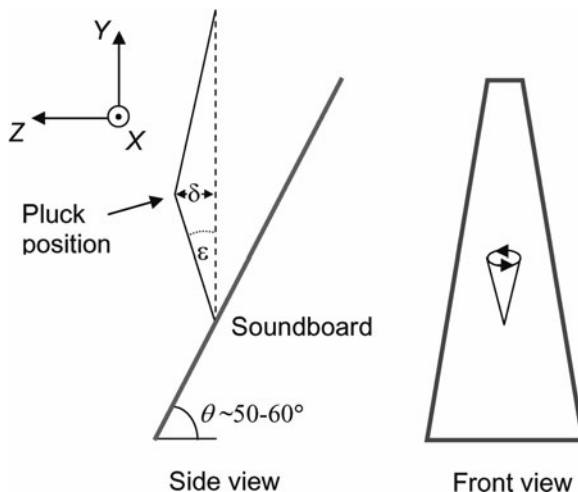


Fig. 9.1 Geometry and coordinate system of the harp soundboard and plucked string. The whirling motion of the string is shown, indicating how the tension force vector varies during one cycle of string vibration

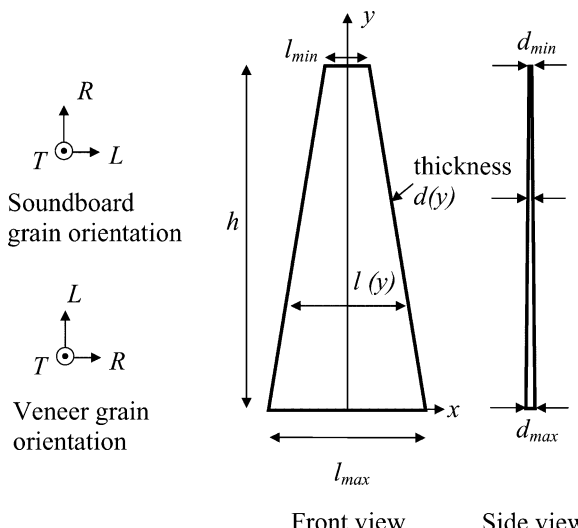


Fig. 9.2 Layout of harp soundboard and the orientation of the wood grain for the soundboard base and veneer. The longitudinal (L), transverse (T), and radial (R) directions refer to the natural cylindrical coordinate system of a tree limb



Fig. 9.3 The configuration of a concert harp, a 47-string Salvi Aurora (photo by author)

In addition, harmonic bars (made of beech or fir) are mounted approximately parallel to the string bars on the inside of the soundboard (Fig. 9.4).

The soundbox of a large harp is typically semi-conical in shape, and is built up by bonding hardwood veneer (e.g., beech) around a mold. The soundboxes of smaller harps are often built the same way, although some have flat sides and back. There are generally four or five soundholes in the back of the soundbox and one in the base. The primary function of these holes is to gain access to mount or replace strings, although they do have acoustical effects. Inside the back of the soundbox are strong U-shaped ribs (of beech, aluminum, or steel) that prevent the box from undergoing too much flexure under the string tension.

A full-size instrument has 46 or 47 strings, running from C1 or D1 to G7. The strings run from the center of the soundboard to the left side (viewed by the player)

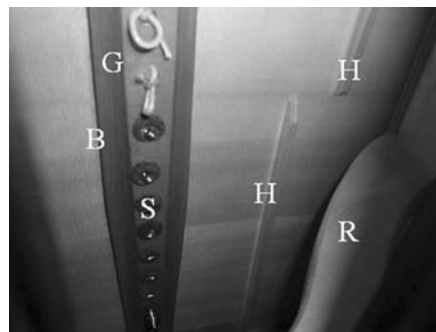


Fig. 9.4 View through one of the soundholes of a Salvi Aurora concert harp. Visible are the central reinforcing bar (*B*) at the division between gut (*G*) and steel strings (*S*), the horizontal strips of the soundboard, the vertical harmonic bars (*H*), and part of the soundbox reinforcement (*R*). The horizontal grain of the spruce can be seen in this view. The precise function of the harmonic bars is not clear. They may have originated in a time when soundboards were not veneered and were more prone to cracking without additional stiffening away from the central bar (photo by author)

of the neck. At the top end they are wrapped around a tuning peg, used for tuning, and a bridge pin, which defines the unsharpened vibrating length of the string. Beneath the bridge pin are the sharpening mechanisms, if any, which raise the pitch of the string one or two semitones (Fig. 9.5a). On a concert harp there are pairs of rotating tuning disks, and the strings are tuned a semitone flat; the first disk raises the string to natural, and the second to sharp. The sharpening mechanisms are controlled from seven pedals (Fig. 9.5b) at the base of the harp, which allow all the As, Bs, Cs, etc. to be played as flat, natural, or sharp. The mechanical connection between the pedals and the sharpening mechanism is extremely complex and runs up the forepillar or post into the neck.

The strings at the bass end are typically copper-wrapped steel with a nylon separator. In the center they are gut, and at the treble end, nylon. The position where steel changes to gut is marked on the shape of the neck by the break, where the curvature changes sign and the neck becomes horizontal.

The neck of the harp needs to be very strong in order to withstand the torque of the string tension on the tuning pegs; it is typically made of maple ply. A sensible engineering solution to this issue would be to split the neck in two and run the strings down the gap in the middle. However, the only harp-making tradition that adopts this approach is the Paraguayan one; all European harps – even baroque examples with two or three chromatically tuned ranks of strings – attach strings on the left. The pillar is carved or turned from hardwood and may be plainly polished or highly decorated. It has to be strong to withstand both the compression and torsion due to the strings, and carries the sharpening linkages along a central channel.

The harpist sits behind the harp and rocks it backward so that his or her right shoulder rests against the upper end of the soundbox. The strings are plucked with the thumb and three larger fingers of each hand, the left for the bass and the right for the treble (Le Carrou et al. 2007). Harp music is written in the treble and bass clefs

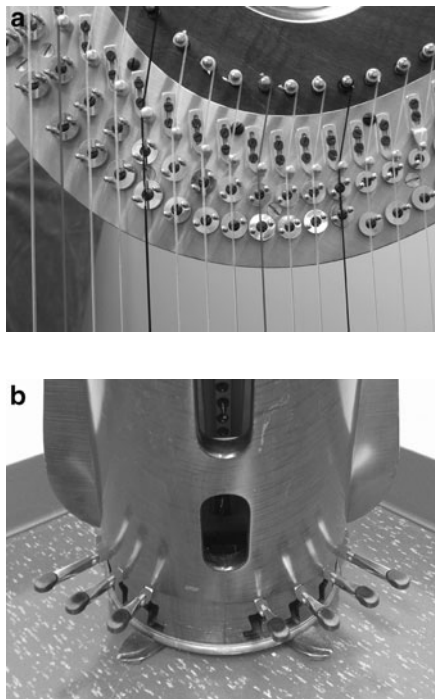


Fig. 9.5 (a) Erard double-action sharpening mechanism on a Salvi Aurora. The upper rank of tuning disks raise the strings from flat to natural; the lower rank raises them from natural to sharp. (b) The order of the pedals from left to right is: D, C, B–E, F, G, A (photo by author)

in the same manner as piano music. The strings are usually plucked between one-third and one-half of the way from the soundboard to the neck, although they may be plucked closer to the soundboard (*près de la table*) to gain a more “guitar-like” sound. Harmonics can be played by touching the center of the string with the base of the thumb and plucking it with that thumb. The extremely long decay times of the strings (see Sect. 9.5.1) – the lower strings can be heard for half a minute after being plucked – make it frequently necessary for the harpist to stop the vibrations with the flat of the hands.

9.3 Strings

9.3.1 History

Over the centuries, strings have been made from the strongest filaments available. In the past, copper, bronze, brass, horsehair, silk, and gut have been used (Firth 1988). Of these traditional materials, only gut remains in common use, mostly for

the midrange of concert harps. Nylon is stronger than gut, and can be made more uniformly, and so it is almost ubiquitous for the higher strings. For the lowest strings, steel is favored, sheathed with silk and wrapped with a helix of thin copper wire to raise the linear density without raising the stiffness and thus the inharmonicity. Before steel was introduced, it was possible to achieve a similar effect in gut by overwrapping or twisting several strands into a rope (Barbieri 2006).

9.3.1.1 Diatonic Versus Chromatic Stringing

Chromatic music has always been a challenge for harp makers and players. The strings have to be typically a finger-width apart, and one has only one arm-length to play with rather than two as in the case of a piano. In addition, the direct connection to the soundboard means one cannot match increasing string tension with a massive iron frame, as in a grand piano.

No solo harp music exists from prior to the sixteenth century, and it is only about this time that written and pictorial information becomes detailed enough to say for sure how harps were strung. Printed illustrations from the first half of the sixteenth century show simple diatonic stringing, with indications of alternative tuning (Morrow 1979). Vincenzo Galilei reports that the Irish harps in Italy in the mid-sixteenth century were strung chromatically, probably with only one rank of strings. Toward the end of that century, Italian harps acquired a second rank of strings, parallel to the first, arranged so that the “white” notes were on the bottom left rank and top right rank, the remaining strings being “black”: this is the classic *arpa doppia* (double harp) or *arpone*. Later, a third rank was added to form a triple harp, strung such that the “white” notes were duplicated on each side and the “black” notes were in the central rank. Spanish harps, on the other hand, often had a separate rank running down the right-hand side of the soundboard. It was the Italian style of triple harp that was exported to Wales, becoming that country’s national instrument even as its popularity waned in Italy.

9.3.1.2 Sharpening Mechanisms

Early attempts at providing a sharpening mechanism for diatonically strung harps consisted of hooks with which the effective length of the string could be shortened. These were similar to the sharpening levers used on modern small harps, and had the same limitations. A major improvement occurred with the invention of the single-action pedal harp, probably by Jacob Hochbrucker (1673–1763), a Bavarian maker, around 1720 (Kastner 1909). All the A-strings, B-strings, etc., together could be raised a semitone (only, hence *single-action*) by pressing one of seven pedals. In Paris, a harpmaker to Queen Marie Antoinette, Jacques-Georges Cousineau (1760–1836) extended this arrangement to include 14 pedals – seven to sharpen the string pitches, and seven to flatten them. Soon afterward, Sébastien Erard (1752–1831), produced a *double-action* version in which each pedal had three

positions: flat, natural, and sharp. Patented in 1810, this mechanism was complex to build, but much simpler to use, and it has since become the standard for concert harps (Fig. 9.5).

9.3.2 Basic String Considerations

The requirements for the strings are as follows (Firth et al. 1986):

String spacing: All the strings need to be accessible in one arm's length and comfortably more than a fingers-width apart from each other. It should be possible to put enough energy into each string without it striking its neighbors.

Tension, T : This should not be so great as to break the soundboard or the strings themselves. As the total tension for even a small harp can be several thousand newtons, the former is not a trivial requirement.

“Feel,” F : This is the ratio of the plucking force to the lateral displacement, and for a string of length L plucked in the center it is given by

$$F = \frac{4T}{L}. \quad (9.1)$$

This value will rise for plucks away from the center, but in any case it should be large enough that sufficient potential energy can be given to each string without displacing it so much that it interferes with adjacent strings. For ease of playing, it should be fairly constant from string to string, and vary only slowly across the whole instrument.

The inharmonicity of each string arises from two sources: one intrinsic due to the stiffness of the string, and one due to the inevitable stretching of the string during plucking – the initial nonlinear pitch shift. To quantify these effects, we can define a factor K , which depends on the elastic modulus, E , and the core diameter d_c ,

$$K = \frac{\pi^3 E d_c^2}{16 T L^2}. \quad (9.2)$$

The intrinsic inharmonicity is

$$\frac{\Delta f_i}{f} = \frac{K}{4} d_c^2 \quad (9.3)$$

and the initial nonlinear pitch shift for a transverse deflection δ is

$$\frac{\Delta f_n}{f} = \frac{3K}{8} \delta^2. \quad (9.4)$$

Hence the latter dominates as the pluck amplitude is related to the string spacing and is likely to be at least an order of magnitude larger than the string diameter, and in fact the value given in (9.4) is a minimum, because we have assumed the string is

plucked in the center. This pitch shift is responsible for the initial *twang* of the string and dies down rapidly after the pluck.

There are many ways of optimizing all these constraints; consider the data obtained from a 47-string Salvi Aurora shown in Fig. 9.6. The strings are made, as is typical for large harps, of copper-wound steel, gut, and nylon. We shall discuss the reasons for these materials below. The characteristically graceful shape of the harp neck is reflected in the plot of string length, Fig. 9.6a. Note the position of the *break*, between the 12th (steel) string and the 13th (gut) string, where the neck flattens out. This is a problematic area for harp builders and players because the string tension is the highest, as can be seen in Fig. 9.6b, so the soundboard is under the most stress here. The highest steel strings tend to be the ones that break, usually at points of highest flexure at the tuning peg or soundboard, because the stress here is the largest fraction of the material yield stress: Fig. 9.6c. For the player, there is a sharp change in feel between the highest steel and the lowest gut string: Fig. 9.6d.

The reason for the change from gut to steel strings is follows. For the Salvi, the following empirical dependencies of length and diameter on pitch are observed for the unwrapped strings: $L \propto f^{-0.8}$ and $d \propto f^{-0.5}$. Because $f \propto \sqrt{T}/(Ld)$ (for a given material), the tension and feel depend on pitch thus: $T \propto f^{-0.6}$ and $F \propto f^{0.2}$. Note the variation in feel is very small; an exponent of 0.2 corresponds to 15% per octave. Extrapolating these forms for the low strings of a uniformly strung harp (i.e., all gut strings) would mean these strings would be an extra meter long, like many old Welsh harps (Rensch 1998), and slack. The break avoids this particular problem, but raises another. Steel and gut/nylon differ by a factor of six in density, and so there is an abrupt jump in feel (and tonal quality). This is an annoyance, but there is no other credible material between these extremes which could ameliorate the sudden change.

The particular pitch dependencies found on the Salvi harp show an interesting feature when one considers the potential energy of the plucked string. If one makes a reasonable assumption that the lowest strings may be pulled back 75% of the string spacing, and the highest somewhat less, say 50%, then the maximum potential energy of the plucked string, as shown in Fig. 9.7a, is essentially constant for all the unwrapped strings. Under these conditions, the actual pitch distortion caused by the deflection (Fig. 9.7b) is mostly tolerable, but rises to a semitone at the extreme treble end of the instrument.

9.3.3 String Motion and Its Influence on the Sound Spectrum

If the string is plucked in the center, then it will vibrate with frequencies that are odd multiples of the fundamental. However, the soundboard will be driven at both odd and even multiples of the fundamental because it can be pulled in both the X (odd) and Z (even) directions as defined in Fig. 9.1. For a string with an elastic modulus E and area A that has been tensioned by stretching it a distance ΔL (i.e., $T = EA\Delta L/L$)

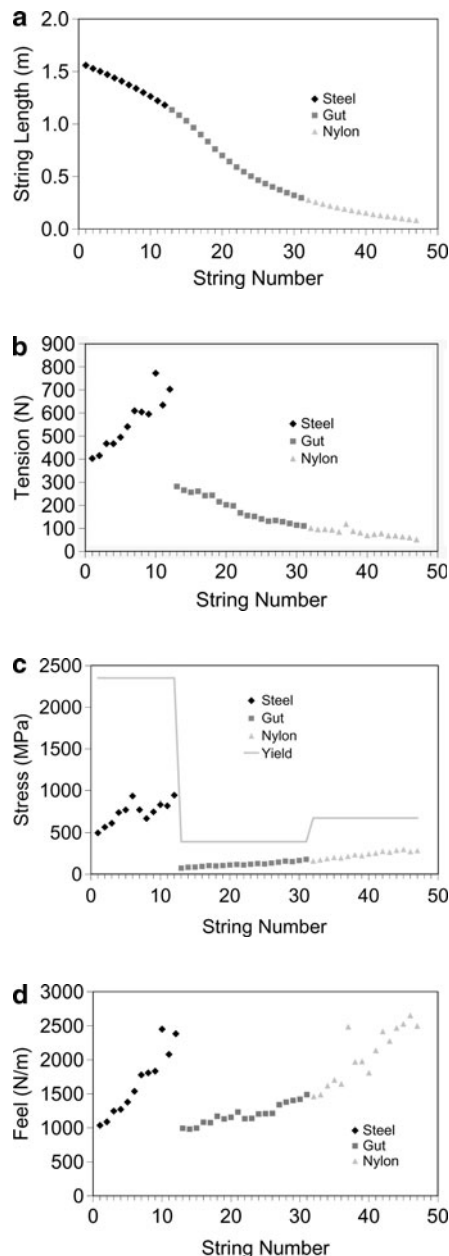


Fig. 9.6 Measurements of string properties for a Salvi Aurora 47-string concert harp: (a) vibrating length, (b) tension, (c) stress, and (d) feel

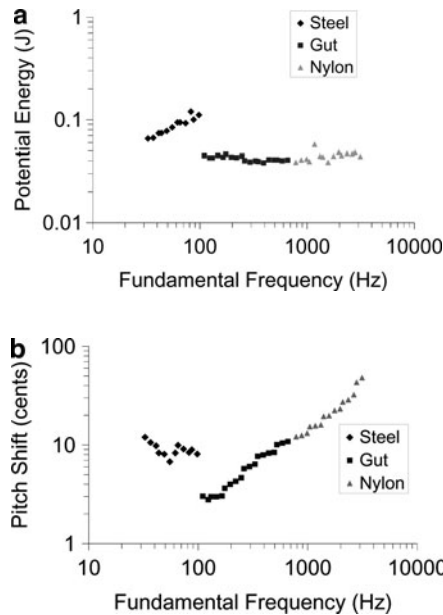


Fig. 9.7 (a) Potential energy stored in the string under typical deflections as discussed in the text.
(b) Pitch shift in cents (1/100th of a semitone) under the same conditions

one can show that the change in force on the soundboard $\vec{\Delta F}$ caused by a central transverse deflection δ , has components given to the lowest order in δ by

$$\Delta F_X = \frac{2EA\delta\Delta L}{L^2} \quad \Delta F_Z \approx \frac{2EA\delta^2}{L^2} \left(1 - \frac{\Delta L}{L} \right) \approx \frac{2EA\delta^2}{L^2}. \quad (9.5)$$

Hence the force normal to the soundboard will have a component $\Delta F_x \sin(\theta)$ vibrating at the fundamental and odd-numbered harmonic frequencies (being proportional to the displacement of the string), and a component $\Delta F_z \cos(\theta)$ vibrating at even-numbered harmonic frequencies (being proportional to the square of the displacement). The form of ΔF_z is at first sight counterintuitive, for not only is it independent to lowest order of ΔL (i.e., the string tension), but the higher order term also causes it to decrease somewhat with string tension (due to the change in angle). Comparing the X and Z components, the magnitude of the second harmonic relative to the fundamental is seen to depend on the ratio $\delta/(\Delta L)$ and $1/\tan(\theta)$ ($\approx 0.6-0.7$). The ratio $\Delta L/L$ is typically small (for the Salvi Aurora it is around 0.2–0.4% for the steel strings and 1–5% for the rest), hence the force ratio is greater than unity for the steel strings and less for the gut and nylon – except at the far treble end, where it rises steeply. Hence, one would expect the second harmonic to be strong for the steel and weak for the gut/nylon strings. Of course, plucking at positions other than the center will change these ratios, and the actual strengths of

harmonics for any given string are complicated by the highly nonuniform frequency response of the soundboard, as will be examined below. The result is that in general both even and odd harmonics are present in all strings but their relative strengths vary with register and the manner of plucking.

9.3.4 String Motion and Temporal Development of the Sound

The strings are connected at one end to a relatively rigid bridge pin, but at the other end the thin soundboard is mobile in one direction (in the Y-Z plane) and rigid in the other (X), as defined in Fig. 9.1. As a result, waves on the string polarized in the Z-direction meet a different soundboard impedance than those in the X, causing a phase-shift due to a difference in effective string lengths, and thus the string develops an elliptical whirling motion, as shown in Fig. 9.1. This can easily be seen by plucking the lower strings on a harp, particularly when viewed under fluorescent lighting. The center of the string executes an elliptical motion in a particular sense that is initially determined by the torque applied to the string by the pluck. This ellipse then collapses until the string is vibrating in the X-direction, and the soundboard produces very little sound. The ellipse then grows back with the opposite direction of rotation, having picked up the necessary angular momentum from the soundboard, and the sound output grows again. The rate of pulsation is dictated by the relationship with soundboard resonances, and the effect on the sound is discussed in Sect. 9.4.2.

These motions can be understood in terms of a simple mechanical model. If one has a 2D harmonic oscillator mounted on a support which is itself allowed to vibrate in one direction, then the orbits generated are very similar to the observed motion of harp strings, especially when the two resonant frequencies are closer together. Such a case is shown in Fig. 9.8. These effects have also been seen in the Finnish *kantele*, a plucked instrument with a peculiar string-anchoring mechanism that gives markedly different vibrating lengths for the two polarizations (Erkut et al. 2002).

9.4 Soundboard and Soundbox

9.4.1 Evolution of the Soundboard

Over the last 1,000 years or so, the body of a European harp has developed from being one carved of solid wood, to one built up of parts glued together (Firth 1989). Early harps from the Celtic seaboard were perforce carved out of solid wood; natural glues would not have survived the damp climate (Hadaway 1980). The construction and heavy stringing of Irish harps favored relatively thick bellies carved out of hardwoods: willow or yew. The word *belly* is appropriate where there was no separate soundboard.

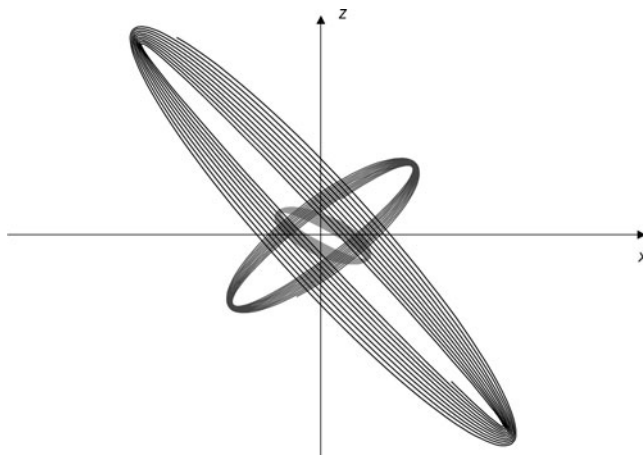


Fig. 9.8 Motion of a damped 2D harmonic oscillator on a mount which itself vibrates in one direction. This motion is similar to that observed in the nonplanar motion of harp strings

The transition from thick hardwoods to thin softwoods started in the seventeenth century. Quite when or where this happened is not clear owing to the tiny number of instruments that have survived from this period. However, two seventeenth-century reconstructions that have been studied (Firth 1989) are a northern Italian one¹ with an 8–10 mm thick one-piece maple soundboard with longitudinal grain, and a Spanish-style harp² (made in Naples) with a thin spruce soundboard made of two halves with the grain arranged in an almost-longitudinal herring-bone pattern. Firth notes that the Spanish-style harp is on average 15 dB louder than its northern Italian cousin. The thinner soundboards tended to have a few horizontal braces to prevent cracking (Bordas 1987). By the mid eighteenth century, when the Italian Triple Harp had become firmly established in Wales, the soundboards of Welsh harps were a mere 3 mm thick (Rimmer 1965). At the end of the eighteenth century, the cross-grain construction of glued strips familiar in modern instruments appeared, a change made necessary for the soundboard to withstand the cumulative tension of the many strings of a large pedal harp.

In order to raise the sound output of a thick soundboard, Italian and early Welsh makers frequently placed bray pins at the base of the strings. Quite how these were configured is now a matter of conjecture (Hobrough 1980); they were either used to make a buzzing sound or for pitch modulation in the manner of a *jawari* bridge on a sitar.

Many pre-1800 harps had closed backs and only small soundholes in the soundboard itself (Firth 1989). The strings were attached from the front using a

¹ A Hadaway copy of an Italian *arpa doppia* from the Brussels Conservatoire Museum (item #1504), dated 1675.

² A Hadaway copy of a Spanish *arpa doblata* in the Vienna Kunsthistorisches Museum.

peg to hold them in place. More recent instruments tend to have large soundholes in the back of the soundbox, as described in Sect. 9.2.2.

9.4.2 *Vibrational Behavior of the Soundboard*

The shape of a modern soundboard is typically a simple, flat trapezoid (Fig. 9.2). The wood, usually spruce, has a transverse grain, with the radial direction of the wood grain parallel to the plane of the board. Because of the grain direction, the soundboard consists of a dozen or more pieces, glued edge to edge. This glue joint can be unsightly, and the soundboard is prone to cracking along the grain under string tension (not necessarily at the glue joints, which may be stronger than the wood). To solve both these problems, a thin veneer of spruce with longitudinal grain is bonded on top of the soundboard.

Consider a small 36-string harp made by the present author, a copy of a George Morley instrument of about 1820.³ The soundboard dimensions are length 1,025 mm, width 344–70 mm, thickness 2.38–4.76 mm, and the material is Sitka spruce. Figure 9.9a shows the modal shapes of the first four nontorsional modes of the soundboard, from a finite-element calculation. Figure 9.9b is a photograph of the finished harp. One can see that for each mode, there is one dominant antinode, and this is the region where the soundboard has the highest mobility. This principal antinode moves up the soundboard as the frequency rises, as does the pitch of the attached strings, and the relationship between the two frequencies is of course, crucial. Firth and Bell (Firth 1977; Firth and Bell 1985) made a systematic study of the lowest modes of soundboards with varying thicknesses and widths and found that the standard trapezoidal shape is quite critical in maintaining this spatial and frequency structure.

The bare soundboard was subsequently veneered, polished, and had string bars mounted on the front and back. The effect of these additions was to spread out the resonances, both in frequency and up the full length of the soundboard, while keeping the fundamental fairly constant at around 200 Hz. A study of the vibrational effects of veneer (Firth and Bell 1988) showed that it effectively reduces the anisotropy of the soundboard from the original spruce value of 12:1 to about 4:1.

9.4.3 *Helmholtz and Pipe Resonances of the Soundbox*

Bell studied the air modes – the Helmholtz and pipe resonances – of a Salvi Orchestra (a 46-string concert harp) soundbox by placing one in sand to prevent the wood from vibrating (Bell 1997). He found the pure Helmholtz mode to lie

³ Plans available from Robinson Harps of California, www.robinsonharp.com.

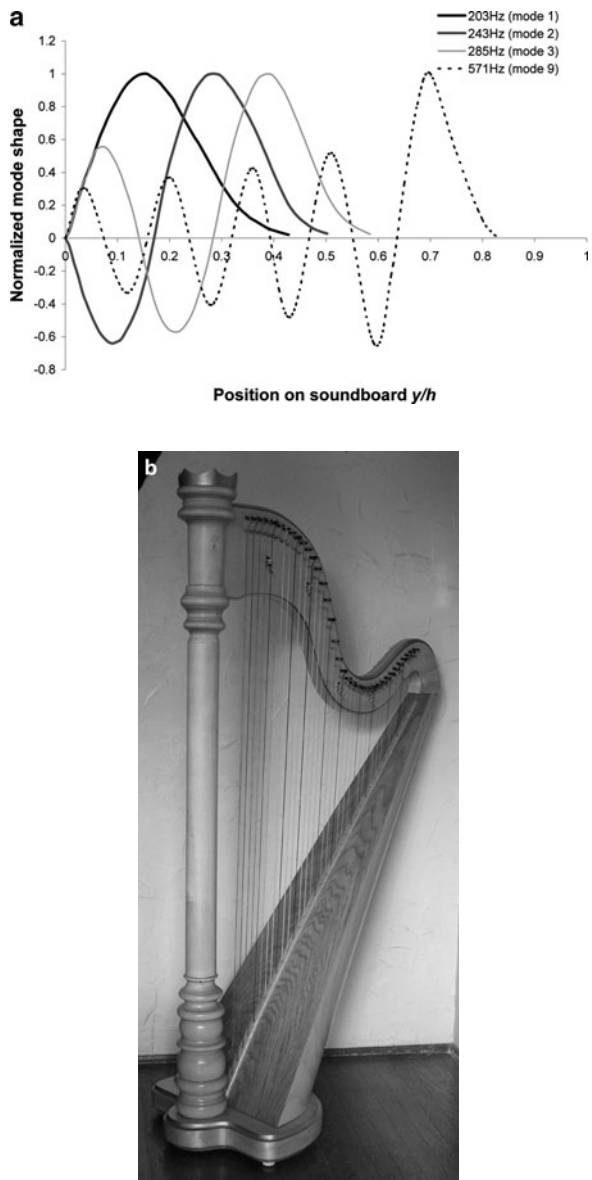


Fig. 9.9 A finite-element calculation of the lowest nontorsional modes of the trapezoidal soundboard of a Morley harp, made of Sitka spruce with transverse grain, with reinforcing bars of maple. The region of highest mobility can be seen to move toward the treble end of the soundboard as the frequency rises

fairly close to that predicted by the standard expression (Kinsler et al. 1999) assuming the air in all the holes moved in phase with one another:

$$f_A = \frac{c}{2\pi} \sqrt{\frac{A}{V(l + 2\Delta l)}}. \quad (9.6)$$

Here c is the sound speed, A the area of hole, V the soundbox volume, l the hole thickness and $2\Delta l$ the end correction (which is approximately equal to the square root of the area of each hole). The value for the Salvi was found both experimentally and theoretically to be 190 Hz, although Bell commented that it is very difficult to isolate the Helmholtz resonance except in the ideal conditions he employed.

9.4.4 Vibroacoustic Behavior of the Soundbox

After a bare soundboard is veneered, polished, given string and harmonic bars, mounted into the soundbox, and strung, the typical modal pattern shown in Fig. 9.9 undergoes considerable modification. In addition to the spreading of frequencies noted above, the strings tighten the soundboard and raise all the frequencies a few tens of Hertz (Waltham and Kotlicki 2008). The air in the soundbox couples to the soundboard and increases the number of possible modes. There are additional bending modes due to the mounting of the soundbox in the harp frame, and in the semi-conical back of the soundbox.

The musical acoustics group at the Université du Maine in Le Mans, France, have made an extensive vibroacoustic investigation of the low-frequency behavior of the soundbox of a Camac Atlantide Prestige 47-string concert harp (Le Carrou 2006). They have focused on the relationship between the movement of air in the soundholes and the motion of the soundboard in order to try and identify the principal low modes of vibration of the soundbox (Fig. 9.10).

Of the first six modes, no. 1 corresponded with the global motion of the soundbox within the frame of the harp; no. 5 was a torsional mode with very weak coupling to excitation by the strings; two (no. 2 and no. 3) had characteristics of the bending of a simply supported free beam; and two (no. 4 and no. 6) were associated with breathing modes of the cavity. The last two are the most important acoustically, as was demonstrated by measuring the air velocity near the soundholes when the soundboard was excited with a driving force. The ratio of air velocity (V_i) to force (F) as a function of frequency is shown in the upper plot of Fig. 9.11. The two breathing modes can be described in the manner of a simple two-oscillator model of the air and soundboard, of the type introduced for the guitar by Caldersmith (1978). Below 150 Hz the soundboard moves outward, while the air moves inward, and vice versa, and above 200 Hz the soundboard and the air both move outward or inward at the same time. The interplay between these two motions typical of any instrument that consists of a wooden shell with a hole; it is crucial for the quality of sound radiation (Weinreich 1993).

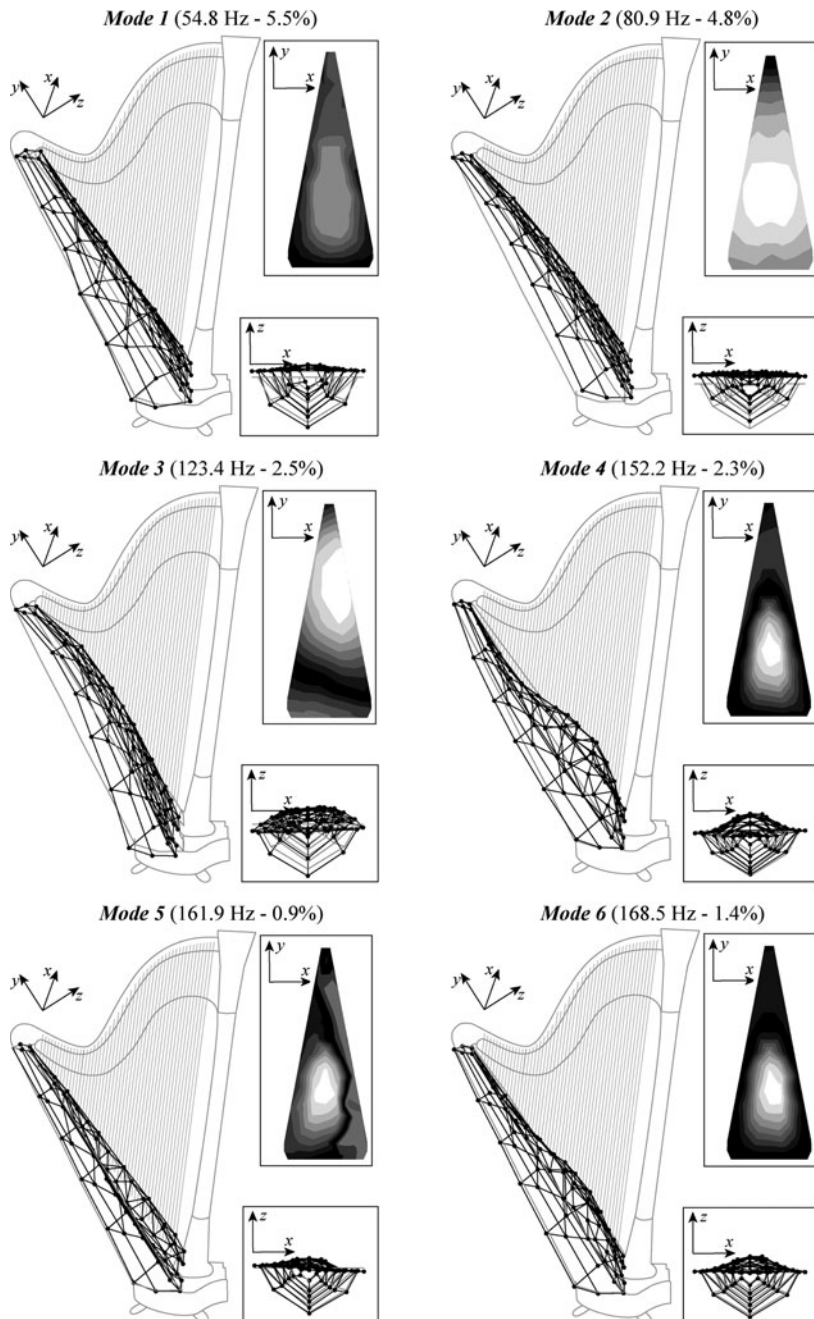


Fig. 9.10 The first six modal frequencies, damping coefficients, and mode shapes of a complete Camac Atlantide harp (from Le Carrou 2006). Modes 4 and 6 are coupled to the lowest mode of the free soundboard as shown in Fig. 9.9

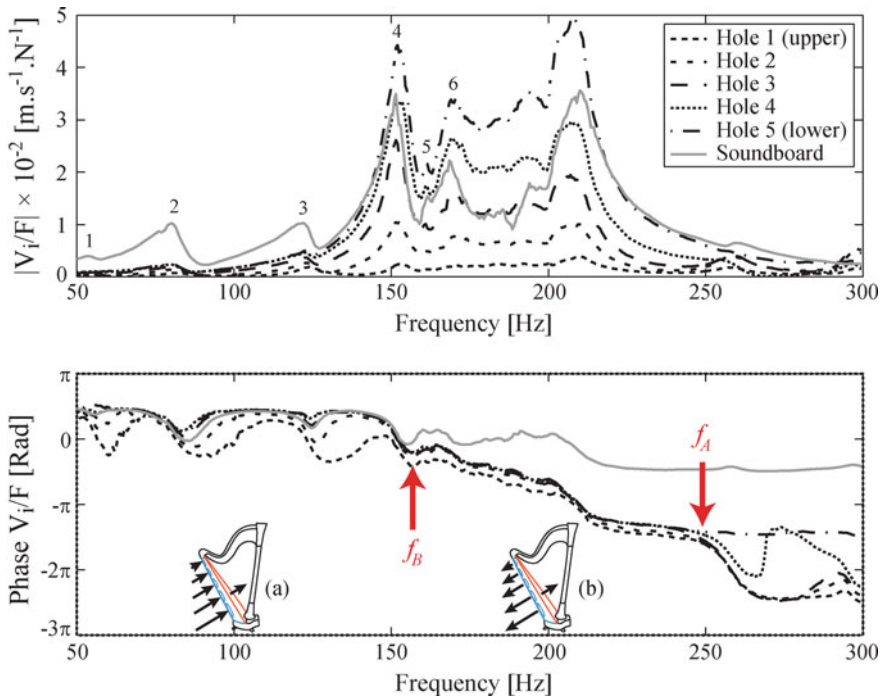


Fig. 9.11 Magnitude and phase of the acoustic velocities (V_i) in the soundholes relative to a force (F) applied to the soundboard for a Camac Atlantide concert harp. Numbers indicate the modal frequencies given in Fig. 9.10. The frequencies f_A and f_B indicate the pure Helmholtz and fundamental soundboard frequencies, respectively. Below f_B , the air and soundboard velocities are in phase; above f_B , they are in antiphase (adapted from Le Carrou 2006)

How do these modes of the whole instrument relate to the spectrum of soundboard modes? Modes 4 and 6 are a result of the fundamental soundboard mode coupling to the air in the soundbox. Above these frequencies, the whole spectrum of soundboard modes is identifiable when the soundboard is mounted on the soundbox (Waltham and Kotlicki 2008). They are shifted up in frequency, but the structure of principal antinodes moving up the soundboard with frequency remains. Makers have had to find the best relationship between the pitches and attachment points of each string, and the frequencies and positions of these principal antinodes. A precise coincidence is not possible for all strings simultaneously (there are many more strings than soundboard resonances), and not desirable for a few strings to sit at these resonances. In this case some strings would *boom* very loud and their neighbors would be *dead*. A discreet distance is therefore best kept between string and soundboard resonance, allowing a more even production of sound from string to string (Waltham and Kotlicki 2008).

9.5 The Harp as a Whole

9.5.1 Strings and Soundbox

We have discussed in Sect. 9.3 the vibration of a single string connected to the soundboard in a frequency region where there are no very strong resonances. Where the fundamental or overtone of the string coincides closely with a soundboard resonance, the result is a loud string and a marked time structure. This coincidence happens in several places on the soundboard of a Salvi Aurora. One such is the F4 (349 Hz) string that is connected to the soundboard near the principal antinode of the second soundboard mode at 335 Hz. This resonance can be seen in Fig. 9.12a next to the fundamental of F4 and also next to the second harmonic of F3. This 14-Hz difference produces beating at the frequency which can be seen in the envelope of the F4 string in Fig. 9.12b. Also visible clearly is the lowest soundboard mode at 230 Hz. This example is typical of the almost random interactions between string pitches, overtones, and soundboard resonances which shape the temporal structure of the sound, and give each harp string an individual character.

In spite of this element of randomness, the decay times for plucked harp strings show a general trend from one end of the instrument to the other, as shown in

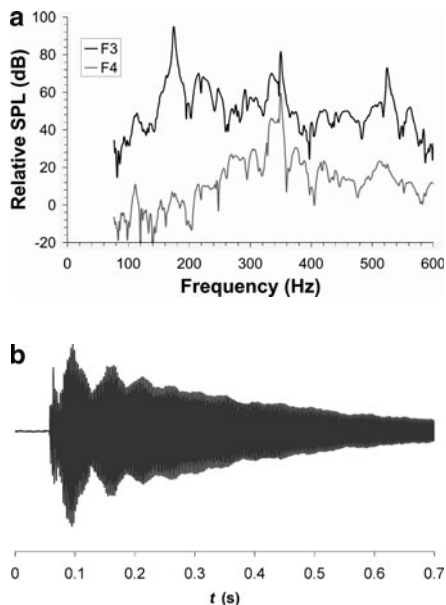


Fig. 9.12 (a) Sound spectra for the F3 and F4 strings of a Salvi Aurora, each plucked in the center, at the instant of plucking. Large soundboard resonances at 223/230 and 335 Hz (corresponding to the two lowest modes of the free soundboard), among others, can be seen. (b) Envelope of sound production from the F4 string plucked at the center. The 14 Hz beating between the string pitch of 349 Hz and a nearby soundboard resonance of 335 Hz can be clearly seen

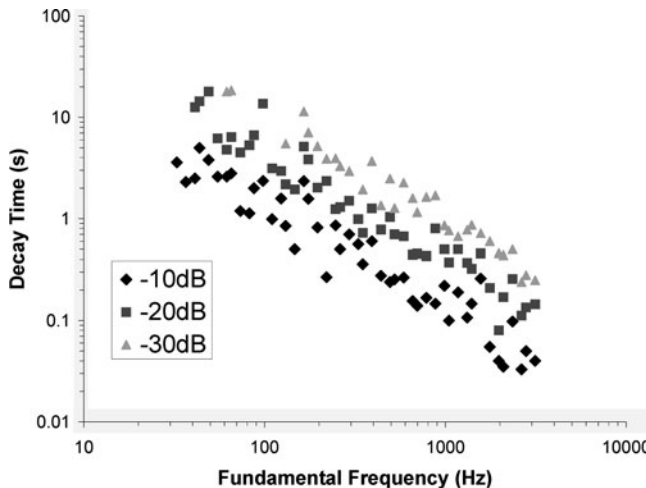


Fig. 9.13 Decay times for plucked harp strings. The strings of a Salvi Aurora concert harp were each plucked at a distance from the soundboard of 40% of the string length. The recording was made in a concert hall and the microphone was placed 1 m in front of the soundboard. The times are recorded from the instant of the pluck to the last occasion when the sound level was 10, 20, and 30 dB lower than the maximum

Fig. 9.13. Here the strings of a Salvi Aurora concert harp were each plucked at a distance from the soundboard of 40% of the string length. The recording was made in a concert hall and the microphone was placed 1 m in front of the soundboard. The times are recorded from the instant of the pluck to the last occasion when the sound level was 10, 20, and 30 dB lower than the maximum. While the decay times of individual strings may vary considerably with those of their neighbors, no change in trend is apparent when the string material changes (the 13th string is the first gut, and the 32nd string is the first nylon string). Thus, it seems that soundboard damping is more important than losses in the strings.

The totality of the string–soundboard interaction is very complicated, as the soundboard couples each fundamental and the harmonics of the strings to fundamentals and harmonics of many other strings. These interactions have been investigated in detail by the Le Mans group (Le Carrou et al. 2005a) who have calculated the vibrational modes of a beam with N strings attached, and identified many of these modes on a Camac Atlantide concert harp.

9.5.2 Sound Radiation

Two studies have been made of the sound radiation from concert harps. Bell and Firth measured a Salvi Orchestra and found three distinct frequency regimes: below 400 Hz the harp is omnidirectional; between 400 and 2,000 Hz it radiates predominantly

in the forward and backward directions; and above 2,000 Hz it radiates in three directions – backward, forward-left, and forward-right (Bell and Firth 1989).

The Le Mans group have studied the Camac Atlantide (Le Carrou et al. 2006) and have attempted to model the radiation with one monopole for the soundboard, and either one or five monopoles for the five soundholes. They found the single monopole model to give reasonable results below 240 Hz, with some improvement by adding more for the soundholes. The phase of these monopoles supports the conclusions from their vibroacoustic measurements discussed above (Le Carrou 2006), that is, that the T_1 mode lies below the A_0 mode. Above this frequency the fit to one monopole was poor, and adding more monopoles yielded little improvement. This is not surprising as above this frequency the soundboard is certainly not moving as a solid body. Another study of the radiated power (Gautier and Dauchez 2004) showed that the sound from the soundholes dominated that from the soundboard in certain frequency bands, namely 150–200 Hz and 400–550 Hz.

9.5.3 *The Sound of the Harp*

If one plays a recording of an isolated note played on the guitar, followed by the same note played on a harp, and then asks an audience to guess which instrument is which, the results are not conclusive. The differences are quite subtle to the ear, the difference being largely that each harp string is coupled strongly to several other strings in the instrument. Much of the character of the harp comes from the physical presence of the instrument and the type of music played. The harp glissando is like nothing else in music, and neither is the ethereal sound of harmonics played with the base of the thumb lightly touching the center of the string.

9.6 Conclusion

Thus far, acoustical physicists have examined various aspects of the harp as a coupled oscillator system with many degrees of freedom. However, the quality of the harp as a musical instrument has not yet been addressed, except in very general terms. The sheer complexity of 47 strings, each vibrating in three dimensions, coupled to a soundbox with many modes of its own, makes it a forbidding problem. Much acoustical work remains to be done.

Acknowledgments I am grateful to the School of Music and the Chan Centre for the Performing Arts at the University of British Columbia for making their Salvi and Aoyama concert harps available. I acknowledge the considerable support and assistance of my UBC colleagues, Andrzej Kotlicki and Domenic diTomaso, and of undergraduate students Gary Chan, Laura Dunwoody, Tina Lee, Billy Lin, Julia Lin, and Charles Zhu. Thanks to Jean-Loïc Le Carrou of the Université du Maine for allowing the use of figures from his PhD thesis. I am also happy to note that I have learned a great deal from Vancouver harpists Mehlinda Heartt, Lori Pappajohn, and Elizabeth Volpé-Bligh, and from Walter Bresch, late harpmaker of Surrey, BC.

References

- Barbieri P (2006) Roman and Neapolitan gut strings, 1550–1950. *The Galpin Society Journal* **LIX**, 147–181.
- Bell AJ (1997) The Helmholtz resonance and higher air modes of the harp soundbox. *Catgut Acoustical Society Journal* **3**, 2–8.
- Bell AJ, Firth IM (1989) The directivity of the concert harp. *Acustica* **69**, 26–30.
- Bordas C (1987) The double harp in Spain from the 16th to 18th centuries. *Early Music* **15**, 148–163.
- Caldersmith G (1978) Guitar as a reflex enclosure. *Journal of Acoustical Society of America* **63**, 1566–1575.
- Erkut C, Karjalainen M, Huang P, Välimäki V (2002) Acoustical analysis and model-based sound synthesis of the kantele. *Journal of Acoustical Society of America* **112**, 1681–1691.
- Firth IM (1977) Acoustics of the harp. *Acustica* **37**, 139–147.
- Firth IM (1988) Harp strings of the 18th century. *Catgut Acoustical Society Journal* **1**, 19–23.
- Firth IM (1989) Harps of the Baroque period. *Catgut Acoustical Society Journal* **1**, 52–61.
- Firth IM, Bell AJ (1985) On the acoustics of the concert harp's soundboard and soundbox. In: *Proceedings of SMAC 83 Conference*, Stockholm: Royal Swedish Academy of Music, pp. 167–183.
- Firth IM, Bell AJ (1988) Acoustic effects of wood veneering on the soundboards of harps. *Acustica* **66**, 114–116.
- Firth I, Bain R, Gallaher A (1986) String design equations. *Catgut Acoustical Society Journal* **46**, 3–6.
- Gautier F, Dauchez N (2004) Acoustic intensity measurement of the sound field radiated by a concert harp. *Applied Acoustics* **65**, 1221–1231.
- Hadaway R (1980) The re-creation of an Italian Renaissance harp. *Early Music* **8**, 59–62.
- Hobrough T (1980) Early harp attitudes. *Early Music* **8**, 507–508.
- von Hornbostel EM, Sachs C (1914) Systematik der musikinstrumente. *Zeitschrift für Ethnologie* **46**, 553–590.
- Kastner A (1909) The harp. In: *Proceedings of the Musical Association, 35th Session*, pp. 1–14.
- Kinsler LE, Frey AR, Coppens AB, Sanders JV (1999) *Fundamentals of Acoustics*. New York: John Wiley.
- Le Carrou JL (2006) Vibro-acoustique de la harpe de concert. PhD thesis, L'Université du Maine, Le Mans, France. *Journal of Acoustical Society of America* **121** 559–567.
- Le Carrou JL, Gautier F, Dauchez N, Gilbert J (2005a) Modelling of sympathetic string vibrations. *Acta Acustica/Acoustica* **91**, 277–288.
- Le Carrou JL, Gautier F, Dauchez N, Gilbert J, Arruda JR. de F. (2006) Low-frequency model of the sound radiated by a concert harp. In: *Proceedings of Forum Acusticum*, Budapest.
- Le Carrou JL, Gautier F, Kerjan F, Gilbert J (2007) The finger-string interaction in the concert harp. In: *Proceedings of ISMA 2007*, Barcelona, Spain.
- Morrow M (1979) The Renaissance harp. *Early Music* **7**, 499–510.
- Otake K, Aoyama K (2007) Aoyama Musical Instrument Manufacturing Company, private communication.
- Rensch R (1972) Development of the medieval harp. *Gesta* **11**, 27–36.
- Rensch R (1998) *Harps and Harpists*. Bloomington, IN: Indiana University Press.
- Rimmer J (1965) The morphology of the triple harp. *The Galpin Society Journal* **XVIII**, 90–103; The morphology of the triple harp II: addendum on a Late Italian example. *The Galpin Society Journal* **XIX**, 61–64.
- Waltham C, Kotlicki A (2008) Vibrational characteristics of harp soundboards. *Journal of Acoustical Society of America* **124**, 1774–1780.
- Weinreich G (1993) What science knows about violins and what it doesn't know. *American Journal of Physics* **61**, 1067–1077.

Chapter 10

Burmese Arched Harp

Robert M. Williamson

Our knowledge of the history, construction, and tunings of the Burmese arched harp (*saìng gauk*) comes from a variety of sources. Conversations with master harpists, together with recordings made of their performances between 1960 and 1980, provide richly detailed examples of the effect of Western music on a non-Western musical tradition. Scholars' essays and conference proceedings complement these first-hand accounts, expanding our understanding of Burmese music and musical instruments.

10.1 History

Prior to the nineteenth century, the Burmese harp was used only for chamber music at the royal court, where it was the most prized of the court instruments. It was employed as solo instrument, in ensembles, and to accompany singers. The most notable harpists held posts at court, and they wrote many of the classical songs that are a major part of the harp repertoire. Members of the royal family who mastered the harp are notable in Burmese history. The Burmese harp tradition “seems to be unique as a classical ancient harp tradition still alive today” (Emmert and Minegishi 1988, p. 257).

Burmese classical songs are part of the chamber music (*saìng*) tradition. The singer, who may be accompanied by a harp or a xylophone (*pattala*), controls the time with small hand cymbals (*si*) and a castanet (*wa*) (Fig. 10.1). These structured, strongly pentatonic songs are performed everywhere in the country by small orchestras and are familiar to most Burmese. Enthusiastically raucous orchestral music comprises a separate (*hsaing*) tradition.

Archeological evidence suggests that the arched harp came to Burma from India prior to AD 800, but there is no linguistic evidence to support this. Figures in a

R.M. Williamson (✉)

Department of Physics, Oakland University, Rochester, MI 48309-4401, USA (retired)
e-mail: williamson23@aol.com



Fig. 10.1 The harpist Daw Khin May and singer U Ba Thin, who holds small hand cymbals and a castanet. Their memories are aided by song-texts (photo taken in Mandalay in 1961 by R.C. Williamson)

Burmese temple relief dated about AD 1090 indicate that the arched harp was in use during the Pagan dynasty. In the early 1800s, the court harpist, Myawadi Wungyi (1766–1853), increased the number of strings from 7 to 13, so that the notes spanned about two-and-a-half octaves, from about C3 to F5. The last court harpist, U Maung Maung Gyi (1855–1933), added a 14th harp string, and the noted harpist U Ba Than created a 16-string harp tuning in the mid-1950s.

The Burmese have no indigenous musical notation. The melodies of their classical songs have been transmitted orally through generations of musicians, whose memories are supplemented by song-texts in which some of the words imply the intervals to be played by the accompanist. Daw Khin May (1911–1964), a pupil of the last court harpist, became the first staff harpist at the State School of Fine Arts in Mandalay, which was established in 1953 to teach and maintain classical Burmese music and dance. She was followed in that post by her distinguished pupil, U Myint Maung. Muriel Williamson, who had the good fortune to be in Mandalay from 1958 to 1962 – just before the country was closed to outsiders – studied the harp and its classical songs with Daw May and consulted widely with other Burmese musicians and scholars. Most of this chapter is a summary of her information about the harp (Williamson 2000a).

10.2 Construction and Playing Techniques

The Burmese arched harp is visually stunning. Its black lacquered, boat-shaped body (resonator) is roughly horizontal, trimmed with an amount of gold leaf and colored stones dictated by the budget and taste of the purchaser. Its dimensions are

about 80 cm × 16 cm × 16 cm. (Ladies' harps are somewhat smaller, though skilled female harpists play full-sized harps.) The top of the harp's body is covered with red-lacquered deerskin, tightly stretched over and around a longitudinal center rib. Sound holes in the cover give an air resonance in the mid-range of the harp frequencies (Lawergren 1981). Thirteen to sixteen silk or nylon strings run from a longitudinal center rib to the gracefully curved, brown varnished neck of the harp, which rises about 60 cm from the front of the body. The strings are attached to the neck by red cords that end in decorative tassels. The wrapped cords are tightened or loosened to tune the harp (Williamson 1968; Emmert and Minegishi 1988). Skilled harpists can tune with a precision comparable to that of Western string players.

The harp is held in the lap. The strings are stroked upward, with the forefinger or thumb of the right hand moving from the shorter strings to the longer ones. This leads to a natural sequence of descending notes, as opposed to the ascending notes of Western harps. A string may also be plucked outward, perpendicular to the plane of the strings. The fingers of the left hand are braced against the neck of the harp so that the thumb can press a string to increase its tension and pitch, creating what are called stopped tones. The left hand is also used to dampen a string.

10.3 Scales and Tunings

The Burmese word for scale is translated as “set of seven tones.” The names for the seven scale notes are different in the chamber music and orchestra traditions. Western transcriptions associate the most important note (*Hnyin-lòn*, or *Hnyin*) with Western C. The pitch of *Hnyin* changed with time, and differed in the harp and orchestra traditions. Before the State School of Fine Arts decided in the 1950s that *Hnyin* should be tuned to Western C, this note was near D in the chamber music tradition and C in the orchestra tradition.

Although frequency measurements of Burmese fixed-pitch instruments vary a great deal, they suggest a scale similar to a Western diatonic scale, with the third and seventh notes lowered about a quarter-tone. It can be represented by the note set C D E* F G A B* C, in which the starred notes B* and E* are lowered about 50 cents. The approximate intervals between notes are 200, 150, 50, 200, 200, 150, and 150 cents (Khin Zaw 1941).

Burmese songs have well-defined modal structures and are classified into four divisions, according to the principal mode of the song. Because the harp tunings are pentatonic within each octave, the two missing tones are played as stopped tones. When moving from one song division to another, several harp strings are re-tuned so that the most important notes will be open-string tones. The tunings are named for the root of the principal modal scale of songs in that division. Master harpists now use compound tunings that allow them to play songs in all the divisions without re-tuning the harp.

The oldest songs are in Hnyìn-lòn (C) tuning; the three newer song divisions and tunings date from the early 1800s. The fourteen-string tunings with their traditional intonations are:

Hnyìn-lòn (C): B2* C3 – E3* F3 G3 – B3* C4 – E4* F4 G4 – B4* C5 D5 – F5
Auk-pyan (F): B2* C3 – E3* F3 – A3* B3* C4 – E4* F4 G4* – B4* C5 D5 – F5
Palè (B*): B2* C3 D3 – F3 G3 – B3* C4 D4 – F4 G4 – B4* C5 D5 – F5
Myin-zaiṅg (E*): B2* C3 – E3* F3 G3 – B3* C4 – E4* F4 G4 – B4* C5 – E5* F5

Only Auk-pyan tuning includes the note A* and all seven scale notes. In 1980, U Myint Maung sent Mrs. Williamson verbal descriptions and precisely played examples of these traditional harp tunings, together with the changes in intonation that were taking place due to the influence of Western music. The measured frequencies of his traditional tunings (Williamson 2000b) match in detail his statement that the notes B*, E*, and A* are distinctively Burmese and tuned about a quarter-tone below the Western notes. The descending fifths between D, G, C, and F and those between B*, E*, and A* are closely Western. Daw May's Hnyìn-lòn tuning sequences support these conclusions. She first tuned the C4 – B3* Burmese second, and then the other notes in fifths and octaves.

Frequency measurements of Daw May's recorded Hnyìn-lòn songs show that the stopped tone A is played as A-natural. In the newer song divisions, E* can be E-natural when played as a stopped tone. Thus, the traditional harp modal scales used the note set C D E*(E) F G A (A*) B* C, in which the intonations of two of the seven notes could be varied a quarter-tone. However, the historically important Hnyìn-lòn C modal scale had only the lowered third and seventh notes that probably characterized the scale of Burmese fixed-pitch instruments.

U Myint Maung learned the traditional intonations of the tunings from Daw May in 1956. Just four years later, she taught Muriel Williamson both the traditional Hnyìn-lòn tuning and revised versions of the three other tunings containing B-flat and E-flat. U Myint Maung remarked that harpists made a special effort to retain the traditional intonations only in Hnyìn-lòn and then performed the revised versions of the other three tunings. Noting that present-day harpists used only the C-major scale notes in all tunings, he went on to demonstrate these modern versions of all four tunings and several compound tunings. Measurements of all three versions (traditional, revised, and modern) of the tunings confirm in detail U Myint Maung's descriptions of the changes that had taken place.

10.4 Measurements of Plucked Tones

The perceived pitch of a plucked tone comes from the slowly decaying vibrations that follow the short frequency burst following the pluck. In order to measure these vibrations, I used a visual stroboscopic method to compare the recorded harp tone with a reference oscillator signal. About one-and-a-half cycles of the two signals

were displayed on the traces of a dual-beam oscilloscope. Both traces were triggered by the reference oscillator. A tunable band pass filter was set to select the fundamental or an overtone of the harp tone. A reference frequency change of 1 Hz caused an easily visible change in the horizontal motion of the harp signal, corresponding to the musically insignificant interval of 6 cents at C4. Although my decision to use this method of measurement was heavily influenced by the equipment that was readily available in a college physics stockroom, this turned out to be an effective way to select the vibrations that determine pitch.

My measurements showed that U Myint Maung's octaves and fifths were within ± 10 cents of Western tempered values. These intervals in the tunings and songs of two other harpists varied by ± 15 cents. Their Burmese C – B* seconds varied from 130 to 170 cents, while those of U Myint Maung's ranged from 135 to 165 cents. The measured frequencies and verbal information show that harpists clearly distinguish the 50 cent difference between the Burmese and Western intonations of B*, E*, and A* that took place in the mid-1900s. The numbers 150 ± 15 and 200 ± 15 cents suffice to describe the unequal intervals of the traditional harp scales and clearly distinguish them from the 171 cent seconds of a seven-interval tempered scale, such as that found in the fixed pitch instruments of Thailand (Morton 1976).

Because of the need to temper the intervals of Burmese fixed-pitch instruments to accommodate different modal scales, the information from master harpists familiar with traditional intonations is the more sensitive evidence about them.

Acknowledgments I am indebted to Muriel Williamson for my interest in the Burmese harp and for recordings of its music. Because twenty-first-century Burmese musicians may no longer know the traditional intonations of the harp scale notes, the information provided by Daw Khin May and U Myint Maung is invaluable. John Okell shared his knowledge of Burmese music and provided the recording of U Myint Maung's tunings. Judith Becker has been generous with her advice and encouragement.

References

- Emmert, R. and Minegishi, Y. (1988). *Musical Voices of Asia*. Heibonsha, Tokyo.
- Khin Zaw, U. (1941). Burmese music. *Bulletin of the School of Oriental and African Studies* 10(3), 717–754.
- Lawergren, Bo. (1981). Acoustics and evolution of arched harps. *Galpin Society Journal* 34, 110–129.
- Morton, D. (1976). *The Traditional Music of Thailand*. University of California Press, Berkeley.
- Williamson, M.C. (1968). The construction and decoration of one Burmese harp. *Selected Reports: Instruments of Ethnomusicology* 1(2), 45–72.
- Williamson, M.C. (2000a). *The Burmese Harp: Its Classical Music, Tunings, and Modes*. SE Asia Publications, Northern Illinois University, DeKalb, IL.
- Williamson, R.M. (2000b). Burmese harp scale pitch measurements. In: Williamson, M.C., *The Burmese Harp: Its Classical Music, Tunings, and Modes* (2000), SE Asia Publications, Northern Illinois University, DeKalb, IL, pp. 131–153.

Chapter 11

Plucked String Instruments in Asia

Shigeru Yoshikawa

In this chapter some distinct characteristics of the plucked string instruments from Asia will be discussed in relation to those from the West. Primary attention will be paid to the interrelation between the instrument wood material, the playing style, and the resulting sound. It will be demonstrated that the philosophy of making string instruments is definitely different in Asia and the Western countries.

11.1 Classification of Asian Musical Instruments Based on Construction Material

Western musical instruments are usually classified according to the method used to produce sound. Wind instruments are divided into three groups (air jet instruments, reed woodwind instruments, and brass instruments) based on the type of sound-producing sources (air jet, reed, and lips). String instruments are also divided into three groups (plucked instruments, struck instruments, and bowed instruments) by the playing methods (plucking, striking, and bowing).

On the other hand, musical instruments in ancient China were classified according to their material. Such a traditional classification was called *eight sounds* (*hachi'in*, or *hachion*, in Japanese). Eight different sounds are produced by eight kinds of materials: metal, stone, thread, bamboo, gourd, earth, skin, and wood. Of course, the material is considered to be important in the West as known from *brass* instruments, *woodwind* instruments, and *string* instruments. However, in China one thinks that the variety of materials used for musical instruments is mutually making a world of sounds, and thus the harmony of the universe is realized.

This Asian musical philosophy is essentially different from the Western philosophy. Therefore, it seems to be appropriate to begin our discussion with wood material for Asian stringed instruments. A very fundamental structure of

S. Yoshikawa (✉)

Graduate School of Kyushu University, 4-9-1 Shiobaru, Minami-ku, Fukuoka 815-8540, Japan
e-mail: shig@design.kyushu-u.ac.jp

string instruments in both the Asian and Western worlds is a box – a sound hole structure, which is commonly seen in the clavichord, harpsichord, guitar, and violin. The box usually consists of top plate, side plate, and back plate. The top plate is the sound board that radiates sound due to its vibration. The side and back plates work as the frame board that supports the vibration of the top plate and forms the cavity for air resonance, the effect of which is radiated from the sound hole(s). As a result, wood material for string instruments should be categorized into two groups: wood for the soundboard and wood for the frame board. It should be noted that the sound board is the prime sound radiator, and the frame board is not usually a significant sound radiator except for the back plate of the violin family, where the back plate is tightly connected with the top plate via the sound post. However, that is not always the case with Asian stringed instruments as shown in Sections. 11.3 and 11.4.

Table 11.1 summarizes fundamental wood properties (the density ρ , Young's modulus E along the grain, and the quality factor Q of the resonance) of traditional and typical woods used for string instruments with the best quality (Yoshikawa 2007).

Norway spruce (*Picea abies*) and Sitka spruce (*Picea sitchensis*) are used for the violin top plate, the piano sound board, the guitar top plate, etc., because of their excellent vibrational properties, as will be explained later. The *paulownia* (*Paulownia tomentosa*; *kiri* in Japanese) is the best for the Japanese 13-stringed long zither, *koto* (or *soh*). The *mulberry* (*Morus alba*; *kuwa* in Japanese) has been traditionally used for the Japanese four-stringed lute, *Satsuma biwa* (for its whole body including top and shell-like back plates). On the other hand, four other woods are for frame boards. That is, Norway maple (*Acer platanoides*) and Japanese maple (*Acer* sp.; *kaede* in Japanese) are used for the violin back plate. The *amboyna wood* (*Pterocarpus indicus*; *karin* in Japanese) is the best for the body and neck of the Japanese three-stringed lute, *shamisen*. The Brazilian/Rio rosewood (*Dalbergia nigra*; often called *jacaranda*) is the best-quality wood for the guitar back and side plates. Note that numerical data are taken from Yoshikawa (2007), Haines (1979), and Aizawa (1998).

Table 11.1 Physical properties of traditional woods for stringed instruments (Yoshikawa 2007)

Wood name	f (Hz)	ρ (kg/m ³)	E (GPa)	Q	c (m/s)	ρ/c (kg/m ⁴)	cQ (10 ⁵ m/s)
Norway spruce ^a	532	560	16	116	5,300	0.11	6.2
Sitka spruce ^a	484	470	12	131	5,100	0.092	6.7
Sitka spruce ^b	617	408	10.0	144	4,940	0.083	7.1
Paulownia ^b	569	260	7.3	170	5,300	0.049	9.0
Mulberry ^c	447	647	6.3	70	3,130	0.21	2.2
Norway maple ^a	470	620	9.8	85	4,000	0.16	3.4
Japanese maple ^b	447	695	11.8	122	4,110	0.17	5.0
Amboyna wood ^b	519	873	20.0	155	4,770	0.18	7.4
Brazilian/Rio rosewood ^a	354	830	17	185	4,400	0.19	8.1

^aHaines (1979)

^bAizawa (1998)

^cYoshikawa (2007)

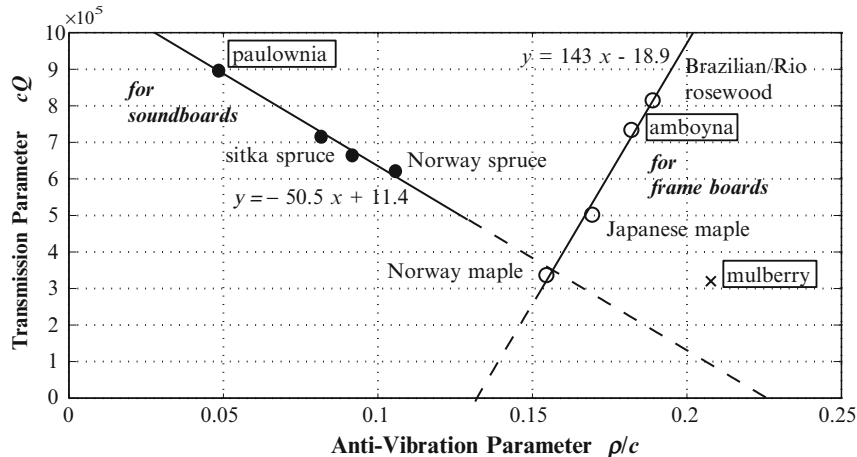


Fig. 11.1 Classification diagram of traditional string-instrument woods (Yoshikawa 2007). Full circles indicate soundboard woods; open circles indicate frame-board woods. Wood names for Japanese string instruments are enclosed by rectangles. Note that the mulberry is used for the top and back plates of the Satsuma biwa

Based on fundamental wood constants given in Table 11.1, a classification diagram of woods for string instruments is illustrated in Fig. 11.1 (Yoshikawa 2007). The abscissa is the *antivibration parameter* ρ/c [c is the propagation speed of the longitudinal wave along the gain; $c = (E/\rho)^{1/2}$]; the ordinate is the *transmission parameter* cQ . Schelleng (1963) derived the constancy of the inverse of ρ/c by considering that both stiffness and inertia of the plate should be invariant between different woods if their vibrational property remains unchanged. Because the vibration of wood plate produces sound radiation, Haines (1979) called the *vibration parameter* c/ρ the “radiation ratio.” The higher c/ρ , the greater the vibration and radiation. In this figure the wood names for Japanese string instruments are marked by a rectangle.

Good radiators (sound boards) are good transmitters of vibration because the excitation is easily transmitted to the edges and corners. Such transmission characteristics can be represented by the inverse of attenuation constant of the longitudinal wave, which is approximately given by $2Q/k = 2cQ/\omega$, where k and ω denote the wave number and the angular frequency, respectively (Yoshikawa 2007). The ω (=2 π times the frequency f) indicates the frequency used to measure the mechanical properties of wood samples, but ω itself is not a property of the wood. Therefore, it should be appropriate to assume that cQ represents the transmission characteristic of wood if the measurement of wood properties is carried out at almost the same frequency.

The c and Q are usually measured by observing the first-mode bending vibration of strip-shaped sample plate with the free-free boundary condition (Obataya et al. 2000; Hearmon 1958). Depending on the sample size, the first-mode frequency (i.e., f) is about 500 Hz. Also, it must be noted that Q is the quality factor of the bending wave, while c is the speed of the longitudinal wave. However, Q

for vibrations along the grain is the same for longitudinal vibrations and bending vibrations if the frequency is the same and the modal vibration frequency is not too high. From now on we call cQ (instead of cQ/ω) the *transmission parameter*.

Four points of sound board wood (except for the mulberry) form a regression line with a negative slope ($y = -50.5x + 11.4$ for $x = \rho/c$ and $y = cQ/10^5$) in Fig. 11.1. These points extend over a narrow range, $0.05 < x < 0.11$ and $6.2 < y < 9.0$. On the other hand, four points of frame-board wood form another regression line with a positive slope ($y = 143x - 18.9$). These points have a narrower range of x ($0.16 < x < 0.19$), but have a wider range of y ($3.4 < y < 8.1$). It is well understood that two parameters ρ/c and cQ clearly separate soundboard wood from frame-board wood.

Interestingly enough, the point of Norway maple almost corresponds to the intersection of these two lines. This implies that Norway maple has unique acoustical properties that make it suitable for both sound boards and frame boards. Such properties are very desirable for the violin back plate. However, mulberry wood lies outside the traditional wood groups, and its position opposite Sitka spruce and Norway spruce with respect to the line with a positive slope for frame boards may seem puzzling.

The idiosyncrasies of mulberry for the Japanese *Satsuma biwa* will be discussed in the next section. Although the amboyna for the Japanese shamisen is in the Western category of frame-board wood, it should be noted that the shamisen's primary vibrator is the cat skin stretched over both sides of the amboyna body. Also, the paulownia for the Japanese koto lies at the leftmost and uppermost of the regression line for sound boards. It will be demonstrated that this kind of wood property is necessary to the koto.

Importantly, the above two regression lines can serve as a reference to select the best substitute woods when traditional woods are not available. In addition, they can guide the design of better-quality artificial composite substitutes for stringed-instrument woods. More detailed discussion is given in Yoshikawa (2007).

11.2 Japanese Satsuma Biwa

There are several kinds of the Japanese biwa. In this section only the *Satsuma biwa* ("Satsuma" is the old name of the southernmost prefecture in Kyushu) of Fig. 11.2 is specifically treated. Fundamentally, it consists of four strings and four frets (called *chuh*, or *juh*, in Japanese, meaning "post"). Its length is less than 1 m. The tuning of four strings depends on the player's voice register. Examples are (1) C3# (about 139 Hz), G2# (104 Hz), C3# (139 Hz), G3# (208 Hz) and (2) A3 (220 Hz), E3 (165 Hz), A3 (220 Hz), E4 (330 Hz). Because the fret is high and the distance between two frets is long, the string tension is relatively freely changed by the pressing force of the player's left-hand fingers. It is thus not difficult for excellent players to produce tones with an interval of a fourth or fifth by fixing the finger position and by subtly adjusting the string tension. Also, the fret width is large, and

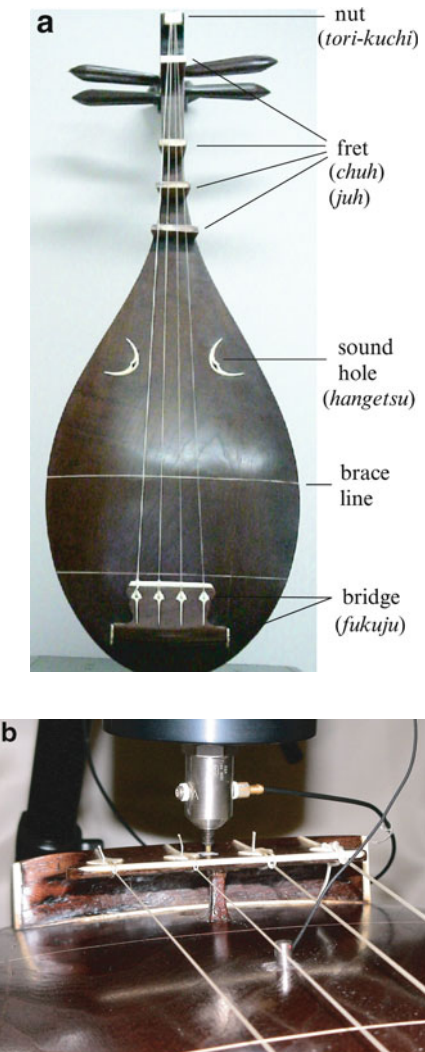


Fig. 11.2 Fundamental biwa structure. (a) A photo of the Satsuma biwa. (b) A setup for the mobility measurement (Yoshikawa et al. 2008). The driving point is at the middle of the bridge (*fukuju*) and right over the post fixed between the bridge and the top plate. An impedance head is inserted between a mini-shaker and the bridge. A small nail is used as the contact point to the bridge. A tiny accelerometer to measure the transmission mobility is seen on the *right-hand side*

this serves to produce the *sawari* (meaning “gentle touch”) sound, as will be explained later.

The Chinese *pipa* (or *p'i-p'a*) is completely different from the Satsuma biwa and is relatively closer to the Western lutes like the guitar family, although the pipa should be the root of the Japanese biwa. Strangely enough, there is no plucked lute

family in Korea. There is an excellent and intensive research book on the Satsuma biwa by Heinz-Eberhard Schmitz (1994) from the viewpoint of musicology. Also, an excellent Japanese biwa player, Kakuryo Tohnai has written a book from historical and acoustical viewpoints (1998).

11.2.1 Structural Response

Physical properties of wood are directly reflected in structural responses of wood against the vibration excitation. A biwa string is extended between a nut (called *tori-kuchi* in Japanese, meaning a bird bill) and a bridge (called *fukuju*, meaning a covering hand). Because string vibration is transformed to the top-plate vibration at the bridge, the driving-point mobility (i.e., the ratio of the vibration velocity v to the driving force F measured at the driving point) at the bridge well represents the structural response of the biwa. Usually v is given by integrating the output of an accelerometer. See Fig. 11.2b for a setup of an impedance head inserted between a shaker and a driving point.

Note that a short post connects the bridge with the top plate as shown in Fig. 11.2b. The driving point is located right over this post. A small accelerometer for the transmission mobility measurement is also seen in Fig. 11.2b. It lies on the vertical centerline of the top plate and about 60 mm below a solid brace that is horizontally built under the top plate near its middle. The location of this brace is usually indicated as a white line on the top plate (cf. Fig. 11.2b). Because the body is made by gouging out a thick plate of mulberry, it is impossible to divide it into back and side plates as in the guitar (the biwa body is called the *shell*).

Measurement results (Yoshikawa et al. 2008) are illustrated in Fig. 11.3. The ordinates of Fig. 11.3a, b indicate $20 \log|Y_d|$ and $20 \log|Y_t|$, respectively, where the driving-point mobility Y_d is the ratio of the vibration velocity at the driving point v_d to the driving force F_d , and the transmission mobility Y_t is the ratio of the vibration velocity at the transmission point v_t to the driving force F_d . The values of Y_d and Y_t are calibrated based on the transducer sensitivities. Therefore, the ordinate values correspond to the calibrated absolute values. The transmission point is given by the position of a small accelerometer shown in Fig. 11.2b. Also, Fig. 11.3c, which plots $20 \log|Y_t/Y_d|$, shows the difference between Fig. 11.3b and Fig. 11.3a. Because $Y_t/Y_d = v_t/v_d$, the curve of Fig. 11.3c can suggest the loops or nodes of normal mode vibrations and the resulting sound radiation characteristic of the top plate.

The Satsuma biwa shows a few strong peaks of the bridge mobility between 500 Hz and 3 kHz as depicted in Fig. 11.3a. On the other hand, the bridge mobility of the cello always shows a few sharp peaks below 500 Hz (Yoshikawa et al. 2008; Woodhouse 1993). This difference in the bridge mobility well reflects the difference in the philosophy of instrument making based on different wood material in Asia and the West. The fundamental component is significantly stressed in Western string instruments; higher frequency (harmonic) components are emphasized in

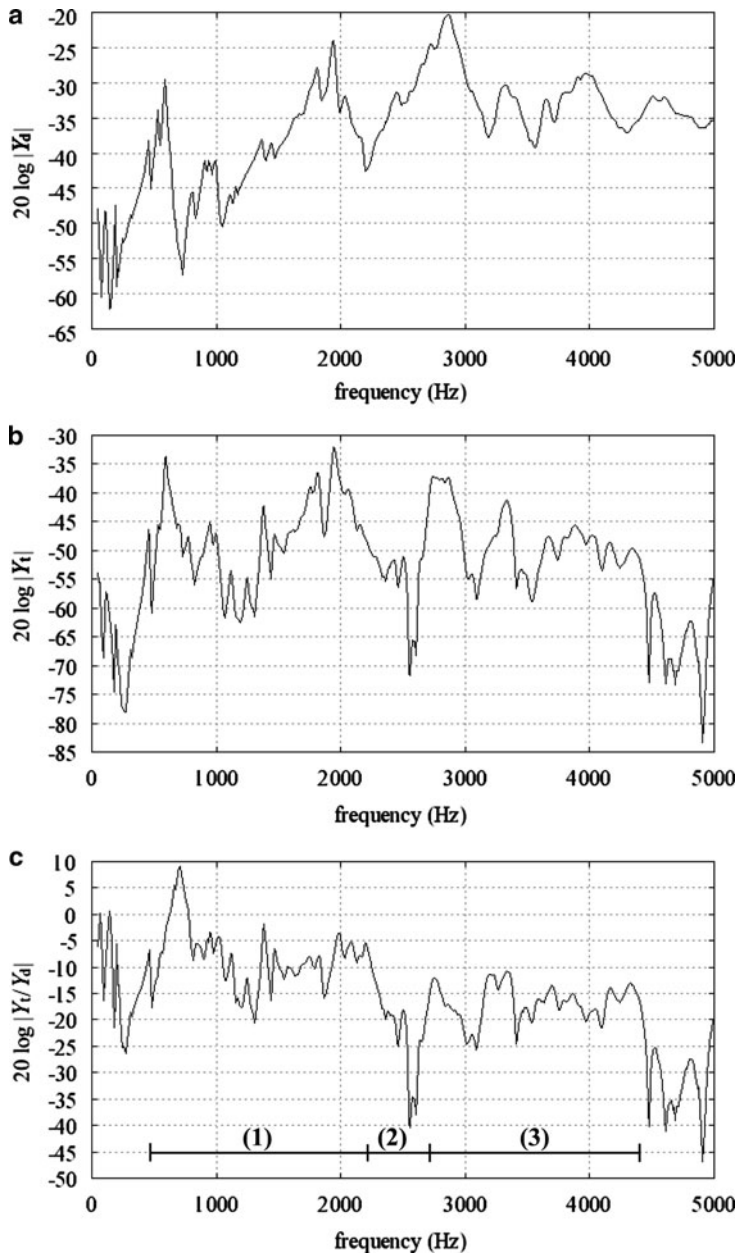


Fig. 11.3 Mobilities of the Japanese Satsuma biwa (Yoshikawa et al. 2008). (a) The driving-point mobility measured on the bridge. (b) The transmission mobility. (c) The difference between (b) and (a). Three important frequency bands are indicated in (c)

Asian ones. A more detailed structure of this high-frequency emphasis in Asian stringed instruments is explained below.

There are three distinct and broad peaks in Fig. 11.3a. The centers of these peaks lie near 600, 1,900, and 2,800 Hz. Also, from Fig. 11.3b, c the vibration response of the top plate seems to be divided by a very deep dip at around 2.6 kHz, which is possibly given by a certain vibration node formed near the acceleration position. Because there is a dip near 2.2 kHz in Fig. 11.3a, a frequency band of weak response, which is denoted as (2) in Fig. 11.3c, can be formed between about 2.2 and 2.7 kHz. The frequency range below this weak response band, which is extended from about 0.4 to about 2.2 kHz, probably yields stronger responses and sustains the resulting sound [see band (1) in Fig. 11.3c]. In addition, a higher-frequency band (3) above the weak response band (2) can sustain the sound, though the relative strength is about 10 dB less than that in the lower-frequency band (1).

According to Taguti and Tohnai (2006), the *fukuju* itself of the Satsuma biwa tends to have three resonant peaks (near 1.0, 1.4, and 2.1 kHz) and two dips (near 0.5 and 2.0 kHz). If we may consider that these peak frequencies are raised by about 0.5 kHz when the *fukuju* (bridge) is integrated onto the biwa body, we can have two broad peaks near 1.9 and 2.8 kHz in Fig. 11.3a. Small peaks near 1.5 kHz in Fig. 11.3a may be attributed from the bridge resonance near 1.0 kHz. Thus, the main structural response of the Satsuma biwa used for the experiment is formed by the top-plate resonances below about 1 kHz and the bridge resonances extending from about 1.5 to 4.5 kHz. In relation to the resulting sound explained in Sect. 11.2.3, the three frequency bands indicated in Fig. 11.3c are important:

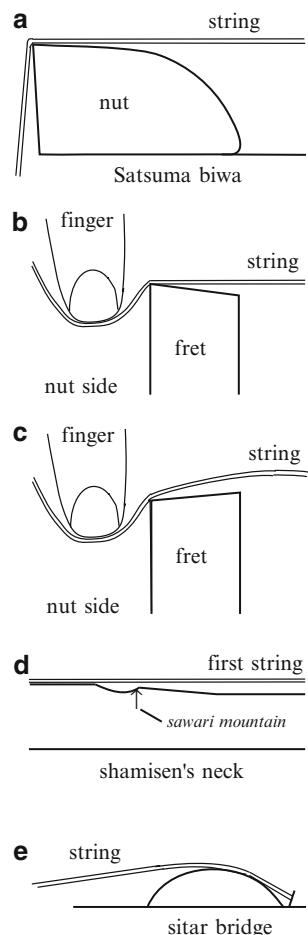
1. a primary sound-sustaining band (0.4–2.2 kHz)
2. a sound-suppressing band (2.2–2.7 kHz)
3. a secondary sound-sustaining band (2.7–4.5 kHz)

11.2.2 Sawari Mechanisms and Their Effects on High-Frequency Emphasis

The whole structure of the Satsuma biwa is constructed to support higher-frequency components above 500 Hz, as explained in the previous subsection. However, this does not work well unless such higher frequencies are created in the string vibration. The vibration amplitude of the plucked string depends on the harmonic order n , and the n th harmonic amplitude decreases as strongly as $1/n^2$. Therefore, some mechanism is needed to create an acoustical emphasis in higher frequencies. The sawari is such a mechanism creating a reverberating high-frequency emphasis.

The sawari is applied to all of biwa tones, that is, to four frets and a nut. However, the shapes of the nut and fret are different from each other. Four strings are gathered at the nut. This nut, which is made of ivory, is called *tori-kuchi* or *shohgen* (or *johgen*, meaning “to get the strings on”). The nut surface is slightly curved as shown in Fig. 11.4a. As a vibrating string gently touches this surface at

Fig. 11.4 Examples of *sawari* mechanisms: (a) *nut-sawari* (*shohgen-sawari*) in the Satsuma biwa (Schmitz 1994; Tohnai 1998; Ando 1996); (b) *fret-sawari* of Kyushu type in the Satsuma biwa, suitable for soft and flexible strings (Schmitz 1994; Tohnai 1998); (c) *fret-sawari* of Tokyo type in the Satsuma biwa, suitable for hard and stiff strings (Schmitz 1994; Tohnai 1998); (d) *nut-sawari* in the shamisen (Ando 1996); (e) *bridge-sawari* (*jawari*) in the Indian sitar (Fletcher and Rossing 1998)



some vibration amplitude, a kind of reverberation is followed with an emphasis of higher frequencies. The degree of this *reverberation* (meaning both an extension of the decay time and an emphasis of higher harmonics in the plucked string sound) depends primarily on the inclination of the curved surface and secondly on the thickness of the string. Also, inharmonic higher frequencies (a kind of noise) are generated. Too strong *sawari* tones tend to be heard as “less refined” or “rough-hewn.” Although this *nut-sawari* (or *shohgen-sawari*) depends on the player’s taste, a subtle adjustment of the curved surface is carried out by a biwa maker with great care and originality.

On the other hand, there are two ways of attaching the *sawari* on the fret (Schmitz 1994; Tohnai 1998). As indicated in Fig. 11.4b, one way is to shave the bridge side of the fret surface. This type of *fret-sawari* is usually seen in the Kyushu area. Another way is to oppositely shave the nut side as depicted in Fig. 11.4c, which is seen in the Tokyo area (Tohnai 1998). It is said that this Tokyo-type of

fret-sawari was preferred by a world-famous master player, Kinshi Tsuruta (Tohnai 1998). The fret-sawari of the Kyushu type in Fig. 11.4b tends to form a much wider sawari clearance when a thick and stiff string is used as in the case of the first and second strings (Schmitz 1994). The Kyushu type can work well on the third and fourth strings because of their high flexibility. In any case, the inclination of the shaved surface is very subtle, and the inclination of the Kyushu type seems to be natural, although the selection of fret-sawari type may depend on the flexibility (or stiffness) of the string and the playing style.

Numerical simulations are appropriate to demonstrate the vibration of a string to one of whose boundaries a fret-sawari is applied. A string is fixed at another boundary, the bridge. For simplicity and ease of demonstration a fret-sawari is assumed to have a flat surface without any inclination and to have a large width ([Sendai and Toshikawa to be submitted](#)). A linear equation on the transverse wave propagating along a flexible string is discretized and solved using the fourth Runge–Kutta method to assure satisfying precision of calculation. For simplicity, the attenuation (temporal decay) of the string vibration is ignored. Numerical assumption is as follows: string length = 1.0 m, fundamental frequency of string vibration = 100 Hz, spatial discretization width (element number) = 2×10^{-4} m (5,000), and temporal discretization width (sampling frequency) = 0.0227 μ s (44.1 MHz). The initial conditions for the plucked string vibration are as follows: initial displacement = -10 mm at the plucking point of 0.2 m from the bridge, and initial velocity = 0.

Soon after the plucked vibration begins, a part of the string contacts with the sawari surface and receives a force from it. This situation resembles a point mass colliding upon the surface. Let us suppose that such a collision occurs at an instant at a point of the string. The velocity of this point mass will be changed from v to $-ev$, where e denotes the collision factor. If a perfect elasticity can be assumed to this collision, e should be 1.0 (real frets are made of very hard magnolia hypoleuca, *ho-no-ki* in Japanese). Although it takes some time for the string point-mass to exchange its momentum with the sawari surface due to the string's compressional deformation, such momentum exchange is supposed to occur momentarily ($e = 1.0$). Because it is essential to find out the instant when the string touches the sawari surface, a very high sampling frequency mentioned above is used.

The actual sawari width is about 10 mm. However, a sawari width of 100 mm is assumed for a clear visualization. The simulation result is shown in Fig. 11.5. The first frame of Fig. 11.5a indicates the initial displacement of the string ($t = 0$), where x denotes the axis along the string and y denotes the axis perpendicular to the top plate and the sawari surface. Usually a guitar string is plucked to the direction (z) parallel to the top plate, but a biwa string is plucked to the y direction. Two frames (a) and (b) depict the string vibration without the sawari because the string is fixed to the right corner of the sawari surface. The string is then released from the sawari surface as depicted in frames (c) and (d). Frame (d) shows the instantaneous displacement at $t \approx T/2$, where T denotes the period of the string vibration. It should be noted that a secondary corner appears on the string near $x = 0.4$ m due to the initial boundary condition in which the string touches the whole of the sawari surface.

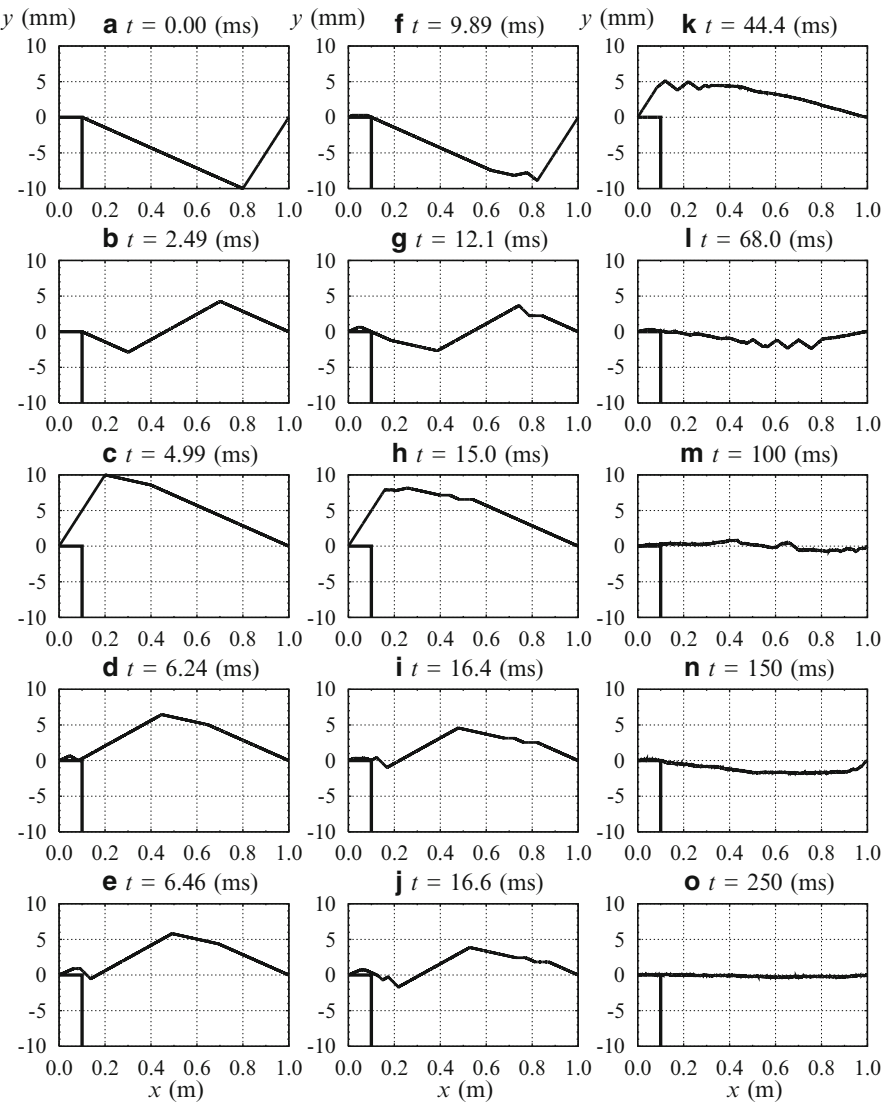


Fig. 11.5 Temporal change of the plucked string vibration ([Senda and Yoshikawa to be submitted](#)). The sawari extends from $x = 0$ to $x = 0.1$ m. The generation of the higher-frequency components is visualized as several small corners appearing on the string

The left segment of the string begins to move toward the right direction after this half a period at frame (d), and meanwhile it touches the sawari surface at a given angle. The repulsive collision between the string and the surface then yields a kind of wave over the surface as depicted in frame (e). The right edge of this wave with a half-wavelength propagates along the surface and is released from the surface as shown in frame (f), and is further moved to the right as shown in frame (g). At this instant we may recognize four corners along the string: an initial corner (near $x = 0.5$ m), a secondary corner (near $x = 0.75$ m), and two other corners (near $x = 0.2$ m). The collision process is still going on as depicted in frame (h). Then, the string returns to almost the same shape as the initial one at around $t = 9.89$ ms as shown in frame (i), where four corners are recognized between $0.1 < x < 1.0$ m (three corners near $x = 0.8$ m and another small corner near $x = 0.6$ m). We may thus say that three small corners are newly generated in a period of the vibration.

Frames (i)–(o) in the right column indicate the string shapes seen almost a period later than frames (a)–(g) on the left column, respectively. A closer look at the right-column frames lets us know the generation of more corners. There exist seven corners along the string in frame (l) and at least ten corners along the string in frame (p). We may thus understand that the collision between the string and the surface generates a few corners on the string every a period of vibration. Also, much smaller corners are possibly buried in the string as disturbances or fluctuations as inferred from frame (p). These appreciable corners and inappreciable disturbances, which have various wavelengths much shorter than the fundamental wavelength determined by the whole string length, produce the higher-frequency emphasis on the biwa sound.

Remember that the total energy of string vibration is conserved in our simulations. However, the vibration amplitude is seen decreased (cf. Fig. 11.5a, p). That is to say, the sawari mechanism transfers the energy of the fundamental to that of the higher frequencies through the string-surface collision process. See Taguti and Tohnai (2006) and Senda and Toshikawa (to be submitted) for more detailed discussions on the sawari mechanism. Also, Taguti (2001, 2005) has developed his numerical simulations from a different viewpoint including a coupling with body resonances.

Different sawari mechanisms are applied to the Japanese shamisen (see the next subsection for more details) and the Indian sitar as shown in Fig. 11.5d, e, respectively. Shamisen's sawari is not a *surface type* but a *point type*. The height of the sawari mountain is carefully adjusted to realize beautiful sawari sounds. Although sawari mechanisms appear on the nut or frets in the Japanese biwa and shamisen, those (*jawari* in Hindi) appear on the bridge in the Indian sitar and tambura (Fletcher and Rossing 1998). This interesting difference should be studied from the standpoints of both musical acoustics and musicology (Odaka and Yoshikawa 2006).

11.2.3 Examples of Characteristic Sounds

The Satsuma biwa has an aspect of a percussion instrument. This is attained by a very hard top plate made of mulberry and by a very large triangular wooden plectrum (called *bachi* in Japanese) made of boxwood (*tsuge* in Japanese). The plectrum often hits the top plate immediately after plucking the string. Poorness of body resonance is required to this striking play to avoid too-loud sounds, and the peculiarity of mulberry (low-resonance nature) is ideal to such a requirement as inferred from Fig. 11.1. An example of biwa's percussive sounds is shown in Fig. 11.6a.

An example of the fret-sawari sound (not striking the top plate) is illustrated in Fig. 11.6b. On this spectrogram it is seen that a reverberating effect is created in higher frequencies above about 3 kHz, which correspond to the secondary sound-sustaining band (2.7–4.5 kHz) in the structural response discussed in the previous subsection. The sounds of Fig. 11.6 were recorded in an anechoic room of Kyushu University when Doriano Sulis, the Italian biwa maker and player living in Fukuoka, played on his biwa shown in Fig. 11.2. Other sound examples are described in Schmitz (1994), Tohnai (1998), Ando (1996), Tohnai and Kishi (1993), and Taguti and Tohnai (2001). It is confirmed that the sawari mechanism

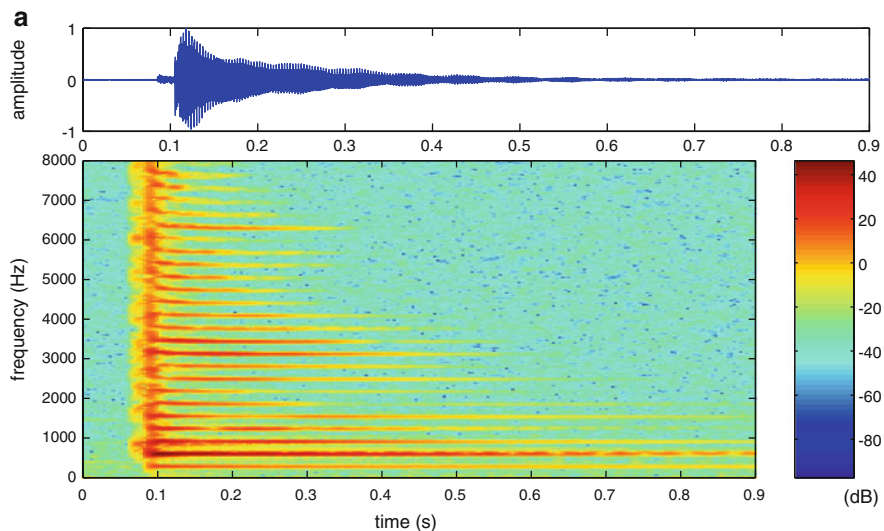


Fig. 11.6 Biwa sound examples (Yoshikawa et al. 2008): (a) a percussive sound when the top plate is struck after plucking a string by a large plectrum (an open fourth string G#3: 207 Hz); (b) a fret-sawari sound (on the fourth string and the third fret, D4: 295 Hz) using a sawari mechanism indicated in Fig. 11.4b

creates a characteristic emphasis of higher harmonics and an extension of the decay time in the plucked string sounds.

11.2.4 Brief Comparison with the Chinese Pipa

The Chinese pipa consists of four strings and many (over 20) frets. Strings are plucked by right-hand fingers or by a plastic pick. This presents a striking contrast to the Satsuma biwa, which has only four frets and where a large plectrum is used for the plucking. Although the pipa sounds are relatively close to the guitar sounds, a high-frequency (or higher-harmonic) emphasis is attained by the body structure of the pipa (Odaka 1998).

The top plate of the pipa is usually made of paulownia and the back shell is made of red sandalwood (close to amboyna) or maple. As inferred from Fig. 11.1, these two woods are very different from mulberry in vibrational properties. Some resonance modes of top plate are measured around 450, 550, and 650 Hz (Feng 1984). These mode frequencies are almost one or two octaves higher than the fundamental frequencies of four strings: A2 (110 Hz), D3 (147 Hz), E3 (165 Hz), and A3 (220 Hz). As a result, an enhancement of the second and third harmonics is realized in the pipa by adjusting mode frequencies of the top plate made of paulownia.

Summing up, Asians prefer the plucked string instrument sound with a high-frequency emphasis to that with a definite pitch given by a fundamental-frequency emphasis seen in the West. There are two ways for such an emphasis: (1) Harmonic enhancement is designed in the Chinese pipa by adjusting lower mode vibrations of the top plate, which is made of soft wood, paulownia. Harmonic enhancement is aimed at the second and third harmonics. (2) The higher-frequency emphasis is designed in the Japanese Satsuma biwa by inventing the sawari mechanisms to cover poor body resonance in lower frequencies. The biwa is made of hard wood, mulberry. The emphasis is reached to a much higher frequency range beyond the third harmonic of the fundamental.

11.3 Japanese Shamisen

The Japanese shamisen (meaning “three-stringed”), which has roots in the Chinese *sanxian* (Odaka 1998), has a long, unfretted wooden neck and a small body, the front and back of which are covered with white cat skin. A bridge is placed on this skin membrane. Strings are plucked by a relatively large (not so large as a biwa’s) plectrum. The cat skin is usually impacted immediately after the string plucking. The vibration of this tightly stretched skin membrane yields the characteristic sounds of the shamisen. Also, the shamisen’s neck and body are traditionally

made of amboyna, which is hard and not so vibrant, but which is excellent in vibration transmission as shown in Fig. 11.1. There are no long-neck lutes like the shamisen or the sanxian in Korea.

11.3.1 Shamisen as an Overall String–Bridge–Membrane System

An averaged spectral envelope obtained from about ten spectra of the shamisen tones indicates a triangular shape with a top located at about 700 Hz (the frequency analysis is carried out at about 40 ms after tonal buildup) (Ando 1996; Ando and Yamaguchi 1983). The fundamental frequencies of string vibration extend from about 140 to 400 Hz. Because a roll-off as much as -25 dB/oct is shown in the lower-frequency side of the envelope, the amplitude of the fundamental is remarkably small.

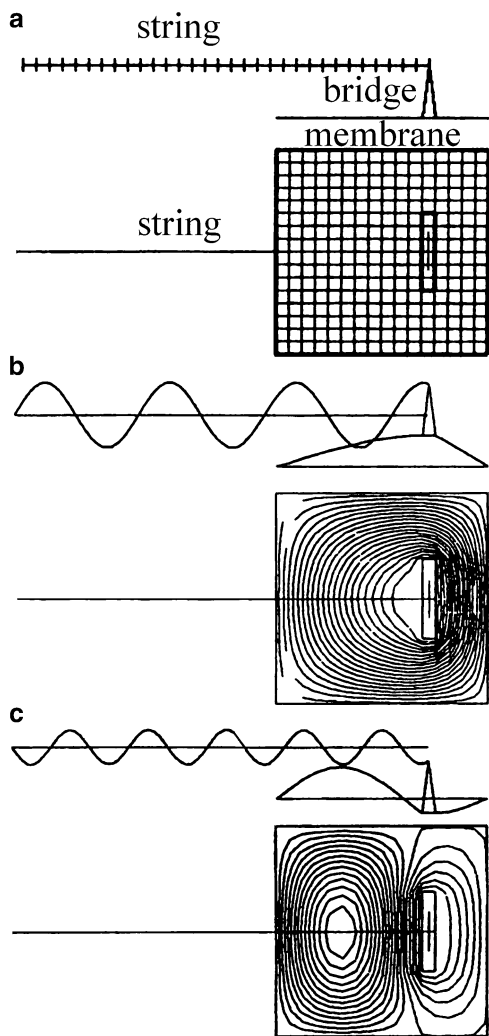
This result suggests that the shamisen may be modeled as a string–bridge–membrane system. The above peak frequency (700 Hz) probably corresponds to the strongest resonance of the overall system, which should be mainly determined by the resonance of the cat-skin membrane. Because the bridge and string move with the membrane, it can be recognized that the resulting sound consists of normal modes of this overall system. Viewing an instrument as a united system like this is very different from the Western traditional view that the instrument body is passively driven by the string vibration.

Takasawa (1993) analyzed such a total system based on the finite-difference method. Numerical data are summarized in Table 11.2. A side of the square membrane is divided into 16 elements and a string into 80 elements (cf. Fig. 11.7a). Numerical simulations show that the normal modes consist of (1) harmonic series of string vibration with the fundamental frequency of about 130 Hz and (2) resonance modes of the overall system (see Fig. 11.7b, c). The first overall resonance (about

Table 11.2 Numerical data for modal analysis of the shamisen as a string–bridge–membrane system (Reinecke 1973)

String	
Length	0.80 m
Density	0.002 kg/m
Tension	80 N
Wave velocity	200 m/s
Frequency	130 Hz
Membrane	
Size	$0.16 \text{ m} \times 0.16 \text{ m}$
Density	0.040 kg/m^2
Tension	2,000 N/m
Wave velocity	220 m/s
Frequency	970 Hz (1, 1) mode 1,500 Hz (1, 2) mode
Bridge	
Mass	0.002 kg
Bottom area	75 mm \times 6.0 mm

Fig. 11.7 Shamisen as an overall string–bridge–membrane vibratory system (Takasawa 1993): (a) discretization of the system elements; (b) the first resonance mode of the system near 840 Hz; (c) the second resonance mode of the system near 1,370 Hz



840 Hz) cuts in between the sixth and seventh harmonic of string vibration. The second overall resonance (about 1,370 Hz) cuts in between the 10th and 11th harmonic. As a result, the harmonics (from 6th to 11th in this simulation) closely lying between these two overall resonances are strongly emphasized and the harmonics far from these resonances are weakened correspondingly to their distance.

The bridge mass is considered to be important in determining the shamisen tone. This mass seriously affects the frequencies of the overall system resonance. According to simulations (Takasawa 1993), the decrease in the rate of these frequencies is about 10% with respect to an increase of 1 g in the bridge mass. Also, the bridge position affects the resonance frequencies. When the bridge is

moved toward the membrane edge (the string is lengthened), the first resonance is increased and the second resonance is decreased in frequency (i.e., the width between these resonances is decreased). Therefore, it seems to be reasonable that some professional shamisen players adjust the bridge position judging from the weather (particularly, the humidity) of the performance day.

Also, Horiuchi et al. (1994) analyzed the plucking motion of the plectrum from its beginning, and the correspondence with the resulting sound was studied.

11.3.2 Sawari and Its Effect on the Tuning

The shamisen has the sawari mechanism as indicated in Fig. 11.4d. The height of the sawari mountain seriously affects the resulting reverberating aftersound. Different from the biwa's sawari, the shamisen's nut-sawari is restricted to only the first (lowest) string. Nevertheless, when the vibrations of the second and third strings (usually tuned a fifth and an octave higher than the first string, respectively) are transmitted to the first string, the sawari effect is appreciable as the result of sympathetic resonance if the tuning is correctly done (Ando 1996). Receiving the

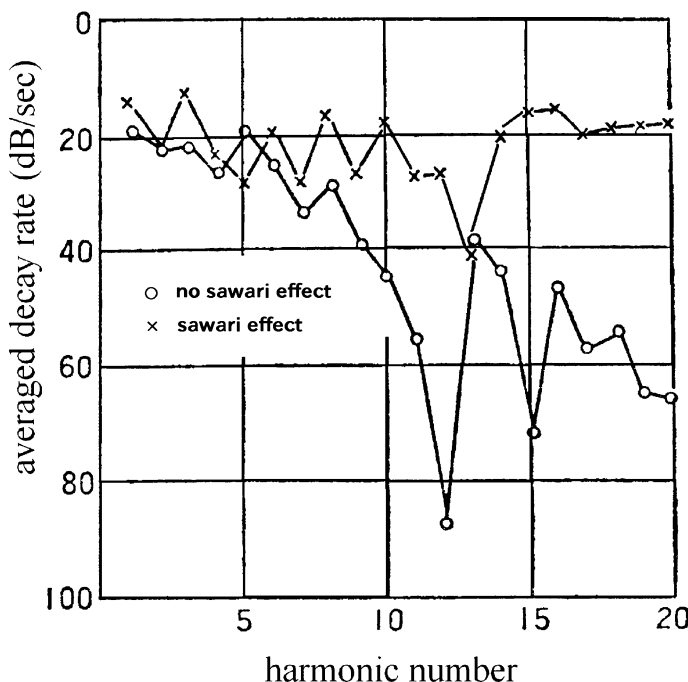


Fig. 11.8 Averaged decay rates (in dB/s) of the harmonics making up shamisen sounds in a lower register (open first string on the *gidayuh shamisen*) (Ando 1996). Open circle: without the effect of the sawari; cross sign: with the effect of the sawari

sawari on the second and third strings serves as a reference to judge whether the tuning is correct or not. The excellence of amboyna in vibration transmission serves very well to receive the sawari on the second and third strings. Amboyna is also the best material for a long neck to realize a very smooth movement of fingers on the strings.

According to Ando's intensive analytical study on the shamisen, it is understood that the sawari makes rich sounds followed with an emphasis on the higher harmonics, as indicated in Fig. 11.8 (Ando 1996). This figure compares the averaged decay rate of each harmonic when the sawari is taken and not taken on the first open string. In this case the harmonics above the eighth are strongly emphasized except for the 13th harmonic. Yako (1991) discussed some interrelations between the amplitude decay of sawari sounds and their perception from the viewpoint of musicology. Also, Ando (1996) stressed the importance of the generation of inharmonic components (above 2 kHz) in the shamisen's aftersound. He explained that such inharmonic components are caused by irregular fluctuations in sawari sounds due to an elliptic string motion with some disturbances as well as by a complex reaction from the membrane vibration to the string vibration through the bridge (cf. Sect. 11.3.1). Moreover, he stressed the indispensability of these noise-like inharmonic components (these themselves sound like cymbal tones) in synthesizing shamisen tones.

11.4 Japanese Koto and Korean Gayageum

The paulownia used for the Japanese long zither, *koto* or *soh*, is a material quite the opposite to the mulberry used for the Satsuma biwa as indicated in Fig. 11.1. The 13 strings, each about 1.5 m long, are stretched between two fixed bridges (called *ryuhaku* in Japanese). In addition, a movable bridge or fret (called *ji* in Japanese) is applied under each string for tuning. The right-hand sections of the strings produce a pentatonic scale, for example G3 A3 Bb4 D4 Eb4 (Ando 1989). Paulownia, which has a very smooth surface, is suitable for the movement of such a bridge on the top plate when a chord change is required during the performance (this may be the case in the Korean *gayageum*, Chinese *ch'in*, and *zheng*, too). Also, the koto strings are plucked with small plectra worn on three fingers (the thumb, index, and middle) of the right hand. Because this plucking is not so strong and the koto body is very large, the material must support vibration well to maintain the sound. The highly resonant nature of paulownia seems to be a relevant requirement. It should be noted that paulownia is better than spruce in both vibration (radiation) and transmission properties as illustrated in Fig. 11.1.

Interestingly, the thickness of the back plate is only about 11 mm, comparing with that of top plate, which is about 37 mm near the middle and about 30 mm at the edges. As a result, the radiation energy is higher from the back plate than from the top plate in the higher-frequency range (Ando 1996). This is a clear exception to instrument-making practice in the West. There are two sound holes near the edges of the back plate. Also, there are usually four ribs under the top plate. Within

the body a large air cavity is formed, about 1.8 m long, 0.25 m wide, and 75 mm thick at the center and about 40 mm thick at the edges.

Normal modes appear near 100 Hz [(0, 2) mode], 210 Hz [(0, 3) mode], 370 Hz [(0, 4) mode], 410 Hz, 450 Hz, 510 Hz, etc., on the top plate alone and near 50 Hz [(0, 2) mode], 80 Hz [(0, 4) mode], 130 Hz [(0, 5) mode], 180 Hz [(0, 6) mode] on the back plate alone (Ando 1996). Because the straight grain is not used for the top plate, mode vibrations above 410 Hz are not simple. When these top and back plates are attached to the koto, the above normal modes are shifted a little in frequency. Structural support of the fundamental and lower-frequency components by these plate normal modes is closer to the philosophy of instrument making in the West (Fletcher and Rossing 1998). This may be a significant reason why young Japanese people seem to easily remember koto sounds but forget biwa sounds (Yoshikawa 2004).

An example of koto sound is illustrated in Fig. 11.9. Its harmonic structure is closer to the Western string instrument sound (e.g., the harp sound) with an emphasis in lower harmonics below 4 kHz. However, it is observed that harmonics higher than 8 kHz usually appear as shown in Fig. 11.9c. This may be because small

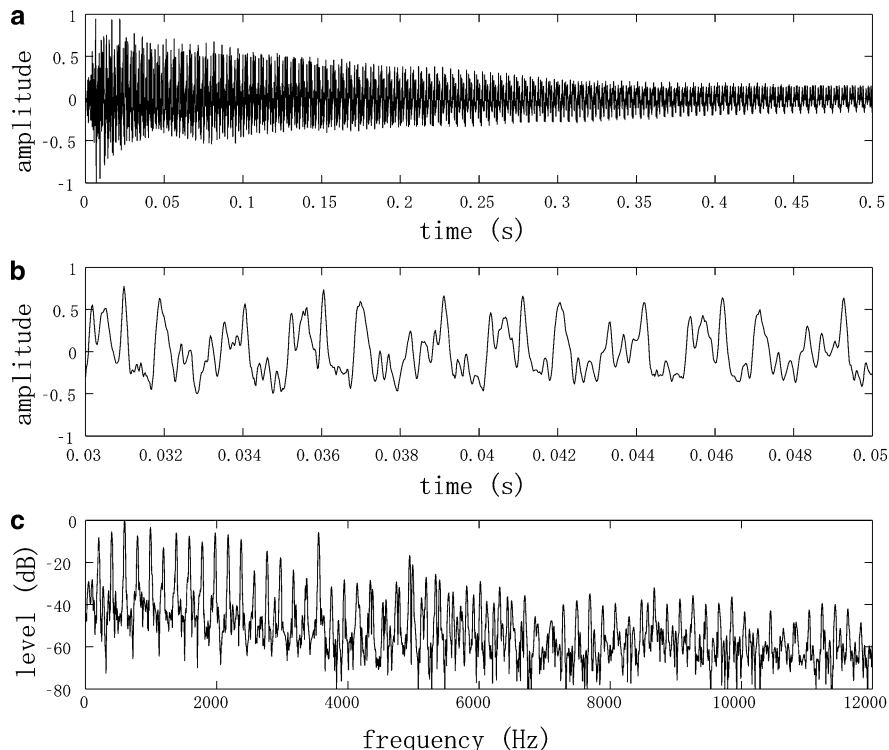


Fig. 11.9 A koto sound example provided by Tamaki Ando (2006). (a) Temporal waveform. (b) Temporal waveform expanded from $t = 0.03$ to 0.05 s. The waveform is very complicated due to higher frequency components. (c) FFT spectrum of the waveform between $t = 0.03$ and 0.13 s. The Hanning window is applied and the DFT point is 8,192

and hard plectrums made of ivory are used for the plucking instead of the player's fingernails (Ando 1996). This type of higher-frequency emphasis in the Japanese koto, which yields a sharp impression at the attack transient, is not usually observed in the Chinese 21-stringed *gu-zheng* and the Korean 12-stringed *gayageum* (Noh et al. 2002). Of course, because higher harmonics attenuate faster, the aftersound of the koto becomes close to that of the *gu-zheng*, *gayageum*, harp, etc.

An important problem of the koto is the difficulty in tuning (Ando 2006). This may be caused by the use of movable bridges, which divide the strings into two. The left-hand sections of the strings, which are not responsible for tuning, can affect the tuning of the sounding strings. Complicated string motion depending on the direction of the plucking (Woodhouse 2004) may be another cause. The complication of string motion may be inferred from Fig. 11.9c, where the single peak spectrum tends to change into a double-peak spectrum above about 4.5 kHz. Particularly, the spectrum structure around 6 kHz seems to be extraordinary.

There are several kinds of long-zither-type plucked string instruments in Korea. The *gayageum* is the most popular among them. It was developed by King Kasil in the Gaya kingdom in the sixth century, based on the Chinese *zheng* (Yoo and Rossing 2006). It is a little smaller than the Japanese *koto*, and has a body of about 1.6 m and a total of 12 silk strings. Also, it is usually played on the right leg of the player seating on the floor, although the Chinese *zheng* and *gu-zheng* players sit on the chair and the Japanese *koto* players usually sit on the floor in front of their instrument. The difference in this playing manner seems to be significant in producing sounds from these traditional instruments. The *geomungo* is a six-stringed instrument with 16 frets and is plucked with a small bamboo stick called a *suldae* (Yoo and Rossing 2006). Also, three strings are supported by the fixed bridges, while the other three strings rest on movable bridges. The *yanggeum* is a traditional Korean hammered dulcimer and it has metal strings. It is quite similar to the Chinese *yangqin* (Yoo and Rossing 2006).

The transfer function of the *anjok* (a movable bridge) of the *gayageum* has been recently investigated (Ko et al. 2006). The transfer function is defined as the ratio of the acceleration measured at the bridge foot to that measured at the bridge top where the driving impulse is given. A high-graded *anjok* that is made of cherry, which is compared with a medium-graded one made of walnut, and a low-graded *anjok* made from an unknown material, shows that the transfer function increases from 100 Hz to 1 kHz with a slope of about 10 dB/octave and has a very sharp dip near 900 Hz. This result is greatly different from the transfer function of a violin bridge, which shows a flat response from 100 Hz to about 2 kHz (Fletcher and Rossing 1998; Reinecke 1973). Because the lower harmonics of the *gayageum* extend from about 150 to 900 Hz, the ascending response of its transfer function yields an emphasis of the lower harmonics rather than the fundamental, just as with other Asian plucked string instruments.

The left-hand sections of the strings are also important to produce vibrato effects and interpolate semitones when the player presses these sections with the left hand. The pitch change by this technique is very drastic in the Korean *gayageum* with the help of relatively weak string tension, and this vibrato technique is called

nong-hyun (Noh et al. 2002). Such a characteristic pitch fluctuation as large as 80–130 cents is peculiar to Korean music, and is not found in Chinese and Japanese music. This character may make it difficult for Japanese young people to fully appreciate Korean music (Yoshikawa 2004).

11.5 Concluding Remarks

An overview of Asian plucked string instruments confirms that neither lutes with a short neck (such as the biwa and pipa) nor lutes with a long neck (such as the shamisen and sanxian) are used in traditional Korean music. This may be because the characteristic pitch fluctuation (bending) is created much less effectively on these lutes than on the long zither-type instruments such as the gayageum, which is played on the player's right leg. On the other hand, a high-frequency emphasis is more important in the traditional music of India, China, and Japan. Particularly, sawari mechanisms were invented for the Japanese biwa and shamisen, and jawari mechanisms were invented for the Indian sitar and tambura, to produce the unique reverberating high-frequency sounds of those instruments.

Why is such an emphasis on reverberating high-frequency sound significant in these countries? Of course, that there is a musical taste for such sounds is one answer. But another interesting reason seems to be hidden. A suggestion is furnished from research into the acoustics of ancient Greek and Roman amphitheaters (Declercq and Dekeyser 2007). The row of stairs (seats for the spectators) with a periodic distance and a slope diffracts the sound waves coming from the foreground of the orchestra (stage). The diffraction from this periodic structure yields a relative amplification of higher frequencies (usually above about 500 Hz) and a relative reduction of lower frequencies. Because the noise caused by the wind and chattering is dominated by the lower frequencies, this noise is depressed by the high-pass filter effect of the stair row. As a result, the higher frequencies rise up and are more easily heard by the audience.

Similarly, the Japanese biwa and Indian sitar were both usually played outside in the past, just on the ground, not in an amphitheater. The environment of their performance must have been quite noisy. Thus, we can conclude that the emphasis on high-frequency sound and long-time tonal sustenance by the sawari/jawari mechanisms was a countermeasure against environmental noise, that is, as an adaptation to the performance environment of the past (Odaka and Yoshikawa 2006).

References

- H. Aizawa, "Frequency dependence of vibration properties of wood in the longitudinal direction," Master's Thesis (Faculty of Engineering, Kyoto University, 1998) (in Japanese).
M. Ando, "Koto scales and tuning," J. Acoust. Soc. Jpn. (E) **10**, 279–287 (1989).

- Y. Ando, *Acoustics of Musical Instruments* (2nd ed., Ongaku-no-tomo-sha, Tokyo, 1996), pp. 193–216 (in Japanese).
- T. Ando, “On the factors for detecting mistuned conditions and guiding their corrections for the koto tuning,” *J. Acoust. Soc. Am.* **120**, 3119 (2006).
- S. Ando and K. Yamaguchi, “Considerations on physical characteristics of samisen tones,” *J. Acoust. Soc. Jpn.* **39**, 433–443 (1983) (in Japanese).
- N.F. Declercq and C.S.A. Dekeyser, “Acoustic diffraction effects at the Hellenistic amphitheater of Epidaurus: Seat rows responsible for the marvelous acoustics,” *J. Acoust. Soc. Am.* **121**, 2011–2022 (2007).
- S.-Y. Feng, “Some acoustical measurements on the Chinese musical instrument P'i-P'a,” *J. Acoust. Soc. Am.* **75**, 599–602 (1984).
- N.H. Fletcher and T.D. Rossing, *The Physics of Musical Instruments* (2nd ed., Springer-Verlag, New York, 1998), pp. 268–269, 298, 334–336.
- D.W. Haines, “On musical instrument wood,” *Catgut Acoust. Soc. Newslet.* **31**, 23–32 (1979).
- R.F.S. Hearmon, “The influence of shear and rotatory inertia on the free flexural vibration of wooden beams,” *Brit. J. Appl. Phys.* **9**, 381–388 (1958).
- R. Horiuchi, T. Kikuchi, S. Sato, and H. Miura, “Sound generation of samisen: Analysis of sound pressure waveform and vibration waveform of skin, bridge, and plectrum,” *Rep. Musical Res. Group MA94-7* (1994) (in Japanese).
- H.-W. Ko, J.U. Noh, and K.-M. Sung, “A study on the anjok (bridge) of the gayageum using impulse response method,” *Proc. 9th Western Pacific Acoust. Conf.*, 722–729 (Seoul, 2006).
- J.U. Noh, C. Choi, H.-G. Moon, and K.-M. Sung, “Acoustical characteristics of the gayageum: A twelve-stringed Korean traditional musical instrument,” *Forum Acusticum, Paper MUS-03-006* (Sevilla, 2002).
- E. Obata, T. Ono, and M. Norimoto, “Vibrational properties of wood along the grain,” *J. Mater. Sci.* **35**, 2993–3001 (2000).
- A. Odaka, “Chinese traditional musical instruments: Some features and their relationships with music,” *J. Acoust. Soc. Jpn.* **54**, 657–663 (1998) (in Japanese).
- A. Odaka and S. Yoshikawa, “Acoustical characteristics of Chinese stringed instruments and their Asian relatives,” *J. Acoust. Soc. Am.* **120**, 3118 (2006).
- W. Reinecke, “Übertragungseigenschaften des Streichinstrumenten-stegs,” *Catgut Acoust. Soc. Newslet.* **19**, 26–34 (1973).
- J.C. Schelleng, “The violin as a circuit,” *J. Acoust. Soc. Am.* **35**, 326–338 (1963).
- H.-E. Schmitz, *Satsumabiwa: Die Laute der Samurai und ihre instrumentalen Spielstücke danpo Untersuchungen zur Musikkultur Japans* (Bärenreiter, Kassel, 1994).
- T. Senda and S. Yoshikawa, “Fundamental aspects of the plucked string vibration with *sawari* constraint at one end,” *J. Acoust. Soc. Am.* (to be submitted).
- T. Taguti, “Unilateral constraint to the string: A model analysis on the *sawari* effect of biwa,” *Proc. Int. Symp. on Musical Acoustics*, 443–446 (Perugia, 2001).
- T. Taguti, “One type of nonlinear vibration of string coupled with a resonator of several resonance frequencies,” *Rep. Musical Res. Group MA2005-8* (2005).
- T. Taguti and K. Tohnai, “Acoustical analysis on the *sawari* tone of Chikuzen biwa,” *Acoust. Sci. Tech.* **22**, 199–207 (2001).
- T. Taguti and K. Tohnai, “Vibro-acoustical measurement of several biwas,” *Rep. Musical Res. Group MA2006-6* (2006) (in Japanese).
- Y. Takasawa, “Analysis of samisen's sounding mechanism by modal analysis approach,” *Rep. Musical Res. Group MA93-16* (1993) (in Japanese).
- K. Tohnai, *A Sequel to the Research of Japanese Modern Biwas* (Kasama Shoin, Tokyo, 1998).
- K. Tohnai and K. Kishi, “Structure and examples of played waves of the Satsuma biwa,” *Rep. Musical Res. Group MA93-19* (1993) (in Japanese).
- J. Woodhouse, “On the playability of violins. Part II: Minimum bow force and transients,” *Acustica* **78**, 137–153 (1993).

- J. Woodhouse, “Plucked guitar transients: Comparison of measurements and synthesis,” *Acustica/Acta Acustica* **90**, 945–965 (2004).
- M. Yako, “Timbre of shamisen tone and perception of decay in amplitude envelope: Preliminary study on the relation between timbre and musical structure,” Rep. Musical Res. Group MA91-6 (1991) (in Japanese).
- J. Yoo and T.D. Rossing, “Traditional plucked string instruments from Korea,” Unpublished technical note (2006).
- S. Yoshikawa, “Measuring the “degree of Asia” of the KID students: From the class of “acoustics of musical instruments”,” *Geijutsu Kogaku J. Des.* **1**, 77–92 (2004) (in Japanese).
- S. Yoshikawa, “Acoustical classification of woods for string instruments,” *J. Acoust. Soc. Am.* **122**, 568–573 (2007).
- S. Yoshikawa, M. Shinozuka, and T. Senda, “A comparison of string instruments based on wood properties: Biwa vs. cello,” *Acoust. Sci. Tech.* **29**, 41–50 (2008).

Chapter 12

Bowed Strings

Thomas D. Rossing and Roger J. Hanson

In the next eight chapters, we consider some aspects of the science of bowed string instruments, old and new. In this chapter, we present a brief discussion of bowed strings, a subject that will be developed much more thoroughly in Chap. 16. Chapters 13–15 discuss the violin, the cello, and the double bass. Chapter 17 discusses viols and other historic string instruments, and Chap. 18 discusses the Hutchins–Schelleng violin octet.

12.1 Kinematics of the Bowed String

As the bow is drawn across the strings of a violin, the string appears to vibrate back and forth smoothly between two curved boundaries, much like a string vibrating in its fundamental mode. However, this appearance of simplicity is deceiving. Over 100 years ago, von Helmholtz (1877) showed that the string more nearly forms two straight lines with a sharp bend at the point of intersection. This bend races around the curved path that we see, making one round trip each period of the vibration. Because of its speed, our eye ordinarily sees only the curved envelope.

During the greater part of each vibration, the string is carried along by the bow. Then it suddenly detaches itself from the bow and moves rapidly back until it is caught by the moving bow again. The motion of the string at the point of bowing is shown in Fig. 12.1.

Up to the point of release *a* and again from *c* to *i*, the string moves at the constant speed of the bow. From *a* to *c*, the string makes a rapid return until it is caught by a different point on the bow. The displacement and velocity at the bow position of a very flexible string during bowing are shown in the oscillograms of Fig. 12.2. The oscillogram on the left, which shows the displacement versus time, is almost

T.D. Rossing (✉)
Center for Computer Research in Music and Acoustics (CCRMA),
Stanford University, Stanford, CA 94302-8180, USA
e-mail: rossing@ccrma.stanford.edu

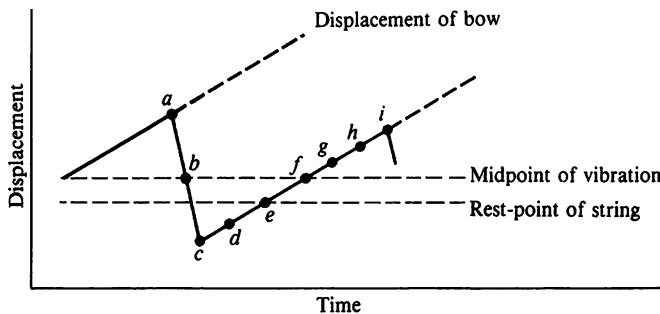


Fig. 12.1 Displacement of bow and string at the point of contact with the bow. Note that the midpoint on the vibration is displaced slightly from the rest position of the string (from Rossing et al. 2002)

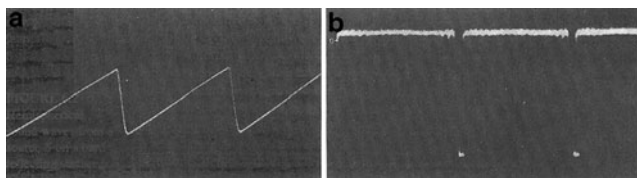


Fig. 12.2 Displacement (a) and velocity (b) of a bowed string as functions of time. The velocity (b) at every time equals the slope of the displacement curve (from Schelleng 1974)

identical to Fig. 12.1, whereas the graph of velocity versus time (on the right) shows rather narrow spikes, which represent the large negative velocity of the string when it slides rapidly along the bow (*a–b–c* in Fig. 12.1).

Figure 12.3 shows the entire string at successive times in the vibration cycle. The letters of the frames correspond to the letters in Fig. 12.1. The sequence at the left shows how the bend races around the envelope, while the sequence at the right shows the velocity of the string at different times in the vibration cycle (bow not shown). At the position of the bow, the arrows in the sequence at the right correspond to the velocity shown in Fig. 12.2b.

At the moment of release, shown in Fig. 12.3a, the bend has just passed the bow. In (b), the bend has reached the bridge, from which it will reflect back down the string in (c), (d), and (e), until it reaches the nut in (f) and is again reflected. At point *c* in Fig. 12.1 and also in frame (c) in Fig. 12.3, the string is captured by the bow, and once again moves upward at the speed of the bow.

The *stick and slip* of the string relative to the moving bow are determined partly by the friction between the string and the horsehair of the bow. It is well-known that the force of friction between two objects is less when they are sliding past each other than when they move together without slippage. After the string begins to slip, it moves rather freely until it is once again captured by the bow. It is important to note, however, that the beginning and the end of the slipping are triggered by the arrival of the bend (slipping begins when the bend arrives from the nut and ends

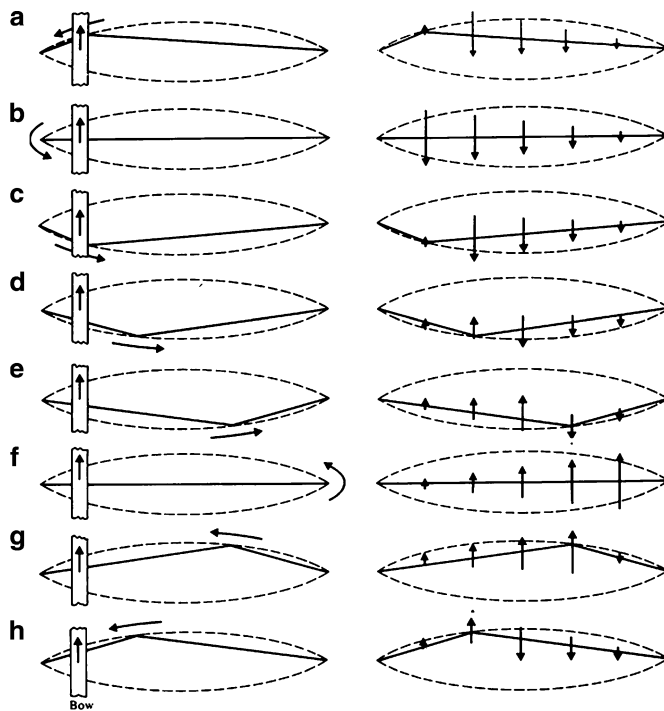


Fig. 12.3 The motion of a bowed string at successive times during the vibration cycle. The configurations shown in (a)–(h) correspond to the points (a)–(h) in Fig. 12.1. (a) The bend races around a curved boundary, which appears to be the profile of the string viewed during bowing; (b) the velocity of the string at different times in the vibration cycle (from Rossing et al. 2002)

when it arrives again from the bridge). Because the time required for one round trip depends on the string length and wave velocity (which, in turn, depends on tension and string mass), the vibration frequency of the string remains the same under rather widely varying bowing conditions. If only friction and the restoring force of the displaced string determined the beginning and the end of slipping, the vibrations would be irregular rather than regular.

The limits on the bowing conditions are the limits on the conditions at which the bend can trigger the beginning and the end of slippage between bow and string. For each position of the bow, there is a maximum and minimum bowing force, as shown in Fig. 12.4. The closer to the bridge the string is bowed, the less leeway the violinist has between minimum and maximum bowing force. Bowing close to the bridge (*sul ponticello*) gives a loud, bright tone, but requires considerable bowing force and the steady hand of an experienced player. Bowing further from the bridge (*sul tasto*) produces a gentle tone with less brilliance, and allows a greater range of bowing force.

It can be inferred from Fig. 12.3 that the amplitude of the vibration is determined by the speed and position of the bow. Because the speed of the bend around its curved path is essentially independent of the speed and position of the bow, the

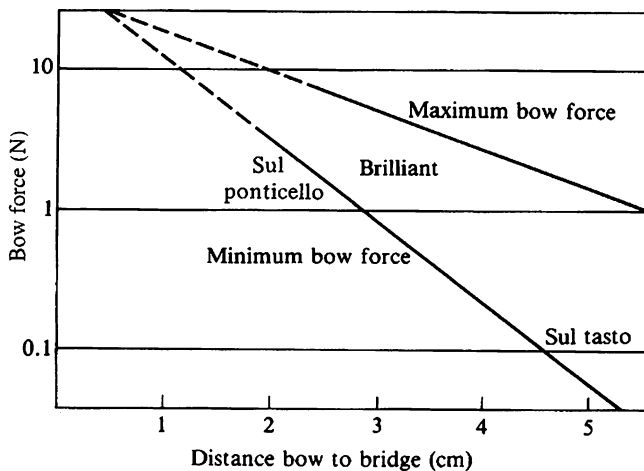


Fig. 12.4 Range of bowing force for different bow-to-bridge distances for a cello bowed at 20 cm/s (after Schelleng 1974)

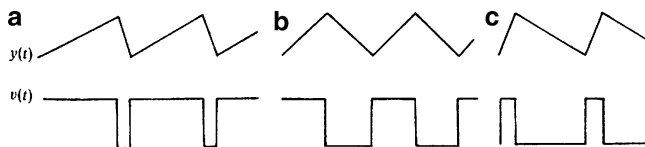


Fig. 12.5 Displacement $y(t)$ and velocity $v(t)$ of a bowed string at three positions (x) along its length L : (a) at $x = L/4$, (b) at the center, and (c) at $x = 3L/4$

amplitude of vibration can increase either by increasing the bow speed or by bowing closer to the bridge.

Figures 12.1 and 12.2 illustrate the motion of the string at one point of contact with the bow. The displacement and velocity at two other points on the string are shown as functions of time in Fig. 12.5. At the center of the string, the velocity (speed) of the string is the same in both directions. When the bow moves in the opposite direction, the curves in Fig. 12.5a, c are exchanged. Also the bend moves clockwise, rather than counterclockwise as shown in Fig. 12.3.

To observe the string motion in a pre-electronic age, von Helmholtz (1877) constructed an ingenious vibration microscope, consisting of an eyepiece attached to a tuning fork. This was driven in sinusoidal motion parallel to the string, and the eyepiece was focused on a bright-colored spot on the string. When Helmholtz bowed the string, he saw a Lissajous figure. The figure was stationary when the tuning fork frequency was an integral fraction of the string frequency. Helmholtz noted that the displacement of the string followed a triangular pattern at whatever point he observed it, as shown in Fig. 12.5. The velocity waveform at each point alternates between two values.

Other early work on the subject was published by Krigar-Menzel and Raps (1891) and by Raman (1918). More recent experiments by Schelleng (1973), McIntyre et al. (1981), Lawergren (1980), Kondo and Kubata (1983), and by others have verified these early findings and have greatly added to our understanding of bowed strings. An excellent discussion of the bowed string is given by Cremer (1981). A detailed analysis is given in Chap. 16.

Raman's model of Helmholtz motion assumed the string to be an ideal, flexible string terminated in real, frequency-independent mechanical resistances. Bowing at a single point x_b divides the string into two straight segments with lengths in the ratio $(L - x_b)/x_b = p$. Raman considered both rational and irrational values of p .

Raman's velocity and displacement curves for the simplest case, with one discontinuity, as discussed in Raman (1918) are shown in Fletcher and Rossing (1998, p. 276). In this case, the positive and negative velocity waves are of the same form, and at the instant at which they are coincident the velocity diagram is a straight line passing through one end of the string with a discontinuity at the other. As this discontinuity moves along the string, the velocity diagram consists of parallel lines passing through its two ends, and the velocities at any point before and after its passage are proportional to the distances from the two ends. The displacement diagrams consist of two straight lines passing through the ends of the string and meeting at the point to which the discontinuity in the velocity diagram has traveled.

Raman (1918) also shows velocity and displacement curves for the case with two discontinuities. The point at which the two discontinuities coincide has been arbitrarily chosen to be the center of the string, which causes the string to vibrate in two segments at twice the fundamental frequency. If the discontinuities cross elsewhere, however (and thus cross twice as often), the frequency of vibration will be that of the fundamental. Note that displacements are measured from the equilibrium configuration of the string under the steady frictional force exerted by the bow, not from the equilibrium position with the bow removed (Fletcher and Rossing 1998, p. 277).

von Helmholtz (1877) observed that the n th partial and its overtones are absent if the string is bowed at a rational fraction m/n of its length. This results in deviations from the idealized displacement curve, which Helmholtz described as ripples.

In practice, two periodic regimes besides the Helmholtz motion are sometimes encountered. If the bow force is insufficiently high, *double-slip* motion can occur. A second slip occurs near the middle of the sticking period, and a double sawtooth wave occurs, as shown in Fig. 12.6a. If the second slip is equal to the first, the note may sound an octave higher, but more commonly the fundamental frequency remains the same although the tone quality changes significantly (string players sometimes describe this as *surface sound*). The second regime is called *multiple-flyback* motion, in which the single flyback of the Helmholtz motion has been replaced by a cluster of them with alternating signs, as shown in Fig. 12.6b (Woodhouse 1995).

Players are well aware of how the amount of bow hair in contact with the string affects bowing. A physical model of the bowed string by Pitteroff (1994) takes into

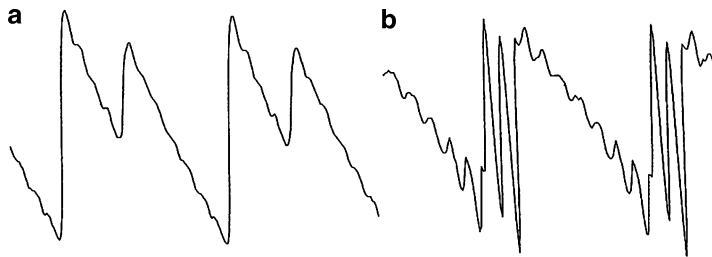


Fig. 12.6 (a) Bridge force waveform in double-slip motion; (b) bridge force waveform in multiple-flyback motion (Woodhouse 1995)

account the width of the bow, the angular motion of the string, bow-hair elasticity, and string bending stiffness. The frictional force for the edge of the bow facing the nut is lower than that of the edge facing the bridge through the entire sticking time.

12.2 Dynamics of the Bowed String

The discussion thus far refers to what might be called the kinematics of the string – a description of its motion. It is also important to examine the dynamics – the forces and energies involved. Why does a bowed string vibrate? Clearly the friction between the moving bow and the vibrating string must transfer enough power to the string to overcome the losses from internal dissipation, viscous drag by the air, and loss through the non-rigid end supports. The energy transfer to the string in each cycle of motion is just the friction force multiplied by the displacement and integrated over the cycle. Because the string returns to its initial position once in each cycle, the energy transferred would be zero unless the frictional force varies with velocity.

We know that there is a difference between *static friction* – the maximum tangential force between two surfaces when their relative velocity is zero – and *dynamic friction* – the tangential force when one surface is sliding over the other. Dynamic friction is generally less than static friction, so that on an inclined plane, for example, after a body begins to slide, it continues to do so. The frictional curve is shown in Fig. 12.7. Dynamic friction is a nonlinear function of relative velocity and static friction is undetermined in sign or magnitude except that its maximum absolute value (which is usually called static friction) has a definite magnitude for the two surfaces in question and for the applied normal force. The exact shape of the curve depends upon the nature of the two surfaces.

If the frictional behavior is as specified by the curve in Fig. 12.7, then we can see the origin of the energy transfer. Suppose that a moving bow is lowered onto a string that is already vibrating with small amplitude. When the string is moving in the same direction as the bow, energy is transferred to it, while when it is moving in the opposite direction to the bow, some mechanical energy is dissipated as thermal energy.

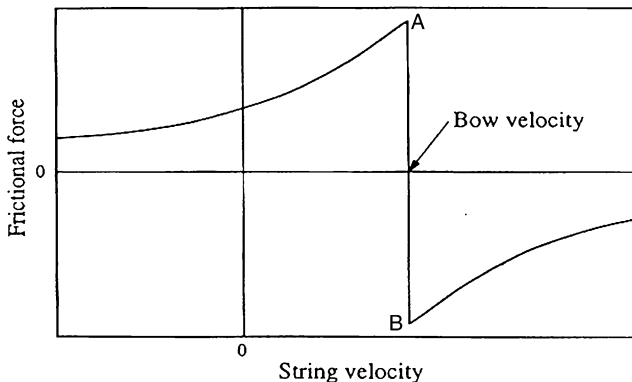


Fig. 12.7 The dependence of frictional force on relative velocity for a bow moving across a string (Fletcher and Rossing 1998)

A more complete discussion of the kinematics of the bowed string is given in Chap. 16 as well as in Fletcher and Rossing (1998).

12.3 Bowing to Achieve Anomalous Low Frequencies

When a bowing force is employed that is within the range of the minimum and maximum forces shown in Fig. 12.4, the string vibrates at very nearly the same frequency as the natural free vibration frequency of the string. This follows from the timing mechanism of the bend traveling around the string. Thus, the bowed string normally yields a sound of approximately the same pitch as when it is plucked and allowed to vibrate freely. There can be small variations up to as much as a semitone due to what is known as the “flattening effect” in which the onset of slip can be slightly modified by fairly large bowing forces still within the limits in Fig. 12.4. Discussions of this effect are given by Boutillon (1991) and Schumacher (1994).

If a bow force is used that is much higher than normal, that is, it exceeds the maximum shown in Fig. 12.4 (referred to here as the Schelleng maximum), the usual result is a raucous nonperiodic sound. Such an unpleasant sound is frequently produced by a beginning violin or viola student. It is possible, however, for an experienced player exercising very careful bow control for bow forces above the Schelleng maximum to produce sustained periodic sounds with a definite pitch much lower than that obtained by normal bowing and hence much lower than that of the plucked string. Experimental studies of this effect have been made by Hanson et al. (1994). Because this is an *anomalous* effect in the sense that it deviates from the usual or normal situation the term *anomalous low frequencies (ALF)* has been applied to the phenomenon. The low frequencies are not referred to as subharmonics because in general they do not correspond to the mathematical definition of a subharmonic of a frequency, f_0 , viz., f_0/n .

A violinist, Mari Kimura, has made extensive use of such low notes in compositions and performances in various locations around the world (Neuwirth 1994) and (Kimura 1999). Pagannini is said to have been heard producing such sounds in private but not in performance (Gold 1995, pp. 83–84). Composer George Crumb in *Black Angels for Electric String Quartet*¹ calls for production of pedal tones an octave low using this technique and also the flattening effect in other parts.

In the studies reported by Hanson et al. (1994), tones were produced roughly a musical third, seventh, octave, ninth, twelfth, and two octaves below that for normal bowing. The musical terms were used for convenience of description rather than for their accuracy in describing the exact frequency. The different frequencies are produced with different bow forces, speeds, and distances from the bridge. Examples of sound spectra are shown in Fig. 12.8. The very small fundamental for the third low is consistent with that for a normally bowed open G string, which vibrates at a frequency too low for efficient radiation from a violin. In the case of the ninth low, the fundamental is completely missing on the plot and the second harmonic is

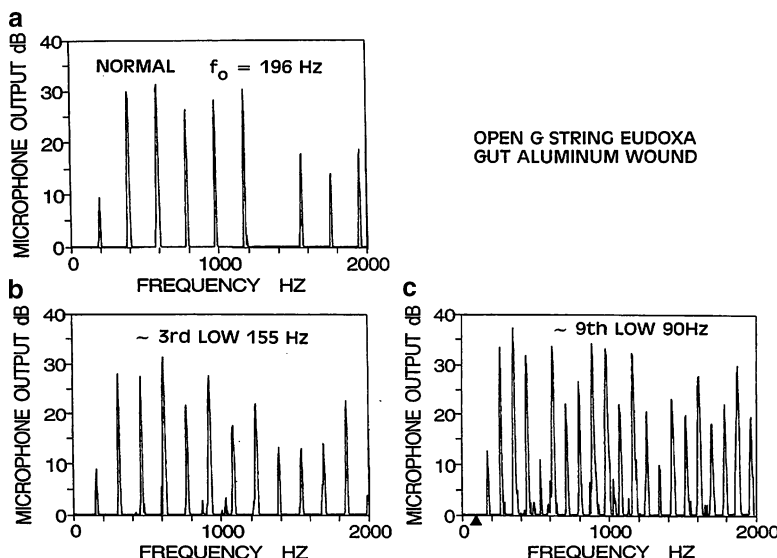


Fig. 12.8 Sound spectra from an FFT analyzer for a bowed open G string on a violin. The microphone is ~0.8 m from the top plate. (a) Normal bowing. (b) High bow force; the pitch is about a musical major third low. (c) High bow force; the pitch is about a musical ninth low. The position for the “missing fundamental” is indicated by *filled triangle*. The second harmonic is also very weak, but the listener hears from the higher harmonics a very definite pitch corresponding to the fundamental frequency of 90 Hz calculated from the other harmonics (from Hanson et al. 1994)

¹On the Crumb score the following note is given: “Pedal tones are produced by moving bow very slowly while exerting great pressure. Since various ‘partials’ are obtainable, the player should calculate carefully [the] distance from [the] bridge and bow pressure in order to produce the lower octave.”

very small for the same reason. The pitch that is heard is, however, definitely that which corresponds to the frequency of the missing fundamental. The clean harmonic sound spectra in Fig. 12.8b, c indicate that the string motion producing the sound output of the violin is indeed periodic. As a result of the altered bowing conditions the string is actually being driven at a frequency lower than the free vibration frequency. There is not a mysterious perception of the lower pitches.

The ALF effect can be interpreted in terms of defeating the Helmholtz mechanism for normal bowing described in Sect. 12.2. In that description the string and bow move together during the sticking portion of the cycle until the traveling bend arrives at the bow to trigger the release of the string for the slipping part of the cycle. Because the traveling bend has a round-trip period the same as that of the freely vibrating string, it serves as a synchronizing mechanism to ensure that the slip-stick process occurs at the natural period of vibration of the string. If, however, the bow force is great enough, the maximum transverse frictional force exerted by the bow on the string is sufficient to prevent the Helmholtz bend from triggering the release of the string from the bow hair, and the Helmholtz process is defeated.

After the failed release, the bow continues in the sticking part of the cycle to displace the string further from its equilibrium position. The restoring force due to the stretched string then becomes great enough that some other small signal coming to the bow may be sufficient to trigger the slipping process. If careful bow control is exercised it is possible for a periodic motion with a longer than normal period to be established as a result of regular triggering by the same part of the waveform for each cycle. Because the bow now serves as a quasi-termination point for the string, there are partial reflections of the waveform of the string at the bow. Thus, the resulting waveform for ALF is much more complex than for the Helmholtz motion as a consequence of multiple bow-nut and bow-bridge reflections of the transverse waves. Reflected torsional waves can probably also play an important role in triggering the release of the string, but the studies of Hanson et al. did not include torsional measurements. Computer modeling of the process of producing ALF for very large bowing forces, taking account of reflections of both transverse and torsional waves, has been carried out by Guettler (1994). Kimura (1999) found that twisting the string can be an important factor in the production of these sounds.

The distance of the bow from the bridge affects the timing for bridge–bow and nut–bow reflections resulting from the bow being a quasi-termination point of the string. Consequently, the slip-stick period and hence the period of the sound is affected by bow position. Hanson et al. measured frequencies ranging from 100 to 106 Hz on the open G string (normal frequency of 196 Hz) for bridge–bow distances varying from 17 to 45 mm. As shown in Fig. 2 in Hanson et al., a linear relationship was found between frequency and bridge–bow distance. Strings of different materials by different manufacturers exhibited similar linear relations, but important differences were found. For example, for one type of string a seventh low was readily produced whereas for another type it was a ninth.

In order to obtain waveforms for the motion of the string at the bridge, bow (nut side), and nut Hanson et al. mounted a violin G string on a rigid steel beam with the ends firmly clamped. Optical detectors were used to sense the position as a

function of time of a point on the string very close to the positions of the “nut,” bow, and “bridge.” The tension of the string on this monochord was adjusted for the normal free vibration frequency of 196 Hz. Periodic vibrations at ALF frequencies were produced by manually bowing with a sufficiently high (and controlled) bowing force. This arrangement facilitated obtaining of data and was judged valid because the same frequencies for the same bowing position were obtained for the same string mounted on a violin and on the monochord. This indicated that the effect was essentially a result of bow-string interaction and not significantly related to the body of the violin itself. The sounds were heard by playing the amplified voltage outputs of the optical detectors through a speaker.

Examples of waveforms at the different positions are shown in Figs. 12.9–12.11. The generation of a very complex waveform at the nut and the bow (*nut side*) is illustrated in Fig. 12.9 where a number of multiple reflections resulting from slips A and B are identified. The waveform at the bridge that would be principally responsible for the sound produced if it were an actual violin is very simple in this case, resembling that for Helmholtz motion except that the period is approximately four times as large as for a normally bowed string. The example in Fig. 12.10 is for the same “bridge”-bow distance but with a lower bow force

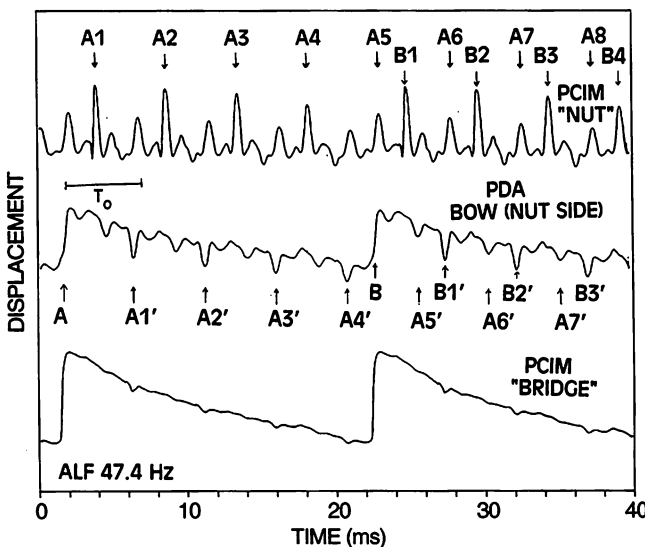


Fig. 12.9 Transverse displacement as a function of time at three positions of a manually bowed Eudoxa aluminum-wound gut G string mounted on a steel beam and tuned to the standard 196 Hz. The bow is 1.8 cm from the “bridge.” The string length between the end clamps is the same as a normal violin bridge-to-nut distance. T_o is the corresponding normal Helmholtz motion period. Arrows labeled A and B point to slip regions at the bow. The displacement pulse at the nut, labeled A1, is a result of slip A; and A2, A3, etc., refer to the series of reflections of A1 from the bow. A1', A2', etc., refer to the reflections from the nut of A1, A2, etc., as observed at the bow. Pulses labeled B1, B2, B1', B2', etc., are correspondingly related to slip B. The ALF of 47.4 Hz (a little more than two octaves below normal) is the lowest frequency that was observed (Hanson et al. 1994)

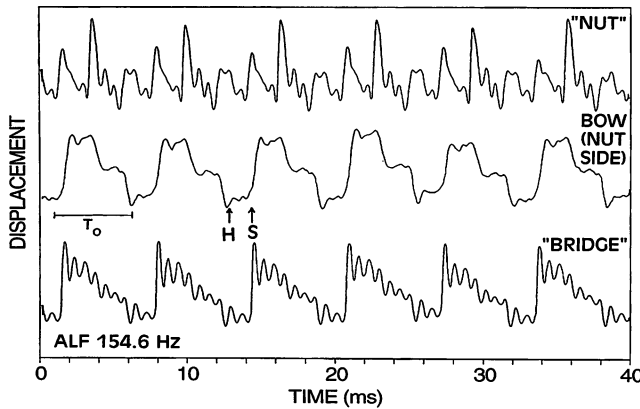


Fig. 12.10 Conditions as in Fig. 12.9 but with a different bowing technique resulting in an ALF of 154.6 Hz, about a musical third below normal. The arrow at S points to a slip region and the arrow at H points to a region where there appears to be a “failed Helmholtz slip” occurring at time T_o (the normal Helmholtz period) after the previous slip (Hanson et al. 1994)

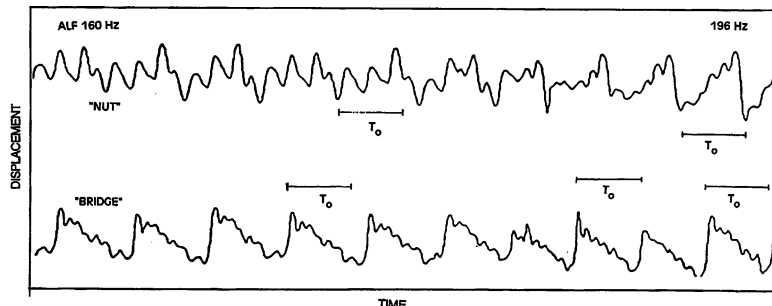


Fig. 12.11 Transitions from ALF of 160 Hz at the *left* to the normal 196 Hz with approximate Helmholtz motion of period T_o at the *extreme right* (Hanson et al. 1994)

resulting in a frequency about a musical third low instead of two octaves low. In this case the waveform at the “bridge” is more complicated exhibiting many “bridge”-bow reflections, but with a definite stick-slip form. Figure 12.11 shows at the end a transition from an ALF frequency about a musical third low toward a Helmholtz motion with a normal period T_o .

References

- X. Boutillon (1991) Analytical investigations of the flattening effect: The reactive power balance rule, *J. Acoust. Soc. Am.* **90**, 745–763.
- L. Cremer (1981) *Physik der Geige*. Hirzel Verlag, Stuttgart. English translation by J.S. Allen, MIT Press, Cambridge, MA (1984).

- N. H. Fletcher and T. D. Rossing (1998) *The Physics of musical instruments* 2nd ed, Springer, New York.
- J. Gold (1995) Paganini: virtuoso, collector, and dealer, *J. Violin Soc. Am.* **XIV**, 67–88.
- K. Guettler (1994) Wave analysis of a string bowed to anomalous low frequencies, *Catgut Acoust. Soc. J.* **6**(II), 8–14.
- R. J. Hanson, F. W. Halgedahl, and A. J. Schneider (1994) Anomalous low-pitched tones from a bowed violin string, *Catgut Acoust. Soc. J.* **6**(II), 1–7. Copies are obtainable from Department of Physics, University of Northern Iowa, Cedar Falls, IA 50614, USA.
- M. Kimura (1999) How to produce subharmonics on the violin, *J. New Music Res.* **28**(2), 178–184.
- M. Kondo, and H. Kubota (1985) A new identification expression of Helmholtzian waves and their formation mechanism, *Proc. SMAC 83*, Stockholm, Royal Swedish Academy of Music 245–261.
- O. Krigar-Menzel, and A. Raps (1891) Aus der Sitzungberichten, *Ann. Phys. Chem.* **44**, 613–644.
- B. Lawergren (1983) Harmonics of S-motion on bowed strings. *J. Acoust. Soc. Am.* **73**, 2174–2179.
- M. E. McIntyre, and J. Woodhouse (1978) The acoustics of stringed musical instruments. *Interdisciplinary Science Reviews* **3**, 157–173.
- R. Neuwirth (1994) From Sciarrino to subharmonics, *Strings* **44**(September/October), 60–66.
- R. Pitteroff (1994) Modelling of the bowed string taking into account the width of the bow. In: *Proc. SMAC 93*, eds. A. Friberg, J. Ewarsson, E. Janson, and J. Sundberg, Royal Swedish Academy of Music, Stockholm.
- C. V. Raman (1918) On the mechanical theory of the vibrations of bowed strings and of musical instruments of the violin family, with experimental verification of the results, *Bull. 15*, The Indian Association for the Cultivation of Science.
- T. D. Rossing, F. R. Moore, and P. A. Wheeler (2002) *Science of Sound*, 3rd ed. Addison-Wesley, San Francisco.
- J. C. Schelleng (1973) The bowed string and the player. *J. Acoust. Soc. Am.* **53**, 26–41.
- J. C. Schelleng (1974) The physics of the bowed string, *Sci. Am.* **230**(1), 87–95.
- R. T. Schumacher (1994) Measurements of some parameters of bowing, *J. Acoust. Soc. Am.* **96**, 1985–1998.
- H. L. F. von Helmholtz (1877) *On the Sensations of Tone*, 4th ed., Translation by A.J. Ellis, Dover, New York (1954).
- J. Woodhouse (1995). Self-sustained musical oscillators. In: *Mechanics of Musical Instruments*, eds. A. Hirschberg, J. Kergomard, and G. Weinreich, Springer-Verlag, Wien.

Chapter 13

Violin

Joseph Curtin and Thomas D. Rossing

13.1 History

The first known violins were built in Italy in the early 1500s. While not much is yet known about the instrument's prior development, European forebears include the *rebec* and the Renaissance fiddle, which themselves evolved from instruments found in the ancient Eastern world. The violin brought together in a particularly happy way features seen in a variety of earlier stringed instruments. Arched plates increased the stiffness-to-mass ratio of the body, creating a more brilliant sound and helping resist long-term deformation. A pronounced waist gave the bow access to the outermost strings, while the precisely calibrated curves of fingerboard and bridge enabled the strings to be played individually as well as in two-, three-, and even four-part chords. In contrast to the *viola da gamba* and guitar, the violin's top and back plates overhung the ribs, allowing easy removal for repairs, thus contributing to the instrument's fabled longevity. A graceful outline, harmonious proportions, and the minimal use of ornamentation together lent the violin a timeless beauty – explaining in part why it has resisted significant stylistic modification to this day. For a discussion of historical string instruments, see Chap. 17.

Though the evolution of the violin is usually told in heroic terms – its sudden emergence and gradual refinement followed by an ascent to perfection at the hands of Stradivari – our current conception of violin sound is the result of a great deal of subsequent development, much of it fueled by the demands of players and composers. The so-called *modern setup* was adopted by French makers in the eighteenth century. It included a longer, slimmer neck and fingerboard, a stiffer bassbar, and a modified bridge. These were retrofitted onto Old Italian instruments to increase brilliance and musical range, and to help sustain the larger string tensions that came with longer strings and a rise in pitch of concert A.

T.D. Rossing (✉)
Center for Computer Research in Music and Acoustics (CCRMA),
Stanford University, Stanford, CA 94302-8180, USA
e-mail: rossing@ccrma.stanford.edu

Important, too, was the creation in the late 1700s of the so-called *modern bow*. Largely credited to Francois Tourte (who pioneered the hot-bending of bow-sticks), its most significant innovations were the reversed camber, a screw for adjusting hair tension, and the adoption of pernambuco wood as the standard stick material. (Bows are discussed in Chap. 16.) While the generally longer, heavier modern bow traded some of its Baroque predecessor's off-the-string agility, it offered the violinist a larger dynamic range together with a more powerful and sustained legato – qualities much exploited by players and composers of the Romantic period. Another important line of development was string technology, especially in the second half of the twentieth century, when synthetic core materials (mainly nylon) began replacing gut. This significantly increased stability and playability, while further contributing to power and brilliance.

So much has the violin changed over the past few centuries that a violinist equipped with a Baroque bow and an instrument straight from Stradivari's work-bench would find most of the standard violin repertoire unplayable – and in a typical concert setting, scarcely audible. That said, a flourishing interest in historical performance practice has ensured that numerous instruments are now built and/or set up in the Baroque manner. More puzzling is that, despite the enormous increases in the standards of instrument and bow making over the past few decades, old French bows and old Italian violins – repaired, rebuilt, and re-engineered, though they may be – are still the combination of choice for most concert violinists.

13.2 Research

Research into stringed instruments goes back at least four centuries and includes many renowned scientists. Marin Mersenne (1588–1648) indicated that he could hear at least four overtones in the sound of a vibrating string. Felix Savart (1791–1841) carried out significant studies of violin, some in collaboration with the well-known violin-maker Jean-Baptiste Vuillaume (1798–1875). Hermann von Helmholtz (1821–1894) did important physical and psycho-acoustical experiments. His pioneering studies of the bowed string were taken up by C.V. Raman (1888–1970), who embarked on a theoretical treatment of bowed string motion.

In twentieth-century Germany, the work of Erwin Meyer, Hermann Backhaus, Hermann Meinel, and Lothar Cremer stands out. Cremer, in particular, was a central figure. His 1981 book, *Physik der Geige* (published in English as *The Physics of the Violin*), remains the essential text on the subject (Cremer 1984). Frederick Saunders (1875–1963) was the pioneering researcher in the USA. In 1963, Saunders, Carleen Hutchins, John Schelleng, and Robert Fryxell founded the Catgut Acoustical Society (CAS), an organization that promoted violin research throughout the world. Among its accomplishments was the development of the violin octet (a scaled ensemble of new violin family instruments; see Chap. 18). More importantly, it began a dissemination of acoustical know-how among violin

makers, which has only increased since the CAS merged with the Violin Society of America (VSA) in 2004.

The viola, cello, and double bass, along with the bow, seem to have fallen into a kind of research shadow thrown by the violin. Still, much of what has been learned about the violin applies to its larger siblings as well, and in this chapter the word *violin* will often stand in for the entire family. Separate chapters are devoted to the cello and double bass.

13.3 Evaluating Violins

A long-standing goal of violin research has been to understand the relationship between the dynamic behavior of a violin and its sound quality. This goal would be more readily attainable if there were a general consensus among violin players, makers, and dealers on how to rate sound quality, and on which particular violins were better than others, and in what ways. Old Italian violins remain the most universally sought-after stringed instruments, and yet it takes an expert opinion based on visual and historical rather than tonal evidence to say whether an instrument is actually an Old Italian – and on occasion, whether it is actually old. Market value is based on an instrument’s provenance and condition, with sound entering the equation only indirectly.

Listening tests, which attempt to rank violins from the audience’s point of view, have generally proved inconclusive. There are at least four possible reasons: (1) many tests are not well-controlled by scientific standards; (2) the length of the excerpts played and the time taken to switch instruments far exceeds the optimal interval for comparing sounds; (3) the acoustics of the listening room can make fine tonal distinctions difficult; and (4) the listener’s impressions tend to be dominated by the musical charisma of the player. Good players make virtually any instrument sound good, and by a certain logic should therefore be excluded from listening tests. Bad players are no more useful!

It is not unusual in a listening test for the audience to prefer one particular violin while the violinist prefers another. There is no a priori basis for assuming that either preference is “correct.” For example, violinists may choose the instrument that most easily delivers the kind of sound they are looking for. The audience, on the other hand, may prefer the instrument that projects the best. Projection (the ability to be heard at a distance) can, by definition, be judged only by a listener. Otherwise, violinists have at least two advantages over their audiences in evaluating an instrument. They are inside a feedback loop, and so base their judgments on interaction rather than passive listening. And they are very close to the instrument, where the *soundscape* is most detailed and intense. In the end, of course, it is violinists who choose their instruments, and whose judgments are therefore most consequential to violin makers, and thus to the development of the instrument.

Violinists typically judge by a number of quality parameters, though these are often loosely defined, and sometimes couched in highly personal language. Various

attempts have been made to refine them; Schleske, for example, polled 120 violinists about the attributes they used for describing violin sound and playability. The results were collapsed into six descriptor pairs: bright/dark; nasal/not nasal; pleasant/unpleasant; even/uneven, and responsive/unresponsive. The subject of violin quality will be taken up again in Sect. 13.6.

13.4 Sound Analysis

In everyday life, the term *spectrum* is commonly associated with light. Our eyes perceive different frequencies of light in terms of color – white light being an equal mixture of all frequencies within the visible range. A prism is a spectrum analyzer in that it separates a beam of light into its color components. The analysis is reversible, because the beam can be re-assembled by passing the spectrum through a second prism. The nineteenth-century scientist Helmholtz devised a simple spectrum analyzer for sound, using a series of resonators tuned to a closely spaced series of frequencies. By listening to a sound through each of the resonators and noting which ones responded, he could list the *frequency components* of the sound. We now know that the human ear works in a similar way: tiny hairs in the inner ear respond selectively to narrow bands of frequencies. The brain then “sharpens” this rather crude analysis to achieve the remarkable pitch discrimination of which we are at best capable.

Breaking down a sound into a number of frequency components might seem a natural thing to do with musical sounds, which typically have a pitch, and therefore at least one frequency associated with them. But what does it mean to speak of the frequency components of a brief, nonmusical sound of no discernable pitch? As it turns out, *any* sound can be completely characterized by a set of frequency components. The mathematical foundation for this kind of analysis was developed by the French engineer Jean Baptiste Fourier in the early 1800s. Each frequency component (or Fourier component) is a sinusoid of specified frequency, magnitude, and phase. When the original waveform is periodic, the components form a harmonic series, that is, each is a simple multiple of the lowest. Most acoustical analysis software is based on a computer-optimized version of the original transform: the fast Fourier transform (FFT), which works for sampled waveforms.

The results of an FFT come in two parts: (1) the magnitude, which gives the strength of each frequency component, and is typically plotted against frequency as a spectrum, often on a decibel scale and (2) the phase of each component. The two together form the *complex spectrum*. This is usually presented as two graphs, with phase placed directly beneath magnitude spectrum, as in Fig. 13.1. The complex spectrum is a complete description of the original waveform. It can be converted back into the original waveform without loss of information.

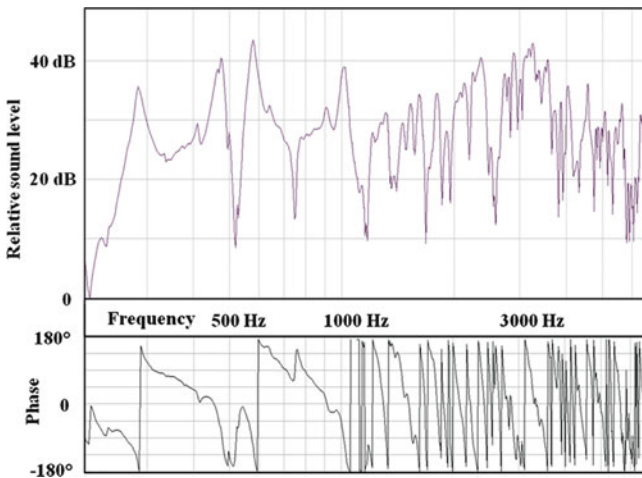


Fig. 13.1 Spectra of sound level (*above*) and phase (*below*) for the output of a typical violin, driven by an impulse at the bass side of the bridge. Frequency is plotted logarithmically. Amplitude is plotted here on a relative scale of decibels (dB). Phase is plotted in degrees, from $+180^\circ$ to -180° . Note that the vertical discontinuities in the line, while suggesting sudden jumps in phase, are in fact an artifact of the scaling: the jump from $+180^\circ$ to -179° represents a shift of just 1° .

13.5 Frequency Response

Acoustical measurements are grounded in the concept of *frequency response*, or how the response of a system varies with frequency. Where audio amplifiers strive for a flat frequency response, a violin's response curve is jagged – and this goes to the heart of its character as a musical instrument. Frequency response is typically measured by driving a system with a known input, measuring the output, and then dividing the complex spectrum of the output by that of the input. This yields a *frequency response function* (FRF), which shows the output per unit input across the frequency range of interest. Two much-used FRFs in violin research are *bridge mobility* (see Section. 13.8.1) and *radiativity* (Section. 13.10).

13.6 Tone Quality

When people speak of violin tone, there is a sense of something best heard in sustained notes – something independent of loudness and clarity and projection. Because of the sensitivity of our hearing, almost immeasurably small details in a sound's waveform may contribute significantly to the perceived sound quality. Bissinger (2008) likens this to the effect of adding tiny amounts of salt to a steak. None of the above suggests that tone quality is easily measured or quantified. Indeed, McIntyre and Woodhouse (1978) warn that “while acknowledging that

standard acoustical measurements have their uses, we must guard against the assumption that such measurements can capture everything significant about a musical sound.”

The standard acoustical measurement most often associated with tone quality is the spectrum of the radiated sound. Meinel (1957) used a bowing machine to measure this for a wide range of instruments. He reported that “superb violin timbre” is associated with (1) large amplitudes at low frequencies, ensuring that “the sounds are agreeably sonorous, and that they ‘carry’ well”; (2) small amplitudes above about 3,000 Hz, lending the sound a “harmonious softness and a fine pure response”; (3) small amplitudes around 1,500 Hz, preventing “a very nasal character”; and (4) an emphasis in the region from 2,000 to 3,000 Hz, giving the sound “a very agreeable, pithy, and dull brightness.”

In 1990, Dünnwald (1991) published a study based on some 700 violins, which he measured in anechoic conditions using an electromagnetic bridge driver. Though his frequency ranges differ somewhat from Meinel’s, his conclusions are similar. The Old Italians were more likely than other instrument makers to concentrate their energy in the ranges Dünnwald associates with “fullness of sound” (190–650 Hz) and “brilliance and clarity” (1,300–4,200 Hz), rather than “nasality” (650–1,300 Hz) and “harshness and in clarity” (4,200–6,400 Hz).

Langhoff (1994) used a Dünnwald-type bridge driver to measure about 60 violins. He cites “evenness” as a quality criterion: Poor instruments may show significant gaps in their response curves, the result being that some of the partials of played notes are only weakly supported. He also cites the general shape of the response curve: A relatively large output at low frequencies yields an instrument with “a powerful bass and often a darker timbre,” and “a general tendency to decline smoothly at high frequencies will generally correlate with a pleasant timbre. If the slope declines too fast, then the instrument will sound ‘covered.’” Langhoff states, presumably from personal experience, that “any musician will tell you immediately whether an instrument he is playing on is an antique instrument or a modern one.” It would be interesting to test this experimentally!

Rodgers (2005) developed an informal method for comparing violins. In semi-anechoic conditions, he played a two-octave glissando on each string while holding the instrument in a standard position relative to a microphone. Twelve award-winning violins at a makers’ competition were compared with a previously measured Stradivari. Rodgers found that (1) none of the new instruments had an A_0 (often referred to as the “Helmholtz” or f-hole resonance; see highlighted box on Namin Modes) of comparable amplitude to that of the Strad; (2) all the new instruments had strong peaks in the 2,000–4,000 Hz region that were higher than those of the Strad in that region; (3) the new instruments that had “many closely spaced [peaks] in the upper frequency region [seemed] to have been favored by the judges”; and (4) none of the new instruments could match the Strad’s virtually unbroken range of peaks in the 2,000–4,000 Hz range.

This last finding echoes Langhoff’s: the existence of significant gaps in the response curve may be detrimental to tone quality. Bissinger confirms this; among seventeen quality-rated violins, the “excellent” violins were more even in terms of sound

output across the measured range. They also had higher levels for A_0 , confirming Dünnwald's first quality parameter. Indeed, Bissinger (2008) found that the level of A_0 was the sole “robust parameter” for distinguishing among bad, good, and excellent instruments. Further discussion appears in Chap. 18.

13.6.1 Sizzle

The jaggedness of a violin's frequency response ensures that the partials of a note played with vibrato will, as they ride the peaks and valleys of the response curve, vary in amplitude as well as frequency. Because of the random distribution of peaks, the amplitude of any given partial is as likely to be rising as falling, and so the overall loudness of the note does not tend to change much. Rather, there is a continuous shifting of the balance of partials, and this contributes to a quality of sound which we will call *sizzle*.

This effect was first pointed out by Fletcher and Sanders (1967). It was investigated experimentally by Mathews and Kohut (1973), using an electric violin and a bank of analog filters. By varying the spacing and Q of the filters, listeners found that a peak-to-valley height of about 10 dB was optimal; if lower, the instrument seemed “unresponsive”; if higher, the sound seemed “hollow.” They point out that “the fact that the best tone is achieved by an intermediate value of damping, which compromises two conflicting factors, helps explain why it is so hard to build a ‘perfect’ violin.” They also mention that the subjective effects are best heard by comparing the sound of a traditional violin with that of a solid-body electric violin, where the relatively flat response curve minimizes the effect.

Melody and Wakefield (2000) explored the relative importance of amplitude and frequency modulation in violin vibrato by artificially removing one and then the other from a recorded note. They found that “the absence of frequency modulation has little effect on the perceptual response to violin vibrato, while the absence of amplitude modulation causes marked changes. . . .”

13.6.2 Directional Tone Color

It has long been known that the sound radiation of a violin becomes increasingly directional as frequencies rise. Weinreich (1997a) showed that above about 1,000 Hz, radiation patterns begin to vary rapidly with frequency, typically changing drastically from one semitone to the next. Directivity becomes so pronounced that the individual partials of played notes radiate in “quill-like” beams. The shifts in frequency within a vibrato cycle are sufficient to cause the direction of these beams to vary, and to do so independently of one another. This creates a *directional modulation* of partials during vibrato that mirrors the amplitude modulation

described above. The overall effect is too complex to be perceived by the ear for what it is. Instead, it is heard as what Weinreich calls *directional tone color* (DTC), which contributes a “flashing brilliance” to violin sound. It also affects the way violin sound seems to fill space. Because normal loudspeakers are designed for minimal directivity, they tend to strip DTC from recorded violin sound. Indeed, a good way to highlight the subjective effect of DTC is to compare live violin playing with a monophonic recording of it.

Note that all musical instruments exhibit some directivity in their sound radiation. With the bowed strings, this is sufficiently pronounced to make DTC a significant feature of their sound quality. Both DTC and sizzle are most strongly exhibited during vibrato, which may help explain the almost continuous use of vibrato in modern performance practice. Weinreich suggests that DTC may contribute to projection: the bowed strings are the only orchestral instruments with appreciable amounts of DTC, and DTC tends to be averaged out within a string section, giving a solo violin part the advantage. Weinreich does not address the question of whether, and under what conditions, one violin might exhibit more DTC than another.

13.6.3 *Projection*

Projection, or *carrying power*, refers to how well an instrument can be heard in a variety of musical contexts. Players know that instruments that sound loud under the ear do not necessarily project well, while some apparently quiet instruments do. We have suggested that both sizzle and DTC may contribute to projection. Another possible factor is transient behavior, though to the best of our knowledge, any relationship between violin transients and projection remains unexplored. More obvious factors affecting projection are the overall amount of sound radiated, and the spectral balance of that sound. The frequency range 2–4 kHz is most often singled out as being important, because it spans the ear’s most sensitive region.

Surprisingly little research has been done on how instruments vary in terms of total sound output. Dünnwald (1991) effectively discarded this information by normalizing to an arbitrary level the response curves of the instruments he studied. Saunders devised a loudness test that involved playing the instrument “as loudly as possible” and recording the results. With regard to this, McIntyre and Woodhouse (1981) pointed out that there is not a definite limit to how loudly an instrument can be played, because the limit depends in part on how much noise can be tolerated. This underscores something noted by Weinreich (1997b): if a player is handed two instruments, he or she will tend to play them at about the same volume level. If one instrument happens to have an inherently lower sound output, the violinist may well *push* the instrument into noisier regions in order to get a *normal* amount of sound. Thus an actual difference in power can lead to a perceived difference in quality. Bissinger (2008) measured the total radiated sound of his 17 quality-related violins (including two by Stradivari and one by Guarneri del Gesù) in absolute terms, but found only slight differences in total output among them.

In one of the few studies directly concerned with projection, Loos (1995) found that it was an instrument's output at *low* frequencies (below about 1.5 kHz) that determined how well it projected. In particular, when the fundamentals of played notes were strong, the instrument seemed “closer” to the listener. This echoes Meinel's remark that large amplitudes at low frequencies help the sound “carry.” It is well-known that the ear becomes less sensitive to low frequencies as sound levels diminish, and because sound levels diminish with distance, a sound with relatively strong low-frequency components may well seem relatively close.

In Loos's experiment, the instruments were played unaccompanied and sequentially, which is how most players test projection. And yet one essential meaning of projection is that given by McIntyre and Woodhouse (1978): “audibility in a concert hall against a background of other sound.” In this sense, projection is the ability to compete with other sounds, rather than with the remembered loudness or apparent closeness of other violins. Loos's results may well have been different if the instruments were tested against a fixed reference, for example, an accompaniment played by a Yamaha Disklavier, or a recorded orchestral part played at a set level. Remember, though, that whether it is the low or high (2–4 kHz) frequency range that is responsible for projection, both Meinel and Dünnwald conclude that good violins radiate well in *both*.

A kind of converse of projection is how well an instrument blends into an ensemble. This is important in orchestral playing, and critically so in chamber music. Clearly, projection and *blendability* may be to some extent mutually exclusive, especially for the lower instruments. For example, a viola that projects over an orchestra with violin-like force and brilliance may not sound quite like a viola, nor is it likely to blend into a viola section or round out the sound of a string quartet in the traditional manner. Research in this area would be useful for violin makers, who are often asked to set up instruments with such considerations in mind.

13.7 Playability

Violinists know that instruments differ greatly in the ease with which they can be played. Differences are described in various ways, including the possibilities for “digging into the string,” playing close to the bridge, producing clean attacks, playing rapid passagework, playing high harmonics, and playing very softly. Though all of these can be affected by the particular bow and strings used, instruments themselves seem to have innate playability characteristics. While assessing them might seem to depend entirely upon subjective reports from players, it is fortunate that [as Woodhouse and Galluzzo (2004) point out], almost all bow strokes have as their goal a readily discernable phenomenon: the so-called *Helmholtz motion* of the bowed string, a *slip-stick* cycle producing a characteristic, sawtooth-like waveform. How easily and under what conditions Helmholtz motion can be initiated and sustained therefore provides a convenient yardstick for assessing playability.

This leads to a rather surprising corollary: playability can (by this model) be assessed by the listener. For just as sustained Helmholtz motion has its characteristic sound, so too do any failures to achieve it. With inexperienced players, these include a library of whistles, crunches, and shrieks. Expert players have an uncanny ability to overcome any difficulties presented by an instrument – at least when playing the kind of sustained passages typically used to demonstrate tone quality. But in rapid or otherwise demanding passagework, there are but limited possibilities for adjusting bowing parameters on a note-by-note basis. The consequences are made public in the starting transients – what players call the “attacks.” Gütter and Askenfelt (1997) have shown that the length of pre-Helmholtz transients is crucially important to violin sound, the maximum acceptable length being about 50 ms. (Note that the details of transient behavior can be muddied by the acoustics of the listening room, and so critical listening is best done at close quarters in a relatively nonreverberant space, using musical excerpts in which articulation is a challenge. Better still, recordings of these excerpts can be played back at reduced speeds. In place of the more-or-less brilliant final effect, one hears what is often a note-by-note struggle for regular Helmholtz motion.)

Pre-Helmholtz transients stem from the interaction of two distinct systems, the bowed string and the violin body. The body is considered linear under normal playing conditions, so its transient behavior is predictable, given the string signal (i.e., the force exerted by the strings at the bridge) and the frequency response of the body. The bowed string, by contrast, is highly nonlinear, which means that tiny changes in bowing conditions can have very large effects on the string signal. Thanks to the work of researchers such as Askenfelt, Galluzzo, Gütter, McIntyre, Pickering, Schelleng, Schumacher, and Woodhouse, a great deal is now understood about the bowed string, its various vibration regimes, and the many factors that determine their excitation. These factors include the mechanical properties of the string, the frictional properties of rosin, the width of the bowhair ribbon, the minimum and maximum required bow force and – most relevant to the playability of an individual instrument – the effects of body vibration on the bowed string. [Chaps. 12 and 16 of this book deal with the bowed string. An excellent overview of the subject can also be found in “The Bowed String as We Know It Today” by Woodhouse and Galluzzo (2004).] Since the string has contact with the instrument at just two points – the bridge and the fingerboard (or upper saddle) – and since the bridge is the primary path for string energy moving into the body, playability effects can presumably be traced to the dynamic behavior of the bridge, as seen at the string notches. This behavior is most naturally measured in terms of *mobility*. More on this is discussed in Sect. 13.8.1.

13.7.1 Helmholtz Motion

About 150 years ago, Helmholtz showed that the smooth curve presented by the bowed string is an optical illusion created by a *kink* traveling up and down

the string, bouncing off the bridge at one end and the player's finger at the other. This motion is described in Chap. 12. Briefly, the rosined bowhair grips the string and pulls it sideways into a shallow V. When the string in due course breaks free, the tip of the V, or *Helmholtz corner*, moves along the string until it meets the bridge and is reflected back toward the bow. The orientation of the corner (which reverses with each reflection) is then aligned with the direction of bow-motion, and so helps re-establish the bowhair's grip on the string, and thus the sticking portion of the cycle. The corner continues along the string until it bounces off the finger, where its orientation is again reversed. Upon reaching the bow, the corner now pulls *against* the direction of bow-motion, causing the string to break free, and reinstating the slipping portion of the cycle.

As long as the string-length remains constant, so too does the time taken for the corner's round-trip. The corner thus enforces the periodicity of the slip-stick cycle. Note that if the corner were absorbed rather than reflected at the termination points, the timing of the cycle would depend on a delicate balance between friction and string tension. This balance would vary with each minute change in bow speed or downward force, making it almost impossible for the player to produce a stable pitch. In reality, losses at the termination points (as well as to string damping and to the bow) are incomplete. They have the effect of rounding the Helmholtz corner, but during the sticking portion of the cycle, the bow quite literally pulls the corner sharp again.

13.7.2 Bow Force Limits

Research on playability has focused mainly on the upper and lower limits of the bow force required to initiate and sustain Helmholtz motion, for a given bow speed and position (Woodhouse 1993). The relationship between minimum and maximum force was made graphic by Schelleng, in a now-famous diagram shown in Chap. 12 of this book. Below minimum force, friction is too weak to hold the string during the sticking portion of the cycle. An untimely slip occurs, and Helmholtz motion degenerates into a surface sound, usually involving more than one slip per cycle. Above the maximum bow force, the bowhair's grip on the string is too strong to be shaken loose by the corner. The sound again degenerates, this time into a "raucous" or "crunchy" sound. Woodhouse (1993) notes that in practice, the violinist is likely to back off before this maximum level is reached, being forewarned by two earlier effects: an increase in bowing noise and a flattening of the pitch of the note.

Woodhouse argues that minimum bow force is the parameter most likely to be associated with playability differences. Unlike maximum bow force, it is strongly influenced by bridge motion: Providing the bow is relatively close to the bridge, motion of the bridge creates a fluctuating force at the point of contact between bow and string. If during the sticking portion of the cycle this additional force is

sufficient to overcome bow friction, an untimely slip will occur. To prevent this, greater bow force is needed. Thus, bridge motion raises the minimum bow force, which in turn narrows the conditions within which the player must work.

When a string waveform is reflected from the bridge, a portion of its energy is transmitted to the instrument body. Because the ring-time of the body (at about one-tenth of a second) is far longer than the period of even the lowest notes on the instrument, a kind of background vibration builds up in the bridge, again raising the minimum bow force. Of course, bridge motion also allows energy to be transferred into the violin body and so radiated as sound. This suggests a trade-off between playability and output power. In the case of the *wolf note* (see Chap. 16), the ringing of a strong body resonance allows bridge motion to build to the point where it catastrophically interferes with Helmholtz motion. Wolf notes are, in a sense, indicators that a limit has been reached to how much power can be extracted from a string. As most violins are built and/or set up so that at least the beginnings of a wolf note show up, it would seem that violin makers try (in a general sense) to increase sound output until playability becomes an issue.

13.7.3 Damping and Playability

From all of the above, it is clear that losses from the string can negatively influence playability. But now consider that the player's fingertip absorbs a greater amount of string energy than does the upper saddle, and yet as every violinist knows, stopped notes speak more easily than open strings. The notion that energy lost from the string can *help* rather than hinder playability is suggested by theoretical models of the bowed string. Using Raman's model, Friedlander (1953) and Keller (1953) showed that for a lossless system, *all* periodic bowed string waveforms (including normal Helmholtz motion) were unstable, meaning that any slight change in bowing conditions would derail them. *Some* damping is therefore beneficial to playability, for it helps to stabilize Helmholtz motion.

While string and finger damping tends to change smoothly with frequency, losses to the violin body vary sharply with the body's uneven response curve. This helps explain why musicians find some notes harder to play than others. It may be that the *range* of note-to-note variation in bridge mobility is what most affects playability. After all, large note-to-note variations require the constant adjustment of bowing parameters, which may well present the violinist with greater difficulties than more stringent but less variable conditions. More research is needed.

13.8 Violin Body Vibrations

Although violin body vibrations have been studied for a very long time, most of our understanding has been gained during the past 60 or 70 years. During the past 30 years, progress has been greatly accelerated by the development of

digital computers and sophisticated optical and electronic instruments. Research from 1930 to 1973 is well documented by the articles reprinted in Hutchins (1975, 1976).

13.8.1 Normal Modes of Vibration

Complicated vibrational motion of a structure may be understood by attempting to determine the *normal modes* of vibration. Normal modes are independent ways in which a structure vibrates. They are characterized by nodal lines (along which vibrational motion is at a minimum) and anti-nodes (where motion is at a maximum), as well as by modal frequency and damping. A normal mode can be excited by applying a force to any point on the structure that is not on a nodal line, excitation being strongest at resonance frequency. The resulting motion can be detected at any point that is not on a nodal line. In practice, the instrumentation used to excite and detect motion may modify the structure slightly by adding mass and/or stiffness.

Mode shapes are characteristic of a structure, whereas the deflection of a structure at a particular frequency, called an *operating deflection shape* (ODS), typically results from the excitation of more than one normal mode. When exciting a weakly damped structure at a resonance frequency, the ODS will be determined mainly by one mode, although if several modes have nearly the same frequency, special techniques may be required to determine their contributions to the ODS. Modes of a structure are functions of the entire structure. A mode shape describes how every point on the structure moves when the mode is excited. The distinction between a normal mode, an operating deflection shape, and a resonance is an important one [see Richardson (1997)].

As discussed in Sect. 13.5, a frequency response function describes the motion-per-force input–output relationship between two points on a structure as a function of frequency. The most commonly used functions are *accelerance* (acceleration/force) and *mobility* (velocity/force, sometimes called *mechanical admittance*). Measuring motion at the same point at which the force is applied gives *driving point* accelerance or mobility, while measuring different input and output points gives *transfer* accelerance or mobility. Frequency response functions in themselves give useful information about a violin, and a series of them at a number of points over the surface of the instrument may be used to determine a mode shape (generally by using an appropriate computer program).

The driving point mobility of a Guarneri violin driven on the bass bar side of the bridge is shown in Fig. 13.2. Note the peak around 275 Hz, which we are going to label A_0 , and prominent peaks around 460, 530, 700, and 1,000 Hz, which we label C_2 , C_3 , C_4 , and A_3 for reasons that we will explain shortly. Comparing Fig. 13.2 to the sound level curve in Fig. 13.1, we notice that the C_4 peak around 700 Hz is missing from Fig. 13.1 because it does not radiate very much sound. We discuss this in a later section.

Naming Modes

Unfortunately for the reader, different violin researchers have labeled the violin's normal modes in different ways. Rossing (2007b) has proposed a relatively simple system of labels, which combines some of the best features of other systems. In this system A_0 refers to the "f-hole" resonance associated with strong sound radiation from the f-holes, as elegantly described by Cremer (1984). A_1 is a mode around 470 Hz in which air "sloshes" from the upper to lower bout in response to plate motion.

B_n (B = beam) labels are attached to modes with beam-like bending motions of the violin body. The lowest is B_1 (called $B\text{-}1$ by some researchers, C_1 by others). It does not radiate appreciably, and because its frequency (at about 185 Hz) is typically below that of the open G string, it is unlikely to have much effect on playability. The second beam mode B_2 (called B_0 by some researchers) is also a poor radiator. It tends to be close in frequency to A_0 ; indeed, the violin maker can deliberately "match" the two modes (by adjusting the fingerboard mass and/or stiffness; see Sect. 13.9.7). This leads to somewhat enhanced radiation in the $A_0\text{--}B_2$ frequency range and a (reportedly) enhanced "feel" in the hands of the player (Woodhouse 1998).

Important modes of the violin body are labeled C_n (C = corpus). C_1 (designated CBR by some researchers, C_2 by others) is a rather symmetrical mode around 400 Hz that does not radiate very well. C_2 (designated B_1^- by some researchers, T_1 by others) is a strong mode that radiates very well and is associated with a peak that has been called W (for "main wood") or P_1 . C_3 (called B_1^+ by some researchers) is a strong mode that radiates very well and is associated with a peak that has been called P_2 . C_4 is a nearly symmetrical mode around 700 Hz with a moderately strong peak in mobility but little sound radiation.

The important collection of peaks in the 2–3 kHz region forms a sort of *violin formant* that we designate as F (called the *bridge hill* or BH by some researchers). The individual peaks can be designated as F_1, F_2, \dots, F_n if they are resolved. This violin formant is analogous to the *singer's formant*, a collection of resonances of the vocal tract that allows an opera singer to be heard over a loud orchestra.

Bissinger and Gregorian (2003) refer to modes A_0, A_1, C_1, C_2 , and C_3 (their A_0, A_1 , CBR, B_1^- and B_1^+) as *signature modes*.

13.8.2 Vibrational Models

The operating deflection shapes (ODSs) of string instruments are often described in terms of the coupled motions of the top plate, back plate and enclosed air. This *two-dimensional* model works well for a guitar, but slightly less well for a violin.

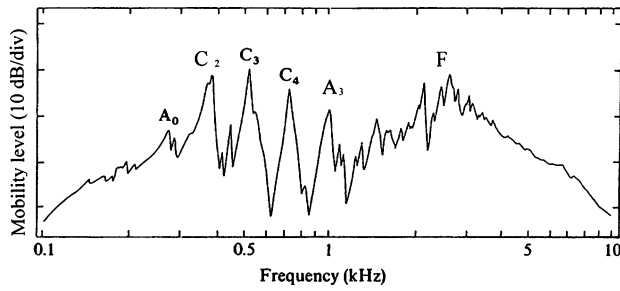


Fig. 13.2 Driving point mobility of a Guarneri violin driven on the bass bar side [adopted from Alonso Moral and Jansson (1982)]. Permanent peaks are labeled with the corresponding normal modes of vibration

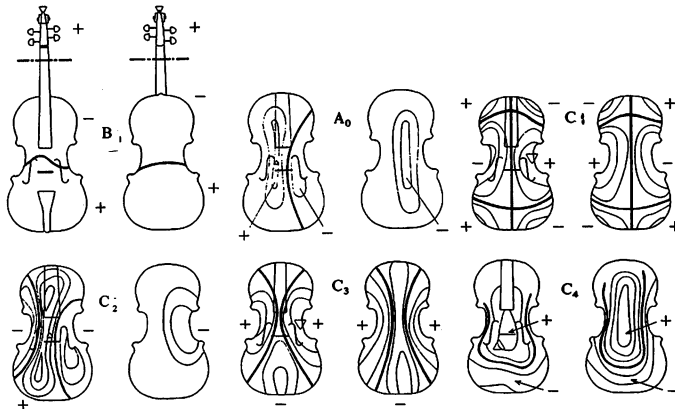


Fig. 13.3 Two-dimensional representation of five modes in a violin. A_0 (285 Hz): air flows in and out of the f-holes; C_1 (405 Hz): symmetrical motion of both plates resulting in weak sound radiation; C_2 (460 Hz): strong motion of the top plate; C_3 (530 Hz): strong two-dimensional motion of both plates; C_4 (700 Hz) symmetrical motion of both plates with weak sound radiation. Top plate and back plate are shown for each mode. The heavy lines are nodal lines; the direction of motion (viewed from the top) is indicated by + or - [after Alonso Moral and Jansson (1982)]

Two-dimensional representations of several prominent resonances are shown in Fig. 13.3.

In Fig. 13.3 it is clear that in several of the stronger modes, the central areas of the top and back plates move in the same direction. This is not surprising since they are mechanically connected by the sound post.

Two-dimensional holographic interferograms of the A_0 and A_1 modes in a violin are shown in Fig. 13.4. The interference lines provide accurate contour maps of the motion, and the nodal lines show up as bright fringes.

Many violins have a strong resonance around 1,000–1,100 Hz, which Roberts and Rossing (1997) identified with lateral air motion and suggested the label A_3 . This mode radiates fairly strongly.

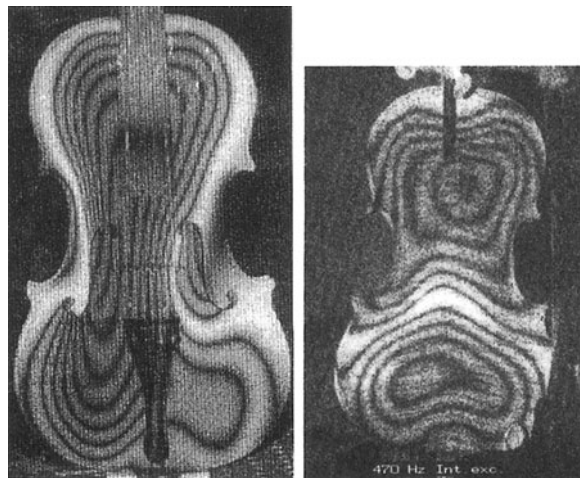


Fig. 13.4 Holographic interferograms of two “air” modes: (a) A_0 (f-hole) mode (Saldner et al. 1996); (b) A_1 mode (Roberts and Rossing 1997)

13.8.3 A Three-Dimensional Model of Vibration

As generally applied, holographic interferometry senses primarily motion normal to the plates. By using mirrors, however, it is possible to sense in-plane motion of the top and back plates, as well as motion of the ribs. When this is done, three-dimensional operating deflection shapes can be accurately determined (Runnemalm et al. 2000). The violin, when sectioned in the bridge plane, can then be interpreted as an *elliptical tube* with nodal diameters. The C_1 and C_2 modes, which have two nodal planes intersecting the cylinder at complementary locations, then form a doublet. The C_3 and C_4 modes, which have three intersecting nodal diameters, form a second doublet. These doublets are not unlike those observed in cylindrical vibrators such as bells, and they remind us that a violin is a three-dimensional object (Rossing et al. 2003). Of course, the violin is really a much more complex structure than either a pair of coupled plates or an elliptical tube, but these simple models help us to understand how it does vibrate.

13.8.4 Modal Analysis

Modal analysis is widely used to describe the dynamic properties of a structure in terms of modal parameters: natural frequency, damping factor, modal mass, and mode shape. The analysis may be done either experimentally or mathematically.

Experimental methods include experimental modal testing (with sinusoidal or impact excitation) and holographic modal analysis. Mathematical methods include finite-element methods and boundary-element methods.

Modal testing is a systematic method for identification of the modal parameters of a structure. In violin testing, the excitation is usually a sinusoidal force or an impulse. Detection methods include: measuring acceleration with an accelerometer; measuring surface velocity with a vibrometer; determining deflection by means of holographic interferometry, and determining nodes via Chladni patterns.

Both experimental and mathematical methods have been applied to violins. Holographic methods for studying vibrations were pioneered by Powell and Stetson (1965) and extensively applied to violins by Jansson et al. (1970) and by Reinecke and Cremer (1970). In recent years, quite a number of researchers have used optical methods such as holographic interferometry and laser vibrometry to study violins. A good review of optical methods for studying vibration is given by Molin (2007).

Experimental modal testing of violins has been described by Müller and Geissler (1983); Marshall (1985); by Jansson et al. (1986); and Bissinger (2003). In experimental modal testing, the violin is excited with a measured force at selected points, and the response is measured at some other point, either with a small accelerometer or with a laser beam. The applied force may be either impulsive or sinusoidal. Modal parameters are determined by the use of curve-fitting routines on a digital computer (Rossing 2007a).

Mathematical modal analysis generally employs either finite-element methods (FEM) or boundary-element methods (BEM). Finite-element methods are based on the premise that an approximate solution to a complex engineering problem can be reached by subdividing the problem into smaller more manageable (finite) elements. Finite-element methods have been applied to violins by Knott (1987); by Bretos et al. (1999); and by Rodgers and Anderson (2001).

One characteristic of both experimental and mathematical methods of modal analysis is that they result in large catalogs of modes without much indication of their relative significance. Still, they do yield a lot of useful information.

13.8.5 What Modes Can a Maker Control?

Woodhouse (2002) identifies two factors determining the extent to which individual modes can be controlled by violin makers, or for that matter tracked by researchers: *modal overlap* and *statistical overlap*. Modal overlap is the ratio of the bandwidth of a series of adjacent modes to their frequency spacing. When the modes are narrow (i.e., lightly damped) and/or widely spaced in frequency, modal overlap is small. Peaks on a response curve can then be reliably attributed to individual modes. When modal overlap is large, peaks tend to be the result of interactions between a number of modes of differing amplitude and phase.

Statistical overlap characterizes the sensitivity of mode frequencies to structural changes, such as plate thickness, or changes in material properties, for example, due to shifts in humidity. Statistical overlap is the ratio of the average frequency shift from structure parameter changes to the mean modal spacing. When statistical overlap is low, individual modes keep their identity despite structural changes. When it is high, their identities are lost in the shifting modal population.

For violins, both modal and statistical overlap go up with frequency. Below about 1,000 Hz, it makes sense to describe individual modes, and for violin makers to perhaps try to manipulate them individually. (The frequency of A_0 , for example, can be readily controlled by changing the area of the f-holes.) At higher frequencies (e.g., the formant or bridge hill region) an irredeemable confusion sets in. Trying to associate individual peaks with specific body modes is usually futile, and a statistical approach involving average levels, peak-spacing, and peak-to-valley height then becomes more useful. Woodhouse points toward wood selection, bridge tuning (see Sect. 13.9.5), adjustments to the “island” area, and the soundpost as means by which violin makers might influence populations of high-frequency modes.

13.9 Component Parts

Section 13.8 began with a discussion of the entire instrument; we will now consider the vibration of some of the component parts. When building an instrument, the maker must deal with these parts individually, and so one goal of research has been to provide workshop guidelines based on empirical relations between the parts and the whole. The top and back plates (in that order), are usually considered most critical to the instrument’s sound. The bass bar, bridge, and soundpost are critical too, but they are considered part of the *setup*, and are routinely adjusted or replaced without affecting the value or integrity of the instrument proper. That said, most makers would agree that changes to almost *any* part of the structure can sometimes have surprising effects.

13.9.1 Top and Back Plates

Violin tops, like the sound boards of so many other stringed instruments, are usually made from quarter-cut spruce. Backs are typically figured maple, though poplar, willow, and other woods have been used successfully, especially for the lower instruments of the violin family. Carleen Hutchins played a significant role in bringing the importance of free-plate modes to the attention of makers. In Fig. 13.5, time-averaged holographic interferograms show the first six free-plate modes for a violin top, and the first seven for the back.

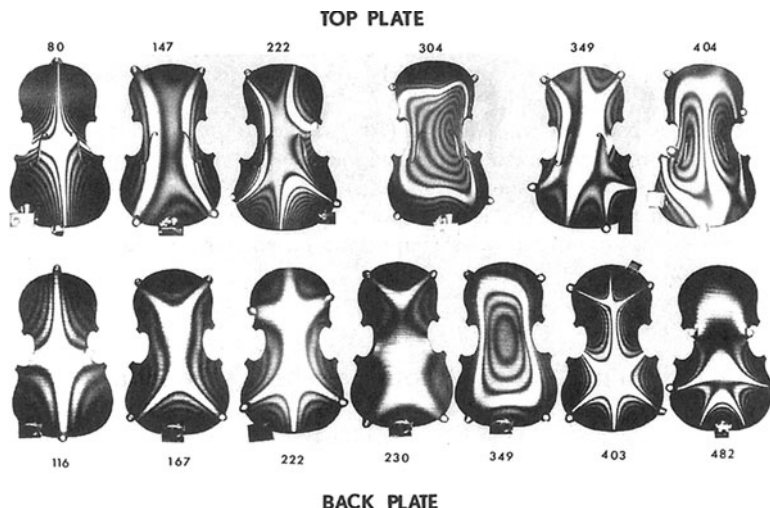


Fig. 13.5 Time-averaged holographic interferograms of a free violin *top plate* and *back plate* (Hutchins et al. 1971)

13.9.2 Tap Tones

If a violin top or back is held lightly between two fingers and tapped, one or more of the lowest plate modes are heard as *tap tones*. Modes 1, 2, and 5 (corresponding to the first, second, and fourth modes in the upper row, and the first, second, and fifth in the lower row) are of special significance, as their frequencies are related to the stiffness properties of the wood – torsional stiffness for mode 1, and stiffness across and along the grain for modes 2 and 5, respectively. These modes can be individually excited by holding the plate along a nodal line and then tapping in the area of an antinode. They can also be made visible as Chladni patterns by using the sine-wave-and-glitter method popularized by Hutchins and shown in Fig. 13.6.

Tap tones have interested both makers and researchers going back at least as far as Felix Savart. In recent decades, researchers such as Jansson, Alonso Moral, and Rodgers have provided many useful guidelines for makers interested in “tuning their plates,” that is, adjusting the tap tones to match target frequencies. Hutchins found an octave relationship between modes 2 and 5 of a Stradivari top, and went on to develop an influential method for bi- and tri-octave plate tuning (1991).

There is scant evidence from either historical documents or the current state of Old Italian instruments that their makers used, or were even aware of, Tap tones. Table 13.1 gives mode 2 and 5 frequencies along with plate mass for nine old Italian violin tops, with and without bassbar. No common norms for either tap tones or mass are apparent. Mode 2 values (without bassbar) range from 117 to 143 Hz, mode 5 from 276 to 332 Hz, and mass from 54 to 65.5 g. The highest value in each case is about 20% greater than the lowest.



Fig. 13.6 Mode 2 (*left*) and mode 5 (*right*) for a typical violin top. Plates are sprinkled with glitter and suspended above a loudspeaker, which is fed by a sinewave generator. When the frequency matches a plate mode, the plate vibrates vigorously, causing the glitter to migrate toward the still areas along the nodal lines

Table 13.1 Tap tones and top plate mass of nine Old Italian violins (from Curtin 2006)

Instrument	Without bassbar			With bassbar			
	M2 (Hz)	M5 (Hz)	Mass (g)	M2 (Hz)	M5 (Hz)	Mass (g)	Bar (g)
“Booth” Stradivari, 1716	127	305	54	150	345	58	4
“Kreutzer” Stradivari, 1727	117	276	55.5	139	324	60	4.5
“Petri” Stradivari, 1700	126	332	65.5				
“Artot-Alard” Stradivari, 1728	127	304	61.7	146	351	66	4.3
Guarneri del Gesu, 1726	143	308	64.1	155	362	68.4	4.3
C. Landolfi, 1762	150	321	59.2	172	371	63.5	4.3
C. Tononi, <i>circa</i> 1730	127	332	62.9	146	384	67.2	4.3
“Spivakov” C.G. Testore	143	322	60.5	164	366	65	4.5
F. Ruggieri, <i>il Per</i> 1685	150	324	61.2	171	375	65.5	4.3
Average	131	309	59.9	155	360	64.2	4.3

M2 and M5 are modes 2 and 5, respectively. Mass is in grams. The shaded values are estimates, used when an instrument could not be measured both with and without the bassbar. Estimates of mass without bassbar were made by subtracting the average bassbar mass (4.3 g) from the total mass. Estimates of frequencies were made by calculating the average percent-frequency-shift produced by the bar, and then “virtually” removing the bar

Schleske (1996) found that there is “no correlation between a tuning of the free violin plates (‘tap tones’) and the resulting frequency spectrum of the violin (up to 1,000 Hz). This makes the meaning of a free-plate tuning method questionable.” Curtin (2006) points to the usefulness of taptones *in combination with plate mass*

for assessing both the stiffness and the material properties of old and new plates. He suggests that, when copying a specific instrument, it makes sense for a maker to try to match the tap tones and mass of the original. The possibilities for matching *both* depend on the mechanical properties of the wood chosen. Schelleng (1963) used the ratio c/ρ to capture something like the stiffness-per-unit-mass for violin wood, where c is the velocity of a compression wave in a given direction, and ρ is the wood density. Haines (1979) called this the *radiation ratio*. Wave velocity can be conveniently measured using a Lucchi Elasticity Tester. Curtin (2006) argues that readings across and along the grain are sufficient for dealing with modes 2 and 5. He also notes a statistical correlation between low-density and high-radiation ratio, so choosing the least dense woods tends to yield those with the highest ratios. Radiation ratio varies somewhat throughout a given piece of wood, making a perfect match between any two pieces unlikely. But in principle at least, if the ratios match both across and along the grain, then two plates can be matched in terms of mode 2, mode 5, and plate mass. If the densities of the woods also match, so too can plate thicknesses. For an in-depth discussion of material properties relevant to musical instrument construction, see Barlow (1997).

13.9.3 The Mass of a Violin

Although most aspects of the violin have been studied in detail, the mass of the body and its component parts has until recently been mostly ignored in the violin literature. The oversight is especially puzzling for tops and backs, which can easily be weighed while an instrument is apart for restoration. Möckel (1930) lists tap tones for numerous Italian tops and backs, but makes no mention of their mass. Hutchins (1991) recommends specific frequency relationships for the plates, but again without reference to plate mass. Alonso Moral (1984) investigated the relationship between free-plate modes and those of the assembled violin using tops with masses from 67 to 93 g, and backs from 115 to 147 g. Harris (2005) cites tops between 59 and 71 g. The above figures, along with those seen in Table 13.1, suggest that the heaviest violin tops are about 60% more massive than the lightest, and that the Old Italians lie at the light end of the scale.

The increasing use of CT (computed tomography) scans to study violins allows detailed measurement of density and mass distribution. Figures are only beginning to emerge, but for violins by Stradivari and Guarneri del Gesu, top plate densities seem to range from about 0.33 to 0.42 g/cm³, and backs from about 0.5 to 0.58 g/cm³. These values are toward the low end of the density range for both woods, suggesting the not-unreasonable idea that Old Italian makers chose lightweight wood. Stoel and Borman (2008) found that the difference in density between early- and late-growth wood for spruce found in Old Italian violins was markedly less than for new instruments, though the average density was about the same in both groups.

13.9.4 Enclosed Air

The violin encloses roughly a liter of air, which contributes both effective stiffness and mass to the vibrations of the violin body. In order to isolate the motion of the air from the motion of the plates and ribs, it is possible to imbed the violin in sand or else construct a cavity with rigid walls having the same size and shape as the violin. The violin cavity can be excited by inserting a small hose or pipe into the cavity and moving a small microphone around inside the cavity to map the pressure maxima and minima (nodes). Seven modes of a violin cavity are shown in Fig. 13.7. The numbers below each drawing give the numbers of nodes in the longitudinal and transverse directions.

The $(0,0)$ mode corresponds to the Helmholtz resonance H_0 which has no internal nodes. The air in the cavity acts as the stiffness, and the air in and around the f-holes acts as the vibrating mass. Note that the frequency is slightly higher than that of the A_0 mode in which the top and back plate are also vibrating. A simplified mathematical model shows that when the modulus of the mobility is plotted as a function of frequency, the resonance of the A_0 normal mode is followed by a dip (anti-resonance) with a minimum very close to the frequency of the Helmholtz resonance in a violin with rigid walls.

In general, modes of the enclosed air interact with plate modes having the same shape. Thus the $(0,1)$ air mode interacts with “rocking” modes of the plates to give the A_1 mode in the violin which typically occurs around 475 Hz. Again, the $(0,1)$ air mode is slightly higher in the cavity with rigid walls.

13.9.5 Bridge

The bridge serves to translate the mainly lateral force of the strings into mainly vertical forces on the top via the bridge feet. Violin makers know that small changes to the bridge can make dramatic differences to an instrument’s sound, and so pay careful attention to everything from the choice of wood to the precise details of thickness, height, and overall proportions. In recent decades, researchers –

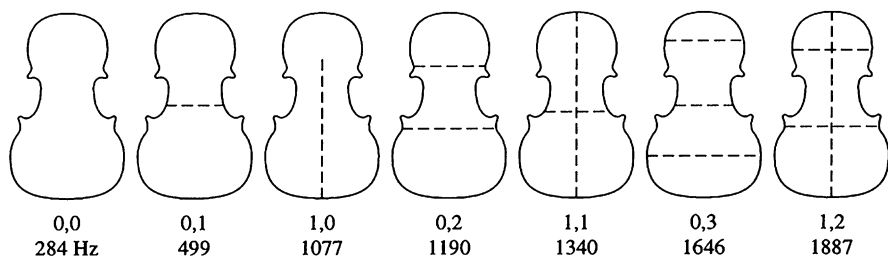


Fig. 13.7 Modes of a violin air cavity having rigid walls (Roberts and Rossing 1997)

especially Jansson et al. (1990) – have shown the importance of the bridge's lowest in-plane resonance to the violin's treble response. More recently, the importance of bridge mass has been investigated by Woodhouse (2005) and Bissinger (2006).

Figure 13.8 shows a typical violin bridge. The upper portion is divided from the lower portion by a distinct waist. This creates the conditions for a resonance, the waist acting as a spring, and the upper portion as a mass that rocks from side to side. This resonance, which we will call simply the *bridge resonance*, is illustrated in Fig. 13.9. It happens to be the bridge's lowest in-plane mode. There are several others, both in-plane and out-of-plane, within the frequency range of interest, most notably a second in-plane mode at about 6,000 Hz, the up-and-down bouncing motion of which is shown in Fig. 13.9. These other modes have not yet been studied much in terms of their effect on violin sound.



Fig. 13.8 A typical violin bridge

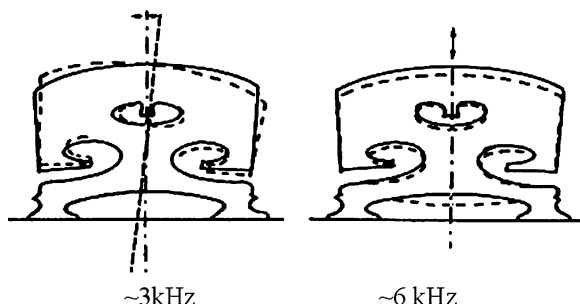


Fig. 13.9 The first and second in-plane modes of a violin bridge mounted on a rigid surface. (After Reinecke 1973)

Well below resonance frequency, the bridge behaves as a rigid body, allowing the strings to act directly on the body. At resonance frequency, the bridge strongly reinforces the transmission of string vibration to the body. As frequencies rise above resonance, string vibration is increasingly reflected from the bridge and back into the string. In this way, the bridge acts as a low-pass filter, a kind of treble control knob that the maker can turn up or down by raising or lowering the resonance frequency. For a normally cut violin bridge, the bridge resonance typically falls between 2,800 and 3,300 Hz (measured with the feet clamped in a massive vise). This happens naturally when makers follow normal workshop practice, but it can be consciously controlled in a process known as *bridge tuning*. For example, narrowing the waist and/or leaving the top portion heavier will reduce frequency. A simple experiment is to place tiny wedges in the cutouts of the bridge. This greatly increases the in-plane stiffness, while hardly affecting bridge mass. Alternatively, bits of modeling clay can be affixed to the top of the bridge, raising the effective mass without changing the stiffness. Müller (1979) did just such an experiment with the bridge mounted on a rigid plate. Figure 13.10 shows the results in terms of the force transmitted from the top of the bridge to the bridge feet. On a strung-up violin, the effects are an increase in the brightness of the sound when the bridge is wedged, and a muting when mass is added.

Rodgers and Masino (1990) used finite-element analysis to predict the first few modes of typical violin and cello bridges, and then suggested where makers might remove wood in order to shift the mode frequencies. Bissinger and a team of violin makers studied two violins set up with a range of bridges and bridge tunings covering a total of 140 different mass/frequency combinations. Their findings clearly showed that both higher bridge frequencies and lower bridge mass were associated with greater high-frequency radiation.

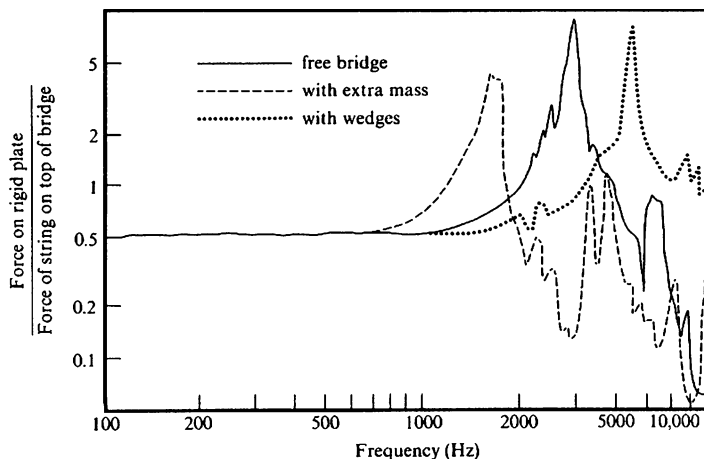


Fig. 13.10 Force transfer function of the bridge with additional mass (1.5 g) and additional stiffness. (Data of Reinecke cited in Müller 1979)

When mounted on a violin, the modes of the bridge more or less disappear into those of the instrument body. Bissinger (2006) found that below about 600 Hz, the bridge is effectively rigid, and motions of the bass bridge-foot predominate. As frequencies rise, the bridge undergoes a variety of in-plane and out-of-plane contortions, and the treble foot becomes the center of motion. At still-higher frequencies, movement of either foot can dominate.

Violin makers consider bridge height important to sound, higher bridges being associated with increased power and brightness. According to Cremer (1984), mobility at the string notches tends to increase as the square of the ratio of bridge-height to bridge-foot spacing. Increasing bridge height (while keeping foot-spacing constant) will therefore increase acoustical output for a given string force, and also make wolf notes more likely. This is one reason why cellos, with bridges that are rather high in relation to their width, are specially prone to wolf notes, and why reducing bridge height can help get rid of them.

13.9.6 Ribs

The sides or *ribs* of a violin are made by hot-bending strips of ~1 mm thick maple about a form, gluing them to the end- and corner-blocks, and then reinforcing their upper and lower edges with *linings* (typically spruce or willow about 2 mm thick by 6 mm wide). The linings broaden the gluing surface to which the plates are attached, and also strengthen the ribs in rather the way that a buttress supports and strengthens a wall.

The finished rib assembly is about 30 mm high, and so has an obvious role in defining the interior volume of the violin body, and hence its A_0 mode frequency. Another important role is in tying the front and back plates together along their edges, resulting in body modes that combine the motions of both front and back. The bending stiffness of the rib assembly (which increases with rib and lining thickness and decreases with rib and lining height) affects the boundary conditions of the plates. If the ribs were very flexible, the plates would vibrate as though hinged along their edges. If very stiff, the edges of the plate would in effect be rigidly clamped – thus raising the frequency of all the flexing modes of the plates. Whatever the rib stiffness, the motions of the back and front in the assembled violin will be very different from those of the free plates, whose low-frequency modes strongly depend on the free boundary conditions.

13.9.7 Fingerboard

The shape and dimensions of the neck and fingerboard are critical to the comfort of the musician and the playability of the instrument. Important too is the angle at which the neck is set into the body, as this determines the height of the bridge.

Dynamically, the fingerboard acts as a cantilevered beam, with one end fixed and the other free.

Schleske (2002) used experimental modal testing to measure the fingerboard modes of a Stradivarius violin. He found a bending mode close in frequency to the instrument's second beam mode (B_2) so that the fingerboard vibrates strongly with that mode. In fact, the interaction of fingerboard and body vibration results in a *splitting* of the B_2 mode into a doublet: In one mode, the end of the fingerboard moves in the same direction as the top plate, in the other it moves in the opposite direction.

A torsional or twisting mode of the fingerboard is observed at 507 Hz, and this mode couples to the strong C_3 corpus mode resulting in a splitting of that mode into a doublet, which has component frequencies of 513 and 524 Hz in one Stradivarius violin. The fingerboard twists in opposite phase for the two components. Another doublet due to fingerboard coupling is observed at 1,620 and 1,690 Hz.

Violin maker sometimes try to bring the frequency of the B_2 beam mode into close proximity with that of the A_0 air mode. Because the B_2 mode involves significant fingerboard motion, this *mode tuning* is most easily done by adding or removing mass from the end of the fingerboard, or by scraping wood from the underside of the fingerboard near the root of the neck, thus reducing fingerboard stiffness.

13.9.8 Bass bar and Soundpost

The bass bar is a gracefully shaped beam of spruce that runs along the inside of the top, its outside edge lying about a millimeter inside the edge of the bass bridge foot. Statics, the bar stiffens the top plate and so helps distribute the downward force of the bridge over a greater area. Dynamically, it raises the frequency of the vibrational modes. The soundpost is a spruce dowel (~6 mm diameter) fitted between the top and back plates. It is typically placed 2–3 mm behind the treble bridge foot, and about a millimeter inside the edge of the foot. The soundpost helps support the top by transmitting some of the downward force of the strings to the back. Unlike the bar, it is not glued in place; indeed, adjusting both its position and length (by as little as a few tenths of a millimeter) is one of the principal means by which makers optimize an instrument's sound and response.

The bass bar and soundpost introduce an important structural asymmetry into the violin's otherwise-symmetrical design. Without this, the rocking motion of the bridge would tend to induce equal but opposite motions in the areas of the top around each bridge foot. The result would be an acoustical "short-circuiting" that would reduce low-frequency radiation.

Saldner et al. (1996) found that removing the soundpost from one violin: (1) lowered the frequencies of the A_0 and C_2 (B_1^-) modes by 8 and 13%, respectively; (2) made the C_2 mode quite symmetrical; (3) raised the frequency of the C_3 (B_1^+) mode by 2%; (4) left the A_1 mode unchanged; and (5) introduced a symmetrical

bending mode in the top plate. Bissinger, on the other hand, found that removing the soundpost left the frequencies of the C_2 (B_1^-) and C_3 (B_1^+) mode frequencies virtually unchanged, but completely changed the mode shapes. He also noted a drastic decrease in the radiation efficiency.

Saldner et al. (1996) also compared several modes of a violin with the soundpost in the normal position to those of the same violin with the soundpost relocated about 10 mm closer to the centerline of the violin. With the soundpost nearer the center line, the C_2 mode was raised about 9% in frequency and the bridge mobility level was increased about 15 dB at the frequency of the C_3 mode, though its frequency was not changed.

13.10 Measuring Sound Radiation

Under normal playing conditions, a violin produces sound in response to the string force at the bridge. For measurement purposes, a transducer typically applies the force, while one or more microphones pick up the sound. A transfer function between microphone and driver signals yields the frequency response in terms of sound pressure at the microphone position, per-unit-force at the bridge, a measure of what Weinreich has termed *radiativity*.

Many possible radiation measurements can be made for a given violin. The bridge can be excited at different driving points and in different directions, and each will excite a different balance of body modes. Because of increasingly directional radiation above about 1 kHz, shifting the microphone position can significantly change the measurements. Furthermore, the response of the instrument itself may change with temperature and humidity, and then there are the complicating effects of room acoustics. All this makes it difficult to measure violin sound radiation in a comprehensive way. Instead, researchers rely on a number of simplifications. The bridge is generally excited with a lateral force, while a limited number of microphone positions are used to sample the sound field. Langhoff (1994) found that eight positions provided a good estimate of total radiation. Schleske (2002) used 36, spaced evenly around the instrument in the plane of the bridge; Bissinger (2008) used 266, arranged spherically.

Many excitation methods have been employed, including bowing machines and electromagnetic bridge drivers. For purposes of illustration, we will consider some results obtained with an impact hammer. Figure 13.11 shows the equipment used. The hammer taps the bass corner of the bridge, while a sensor in its tip records the force waveform of the blow. The microphone, which can be moved 360° around the instrument, is held in the plane of the bridge at 37 cm from the central axis of the instrument, here defined as a line rising vertically through the end-pin. To increase the signal-to-noise ratio, the complex average of several impacts is taken for each microphone position. The measurements cited below are all for a single, good-quality, modern violin. To avoid problems with reflected sound, measuring was



Fig. 13.11 Apparatus for measuring sound radiation using an impact hammer. It can be set up in a violin maker's workshop

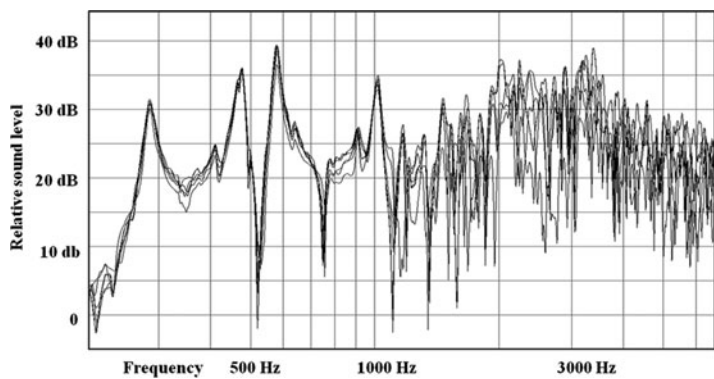


Fig. 13.12 An overlay of five microphone positions, one directly in front, the others at 30° and 60° to either side. Though there is good correspondence at low frequencies, the spread above about 1 kHz indicates radiation patterns that change significantly with frequency

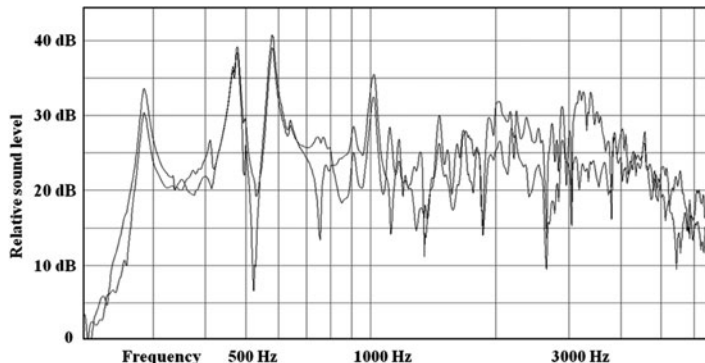


Fig. 13.13 The average magnitude of five front microphone positions overlaid on the average of five rear positions. The higher level of the front microphone average shows that high frequencies are most strongly directed forward from the instrument

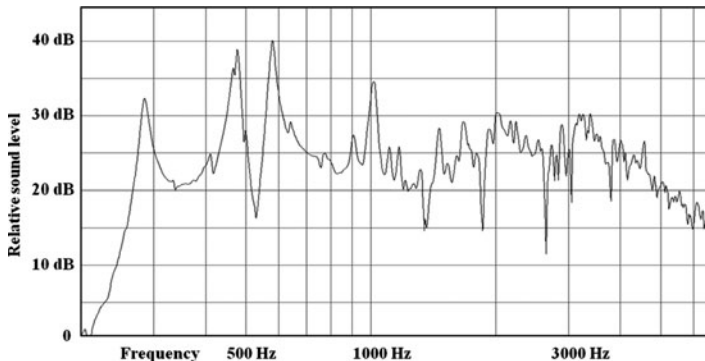


Fig. 13.14 Average magnitude for 12 microphone positions

done in an anechoic chamber. Twelve microphone positions were used, one directly in front of the bridge, the others spaced at 30° intervals around the instrument.

There are many ways of deriving single response curves from multiple readings. Figure 13.14 shows the average magnitude for all 12 microphone positions, while Fig. 13.15 shows a single, front-central position. Which curve better represents the sound of the instrument?

While the two graphs have a very similar overall shape, note that above 1 kHz, the peak-to-valley heights are far greater for the single-microphone measurement, and as we saw in Sect. 13.6.1, this *spikiness* is important to sound quality. The averaged measurement provides an estimate of the total radiated sound (assuming that radiation in the plane of the bridge is representative). The single-microphone measurement represents what might be heard by listening with one ear held 37 cm from the violin in an anechoic chamber. This is further than the violinist's ear, but much closer than a typical listener's, though neither player nor listener is likely to

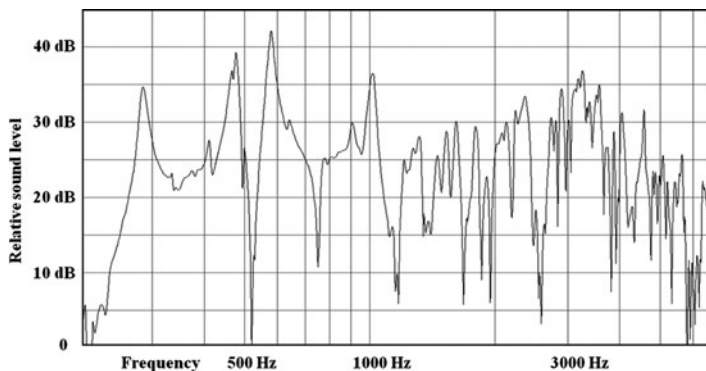


Fig. 13.15 Single, front-center microphone position

be found in an anechoic chamber! Without further laboring the point, there is no single radiation measurement that fully captures the sound of a violin. The meaningfulness of any particular measurement depends on how well the measurement conditions are specified. The usefulness depends on how much light is shed on the question at hand.

13.11 Low-Frequency Radiation

For each body mode, the violin subdivides into a number of vibrating regions bounded by nodal lines, with neighboring regions moving in opposite phase to one another. Each vibrating region generates a pressure wave in the air adjacent to it, but when the dimensions of the body are small compared with the wavelength of sound in air, a kind of short-circuiting occurs: One region moves up while another moves down, and their respective pressure waves cancel out. For radiation to occur under these conditions, the combined displacements of all vibrating regions *must not be zero*. Put another way, their combined displacements must produce a change in the instrument's volume. The resulting monopole radiation is omni-directional, and its level depends only on the amplitude of volume fluctuation.

Volume fluctuation can occur when a body mode has an odd number of vibrating regions, and/or when the vibrating regions displace unequal amounts of air, for example, when the regions differ in area or net displacement. For violins, the off-center placement of soundpost and bassbar introduces a major asymmetry into the otherwise-symmetrical design. This asymmetry is compounded by the many irregularities in geometry and material properties found in handmade wooden instruments. The result is that no violin modes are perfectly symmetrical, making it unlikely that their vibrating regions will exactly cancel out. For this reason, all modes are likely to produce some volume fluctuation. This is large for a few of the lowest modes (notably C_2 or B_{1-} and C_3 or B_{1+}), but at higher frequencies, vibrating

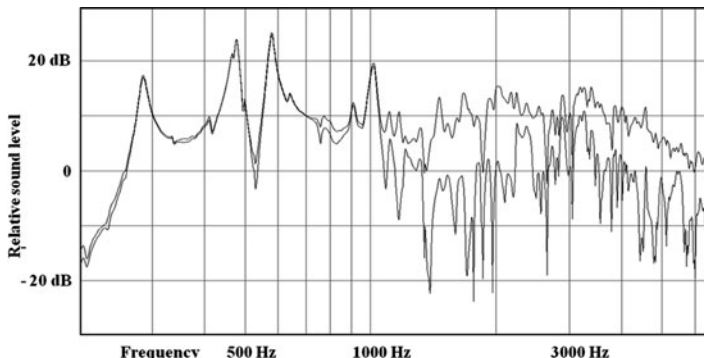


Fig. 13.16 Estimated total radiation (upper line) and monopole radiation (lower line). The first was arrived at by taking the average magnitude for 12 microphone positions, and the second by the complex average, which allows for cancellation due to phase differences

regions of mutually opposing phase become ever more finely distributed throughout the structure. As a consequence, the chances that summing their displacements will add up to a significant change in volume grows steadily smaller.

Weinreich et al. (2000) have termed the frequency region in which monopole radiation predominates the *monopole regime*. Its upper limit is easily specified for a spherical structure: it is the frequency for which the wavelength of sound in air is equal to the sphere's circumference. For an irregular structure such as a violin, however, the situation is complicated by the instrument's narrow waist, which presents an obvious acoustical shortcut. For a typical violin, the distance from the center of the top (in the C-bout region) to the center of the back is about 16 cm, or a half-wavelength at about 825 Hz. Figure 13.16 shows estimates of monopole and total radiation for a typical violin. The coincidence of the two lines below about 1 kHz confirms that virtually all low-frequency radiation is indeed monopole. At higher frequencies, directional radiation becomes a large fraction of the total output.

13.12 High-Frequency Radiation

When the speed of a bending wave in a plate matches the speed of sound in air, the well-known *coincidence frequency* is reached. At this and all higher frequencies the plate will radiate well, and in an increasingly directional fashion. While the speed of sound in air is constant with frequency, that of bending waves increases with the square root of frequency. This is because shorter wavelengths entail a more acute bending of the material, and thus a greater restoring force. Consequently, the velocity of bending waves will *at some frequency* reach that of sound waves in air. The higher the stiffness-to-mass ratios of a plate, the lower this coincidence frequency will be. Cremer (1984) estimates values of about 5 and 18 kHz (along and across and the grain, respectively) for a flat, 2.5-mm-thick top plate. Because

the stiffness-to-mass ratios of a violin plate are advertized by the frequencies of its lowest free-plate modes, the usefulness of tap tones to violin makers is underscored.

For a flat, isotropic plate of uniform thickness, bending wave velocities are the same in all directions. For a complex structure made with an orthotropic material such as wood, velocities tend to vary both with direction and local changes in plate stiffness. For this reason, it is neither possible nor meaningful to determine a single coincidence frequency for a violin. Still, two aspects of the instrument's behavior point to what might be called a *coincidence frequency region* – a region in which coincidence frequency is approached and then achieved in at least one direction: (1) an increasing amount of directional radiation above about 1 kHz and (2) a plateau in *radiation efficiency* beginning at about 3.5 kHz.

The term *radiation efficiency* [as used by Bissinger (2004)] compares a mode's radioactivity with that of a very efficient and well-studied radiator – the baffled piston. Radiation efficiency (R_{eff}) is the ratio of a mode's total radiation to that of a baffled piston of the same surface area and mean-squared velocity. Well below coincidence frequency (and barring a strong monopole component), R_{eff} tends to be low. But as wave velocities increase, so does R_{eff} , reaching a maximum value of about 1. Bissinger (2004) finds a *plateau* in radiation efficiency at about 3.4 kHz for the “good” violins he measured, and about 4.8 kHz for the “bad” violins. Just where this plateau is reached is presumably related to the geometry and material properties of the particular instrument. For example, a violin with plates that have low stiffness-to-mass ratios will plateau at a relatively high frequency. This is the case for Bissinger’s “bad” violins, suggesting relatively thin plates and/or dense wood. One can equally well imagine bad violins with excessively thick plates, and a correspondingly low plateau frequency. Indeed, the re-graduation of too-thick factory instruments has long been a way for violin shops to provide good-sounding instruments at reasonable prices.

13.13 Radiation Damping

In the context of violin acoustics, radiation damping is the damping associated with energy carried away from the instrument by sound waves. It is related to the instrument's radiation efficiency and to its vibrating mass.

If each mode of a violin is represented by a baffled piston attached to a damped spring, then the radiativity of the mode can be modeled by making the area of the piston equal to the area of the mode multiplied by its radiation efficiency. Thus a poorly radiating mode will be represented by a piston with a very small surface area, while one which radiates well will have a correspondingly larger area. Now consider two pistons with the same area, resonance frequency, and excitation level, but one having twice the mass of the other. Both will radiate energy at the same rate, but the heavier piston, having twice the stored energy, will have half the radiation damping. Radiation damping, then, is proportional to radiation efficiency and *inversely* proportional to vibrating mass. As radiation efficiency tends to go up

with frequency, so too will radiation damping. When radiation efficiency reaches 1, radiation damping is governed entirely by mass.

As an approximation, Bissinger (2008) computes radiation damping by dividing radiation efficiency by the total mass of the instrument (without chinrest). He finds that his “excellent” violins have slightly higher radiation damping across the frequency span, though more so at lower frequencies. Above 2 kHz, violins of all quality classes were similar in terms of radiation damping, and propagated errors were too large to make much of any differences.

13.14 Electric and Virtual Violins

The practical difficulties of manipulating violin body modes can be nicely sidestepped, at least for research purposes, by emulating the modes electronically with filters, as described in Chap. 22. The signal to the filter bank can come from an appropriately designed electric violin, or from a traditional violin with force sensors at the string notches. Pioneering work was done by Mathews and Kohut (1973), who used a solid-body electric violin to drive an analog filter bank. As described in Sect. 13.6.1, the filtered output was then amplified and sent to a speaker. Gorrell (1975) built a loudspeaker into a modified traditional viola. The string signal from the viola was fed through an external filter bank and then back to the onboard speaker. In both the above cases, the resulting sound could be changed by adjusting the filters.

The term *virtual violin* is most often applied to systems for synthesizing violin sound, but also to various electronic and digital methods for driving traditional violins and/or modifying their sound. For example, Farina et al. (1995) derived the string signal from a traditionally played violin, recorded it, and then convolved it with the impulse response from the same violin. The result, they reported, was a plausible emulation of the instrument played in the normal manner.

Weinreich and Caussé (1991) developed a *digital bow*, in which a photoelectric sensor was used to determine the string velocity at an imagined bowing point. A computer calculated the corresponding bowing force, using previously programmed frictional characteristics. The bowing force was then applied by passing a current through the string, which had a magnetic field applied at the bowing point. Experiments with the digital bow shed some light on the stability of the Helmholtz motion of a bowed string (see Chap. 12). A digital bow was used by Müller and Lauterborn (1996) to demonstrate nonlinear effects at high bow speeds.

The *reciprocal bow*, developed by Curtin (1997), is a direct descendent of Weinreich’s technique for measuring radiativity: the violin is excited by a loudspeaker playing a swept sine wave, and the bridge vibrations are picked up with a phono cartridge. With the reciprocal bow, a string signal is fed to the loudspeaker, so that the violin is, in effect, played backward. It absorbs sound rather than radiating it, and the bridge becomes the output rather than the input. If we think

of the violin as a complex filter, removing or enhancing portions of the string signal, the filter works equally well in both directions.

Recent use of *virtual violin* technology by Fritz et al. (2007) takes the string signal from a real violin and uses it to drive digital filters corresponding to the modified admittance curves of actual violins. Initial studies focused on the perceptual thresholds for detecting amplitude and frequency changes to a violin's three lowest radiating modes, as well as changes to the frequency bands specified by Dünnwald (1991).

Boutin and Besnainou (2008) inserted piezoelectric actuators into the violin bridge, the resonance frequency and damping of which could then be modified electrically, allowing the treble response of the instrument to be changed while the instrument was being played. This kind of experiment suggests possibilities for developing hybrid digital/acoustical instruments that allow players an unprecedented degree of control over the sound. For further discussion of virtual string instruments, see Chap. 23.

Acknowledgments The authors wish to thank Colin Gough, Gabriel Weinreich, and Jim Woodhouse for their many valuable comments, insights, and suggestions.

References

- Alonso Moral J, Jansson E (1982) Input admittance, eigenmodes, and quality of violins. Report STL-QPSR 2-3/1982, pp. 60–75. Speech Transmission Laboratory, Royal Institute of Technology (KTH), Stockholm.
- Barlow CY (1997) Materials selection for musical instruments. *Proceedings of the Institute of Acoustics*, **19**, part 5, 69.
- Bissinger G (2003) Model analysis of a violin octet. *J. Acoust. Soc. Am.* **113**, 2105.
- Bissinger G (2004) The role of radiation damping in violin sound. *ARLO* **5**(3), 82.
- Bissinger G (2006) The violin bridge as filter. *J. Acoust. Soc. Am.* **120**, 482.
- Bissinger G (2008) Structural acoustics of good and bad violins. *J. Acoust. Soc. Am.* **124**, 1764.
- Bissinger G and Gregorian A (2003) Relating normal mode properties of violins to overall quality signature modes. *J. Catgut Acoust. Soc.* **4**(8), 37.
- Boutin H, Besnainou C (2008) Physics parameters of the violin bridge changed by active control. *Proceedings of the Acoustics 2008*, Paris, 4189.
- Bretos J, Santamaría C, Alonso Moral J (1999) Vibrational patterns and frequency responses of the free plates and box of a violin obtained by finite-element analysis. *J. Acoust. Soc. Am.* **105**, 1942.
- Cremer L (1984) *The Physics of the Violin*. MIT Press, Cambridge, MA.
- Curtin J (1997) The reciprocal bow as a workshop tool. *J. Catgut Acoust. Soc.* **3**(3), 2d Series, 15.
- Curtin J (2006) Taptones and weight of Old Italian violin tops. *VSA Papers* **1**(2), 161.
- Dünnwald H (1991) Deduction of objective quality parameters on old and new violins. *J. Catgut Acoust. Soc.* **1**(7), 2d Series, 1.
- Farina A, Langhoff A, Tronchin L (1995) Realization of “virtual” musical instruments: measurements of the impulse response of violins using MLS technique. *Proceedings of the CIARM95*, Ferrara (Italy), 19.
- Fletcher HA, Sanders LC (1967) Quality of violin vibrato tones. *J. Acoust. Soc. Am.* **41**, 1534.
- Friedlander FG (1953) On the oscillations of the bowed string. *Proc. Camb. Philol. Soc.* **49**, 516.
- Fritz C, Cross I, Moore BCJ, Woodhouse J (2007) Perceptual thresholds for detecting modifications applied to the acoustical properties of a violin. *J. Acoust. Soc. Am.* **122**, 3640.

- Gorrill S (1975) A viola with electronically synthesized resonances. *Catgut Acoust. Soc. Newsletter* **24**, 1.
- Güttler K, Askenfelt A (1997) Acceptance limits for the duration of pre-Helmholtz transients in bowed string attacks. *J. Acoust. Soc. Am.* **101**, 2903.
- Haines DW (1979) On musical instrument wood. *Catgut Acoust. Soc. Newsletter* **31**, 23.
- Harris N (2005) On graduating the thickness of violin plates to achieve tonal repeatability. *VSA Papers* **1**(1), 111.
- Hutchins CM (1975) *Musical Acoustics, Part I: Violin Family Components*. Dowden, Hutchinson and Ross, Stroudsburg, PA.
- Hutchins CM (1976) *Musical Acoustics, Part II: Violin Family Functions*, Dowden, Hutchinson and Ross, Stroudsburg, PA.
- Hutchins CM (1991) A rationale for bi-tri octave plate tuning. *J. Catgut Acoust. Soc.* **1**(8), 2d Series, 36.
- Hutchins CM, Stetson KA, Taylor PA (1971) Clarification of “free plate tap tones” by holographic interferometry. *Catgut Acoust. Soc. Newsletter* **16**, 15.
- Jansson EV, Molin N-E, Sundin H (1970) Resonances of a violin studied by hologram interferometry and acoustical methods. *Phys. Scripta* **2**, 243.
- Jansson EV, Bork I, Meyer J (1986) Investigation into the acoustical properties of the violin. *Acustica* **62**, 1.
- Jansson EV, Frydén L, Mattsson G (1990) On tuning the violin bridge. *J. Catgut Acoust. Soc.* **1**(6), 2d Series, 11.
- Keller JB (1953) Bowing of violin strings. *Comm. Pure Appl. Math.* **6**(4), 483.
- Knott G (1987) A modal analysis of the violin using MSC/Nastran and Patran, MS thesis, Naval Postgraduate School, Monterey, CA.
- Langhoff A (1994) Measurement of acoustic violin spectra and their interpretation using a 3D representation. *Acustica* **80**, 505.
- Loos U (1995) Investigation of projection of violin tones; reviewed by Martin Schleske (2003) *J. Catgut Acoust. Soc.* **4**(8), 72.
- Lucchi Elasticity Tester, developed by and available from G. Lucchi & Sons Workshop, Cremona, Italy: <http://www.lucchi-n-sons.com>
- Marshall KD (1985) Modal analysis of a violin. *J. Acoust. Soc. Am.* **77**, 695–709.
- Mathews MV, Kohut J (1973) Electronic simulation of violin resonances. *J. Acoust. Soc. Am.* **53**, 1620.
- McIntyre ME, Woodhouse J (1978) The acoustics of stringed musical instruments. *Interdiscip. Sci. Rev.* **3**, 157.
- McIntyre ME, Woodhouse J (1981) Aperiodicity in bowed string motion. *Acustica* **49**, 13.
- Meinel HF (1957) Regarding the sound quality of violins and a scientific basis for violin construction. *J. Acoust. Soc. Am.* **29**, 56.
- Mellody M, Wakefield G (2000) The time-frequency characteristics of violin vibrato: modal distribution analysis and synthesis. *J. Acoust. Soc. Am.* **107**, 598.
- Möckel O (1930) *Die kunst des geigenbaues*. Verlag von Bernh. Friedr. Voigt, Leipzig.
- Molin N-E (2007) Optical methods for acoustics and vibration measurements. In: Rossing TD (ed) *Springer Handbook of Acoustics*. Springer, New York, pp. 1101–1125.
- Moral JA (1984) From properties of free top plates, of free back plates and of ribs to properties of assembled violins. *STL-QPSR* **25**(1), 1.
- Müller HA (1979) The function of the violin bridge. *Catgut Acoust. Soc. Newsletter* **31**, 19.
- Müller HA, Geissler P (1983) Modal analysis applied to instruments of the violin family. SMAC 83, Royal Academy of Music, Stockholm.
- Müller G, Lauterborn W (1996) The bowed string as a nonlinear dynamical system. *Acustica* **82**, 657.
- Powell RL, Stetson KA (1965) Interferometric vibration analysis by wavefront reconstruction. *J. Opt. Soc. Am.* **55**, 1593.

- Reinecke W (1973) Übertragungseigenschaften des Streichinstrumentenstegs. *Catgut Acoust. Soc. Newsletter* **13**, 21.
- Reinecke W, Cremer L (1970) Application of holographic interferometry to vibrations of the bodies of string instruments. *J. Soc. Am.* **48**, 988.
- Richardson MH (1997) Is it a mode shape or an operating deflection shape? *Sound Vib* **31**(1), 54.
- Roberts M, Rossing TD (1997) Normal modes of vibration in violins. *J. Catgut Acoust. Soc.* **3**(5), 3.
- Rogers O, Anderson P (2001) Finite-element analysis of a violin corpus. *J. Catgut Acoust. Soc.* **4**(4), 12.
- Rodgers OE, Masino TR (1990) The effect of wood removal on bridge frequencies. *J. Catgut Acoust. Soc.* **1**(6), 2d Series, 6.
- Rodgers OE (2005) Tonal tests of prizewinning violins at the 2004 VSA competition. *VSA Papers* **1**(1), 75.
- Rossing TD (2007a) Modal analysis. In: Rossing TD (ed) *Springer Handbook of Acoustics*. Springer, New York, pp. 1127–1138.
- Rossing TD (2007b) Observing and labeling resonances of violins, Paper 3-P1-1, *Proceedings of ISMA 2007*, Barcelona.
- Rossing TD, Molin N-E, Runnemalm A (2003) Modal analysis of violin bodies viewed as three-dimensional structures. *J. Acoust. Soc. Am.* **114**, 2438.
- Runnemalm A, Molin N-E, Jansson EV (2000) On operating deflection shapes of the violin body including in-plane motions. *J. Acoust. Soc. Am.* **107**, 3452.
- Saldner HO, Molin N-E, Jansson EV (1996) Vibration modes of the violin forced via the bridge and action of the soundpost. *J. Acoust. Soc. Am.* **100**, 1168.
- Schelleng JC (1963) The violin as a circuit. *J. Acoust. Soc. Am.* **35**, 326.
- Schleske M (1996) Eigenmodes of vibration in the working process of the violin. *J. Catgut Acoust. Soc.* **3**(1), 2.
- Schleske M (2002) Empirical tools in contemporary violin making. Part II: Psychoacoustic analysis and use of acoustical tools. *J. Catgut Acoust. Soc.* **4**(5), 2d Series, 43.
- Schleske M Criteria for rating the sound quality of violins. <http://www.schleske.de/en/our-research/handbook-violinacoustics/rating-the-sound-quality.html>.
- Stoel BC, Borman TM (2008) A comparison of wood density between classical Cremonese and modern violins. *PLoS One* **3**(7), e2554. doi:10.1371/journal.pone.0002554.
- Weinreich G (1997a) Directional tone color. *J. Acoust. Soc. Am.* **101**, 2338.
- Weinreich G (1997b) Personal conversation.
- Weinreich G, Caussé R (1991) Elementary stability considerations for bowed-string motion. *J. Acoust. Soc. Am.* **89**, 887.
- Weinreich G, Holmes C, Mellody M (2000) Air-wood coupling and the Swiss cheese violin. *J. Acoust. Soc. Am.* **108** (5 Pt 1), 2389.
- Woodhouse J (1993) On the playability of the violin. Part II: Minimum bow force and transients. *Acustica* **78**, 137.
- Woodhouse J (1998) The acoustics of “ A_0-B_0 mode matching” in the violin. *Acustica Acta Acustica* **84**, 947.
- Woodhouse J (2002) Body vibration of the violin – What can a maker expect to control? *J. Catgut Acoust. Soc.* **4**(5), 2d Series, 43.
- Woodhouse J (2005) On the ‘bridge hill’ of the violin. *Acustica/Acta Acustica* **91**, 155.
- Woodhouse J, Galluzzo PM (2004) The bowed string as we know it today. *Acta Acustica/Acoustica* **90**, 579.

Chapter 14

Cello

Eric Bynum and Thomas D. Rossing

14.1 The Cello

The violoncello, or cello, is a member of the violin family of string instruments, but it is distinctly different from the violin. Its strings are tuned to C2, G2, D3, and A3, an octave below the viola and a twelfth (octave plus a fifth) below the violin. Although the strings vibrate at one-third the frequency of those on a violin, the length and width of its body are closer to twice rather than to three times those of the violin. Increased rib height and relatively thinner construction help to keep the resonances sufficiently low for bass enhancement. An exploded view of a cello is shown in Fig. 14.1.

The cello has a rich history. The oldest surviving cello is thought to be the work of Andrea Amati, and is dated 1572. It was made as part of a group of instruments for Charles IX, King of France, and shows that the cello was established as a member of the violin family at an early time (Dilworth 1999). The early instruments made in Cremona by Amati and his family were 79 cm in length, whereas smaller cellos of about 71 cm (twice the length of the violin) were made in Brescia. These two sizes persisted well into the eighteenth century. The standard length today is about 75 cm (Dilworth 1999). A comparison of cello and violin dimensions is given in Table 14.1.

Most acoustical research on bowed string instruments has been concentrated on the violin. Although in a typical orchestra there are about one-third as many cellos as violins, published material on cello acoustics is relatively scarce (see Firth 1974, Egger 1991, Langhoff 1995, Woodhouse and Courtney 2003).

T.D. Rossing (✉)
Center for Computer Research in Music and Acoustics (CCRMA),
Stanford University, Stanford, CA 94302-8180, USA
e-mail: rossing@ccrma.stanford.edu

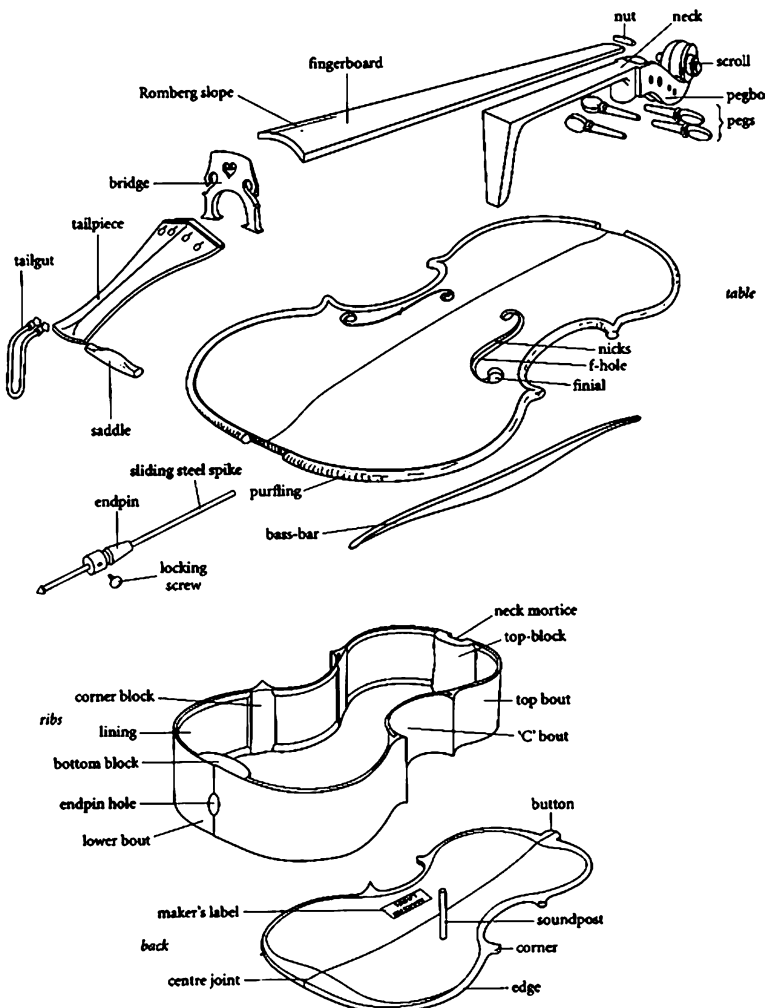


Fig. 14.1 Exploded view of the cello

Table 14.1 Comparison of cello and violin dimensions (Bynum 1997)

General part description	Cello	Violin
Lower bout width (cm)	43	20
Upper bout width (cm)	34	16
C-bout width (cm)	24	10.5
Sound cavity length (cm)	76	35
Rib depth (cm)	12	3.5
f-hole surface area (cm^2)	42.5	9.25

14.2 Modal Analysis of Cellos

Probably the most important determinant of the sound quality and playability of a string instrument is the vibrational behavior of its body. The rather complex vibrations of the body are conveniently described in terms of normal modes of vibration or eigenmodes. Violin body vibrations have been studied for 150 years or more, although the development of optical holography and digital computers has greatly contributed to our understanding in the past 20 years. Vibrations of cello bodies are equally complex, and their vibrations have been studied in more recent years.

The normal modes of vibration of violins and cellos are determined mainly by the coupled motions of the top plate (table), back plate, and enclosed air. Smaller contributions are made by the ribs, neck, fingerboard, and other parts. The coupling between the various oscillators is more difficult to model than in the guitar, for example, because of the soundpost. Although the free plates of violins have been successfully modeled by finite-element methods, most of our knowledge about cello vibrations is based on experimental studies.

14.2.1 Frequency Response

The frequency response of an instrument is a good indication of how it behaves (i.e., vibrates or radiates sound) at different frequencies throughout its playing range. One way of expressing the vibrational frequency response is to apply a sinusoidal force at one point (often the bridge) and observe the response at some other point. If the response is the observed velocity of some point, the *mobility* (or mechanical admittance) is obtained by dividing the velocity by the applied force. This is a very useful expression of the frequency response. (Closely related to mobility is *accelerance*, which is acceleration divided by applied force). Another useful expression of frequency response is the *radiance*, which is the pressure of the radiated sound, measured with a microphone, divided by the force.

The mobility of a cello is compared to that of a violin in Fig. 14.2. The frequency scale in the violin is twice that of the cello so that the corresponding peaks (resonances) and valleys (anti-resonances) are easier to compare. A peak in the mobility curve indicates a frequency at which the driving point moves relatively easily, while a valley indicates a frequency at which the driving point moves with great difficulty (although vibrations at that frequency may be excited easily at some other drive point).

Note the close spacing of the C_2 (T_1 or B_1^-), C_3 (B_1^+), and C_4 peaks in the mobility graph in Fig. 14.2b, unlike the violin (Fig. 14.2a) where they are spread out over nearly an octave. One luthier noted that in a cello the C_2 and C_3 peaks often blend into one broad resonance peak around 140–190 Hz. “I have found that by using slightly higher arching profiles (max 32 mm instead of 26–28 mm normal) and a lighter bass bar and thinning the plate around the edges those modes can be

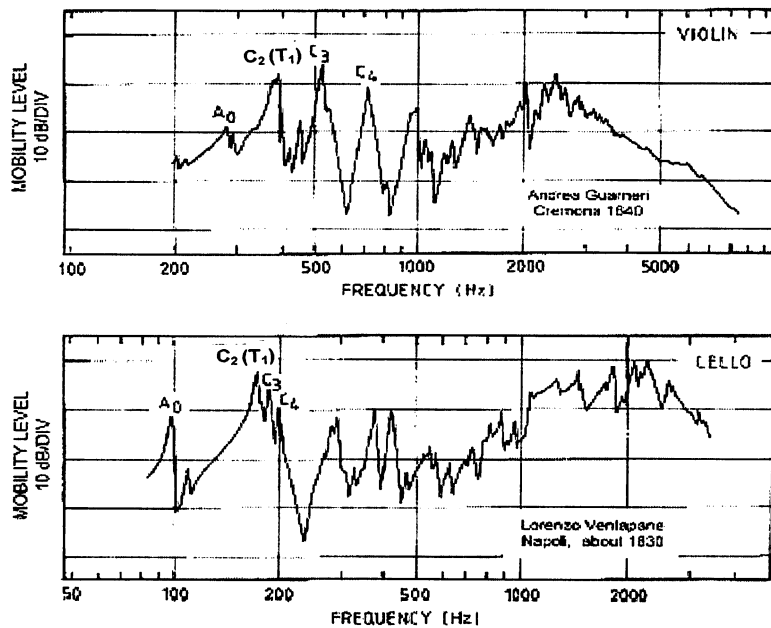


Fig. 14.2 Mobility curves for a violin (top) and a cello (bottom). Note the different frequency scales (Askenfelt 1982)

spread out between 165 and 200 Hz which reduces the wolf problem and gives a much more useable resonance band" (Caldersmith 1997).

14.2.2 Modes of Vibration

The complex vibrations of a complex structure, such as a musical instrument, can be described in terms of *normal modes of vibration*. A normal mode of vibration represents the motion of a linear system at a normal frequency. Each mode is characterized by a natural frequency, a damping factor, and a mode shape. *Normal* implies that each shape is independent of all other mode shapes for the structure.

The vibration of a structure when an oscillating force is applied is often called the *operating deflection shape* (ODS). The operating deflection shape at each frequency will generally be a combination of normal mode shapes. If the normal mode frequencies are well separated and the mode damping is small, the ODSs correspond closely to the normal modes of vibration. In a cello, they represent the normal modes fairly well at low frequency, but at higher frequencies rather special techniques are required to observe the normal modes of vibration.

In a cello, sound radiation from the large top and back plates dominates, but sound is also radiated through the f-holes, and so the motion of the air inside the

cello is of considerable interest. By applying appropriate constraints it is possible to study the vibrations of the top plate, back plate, and enclosed air alone, but in general when a force is applied to any part of the cello, or when the cellos is played, the resulting vibrations are due to coupled vibrations of many parts of the cello. Although we sometimes speak of *plate modes* or *air modes* at frequencies where the motion of one part of the cello is especially strong, most modes of vibration involve the motion of several different parts of the instrument.

14.2.3 Observing the Modes

Modal testing is a systematic method for identification of the modal parameters of a structure. Modal testing may use sinusoidal, random, pseudo-random, or impulsive excitation (each has its advantages and disadvantages). The response may be measured mechanically, optically, or indirectly (e.g., by observing the radiated sound field). The first step in experimental modal testing is generally to obtain a set of frequency response functions.

Whereas resonance frequencies can generally be identified from a single frequency response function (FRF), obtaining modal shapes and damping parameters requires a more complete modal analysis. Most experimental modal analysis relies on a modal parameter estimation (curve fitting) technique to obtain modal parameters from the FRFs (see Rossing 2007a).

Optical methods, such as holographic interferometry and scanning laser vibrometry, offer the best spatial resolution of operating deflection shapes. In cases where the damping is small and the modes are well separated in frequency, the operating deflection shapes correspond closely to the normal mode shapes. Modal damping can be estimated with a fair degree of accuracy from half-power points determined by counting fringes. Phase modulation allows analysis to be done at exceedingly small amplitudes and also offers a means to separate modes that overlap in frequency (see Molin 2007).

14.2.4 Labeling the Resonances

Different researchers have used different systems for naming and labeling resonances of cellos as well as violins, and a certain amount of confusion has resulted. We recently proposed a labeling system that combines some of the best features of the systems used by various researchers. A_0 refers to the f-hole resonance. B_n (B = beam) labels are attached to bending modes of the body. Important modes of the cello or violin body are labeled by C_n (C = corpus). The important collection of peaks in the 800–1,200 Hz region forms a sort of *formant*, which we designate as F (called the *bridge hill* by some researchers). The individual peaks can be designated as F_1, F_2, \dots, F_n if they are resolved (Rossing 2007b).

14.3 Modes of Component Parts

14.3.1 Cello Plate Modes

Violin and cello makers have traditionally attached considerable significance to the vibrations of free top and back plates as determined by listening to tap tones and more recently by visual observation of the mode shapes (see Chap. 13). Many makers use Chladni patterns to map the nodal lines in free plate modes. Holographic interferograms of a well-tuned top plate and back plate are shown in Fig. 14.3 (Hutchins et al. 1971). Particularly important are the X-mode (mode no. 2) and the ring mode (mode no. 5), which correspond to the tap tones that luthiers hear and use to gauge thickness and stiffness of the plate while carving it to shape. Less has been published about the free plate modes of cellos, but they are quite similar to those of violins.

Wilkins (2003) compares Chladni patterns of free cello plates, the top and back plates with ribs attached, and the same plates in the assembled cello.

14.3.2 Cello Air Cavity Modes

The first seven modes of a cello air cavity are shown in Fig. 14.4. These are observed by constructing a cello-like cavity with rigid walls or by imbedding the cello in a sandbox so that the plates cannot vibrate. The modes are labeled by two

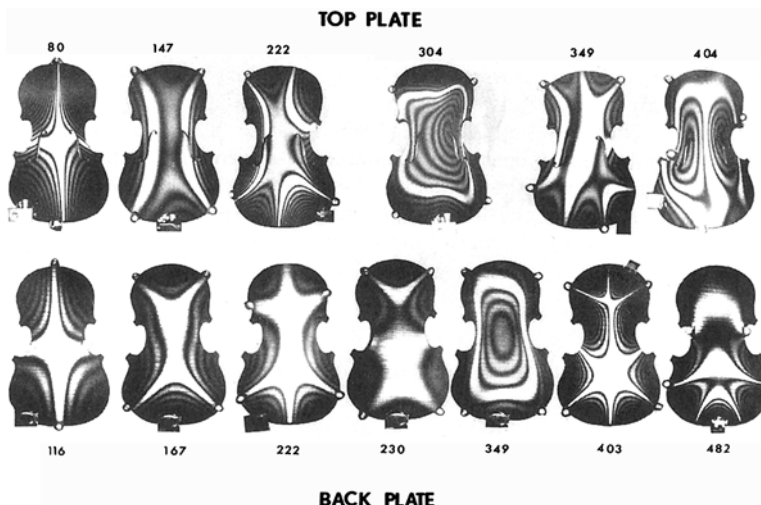


Fig. 14.3 Holographic interferograms showing modes of a free violin *top plate* and *back plate* (Hutchins et al. 1971)

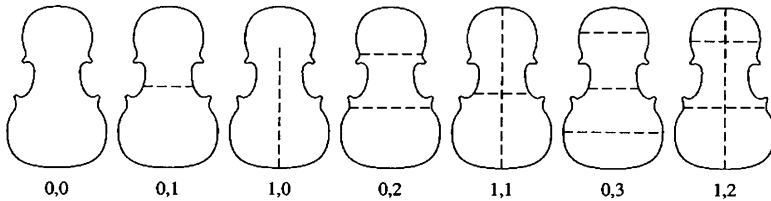


Fig. 14.4 Modes of a cello air cavity

integers m and n , which denote the number of transverse and longitudinal nodes, respectively. The nodes are observed by moving a probe microphone inside the cavity and observing the locations where the phase shifts by 180° .

The first air mode, the (0,0) or Helmholtz resonance, is found at 104 Hz. This is followed by a longitudinal (0,1) air mode at 226 Hz and a transverse (1,0) mode at 496 Hz. The (0,2) longitudinal air mode at 547 Hz is followed by a (1,1) mode at 609 Hz and a (0,3) air mode at 742 Hz. The (1,2) mode is observed at 820 Hz. Other air modes are the (2,0) at 893 Hz, the (1,3) mode at 980 Hz, the (0,4) mode at 1,016 Hz, and the (1,4) mode at 1,129 Hz (Bynum 1997).

14.4 Cello Body Modes

The best spatial resolution of modes of vibration is obtained with holographic interferometry (see Chap. 13). On a time average holographic interferogram, vibrational nodes show up as bright lines, and the fringes between the nodes allow the displacement to be determined to within a fraction of the optical wavelength. The fringes provide a sort of contour map showing the out of plane component of displacement of every point on the structure.

The first important mode is the A_0 or f-hole mode. The top and back plates vibrate in such a way as to change the volume of the cavity, and air is pumped in and out of the f-holes, resulting in considerable sound radiation. Typically the resonance associated with this mode occurs around 90–100 Hz, close to the frequency of the open G string (98 Hz). A holographic interferogram of a cello vibrating in its A_0 mode is shown in Fig. 14.5a. Because the cello radiates well at the frequency of this mode, it can be driven with an oscillating sound field as well as by a mechanical force applied to the bridge (Bynum 1997).

Another mode in which the air in the cavity interacts strongly with the top and back plates is the A_1 mode at around 200 Hz, shown in Fig. 14.5b. Both plates rock around a nodal line across the waist of the cello, so air sloshes back and forth between the upper and lower bouts (as in the (0,1) mode of the rigid cello cavity). Because the volume change is opposite in phase in the two bouts, relatively little sound is radiated from the f-holes. Another mode showing similar nodal patterns

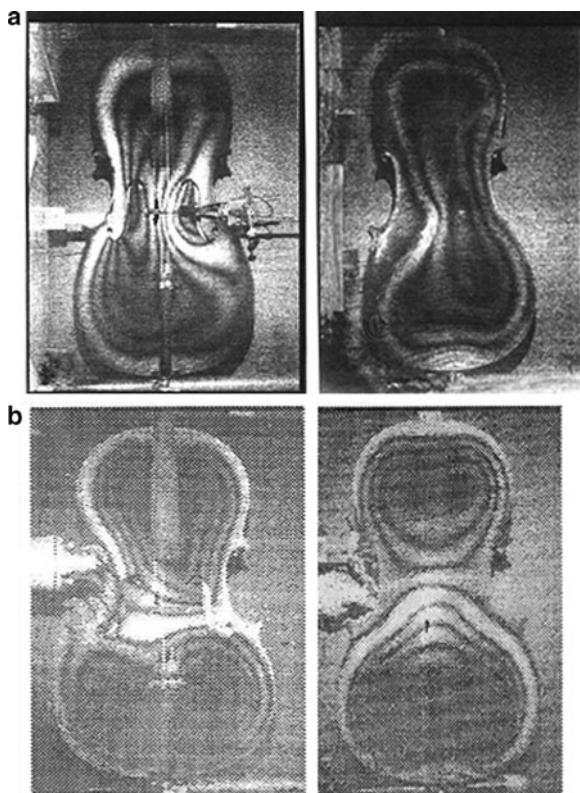


Fig. 14.5 Holographic interferograms of two cello modes with considerable air motion. (a) A_0 mode, top and back plates; (b) A_1 mode, top and back plates (Bynum 1997)

in the top and back plates is the A_2 mode around 300 Hz, but in this case the two plates move essentially in the same direction so there is much less motion of the air in the cavity.

The B_1 mode at 57 Hz is essentially a bending mode of the entire cello, and it radiates very little sound, but it does contribute to the “feel” of the instrument. The C_1 mode is a rather symmetrical mode that does not radiate very well either. The C_2 mode around 140 Hz, however, is an important resonance that results in considerable sound radiation (this mode has been called the T_1 mode by some researchers, because the top plate moves strongly; other researchers have called this the B_1^- mode). Another important radiating mode is the C_3 mode around 220 Hz (called the B_1^+ by some researchers). The rather symmetrical C_4 mode around 195 Hz, (Fig. 14.6) although it shows prominently in the mobility curve (see Fig. 14.2), does not radiate very well.

Table 14.2 compares frequencies of certain cello modes (resonances) reported in the literature. The modal frequencies are fairly similar, which is not surprising because cello makers have many years of experience to follow.

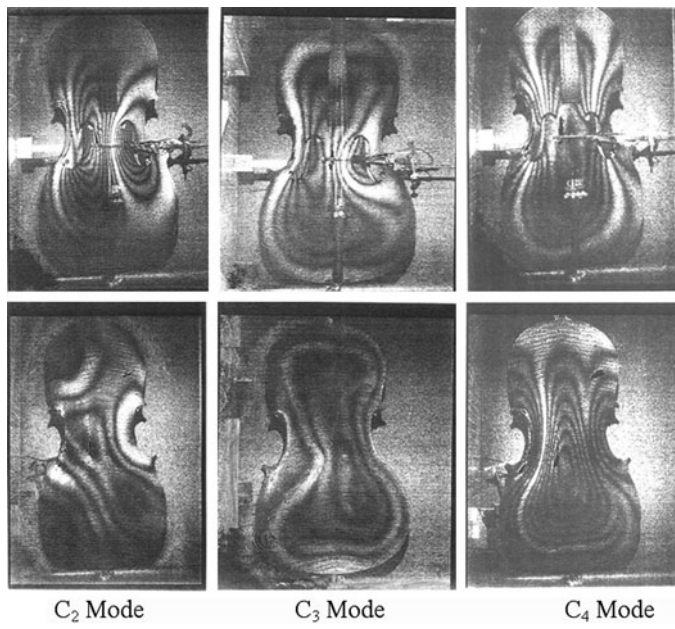


Fig. 14.6 Holographic interferograms of C_2 , C_3 , and C_4 modes in the same cello (Bynum and Rossing 1997)

Table 14.2 Mode frequencies in cellos reported by several researchers

Mode	Bynum (1997)	Eggers (1991)	Askenfelt (1982)	Langhoff (1995)	Firth (1974)	Comment
B_1 (Hz)	57					aka B_1 , C_1 mode; bending of whole cello
A_0 (Hz)	102	82	90	85	90, 104	f-hole mode
C_2 (Hz)	144	132	168	146	165, 185	aka T_1 , B_1^- , P_1 mode; strong radiator
B_2 (Hz)					178, 205	aka B_0 mode
C_1 (Hz)	170	186	163			aka C_2 mode; torsional motion
C_3 (Hz)	219	218	185			aka B_1^+ , P_2 mode; strong radiator
C_4 (Hz)	195	202				Symmetrical mode; weak radiator
A_1 (Hz)	203					Longitudinal air motion
A_3 (Hz)	277	260				Longitudinal air motion
A_2 (Hz)	302	312				Symmetrical mode; weak radiator
C_5 (Hz)	297					
C_6 (Hz)	336					

Table 14.3 Comparison of resonance (mode) frequencies in violin and cello

Mode	Cello (Hz)	Ratio to violin
B_1	57	0.33
A_0	102	0.36
C_2	144	0.32
C_1	170	0.42
C_4	195	0.29
A_1	203	0.43
C_3	219	0.39
A_3	277	0.25
A_2	302	0.37

14.4.1 Comparison with Violin Resonances

A comparison of the violin and cello frequency response functions in Fig. 14.2 shows that the cello is not a violin scaled up in size. Three resonances cluster around 200 Hz in the cello, whereas the corresponding resonances in the violin are more evenly spaced. Table 14.3 compares the resonance frequencies in a cello and a violin.

Because the cello is tuned a twelfth lower than the violin, one might expect the ratios to be close to 0.33, which several of them are. However, the ratios range from 0.25 to 0.43, from which it is evident that a cello is not a scaled-up violin. The dimensions in Table 14.1 are further evidence of this fact.

14.5 Sound Spectra of the Cello

The sound spectrum depends on the way the cello is supported. Sound spectra for a cello supported on rubber bands and the same cello supported by a cellist in normal playing position are shown in Fig. 14.7. In addition to spectral peaks corresponding to the low-frequency modes that we have discussed, a *formant* is seen in the range of 800–1,000 Hz. This formant is somewhat less prominent than the formant in the sound of a violin or the *singer's formant* in the human voice.

Like all string instruments, the cello has a directional radiation pattern that varies with frequency as shown in both the horizontal and vertical planes in Fig. 14.8. The shaded sectors in the figure represent the main directions of the radiated sound in the indicated frequency ranges. The lower frequencies are broadly radiated toward both the sides and front, whereas the higher frequencies have much more directionality. The timbre of cello sound thus varies with position in the audience. Different conductors prefer different seating arrangements for their cello sections.

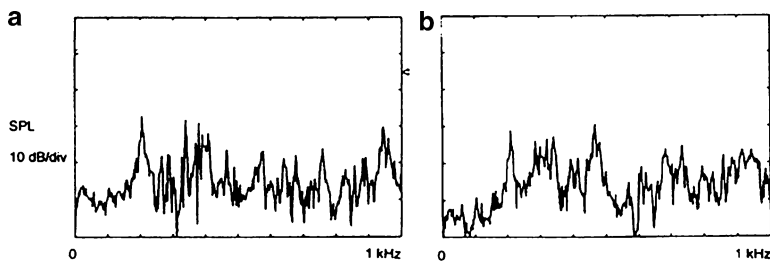


Fig. 14.7 Room-averaged sound spectra of a cello: (a) freely supported on rubber bands; (b) hand-held in playing position (Bynum and Rossing 1997)

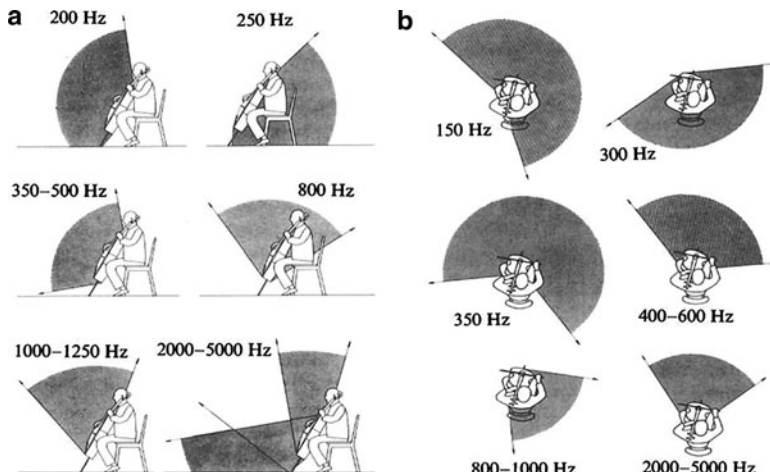


Fig. 14.8 Principal radiation directions for a cello at different frequencies: (a) in the vertical plane; (b) in the horizontal plane (Meyer 1972)

14.6 Mobility (Admittance) at the Bridge

An important way to characterize the behavior of a cello is the input admittance (mobility) at the bridge. This is the only aspect of the body behavior that influences the string and hence the only aspect that can contribute to variations of *playability* between instruments. Woodhouse and Courtney (2003) have measured the 3×3 admittance matrix at the center of a cello bridge using a miniature impulse hammer and a laser vibrometer. They show evidence of longitudinal string resonances and out-of-plane resonances of the bridge.

Tronchin and Cocchi (1998) measured mobility at different points on the cello bridge, and showed how they change when the cello is *toned*, that is, when the maker or the player makes adjustments such as moving the bridge or soundpost.

14.7 The “New Violin Family”

We have shown that the cello is not a scaled up violin but a distinctively different member of the family of bowed strings. The so-called “new violin family,” however, is an octet of string instruments that are scaled according to acoustical rules. These instruments, created by Carleen Hutchins and co-workers in the Catgut Acoustical Society, will be discussed in Chap. 18. The baritone in this family is similar in size and range to the cello.

14.8 Conclusion

The cello is a cherished instrument, widely used as a solo instrument as well as in string quartets and orchestras around the world. Although its acoustical properties have been studied far less intensively than the violin, nevertheless a growing body of knowledge is appearing in the scientific literature. We sincerely hope that this body of knowledge will continue to grow in the future.

References

- Askenfelt A (1982) Eigenmodes and tone quality of the double bass, *Quarterly Progress and Status Report*, Dept. of Speech, Music, and Hearing, Royal Institute of Technology (KTH) Stockholm, STL-QPSR 4/1982, 149–174.
- Bynum E (1997) Modal Analysis of the Violoncello, MS thesis, Northern Illinois University, DeKalb.
- Bynum E, Rossing TD (1997) Holographic studies of cello vibrations, *Proc. ISMA97*, Edinburgh.
- Caldersmith G (1997) Private communication.
- Dilworth J (1999) The cello: origins and evolution, in *The Cambridge Companion to the Cello*, R. Stovell (Cambridge Press, Cambridge).
- Eggers F (1991) Mechanical impedance measurements around the violoncello, *Acustica* **74**, 264–270.
- Firth IM (1974) The wolf tone in the cello: Acoustic and holographic studies, *Quarterly Progress and Status Report*, Dept. of Speech, Music, and Hearing, Royal Institute of Technology (KTH) Stockholm, STL-QPSR 4/1974, pp. 42–56.
- Hutchins CM, Stetson KA, Taylor PA (1971) Clarification of ‘free tap tones’ by holographic interferometry, *CAS News!* **16**, 15–23.
- Langhoff A (1995) Modal analysis of violin, viola and cello compared to the acoustical spectrum, *Proc. ISMA95*, pp. 286–290.
- Meyer J (1972) Directivity of bowed stringed instruments and its effect on orchestral sound in concert halls, *J. Acoust. Soc. Am.* **51**, 1994–2009.
- Molin N-E. (2007) Optical methods for acoustics and vibration measurements, in *Springer Handbook of Acoustics*, ed. T. D. Rossing (Springer, Heidelberg).
- Rossing TD (2007a) Modal analysis, in *Springer Handbook of Acoustics*, ed. T. D. Rossing (Springer, Heidelberg).

- Rossing TD (2007b) Observing and labeling resonances of violins, *Proc. ISMA07*, Barcelona.
- Tronchin L, Cocchi A (1998) On the toning of the cello: the effect on damping in the sound board, *Proc. ISMA98*, eds. D. Keefe, T. Rossing, C. Schmid, Acoustical Society of America. pp. 65–70.
- Wilkins RA (2003) Cello modes throughout three stages of construction, *CAS J* 4(8), 64–71.
- Woodhouse J, Courtney PE (2003) The Admittance Matrix of a Cello, *Proc. SMAC 03*, Stockholm, Sweden.

Chapter 15

Double Bass

Anders Askenfelt

The study of the acoustics of bowed instruments has for several reasons focused on the violin. A substantial amount of knowledge has been accumulated over the last century (see Hutchins 1975, 1976; Hutchins and Benade 1997). The violin is discussed in Chap. 13, while the cello is discussed in Chap. 14. The bow is discussed in Chap. 16.

It should be noted that that the cello and double bass are not just scaled-up versions of the violin (see Fig. 15.1). The cello and double bass differ from the violin in many aspects. The proportions between the upper and lower bouts are different and the rib height of the cello and bass is much higher, to mention just some differences. In particular, the double bass comes in a variety of shapes and sizes, in contrast to the “standardized” violin. Flat or carved back, violin-like bouts with sharp corners or viol-like sloping shoulders and round corners, the shape of the bridge, string length, and the number of strings are all examples.

15.1 Modes of Vibration

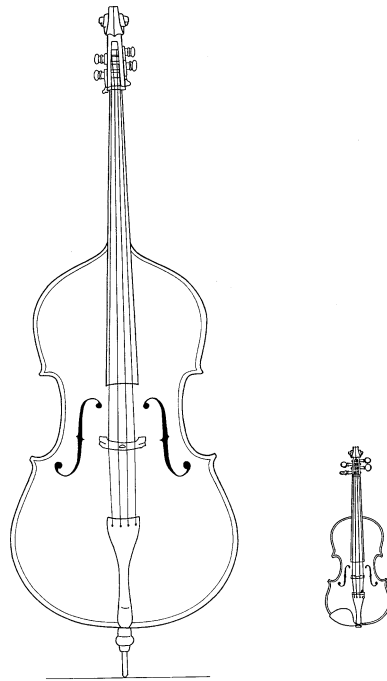
The history of research on the bowed instruments is closely associated with studies of modes of vibration (colloquially referred to as *resonances*). The body of a bowed instrument – a wooden structure made up of two thin and arched wooden plates connected by the ribs and supported by the sound post – is in itself a complicated structure. Adding the neck, finger board, bridge, tail piece and strings gives a vibrating structure of unusual complexity. Nevertheless, the basic properties of modes of vibration apply. Among other things this means that when driven by the vibrating string, the response of the instrument is determined by the particular set of modes of the instrument (mode frequencies, mode shapes, and damping).

A. Askenfelt (✉)

Department of Speech, Music, and Hearing, Royal Institute of Technology (KTH),
Stockholm, Sweden

e-mail: andersa@speech.kth.se

Fig. 15.1 A double bass and a violin



The mode shapes can be measured using holographic techniques, as we have seen in Chaps. 13 and 14. Unfortunately, several different systems for labeling the modes are in use. For example, the C_2 resonance associated with the first large peak in Fig. 15.2 has also been called T_1 , B_1^- , P_1 , and *main wood* by various researchers.¹ Modal analysis is discussed by Rossing (2007) and holographic techniques are discussed by Molin (2007)

15.1.1 *The Modes in Playing*

It is important to remember that individual modes can only be studied under laboratory conditions. Examples were given in Chaps. 13 and 14, in which violins and cellos were driven at a single frequency at a time. In real playing, *all* modes will be excited simultaneously, some more and others less, both when plucking the string and in bowing. The vibrating string provides a driving force with a large number of harmonically related partials (fundamental and overtones), each of which tries to vibrate the instrument body via the bridge. If a partial of the string happens to be close in frequency to a mode frequency of the instrument, this mode will be strongly

¹In this chapter the label T_1 is used in all figures to indicate mode C_2 .

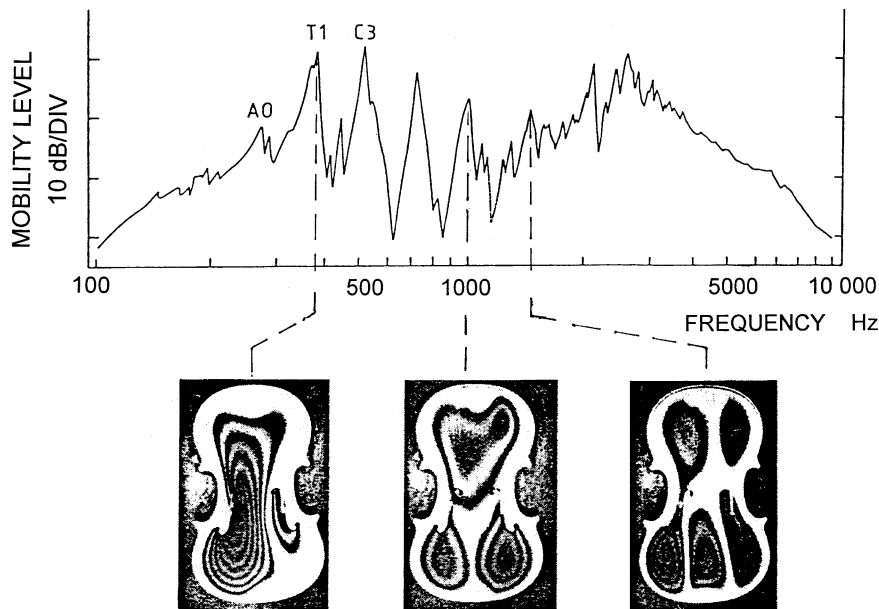


Fig. 15.2 Mobility curve of a violin. The peaks represent modes of vibration (resonances). A few important modes are labeled; A_0 , C_2 (T_1) and C_3 (see Chap. 13). The mode shapes (amplitude distributions) for three modes are illustrated below the mobility curve (from Alonso Moral and Jansson 1982a; Jansson et al. 1970)

excited. Changing the pitch only slightly (which is equivalent to shifting the frequencies of all partials), will be enough to change the driving conditions for the different modes, and the amplitude relations between the partials in the radiated sound will change. Such temporal variations in the spectrum envelope, which occur, for example, at a regular rate in a note played with vibrato, is a characteristic of the bowed instruments that we appreciate. At the onset of a note, and in particular in sudden attacks such as *sforzando* or *martellato*, the instrument receives a “shock” excitation and all modes of the instrument are momentarily excited vigorously. This massive excitation of many modes may sometimes be apparent as a “clunk”-like component in the attack sound, particularly in close-microphone recordings.

15.1.2 Mobility Curves and Instrument Identity

A bowed instrument exhibits numerous modes of vibration, far more than can be detailed in an acoustical analysis. Several ways of documenting the modes by measurements have been used. A common way is a frequency response curve. A very useful type of frequency response curve (as we have seen in Chaps. 13 and 14) is a *mobility curve*, which shows the mobility over the frequency range of interest. An example of such a curve for a violin is given in Fig. 15.2. Mobility is defined as

velocity (at some point) divided by force (applied at that point or a different point), and so a mobility curve represents the “willingness” of an instrument to vibrate at different frequencies. A high mobility value (*peak*) means that the structure is easy to set into vibration at that particular frequency. This condition applies at the mode frequencies, and consequently each peak in the mobility curve represents a mode (*resonance*) of the instrument. The higher is the peak, the larger is the vibration amplitude of that mode when excited by a vibrational force from the string.

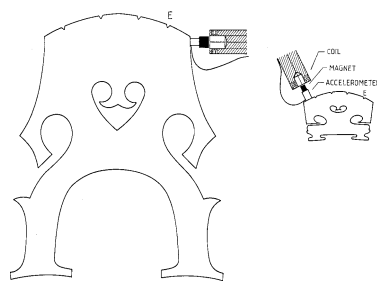
The frequency scale in Fig. 15.2 covers the range 100–10,000 Hz. We see several individual modes in the left part of the figure below 1,000 Hz, some of them which are labeled (A_0 , $T_1(C_2)$, etc.). In the right part the peaks are so numerous and close in frequency that they form a continuum.

Each mode has its own characteristic distribution of vibration amplitudes across the instrument (*mode shape*). The mode shapes for three modes in Fig. 15.2 are shown below the corresponding peaks in the mobility curve. These pictures should be read as topographical maps, with large white areas representing no motion (nodal lines), and alternating black and white lines representing “vibration mountains” with the highest vibration amplitude at the top of the mountain.

The mobility curve can be measured in several ways. In Fig. 15.3, two setups for measuring the mobility curve of a violin and a double bass, respectively, are shown, based on the same principle as in a common electro-dynamic loudspeaker. A fixed coil and a magnet mounted on the bridge provide a vibrational force with a certain frequency when the coil is fed with a sinusoidal current. The resulting vibration amplitude of the instrument at the driving point is picked up by a sensor (accelerometer) mounted under the magnet. By sweeping the frequency of the current over the measurement range, a mobility curve, such as Fig. 15.2, is obtained.

A main reason for the large interest in the modes of bowed instruments, and mobility curves in particular, is that each instrument has a unique set of modes. In other words, each instrument has its own characteristic mobility curve – a sort of acoustical fingerprint – which can be compared with other instruments. Further, the mobility curve is relatively easy to measure, much easier than the radiated sound.

Fig. 15.3 A method for measuring mobility curves of stringed instruments. A small magnet is mounted on the bridge. A fixed coil is positioned close to the magnet, with a small gap of air in between. The system exerts an excitation force on the bridge when a periodic (sinusoidal) current is fed through the coil. A sensor (accelerometer) under the magnet measures the resulting motion of the bridge (from Askenfelt 1982)



This is because the fundamental and the overtones all have individual directional radiation patterns. In order to measure the radiated sound properly, specially designed rooms such as anechoic chambers, need to be used.

15.2 The Double Bass Compared to the Violin and Cello

A comparison of the mobility curves of a violin, cello, and a double bass is shown in Fig. 15.4. All three instruments are of high quality and by renowned makers. We see similarities as well as differences. Above all, the larger the instrument, the lower the frequencies of all the modes.

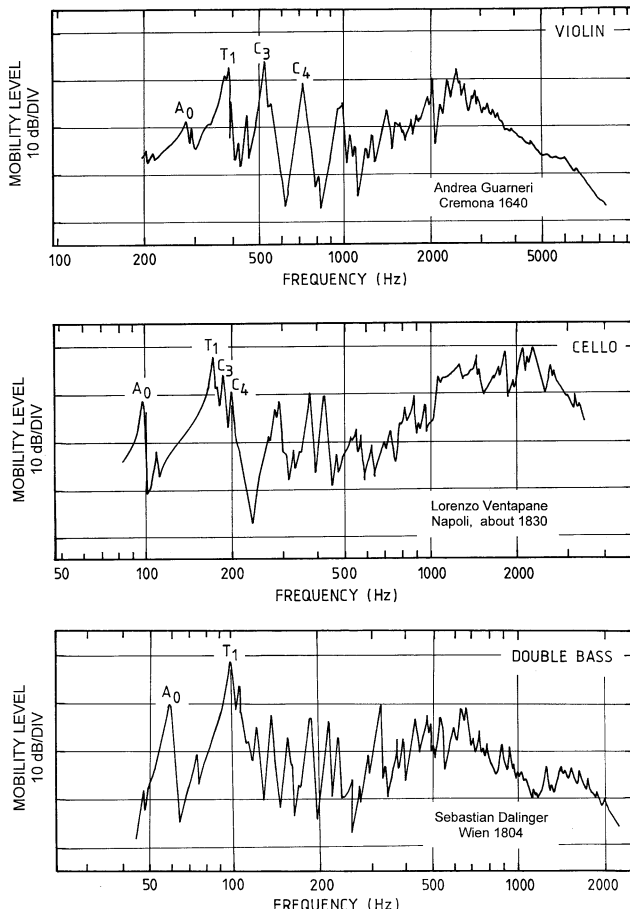


Fig. 15.4 Mobility curves for a violin (top), a violoncello (middle), and a double bass (bottom) by recognized makers (Askenfelt 1982). The violin is labeled Andrea Guarneri 1640, but recently ascribed to Francesco Ruggieri, ca. 1685. Violoncello by Lorenzo Ventapane, Napoli, about 1830; double bass by Sebastian Dalinger, Wien, 1804

Compared to the violin, the frequency scale in the mobility curve of the cello is one octave lower, and two octaves lower for the double bass. This is essentially a reflection of the sizes of the instruments. We recognize some of the lower modes in all three instruments. The air resonance A_0 , which appears at about 270 Hz in the violin, is lowered to about 100 Hz in the cello and to 65 Hz in the double bass.

For the violin, the next higher modes C_2 (T_1), C_3 , and C_4 are separated in frequency, but in the cello and the double bass they are clustered in a main peak. Above this range a handful of individual modes can be seen in the cello and bass. These are probably higher plate modes, in which the top and back plates are broken up in several small vibrating areas separated by nodal lines. A common feature of all three instruments is the broad hump at higher frequencies, between 2 and 3 kHz in the violin, 1 and 2.5 kHz in the cello, and 500 and 1,000 Hz in the double bass. This is often called the *bridge hill* (so-named because it is connected to the interaction between the bridge modes and the top plate) (Durup and Jansson 2005; Woodhouse 2005). Most high-quality violins show a pronounced bridge hill. This region of the mobility curve can be changed considerably by trimming of the bridge shape and thickness, and to some degree by the final adjustment of the position of the sound post relative to the bridge.

A measurement of the mobility of a double bass bridge (French model) in isolation is shown in Fig. 15.5. The bridge was clamped rigidly to a steel plate and driven by a magnet and coil as in Fig. 15.2. Three bridge modes are seen with frequencies at about 700, 1,100, and 1,500 Hz. The lowest mode is connected with the bridge hill below 1,000 Hz, and the other two may form a separate hump in the mobility of curve of some basses.

The motion of the bridge at the mode frequencies has some resemblance with some popular exercises in gymnastics (Reinecke 1973). In the lowest mode the whole bridge moves sideways as the legs lean from left to right and back again. In the highest mode the legs are fixed and the upper part of the bridge tilts from side to side.

15.3 Double Basses of Different Quality

The mobility curves of four double basses ranging from very poor to excellent quality are compared in Fig. 15.6. Many features are of course common, being determined by the size of the instruments. All four instruments were comparable to a three-quarter size, or slightly larger, bass. The A_0 mode is seen to range from 58 to 68 Hz, and the $T_1(C_2)$ mode from 82 to 114 Hz. A general conclusion about desired properties of a double bass as reflected in the mobility curve is difficult to draw from this limited sample of instruments. However, pronounced A_0 and T_1 (C_2) modes, occurring at relatively low frequencies, followed by a broad dip with lower mobility above C_2 , and finally a boosted bridge hill seem advantageous.

A reason for preferring instruments with low frequencies of the A_0 and T_1 (C_2) modes could be that they enhance a full tone quality in the lowest register of the bass. In this pitch range, the fundamental and first overtone are weakly radiated in the sound.

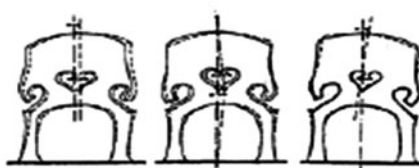
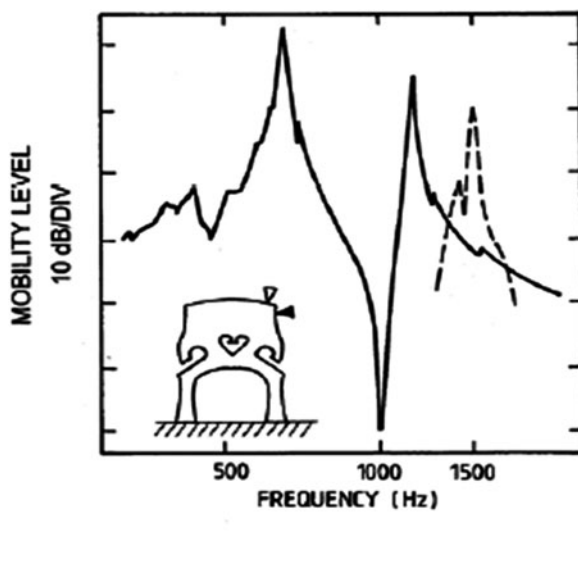


Fig. 15.5 Mobility curves of a double bass bridge measured with the bridge feet clamped to a rigid support. The two lower bridge modes (peaks) at about 700 and 1,100 Hz were obtained by driving the bridge in the direction parallel to the top plate, the bowing direction (*black triangle*). The highest mode at about 1,500 Hz (*dashed line*) was driven perpendicular to the top plate (*white triangle*) (Askenfelt 1982). The illustrations of the mode shapes are from Reinecke (1973)

The A_0 and C_2 modes can assist in boosting the low partials as their frequencies come close to the mode frequencies. We shall return to these matters below.

In Fig. 15.7, an important double bass made in 1611 by the brothers Antonio and Hieronymus Amati, Cremona, is compared to the high-quality Dalinger bass in Fig. 15.6. This instrument (see Fig. 15.8) was once played by the great Russian bass virtuoso Serge Koussevitzky, later more famous as a conductor. The Amati bass has higher A_0 and T_1 (C_2) mode frequencies than the Dalinger bass, but the characteristics of the mobility curve are otherwise similar. As is apparent from the many recordings of the Amati bass it has a very sonorous tone quality.² The comparatively higher mode frequencies may have made it particularly suited for solo playing.

²The Amati bass was passed from Koussevitzky to the American bass virtuoso Gary Karr who kindly put the bass at our disposal for measurements (<http://www.garykarr.com>).

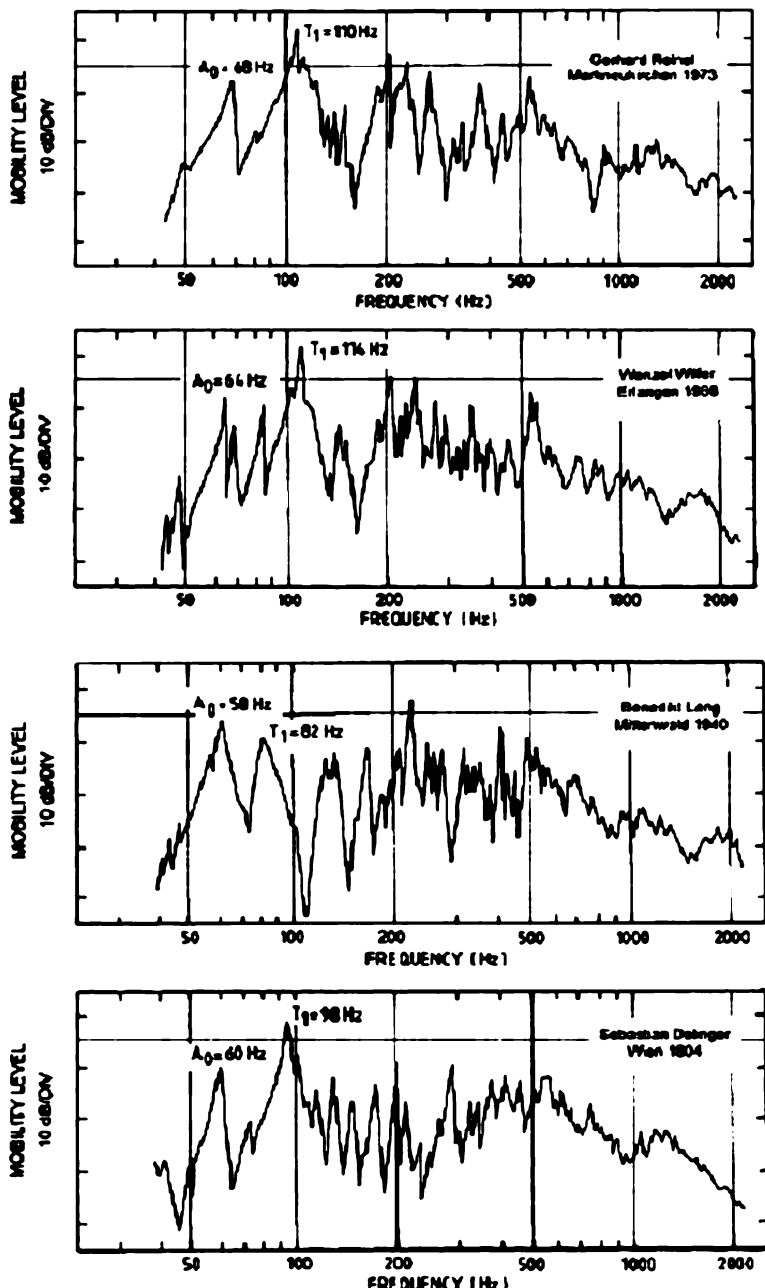


Fig. 15.6 Mobility curves of four double basses by Reinel 1973, Wilfer 1968, Lang 1940, and Dalinger 1804, ranging from poor (top) to high quality (bottom) (from Askenfelt 1982)

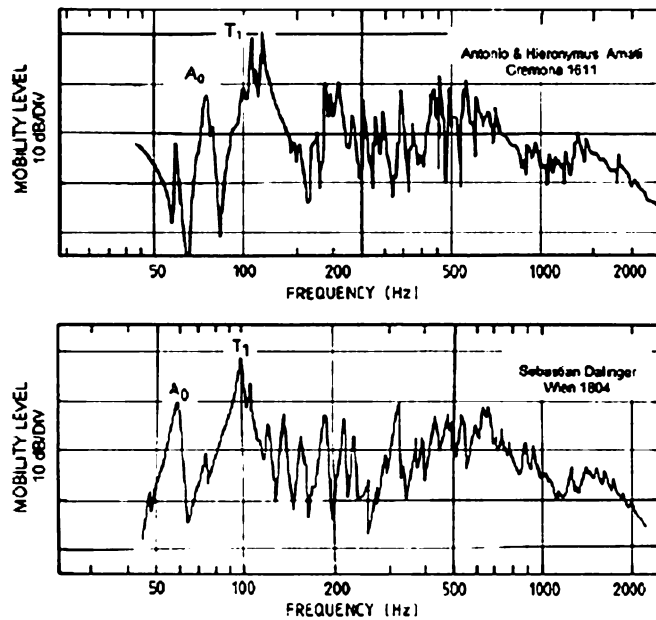


Fig. 15.7 Mobility curve of an important double bass by the brothers Antonio and Hieronymus Amati, Cremona, 1611. The mobility curve of the Dalinger bass in Fig. 15.6 is shown below for comparison



Fig. 15.8 The 1611 Amati bass, here played by Serge Koussevitzky

15.4 The Violin Octet

Of particular interest are two basses from a set of eight instruments designed in the 1960s by the American violin maker Carleen Hutchins and co-workers in the Catgut Acoustical Society, which are shown in Fig. 15.9 (Hutchins 1967). The instruments of the Violin Octet, discussed in Chap. 18, have been scaled according to acoustical rules so that they should have as similar tone quality as possible, but projected in different pitch ranges. All bodies have the same shape. The scaling constraints have resulted in body sizes and proportions, as well as string lengths, somewhat different compared to conventional instruments. The octet includes two bass instruments, *large bass* and *small bass*, the former of extraordinary dimensions (total height 214 cm, body length 130 cm). The string length is, however, in the normal range (110 cm) and the bass is tuned to standard orchestra tuning G2, D2, A1, E1, (98, 73, 55, and 41 Hz, respectively). The small bass is of about the size of a three-quarter bass and tuned a fourth higher (C3, G2, D2, A1).

The mobility curves for a small and large bass are shown in Fig. 15.10. The small bass has about the same A_0 and T_1 (C_2) frequencies (62 and 118 Hz) as conventional basses of the corresponding size in Fig. 15.6, and also the general appearance of the mobility curve is similar. The large bass has a very low A_0 mode (42 Hz) due to the large enclosed air volume. The frequency for C_2 , too, is low (81 Hz), but such a low value can in exceptional cases be reached also for a bass of normal size (cf. Fig. 15.6). The large bass can be expected to possess a full tone quality in the low register, which has been verified by players. The size, however, makes it somewhat awkward to play and handle.



Fig. 15.9 The Violin Octet
(by permission of Catgut Acoustical Society, Inc.)

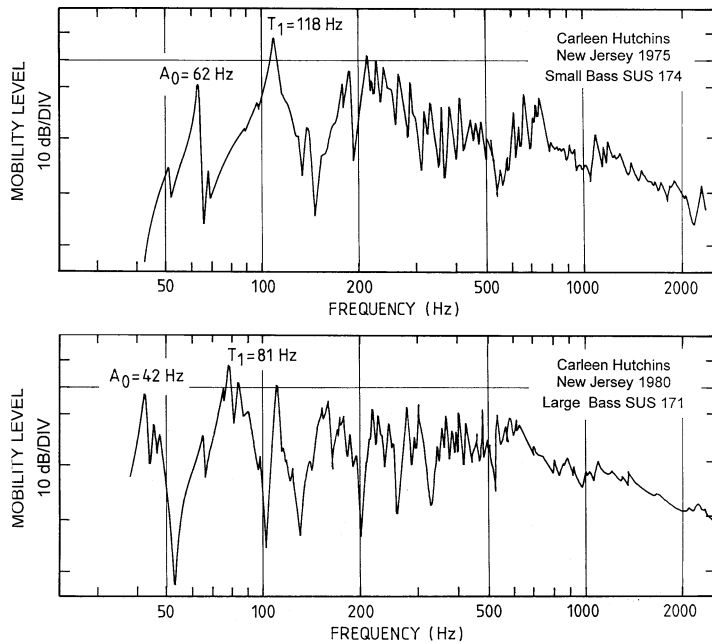


Fig. 15.10 Mobility curves of the Small Bass and Large Bass of the Violin Octet (Askenfelt 1982)

15.5 The Player's Support

The mobility curves offer an easy way of characterizing a string instrument in terms of its individual sets of modes. In order to facilitate comparisons between instruments, mobility measurements should be made under identical conditions, as far as possible. Usually, the basses are measured lying down on the side, supported on foam rubber cushions and with the strings damped. In this way reproducible measurement conditions are ensured. In playing, the player supports the instrument by the hip and often also by the knee, and the left hand holds the neck. A number of modes are influenced by this support. A comparison between the mobility curves when a bass is supported as little as possible (suspended from rubber bands), and under normal playing conditions, respectively, is shown in Fig. 15.11.

As seen in the figure, the mobility curves change considerably due to the player's support. Many modes are damped substantially (reduced height and rounded peaks) and the frequencies are also shifted slightly. The figure illustrates the importance of measuring instruments under identical conditions in order to allow comparisons of the data. The actual change in tonal quality is less than might be expected from the differences between the mobility curves, but nevertheless the support of the instrument influences the tone quality to some extent.

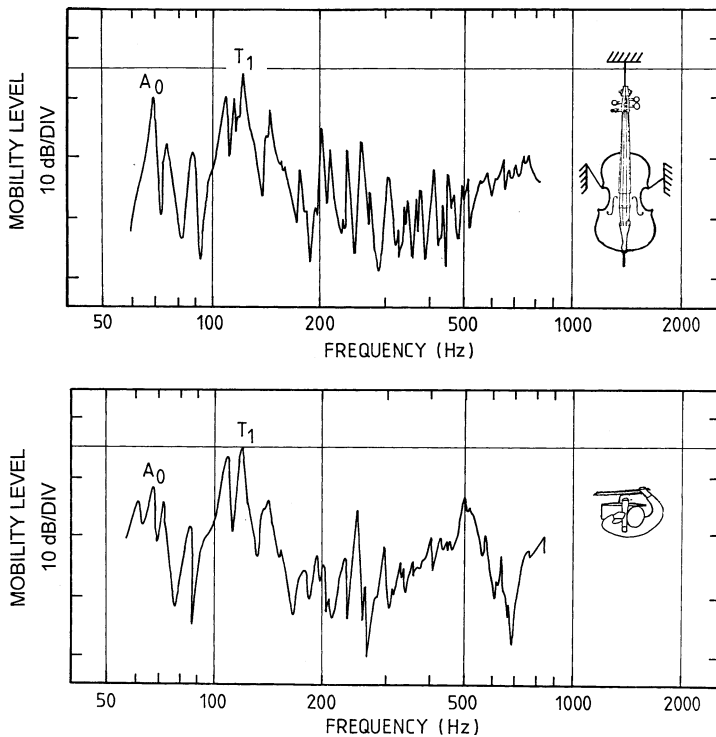


Fig. 15.11 Illustration of the influence of the player's support of the bass. Mobility curves for a bass suspended from rubber bands (*top*) and as supported in normal playing (*bottom*) (from Askenfelt 1982)

15.6 Scaling

As mentioned in the introduction, the cello and double bass are not just scaled-up versions of the violin. This is reflected in the mode frequencies as discussed above (Fig. 15.4). A comparison of the mode frequencies with the tuning of the instruments gives an idea of the acoustical scaling of the conventional violin, cello, and double bass. Figure 15.12 shows the average frequencies for the four modes B_1 (C_1), B_2 (N), A_0 , T_1 (C_2) for sets of four violins, five cellos, and four double basses in comparison to the tuning of the open strings.

For the violin, the A_0 resonance falls below the frequency of the second lowest string ($D4 = 295$ Hz). For the cello, the frequency of A_0 is comparatively higher and falls approximately at the frequency of the second lowest string ($G2 = 98$ Hz). For the double bass, A_0 lies well above the frequency of the second lowest string ($A1 = 55$ Hz). Similarly, the frequency of the T_1 (C_2) resonance corresponds approximately to the frequency of the second highest string ($A4 = 440$ Hz) on the violin, but to the frequency of the highest string ($G2 = 98$ Hz) on the double

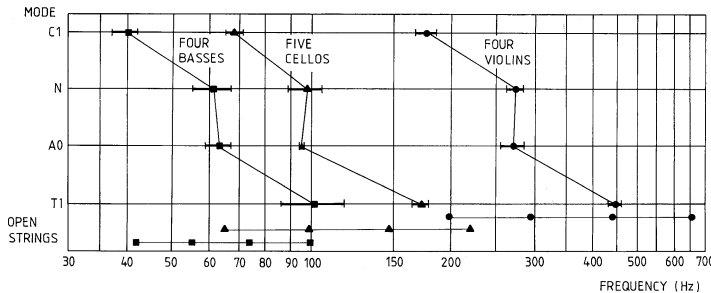


Fig. 15.12 Comparison of average mode frequencies $B_1(C_1)$, $B_2(N)$, A_0 , and $C_2(T_1)$ of four violins (circles), five cellos (triangles), and four double basses (squares). The tuning of the open strings is shown at the bottom (from Askenfelt 1982)

bass, the cello taking an intermediate position in this case too. The conclusion is that the tuning of the cello and double bass is too low compared to the violin, if we want an *acoustically scaled* set of instruments. By acoustical scaling is here meant a design criterion in which the mode frequencies of the instrument have a fixed relation to the frequencies of the open strings. Turned the other way around, with the present tuning, the bodies of the cello and bass would need to be much larger to be properly scaled to the violin acoustically.

The question is, then, whether such an acoustical scaling is desirable. For the Violin Octet in Fig. 15.9 acoustical scaling is *the* design criterion. This is the reason why the Alto Violin is so large that it cannot easily be played under the chin but is generally played vertically, supported by a peg as on the cello. The “cello” (the Baritone of the Octet) is larger than usual and the Large Bass is indeed large. A main argument for acoustical scaling is that the instruments will blend very well, forming a consort sound. The same argument can be turned against scaling as a design criterion: The individual character of the instruments in different pitch ranges is lost, and it will be harder to follow the individual parts of the score. Moreover, an equalized timbre may be uninteresting in the long run. An acoustically scaled set of bowed instruments conceivably could co-exist with the conventional instruments, perhaps playing a different repertoire that brings out the features of the scaling. In any case, the string sections in today’s ensembles (violin, viola, cello, double bass) are far from being acoustically scaled. This has been the fact for centuries, and the classical repertoire is most likely adapted to this acoustical criterion.

15.7 Body Size and Radiated Sound

The lack of acoustical scaling of the conventional string instruments is clearly apparent when studying the radiated sound. Here, too, body size is of primary interest. Among other things, body size influences the ability of the instruments to

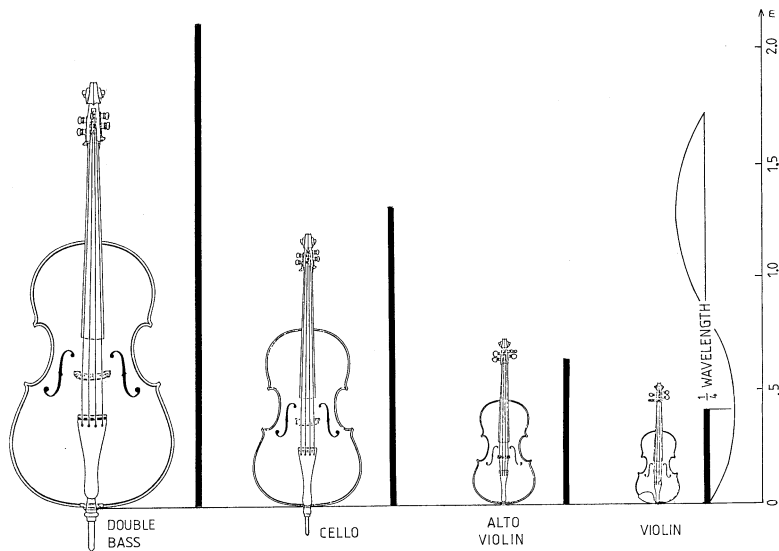


Fig. 15.13 All bowed instruments are small compared to the wavelength of sound in their lowest register. Comparison of the body length with the wavelength of the fundamental for the lowest note on the violin, viola, cello, and double bass. The black bars correspond to one-quarter of the wavelength of the lowest notes (from Askenfelt 1986)

radiate sound in their low registers, particularly the fundamental and lowest overtones. A general result in acoustics states that a vibrating body that is small compared to the wavelength of sound in the air will be very inefficient as a sound radiator. In Fig. 15.13, the body sizes of the violin, viola, cello, and double bass are compared with the wavelengths of the fundamental of their lowest note. For the violin, the size of the body is only about one-quarter of a wavelength of the fundamental of the lowest note. Consequently, the fundamental of the lowest notes on the G string could be expected to be rather weak in the radiated sound. Compared to the other instruments, however, the violin is in a relatively favorable position. For the double bass, a quarter of a wavelength of the low E string corresponds to about twice the body size. As a consequence, the fundamental will be even weaker than for the violin. The viola and cello fall between these two extremes.

Measured spectra of the radiated sound of four notes in the low register of a double bass with fundamentals from 41 to 82 Hz (E1, G1, B1, E2) confirm these assumptions (see Fig. 15.14). Not surprisingly, the fundamental is seen to be about 20 dB weaker than the first overtone for the lowest note (E1). A minor third higher (G1), the difference is much smaller, and one octave above the lowest note (E2) the fundamental is about 12 dB stronger than the first overtone. A weak fundamental in the low register is a consequence of the relation between body size and tuning. It can be changed to some extent by a redesign of the instruments, but apparently we accept this change in timbre in the bottom register of the bowed

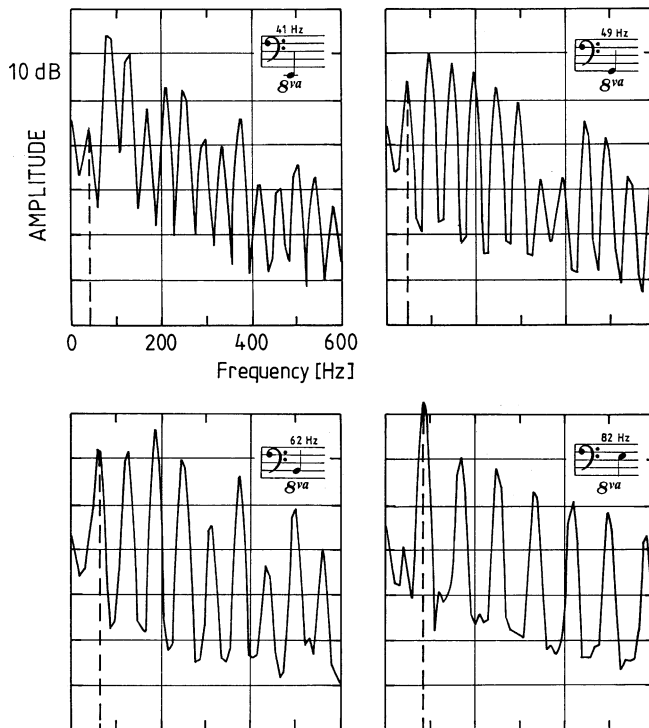


Fig. 15.14 The double bass produces a weak fundamental in the lowest register. A comparison of spectra of radiated sound for four low notes ($E_1 = 41\text{ Hz}$, $G_1 = 98\text{ Hz}$, $B_1 = 62\text{ Hz}$, $E_2 = 82\text{ Hz}$) illustrates how the fundamental increases in strength with rising pitch. The dashed lines indicate the fundamental (from Askenfelt 1986)

instruments. In speculating about possible reasons for this preference it should be noted that the singing voice shows the same characteristics, both for male and female voices.

15.8 Stage Risers

As concluded above, a weak fundamental in the lowest register is unavoidable with the present design and tuning of the family of bowed instruments. For the double bass this condition may not be completely satisfactory. A strong fundamental in the low register gives a full, mellow bass sound, which often is highly desired in an orchestra. A comparison can be made with the organ. An open organ pipe with a wide diameter compared to its length (e.g., *Subbaß 16'*) gives a strong fundamental. When this stop is added to the organ sound, a full, warm bass quality is obtained. Because of the obvious difficulties in playing and reaching higher positions with the

left hand, the body of the double bass can hardly be made much larger in order to enhance a full bass quality. The stage floor, or separate stage risers, may, however, provide some assistance in this respect.

Because the bass cannot radiate the fundamental and low overtones efficiently, their energy is trapped in the instrument as vibrations. Some of the vibrations may be transmitted to the stage floor (or riser) via the end pin or by nearfield sound radiation. Under favorable conditions the floor and bass may interact, contributing to the radiation of the low partials (Cremer 1981; Askenfelt 1986). In a sense, the floor can be viewed as an extension of the instrument body. A comparison between the partial amplitudes in the radiated sound when a bass is played on a riser and a stiff stage floor, respectively, is shown in Fig. 15.15.

As seen, the gain in radiated sound can be substantial over a considerable frequency range. For the notes played on the low E string (E1 and G1) the boost of the lower partials reaches about 6 dB. These measurements are in accordance with the experience of professional bass players. Some stage floors, or certain types of risers, are considered to have a profound effect on the bass sound. In fact, there are some concert halls that are famous for a full bass sound, a feature that has been attributed to the properties of the stage floor. Neues Gewandhaus in Leipzig (destroyed during World War II) was a famous example, and Boston Symphony Hall is claimed to have similar properties. When designing a new

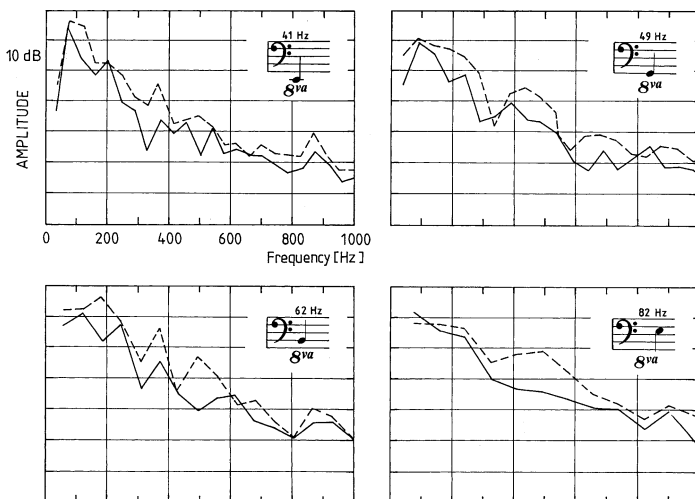


Fig. 15.15 The amplitude of the fundamental and low partials can be boosted by supporting the bass on a riser. Comparison of the partial amplitudes in the radiated sound when a double bass is played on a stiff stage floor (*full line*) and on stage risers (*dashed line*). The pitches are the same as in Fig. 15.14 (E1, G1, B1, E2) (from Askenfelt 1986)

concert hall, the effects of the stage floor on the bass sound should certainly be taken into account (Guettler, Buen and Askenfelt 2008; Guettler, Buen and Askenfelt 2010).

15.9 Directional Radiation

Like the other stringed instruments, the sound of a double bass is radiated in different directions depending on frequency, as shown in Fig. 15.16 (Meyer 1972). The shaded sectors in the figure represent the main directions of the radiated sound in the indicated frequency ranges. In short, the fundamental and low partials (up to about 160 Hz) are radiated mainly in a wide sector in front of the bass, while the higher partials radiate in narrower sectors in slightly other directions. For example, when playing on the open A string, the fundamental ($A_1=55$ Hz) and two lowest overtones (110 and 165 Hz) will be radiated mainly in a half-circle in front of the player. The third and fourth overtones (220 and 275 Hz) will be radiated mainly front-left and back-right, while the following (330 and 385 Hz) will be directed towards the right quadrant. The highest frequencies (above 1,000 Hz) are radiated frontally.

In all, the amplitudes of the partials in the direct sound that reaches the listener will depend on the position of the listener in relation to the bass, and hence influence the perceived timbre. It is true that the sound radiated in almost all directions will reach the listener after a slight delay, due to so-called *early reflections* from the stage walls and ceiling. However, the direct sound carries important information about the timbre of the instrument, in particular the high-frequency content. According to many professionals, a standing playing position with the bass oriented vertically (no tilt) so that the top plate faces the audience gives the best projecting sound.

It can be noted that the directional radiation from a bass does not seem to be drastically dependent on pitch. In the normal orchestra playing range with fundamental frequencies from 41 Hz to about 200 Hz, the direction of the overall radiation shifts slightly towards the right as the pitch is raised.

The directivity patterns have implications for the seating in the orchestra. In the so-called American seating with the basses to the far right of the conductor, the players' normal turning of the instruments (slightly clockwise as seen from above) will direct the frontal radiation into the orchestra instead of toward the audience. This is not advantageous and in this respect it would be better to put the basses to the left of the conductor behind the violins. On the other hand the distance to the cello group may then be rather large. A third solution is to place the basses in a row against the back wall as in the Vienna Philharmonic Orchestra. In addition to the desired frontal radiation toward the audience, the basses will benefit from being close to a wall. This condition may reinforce the sound radiation of the lower notes by an acoustical mirroring effect, provided that the basses are sufficiently close to the wall.

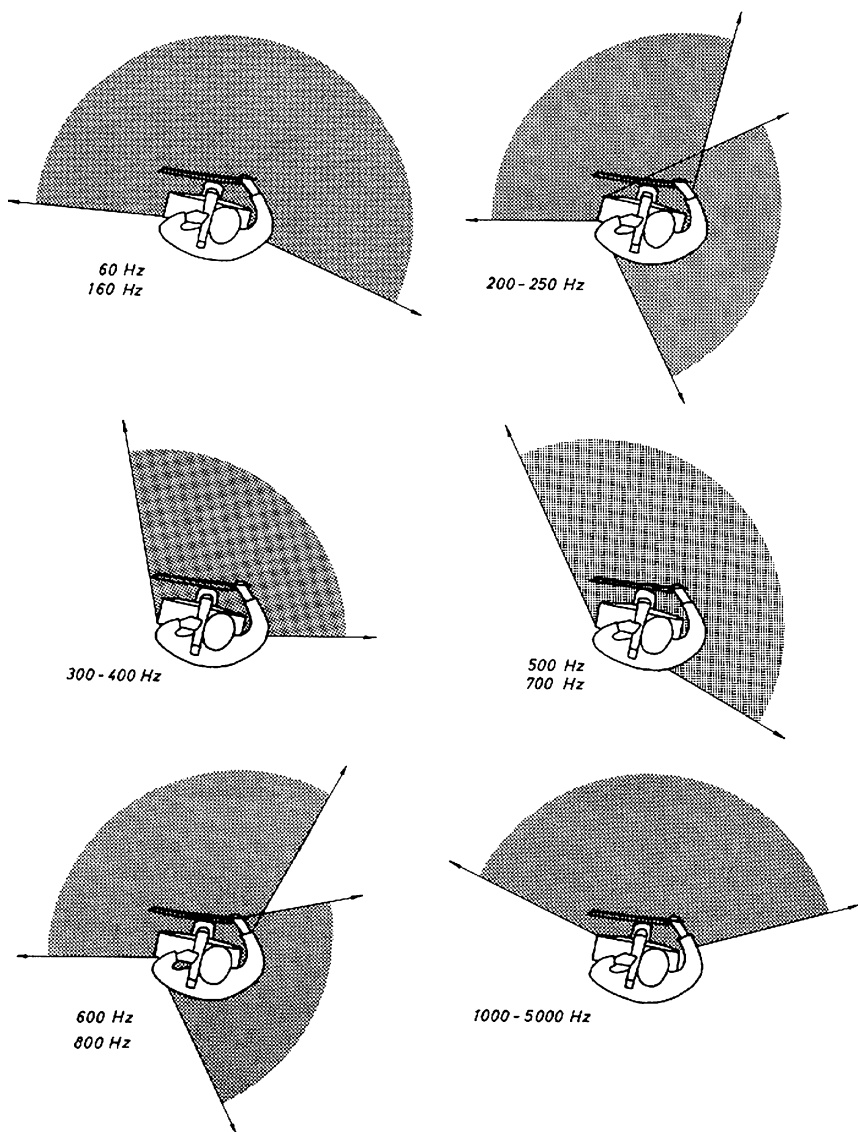


Fig. 15.16 Directional sound radiation from a double bass. The *shaded areas* indicate the main radiation sectors in the horizontal plane for the indicated frequency ranges. At the borders of the *shaded areas* the sound level is 3 dB lower than the maximum value in the sector (from Meyer 1972. By permission of Verlag Das Musikinstrument)

15.10 Further Reading

A number of aspects on the history, making, playing, and acoustical properties of stringed bass instruments can be found in *Geschichte, Bauweise und Spieltechnik der tiefen Streichinstrumente*, Michaelsteiner Konferenzberichte 64, Stiftung Kloster Michaelstein und Verlag Janos Stekovics, Dössel, 2004.

References

- Alonso Moral J and Jansson EV (1982a) “Eigenmodes, input admittance, and the function of violin,” *Acustica* **50**, 453–461.
- Askenfelt A (1982) “Eigenmodes and tone quality of the double bass,” *Quarterly Progress and Status Report*, Department of Speech, Music and Hearing, Royal Institute of Technology (KTH), Stockholm, STL/QPSR 4/1982 149–174. <http://www.speech.kth.se/qpsr/>
- Askenfelt A (1986) “Stage floors and risers: supporting resonant bodies or sound traps?” in *Acoustics for Choir and Orchestra* (ed. S. Ternström), Royal Swedish Academy of Music, Stockholm, No. 52, 43–61.
- Cremer L (1981) *Physik der Geige*, Hirzel Verlag, Stuttgart (also available in English: *The Physics of the Violin*, MIT Press, Cambridge, MA 1982).
- Durup F and Jansson E (2005) “The quest of the bridge hill,” *Acta Acustica/Acoustica* **91**, 206–213.
- Guettler K, Buen A and Askenfelt A (2008) “On the interaction between double basses and the stage floor,” Proceedings of Acoustics’ 08, June 29 – July 4, 2008, Paris, France.
- Guettler K, Buen A and Askenfelt A (2010) “The Lindeman Hall of Oslo — Evidence of low-frequency radiation from the stage floor,” Proceedings of 20th International Congress on Acoustics (ICA 2010), 23–27 August 2010, Sydney, Australia.
- Hutchins CM (1967) “Founding a family of fiddles,” *Phys. Today* **20**(2), 23–37.
- Hutchins CM, ed. (1975) *Musical Acoustics, Part I: Violin Family Components*, Dowden, Hutchinson & Ross, Inc., Stroudsburg, PA (John Wiley & Sons, Inc. USA).
- Hutchins CM, ed. (1976) *Musical Acoustics, Part II: Violin Family Functions*, Dowden, Hutchinson & Ross, Inc., Stroudsburg, PA (John Wiley & Sons, Inc. USA).
- Hutchins CM and Benade V, eds. (1997) *Research Papers in Violin Acoustics, 1975–1993*, Acoustical Society of America, New York.
- Jansson EV, Molin N-E and Sundin H (1970) “Resonances of a violin body studied by hologram interferometry and acoustical methods,” *Physica Scripta* **2**, 243–256.
- Meyer J (1972) *Akustik und musikalische Aufführungspraxis*, Verlag Das Musikinstrument, Frankfurt am Main.
- Molin N-E (2007) “Optical methods for acoustics and vibration measurements,” in *Springer Handbook of Acoustics* (ed. T.D. Rossing), Springer, Heidelberg.
- Reinecke W (1973) “Übertragungseigenschaften des Streichinstrumentenstegs,” *Catgut Acoust. Soc. Newsrl.* **19**, 26–34.
- Rossing TD (2007) “Modal analysis,” in *Springer Handbook of Acoustics* (ed. T.D. Rossing), Springer, Heidelberg.
- Woodhouse J (2005) “On the ‘bridge hill’ of the violin,” *Acta Acustical Acustica* **91**, 155–165.

Chapter 16

Bows, Strings, and Bowing

Knut Guettler

16.1 The Bow

16.1.1 Effect of Camber on Transverse Hair Stiffness

It is to the credit of François Tourte (Paris, ca. 1747–1835) that modern bows give a more direct impact on the string than their predecessors. This feature is of utmost importance when applying off-string, bouncing techniques such as *spiccato* and *ricochet*, but even for a stroke such as *martelé*, where quick reduction of bow force is required during the attack. With Tourte's concave-cambered bow, the bow force increases rapidly when the bow stick is falling or pressed against the string. With the old concave or straight bows, more movement, and thus time, was required for establishing comparable bow force.

Figure 16.1 gives a geometrical explanation to what is happening: As is seen in the lower panel, the hair stretches the farthest when the bow stick has the greatest camber,¹ that is, when pressed down until (nearly) touching the hair. (You can check this by placing the bow on a tabletop, with the frog's ferrule/ring touching the table edge for a fixed reference, and with the entire frog outside it. Loosen the hair and press the stick down until it touches the hair/tabletop.) Notice that as the bow stick is pressed down, the change of frog and head angles causes an increase of the hair length, frog to tip from, say, *F-B* to *F-A*. Had we straightened the stick (i.e., given it 0 percent camber), the distance between frog and head *at the stick level* would have increased, but this would be more than compensated for at the hair level, due to the implicit change of absolute frog and head angles. As the stick

¹Bow camber is often measured as deflection of stick compared to a straight line from top of head to the frog's button. However in the present context it refers to the part of stick that actively participates in defining the hair's tension, that is, the deflection *between* the head and the frog. In other connections a positive camber refers to a convex arch, but here we follow the convention of bow makers to give concave arches positive camber values.

K. Guettler (✉)

The Norwegian Academy of Music, Eilins vei 20, Jar 1358, Norway

e-mail: knut.guettler@tele2.no

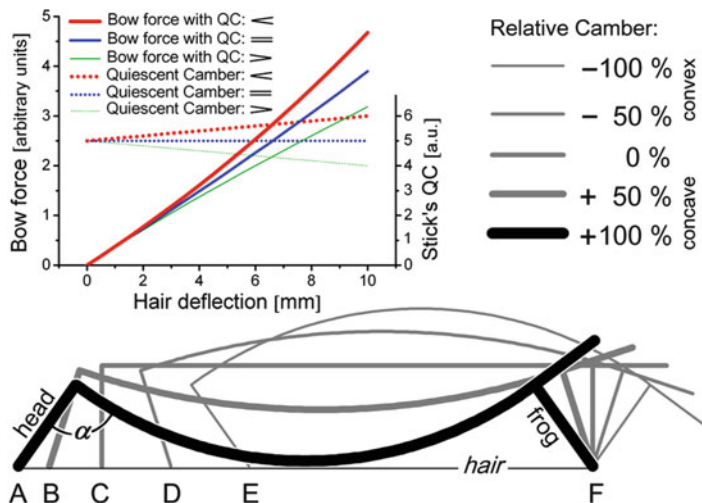


Fig. 16.1 Effect of the bow's camber on bow-hair stiffness (schematic). Lower panel shows fundamental bow geometries with relative cambers ranging from -100% (convex stick) to $+100\%$ of maximum possible concaveness. Upper-left panel shows bow force (bow pressure) as function of quiescent camber (QC) and string-provoked hair deflection (see text)

assumes a *convex* curve, the tip–ferrule distance decreases at an increasing pace (see how the intervals between A, B, C, D, and E become progressively wider). This also implies that any force trying to narrow the distance between the bow hair's endpoints will have an easier match when the bow's camber is smaller (or negative), simply because it requires less stick bending to do so.

In order to see the effect during playing, one might imagine two different cases. I will refer to the camber of the hairless/untensioned bow as the *quiescent camber* (QC):

1. If you increase the bow force by pushing the bow against the string with your index finger, you are actually *increasing* the stick's effective QC. The hair tension will increase quickly because you are trying to lengthen the tip–ferrule distance.
2. If you throw the bow onto the string in a rotational way with the frog as an axis, as you would in a normal ricochet and spiccato, the bow will in many cases (depending on contact point and bow properties) bend somewhat over the string, which means that the QC will dynamically *decrease* somewhat. The tip–ferrule distance will be shortened.

In the upper-left panel of Fig. 16.1 the effects of these two examples are illustrated along with a “neutral” situation, where the quiescent camber remains unchanged. The dotted lines indicate QC, while the solid lines show bow force as function of string-provoked hair deflection. In both cases the upper (thick) line refers to *increasing* QC ($<$), describing situation (1), while the lower (thin) line refers to situation (2) with decreasing QC ($>$). As can be seen, with increasing QC

the bow-force curve bends upward, meaning that the force increases more than proportionally to the hair's deflection. In situation (2) the opposite is true: This force curve is nearly straight, bending slightly downward. In the latter case the string has to dig substantially deeper into the hair before the same bow force is established. With a negative QC, or $QC = 0$ (a straight stick), the resulting curve would have nearly flattened out at a relatively low force level.

The nice thing about these contrasting features is that they are both very useful in practical playing. With the index finger on the stick the player has very quick access to high bow force, for example, at the onset of a martelé stroke. On the other hand, when you throw the bow onto the string, as in spiccato, the force initially builds up quickly with the Tourte bow, but as the bow bends somewhat over the string the force buildup becomes less steep, which implies that excess force values can be avoided: The well-designed bow remains on the string long enough for a sonorous tone to be created, during which time the stick is actively (but smoothly) storing and restoring energy.

16.1.2 Wood

François Tourte is said to have experimented with a number of materials for his bows, including steel, before settling with Pernambuco (a trade name for the core wood of *Guilandia echinata* of family *Caesalpiniaceae*, or synonymously: *Caesalpinia echinata*). Tourte chose this wood for its rare combination of density and stiffness. The preferred quality has density and Young's modulus of about $0.94\text{--}1.00 \text{ g/cm}^3$ and $21\text{--}23 \text{ GPa}$, respectively. Another type of wood, often used for historical bows, is snakewood (*Brosimum guianense*, or synonymously: *Piratinera guianensis*), which compared to Pernambuco has typically about the same Young's modulus, but a density some 20–40% greater (calling for slimmer bows). To some extent it is possible to compensate a lower stiffness by increasing the stick's diameter, but only minor adjustments can be done in this way because stiffness and density are so closely interwoven: If the material is homogeneous, a doubling of a rod's diameter will increase its mass and stiffness by factors 4 and 16, respectively: While the mass is proportional to density times the diameter squared, the stiffness is proportional to Young's modulus times the diameter raised to the power of four. With modern materials, such as carbon fiber, the problem can be solved by making the sticks hollow, which permits bending stiffness and mass to be adjusted separately. A wooden Tourte-model bow stick has a bending stiffness nearly seven times higher near the frog than near the head.

16.1.3 Tonal Quality

What makes one bow sound different from another one is not yet scientifically well understood. However, when a tone is established and the string oscillating in steady

state, any resonant vibration in the bow can only drain energy from the string, not the other way around. Askenfelt (1995) reports the transverse modes of the freely suspended stick typically to lie around 60, 160, 300, 500, 750, 1,000, 1,300, and 1,700 Hz in the lower range – comparable to the resonances of a free-free bar. It may be that the bow's *fingerprint* on the sound is more detectable during tone onsets and other transients, but certainly the differences in action are more noticeable for the player than for the audience. Anyhow, there is some evidence that violinists are able to recognize and discriminate between bows from their sound alone (Askenfelt and Guettler 2001).

16.1.4 Effect of Hair Elasticity and Surface Roughness

It is sometimes claimed that the hair should be elastic and have pronounced scales to play well. Both statements must be considered to convey myths. Hair is by nature very stiff. For a hair-bundle length of 650 mm, Askenfelt reports a value of 16 N (≈ 1.6 kg force) per mm static elongation, equal to 0.2 N/mm per fully engaged hair. In a dynamic, more realistic, situation the force required to elongate the hair bundle 1 mm was measured to about 30 N. Compared to that, the compliance of the hand's bow hold is many times higher: During playing, the entire bow can vibrate with amplitudes as much as 10% of the bow speed. With more compliant hair the effect of Tourte's brilliant design had been substantially reduced, making the bow force less sensitive to the bow's camber in both directions. (The same is actually true for the head compliance, that is, had the head been more giving.)

A persistent myth describes the hair scales as a main contributor to friction, but the tallest of those stands out less than 1/2,000 mm (Rocaboy 1990), which compared to the string diameter is negligible. But, more importantly – as discussed below – a friction *difference* is needed for the string to start oscillating. Bow hair should be judged on its chemical ability to hold rosin rather than on its surface roughness. Figure 16.2 shows bow hair without and with rosin, respectively. Notice that the scales are completely covered with melted or dusty rosin in picture *b*, and their orientation is no longer visible.

16.1.5 Rosin/Friction

During tone onsets and other transients it is important that the static-friction limit is significantly higher than friction during slip. Rosin has this property. It was earlier believed that the resulting friction force was a simple function of the relative speed between the bow and the string surface, and that friction was decaying as speed increased. A more updated theory, in better accordance with experiments, suggests that during slip dissipated heat is softening the rosin, which then, depending on *temperature*, contributes with a greater or lesser frictional resistance (Smith and

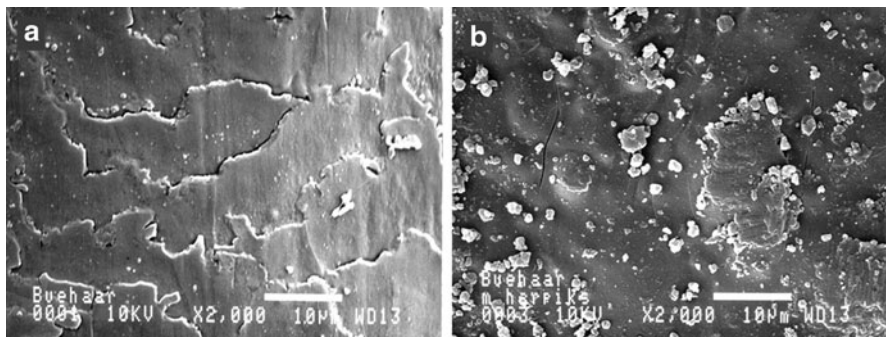


Fig. 16.2 Bow hair (a) without and (b) with rosin. The white lines low in the pictures indicate 10 μm , equal to 1/100 of a millimeter. Scales, sticking out less than 0.5 μm , are completely covered when rosined (photographs by Norwegian Institute of Technology, Trondheim)

Woodhouse 2000). Rosin has the property that it starts to soften right above room temperature, and has low enough specific heat to enable extremely quick temperature changes.

Although temperature seems to be determining the sliding friction, this does not imply that the string's slide on the bow hair is a smooth one. The rosin is never a uniform viscous substance, but rather a substance mixed with hard particles and other irregularities creating *noise* or *hiss* during slip (Schumacher 1996; Woodhouse et al. 2000). Another characteristic effect is *aperiodicity*: The string's fundamental frequency is constantly modulated by a small jitter due to minor deviations in the stick-slip intervals. More when the corner rounding occupies a greater part of the string (e.g., when playing high on a violin G string), less if the corner is sharp and stick-slip triggering is well defined (McIntyre et al. 1983); see Fig. 16.3.

16.2 Strings

16.2.1 The Concept of Wave Resistance or Wave Impedance

Only a small number of materials can withstand the tensile stress required for strings of a bowed or plucked instrument. Traditionally, gut, silk, and later steel and polyamides (with a variety of brand names) have been utilized for core material in such strings. As far as homogeneous bowed strings are concerned, only gut and steel display desirable combinations of density and tensile strength. Density plays an important role, because it largely determines how much energy is fed into the instrument's body: While the bridge has a natural resistance (mechanical impedance) to pivoting from side to side and in that way exciting the instrument body, the string has a natural resistance to changing its wave pattern, called *characteristic*

wave resistance or *characteristic wave impedance*. The concept of wave impedance can be described like this: Imagine a wave initiated at one end of a very long, tensioned string. The characteristic wave impedance (specified in units of mass per second) is then equal to the mass of the string section, over which the wave propagates per second. The higher the string tension, the further the wave will travel, and thus the impedance increases proportionally to the speed. On a violin's A string the propagation speed is some 290 m/s (!) and the typical impedance is around 200 g/s.

In a string instrument, where the string has boundaries at the bridge and nut (or the finger), causing waves to repeatedly reflect and change direction of propagation, a certain amount of energy goes to moving the boundaries, and on the bridge side, to produce sound. How much is determined by the ratio between the impedances of the string and the bridge, the latter always possessing the higher impedance. There is a trade-off between how much energy to keep in the string and the energy to be used to excite the body. The string itself does not radiate sound, its physical dimensions being far too small for "pumping" air.

Wolf tones represent examples where the bridge and string impedances are too closely matched. That is, at certain frequencies the bridge impedance is too small compared to the string impedance, causing the bridge to move "too much," at the cost of reduced reflections. This implies that so much wave energy leaves the string that maintaining a consistent stick-slip pattern with the bow becomes impossible (the smaller the impedance difference, the smaller the reflection at the boundary). In some cases one quick solution to the wolf tone problem may therefore be to use a lighter string, thus increasing the difference.

Nowadays some manufacturers print tension values on the string envelope. These give all the information needed to figure the string's impedance, which is equal to the tension divided by the product of frequency and twice the string length, which again for a given tuning is proportional to the square root of the tension. For most frequencies, increasing the string's wave impedance will lead to a proportional increase in body/sound excitation at the expense of increased string damping as well as *heaviness* of bowing. However, higher tension also implies greater brilliance when other parameters are kept unchanged.

To get a good sound balance between strings, the lowest strings on a bowed instrument are normally designed with the highest impedances. In practice this means that you will have to bow these strings a little bit more slowly, or with greater *bow pressure* compared to the lighter strings.

16.2.2 Tension

On a violin, the modern A, D, and G string tensions are typically some 30, 35, and 45% lower, respectively, than the tension of the E string. On the other hand, the resulting *impedances* are then 5, 46, and 85% higher, respectively, than the E string impedance. Equal string tension is claimed to have been recommended by Leopold

Mozart, but is today, except for double-bass strings, mostly manufactured for certain ancient music strings, the balance of which leaves a rather deep and mellow impression. Bigger concert halls call for more brilliance, and one way to achieve it is to increase the tension for the higher strings (see Table 16.1). Soloists tend toward high tension, at least for their top strings. The introduction of good-quality synthetic and steel cores in the 1970s opened the way for higher tensions, which led to a general shift in preferences. As the damping of steel-core strings became better balanced (was increased) some ten years later – resulting in better playing properties and reduction of shrillness – more players would accept these. Generally, the acceptance of steel-core strings increases with the size of the instrument, and most bass players today would use steel-core strings only, even though some bass groups have returned to modern gut- or synthetic-core strings.

16.2.3 Damping

Strings need to be damped in order to be “bowable.” We know from experience that open strings are harder to bow than stopped strings. When a soft finger pad provides additional damping, the whistling or shrill attacks we sometimes experience with open strings, are usually avoided. In fact, such extra damping is only needed for the attack itself. After the transient, strings behave stably and reliably with very little damping, even the open ones. Many strings of older design had the unintentional and undesirable property that damping increased with string amplitude (as windings were pulled more apart) (Pickering 1989). It would actually been better if the opposite were true! Nowadays, some manufacturers offer strings where damping is more or less linear over a good part of the amplitudes in question, making the strings noticeably easier to attack. More on damping can be read in Valette (1995).

Internal string damping is controlled by choice of materials, or rather *material combinations*. Two materials that individually give little friction may well provide high friction when rubbed against each other, due to molecular level interactions and other effects. Another important part of the internal damping comes from residual metal dust left over from the sanding process where the windings are smoothened to minimize friction during position shifts. Internal damping in the string goes to heating it. The internal string damping is, however, only part of the total damping; a good half comes from reflectional losses at the bridge and the finger/fingerboard/nut, and a small part from the air resistance. The string’s bending stiffness smoothes sharp corners, and thus to some degree limits creation and propagation of high frequencies. Increasing the string’s tension will, nevertheless, sharpen the corner again, and to some extent counteract the spectral effect seen at the bridge. In some strings a thin layer of nylon or similar monofilament material is applied as intermediate wrapping or as a braiding knitted around the core. Apart from giving the next layer a better fix to the core, this wrapping influences bending stiffness, which apparently becomes lowest when the wrapping is applied as simple floss, while braiding might provide better quality control during manufacture (Firth 1987).

Table 16.1 Transverse impedances and tension for commonly used strings[†]

Instrument	Tuning pitch	Frequency (Hz)	String length (cm)	Mass per unit length (g/m)	Propagation speed (m/s)	Transverse impedance (g/s)	Tension (N)
Violin	E5	659.3	32.8	0.38–0.48	432.50	165–210	71.4–90.7
	A4	440.0		0.58–0.75	288.64	167–217	48.3–62.7
	D4	293.7		0.92–1.63	192.67	178–193	34.3–60.6
	G3	196.0		2.12–3.09	128.58	272–397	35.0–51.1
Viola	A4	440.0	37.5	0.56–0.92	330.00	184–304	60.6–100.2
	D4	293.7		0.98–1.25	220.27	220–276	47.6–60.7
	G3	196.0		2.20–2.81	147.00	324–413	47.6–60.7
	C3	130.8		4.95–6.31	98.10	485–619	47.6–60.7
							Sum: 189.0–265.1
Cello	A3	220.0	69.0	1.50–1.92	303.6	456–584	138.3–177.2
	D3	146.9		2.94–3.57	202.7	597–725	121.0–146.9
	G2	98.0		6.38–7.56	135.2	863–1,023	116.7–138.3
	C2	65.4		14.33–16.98	90.3	1,293–1,532	116.7–138.3
Double bass; solo tuning	A2	110.0	106.0	4.95–6.00	233.2	1,154–1,398	269.1–326.1
	E2	82.4		9.18–9.78	174.7	1,604–1,708	280.2–298.3
	B1	61.7		16.59–17.78	130.8	2,170–2,326	283.9–304.2
	F#1	46.2		29.59–34.04	97.9	2,899–3,335	283.9–326.5
							Sum: 492.7–600.7
Double bass; orchestra tuning	G2	98.0	106.0	5.98–7.25	207.8	1,242–1,506	1151.1–1255.1
	D2	73.4		10.96–13.12	155.6	1,705–2,041	258.0–312.8
	A1	55.0		20.45–23.88	116.6	2,384–2,785	265.3–317.6
	E1	41.2		37.32–44.12	87.3	3,260–3,854	278.0–324.7
	B0	30.9		68.81–81.35	65.5	4,507–5,329	284.7–336.6
							295.3–349.1
Sum:							
1381.3–1640.8							

Note: 1 N \approx 0.098 kg force \approx 0.216 pound force.[†]The author is indebted to Fan Tao of D'Addario & Company and Michel Simane of Corelli/Savarez for their insightful comments on strings and contribution of values to this table.

16.2.4 Torsion

Because the string is not driven by the bow through its center, but tangentially at one side, the string is bound to be twisted when friction force is applied. This torsional motion is most pronounced during transients and when high bow force is employed. In these situations torsion might provide additional damping, but its effect on sound is not entirely clear. Torsion introduces a *shadow fundamental* with a complete set of overtones. On a violin, torsional frequencies are normally two to eight times higher than the transversal ones (as seen for homogeneous gut and steel, respectively). Luckily, we won't hear these frequencies unless they couple to the transverse modes, like they sometimes do in "whistling" violin E strings (Stough 1999).

Torsional propagation speed is determined by torsional stiffness (function of the string's internal shear modulus) and the moment of (rotational) inertia, and is largely independent of the transverse propagation speed. The torsional propagation speed in nonhomogeneous strings can, however, be manipulated (reduced) by twisting the string against the direction of top winding or winding of the string core, before mounting on the instrument. This might have practical applications when employing novel techniques such as playing *subharmonics* or anomalous low frequencies (ALFs) beyond the range of the instrument, as will be described later in this chapter. Strings with low torsional impedance (e.g., some synthetic-core strings) are more difficult to bow with high force close to the bridge when attempting to produce maximum output.

16.3 Bowing Techniques

16.3.1 The Main Three Bowing Parameters

The main three parameters controlling the string's wave form when bowing are:

- Bow speed
- Bow force (usually termed *bow pressure* by musicians)
- Bow's distance from the bridge

Together, these three parameters control what kind of *mode* the string will take, that is, whether the only nodes (*quiet points*) will appear at the reflecting string ends, or if one or more additional nodes will appear on the active string length, as when harmonics are played. With no additional nodes on the vibrating string length, and one slip-stick phase per nominal period, the string is most likely moving in the so-called "Helmholtz mode," named after the German scientist who around 1850–1860 analyzed the string motion in a very ingenious way by use of a vibrating microscope (von Helmholtz 1954).

The Helmholtz mode produces the fullest, most sonorous sound, and is what classical string players in most situations make an effort to achieve. But, as we shall

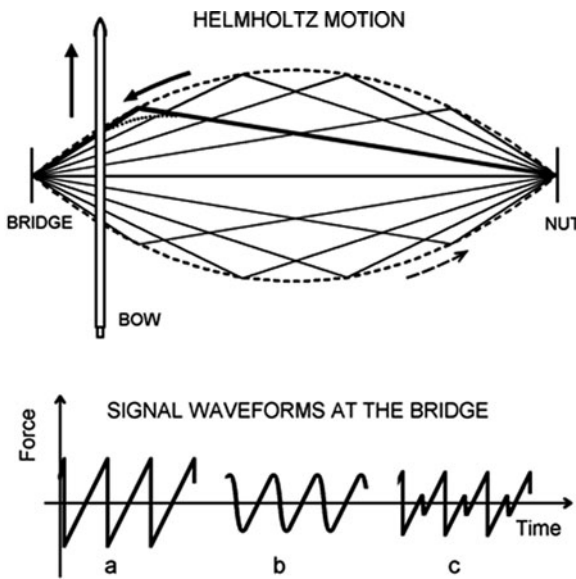


Fig. 16.3 String motion and resulting force signal in the (idealized) Helmholtz mode. The string is composed of two straight lines joined in a sharp corner. The corner rotates anticlockwise when the bow direction is up, and clockwise when down. Damping causes the corner to be rounded (see *fine dots*), while high bow forces counteract the effect by sharpening it every time it passes the bow (of *lower panel* see force signals *b* and *a*, respectively). *Lower panel c* indicates a force signal resulting from a non-Helmholtzian waveform with two rotating corners

see, there are numerous “special effects” that can be called upon with proper bowing technique. In the Helmholtz mode, however, the string moves as shown in Fig. 16.3. For most of the period, while the corner is moving on the nut side of the bow, the bow has a good grip on the string, which follows with the same speed. While the corner is moving on the bridge side, the string slips back with a much higher speed. The ratio between the slip speed and the stick (bow) speed is proportional to the ratio of the string lengths on the nut side and bridge side of the bow, respectively.

Damping causes the corner to be rounded (see the fine dots right below the corner of the bold line), but every time the rounded corner passes, the bow sharpens it. How much depends on the bow force. Regard the force signals in the lower panel, where (a) represents high bow force, and (b) low bow force with little corner sharpening. If Helmholtz mode is not achieved, the string may end up with two or more rotating corners, and produce a force signal like (c), where the fundamental frequency and several overtones are weakened; the tone will be “lacking core.”

Figure 16.4 outlines the force range required for maintaining the Helmholtz motion as function of the bow’s position on the vibrating string. The relative position (β) is the ratio between the bow’s distance to the bridge and the active string length. The force is shown relative to the highest force that can be applied at any point on the string, while still maintaining Helmholtz motion. If allowing for

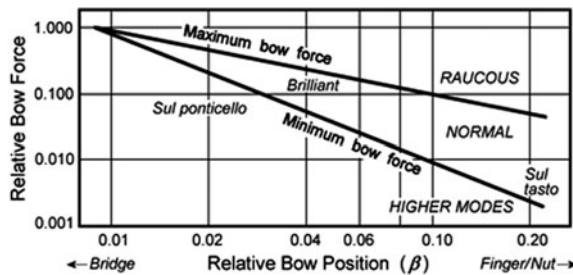


Fig. 16.4 The Schelleng diagram. Schelleng calculated the criteria for maintaining Helmholtz motion for a given bow speed and found that the maximum and minimum bow forces form a wedge when represented in logarithmic coordinates. As can be appreciated, playing close to the bridge demands higher bow force, and will therefore produce a more brilliant sound

change of bow position, the ratio between maximum and minimum usable bow force is seen to be more than 300.

One note on the logarithmic scales: the diagram may leave the impression that the usable force range diminishes as the distance to bridge becomes smaller. This illusion is due to the logarithmic scaling. In absolute values the force range *increases* as β becomes smaller, until a point very near the intersection between the two straight lines in the log–log plot. The Schelleng diagram describes the Helmholtz regime in terms of normalized bow-force values, for a given bow speed (Schelleng 1973). In Schelleng's equations there is proportionality between bow speed and bow force. This implies that lowering the bow speed while keeping the bow force unchanged will move the force-position coordinate upward in the normalized diagram, and make the tone color brighter as long as the combination satisfies the Helmholtz requirements. Recent research has shown that the minimum bow force is rather independent of the bow speed, but Schelleng's equation holds well for the upper part of the wedge (Schoonderwaldt et al. 2008).

If maximum bow force is surpassed, the waveform most likely becomes irregular and the sound raucous or creaky. A third possibility also exists: the pitch could drop to a substantially lower frequency, for example, about one second or third, one octave, or even one octave plus a fifth, or more. If this happens, the rotating corner fails to trigger a string release when hitting the bow on its way toward the bridge. This gives rise to two reflected waves, one torsional and one transversal, both capable of triggering a delayed release when passing the bow after one or more additional nut reflections (Guettler 1994; Hanson et al. 1994). Acousticians refer to this phenomenon as *anomalous low frequencies*, or simply ALF, while musicians would prefer (the physically less correct) *subharmonics*. (The violinist Mari Kimura (1999) has a point when she says: “Anomalous low frequencies could hardly be a musical term.”) These tones, which are fragile and only sustainable with extremely precise bowing, differ from tones pressed down a semitone or so – the latter referred to as *pitch flattening*, a phenomenon that always takes place to some degree and is a result of delayed string release within the normal Helmholtz regime.

Below minimum bow force, two or more slips will happen within each nominal period. The sound is weak and scratchy unless it develops to a pure harmonic with no trace of the nominal fundamental. Near the bridge, the sound is *glassy* and referred to as *Sul ponticello*. Here a number of slips take place within the nominal period. Typically, a spectral peak will occur at the frequency with the same harmonic number as the number of slips per nominal period.

16.3.2 *Flautando*

Near minimum bow force, when combined with a large β (i.e., the bow positioned closer to, or above the fingerboard), a “breathy” sound is obtainable, to some extent resembling tones of the flute. This happens because random noise is created every time the string slips on the bow-hair ribbon, where rosin dust and other irregularities prevent a smooth slide. When the bow is pulled away from the bridge, the sliding intervals increase, thus giving more time for hiss to be created. With the idealized Helmholtz motion the slip interval is β times the nominal fundamental period. However, near minimum bow force corner rounding causes the slipping interval to expand well beyond that. Also, during the sticking interval minor partial slips across the bow-hair ribbon will occur, adding to the total amount of hiss. This *rosin noise* is a characteristic part of the bowed-instrument sound, whether the instrument is played *flautando* or not, and should not be understood as something undesirable. *Noise* is here merely a technical term for random frequencies.

16.3.3 *Harmonics*

Figure 16.5 gives an example of harmonic B_5 played on an open violin G string. If played in slow motion, no less than five rotating Helmholtz corners would be seen; all separated by quiet nodes. The fundamental frequency of B_5 is five times higher than the open G_3 fundamental. Because five is a prime number, all of the four nodes can be used for producing the pitch of B_5 by touching the open string gently. Notice that such nodes are always spaced with equal intervals. If performed as artificial harmonics, as indicated at the bottom staff of Fig. 16.5, the spacing between the stopping and the lightly touching finger hence remains the same in all cases although the fingered musical intervals differ.

One should also notice that when playing a harmonic after having played the same string open, the bow speed might need adjustment. The bow speed of the harmonic should ideally be the same as if the note were played *stopped* on the string in question. A rule of thumb might be to increase the bow speed in proportion to the frequency change; for example, for playing the fifth harmonic B_5 (980 Hz) such a rule would suggest five times the speed of the open G_3 (196 Hz): When the number

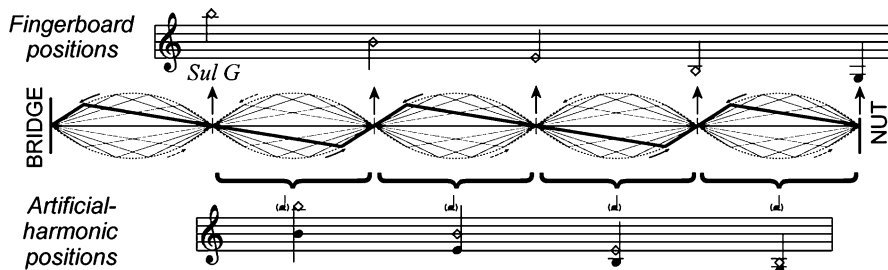


Fig. 16.5 String movement when playing the fifth harmonic. By lightly touching the string in one of the shown node positions, the pitch of the fifth harmonic will be produced. The string motion will be composed of five jointed Helmholtz rotations separated by quiet nodes. The bow can excite the string anywhere outside of these

of string slips per second increases by a factor of five, maintaining the string amplitude under the bow requires fivefold bow speed.

16.3.4 Harmonics and Intonation

Natural harmonics are often claimed to be flat. Physically, they seldom are (in fact, due to string stiffness they are usually *sharp* compared to the mathematical intervals), but there exist a number of well-founded explanations as to why they are *perceived* as flat:

- Lack of high overtones. Because harmonics bend the string in a number of Helmholtz corners, of which only one is sharpened by the bow, harmonics will normally turn out less brilliant than stopped notes. Tones lacking overtones tend to be perceived lower-pitched than brilliant ones.
- The ear has a preference for stretched octaves, meaning that high notes by preference are tuned slightly higher than the mathematical frequency doubling per octave. Octaves of the piano are tuned that way. Played together with string harmonics, conflicts are bound to occur.
- Difference between true and tempered pitch. Harmonics are close to the true-interval pitches. The fifth and seventh harmonics (two octaves + a major third, and + a minor seventh, respectively) are therefore by nature much lower than the equally tempered intervals. While the first major third is 14 cent lower than the tempered pitch, the latter is simply out of tune by all measures. True fifths are 2 cent higher, while octaves are mathematically in tune.
- Pitch distortion. When bowing with high speed and large string amplitudes, the string is stretched and the increased tension causes the pitch to rise in spite of a slight string lengthening. Harmonics, however, are less prone to this distortion since maximum amplitude remains somewhat restricted due to the relatively wider corner rounding.

- String players tend to gradually raise the pitch during performance, while harmonics remain unaffected.

16.3.5 Double Stops

Double stops need special attention in order to sound good, particularly if the interval is large and the goals are secure intonation and voices of equal tone quality. The richest sound (i.e., with most audible difference tones) will occur when the two voices show similar spectra, as opposed to one sounding dull while the other sounding bright. Again we are dealing with two different frequencies that ideally should have been bowed with different speeds. Because this is not possible in a double stop, the bow *pressure* (force) must be adjusted so that the lower-sounding string takes the greatest amplitude under the bow, even if the top voice carries the melody. The ratio between amplitudes of low and high voices should preferably be near the inverse ratio of their fundamental frequencies, that is $f_{\text{High}}/f_{\text{Low}}$. So, in order to have comparable corner sharpening of the two strings, the one sounding with the lower voice should always have the greatest pressure. Several factors come into play here, such as impedances, bending stiffness, β , etc., but to once more suggest a rough rule of thumb, the bow force ratio might be chosen to match the amplitudes, that is, inversely proportional to the frequencies. If playing large intervals with the bow force equally distributed between the two strings, chances are significant for pressing the pitch of the upper voice flat.

16.3.6 Tone Onsets, Attacks

While the bow's *speed, force and position* constitute the main controlling parameters during the sustained tone, *acceleration, force and position* have the same functions during attacks and transients (Guettler 2002). Acceleration is necessary for the Helmholtz pattern to develop quickly, but the accelerating phase does not have to last long. If acceleration is too high for the chosen bow force and position, higher modes (as described below minimum force in the Schelleng diagram) will prevail until the string's damping suppresses the noisy extra slips. Sometimes damping is not enough, and the string whistles during the entire note. When acceleration is too low, the attack will sound a bit raucous or creaky, but as soon as the bow has gained appropriate speed, the wave pattern will normally be replaced by Helmholtz motion. With appropriate acceleration the stick–slip action will be periodic from the very onset, which of course produces the cleanest attacks.

This is not to say that there exists an ideal acceleration or perfect attack sound. In a study published in the *Journal of Acoustical Society of America* it was shown that professional violinists choose the character of the attack (with or without

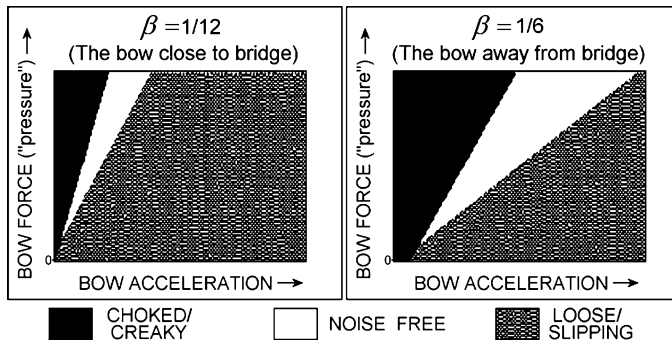


Fig. 16.6 Relation between bow acceleration, bow force and sound quality. When playing further away from the bridge or increasing the bow force, the range of permitted bow acceleration for noise-free attacks increases

noise), quite precisely in accordance with the musical style and expression of the piece (Guettler and Askenfelt 1997). This implies sometimes giving the attack a choked creaky sound, while in other situations giving the attack a loose, slipping character. However, for a *neutral* attack (such as when practicing scales), noise-free attacks were commonly preferred.

Figure 16.6 describes schematically the relation between acceleration, force, and position with respect to three categories of sound output. As can be seen, the range of acceleration/force combinations leading to clean tone onsets gets smaller as the bow is brought closer to the bridge. Also, the acceleration must be less with the bow in that position in order to avoid scratchy sounds. When starting the stroke with little or no bow pressure, both acceleration and pressure must build up gradually.

But how is acceleration controlled? Before answering that question it might be a good idea to inspect the forces that work against the bow movement, namely the friction between the string and the bow hair. Look at the friction plot in Fig. 16.7: As the bow is accelerating from zero while holding a constant pressure against the string, the friction force builds up smoothly until a first release takes place at time = 0, when the static-friction limit is reached. After that, the buildup of a rotating corner causes force spikes to occur at regular intervals, each one forcing the string to make a short slip back on the bow-hair ribbon. However, between these slips, during the static-friction interval, peaks *nearly* reaching the friction limit represent a threat against the periodicity of the stick/slip action. If bowing is too fast, one of these peaks will reach the limit and a premature slip occur, causing the string to fall into higher modes for a shorter or longer time. If on the other hand bow speed is too slow, spikes won't be high enough to cause slips with intervals equal to the nominal period. The string will sound choked, creaky, or will synchronize to a lower fundamental. With adequate bowing, the static-interval force peaks will have faded away completely after a small number of periods, opening for great bowing liberty within the Helmholtz regime.

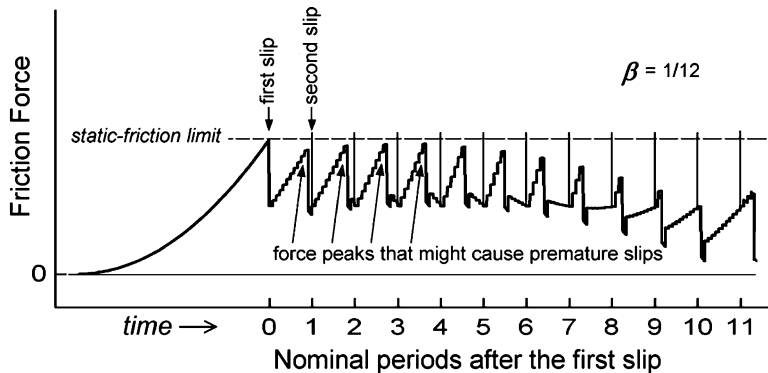


Fig. 16.7 Friction force during an attack with steady bow force and acceleration. The first slip happens when friction can no longer hold the string (reaching the static-friction limit). Later, periodic force spikes trigger string releases. However, between these spikes (drawn above friction limit for clarity), peaks of high friction might cause premature string releases if the bowing speed gets too high

Back to the question about controlling the acceleration: If starting the stroke “from the string,” that is, with a near-constant bow force, the string resistance will be felt at peak just before the first slip, before any sound has been made. When the string slips and the tone starts, a sudden drop in the friction force is experienced, not only during the slip interval, but also during much of the stick intervals that follow. To prevent the bow from shooting forward now (with the hand still pushing or pulling) it is important to have *adequate mass* connected to it. When a given force is working on a mass, the resulting acceleration is inversely proportional to the mass value, implying that if more mass is involved, acceleration will be less, and vice versa. When the situation calls for low and smooth acceleration, for example, if starting a stroke on a low string very close to the bridge, a slightly more rigid bow grip combined with a reduction in wrist flexibility might be just what does the trick. By temporarily reducing joint flexibility, the masses of fingers, hand, forearm, upper arm, or even the whole torso may be added to the minor mass of the moving bow, and thus significantly reduce unwanted fluctuations of the acceleration. This is not an attempt to introduce a new bowing style, just a description of the underlying physics in situations where the player easily could face an uninvited ponticello. In other situations where the music calls for quick and crisp articulation, which involves rapid changes of the bow acceleration, minimizing the active moving mass might be the right thing to do.

16.3.7 *Détaché*

Détaché (separated) is the term for broad strokes with clear onsets, such as employed in national anthems, and when practicing scales slowly. Here the attacks

should be in the category noise-free of Fig. 16.6, and most players will maintain bow pressure (force) during bow changes.

16.3.8 *Martelé*

Martelé (hammered) is a term for short tones with very distinctive onsets, mostly produced by starting the stroke with *excess* bow force near the frog, so that the first periods fall in the category *choked/creaky* with respect to Fig. 16.6. However, after a few milliseconds the high bow force is released, and a normal Helmholtz-type tone is produced.

16.3.9 *Light Bowing*

When playing ancient music, many violinists prefer to avoid too distinctive attacks by playing “on the surface”. This is particularly valid for rapid passages. Typically, these will be played at the outer half of the bow, with a combination of force/acceleration that places the attacks in the *loose/slipping* category of Fig. 16.6.

16.3.10 *Spiccato/Sautillé/Ricochet*

In *spiccato* (cut off) and *sautillé* (jumping) the bow bounces off (or nearly off) the string between attacks that are executed with alternating bowing directions. In *ricochet* (rebounding) the bow makes a series of jumps in one direction. The fact that the bow directions alternate in spiccato and sautillé calls for an efficient damping of the string between tones in order to make the attacks crisp: Keep in mind that the rotational direction of the Helmholtz corner is changed for every new stroke and reminiscences of the old wave pattern are likely to conflict with the new one. A closer inspection explains what is happening when the spiccato is crisp and clean (see Fig. 16.8).

In Fig. 16.8 the contact force between the bow hair and the string is superimposed on the bow velocity and the velocity of the string under the bow. The slip backs of the string are seen as regularly paced spikes, indicating that there is no noise in these tones. The first slip (a) is happening when bow force (dashed line) is near maximum. In the interval (a) to (b) the bow speed is still increasing and the tone building up in spite of a decreasing bow force. Between (b) and (c) there is no contact between the bow and the string, so the string waves fade out exponentially (like reverberation). At (c) the bow returns to the string – *still moving in the old direction* – and now a forced damping of the string waves starts. At (d) the waves are so much damped that the string can no longer produce slips, but stays stuck on the bow hair. In the interval (d) to (a) again, the remaining torsional waves are further damped (quietly), while the bow changes

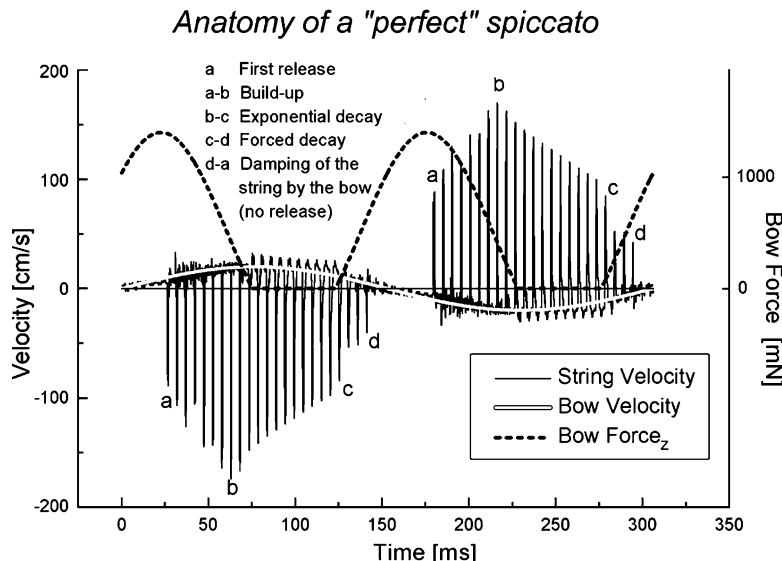


Fig. 16.8 String velocity and bowing parameters during a clean spiccato (simulated). The velocity spikes seen in the plot are string slips, just once per nominal period. The first string release (a) comes when the bow force is near maximum (dashed line) and while the bow speed is increasing (gray line). The bow/string interaction has four distinct phases (see text)

direction and the bow force approaches a new maximum. And thereafter the cycle repeats. See Guettler and Askewelt (1998).

Notice that while the bow *speed* is controlled by a back-and-forth *translational* movement of the frog in a cycle lasting the entire time span of the plot, the *force* is controlled by a *rotational* movement around an axis near the frog, with a cycle lasting only half that time. It is actually the timing between these two cycles that determines the quality of the attacks. If putting a small mark on the bow-sticks' midpoint, a lying figure eight (∞) should be seen when playing a fast sautillé when timing is right.

In ricochet, there is no damping of the string between tones, since there is only one rotational direction of the Helmholtz corner. The bow can merely pick up and refresh the waves fading between attacks. See Fig. 16.9 for recorded examples of spiccato and ricochet.

16.3.11 Bouncing Rate

All the bouncing techniques mentioned above take advantage of the natural (rotational) bouncing rate of the bow's stick–hair combination, where (1) stick stiffness and (2) hair tension play crucial roles. In addition to those two, no less than six additional parameters are involved in the determination of the final bouncing rate: (3) distance from the bow/string contact point to the effective rotational axis near the frog, (4) firmness of the bow hold, (5) tension of the played string, (6) distance from contact point to the bridge, (7) tilt of bow hair, (8) time interval

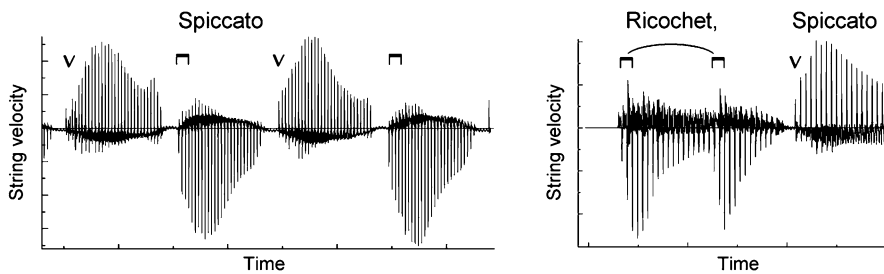


Fig. 16.9 Examples of spiccato and ricochet in actual playing. Measurements of a violin string during a crisp spiccato (left panel) and two ricochet tones followed by one spiccato tone (right panel). Notice the nearly total damping of the string before each spiccato attack, while between ricochet attacks the stick-slip action continues

when the bow is in the air. If parameters 1–5 are increased, the bouncing rate goes up; if parameters 6–8 are increased, the bouncing rate goes down – and vice versa.

With normal hair tension (55 ± 5 N) the natural bounce rate for a violin bow resting on a string varies from about 4–5 Hz close to the frog to about 40 Hz close to the tip (Askenfelt and Guettler 1998). When the bow bounces off the string, the rate becomes lower, because the restoring force downward (e.g., gravity) is less than the force exerted by the string upward. But here the firmness of the bow hold will act as a restoring force too, potentially increasing the rate again. If a series of ricochet notes of equal values is to be played on a down bow, from the middle to the tip, the bow hold needs to be continually adjusted (relaxed) in order to counteract the natural rise in the bow's bounce rate. A gradual increase of the hair-ribbon tilt angle, works in the same direction, as well as pulling the contact point slightly away from the bridge during the sequence.

For spiccato and sautillé, each tempo has a *sweet spot* along the bow-hair ribbon. To find the sweet spot one can (while holding the bow with the firmness one is going to use when playing) make a quiet ricochet by moving the frog no more than a couple of centimeters. Listen to the bouncing rate: it should be close to the rate applicable for the musical rhythm in question. Try different bow/string contact points until the applicable rate is found.

Because tilting the hair ribbon lowers the bouncing rate by a couple of hertz, a loud and fast sautillé is most easily performed with the hair flat on the string.

16.3.12 Parameters That Affect the String's Spectrum

This section offers an overview in table form of parameters that influence the sound spectrum when playing within the Helmholtz regime (see Table 16.2). Notice that only one parameter is changed at a time.

Table 16.2 Parameters capable of changing the string's spectrum during playing

Parameter value increased – see footnotes	Effect on tone color – spectral profile
Bow force (“bow pressure”)	Increased sharpness/brilliance
Bow speed	Decreased sharpness/brilliance
Tilting of bow-hair ribbon with respect to the string (only if tilted the correct way, i.e., toward the fingerboard)	Increased sharpness/brilliance (moderate effect only)
Width of bow-hair ribbon	Decreased sharpness/brilliance (moderate effect only), and increased noise due to partial slipping across the hair ribbon during “stick” intervals (particularly when bowing near the bridge)
Length of string (with constant bending stiffness and impedance but with the fundamental frequency decreasing)	Increased sharpness/brilliance (relative to the fundamental frequency)
Finger-pad damping	Decreased sharpness/brilliance
Relative bowing position (β)	Only local spectral deviations – no general trend except increased slipping noise due to the increased slipping intervals

Notes:

1. Increased bow force sharpens the rounded corner and moves the working point upward in the Schelleng diagram (Fig. 16.4). The brilliance increases.
2. Increasing the bow speed implies a movement down in the Schelleng diagram, because in absolute force values the diagram is shifted upward. The Helmholtz corner gets more rounded.
3. Tilting the bow-hair ribbon boosts the higher partials slightly and gives a “freer sound” (Schoonderwaldt et al. 2003). Even more importantly for violin and viola is that tilting allows for more gentle onsets and onsets closer to the bridge.
4. Width of bow-hair ribbon is closely linked to bow-hair tilting. What causes the slight corner rounding when a 7–8 mm wide hair ribbon lies flat on a violin string is not clear, but the effect is probably related to frictional properties rather than *signal averaging*, which would suggest a higher roll-off frequency.
5. When making a downward glissando, the section with the rounded corner becomes a relatively smaller part of the vibrating string, so although the cutoff frequency remains the same, its harmonic number increases. On a violin the relatively widest kink is experienced when playing high positions on the comparably thick G string.
6. A soft finger pad (or more pads on a double bass/cello) will contribute to further corner rounding and put greater demand on the bow’s sharpening function.
7. The bowing position has less spectral influence than one would imagine. Bringing the bow closer to the bridge does not sharpen the corner and thus lift the upper part of the spectrum. The necessary adjustment in terms of increased bow force does. However, in pizzicato, where the string takes a completely different waveform, the spectral envelope is very much influenced by the plucking position (Guettler et al. 2003).

References

- A Askenfelt, Observations on the violin bow and the interaction with the string. *Proc. International Symposium of Musical Acoustics*, Paris (1995).
- A Askenfelt and K Guettler, The bouncing bow – an experimental study. *Catgut Acoust. Soc. J.* **3**(6) (series II), 3–8 (1998).
- A Askenfelt and K Guettler, Bows and timbre – myth or reality? *Proc. International Symposium of Musical Acoustics*, Perugia (2001).
- I Firth, Construction and performance of quality commercial violin strings. *Catgut Acoust. Soc. J.* **47**, 17–20 (1987).
- K Guettler, Wave analysis of a string bowed to anomalous low frequencies. *Catgut Acoust. Soc. J.* **2**(6) (series II), 8–14 (1994).
- K Guettler, On the creation of the Helmholtz motion in the bowed string. *Acta Acustica/Acoustica* **88**, 970–985 (2002).
- K Guettler and A Askenfelt, Acceptance limits for the duration of pre-Helmholtz transient in bowed string attacks. *J. Acoust. Soc. Am.* **101**(5 Pt. 1), 2903–2913 (1997).
- K Guettler and A Askenfelt, On the kinematics of spiccato and ricochet bowing. *Catgut Acoust. Soc. J.* **3**(6) (series II), 9–15 (1998).
- K Guettler, E Schoonderwaldt and A Askenfelt, Bow speed or bowing position: which one influences the spectrum the most? *Proc. Stockholm Music Acoustics Conference (SMAC'03)*, Sweden, 67–70 (2003).
- R J Hanson, A J Schneider and F W Halgedal, Anomalous low-pitched tones from a bowed violin string. *Catgut Acoust. Soc. J.* **2**(6) (series II), 1–7 (1994).
- M Kimura, How to produce subharmonics on the violin. *J. New Music Res.* **28**(2), 178–184 (1999).
- M E McIntyre, R T Schumacher and J Woodhouse, Aperiodicity in bowed-string motion. *Acustica* **49**, 13–32 (1983).
- N C Pickering, Nonlinear behavior in overwound violin strings. *Catgut Acoust. Soc. J.* **1**(2), 46–50 (1989).
- F Rocaboy, The structure of bow-hair fibres. *Catgut Acoust. Soc. J.* **1**(6), 34–36 (1990).
- J C Schelleng, The bowed string and the player. *J. Acoust. Soc. Am.* **53**(1), 26–41 (1973).
- E Schoonderwaldt, K Guettler and A Askenfelt, Effect of the bow hair width on the violin spectrum. *Proc. Stockholm Music Acoustics Conference (SMAC'03)*, Stockholm, Sweden, 91–94 (2003).
- E Schoonderwaldt, K Guettler and A Askenfelt, An empirical investigation of bow-force limits in the Schelleng diagram. *Acta Acustica/Acoustica* **94**, 604–622 (2008).
- R T Schumacher, Bowing with a glass bow. *Catgut Acoust. Soc. J.* **3**(2), 9–17 (1996).
- J H Smith and J Woodhouse, The tribology of rosin. *J. Mech. Phys. Solids* **48**, 1633–1681 (2000).
- B Stough, E string whistles. *Catgut Acoust. Soc. J.* **3**(2), 28–33 (1999).
- C Valette, The mechanics of vibrating strings. In: *Mechanics of Musical Instruments*. A Hirshberg, J Kergomard and G Weinreich (eds). Springer-Verlag, Vienna (1995).
- H von Helmholtz, *On the Sensations of Tone*. Dover, New York (1954). Original publication: *Lehre von den Tonempfindungen*. Braunschweig: Vieweg (1862).
- J Woodhouse, R T Schumacher and S Garoff, Reconstruction of bowing point friction force in a bowed string. *J. Acoust. Soc. Am.* **108**(1), 357–368 (2000).

Chapter 17

Viols and Other Historic Bowed String Instruments

Murray Campbell and Patsy Campbell

While plucked strings have been used for musical purposes since at least the third millennium BCE, the idea of sounding a string by bowing it is a much more recent development. Bowed string instruments seem to have originated in Asia toward the end of the first millennium CE, and were in widespread use in Western Europe by the end of the eleventh century. For the next three centuries many different types of bowed instrument, with a bewildering variety of names, were in common use throughout Europe.

By 1500, two distinct families of bowed string instruments were emerging: the viols and the violins. It has often been stated that the violin evolved from the viol, but this is not the case; the two families developed at roughly the same time, with different physical characteristics and musical functions. The viol family maintained an important independent musical role until the eighteenth century, but changes in musical taste resulted in a period of neglect in the nineteenth century. The revival of interest in early music and the search for historically informed performances led to a remarkable resurgence in the making and playing of viols in the twentieth century.

This chapter begins with a short survey of the musical and acoustical properties of some of the more important medieval bowed string instruments. The nature of the viols that were made and played in the late fifteenth and sixteenth centuries is then described, and the evolution that led to the instruments written for by Baroque composers such as Couperin, Handel, and Bach is charted.

M. Campbell (✉)

School of Arts, Culture and Environment, University of Edinburgh, Edinburgh EH1 1JZ, UK
e-mail: j.p.campbell@ed.ac.uk

17.1 Medieval Bowed String Instruments

It is evident from the diversity of types of bowed instruments illustrated in contemporary manuscripts and paintings that the Middle Ages was a period of intense experimentation in musical instrument making. Two broad groups of instruments can be distinguished in these illustrations. One group, which can be loosely described as medieval fiddles, consists of instruments with a body shape characterized by a relatively distinct and narrow neck, opening out fairly quickly into a much wider body. The other group, which can be described loosely as rebeccas, consists of instruments without a distinct neck, with a body shape that resembles an elongated pear.

17.1.1 Medieval Fiddles

Medieval fiddle is a term that covers a wide range of differently shaped and sized bowed instruments that were developing in Northern Europe during the twelfth and thirteenth centuries. Although a fiddle held with the neck vertically above the body has sometimes been described as a *medieval viol*, there does not seem to have been a direct link between these instruments and the viol family that developed in the fifteenth century.

Early medieval fiddles, often used by troubadours, were hollowed out from a solid piece of wood, with a top soundboard usually of soft wood perforated with groups of sound holes. Unlike the rebec with its deep bowl, the fiddle had a flat back. Strings were made of twisted strands of sheep gut, though silk and horsehair were also used in Germany and England. We see from twelfth-century manuscripts that some body outlines were oval and some were rectangular; gradually, more and more became waisted. The addition of a tilted, wedged fingerboard and a pegbox became customary, with a tailpiece and bridge to support the tension of the strings. From the thirteenth century onward, shallow bouts appeared between the back and top plates, with large C holes above or near the bridge; the construction became lighter, with bridges more curved and higher so that the most complex tunes could be bowed. Necks were normally unfretted, although frets are shown in some depictions. Bows typically had a simple arched shape.

Hans Memling, one of the most eminent early Netherlandish painters of the late fifteenth century, frequently depicted angels playing extremely highly decorated medieval fiddles which were certainly created as expensive luxury items as well as musical instruments. As a very similar instrument appears from different viewpoints in several paintings, one can deduce that Memling had access to a specific medieval fiddle and copied its features accurately. Another sophisticated medieval fiddle is clearly and carefully depicted in the *Coronation of the Virgin* (ca. 1465), now in the Alte Pinakothek in Munich, by a painter known only as the Master of the Life of the Virgin. An angel holds the shallow instrument steady below his shoulder tilting downward; a forked bridge supports each of the four strings on an individual

flattened prong of the bridge, and the long tailpiece is secured by a basal nut. The instrument clearly has front and back plates that overlap the bouts; there are large C-holes at either side and slightly below the bridge; the fingerboard is wedged above the neck; and there is a hollow peg board carrying the four pegs. The medieval fiddle shown on the left in Fig. 17.1 is a reconstruction by Bernard Ellis based on this painting.

17.1.2 Rebecs

The *rebec's* antecedents are considered to lie in Arabic, Moorish, and Spanish *rababs*, which originally had a resonant gourd body, later a cupped wooden body with a top covering of skin, and a crude wooden fingerboard. Developing to prominence in Europe from the tenth century to the end of the Renaissance, Western rebeccas were made in a great variety of sizes and shapes, but contemporary manuscript illustrations generally show a smoothly tapering tear or pear-shaped wooden body, often with the body and straight fingerboard carved from a single piece of hard wood. As with the medieval fiddle, bows are usually a simple arched shape. Many variations on the number of strings from one to five (occasionally including a drone string) and of playing positions (sometimes including playing with the instrument between the knees, “a gamba”) appear in contemporary



Fig. 17.1 Left: medieval fiddle by Bernard Ellis (ca. 1982). Right: alto rebeck by Bernard Ellis (ca. 1982)

illustrations, but all instruments are within dimensional constraints that allowed a comfortable playing posture while standing and walking. It is quite evident from descriptions and illustrations that Western stringed instruments overall were not standardized in the early centuries of development: considerable overlap between the shapes of bowed medieval fiddles and rebecs and plucked lutes and citoles existed.

Due to its relative loudness, the rebec was often considered an instrument for outside use and not a court instrument. Rebecs did, however, perform art music in the late medieval period and Renaissance. Massed small rebecs and violins gathered to greet Queen Mary with psalms in 1560 after she arrived in Edinburgh from France, although the music was reported to be “out of tune.” Many visual and documented references to the use of rebecs in taverns or rural processions give an idea of the power and clarity of its sound. The characteristic sound of modern reconstructed rebecs such as that shown in Fig. 17.1 is certainly penetrating, and suitable to convey a clear dance tune over the noise of the dancing, but as the instrument was also used at court entertainments in combination with other wind, string, and keyboard instruments, there must have been a great range of quality of sound dependent on the skill of the maker.

In the fifteenth century, different sizes of high pitched rebecs are mentioned. By the beginning of the sixteenth century, convincing illustrations of fully developed, sophisticated rebecs appear in Flemish paintings, in which they are represented as instruments appropriate for prestigious occasions, and are played by angel instrumentalists, as in the *Virgin and Child with Female Saints* by Gerard David in the Musée des Beaux-Arts, Rouen. Structural features retained at this period include the pear-shaped body with three strings (probably gut), but this painting defines a more complicated, sectionally constructed instrument with a top plate featuring C-holes and a rose, a separate, inlaid fingerboard, an angled and hollowed peg box with scroll, and a fairly high curved and hollowed bridge. By this stage the practical and effective outdoor instrument had clearly extended its role; in 1532, the German Hans Gerle published his text on the tuning and performance practice of families of rebecs in four different sizes, tacitly acknowledging that rebecs had the potential for subtlety of expression in experienced hands.

17.1.3 Acoustics of Medieval Bowed String Instruments

Because no bowed string instruments have survived from the medieval period, a discussion of the acoustical properties of these instruments must of necessity be somewhat speculative. The general shape and scale of the instruments can be judged from paintings, but important internal details such as the presence or absence of a soundpost cannot be determined. These limitations have not inhibited makers from experimenting with reconstructions, and it is interesting to explore the acoustical properties of reconstructions that have been judged by musicians to be successful from the standpoint of performance.

17.1.3.1 Acoustical Properties of the Medieval Fiddle

The instrument shown on the left of Fig. 17.1 is a medieval fiddle reconstructed by Bernard Ellis. It has four strings, which can be tuned to G3-D4-A4-E5 as on a modern violin. The reconstruction is approximately the same overall size as a modern violin, but has a flat top plate with C-holes instead of f-holes. The back plate is also flat. There is no soundpost, but the top plate is braced by a transverse strut below the C-holes and an axial bar approximately underneath the top string.

The vibrational properties of the Ellis reconstruction were compared with those of a modern violin by measuring the bridge admittance, which is the frequency-dependent ratio of the velocity of a point on the bridge to the amplitude of the driving force at that point. The measurements of bridge admittance, like the others reported in this chapter, were carried out by Professor J. Woodhouse in his laboratory at the University of Cambridge, using a method similar to that described by Jansson (1997). A small hammer was swung so as to deliver an impact at a point on the treble side of the bridge close to the crossing of the top string. An accelerometer mounted in the hammer head gave a signal from which the force applied to the bridge could be deduced. The resulting motion of the bridge was measured by a laser vibrometer.

The solid line in Fig. 17.2 shows the bridge admittance for the Ellis medieval fiddle over the frequency range 180–5,000 Hz. For purposes of comparison, the measured bridge admittance for a twentieth-century violin made by David Rubio is shown in the same figure by a dotted line. Considering the major structural

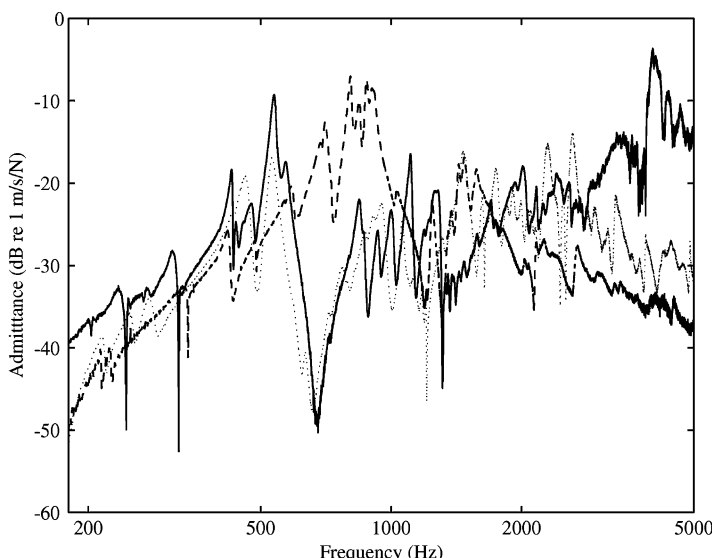


Fig. 17.2 Solid line: bridge admittance for a reproduction medieval fiddle by Bernard Ellis. Broken line: bridge admittance for a reproduction alto rebec by Bernard Ellis. Dotted line: bridge admittance for a violin by David Rubio (courtesy of J. Woodhouse)

differences between the two instruments, the overall similarity between the two curves is remarkable. The cluster of *signature modes* of the body is evident around 500 Hz in the two instruments, as is the dramatic dip in admittance around 700 Hz, and a second cluster of body modes around 1,000 Hz. A *bridge hill* around 2,000 Hz may also be distinguished. Above 3,000 Hz the bridge admittance of the modern violin dies away while that of the medieval fiddle increases dramatically; this may be related to the fact that the medieval fiddle bridge has a toothed construction, with each string supported on a separate pillar of the bridge.

The A_0 mode, formerly described as the *main air resonance*, can be identified with the peak-and-dip feature at 275 Hz in the Ellis fiddle. This identification was confirmed by a simple experiment in which a miniature lapel microphone was inserted into the internal air cavity of the fiddle through one of the C-holes. When air was blown across the other C-hole the resulting broadband noise excited the cavity resonance, and the spectrogram of the sound recorded by the internal microphone showed a pronounced peak at 275 Hz.

The A_0 mode frequency corresponds to a pitch a semitone below the open D string, which is close to its pitch on a modern violin. It is not necessarily the case, however, that this cavity mode plays the same important role in boosting the low-frequency radiation efficiency of the medieval fiddle as it does in the case of the violin. In the A_0 mode the radiation efficiency is reduced by destructive interference between the air flowing through the C-holes and the air displaced by vibration of the external surfaces of the instrument. This reduction is less pronounced in the violin because of the asymmetry introduced by the placing of the soundpost under the treble foot of the bridge (Saldner et al. 1996). It is interesting that Ellis chose an unsymmetrical bracing pattern for the top plate; because no original medieval fiddles have survived, it is impossible to say whether a similar stratagem was adopted by the fifteenth-century makers.

17.1.3.2 Acoustical Properties of the Rebec

The instrument on the right in Fig. 17.1 is a reconstruction of a rebec by Bernard Ellis. This is an instrument designed to play in the alto register, with three strings tuned G3-D4-A4; both smaller and larger instruments are also commonly depicted in medieval sources. The body and neck of the Ellis rebec are carved from a single piece of wood, to which a flat top plate and a fingerboard have been glued. The top plate has two f-holes and bracing struts, but there is no soundpost.

The bridge admittance curve for the Ellis rebec is shown by the broken line in Fig. 17.2. It is strikingly different in overall shape from the admittance curves for the medieval fiddle and the violin. The response is dominated by a very large peak just below 1,000 Hz, with a subsidiary peak at around 1,800 Hz. Using the internal microphone, the A_0 air cavity resonance was found at 373 Hz.

Dünnwald (1991) found that a strongly radiating air cavity mode around 280 Hz on a violin was correlated with perceived excellence in sound quality; this finding was confirmed in a recent study by Bissinger (2008). Although the strings of the

Ellis alto rebec are tuned to the same pitches as the bottom three strings of the violin, the A_0 mode appears to be nearly 100 Hz higher on the rebec. This, together with the absence of a soundpost, means that there is little to support radiation of the lower harmonics of notes played on the G3 string of the rebec. In contrast, the highest (A4) string has a powerful, vigorous sound.

Dünnwald has also proposed that a strong response in the frequency band between 650 and 1,300 Hz is associated with a nasal timbre in violins. Although Dünnwald's conclusions have been called into question by more recent research (Fritz et al. 2009), it is certainly the case that the penetrating sound of the rebec is frequently described as nasal.

17.2 Renaissance Viols

Throughout most of the twentieth century, the term *viol* (or the Italian equivalent *viola da gamba*) normally referred to the Baroque type of instrument, made in the seventeenth and eighteenth centuries. In the last few decades, interest has grown in the rather different styles of viol that were made in the preceding century, and it has been recognized that in many ways these early viols are particularly well adapted to the performance of Renaissance polyphony. In this section the musical and acoustical properties of the Renaissance viol are described.

17.2.1 *The Development of the Renaissance Viol*

Woodfield (1984) has demonstrated that the viol or viola da gamba family developed in the fifteenth century from the Arabian *rabab* and the Spanish *vihuela da mano* as a bowed string instrument with longish fretted neck, held in the lap between the knees with clearance for the bowing action. One of the first identifiable viols is represented in a Valencian painting, which depicts a rather chubby, long-necked, guitar-like instrument but with a highly curved bridge allowing the free use of an arched bow. By 1493, viols "taller than a man" were brought from Spain to Mantua, and a type of tall, thin viol subsequently was featured in early sixteenth-century paintings in northern Italy.

In 1497, Lorenzo Costa, a sophisticated painter at the Mantuan court of Isabella d'Este, included a pair of viol players in his *Ghedini Altarpiece* in the church of San Giovanni in Monte, Bologna. The perspective system used to represent these two viols slightly precedes the general use of systematized perspective principles in mainstream art. However, two sizes of viol are indicated, and the angled views of the viols provide a lot of information about the instruments. They have fairly flat front plates extending beyond the bouts, pairs of C-holes in the front plates, very shallow ribs, thin necks with narrow fingerboards, a curved angled peg box with a scroll, and six paired strings and flattish bridges. The back seems to be fairly straight, but cannot be properly seen.

Less than a decade later, Raphael painted his *St. Cecilia* for the same church, and included in the picture a very different viol. It has much deeper sides, steeply sloping shoulders, an angled and curved peg box for six pegs, a wedged neck with a fretted fingerboard and six gut frets. The gut strings themselves are all broken, but a high arched bridge and a tailpiece are clearly shown in place, and above the bridge, on the fairly thick front plate, are two tear-shaped sound holes. A short, stocky bow rests at the side of the viol. The symbolism of the image makes it clear that this damaged viol was intended to represent a state-of-the-art instrument in 1506, and that it had failed, like the portative organ and other discarded man-made instruments in the picture, to out-class the musically pre-eminent natural human voice.

Very few sixteenth-century viols have survived to the present day without suffering significant alteration and repair, but at least one tenor viol of ca. 1540 by the famous Venetian maker Francesco Linalol exists in essentially its original state in the collection of the Kunsthistorisches Museum in Vienna. X-rays of the instrument have revealed some surprisingly crude technical processes for attaching the neck, as well as some subtle dovetailing in the rib woodwork and a light top plate. Reconstructions of this tenor instrument have been made by Richard Jones from working drawings by Benoit Gervaise. By scaling the measurements upward and downward, after consulting a range of Northern Italian paintings of differently



Fig. 17.3 Left: Renaissance tenor viol by Richard Jones (2003), after Francesco Linalol. Right: Renaissance bass viol by Richard Jones (2004), after Francesco Linalol

sized Linarol viols, Jones has created very successful chests of viols with A tenor, G tenor, D bass, and A great bass, which produce a rich and clear sound when played in consort. G tenor and D bass viols by Jones are illustrated in Fig. 17.3.

17.2.2 Acoustics of Renaissance Viols

The bridge admittance curve for the copy of the Francesco Linarol tenor viol by Richard Jones, illustrated in Fig. 17.3, is shown by the solid line in Fig. 17.4. The response is dominated by a closely grouped set of body modes between 400 and 500 Hz, with a second peak just below 1,000 Hz. The A_0 air cavity resonance is not evident in the bridge response curve, but was found at 135 Hz using an internal microphone.

The relatively high frequencies of the main body modes is probably related to the fact that the top plate is bent and braced rather than carved, because carving cuts through the fibers of the wood and lowers its stiffness. In the absence of a sound-post, the structural integrity of the instrument requires relatively stiff transverse bracing bars. An interesting feature of the original Linarol viol is that there is a bass bar under the top plate that is slanted relative to the main axis of the plate. This asymmetry can be significant in allowing the A_0 mode to radiate more efficiently, boosting the low frequency output.

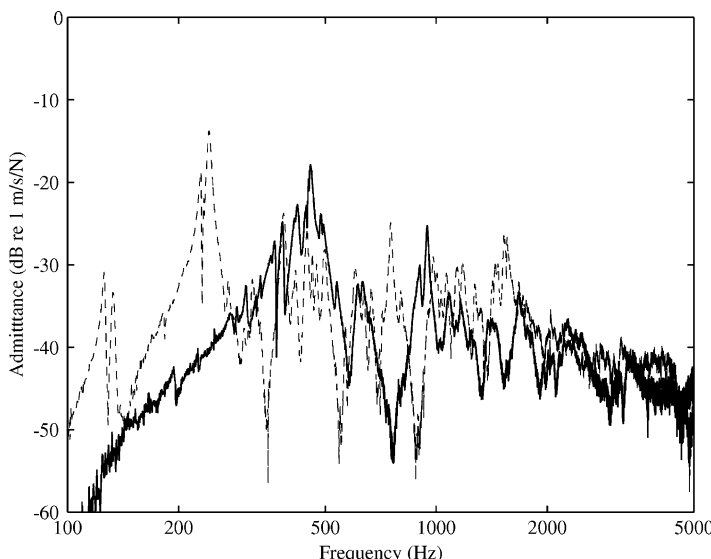


Fig. 17.4 Solid line: bridge admittance for a reproduction Renaissance tenor viol by Richard Jones. Broken line: bridge admittance for a Baroque tenor viol by Norman Myall (courtesy of J. Woodhouse)

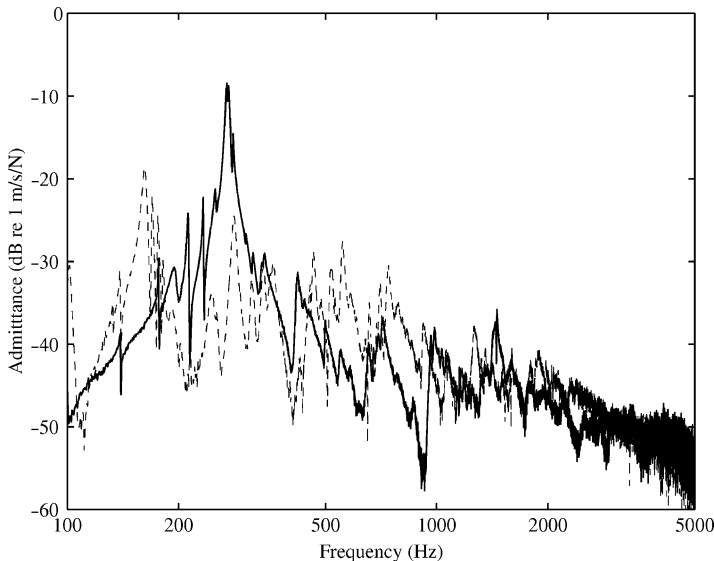


Fig. 17.5 Solid line: bridge admittance for a reproduction Renaissance bass viol by Richard Jones. Broken line: bridge admittance for a reproduction Baroque seven-string bass viol by Anthony Edge

The viol is tuned as a tenor in G (G2-C3-F3-A3-D4-G4). The main body resonances thus correspond to notes played on the top string, which has a strong singing quality. Notes played on the lower strings have an edgier timbre; while the sound is less full than that of a Baroque tenor viol, the emphasis on upper harmonics is valuable in allowing each strand in a polyphonic texture to retain its distinctness and clarity.

The solid line in Fig. 17.5 shows the measured bridge admittance curve for a Renaissance D bass viol, illustrated in Fig. 17.3. Because no complete Francesco Linarol bass viol has survived, Richard Jones designed and constructed this instrument by scaling up the Linarol tenor viol. The main body modes appear between 200 and 400 Hz, with a very strong peak at around 250 Hz. Because the bass is tuned D2-G2-C3-E3-A3-D4, the strong peak in the response occurs between the two top strings. The A_0 air resonance is found at 97 Hz, close to the frequency of the G2 string. As with the Renaissance tenor, the breaking of symmetry by the bass bar may help the A_0 mode to radiate efficiently even in the absence of a soundpost.

17.3 Baroque Viols

Many viols made in the late sixteenth and seventeenth centuries have survived, some in good playing condition, allowing modern makers to make accurate copies that can be reliably taken to represent the musical and acoustical properties



Fig. 17.6 *Left:* Baroque treble viol by Norman Myall (1999). *Center:* Baroque tenor viol by Norman Myall (1999). *Right:* copy of Colichon seven-string bass viol by Anthony Edge (2001)

of instruments of the Baroque period. Examples of viols of different sizes, modeled on seventeenth-century originals, are illustrated in Fig. 17.6.

17.3.1 *Development of the Baroque Viol*

In the seventeenth century, several major illustrated organological texts were published that charted the evolving characteristics of viol structure, but the communication of practical information and hard data seem to have been restricted largely to the makers' workshops. It is clear that many sizes and elaborate shapes were experimented with. By the time that Praetorius (1618) was writing the second volume of his magisterial *Syntagma Musicum*, families of different-sized viols were in common use for consort playing in amateur domestic situations and for performance at court. A rich repertoire of music was created especially for the viola da gamba in England, while music for solo *lyra* or *bass viol* also developed. The bass viol held an important role in supporting the solo voice, and as continuo in broken consorts where viols of different sizes often contributed their own particular timbre.

Baroque viols usually have six strings, although the *Instrumentalischer Bettlermantl*, a manuscript book of ca. 1635–1650 in the Edinburgh University Library, describes viols with five strings as well as six strings, with the addition of a seventh string on some basses. The most common sizes are D bass, G tenor, and D treble. Viols are normally tuned in fourths with a major third in the middle, but tuning systems vary and texts from the seventeenth century to the present day spill a lot of ink on this topic. The construction of Baroque viols is largely directed toward

enhancement of volume, brightness, and variety of sound, rather than the softer, buzzing nasal sonority so characteristic of Renaissance viols. The front plate is usually sectional and can be very thin indeed; ribs are deep with strengthening bars; bridges are higher and pierced; and a soundpost is invariably present. The strings are still made of gut, but the lower strings are often wire wound to achieve a greater volume of sound, especially for bass viol solos, which became an increasingly important part of the Baroque viol repertoire.

17.3.2 Acoustics of the Baroque Viol

By the end of the sixteenth century, the introduction of the soundpost had transformed the acoustical and musical character of the viol. The first few decades of the seventeenth century saw an outpouring of musical compositions, especially in England, for consorts of up to six viols including treble, tenor, and bass instruments. In these compositions all voices are equally important, and homogeneity of timbre among the different sizes of viol was therefore desirable.

17.3.2.1 The Baroque Treble Viol

There is very little information about the acoustical properties of viols in the published scientific literature (see Fletcher and Rossing 1998). It is therefore remarkable that the first instrument to be studied by interference holography appears to have been a Baroque treble viol. Carl-Hugo Agren used this technique in the late 1960s to guide a redesign of the classic treble viol, which he felt to be musically unsatisfactory (Agren and Stetson 1972). His approach, which resulted in an increased body length and drastically reduced rib height, proved controversial in the viol-playing community (see Rutledge 1979; Agren 1980). A more conventional treble viol made by Norman Myall is illustrated in Fig. 17.6.

The bridge admittance curve for the Myall treble viol is shown by the solid line in Fig. 17.7. The admittance curve for the Rubio violin is shown for comparison by the dotted line. The general pattern of admittance peaks for the treble viol below 1,000 Hz is similar in both form and magnitude to that for the modern violin, but transposed downward by about a musical fifth: there appears to be a group of body modes centered at around 320 Hz, and a second group of modes between 600 and 700 Hz. The A_0 resonance is at 180 Hz.

The treble viol is tuned D3-G3-C4-E4-A4-D5. The top string is a tone below that of the violin, and the range of treble viol parts in the early decades of the seventeenth century is similar to that of contemporary violin parts. The bottom string is rarely used in consort music, so that the practical ranges of the treble viol and early Baroque violin were effectively the same. The violin, however, was starting to develop as a solo instrument with a strong individual voice, while the primary role of the treble viol was to blend euphoniously with larger instruments of lower pitch in consorts. The relatively low frequencies of the main body modes, and

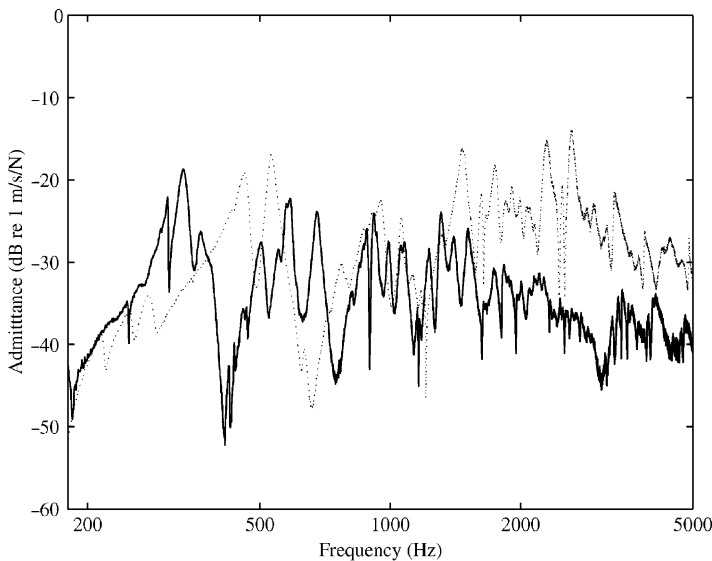


Fig. 17.7 Solid line: bridge admittance for a reproduction Baroque treble viol by Norman Myall. Dotted line: bridge admittance for a violin by David Rubio (courtesy of J. Woodhouse)

the lack of strong admittance maxima in the frequency band between 1,500 and 3,000 Hz, are consistent with the less obtrusive function expected of the treble viol. The A_0 resonance is well placed to strengthen notes down to F3, allowing the instrument to function effectively as an alto voice when required.

17.3.2.2 The Baroque Tenor Viol

The bridge admittance of the reproduction Baroque tenor viol by Norman Myall, illustrated in Fig. 17.6, is shown by the broken line in Fig. 17.4. The A_0 mode peak is at 132 Hz and low frequency body modes are clustered between 220 and 240 Hz. A second cluster of peaks is evident between 400 and 500 Hz. The general pattern of admittance peaks is similar to that of the Baroque treble viol, but transposed downward by a little less than a musical fifth, which is consistent with the tuning of the tenor a fifth below the treble. A group of admittance peaks in the region between 900 and 1,500 Hz adds some brightness to the timbre, but the admittance drops sharply above 1,500 Hz.

17.3.2.3 The Baroque Bass Viol

The final instrument discussed in this chapter is a copy by Anthony Edge of a seven-string bass viol made by Michel Colichon in Paris in 1683. This instrument,

illustrated in Fig. 17.6, is typical of the powerful solo instruments that were developed in the later seventeenth century. It is tuned A1-D2-G2-C3-E3-A3-D4.

The bridge admittance curve of the Colichon copy is shown by the broken line in Fig. 17.5. Because this instrument resembles the cello quite closely in body length, string length, and playing range, it is interesting to compare its admittance curve with the cello mobility curve reproduced in Chap. 13. The A_0 air resonance of the bass viol is close to 100 Hz, and a set of strong body modes are evident between 150 and 170 Hz. The admittance dips strongly just above 200 Hz, and a more widely spaced set of maxima appear between 400 and 800 Hz. These features parallel quite closely those of the curve for the nineteenth-century cello reproduced in Fig. 13.2.

The most striking difference between the admittance curves for the cello and the bass viol is in the frequency range above 1,000 Hz. The cello curve has a pronounced bridge hill: the peak value of the admittance, just above 2,000 Hz, is higher than at any of the strong signature body modes. There is no evidence of a bridge hill in the curve for the bass viol, and the admittance around 2,000 Hz is 20 dB lower than it is at the 160 Hz signature mode peak. This contrast is a useful reminder that, despite many superficial similarities, the cello and the bass viol are very different instruments, with distinct musical personalities. The cello developed a power and brilliance which matched those of the violin, and fitted it for a solo role in large concert halls; the viol, with its lighter construction and lower string tensions, remained an instrument more suited to intimate chamber music and to blending with human voices. It was the flexible, vocal quality of the viol that led Mersenne (1636) to praise it above all other musical instruments in his *Harmonie Universelle*:

It is certain that if the instruments are taken in proportion that they best imitate the voice, and if of all the artifices one esteems most that which best represents the natural, it seems that one must not refuse the prize to the viol, which imitates the voice in all its modulations, and even in its accents most significant of sadness and joy

Acknowledgments The authors are profoundly grateful to Jim Woodhouse for his enthusiastic and expert collaboration on the bridge admittance measurements described in this chapter, and for many helpful discussions on the science of bowed strings. Richard Jones and Anthony Edge provided invaluable guidance on the structural properties of Renaissance and Baroque viols, and Alison Crum showed us how they should be played.

References

- Agren, C.H.: The sweet sound of the viol. *Early Music* **8**(1), 72–77 (1980)
- Agren, C.-H., Stetson, K.A.: Measuring the resonances of treble viol plates by hologram interferometry and designing an improved instrument. *J. Acoust. Soc. Am.* **51**, 1971–1983 (1972)
- Bissinger, G.: Structural acoustics of good and bad violins. *J. Acoust. Soc. Am.* **124**, 1764–1773 (2008)
- Dünnewald, H.: Deduction of objective quality parameters on old and new violins. *Catgut Acoust. Soc. J.* **1**, 1–5 (1991)

- Fletcher, N.H., Rossing, T.D.: *The Physics of Musical Instruments*, 2nd ed. Springer, New York (1998)
- Fritz, C., Cross, I., Blackwell, A.F., Moore, B.C.J., Feygelson, E., Woodhouse, J.: Acoustical correlates of violin timbre descriptors. Abstracts of the Fifth Conference on Interdisciplinary Musicology (CIM09), 80–81 (2009). http://cim09.lam.jussieu.fr/CIM09en/Proceedings_files/Fritz-Cross.pdf. Accessed 5th February 2009.
- Jansson, E.V.: Admittance measurements of 25 high quality violins. *Acustica/Acta Acustica* **83**, 337–341 (1997)
- Mersenne, M.: *Harmonie Universelle* (1636); transl. Chapman, R.: *The Books on Instruments*. Nijhoff, The Hague (1957)
- Praetorius, M.: *Syntagma Musicum II: De Organographia* Parts I and II (1618–19); transl., ed. Crookes, D.Z. Oxford University Press, Oxford (1986)
- Rutledge, J.: How did the viola da gamba sound? *Early Music* **7**(1), 59–69 (1979)
- Saldner, H.O., Molin, N.E., Jansson, E.V.: Vibration modes of the violin forced via the bridge and the action of the soundpost. *J. Acoust. Soc. Am.* **100**, 1168–1177 (1996)
- Woodfield, I.: *The Early History of the Viol*. Cambridge University Press, Cambridge (1984)

Chapter 18

The Hutchins–Schelleng Violin Octet After 50 Years

George Bissinger

18.1 Introduction

Scientifically speaking, the Hutchins–Schelleng violin octet is the most interesting of all the bowed string instruments. We refer specifically to those instruments resulting from the first application of physics to the design of bowed string instruments, viz., the scientific resonance scaling process developed by John Schelleng to dimension the violin – certainly the most “successful” and mature bowed string instrument – to cover a 3½ octave range.

What do “successful” and “mature” mean here? Just that the outline shape, archings, plate tunings, materials, and dimensions used in violin construction are pretty much settled compared to the viola or cello. Of course, it is just these very parameters that affect the way the violin vibrates. Thus, our story begins here, at resonances – those specific frequencies of vibration where the violin’s various parts move maximally in a well-defined collective way called a *mode* – and whose specific properties determine how strongly each participates in the overall vibrations *and* how well each radiates. Consider these modes as being the *atoms of vibration* that, properly understood, form the “molecule” of each violin’s overall response to what is making it move.

Fifty years have now passed since the violin octet project was conceived. Considerable scientific research and major technical developments of relevance to bowed string instrument vibration and radiation has accumulated since then. In just the last decade computer-based measurement and analysis technologies have allowed us to determine for the first time such violin properties as critical frequency, normal mode (or modal average) radiation efficiency and damping, fraction of vibrational energy radiated, fraction of acoustic energy from the f-holes, and two new, important indirect radiation mechanisms. Yet *the* hallmark measurable

G. Bissinger (✉)

Acoustics Laboratory, East Carolina University, Howell Science Complex,
Room E208, Greenville, NC 27858, USA
e-mail: BISSINGERG@ecu.edu

property for determining violin quality is still elusive after more than two centuries of scientific investigation.

What is it exactly – modewise – that makes the violin what it is? Even though our understanding of the structural acoustics of the violin has expanded enormously over the past 20 years, and even after more than two centuries of scientific investigation of the violin, the parameter relationships among octet members have exposed some entirely new aspects in bowed instrument design that in turn help us to understand the violin. Consider just this one example: All properly constructed traditional violins *and* all members of the violin octet measured to date have the same basic *signature* modes in the open string frequency region (where wood-variability scales are much smaller than wavelengths), irrespective of perceived quality! Perhaps a simile from biology would be apt here? Such modes constitute violin DNA, a veritable genetic code for violins and thus the octet.

Given the continuing scientific inability to characterize violin quality, the presumption that the placement of the lowest strongly radiating cavity and corpus mode frequencies relative to the open string pitches mainly determined the violin's characteristic sound was quite audacious. (Little if any attention was paid to psychoacoustic matters such as our frequency-dependent hearing sensitivity.) The hypothesis underlying violin octet scaling then was that by moving these mode frequencies to coincide similarly with the open string pitches of various proposed higher or lower pitched instruments the violin's *sound* would somehow carry along into these pitch regions.

Contrast the violin's "fixed" shape/size, but not its measured dynamics, with the broad range of shape/sizes in the octet, constructed with a common physics-based scaling, that, though unsuccessful at times, was then modified to achieve a desired design goal. The enormous range of octet shape/size variations tends to dwarf the natural variability of wood materials, thus allowing general trends in resonance properties across a large range of sizes, volumes, rib heights, archings, etc., to emerge. The violin octet is able to shine a general scientific light on how to achieve "violin sound" by resonance placement across their pitch range that seems unrealizable by examining any number of traditional violins closely.

In this chapter, we will review the basics of Schelleng's (1963) scaling procedure, give a précis of important developments since then, provide an overview of the most recent octet modal and acoustical analysis results for a complete set of the instruments (including cavity air mode analysis), compare scaling predictions with experiment, discuss the importance for the octet of the coupling between the two lowest cavity modes A0 and A1 inherent in the first significant advance in cavity mode theory model for the violin since Rayleigh's relationship for the Helmholtz resonator, explore the surprisingly dominant acoustic contribution from the A1 cavity mode to the "main wood" region for the largest octet instrument, clarify the status of A1 in the octet scaling as amended by Hutchins, and conclude with present and near-future activities involving the violin octet. Such a necessarily brief outline of the original scientific work underlying the development and implementation of the violin octet is certainly no substitute for a reading of the published summary works by Carleen Hutchins and John Schelleng (or, for that matter, for necessary details from the references included here).

Here is some useful nomenclature:

- **VIOCADEAS** – Acronym for a systematic computer-based approach to measuring each violin’s material (aided by CT scans for shape and density), vibration and acoustic properties and integrating these with computer simulations of the dynamic properties based on material properties to provide a comprehensive computer solid model for each violin.
- *Linear system* – A vibrating system where, for example, doubling the driving force F doubles the vibrational response (acceleration, velocity, or displacement).
- *Experimental modal analysis* – Computer-based vibrations analysis technique that uses a known force exciting/striking the object at a known place from a known direction in conjunction with a measured response *profile* to extract frequencies, dampings, and vibrational mode shapes. By computer-fitting the response curves it is possible to extract the normal modes of a vibrating linear system. (Our measurements used a force hammer striking a bridge corner and a scanning laser for surface motion studies.)
- *Normal modes* – The individually unique vibrational building blocks that, properly summed, create the total response of any linear system irrespective of how it is made to vibrate.
- *Mode shape* – The often-animated vibrational profile of an object set into motion by an applied force. Characterized often by connecting surface points of no motion (nodes) into nodal lines.
- *Mobility Y* – The ratio of response velocity to driving force v/F ; used for all octet vibration measurements.
- *Radiativity R* – The ratio of far-field pressure to driving force p/F ; used for all VIOCADEAS violin acoustic measurements.
- *FEA* (finite-element analysis) – A computational technique requiring accurate shape as well as material density and elastic moduli that is capable of accurately simulating the way the violin vibrates. Generally computed without air loading (i.e., vacuum FEA).

18.2 Brief Octet History

By the 1950s, Frederick Saunders (widely known in the physics community for his work in atomic structure that led to the Russell–Saunders coupling theory) had established himself as the foremost American researcher on bowed string instruments. He had gathered a group of like-minded individuals around himself who jokingly called themselves the Catgut Acoustical Society. Shortly before his death in 1963 this name became official as did the organization. (Interested readers are referred to Hutchins’ 1992 paper, “A 30-Year Experiment on the Acoustical and Musical Development of the Violin-Family Instruments,” for an enjoyable description of the personal and technical trials and successes of this endeavor

(Hutchins 1992a). So when Henry Brant had the idea in 1957 for an octet of bowed string instruments with sound characteristics similar to the violin that would cover a 3½-octave range, it was natural that he would approach this research group to see if there was any interest in pursuing such an endeavor. In this group was Carleen Hutchins, an amateur violin maker who had been working with Saunders for years helping to construct experimental instruments. She was immediately attracted to the idea and subsequently played the major experimental part in the design and construction of these instruments. Her main partner in this endeavor was John Schelleng, a retired electrical engineer who went on to publish a landmark paper with the first application of physics to violins, scaling the violin's resonance properties into different pitch regions (Schelleng 1963).

18.2.1 Identification of Important Resonances

The violin has a lot of resonances. Some, due to collective air motions inside the violin in well-defined patterns at particular frequencies, are called *cavity modes*. Others are due to the body itself in the aforementioned modes of vibration. A few have quite strong interactions between the air motions inside and the violin body walls. Which ones are important? The ones that can be heard when the violin is bowed, of course!

When the Saunders group settled on this project they began a search through voluminous violin tests that Saunders and the others had made to try to identify what resonance properties typified the best violins, and to determine the character of these resonances. One principal resource was the bowed instrument *loudness* curves developed by Saunders (1953). These were plots created by standing in front of a sound level meter (SLM) and bowing the instrument as loudly as possible without the tone breaking up, over many semitones, then plotting the SLM reading in dB vs. the fingered pitch. These measurements provide an *integrated* loudness measurement over all the harmonics for violins bowed in semitones up to an octave or so above the open E string (660 Hz). Unfortunately these plots are prone to misreading because, for example, the second harmonic could coincide with a prominent higher resonance for a certain fingered pitch causing a significant enhancement, but with the SLM reading attached to the fingered pitch (the fundamental), not the second harmonic. These plots suggested two main regions of acoustic strength in the open string pitch region, originally labeled as the *main air* associated with the lowest cavity resonance near C# on the G string and the *main wood* near B-C on the A string. These plots offered no clues as to the cavity or corpus (top + ribs + back) character of the resonances, which had to be gained by other means.

Saunders had developed a number of different techniques to measure violin resonances and their character reliably. One involved placing a silk fiber or feather closely over the f-hole and observing its motions with a microscope, an especially apt technique for what was called the main air resonance where there are large air

volume flows in and out of the f-holes. He used this technique as well as others on violins and violas for confirmation, but Hutchins has reported that his apparatus was not suitable for larger instruments and that his main air identification for the cello was based on loudness curves alone (Hutchins 1976). Unfortunately, the lack of mode character specificity in these plots led to a faulty cello identification that, propagated in the scaling process, created scaled predictions that led to too-high ribs in the larger instruments and correspondingly too-low main air frequencies.

In 1963, Schelleng's scaling included only the main air and main wood resonances. After 1963, the analysis of violins was greatly aided by the advent of miniature microphones that could be dropped through the f-holes, miniature force hammers, very low mass accelerometers, and scanning lasers. By the 1980s, the remarkable technological advances in computer-based vibration–radiation measurement and analysis completely revamped our understanding of the character of violin resonances over a broad frequency range, providing a degree of detail in measurement and simulation of violins not previously possible. Accompanying these much-enhanced analysis capabilities was a blossoming in graphical presentation capability that led to animations of the various modes of vibration, a truly wonderful gift for our understanding of how the violin vibrates, and thus radiates.

18.3 What Do We Know Now?

What did Saunders, Hutchins, Schelleng and other violin researchers not know back when the scaling procedures for the main air and main wood resonances was worked out in the 1960s? The accepted view during octet development was that there were only two violin radiation mechanisms of importance, viz. direct radiation from the f-holes (as for the main air Helmholtz-like resonance hereinafter labeled A0 – always the lowest strongly radiating resonance in the violin) and direct radiation from the vibrating surface. (The “A” prefix will always denote air modes, labeled in order of increasing frequency.) Schelleng in fact stated that, except for A0, all other cavity modes were unimportant radiators because they all had a node at the f-holes and thus acted essentially as acoustic shorts. Much has changed since 1963.

18.3.1 *Summary of Octet-Related Developments, 1964–2007*

Over the next 4 decades, many scientific developments relevant to our understanding of the octet were published. The following summary outlines the evolution in our understanding of the violin octet:

1. In 1973 Jansson (1973, 1977) published an experimental investigation of the violin cavity air resonances with the f-holes closed then open. The cavity modes were labeled in order of increasing frequency as A0, A1, A2,

A3, A4, . . . , but opening f-holes eliminated some modes by creating a pressure node, for example, A3 drops out. For the first time Jansson's work exposed the *geometry* of these higher cavity modes.

2. In 1974 Jansson and Sundin used a network model to show possible coupling between A1 and the lower first corpus bending mode a first indication of vibro-acoustic coupling in the violin.
3. In 1976 Hutchins published a report on the A0 frequency for the cello and baritone, comparing cavity resonance plots made with air vs. CO₂ that clearly showed Saunders had mistakenly identified A0 in the cello. This experiment followed remarks by Skeaping of the London Royal College of Music that the sound of the four larger octet members all seemed "bottom heavy." This error, propagated through the larger instruments, led to a later misreading of the loudness plots by Hutchins.
4. In 1985 Marshall published an experimental modal analysis of a violin, characterizing the vibrational modes and showing that the violin is a linear system and thus at any frequency vibrates as the sum of normal modes. Marshall also showed: (a) top and back plate motions with no mode localization to either plate, (b) the main wood (B1) resonance contained *two* first corpus bending modes B1⁻ and B1⁺ (evidence for two peaks can sometimes be seen in the loudness plots), and (c) evidence for A1 (and higher) cavity-mode-induced corpus motion.
5. In 1987 Knott's master's thesis provided the first complete vacuum finite-element analysis of the playable violin, using generic wood properties and a standard violin shape that agreed quite well with the experimental frequencies and mode shape results of Marshall, confirming that the violin was a linear system. It also showed that no vibro-acoustic coupling was necessary to create the observed first corpus bending modes.
6. In 1988 Heavier-than-air gas through the f-holes was used to drop the frequency of A1 significantly below B1 (Bissinger and Hutchins 1988). Clear evidence was then seen for an A1 radiation in the frequency-analyzed sound spectra while the violin was bowed, indicating that A1 indeed radiated, but leaving uncertainty as to the origin – from the f-holes or from induced surface motion?
7. In 1990 Shaw published an important new network model to describe A0 that introduced another degree of freedom by adding the next lowest cavity mode A1. We will refer to this model as the 2DOF model. This model, the first significant improvement in describing A0 since the Rayleigh relationship a century earlier, was crucial to understanding the behavior of the A0 and A1 modes as various octet parameters were changed.
8. In 1992 Hutchins claimed that A1 was an integral part of the original scaling process Hutchins (1992b).
9. In 1996 Schleske performed a systematic experiment that investigated the dependence of low-lying corpus mode frequencies on top and back plate mode frequencies by sequentially thinning the plates and reassembling the violin in stages. He concluded that plate mode frequencies had little effect on

low-lying corpus mode frequencies, hence the traditional practice of tuning plate frequencies to specific values seemed of little value in determining corpus mode frequencies. However, if the rib stiffness dominates plate stiffnesses (as flat plate calculations indicate), this experiment can be interpreted quite differently. The larger instruments originally had too-high ribs as a consequence of incorrect scaling of A0, which would then put the first corpus bending modes too high also. (Ribs were neglected in Schelleng's scaling.)

10. In 1998 a water-fill experiment on a rigid violin-shaped cavity revealed coupling between A0 and A1 inherent in the 2DOF model (Bissinger 1998). This coupling dramatically reduced the volume dependence for a rigid violin-shaped cavity from the expected Helmholtz resonator result, $f(A0) \propto V^{-0.5}$ to $f(A0) \propto V^{-0.25}$, in excellent agreement with experimental results from an earlier water-fill experiment on the same cavity (Bissinger 1992b). A0–A1 coupling was the origin of Hutchins' difficulties in trying to raise A0 by reducing rib height in the large octet instruments (Hutchins 1992a).
11. In 2003 cavity analysis of the A0 and A1 modes for a complete violin octet underlined the superiority of the Shaw 2DOF predictions over the Rayleigh relationship for A0 frequency, although discrepancies between measurement and prediction still existed. Subsequent incorporation of a semi-empirical wall compliance correction consistent with a network theory approach significantly improved agreement with A0 and A1 experimental frequencies to within $\pm 10\%$ over the entire octet, a range of 4.5:1 in length, 10:1 in the f-hole area, 3:1 in top plate thickness, and 128:1 in volume (Bissinger 2003a).
12. In 2003 modal and acoustic analyses of a complete octet were compared with the Schelleng scaling predictions for A0 and B1 (Bissinger 2003b). Except for the baritone, the measured B1 frequencies (computed as the average of the B1⁻ and B1⁺ values) were in good agreement with the desired scaling goals. Surprisingly, the acoustic output of the large bass in the B1 region was dominated by A1, an unexpected intruder into the main wood resonance region.
13. In 2007 the radiation from the f-hole region only was measured using *patch* near-field acoustical holography (pNAH). Combining the pNAH results with modal analysis and far-field acoustical radiativity results showed that within experimental error A0 did indeed radiate completely, while A1 radiated hardly at all, through the f-holes, as expected from basic acoustic considerations (Bissinger et al. 2007). Hence A1 far-field radiation must come from A1-*cavity-mode-induced* wall motion, adding an important indirect radiation mechanism. Remarkably this same experiment exposed *corpus mode-driven volume-change f-hole radiation* as an important indirect radiation mechanism, contributing a remarkably large percentage ($\sim 50\%!$) to the B1 modes' overall far-field radiation.

In all discussions we refer to just five basic modes in the critical open-string region, known as the signature modes:

1. A0 – always the lowest resonance (violin ~280 Hz); always prominent and extremely important for sound from the lowest string;

2. A1 – the next higher air resonance (violin ~450 Hz, near B1⁻ usually), sometimes important, even dominant in the large bass main wood region, *and* coupled to A0, thereby enhancing its overall importance;
3. CBR – (C-bout rhomboid in cross-section) the lowest corpus mode (labeled C_1 by Jansson), nominally 400 Hz in the violin with double dagger (\ddagger) nodal line pattern on top and back plates and a shear-like motion between them; never radiates strongly and hence never showed up in SLM-bowing tests;
4. B1⁻ – (Jansson T₁) the lowest major corpus radiator, the lower first corpus bending mode, violin nominally 460 Hz.
5. B1⁺ – (Jansson's C3) the upper first corpus bending mode, violin nominally 530 Hz (4–5 collectively referred to here as the B1 modes, replacing main wood resonance).

Note that these corpus or cavity modes may couple to a low-lying tailpiece or neck-fingerboard mode and show up at multiple frequencies. The tenor was the most obvious example of this coupling.

18.3.2 How Bowed-String Instruments Radiate

Because violin strings are tuned in musical fifths, and A0 and B1 typically fell close to the lower and upper middle strings of the violin, respectively, the nominal goals in Schelleng's scaling were to place A0 at $1.5 \times$ and B1 at $2.25 \times$ the lowest string frequency. A0 was expected to be the *only* cavity mode capable of significant direct radiation from the f-holes. Schelleng did not expect any of the higher cavity modes to radiate directly through the f-holes because all had a node at the f-holes, but A1, the next higher cavity air mode, was capable of inducing indirect surface motion consistent with its pressure profile that sometimes led to strong radiation at its frequency.

The possibility that significant cavity-mode-induced surface motion could lead to significant radiation does not seem to have ever been seriously considered by Schelleng or any of his contemporaries. The main wood resonance loudness peak conglomerated direct surface radiation from both first corpus bending modes (labeled together as B1), but enhanced these by indirect volume-change-driven radiation through the f-holes. Thus, we now have *four* important radiation mechanisms. The traditional two *direct*: (1) cavity mode directly through the f-holes (A0) and (2) *corpus* modes radiating directly from the surface (most modes) are now accompanied by two new *indirect*: (3) cavity-mode-induced surface vibrations (A1) and (4) corpus-mode-driven volume flows through the f-holes. The four violin radiation mechanisms vary in relative importance through the octet, although generally all must be considered for all the instruments.

The structural acoustics of bowed string instruments has now evolved to where contributions from individual normal modes of vibration can be summed to determine the overall instrument sound. While it is no longer realistic to consider pure

corpus modes (such as vacuum finite-element analysis, FEA, gives) or pure cavity modes (requiring a rigid corpus such as in cavity mode boundary-element calculations (Bissinger 1996), most modes can be considered as (mostly) corpus or (mostly) cavity in character. However, corpus–cavity coupling is always important and sometimes dominant, as for A1 in the large bass.

Various structural acoustics parameters dealing directly with sound production by violins that were measured for the first time over the last decade – radiation efficiency and radiation damping, effective critical frequency, fraction-of-vibrational-energy-radiated, fraction-of-acoustic-energy-from-f-holes – show that the violin indeed is not unique in its vibratory and radiative behaviors compared to other simpler-shape structures, nor are “bad” violins markedly different from “good” ones. All of these parameters theoretically can be computed with a good FEA solid model that incorporates coupling of the corpus with the air motions inside. Quantitative correlations to quality judgments must take into account the fact that the proper setup and a well-cut bridge are as essential to making any violin sound good as the best materials and construction, although this is certainly not a new insight into violin sound.

18.3.3 *Where Do Materials Come in?*

Linear systems with their unique “normal” (mathematically “perpendicular”) modes are crucial to our evolving modern understanding of bowed string instruments. (What does linear mean for a violin? Only that if we apply a force and the violin responds, applying twice the force will give twice the response, hence response divided by force is constant.) For linear systems there is a *fundamental physics linkage between actual vibrational behavior and simulations based on detailed knowledge of material properties* such as shape, density, and stiffness (elastic moduli). The vibrational behaviors of any violin can be characterized by its individual normal modes – in properly phased superposition these provide the response of the whole instrument to any frequency driving force called the *operational deflection shape* (ODS) – computed from purely material properties.

In fact, comprehensive CT scans over the whole strung-up violin can provide accurate *fixed* densities and shape for a certain violin that, in combination with starter-generic wood stiffness properties, allow an FEA program to compute a violin’s normal mode frequencies and shapes. And here is where the importance of signature modes emerges; because these are readily recognizable in all violins their measured frequencies can be compared with their computed values, and FEA wood stiffness values varied until there is agreement. In this way it is possible to reverse-engineer a violin back to the basic material properties, which is the essence of the VIOCADEAS Project (Bissinger 2005)! All these linkages are essential for a comprehensive understanding of the violin, and underscore the importance of experimental modal analysis in characterizing the fundamental ways a violin vibrates.

18.3.4 A1 Radiation in the B1 Region

In the 1990s, Hutchins surprised the violin community by stating that A1 and its frequency relationship to the B1⁽⁺⁾ corpus mode was the underlying determiner of violin quality, and furthermore that it was used in the scaling of the octet. Schelleng, on the other hand, while understanding that the violin cavity was not rigid, presumed it so in order to compute frequencies for A0, assuming that higher cavity modes such as A1 could not possibly radiate strongly because all had nodes at the f-holes. The unanticipated result of the modal and acoustic measurements on the violin octet (and 17 violins of varying quality) was the common presence of A1-induced vibrations in the B1 region. Radiation accompanying A1, however, was generally weak compared to nearby B1 – main wood – mode radiation and thus should not show up in SLM-based loudness plots. No quality-A1 radiation strength correlation was seen in our 17 violin sample, for example, the *Plowden Guarneri del Gesu* demonstrated A1 radiation competitive with the B1 corpus modes below 600 Hz (Bissinger and Rowe 2007), while the *Titian Stradivari* was considerably weaker. Furthermore a violin with prominent A1 radiation was rated as “bad.”

Because VIOCADEAS analysis provided vibration *and* radiation measurements, it was simple to compare these and thus determine which modes radiated well. As an example, superimposed averaged-over-corpus vibration (mobility $\langle Y \rangle$ in m/s/N)

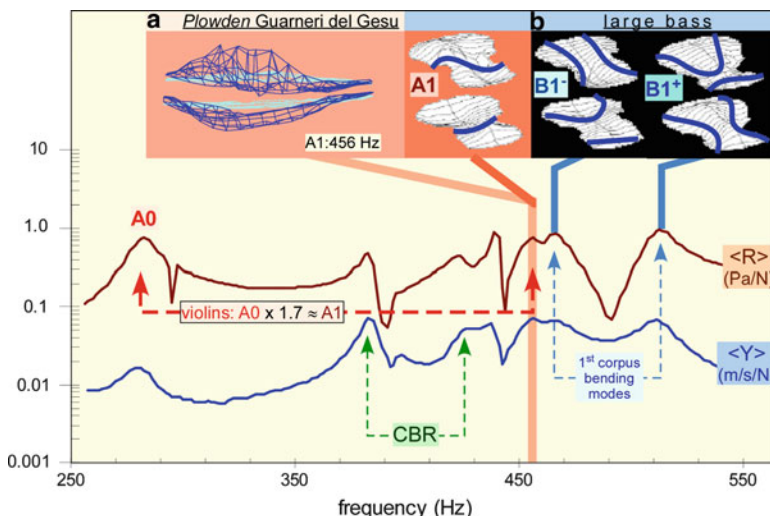


Fig. 18.1 Average corpus vibration (lower blue curve mobility $\langle Y \rangle$, m/s/N) and top hemisphere radiativity $\langle R \rangle$ (upper dark red curve, Pa/N) for *Plowden Guarneri del Gesu* (1735) with noted signature modes A0, A1, CBR, B1⁻ and B1⁺ generic to all bowed instruments tested (strings cause sharp dropoffs). Strong A1 is apparent. Insets: (a) Plowden A1 mode shape at 456 Hz, undeformed shape *light blue*; (b) large bass (discussed later) A1 (showing opposite phase motions in lower and upper bouts), and B1⁻ and B1⁺ modes with superimposed nodal lines. B1 nodal line patterns switch between top and back plate. Helmholtz-like mode A0 has much weaker induced surface vibration relative to radiativity as expected (nodal line patterns common across octet and all violins)

and averaged-over-top-hemisphere radiation (radiativity $\langle R \rangle$ in Pa/N) for the *Plowden* are shown in Fig. 18.1, along with the nodal line patterns for A1 and B1⁻ and B1⁺ obtained for the large bass. It is important to keep in mind that these mode shapes were common across the octet and all violins, varying only in frequency as the pitch range of the instruments was varied. An insert showing in side view one frame of an A1-induced vibration animation for the *Plowden* (using a greatly magnified motional profile superimposed over the undeformed surface) clearly shows the lower bout region above – and the upper bout region below – the undeformed shape. Strong A1 radiation is associated with the larger lower-bout deformations.

18.4 Scaling Basics

Attempts to scale an instrument of such geometric complexity as the violin cannot proceed without introducing major simplifications. It was by turns a measure of groundbreaking scientific insight and more-than-usual audacity that the violin's essential sound properties were pared down so far as to seem simplistic, while still yielding a harvest of valuable information about string instrument vibrations and sound in general. Here we look at the original “complete” scaling assumptions, the crucial practical steps to go from a desired B1 frequency placement back to plate mode frequency, ergonomic scaling realities to cover 3½ octaves, and an updating on A0 scaling approach.

18.4.1 Scaling Assumptions

The first major scaling simplification was the restriction to only the two lowest strongly radiating modes, one a cavity and the other a corpus mode (later modal and acoustical analyses have certainly changed our view of the latter). A0 was scaled from near-in-size measured instruments using the Rayleigh relationship $\omega = c\{A/(LV)\}^{1/2}$, where A is the f-hole area, L is the port length (here the plate thickness), and V is the cavity volume.

To estimate plate dimensions for various octet members, a second major simplification – violin plates were treated as flat plates – was necessary because analytic expressions relating important parameters such as density, elastic moduli, and geometry to the vibration frequencies did not (and still do not) exist for violin plate shells. When the required B1 mode frequency was determined for any particular octet instrument, *back-scaling* was done by first dividing the desired B1 frequency by 1.5 (Hutchins 1967) and then adjusting the average top and back plate traditional *tap tone* frequencies (or mode #5, the *ring* mode if Chladni patterns were used) until they achieved this value.

Hutchins (1986) later reported target plate frequencies for the octet and from these numbers the B1/#5 ratio was computed as 1.47 for all except for the small and large

bass, where values of 1.65 and 1.85 were computed. The latter two instruments were tuned in fourths, however, so putting their target frequencies at 16/9 of the low string pitch, drops the ratio to 1.30 and 1.45. There does appear to be some disagreement here with Hutchins' statement that these resonances were tuned nominally to be $2.25 \times$ the low string frequency. However, this is more a theoretical than practical problem because Schleske's 1996 experiment shows the tradition of specific plate tunings does not strongly affect the corpus mode frequencies, unintentionally exposing the importance of rib stiffness for these corpus modes. Note that rib parameters were involved in the scaling only through adjustments to the A0 frequency, although Schelleng did note that perhaps scaling by mass might be useful.

The last major simplification was the assumption of *similarity of shape* and materials. Scaling by plate length (discussed later) combined with shape similarity meant that plate width and rib height also were scaled, and thus the volume of the instrument can be directly related to the scaling parameters. By collecting a wide range of data about arching, rib height, plate sizes, etc., and correlating these with A0 and B1 frequencies it was possible to interpolate various octet geometry parameters. It was more difficult to reliably estimate parameter values outside of the data range, consequently Schelleng was always interested in additional measurements on instruments close to the proposed octet member, especially so on larger instruments. The obvious question arises. Why not take the most apparent scaling – size varying inversely with desired pitch of lowest string (*complete scaling*, as Schelleng labeled it) – as the obvious solution? The answer was immediate and quite simple. If the desired $\sim 3\frac{1}{2}$ -octave range was to be covered, reality intrudes.

18.4.2 The Practicalities

If complete scaling was to be maintained the enormous size range for the violin octet to cover a 12:1 pitch range ($\sim 3\frac{1}{2}$ octaves) was highly problematical. For example, the treble violin, tuned an octave above the violin, would have to be one-half its length, or about 17 cm (the thumb–little finger span usually exceeds this value). At the other end of the octet, $2\frac{1}{2}$ octaves down from the violin, the large bass corpus would need to be approximately 2.1-m high; adding endpin and neck/peg-box would then put the lowest fingered-pitch positions beyond the reach of any normal adult. In short, if actual playing of these instruments was desired, small instruments must be made larger, while large instruments must be made smaller than complete scaling would indicate. Complete scaling thus became subservient to ergonomics and practicality (hence our shorthand label *ergonomic scaling*), and in so doing considerably more complication was introduced into the scaling process. The size problem with the large bass if complete scaling was used vs. ergonomic scaling can be seen from Fig. 18.2 which includes photos of a full octet in proper relative scale along with one complete scaling example.

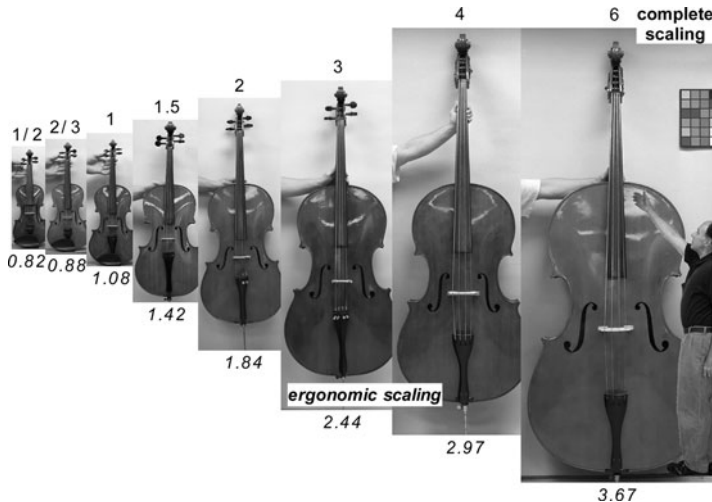


Fig. 18.2 Pictures of the St. Petersburg violin octet in proper relative size (*left to right*): treble, soprano, mezzo, alto, tenor, baritone, small bass and large bass. The bracketing numbers are: *top*, complete scaling (ratio of length to traditional violin length of ~35 cm); *bottom*, ergonomic scaling of plate length (Hutchins 1992a). (Mezzo violin is scaled version of traditional violin.) Instrument size can also be estimated relative to the size of the hand holding each instrument. A large bass, sized via complete scaling, would appear as compared with author's 1.83-m height (*right side*)

18.4.3 Flat Plate Scaling Equations

The flat plate scaling equations presented by Schelleng (1963) are included here for reference (using his notation; hence “*Y*” here is not mobility):

- Thickness H : $H_2 = H_1 \cdot (f_2/f_1) \cdot (L_2/L_1)^2$
- Stiffness S : $S_2 = S_1 \cdot (f_2/f_1)^3 \cdot (L_2/L_1)^4$
- Mass M : $M_2 = M_1 \cdot (f_2/f_1) \cdot (L_2/L_1)^4$
- Ultimate strength Y : $Y_2 = Y_1 \cdot (f_2/f_1)^2 \cdot (L_2/L_1)^4$

The subscript 1 stands for the initial known value while subscript 2 denotes target value. The similarity of shape assumption means that there is a fixed plate width/length ratio. As an example for thickness and stiffness, let 1 denote the violin, nominally $H_1 = 0.3$ cm, $L_1 = 35$ cm, $f_1 = 340$ Hz (average of plate mode 5 for top and back). Let 2 be for a cello-pitched (lowest string pitch down by a factor of 3), but *violin-resonance-scaled* instrument with lowest string $f_2 = 196/3 = 65$ Hz (can also choose $f_2 = B1$ frequency = 480 Hz/3, but be consistent across octet), and an arbitrarily chosen plate length of 70 cm (shorter than cello), then $H_2 = 0.3 \cdot (65/196) \cdot (70/35)^2 = 0.39$ cm, and $S_2/S_1 = 2^4/3^3 = 0.59$. A complete scaling table (Table I.A and I.B) of measured and deduced parameters for traditional and octet bowed string instruments can be found in Hutchins (1992a).

Ribs are truly the skeleton of the violin, yet while Schelleng did mention scaling the ribs by mass, there were no rib scaling parameters in Hutchins' Table I.A and I.B of the scaling parameters for each instrument. Rib height was adjusted to scale A0 after plate length and f-hole dimensions were set. An important result common to all the modal analysis data was that top and back plates in both B1 modes bent similarly along the ribs, which means considerable *in-plane* rib bending was involved too. Rib stiffness is the dominant contributor to the B1 bending modes stiffness, and the neglect of rib stiffness was the fundamental reason why Schleske's (1996) experiment showed so little dependence of these bending mode frequencies on plate mode frequency. A simple *flat plate* rib-plate bending stiffness ratio calculation for a typical violin shows the ribs in bending are approximately $5\times$ stiffer than the plates (Bissinger 2007).

Schleske concluded from his experiment that it made little sense to tune the plates to specific frequencies since these had little influence on the final B1 frequencies. Dominant rib stiffness was the reason why the B1 mode frequency was always nominally about 1.3–1.5× the average tap-tone (plate mode #5) frequency for the Schleske violin experiment. This is a matter of some practical importance for the octet since the B1 modes were frequency-scaled using a nominal 1.5× multiplicative factor for the tap-tones.

18.4.4 Important A0 Scaling Equation Modification

Schelleng's (1963) violin-as-circuit model was the first attempt at a comprehensive network model of the violin. It included all the major dynamic parts of the violin responding to the nonlinear bow driving force. It incorporated the Helmholtz resonance specifically and corpus resonances in a general way. The frequency of A0, however, was estimated from the Rayleigh relationship for a simple-shape rigid cavity of volume V terminating in a port tube of length L (it is unclear what Schelleng's L value was, but his footnote 13 indicates that air mass added by plate thickness drops A0 by one-fifth tone) and cross-sectional area A . Because the A0 mode must be excited via wall motions driven by the bridge feet the violin clearly could not be truly rigid, while a port *tube* only 3–4 mm long leads to unreliable calculations of the mass plug. These problems led to discrepancies between computed and measured A0 values, to inaccurate scaled values, or even to unreliable predictions for rib height reduction changes. Schelleng preferred to interpolate/extrapolate from traditional instruments similar in size with reliable A0 frequencies if possible. Fortunately a wide range of traditional instruments from such sources as student fractional-size violins, violas and cellos, and double basses were readily available for this purpose.

It is no longer appropriate to use the Rayleigh relationship to scale A0, however. Our understanding of cavity modes has undergone a radical shift since 1963, and this relationship has been completely supplanted by relationships innate to the Shaw 2DOF A0–A1 cavity mode model (Shaw 1990). The 2DOF model is

inherently sensitive to interior cavity geometry in a way that the Rayleigh relationship cannot be, for example, there are now upper and lower bout volumes, arching, and various division parameters to apportion the partial volumes properly; it provides upper/lower bout pressure ratios (important for the vibro-acoustic back-coupling between cavity mode pressure variations and induced wall motion) and naturally incorporates coupling between A0 and A1 due to the interaction between the in-out A0 and the back-forth A1 air motions (Bissinger 1998). The 2DOF model has been extended to include arching (via modular volume increments changing the volumes in the upper, C and lower bout regions) and semi-empirical wall compliance corrections (Bissinger 2003a).

The A0–A1 coupling was exposed by changing the orientation of a rigid violin-shaped cavity filled with varying amounts of water from horizontal to vertical (two orientations). It was observed that the same cavity volume led to *three* different A0 frequencies, a clear indication of a coupling between A0 and A1. Of course the Helmholtz resonance equation would predict exactly the same frequency for each orientation because the effective volume and f-hole geometry were unchanged. Because A1 is primarily a length-determined mode, and the violin's upper bout is significantly narrower than the lower, a certain volume of water in the upper bout would make the effective cavity length shorter than when it was in the lower bout; both vertical orientations create shorter effective cavity lengths than the horizontal orientation. Such A0–A1 frequency shifts are important because ergonomic scaling greatly shortened the length of the larger instruments, while extending the length of the smaller.

The relative complexity of the 2DOF model equations (although the compliance correction term is quite simple) means that for detailed discussions of the particulars the reader is best referred to the original papers. However, there are important qualitative implications in the 2DOF model directly dealing with violin-like instruments with geometric properties that vary from the model violin that will be addressed in later sections.

18.4.5 Similarity of Shape

Although one of the fundamental assumptions in the scaling process was similarity of shape, it is clear from Fig. 18.2 that there are definite trends in shape from the treble to the large bass violin. This violin octet, played in St. Petersburg, Russia, on loan, was the one on which all the modal and acoustical analyses were performed, and geometry parameters determined. (*Note:* All larger instruments had ribs trimmed down from original values. See Hutchins (1992) octet for additional discussion.) There are additional interesting normalized-to-body-length geometrical properties such as arch height, f-hole length, rib height H_{rib} , and bridge–upper bout top distance X shown in Fig. 18.3. (Note that some of these normalized values have been multiplied by ten for ease of reading values.) For example, the ratio of maximum upper-bout W_{UB} and lower-bout widths W_{LB} to length for the treble

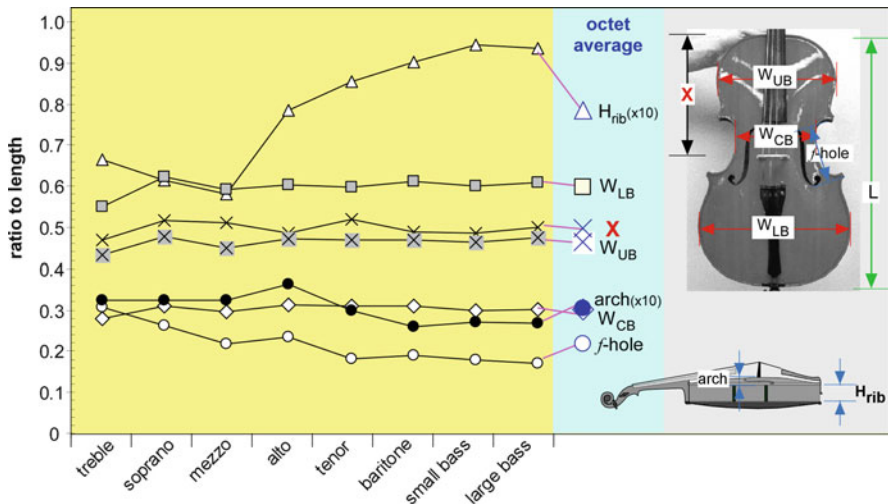


Fig. 18.3 Shape similarity summary of violin octet geometry (all normalized to body length): rib height $H_{\text{rib}}(\times 10)$, f-hole length, arch height($\times 10$), bridge-top distance X , upper-, C-, and lower-bout widths (see annotated graphics for geometry parameters). Also included in figure is average over octet. Perfect shape similarity would show horizontal lines for each parameter across octet

violin are 43 and 54%, respectively, while for the alto the ratios are 46 and 59%, respectively, and for the large bass 46 and 60%, respectively. These graphical results show that a fundamental basis of scaling was weakened slightly as the instruments evolved from the slimmer, broader-shouldered, high-pitch instruments to the broader, fatter-bottom, lower-pitch large octet members.

The length-normalized parameters shown in Fig. 18.3 are quite variable across the octet, especially rib height. Using the ratio (maximum minus minimum) divided by average as an index of variability, in order of increasing variability: f-hole length varies 63%, H_{rib} 46%, arch 33%, W_{LB} 13%, W_{CB} 11%, W_{UB} 10%, and bridge-top distance $\times 10$. The greatest variability was related to those parameters needed to place A0 at 1.5× the lowest string pitch. Surprisingly the arching, which generally decreased with increasing size, was quite variable too. The mezzo violin was the octet's replacement for the traditional violin. Because it was scaled to have more area to improve its loudness ($1.08 \times$ traditional violin length, hence about 16% more area) it was necessary to reduce rib height to maintain A0 at the desired pitch. This length increase also dropped A1 frequency somewhat, a matter that will be examined more closely later.

18.5 Modal and Acoustical Analyses

All the earlier tests that Hutchins and Schelleng relied on to settle the character of the resonances had, in the scientific sense, effectively been swept away by the mid-1980s application of then nascent, computer-based, normal mode analysis and

simulation techniques to the violin, viz., experimental modal analysis and its complementary companion, finite-element analysis. Our current technical sophistication and breadth in measuring bowed-string instrument normal mode vibrational and acoustical properties, including motions of the bridge, tailpiece, and neck-fingerboard, permits us to understand resonances and their radiation, corpus or cavity character, possible vibro-acoustic coupling, as well as material properties in ways so much more definitive than anything available before the 1980s that earlier research has essentially been superseded. It has also made mode-specific comparisons across the octet straightforward. Here we look at the EMA-acoustic experiment and compare measurement results to see how well the scaling goals were met across the complete octet. There are some surprises here both for cavity and corpus modes.

18.5.1 *Modal and Acoustical Analyses of the Octet*

All the octet modal and acoustical analyses were performed with force hammer excitation at the bridge corner parallel to the plane of the violin and bridge; mobility response measurements were made with a scanning laser vibrometer at hundreds of points on a grid over the top, ribs, back, and the various smaller substructures (see Bissinger 2003b for complete experimental details). For the vibration (velocity) and radiation (pressure) measurements the instruments were suspended in an approximate free-free support system using two elastics under the in-curved C-bout region. Such a support arrangement is essential for measuring the instrument's vibrational properties free of support fixture (including player!) interactions. For the room-average acoustic analysis the instruments and their support fixture were moved to another, much quieter reverberant room. The experimental setups are shown in Fig. 18.4. Using the same excitation arrangement acoustical measurements were RMS-averaged for hundreds of hammer strikes using dual microphones in a sound quality head.

Some unexpected behaviors were observed. By superimposing averaged-over-corpus vibrations (mobility = velocity/force) on room-averaged radiation (pressures) both amplitude-normalized to their maximum values in the same plot, it was possible to see the most prominent vibration and radiation peaks in both spectra, and how well each mode radiated relative to its vibration peak. To compare with scaling predictions, these spectra were all frequency-normalized to the lowest string pitch f_{low} so that A0 and B1 should fall at 1.5 and 2.25, respectively, as indicated on the graph. Also note that the A1 and CBR modes are notated. The comparison is furthered by showing frequency bands for the traditional violin A0, B1⁻ and B1⁺ modes from the VIOCADEAS database.

While A1 often was buried by nearby peaks in the vibration spectra for the treble-soprano-mezzo instruments, it could be extracted by special peak fitting procedures that isolated only those regions where the A1 anti-nodal response fell near nodal regions for close-by modes. However, cavity mode frequencies were



Fig. 18.4 Small bass in testing support fixture. Vibration measurements: force hammer impact excitation; scanning laser vibration response measurement (*left*). Room-average acoustic measurements: excitation and support as for vibration, but with acoustic measurement corner setup using dual microphones in sound quality head ~1.5 m distant from instrument (*right*)

also determined directly by cavity excitation-response measurements (Bissinger 2003a). From the alto onward, A1 was readily apparent in the vibrational spectra.

Comparing A0 frequencies with desired scaling targets, A0 lay lower than the target value, but was generally consistent with its relative placement in the traditional violin near 270–280 Hz. Predictably, the greatest deviations from target values were for the treble and large bass – the octet size extremes. The baritone’s A0 (and its low-frequency radiation, in general) was weak relative to the other octet members. A1 moved from $1.8 \times f_{\text{low}}$ (coincident with the treble B1⁻) to $2.3 \times$ for the largest instruments.

The B1 modes generally bracketed the target 2.25 value, except for the treble where both were below 2.25 and the baritone where both were above 2.25. Overall this is quite good agreement with the target goals. Because the treble ribs had to be trimmed significantly to move A0 up in frequency (Hutchins 1992a), their stiffness contribution to the B1 dynamic bending stiffness was significantly reduced, thereby reducing B1 frequency. By this same argument the baritone – where the ribs were also trimmed to raise A0 – could benefit from a further rib shortening, simultaneously raising A0 and dropping B1.

There was no obvious pattern to whether B1⁻ or B1⁺ radiated more strongly relative to their vibration amplitude (and the same conclusion pertains to violins). For example B1⁺ was larger for the soprano and smaller for the mezzo, vs. approximately the same for the alto. In substructure-coupled cases for either B1 mode the result would be split peaks; sometimes with both B1⁻ or B1⁺ split, giving four peaks, as for the tenor (see Fig. 18.5). Generally A1 radiated increasingly more relative to B1 with increasing instrument size.

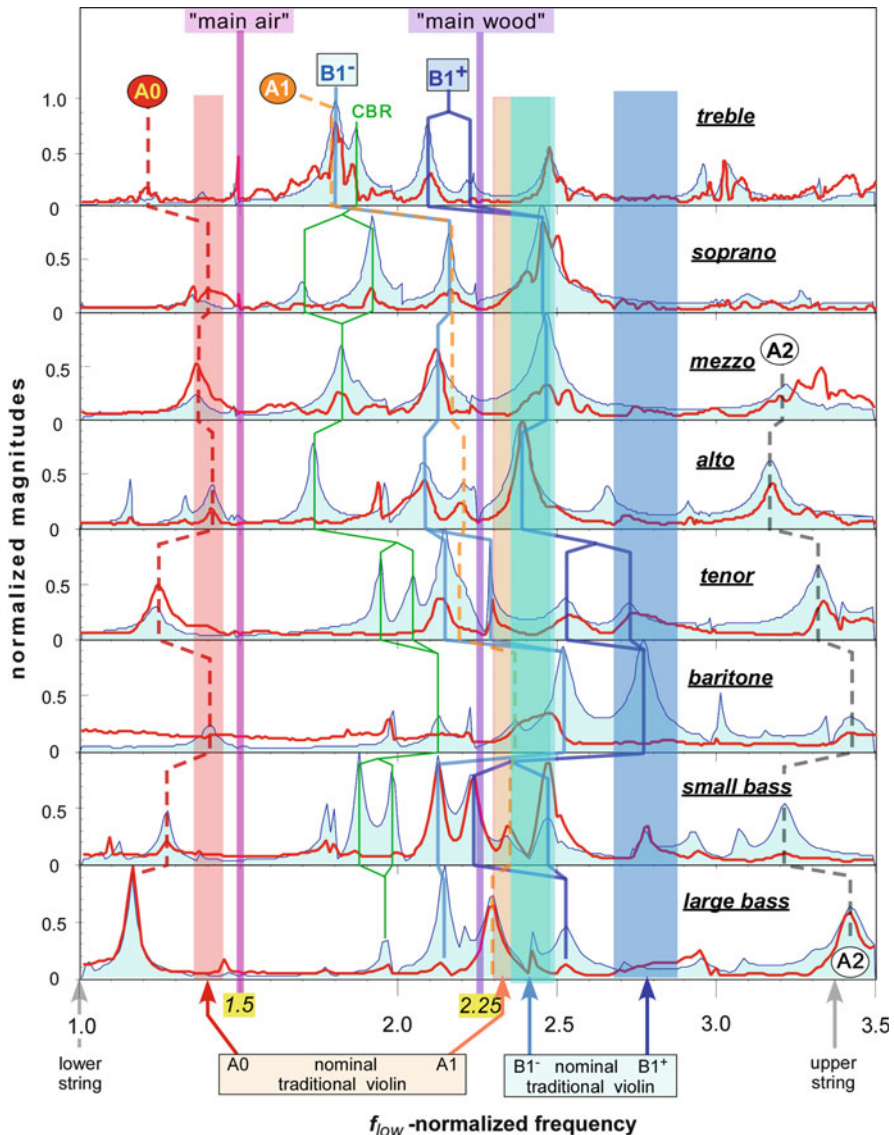


Fig. 18.5 Averaged corpus vibration (blue shaded curve) superimposed on room-averaged radiation (red curve) for St. Petersburg octet vs. frequency (low-string normalized). Magnitudes normalized to maximum (sometimes at off-scale frequency). Scaling targets for A0 and B1 at $1.5 \times$ and $2.25 \times f_{low}$. Lines follow A0, A1, A2 (dashed lines) and CBR, B1⁻ and B1⁺ through octet (doubled lines for some modes from corpus-tailpiece/neck/fingerboard coupling, especially the tenor). VIOCADEAS frequency bands (± 1 standard deviation width) for traditional violins (includes two old Italian violins) shown for A0 and A1, B1⁻ and B1⁺. Note: Weakness of CBR radiation compared to vibration, strength of large bass A1 compared to B1

18.5.2 A0 and A1: Coupling

The coupling in the 2DOF model (Shaw 1990) leads to some unexpected effects, some of which are pertinent to the experimental octet geometry information in Fig. 18.3. Overall as the octet instruments got larger: (1) rib height/length ratios generally increased (albeit with some drops), while (2) arch height/length ratios generally decreased (albeit with some increases). The 2DOF model calculations were used to look for trends in octet A0 and A1 frequencies as the rib and arch heights were varied. These have been summarized in Fig. 18.5 of Bissinger (2003a). Very interesting differences between the arch- and rib-height-dependent frequency variations of A0 and A1 were exposed in these calculations: (1) if rib height was increased, both A0 and A1 dropped in frequency, with A0 dropping more than twice as fast as A1, hence the A1/A0 ratio increases; (2) if arch height is decreased, A0 frequency rose, but A1 frequency *dropped* (!), hence A1/A0 ratio will drop. Even if A0 were somehow kept constant, these results imply that A1 can be moved relative to A0 merely by changing the arching. The 2DOF model clearly shows the theoretical behavior of these two lowest coupled cavity modes is much more complex than previously thought.

The question of whether the rib- or arch- height effect dominates can be settled by looking at Fig. 18.3 above and Fig. 18.5; rib height variations across the octet were significantly larger than those related to the arch (both must be converted to cm scales to use Fig. 18.5 of Bissinger 2003a). Thus, we expect the A1/A0 frequency ratio to increase as octet instrument size increases, in agreement with the trend observed in Fig. 18.6 for this octet. An earlier 11-instrument data set that

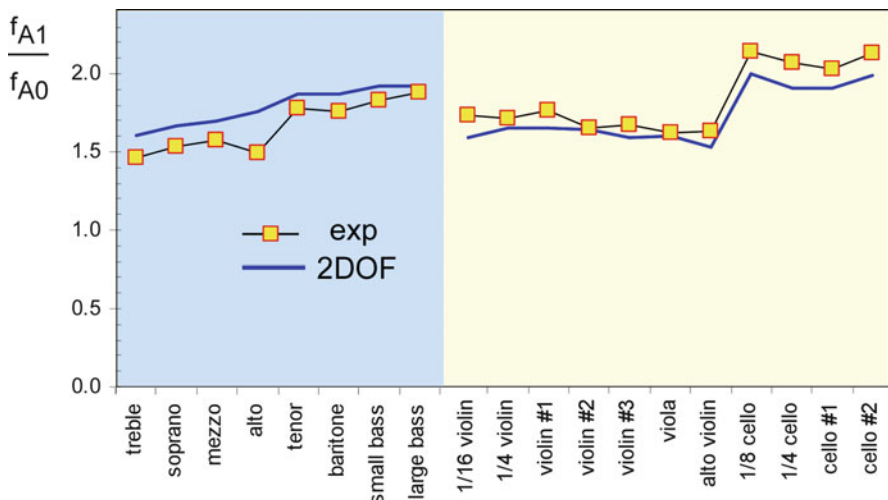


Fig. 18.6 Experimental ratio of A0 and A1 frequencies across the violin octet (blue shaded) and from an earlier 11-instrument (yellow-shaded; 1/16th violin to full-size cello) survey (Bissinger 1992a). Also shown are the 2DOF model calculations for all instruments. The abrupt jump in the 11-instrument frequency ratio is due to the increase in the rib height/length ratio from violins and violas to cellos. Traditional violins have $f_{A1}/f_{A0} = 1.71 \pm 0.05$ (VIOCADEAS 15-violin database)

ranged from one-sixteenth violins to one-eighth, one-quarter, and full-size cellos is also interesting in this regard (Bissinger 1992a). Cello rib height is much larger relative to length than violins and this A1/A0 ratio transition is seen clearly in Fig. 18.6 both in the experimental and computed 2DOF ratios. (Note that the semi-empirical compliance correction – Bissinger 2003a – canceled in the A1–A0 frequency ratio, so rigid and compliant cavity wall ratios were the same.) The 2DOF model on the whole follows the ratio variations over a remarkable range of volumes (>200) quite well.

18.5.3 Wall Compliance and Cavity Mode Frequencies

Schelleng could not avoid assuming rigid cavity walls (here the top and back plates mainly) in scaling A0 frequencies because there was no compliant-wall version of the nineteenth-century Rayleigh relationship for the Helmholtz resonance frequency. Obviously octet cavity walls must vibrate just to be able to radiate from the surface. This wall flexure also squeezes the air inside, putting energy into the A0 and A1 cavity modes. This flexure would be expected to increase with instrument size consistent with increasing plate compliance (obtained by inverting the stiffness ratio presented in Hutchins' Table 1.A and 1.B (Hutchins 1992a). Because wall flexure is practically impossible to compute due to the complex shape of the violin, a semi-empirical correction to the rigid cavity values based on instrument cavity volume, which scales by length, was used instead. The basics of this approach are outlined below.

For simplicity, consider a frictionless piston compressing the air – maintained at constant temperature – in a closed metal cylinder. It is then released and oscillates at a certain frequency. The $PV = nRT$ gas law equation tells us that compressing a gas into smaller volumes leads to higher pressures. Because the compressed air behaves like a spring with stiffness K acting on the piston mass m , the frequency of piston vibration $f = (K/m)^{1/2}/2\pi$. Now allow the cylinder walls to flex outward under the influence of the air pressure. This flexure increases the volume, so the pressure must drop below the rigid wall case, reducing the air spring stiffness, in turn dropping the oscillation frequency. Applying this analogy to A0 for the octet, there is a mass *plug* oscillating in the f-holes (plug mass can be computed approximately from air density, f-hole area, and top plate thickness). If the f-holes are unchanged, allowing wall flexure will drop the mass plug oscillation frequency, so the A0 frequency will decrease. Increasing the wall stiffness (e.g., by inserting a soundpost) raises the frequency of A0.

Wall compliance has turned out to be of great acoustical importance for the A1 mode also. For the largest instruments ergonomic scaling greatly shortened body length relative to complete scaling. For the large bass complete scaling would have created a corpus length six times longer than the violin's, so A1 would drop a factor of 6 from the violin's nominal 470–480 Hz. In ergonomic scaling the length was

scaled by just 3.67, so A1 should have fallen only to 130 Hz, which would have placed it far above the B1 modes at $2.25 \times$ the lowest string frequency (actually off-scale in Fig. 18.5) vs. the measured value of 95 Hz. The ever-increasing compliance of the larger instruments thus was offset by the ever-decreasing ergonomic/complete scaling length ratio, the combined effect being A1 always falling in the B1 region (Bissinger 2003b). Concurrently, increasing compliance enhances back-coupling with the corpus to drive plate motion more effectively, an important effect for A1's radiation.

18.5.4 Rib Heights and Pressure Ratios

There are more complications in the cavity mode story. The 2DOF model provides estimates for the upper-bout (UB)/lower-bout (LB) pressure ratios for A0 and A1 that implicitly relate to the back-coupling effect of A1 on the top and back plates. One fundamental 2DOF prediction is that the UB and LB pressures are not uniform for A0 or A1. For a rigid violin cavity the A0 UB/LB pressure ratio is >1 , while for A1 it is <1 . (*Note:* The A1 ratio is actually always negative due to the pressure phase-reversal, but we will suppress the minus sign in our discussion, using only absolute values.) Over the compliant-wall octet, gross UB/LB pressure ratio trends were similar between measurement and 2DOF prediction; the A0 pressure ratio decreased while A1's increased with increasing instrument size. Unsurprisingly there were large disparities between individual experiment and prediction because wall compliance and back-coupling to the wall significantly affect measured pressures.

Hutchins had experienced great difficulties in raising the frequency of A0 near the target value by reducing rib height. Because A0–A1 coupling significantly reduced the volume dependence of A0 (as noted above) the larger instruments had all needed significant rib height reductions to raise A0 frequencies. However another, more subtle effect accompanies these rib height variations for A1: decreasing rib height raises lower bout pressure relative to upper bout pressure, while the A0 UB/LB ratio lowers, yet another result of the A0–A1 coupling.

18.5.5 Clarifying A1 Status

Unexpectedly, Hutchins in her 1992 article, “The future of violin research,” stated: “In the development of the violin octet, the A1 mode was adjusted to the desired frequency either by finding an instrument that had the proper body length for a given tone range, or by constructing a new one. Then the A0 mode, which is dependent primarily on the volume of the violin cavity, as well as the area of the f-holes and the compliance of the walls, was adjusted by progressively slicing sections off the ribs and

reassembling the instrument until the A0 mode was raised to the desired frequency.” Contrast this with Schelleng’s statement about higher cavity modes in his 1963 scaling paper: “The experimental evidence, however, is that they are of little or no value.” How did Schelleng’s complete indifference to A1 evolve into A1 being central to the scaling procedure?

There are many problems with Hutchins’ statement, beyond the obvious incongruity of A1 being part of the main wood resonance:

1. Violin cavity mode geometries were first categorized 10 years after Schelleng’s 1963 paper by Jansson, who provided the very first indication of A1’s longitudinal character by measuring cavity mode shapes and frequencies up to about 2 kHz (Jansson 1973, 1977).
2. Mezzo violins designed by Hutchins and Schelleng in 1967 to replace the traditional violin in the octet had a nominal 15-in. length, not the traditional 14-in. (Hutchins and Schelleng 1967). The mezzo’s stated design goal was creating more sound by increasing vibrating plate area, with no mention of A1 placement. Scaling A1 frequency purely by body length from the violin average would give ~14/15ths of 469 Hz, or 437 Hz for the mezzo. Later measurements of A1 for two mezzo violins put A1 at 422 or 433 Hz, compared to a 13-sample average of 469 ± 19 Hz (range 430–494 Hz for the traditional violin).
3. The first published violin modal analysis in 1985 saw evidence for A1 back-coupling to the corpus (Marshall 1985).
4. Vacuum FEA results in 1987 (Knott 1987) definitely showed $B1^-$ and $B1^+$, indicating that no cavity mode interaction was necessary to form $B1^-$.
5. Because A0 was the only cavity mode used in Schelleng’s scaling, placing A0 near 280 Hz would then coincidentally place A1 near 476 Hz, close to $B1^-$.
6. A1-related radiation was first seen in a 1988 gas-exchange experiment, but only when A1 was dropped below all the corpus modes by heavier-than-air gas exchange (Bissinger and Hutchins 1988). Commencing in 2002, VIOCA-DEAS radiativity measurements on 15 violins over a sphere in an anechoic chamber with accompanying modal analysis data clearly showed examples of A1 radiation.
7. Patch NAH measurements showed no significant A1 radiation from the violin f-holes, which was consistent with Schelleng’s expectations; A1 radiation originated in cavity-mode-induced surface motion (Bissinger et al. 2007).
8. Octet body lengths were driven primarily by ergonomic considerations, with the instruments of highest pitch being significantly longer and those of lowest pitch significantly shorter than pure scaling would suggest [cf. Table I in Hutchins’ (1992a) summary report on violin octet development].
9. Ergonomic scaling would raise the A1 frequency significantly above the B1 region as the instruments got larger, for example, for the large bass A1 would fall at $3.75 \times f_{\text{low}}$ (rigid cavity) vs. $2.25 \times$ for B1; it is wall compliance, however, that drops A1 close to B1.

We conclude that Hutchins’ 1992 statements concerning the importance of A1 in the original scaling of the octet are incorrect. However, our results do support

incorporating it as a component of the radiation sources in the B1 region, especially so for the large bass. The main wood label, already outdated by the first violin modal analysis, now needs an alternative, more descriptive label to properly encompass all loudness contributions – possibly the B1–A1 complex?

18.5.6 Fat Bottoms, Wall Compliance, and Pressure Ratios

Why does A1 radiate so strongly for the large bass? After all, A1-induced wall motions come about because the energy passing through the bridge into the corpus couples indirectly with air in the cavity, exciting the cavity modes. Each cavity mode's pressure oscillations in turn must back-couple to the corpus, forcing it into induced motion that to some extent mirrors the cavity mode pressure profile. It seems self-evident that such an indirect energy path cannot compete with a direct energy flow into the corpus modes, yet sometimes it does. Furthermore the induced motions are anti-phase, creating essentially a dipole (and thus inefficient) radiator, yet sometimes A1 radiates quite well. Such ostensibly self-contradictory matters demand closer scrutiny, and at least an attempt at a plausible physical basis.

We start with important clues gleaned from Fig. 18.1 for a typical instrument with strong A1 radiation: (a) lots of A1-induced vibration, and (b) an imbalance between upper and lower bout motions that creates a simplified *monopole + dipole* vibrational configuration with a *monopole* component that is an efficient radiator. We have a number of important leads in our pursuit of these clues: (1) experimental from the relative radiation strengths of A1 to B1; (2) theoretical for relative plate stiffness (or its inverse, compliance) from Schelleng's scaling parameters; (3) theoretical A1 cavity pressure trends from the 2DOF model and experimental measurements of these ratios, and (4) geometrical trends over the octet for upper and lower bout areas, which respond to the internal pressure oscillations and thus lead to the observed radiation. Not one of these leads is sufficient to explain why radiation from A1-induced surface motion can compete with surface motions instigated directly by bridge motions, or even exceed it as in the case of the large bass. Our scenario seems to require a certain synergism of multiple, seemingly unrelated phenomena.

We list a number of factors that, taken all together, can evolve A1 into being the dominant radiator in the B1 region for the large bass:

Schelleng's ratio of compliance for the entire octet is shown in Fig. 18.7. The large bass is by far the most compliant in the octet relative to the violin (compliance ratio computed from inverse of Schelleng's stiffness ratio). This means its plates, for a certain applied force, will move more than for a less-compliant instrument.

The lower/upper bout area ratio A_{LB}/A_{UB} slowly increases from about 1.4 to 1.9 as the instruments increase in size (see Figs. 18.3 and 18.7). Even the same average motion in both bouts would therefore lead to the lower bout out-radiating the upper bout. If the upper and lower bout *pressure* oscillations were the same, this would result in a larger force over the lower bout that would lead to larger lower bout motions, further enhancing a *monopole* component in the vibration.

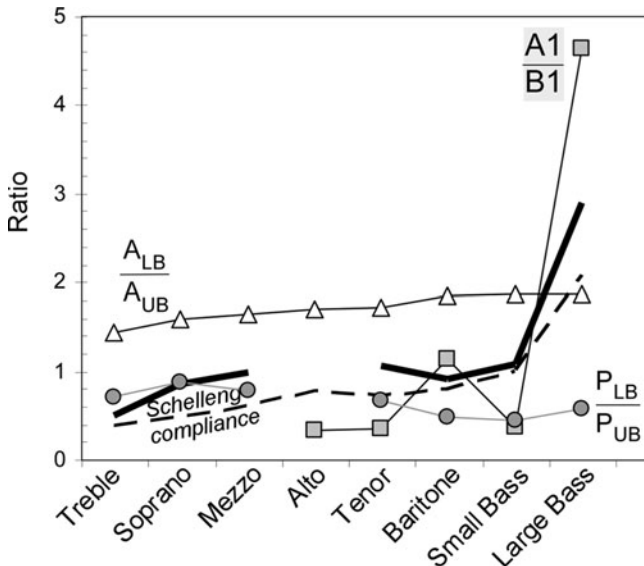


Fig. 18.7 A1 radiation strength quantified as the experimental ratio of room-averaged pressures for A1 to B1 (shaded square). Estimates of this ratio (thick solid line) were computed by multiplying plate compliance (dashed line, relative to mezzo violin), lower/upper bout area ratio (triangle), and lower-upper bout pressure ratio P_{LB}/P_{UB} (shaded circle)

The experimental lower/upper bout pressure ratio P_{LB}/P_{UB} shown in Fig. 18.7 tends to decrease with instrument size in general agreement with 2DOF calculations. This by itself would tend to reduce induced motion in the lower bout relative to the upper bout, reducing the monopole component. However, the measured P_{LB}/P_{UB} pressure ratio in the large bass actually increases relative to the baritone (19%) and small bass (23%).

An imbalance between UB and LB cavity volume flows induced by the respective wall motions in these cavities, creating in effect a *slosh* cavity volume flow component. A network model of A0 and A1 excitation as dual wall-driven Helmholtz resonators joined at the neck with an offset port predicts a clear minimum in A1 excitation for a certain ratio of upper to lower bout cavity volume flows, a possible explanation for why the small bass, which falls between the baritone and large bass has relatively little A1 strength compared to them.

With factors 1–3 quantified we were able to estimate the relative A1/B1 strengths shown in Fig. 18.7 by multiplying them together. This crude estimate follows the experimental A1/B1 ratio trends for the larger instruments surprisingly well. Note that 2DOF calculations, consistent with cavity water-fill experiments (Bissinger 1998), predict that trimming rib heights, as Hutchins did to bring A0 up in frequency in the larger instruments, makes the A1 P_{LB}/P_{UB} pressure ratio even larger.

In summary, the large bass plates are the largest in area, the most compliant, the most responsive to the cavity pressure variations, with the largest lower/upper bout

area ratio, all of which combine to create the strongest monopole component in our monopole+dipole simplification. In the far-field this $\lambda > L$ mode radiates well via the monopole component, hence the dominance of A1 radiation in the so-called main wood region for the large bass.

18.6 Future of the Violin Octet

When Hutchins retired from octet building, the future of the violin octet became quite uncertain. Its long-term success seems to depend on performance groups – playing music written or transcribed for the violin octet – entering the commercial world and being successful. Success in the commercial sphere should allow the octet to evolve beyond the novelty stage. Makers will have to optimize the sound quality of each instrument by tweaking the basic design, a process already started by Robert Spear (2003) who has integrated classical Cremonese proportions with the scientific scaling work to move A0 into optimal relationships with the open strings, especially on the larger instruments.

Continuity will require a new generation of makers to step into Hutchins' shoes. The New Violin Family Association (NVFA, <http://www.nvfa.org>), which split off from the Catgut Acoustical Society before the latter's demise and eventual partial reformation as a Violin Society of America Forum, will have to evolve into something quite different than a scientifically oriented association. While scientific research activity on bowed string instruments is declining, the numbers of makers starting to use instrumentation to test plates and violins has grown substantially. Martin Schleske in Germany was the first maker to consistently incorporate modal analysis into his work in the 1990s, testing over 100 violins, and creating the concept of *tonal copies*. In 2002, the author noted no one using instrumentation at the Oberlin Workshop on Violin Acoustics (sponsored by Violin Society of America). However, by 2007 the renowned violin maker Joseph Curtin was delivering an introductory talk on hammer-impact vibration analysis and frequency response functions to the participants there, in the meantime producing a practical violin testing rig for makers. It is a very promising sign that a coterie of makers, professional and amateur, have embraced the computer-based signal analysis capabilities in all modern personal computers and are starting to incorporate it into their work. If modern makers act like Carleen Hutchins – who was truly the “Tom Sawyer” of violin makers, enticing others with specialized skills to help her “paint her fence,” and freely sharing her results with anyone interested – then whatever branch of lutherie they occupy will benefit, as will players of all future bowed string instruments.

To date there is only one performing group on the violin octet, the Hutchins Consort, a nonprofit organization based in Southern California. With few active octet makers in the world willing to continue the work of Carleen Hutchins constructing these instruments, without sufficient financial support, and few performing groups, the present level of activity is not promising. Octet violins must be made available in sufficient quantities and at reasonable cost so that

musicians can afford to buy them. This will require a major funding commitment that has yet to materialize. In the meantime, hope lies with individual makers, but no professional maker is likely to build an instrument for which there is no market. There are a few positives in this scene however. The treble violin has shown some potential as a soloist instrument, while the small and large bass instruments look promising as a substitute for the double bass.

The actual number of octet instruments is quite uncertain. In terms of full or nearly full octets by professional builders the matter is relatively clear. Six full octets on the original Hutchins–Schelleng design exist. The last full octet by Hutchins and colleagues was completed in the mid-1980s. In addition, two other octets lack only the large bass. Four of the complete octets are now in collections at the Music Museet in Stockholm, Sweden; the National Music Museum in Vermillion, South Dakota; the University of Edinburgh, Scotland (previously at the Royal College of Music in London); and at the Metropolitan Museum of Art in New York. The Hutchins Consort owns two full octets. Robert Spear (2003) has built one full octet based on his second-generation pattern that is used for public performance in Central New York. Joris Wouters of Westerlo, Belgium, has built six octet instruments on which public performances have been given. Pio Montenari of Genoa, Italy, has built four or five instruments of the set. Spear's and Wouters' instruments were completed in the early 2000s. Spear has started his second octet.

Contrast this situation with that pertaining to professional or amateur makers making individual instruments for which there is no accurate tabulation. Hutchins says that she, her colleagues, and a number of others produced 200–300 instruments up to approximately the mid-1980s. Some reside in private hands while many remain Hutchins' personal property. Of these about 100 were made by amateurs and are currently at the NVFA office in Wolfeboro, NH, facing an uncertain future. Many sets of construction drawings have been sold, but no records have been kept about instruments that may have resulted.

The Supersensitive String Company, for many years a strong supporter and the sole manufacturer of strings for all octet violins except the basses, has begun research on new strings for the octet, including a set for professional players. Using a new string core material shows promise in creating a proportionally sized string length for the treble violin (the present string length is very short, due to the physical limitations of steel strings), as well as replacing the more problematic strings of other octet violins, such as the tenor E string and the alto A string.

18.7 Conclusions

Whether or not the violin octet is successful in entering our musical life in the long term, its scientific merits are unquestioned. It has been a treasure trove of interesting and enlightening acoustics phenomena that at the very least has the potential to return to its very violin origins and enrich them for the benefit of future makers and players.

Acknowledgments My contribution to violin octet research discussed here owes much to the active support of Carleen Hutchins who loaned me a complete octet for modal testing and the National Science Foundation who funded the materials-dynamics approach embodied in VIOCA-DEAS. I also want to acknowledge discussions with Robert Spear concerning the present and future status of the violin octet.

References

- Bissinger G (1992a) "Semiempirical relationships for A0 and A1 cavity mode frequencies for bowed string instruments of the violin, viola and cello family" *Catgut Acoust. Soc. J.* (series II) **2**(1), 8–12.
- Bissinger G (1992b) "The effect of violin cavity volume (height) changes on the cavity modes below 2 kHz" *Catgut Acoust. Soc. J.* (series II) **2**(2), 18–21.
- Bissinger G (1996). "Acoustic normal modes below 4 kHz for a rigid, closed violin-shaped cavity" *J. Acoust. Soc. Am.* **100**, 1835–1840.
- Bissinger G (1998) "A0 and A1 coupling, arching, rib height, and f-hole geometry dependence in the 2-degree-of-freedom network model of violin cavity modes" *J. Acoust. Soc. Am.* **104**, 3608–3615.
- Bissinger G (2003a) "Wall compliance and violin cavity modes" *J. Acoust. Soc. Am.* **113**, 1718–1723.
- Bissinger G (2003b) "Modal analysis of a violin octet" *J. Acoust. Soc. Am.* **113**, 2105–2113.
- Bissinger G (2005) "A unified materials – normal mode approach to violin acoustics" *Acta Acustica/Acoustica* **91**, 214–228.
- Bissinger G (2007) "Surprising regularity between plate modes 2 and 5 and the B1 corpus modes: Part I" *J. Violin Soc. Am. VSA Papers* **21**, 83–101.
- Bissinger G, Hutchins CM (1988) "A1 cavity-mode-enhanced fundamental in bowed violin and viola sound" *Catgut Acoust. Soc. J.* (series II) **1**(2), 11–13.
- Bissinger G, Rowe D (2007) "Three-dimensional normal mode vibration plus acoustic analysis of two exemplary old Italian violins (abstract)" *J. Acoust. Soc. Am.* **121**, 3061.
- Bissinger G, Williams EG, Valdivia N (2007) "Violin f-hole contribution to far-field radiation via patch near-field acoustical holography" *J. Acoust. Soc. Am.* **121**, 3899–3906.
- Hutchins CM (1967) "Founding a family of fiddles" *Phys. Today* **20**(2), 23–37.
- Hutchins CM (1976) "The Helmholtz air resonance of the cello and baritone" *Catgut Acoust. Soc. Newsrl.* **26**, 5–6.
- Hutchins CM (1986). "Free plate tuning frequencies for the violin octet instruments" *J. Catgut Acoust. Soc.* **45**, 12–14.
- Hutchins CM (1992a) "A 30-year experiment in the acoustical and musical development of violin-family instruments" *J. Acoust. Soc. Am.* **92**, 639–650.
- Hutchins CM (1992b). "The future of violin research" *Catgut Acoust. Soc. J.* (series II) **2**(1), 1–7.
- Hutchins CM, Schelleng JC (1967) "A new concert violin" *J. Audio Eng. Soc.* **15**, 4–6.
- Jansson E (1973) "On higher air modes in the violin" *Catgut Acoust. Soc. Newsrl.* **19**, 13–15.
- Jansson E (1977) "Acoustical properties of complex cavities: prediction and measurements of resonance properties of violin-shaped and guitar-shaped cavities" *Acustica* **37**, 211–221.
- Jansson E, Sundin H (1974) "A pilot study on coupling between top plate and air volume vibrations" *Catgut Acoust. Soc. Newsrl.* **21**, 11–15.
- Knott GA (1987) "A modal analysis of the violin using the MSC/NASTRAN and PATRAN", MS thesis, Naval Postgraduate School, Monterey, CA.
- Marshall KD (1985) "Modal analysis of a violin" *J. Acoust. Soc. Am.* **77**, 695–709.
- Saunders F (1953) "Recent work on violins" *J. Acoust. Soc. Am.* **25**, 491–498.
- Schelleng J (1963) "The violin as a circuit" *J. Acoust. Soc. Am.* **35**, 326–338 (erratum, p. 1291).

- Schleske M (1996) “Eigenmodes of vibration in the working process of a violin” *Catgut Acoust. Soc. J.* (series II) **3**(1), 2–8.
- Shaw EAG (1990) “Cavity resonance in the violin: network representation and the effect of damped and undamped rib holes” *J. Acoust. Soc. Am.* **87**, 398–410.
- Spear R (2003) “Influence of form on the signature modes of a second-generation new violin family quintet” *Catgut Acoust. Soc. J.* (series II) **4**(8), 19–24.

Chapter 19

Hammered Strings

Thomas D. Rossing

In the next three chapters we consider the science of hammered string instruments. In this chapter, we present a brief discussion of vibrating strings excited by a hard or soft hammer. Chapter 20 discusses the most important hammered string instrument, the piano – probably the most versatile and popular of all musical instruments. Chapter 21 discusses hammered dulcimers, especially the American folk dulcimer.

19.1 Dynamics of the Hammer–String Interaction

The dynamics of the hammer–string interaction has been the subject of considerable research, beginning with von Helmholtz (1877). The problem drew the attention of C.V. Raman and Banerji (1920), R.N. Ghosh (1926), and other Indian researchers in the 1920s and 1930s. More recently, the subject has been reviewed by Askenfelt and Jansson (1985, 1993), Chaigne and Askenfelt (1994), Conklin (1996), and Hall (1986, 1987a–b, 1992), Hall and Askenfelt (1988).

When a string is plucked, we assume an initial displacement but zero initial velocity (see Chap. 2). The opposite set of initial conditions, zero initial velocity with a specified initial velocity, could be imparted by hard hammer striking the string at $t = 0$. Of course, a blow by a real hammer does not instantly impart a given velocity to the string. The initial velocity depends in a rather complicated way on a number of factors, such as the width, mass, and compliance of the hammer (Hall 1986, 1987a–b).

Suppose that the string is struck by a hard, narrow hammer with velocity V . After a short time t , a portion of the string with length $2 ct$ is set into motion. Because this mass increases and becomes comparable to the hammer mass M , the hammer is slowed down and will eventually be stopped. With a string of finite length,

T.D. Rossing (✉)
Center for Computer Research in Music and Acoustics (CCRMA),
Stanford University, Stanford, CA 94302-8180, USA
e-mail: rossing@ccrma.stanford.edu

however, reflected impulses return while the hammer has appreciable velocity, and these reflected impulses interact with the hammer in a rather complicated way, causing it to be thrown back from the string.

At the point of contact, the string and hammer together satisfy the equation

$$M \frac{\partial^2 y}{\partial t^2} = T \Delta \left(\frac{\partial y}{\partial x} \right), \quad (19.1)$$

where elsewhere the string continues to satisfy the equation for transverse waves on a vibrating string.

$$\frac{\partial^2 y}{\partial t^2} = \frac{T}{\mu} \frac{\partial^2 y}{\partial x^2} = c^2 \frac{\partial^2 y}{\partial x^2} \quad (19.2)$$

The discontinuity in the string slope $\Delta(\partial y / \partial x)$ according to (19.1) is responsible for the force that slows down the hammer. Equation (19.1) is satisfied at the contact point by a velocity

$$V(t) = V e^{-t/\tau}, \quad (19.3)$$

where $\tau = Mc/2T$ may be termed the deceleration time (Hall 1986). The corresponding displacement is

$$y(t) = V\tau(1 - e^{-t/\tau}). \quad (19.4)$$

The displacement at the contact point approaches $VMc/2T$, and the velocity approaches zero. If the string were very long, the displacement and velocity elsewhere on the string could be found by substituting $t - [(x - x_0)/c]$ for t in (19.2) and (19.3), as shown in Fig. 19.1.

Only when the string is very long or the hammer is very light does the hammer stop, as in Fig. 19.1. In a string of finite length, reflected pulses return from both ends of the strings and interact with the moving hammer in a fairly complicated way. Eventually the hammer is thrown clear of the string, and the string vibrates freely in its normal modes.

In general, the harmonic amplitudes in the vibration spectrum of a struck string fall off less rapidly with frequency than those of plucked strings (see Chap. 2). For a very light hammer with mass M much less than the mass of the string M_s , the spectrum dips to zero for harmonic numbers that are multiples of $1/\beta$ (where the string is struck at a fraction β of its length), but otherwise does not fall off with frequency, as shown in Fig. 19.2a. (The spectrum of sound radiated by a piano may be quite different from the vibration spectrum of the string.)

If the hammer mass is small but not negligible compared to the mass of the string, the spectrum envelope falls off as $1/n$ (6 dB/octave) above a mode number given by $n_m = 0.73 M_s/M$, as shown in Fig. 19.2b. Note that for high harmonic (mode) numbers, there are missing modes between those in Fig. 19.2a.

Fig. 19.1 Displacement and velocity of a long string at successive times after being struck by a hard narrow hammer having a velocity V

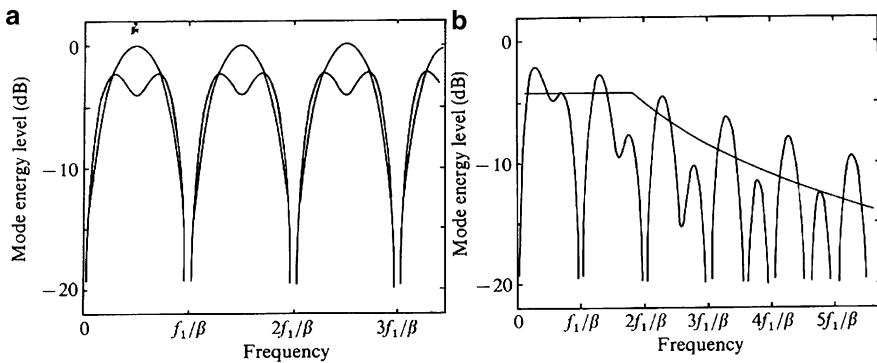
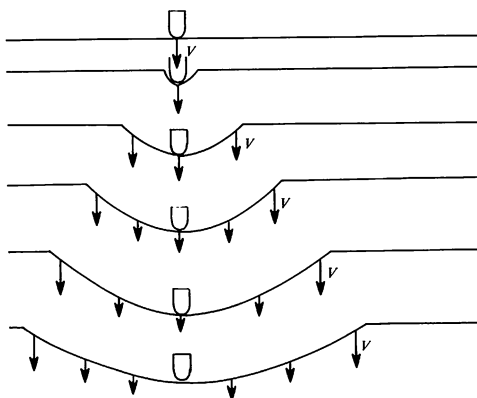


Fig. 19.2 Spectrum envelopes for a string struck at a fraction β of its length. (a) Hammer mass $M \ll$ string mass M_s ; (b) $M = 0.4/\beta M_s$ (from Hall 1986)

19.2 Piano Hammers

Hammer masses in a modern grand piano vary over a factor of 2–3, from about 10 g (bass) to 3.8 g (treble). The ratio of hammer mass to string mass varies even more widely (about 8–0.08). The hammers have hardwood cores of graduated sizes, which are covered by one or two layers of felt that increase in thickness from treble to bass. The outer layer for each set of hammers is formed from a strip of felt that increases in thickness lengthwise from treble to bass, and this strip is attached to the hammer in a press that is long enough to accommodate a complete set of 88 hammers. After pressing, the outer felt generally has a density in the range of 0.6–0.7 g/cm³ (Conklin 1996).

Hammer hardness is an important factor in piano sound. Hard hammers better excite high-frequency modes in a string than soft hammers, and thus treble hammers are considerably harder than bass hammers. The static hardness of hammers

can be tested with a durometer or hardness tester. Felt does not obey Hooke's law but rather behaves as a hardening spring. Force-compression measurements on piano hammers can be characterized by a power law

$$F = K \xi^p, \quad (19.5)$$

where F is force, ξ is the compression, K is a generalized stiffness, and the exponent p describes how much the stiffness changes with force, ranging from 2.2 to 3.5 for hammers taken from pianos and 1.5–2.8 for unused hammers (Hall and Askenfelt 1988).

Dynamic measurements of the force and compression show hysteresis: K and p take on different values for compression and relaxation. Hard hammers tend to have a larger value of the exponent p than soft hammers. Using a nonlinear hammer model along with a flexible string, Hall (1992) found that increasing exponent p leads to a smoother and more gradual rise of force as the hammer compression begins and a correspondingly steeper falloff in string mode amplitudes toward higher frequencies.

One way to test the dynamic hardness of a piano hammer is to observe the force-time pulse shape of the hammer as it strikes a rigid surface. Hall and Askenfelt (1988) determined that the contact duration τ is related to the maximum force F_{\max} by $\tau \propto (F_{\max})^{(1-p)/2p}$, where p is the same as in (19.5). The residual shock spectrum provides related information about what string modal frequencies would be most effectively excited by a given hammer (Russell and Rossing 1998).

19.3 String Excitation by a Piano Hammer

In Sect. 19.1 we discussed what happens when a string is struck by a hammer having considerably less mass than the string. In the most extreme case (which may apply at the bass end of the piano), the hammer is thrown clear of the string by the first reflected pulse. The theoretical spectrum envelope (shown in Fig. 19.2a) is missing harmonics numbered n/β (where β is the fraction of the string length at which the hammer strikes), but it does not fall off systematically at high frequency. When the hammer mass is a slightly greater portion of the string mass, as in Fig. 19.2b, the spectrum envelope falls off as $1/n$ (6 dB/octave) above a certain mode number.

A heavier hammer is less easily stopped and thrown back by the string. It may remain in contact with the string during the arrival of several reflected pulses, or it may make multiple contacts with the string. Analytical models of hammer behavior are difficult to construct, but simulations can be of some value. Hall (1987a–b), for example, showed that in the case of the hard, narrow hammer a mode energy spectrum envelope with a slope of –6 dB/octave at high frequency emerges, although the individual mode amplitudes are not easily predicted.

Askenfelt and Jansson (1985) investigated the effect of hammer mass by exciting the C4 string with three hammers: the original one, a heavy bass hammer, and a light treble hammer. They obtained a longer than normal contact time with the bass hammer and a shorter than normal contact time with the treble hammer, as expected. Although the shapes of the string vibrations did not look very different for the different hammers, the sounds they produced were markedly different. The lighter, harder treble hammer, for example, produced a sound somewhat like that of a harpsichord.

19.4 Hammer Position on the String

Figure 19.3 compares the hammer striking position along the strings d/L for a 1720 Cristofori piano with a modern grand piano. The striking position d/L varies considerably in Cristofori pianos for no apparent purpose. Later in the eighteenth century, a consensus developed that for the best tone the hammers should strike the strings between 1/7 and 1/9 of the speaking length. Figure 19.3 suggest that nowadays that criterion is followed in the lower half of the piano, but that the striking position d/L is smaller in the treble. The optimum striking position at key 88 varies with hammer weight and shape and also with string size and contact conditions but normally occurs for d/L between 1/12 and 1/17 (Conklin 1996).

In theory, an ideal stretched string struck at a certain point will not vibrate at frequencies for which vibrational nodes exist at the striking point. For actual piano strings, a large (~40 dB) but finite attenuation of the L/d -th partial does occur, but this is not a major factor in selecting the striking position. In the mid-treble, the best value is often a compromise between fundamental strength and best tone. Reducing d/L will generally make the tone sound “thinner” because of less fundamental, but too large a ratio will reduce clarity due to excessive hammer dwell time (Conklin 1996).

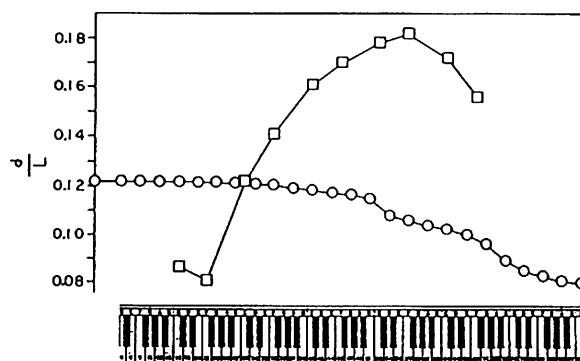


Fig. 19.3 Hammer striking ratio d/L for a Cristofori piano (open square) and a modern grand piano (open circle) (Conklin 1996)

19.5 String Excitation in a Hammered Dulcimer

Hammered dulcimers are typically played with wooden hammers having a mass of about 8 g. Because that mass is distributed along the length of the hammer, however, they act as light hard hammers. Unlike a piano hammer, which is essentially free of the action at the moment it strikes the string, the dulcimer hammer is still in contact with the player's fingers. It is not uncommon for the wooden hammer to lose and regain string contact one or more times (Peterson 1995).

The strike position in the hammered dulcimer is not only variable, but it is also near the bridge, rather than near the terminal end as in a piano. The strike ratio α , the strike point to bridge distance divided by the string length, is of particular interest. Increasing the strike ratio α increases the hammer contact time, decreases the hammer force, and generates a more complex hammer force (see Chap. 21).

References

- Chaigne, A. and Askenfelt, A. (1994). Numerical simulation of piano strings II. Comparisons with measurements and systematic exploration of some hammer and string parameters. *J. Acoust. Soc. Am.* **95**, 1631–1641.
- Askenfelt, A. and Jansson, E. (1985). From touch to string vibrations. III. String motion and spectra. *J. Acoust. Soc. Am.* **93**, 2181–2196.
- Conklin, H. A. Jr. (1996). Design and tone in the mechanoacoustic piano. Part II. Piano structure. *J. Acoust. Soc. Am.* **99**, 3286–3296.
- Ghosh, R. N. (1926). Acoustics of the pianoforte. *Phys. Rev.* **28**, 1315–1320.
- Hall, D. E. (1986). Piano string excitation in the case of small hammer mass. *J. Acoust. Soc. Am.* **79**, 141–147.
- Hall, D. E. (1987a). Piano string excitation II: General solution for a hard narrow hammer. *J. Acoust. Soc. Am.* **81**, 547–555.
- Hall, D. E. (1987b). Piano string excitation III: General solution for a soft narrow hammer. *J. Acoust. Soc. Am.* **82**, 1913–1918.
- Hall, D. E. and Clark, P. (1987). Piano string excitation IV: The question of missing modes. *J. Acoust. Soc. Am.* **82**, 1913–1918.
- Hall, D. E. and Askenfelt, A. (1992). Piano string excitation VI. Nonlinear modeling. *J. Acoust. Soc. Am.* **92**, 95–105.
- Hall, D. E. and Askenfelt, A. (1988). Piano string excitation V. Spectra for real hammers and strings. *J. Acoust. Soc. Am.* **83**, 1627–1638.
- von Helmholtz, H. L. F. (1877). “On the Sensation of Tone,” 4th ed. Translated by A. J. Ellis, Dover, New York, 1954.
- Peterson, D. R. (1995). Hammer/string interaction and string modes in the hammered dulcimer. *Proc. Int. Symp. Mus. Acoust.*, Dourdan.
- Raman, C. V. and B. Banerji (1920). On Kaufmann’s Theory of the Impact of the Pianoforte Hammer. *Proc. Roy. Soc. A* **97**, 99.
- Russell, D. A. and Rossing, T. D. (1998). Testing the nonlinearity of piano hammers using residual shock spectra. *Acta Acustica/Acoustica* **84**, 967–975.

Chapter 20

Some Remarks on the Acoustics of the Piano

Nicholas Giordano

20.1 Introduction

Much has been written about the piano. There are a number of excellent books and research articles that discuss the history, evolution, and acoustics of the instrument (Fletcher and Rossing 1991; Pollens 1995; Suzuki and Nakamura 1990; Conklin 1996a, b, c; Good 2001). However, most of these sources are either at a very qualitative level or aimed at the dedicated acoustician. Our goal in this chapter is to bridge these two extremes and to show how some elementary knowledge of physics and acoustics in general, and of the piano in particular, give interesting insight to the nature and composition of a piano tone. We hope that the next few pages will be of interest to scientists and nonscientists alike.

We begin with a little history. While the modern piano is certainly quite different from its early ancestors, there are certain key features that both versions share that differentiate them from other stringed keyboard instruments. We then describe some properties of vibrating strings, piano hammers, and soundboards, and discuss how they all contribute to the piano's sound. The way the human auditory system perceives piano tones is also important, and is discussed as well. An expanded discussion of some of the topics covered in this chapter has been given by the author elsewhere (Giordano 2010).

20.2 History of the Instrument

The invention of the piano is generally credited to Bartolomeo Cristofori, an employee of the Medici family in Florence. Three of Cristofori's pianos survive, all of which were built around 1700 (Pollens 1995). Like most inventions and

N. Giordano (✉)
Department of Physics, Purdue University, 525 Northwestern Avenue,
West Lafayette, IN 47907-2036, USA
e-mail: giordano@purdue.edu

inventors, Cristofori's work was a product of his environment – he was stimulated by a desire to overcome limitations of other keyboard instruments available at the time, specifically the harpsichord and clavichord. Other inventors contemporary with and even previous to Cristofori had also studied this problem, but the historical evidence strongly suggests that Cristofori was the first to actually build a working instrument (Pollens 1995).

So why was the piano invented? Prior to and well into the 1700s, the harpsichord was the dominant keyboard instrument. The harpsichord produces sound by plucking its strings with a flexible element called a *plectrum*; this was initially a piece of bird quill, but most harpsichords now use a plastic plectrum (Ripin et al. 1989). The control and motion of the plectrum are such that the string is always released with the same initial displacement: the amplitude of the pluck is always the same no matter how quickly or slowly the key is depressed. As a result, the player has no control over the volume of an individual tone. This limits the expressiveness of the instrument, with important implications for both the composer and the player.

Another common keyboard instrument of the time was the clavichord, which produces sound by striking a string with a metal blade called a *tangent* (Ripin et al. 1989). The tangent is held against the string, and thus acts as one end of the vibrating portion of the string. Setting a string into motion by abruptly displacing one end is not an efficient method of excitation; the volume attainable with the clavichord is thus very small, making it unsuitable as a concert instrument. It is perhaps best used for an audience of one: the performer. While the maximum volume of a clavichord is small, the player has great control within the available dynamic range. For this reason, the clavichord was reportedly a favored instrument of J.S. Bach.

These features of the harpsichord and clavichord provided strong motivation for a keyboard instrument capable of enough volume to be part of an ensemble or orchestra, and which also gives the player the ability to vary the volume of individual notes over a wide range. In fact, Cristofori called his instrument a *Gravecembalo col piano e forte* [“large keyboard instrument with soft and large” (Pollens 1995)], indicating that it could produce both soft and loud tonal volumes. Cristofori's invention is often referred to as a *pianoforte* to distinguish it from the modern piano.

Cristofori's pianoforte accomplished his goals by striking the strings with a hammer. This solution is similar in some ways to the hammered dulcimer. In particular, in the late 1600s a very talented virtuoso named Pantaleon Hebenstreit took the playing of the hammered dulcimer to a level never before heard, and it is believed that his performances inspired some early piano makers, especially a German named Gottfried Silbermann. Because both the dulcimer and piano excite their strings by blows with a hammer, an understanding of both instruments requires that we consider the hammer–string interaction and the properties of hammers. We discuss this problem in Sect. 20.5; it is also discussed in Chaps. 20 and 21 in this volume (Peterson 2010; Rossing 2010).

The piano has evolved considerably since the first instruments of Cristofori; his instruments covered a range of just four octaves (49 notes) while the modern piano covers more than seven octaves (88 notes). However, Cristofori was an extremely

skilled and innovative instrument maker, and his other surviving instruments (mainly harpsichords) are recognized for their craftsmanship. It is thus not surprising that his pianofortes incorporated several very creative innovations, many of which survive (although in somewhat altered form) to this day.

20.3 Overall Design

The overall structure of a grand piano is shown in Figs. 20.1 and 20.2. Figure 20.1 shows the general layout of the keys, rim and case, soundboard, strings and bridges, while a simplified version of the hammer–string system is shown in Fig. 20.2.

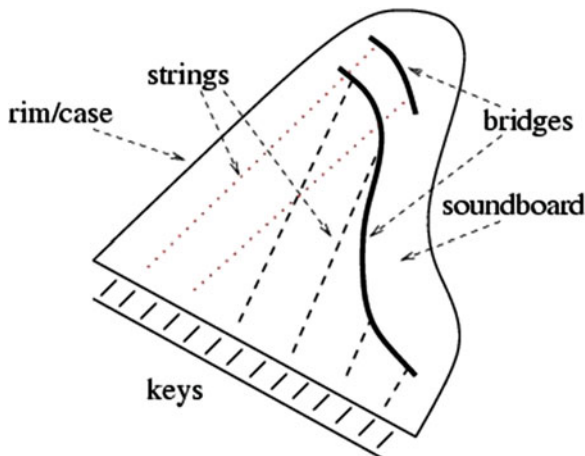


Fig. 20.1 General design of a grand piano.

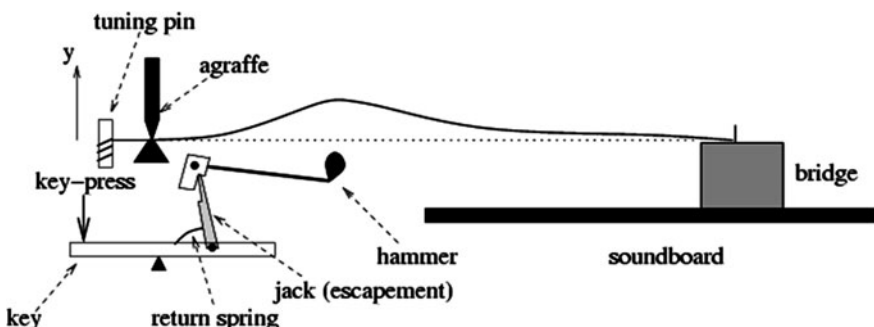


Fig. 20.2 Simplified sketch of the piano action, hammer, and string. The player exerts a force (the *key-press*) on the key, setting the hammer in motion. The jack slips free of the hammer just before the hammer collides with the string. This drawing is not to scale. The hammer–string strike point is usually much closer to the end of the string. Modern piano actions are much more complicated than the simple design shown here.

When the key is depressed, a lever system called the *action* is set into motion. The action ultimately exerts a force on the hammer, sending it on its way toward the string. There are a great many designs of the action; indeed, the action has probably evolved over time more than any other single element of the piano. Moreover, the feel that the action provides to the player is extremely important for the player's affection for an instrument.

While there is much interesting physics and mechanical engineering involved in action design, we can understand the piano tone itself without worrying about the details of the modern action. The crucial point is that the action releases the hammer *before* it contacts the string, so that the hammer is moving freely just before and after colliding with the string. This is usually accomplished using a lever called the *jack* or *escapement* (Fig. 20.2). This lever pushes on the hammer, but loses contact before the hammer reaches the string. The escapement lever also falls away so that the rebounding hammer can be caught by a separate element called a back-check (not shown in Fig. 20.2).

The hammer velocity just prior to its collision with the string is controlled by the speed with which the player depresses the key, with typical hammer velocities in the range of 1–4 m/s. It is this ability to control the hammer velocity that gives the player control over the volume of the resulting piano tone.

Each string is connected to a tuning pin, on the far left in Fig. 20.2, where the tension can be adjusted so as to tune the vibration frequency of the string. The string is held against a rigid surface at the end near the player; in many modern pianos it is held by what is called an *agraffe*, but some pianos used different designs. The other end of the string passes over the bridge. The bridge is a piece of wood (typically maple) that is glued to the soundboard (spruce). The collision with the hammer sets the string into motion, with the displacement in the *y* direction (Fig. 20.2). While the string also exhibits vibrations in the other two directions, the vibration along *y* provides by far the greatest motion of the bridge. This force is perpendicular to the soundboard and sets the soundboard into motion, much like a large speaker. This speaker action sets the surrounding air into motion, producing the pressure waves (sound) that we hear.

Figures 20.1 and 20.2 show all of the major components of the piano: the strings, action, hammer, soundboard, and bridge. In the following sections we discuss each of these components and their role in making the characteristic piano tone.

20.4 Vibrating Strings

Figure 20.2 shows the arrangement of a single string. Most notes on a piano, starting from about an octave below middle C and continuing up the highest note, are produced by the vibrations of three strings. The hammer strikes all three strings simultaneously, and the force from all three sets the bridge and soundboard into motion. Moving down the keyboard, the notes in the next two octaves or so each involve two strings, and the lowest bass notes are produced by a single string.

The different strings of a given note are all connected to the bridge, and they interact through the common bridge motion. This interaction leads to some interesting effects, and helps explain the long decay time of a tone (Weinreich 1977). However, we can get a good understanding of a piano tone by considering the motion of just a single string.

The vibrating string has an important place in the science and practice of musical instruments. Pythagoras reportedly used a single string suspended between two rigid supports, called a *monochord*, to elucidate the connection between wavelength and musical pitch, and by implication, frequency. Using this device he studied how the pitch of the sound produced by a vibrating string depends on its length. Pythagoras showed that if two identical strings have the same tension, they sound the “same” when their lengths differ by a factor of two; that is, when their lengths are in the ratio 2:1. In modern terms we would say that these strings produce notes that differ by exactly one octave.

An explanation of Pythagoras’ result is sketched in Fig. 20.3. The vibrational frequencies of a string are determined by the standing waves that can exist on the string. The top panel shows two possible standing wave envelopes of a vibrating string. The curve labeled *fundamental mode* is the standing wave with the longest wavelength and lowest frequency possible for the string. The ends of the strings are held fixed (at the agraffe and the bridge), so they cannot move. For the fundamental

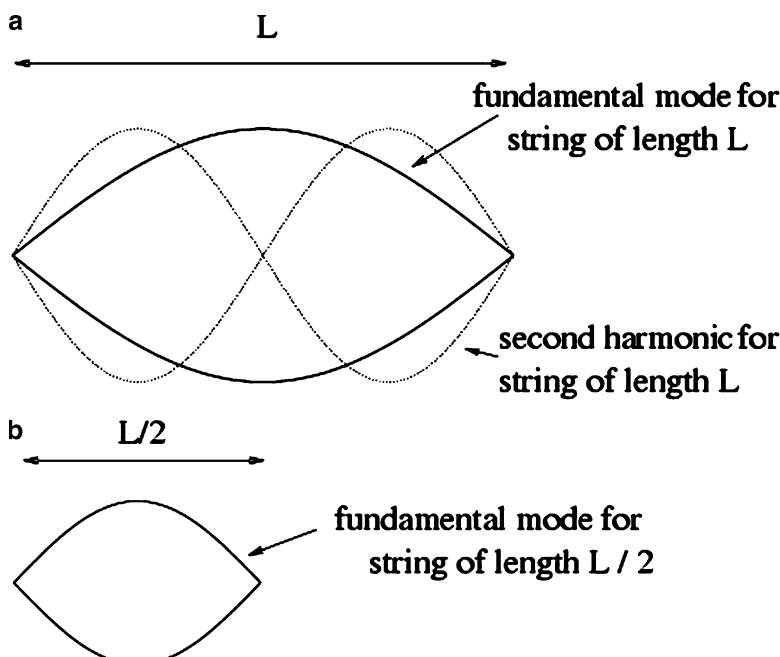


Fig. 20.3 (a) Two possible standing waves on a string, corresponding to the fundamental and the second harmonic. (b) Fundamental standing wave for a string half as long as at the top.

standing wave, the vibration amplitude is largest at the center, giving an envelope as shown. Also shown in the top panel is a standing wave called the *second harmonic*. Its wavelength (the distance between “equivalent” points along the envelope) is half as long as the wavelength of the fundamental. If the fundamental mode has a frequency f_1 , the frequency of the second harmonic is $f_2 = 2 \times f_1$. While Fig. 20.3a shows two possible standing waves on a string of length L , an infinite number of standing waves is possible, with the frequency of the n th harmonic given by $f_n = nf_1$.

Figure 20.3b shows the behavior for a string half as long as in the top panel. If these two strings have the same tension, diameter, and density, the fundamental standing wave of the shorter string has a wavelength and frequency equal to those of the second harmonic of the longer string. Hence, the fundamental frequency and pitch of the shorter string are double those of the longer string – and the two strings produce tones that differ by an octave.

A key result from Fig. 20.3 is that the allowed standing wave vibrations of an ideal string form what is called a *harmonic series*, meaning that the frequency of the n th harmonic is $n \times f_1$, where f_1 is the fundamental frequency. Figure 20.3a shows two standing waves separately on the same string, but when a string is struck by a hammer the string vibration will be a combination of many different standing wave patterns. Hence, when a particular note is played, the string vibration is a combination of many different standing waves, and all of these standing wave frequencies are present in the tone. The pitch of a tone corresponds to the frequency of the fundamental, but the higher harmonics play an important role and give rise to the *color* or *timbre* of a tone. After all, the note middle C (fundamental frequency approximately 262 Hz) can be played on a piano or a violin, but it is easy to distinguish them because the relative strengths of their harmonics are different.

The harmonic frequencies for a ideal string follow the pattern $n \times f_1$, but real strings do not quite follow this simple pattern. Figure 20.4 shows results for the note one octave above middle C (denoted C5) for the author’s grand piano (a Steinway model M). Here we have plotted f_n/n as a function of n . For an ideal string this ratio would be a constant, equal to the fundamental frequency. However, for a real string the harmonic frequencies are shifted to progressively higher frequencies with increasing n . These harmonics are thus not really *harmonic*, and for this reason are usually called *partials*. The effect does not seem large; here it is about a 1% shift for the fifth partial, corresponding to a frequency shift of about 30 Hz. Even so, it is quite noticeable for a listener.

To understand why the partials for a real string deviate from a perfect harmonic series, we must first understand why a string vibrates in the first place. By definition, an ideal string is perfectly flexible, meaning that it does not “spring back” when bent. An ideal string will only vibrate if it under tension, as in a musical instrument. When such a string is plucked or otherwise displaced, it experiences a restoring force due this tension, which tends to pull the string back to its undisplaced profile (i.e., a straight string stretched between two supports). Mathematically, a restoring force due solely to the tension leads to what is known in physics as the *standard wave equation*, which leads in turn to the perfect harmonic series. The same basic

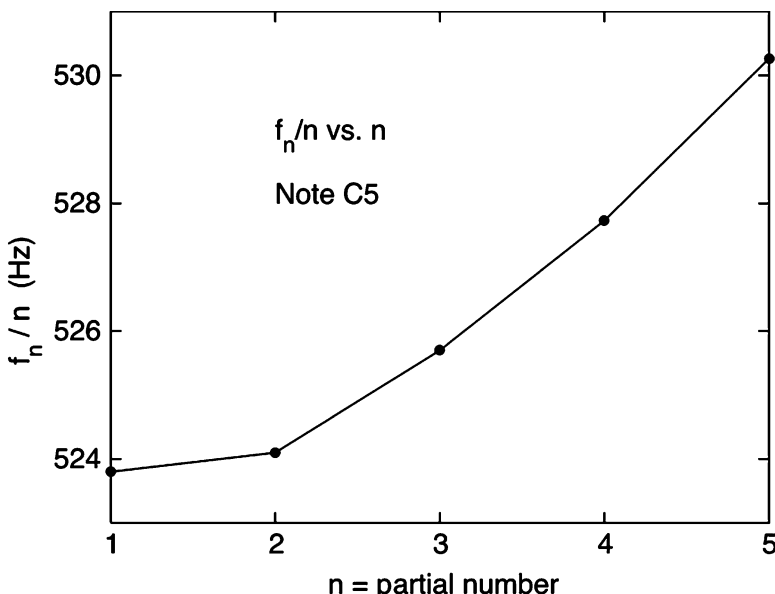


Fig. 20.4 Frequencies of the lowest few partials f_n for the note C5 (one octave above middle C). Here we have normalized f_n by partial number n . For an ideal string f_n is independent of n , so f_n/n is constant. For a real string, f_n/n increases with increasing n as shown here.

wave equation and a similar harmonic series of frequencies are found for many other types of waves, including sound waves and electromagnetic waves.

A real piano string experiences a restoring force due to the tension, so it approximates an ideal string. However, a real string also exhibits a second contribution to its restoring force, due to the elastic properties of the string material. In words, a real string will “spring back” when it is bent, even if the tension is zero. This elastic restoring force is due to material a property called the *Young's modulus*. For a piano string, this elastic stiffness force is much smaller than the tension force, but it does give a slight increase in the vibration frequency. More importantly, the stiffness force depends on how sharply the string is bent. Figure 20.3a shows the standing wave pattern for the fundamental and the second harmonic, and we see that the second harmonic is “bent” more sharply than the fundamental. For this reason, the effect of the stiffness is greater for the second harmonic; in fact, its effect increases with partial number, leading to the behavior in Fig. 20.4.

We now have a qualitative understanding of the partial frequencies for a real string. But do the deviations from a perfect harmonic series really matter? The answer is yes – they lead to an effect called *octave stretching*. When you simultaneously play two notes separated by an octave, the second partial of the lower note has a frequency that is very close to the fundamental of the higher note. To your ear, these notes “sound best” if those two frequencies are equal. However, due to the stiffness the frequency of the second harmonic of the lower note is slightly greater than twice its fundamental, so the fundamental of the higher note must be tuned to

be slightly higher the perfect octave ratio – we say that the octave has been *stretched*. This effect is well known to piano tuners, and helps to give the piano its distinctive tone color. Octave stretching is largest for shorter strings, because (all else being the same) shorter strings are bent more severely than longer ones. This is one reason why small pianos, with shorter strings, are judged inferior to large pianos. It seems that listeners find a small amount of octave stretching to be pleasing, but that the tone suffers if the deviations from perfect octaves are too large.

20.5 The Hammers

Piano hammers have evolved considerably since the time of Cristofori. The earliest hammers were covered with parchment or leather, but by the mid- to late 1800s felt was adopted as the material of choice. Figure 20.5 shows two modern hammers – they are essentially mallets with felt wrapped around a wooden core. The felt is wrapped in several layers with the outer layers being softest. The hammers vary from the bass to the treble, with gradations in both total mass and thickness of felt.

When a hammer collides with the string (Fig. 20.2) the felt layer compresses, much like a tennis ball compresses when it hits the strings of a tennis racket. Continuing with this analogy, the speed of the rebounding tennis ball then depends on the compression characteristics of the ball. In the same way, the compression characteristics of a piano hammer determine how a piano string is displaced by the hammer–string collision. For many materials, the compression characteristics are linear; this means that doubling the compression doubles the resulting force, so that a graph of force versus compression is a straight line. However, piano hammers exhibit distinctly nonlinear compression behavior. An example is given in Fig. 20.6, which shows results for the hammer force F_h as a function of compression for a typical piano hammer. In words, the force increases faster than the compression, giving a hammer that becomes harder as it is compressed.

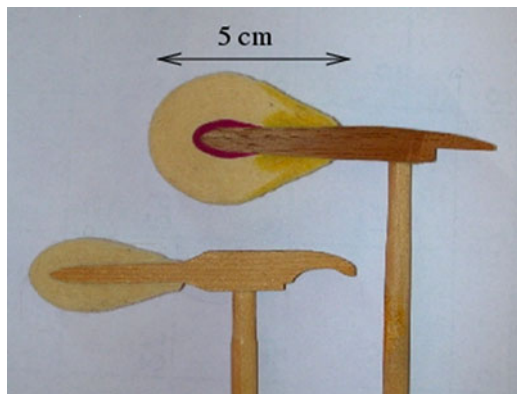


Fig. 20.5 Several modern piano hammers. The hammer at the *top* is for notes near middle C, while the *bottom* hammer is for notes in the treble.

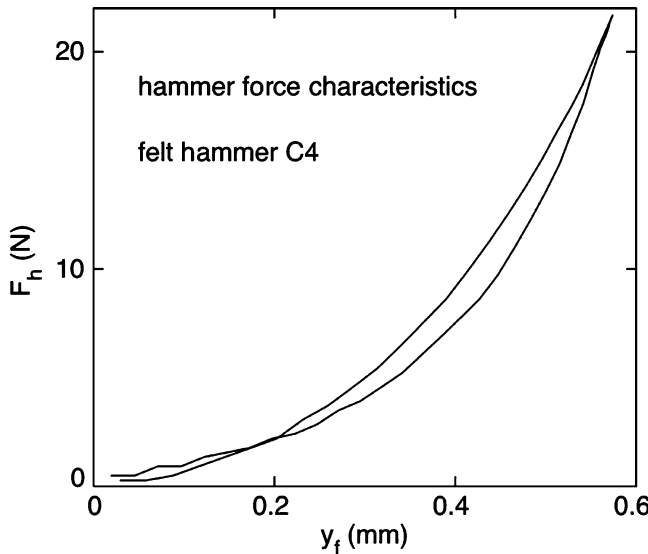


Fig. 20.6 Hammer force as a function of y_f , the amount the felt surface is compressed, for a hammer designed for the note middle C (after Giordano and Winans 2000; Giordano and Jiang 2004).

When a hammer strikes a piano string, the string is set into vibration at many different frequencies; these are just the partial frequencies described in Sect. 20.3. To understand the timbre of a tone, we need to know how the relative amplitudes of these different frequency components depend on the hammer characteristics. This can be understood qualitatively by considering the extremes of a very soft and a very hard hammer. A very soft hammer will compress a lot when it hits the string, staying in contact for a relatively long time. The string is thus released “gently,” giving most of its energy to the “slowest” components, and favoring the partials with the lowest frequencies. On the other hand, a very hard hammer is in contact with the string for a very short time, preferentially exciting the higher frequency partials. An analogy is the sound produced by a ball bouncing from a hard floor. A hard steel ball produces much more sound at higher frequencies than a soft rubber ball.

Because of its nonlinearity, a real piano hammer behaves as a relatively soft hammer when the hammer–string collision is gentle, and as a relatively hard hammer when the collision is violent. Here a gentle collision corresponds to a low hammer velocity just prior to the collision (typically 1 m/s) while a violent collision corresponds to a high velocity (typically 4 m/s). The change in the resulting tone color can be seen by analyzing the piano tones produced by low and high hammer velocities.

Figure 20.7 shows a spectral analysis of several piano tones. These were all obtained for the same note (middle C); the only difference was the volume level of the tone. Here we recorded the tone and then performed a Fourier analysis, which gives the amount of power in all of the different frequency components present in

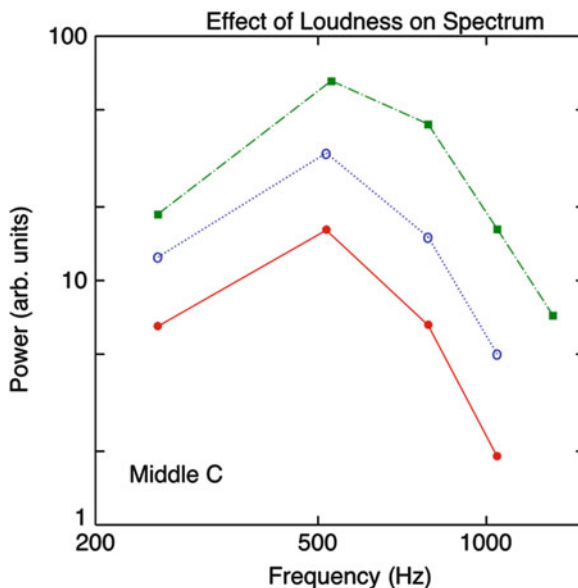


Fig. 20.7 Spectrum of three piano tones. The *bottom curve* (filled circles) was obtained for a pianissimo tone, the *middle curve* (open circles) for a mezzoforte tone, and the *upper curve* (filled squares) for a *fff* tone. The symbols show the relative power in each partial. The lines are just guides to the eye. Data obtained for the note middle C with the author's grand piano.

the tone. These components are just the partials discussed in Sect. 20.3, so for each curve there are points only at the partial frequencies of approximately 262 Hz (the fundamental), 524 Hz (the second partial), etc.

The results in Fig. 20.7 have several remarkable features. In all three tones, the second partial is strongest. For the pianissimo tone the fundamental is next in strength followed closely by the third partial. In contrast, for the *fff* tone the third partial is much stronger than the fundamental, and is nearly as large as the second partial. Thus, as we go from soft to loud tones, the power is redistributed from the lower frequencies to the higher ones. This is precisely what we expect from the effects of hammer nonlinearity, as we have argued above.

So, we have shown that piano hammers are nonlinear and have managed to measure the effect of this nonlinearity by careful analysis of piano tones. But is it really important for the way we perceive the music? The answer is a definite yes. Recall that the piano was invented and accepted because it gives a way to vary the volume of a tone, from note to note. This ability to vary the volume from note to note is crucial to the expressiveness of the instrument. According to Fig. 20.7, a soft note is weighted (relatively) toward low frequencies (a “softer” tone), while a loud note is weighted toward high frequencies (a “brighter” tone). This change in the tone color is also essential to the expressiveness. When listening to recorded music, it is usually very easy to tell if a note is played loudly or softly, even if the

overall volume level of a recording is turned down. This is because of the change in tone color, which is apparent irrespective of the volume.

The change in tone color in going from pianissimo to *fff* is a key property of all piano tones. In fact, a similar change in tone color occurs for many other instruments, including violins, woodwinds, and brass instruments. Indeed, it is hard to find instruments that do not exhibit such a change in tone color!

20.6 The Soundboard as a Speaker

In Fig. 20.7, we saw that the amount of power at the fundamental frequency is smaller than the power in other higher partials, and we explained how hammer nonlinearity can give this behavior. However, another effect also contributes. The soundboard acts like a large speaker – as it vibrates it generates pressure waves (sound) in the surrounding air. As a next step in understanding piano tones, we must consider the properties of this speaker. The speed of sound in air at room temperature is about $v_{\text{sound}} = 343 \text{ m/s}$. This number is important because the frequency f and wavelength λ of a sound wave are related by $f\lambda = v_{\text{sound}}$.

It turns out that the sound production efficiency of a soundboard is small for sounds with wavelengths much larger than the size of a soundboard. Roughly speaking, this is because sound waves generated by the two sides of the soundboard tend to cancel (interfere) when the distance from one side of the board to the other is smaller than λ . The fundamental frequency of middle C is about $f = 262 \text{ Hz}$, so its wavelength is about 1.3 m. This is roughly the width and length of the soundboard of a small grand piano, so this soundboard has a fairly good efficiency for middle C and above. However, for lower notes the wavelength becomes progressively longer – for the note C2, which is two octaves below middle C, the wavelength is more than 5 m, which is larger than any grand piano.

We have seen that a real piano tone is a combination of frequencies: the fundamental plus the partials whose frequencies form an approximate harmonic sequence $f_n \approx nf_1$. For C2 these frequencies are (approximately) 65, 131, 262, 524 Hz, ... For the lowest of these frequencies the wavelength is larger than the soundboard, so their amplitudes are suppressed relative to the amplitudes of the higher partials. An example of this is given in Fig. 20.8, which shows the power in the different partials for C2. The dashed curve shows the general, *averaged* behavior – except for the second partial (which we will discuss more below), the strongest partial is $n = 5$, and the fundamental is weaker by about a factor of nearly 100. This difference is much greater than found for C4 in Fig. 20.7; the suppression of the fundamental for C2 is due almost entirely to the inefficiency of the soundboard at these low frequencies.

Let us now consider the behavior of the second partial for C2 in Fig. 20.8, and why it is so much stronger than expected from the average behavior (dashed curve). To address this problem, it is simplest to first consider the vibrations of a thin membrane, such as a drumhead. A membrane has distinct modes of vibrations, each

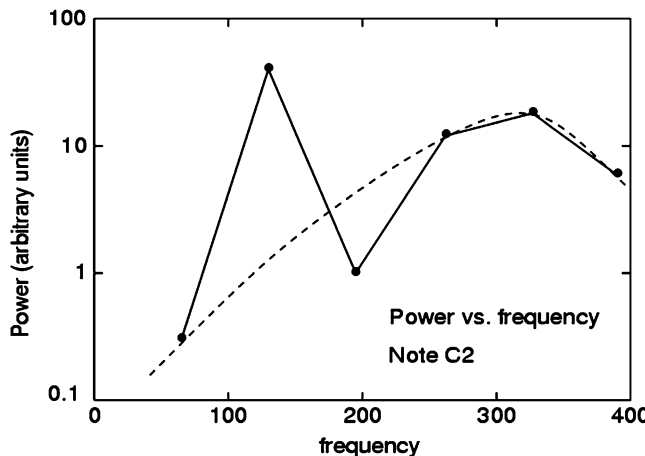


Fig. 20.8 Power at different partials for the note C2 for the author’s grand piano. This was a *mf* tone.

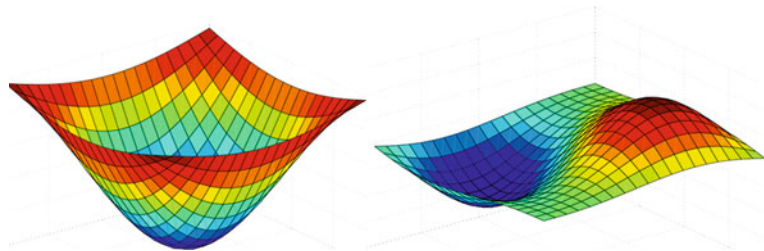


Fig. 20.9 Modes of vibration of a square membrane. (*Left*) Lowest frequency (fundamental) mode. (*Right*) Mode with the second lowest frequency (after Giordano and Nakanishi 2006; Fletcher and Rossing 1991).

with their own frequency and vibration pattern, just as we found for a string (Fig. 20.3). Unlike a string, the modes of a membrane do not form a simple harmonic series, but we can still define the fundamental mode as the one with the lowest frequency. The vibration pattern for the fundamental mode for a square membrane is shown on the left in Fig. 20.9. This is similar to the standing wave pattern for the fundamental string mode (Fig. 20.3) – the center of the membrane has a large vibration amplitude, while the edges are held fixed and do not move. The right panel in Fig. 20.9 shows the membrane vibrational mode with the next highest frequency – there are now two locations with a large vibration amplitude. The point at the center of the membrane, which is midway between these two locations, does not vibrate.

The lowest two vibrational modes of a piano soundboard are shown schematically in Fig. 20.10. [Quantitative results are given by Conklin (1996b).] The fundamental mode is shown on the left. As with the membrane in Fig. 20.9, the

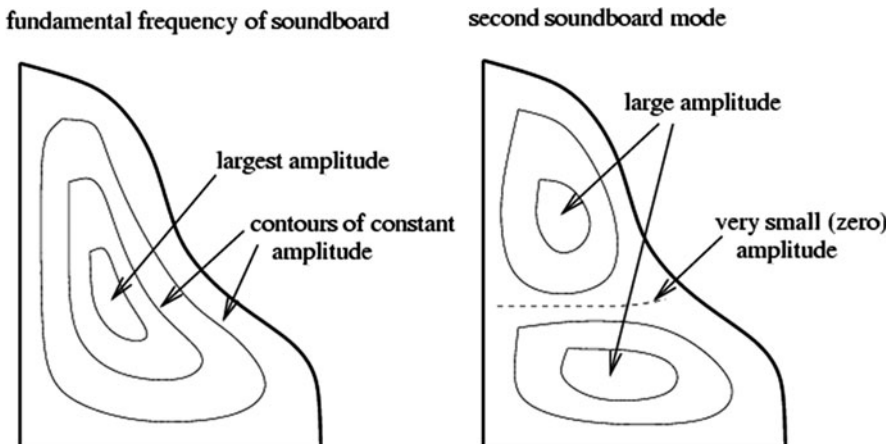


Fig. 20.10 Two lowest vibrational modes of a piano soundboard. These are only schematic diagrams; see Conklin (1996b) for quantitative results.

approximate center of the soundboard has the largest vibration amplitude. For a typical grand piano this mode has a frequency near 100 Hz. The mode with the next highest frequency (typically around 150–200 Hz) is shown on the right in Fig. 20.10. This mode has a large amplitude at two locations, again as found with the membrane (Fig. 20.9). The dashed line separates these two regions; for this mode, this line on the soundboard is approximately stationary.

In addition to the modes in Fig. 20.10, a soundboard has many other modes of vibration. These modes have higher frequencies and also possess regions of large and small amplitude, with the higher modes having more such regions. We have already seen that when struck by a hammer, a piano string vibrates at many different frequencies (at its different partials). The force from the string on the soundboard then sets the soundboard into motion at each of these string frequencies. The result is that the soundboard vibrates in many of its different modes.

The frequencies of these soundboard modes and their vibration patterns affect the composition of a piano tone in two ways. First, the fundamental mode has the lowest frequency of all the modes, and is near 100 Hz. When a soundboard vibrates, the amplitude of this mode is largest when the string frequency matches this value. The board will still vibrate at lower frequencies, but its amplitude will be lower for the same applied force. This effect is important for the note C2 and other notes in the bass. The fundamental frequency for C2 is at 65 Hz, well below the fundamental frequency of the soundboard, while the second partial for C2 is much closer to the fundamental soundboard frequency. As a result, the amplitude of vibration for the soundboard at 65 Hz is suppressed, reducing the strength of this frequency component in the resulting sound. This contributes to the small amplitude of the 65 Hz component in Fig. 20.8, and is why the amplitude of the 131 Hz component is larger than the average behavior (dashed curve).

The mode patterns in Fig. 20.10 lead to another, related effect. Each string is connected to the soundboard at a particular point. If the string is connected at a point where a particular soundboard mode has a very small or zero amplitude, the string will not efficiently excite this mode. On the other hand, if the string is connected in a region where the soundboard vibration amplitude is large for a particular mode, the string will readily excite the board at that frequency. Hence the spatial variation of the soundboard mode pattern also affects the relative strength of the components of a piano tone. This is illustrated in Fig. 20.11, which shows how a piano soundboard responds to forces of different frequencies.

Here we applied forces of different frequencies at the point where the string for middle C (C4) is connected to the soundboard. This plot shows a quantity called the mechanical impedance, Z , which is the ratio of the applied force divided by the resulting soundboard velocity at the driving point. A large board velocity corresponds to a small value of Z , so each dip in Z corresponds to a soundboard mode. The dip near 100 Hz corresponds to the fundamental frequency of this soundboard – there are no modes at lower frequencies.

An interesting feature of Fig. 20.11 is that values of Z vary over a wide range. One of the goals for a piano designer is to achieve a “smooth” response, since one does not want the soundboard to excessively suppress or enhance any particular frequencies for a given note. The large variations in Z in Fig. 20.11 work against this goal. The piano designer must avoid places where Z is extremely large or extremely small, by carefully locating the places where the different strings connect to the soundboard, and by adjusting the shape and other properties of the soundboard.

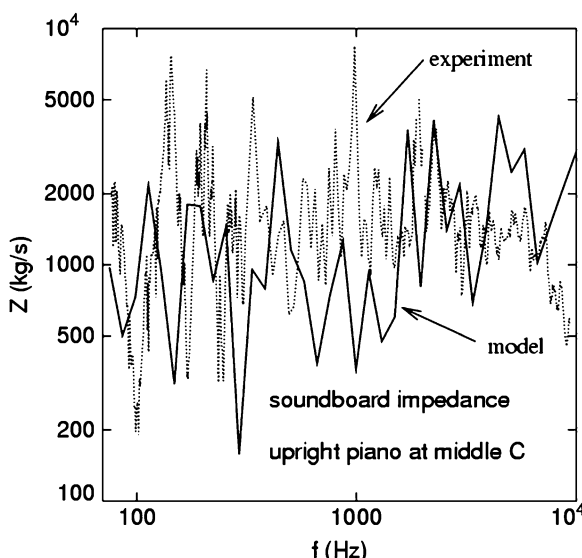


Fig. 20.11 Mechanical response of a grand piano soundboard to forces applied at the bridge point for middle C. Z is the amplitude of the applied force divided by the amplitude of the resulting soundboard velocity. The *dotted curve* shows the experimental measurement, while the *solid curve* is a model discussed in Sect. 20.8 (after Giordano 1998; Giordano and Jiang 2004).

20.7 How We Perceive Piano Tones

The “quality” of a piano tone is affected by many things – the properties of the hammers, and the way the strings and soundboard vibrate are all important. The way that we as listeners perceive tones is also very important. For example, we have seen (Fig. 20.8) that the amplitudes of different partials may vary widely from one partial to the next, but this variation is still tolerated by a listener. For note C2 in Fig. 20.8, the power in the fundamental is smaller than in the second partial by a factor of about 100. This effect becomes even greater for lower notes; at the extreme bass end (the note A0, with a fundamental frequency of 27 Hz), the power in the fundamental is essentially zero, as shown schematically in Fig. 20.12. Moreover, the human ear is very insensitive at such a low frequency, so a listener would not know if the fundamental is present or not! Why does a listener still identify the pitch of this note as corresponding to 27 Hz, and not the frequency of one of the stronger partials?

The answer to this puzzle was first given by Hermann von Helmholtz in the mid-1800s (Helmholtz 1954). He pointed out that because the frequencies of the various partials follow an approximate harmonic series ($f_n \approx nf_1$), the separation of two adjacent partials is approximately equal to f_1 , the fundamental frequency. Helmholtz suggested that such tones the perceived pitch is determined not by the frequency of the lowest nonzero component, but by the spacing of the components. Hence, if the fundamental and other low-frequency components are weak or missing, we can still identify the pitch of the tone through the spacing of the higher partials. Much research has been conducted on how we perceive pitch, and it is now known that many other factors (in addition to the spacing of partials) affect pitch perception. Even so, Helmholtz’s model is still central to our current understanding of pitch perception.

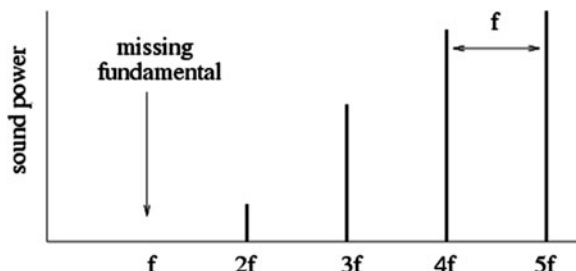


Fig. 20.12 Schematic of how the power in different partials of a piano tone varies with frequency, for a note in the extreme bass. The power in the fundamental and the first few partials is much smaller than the power in the higher partials.

20.8 Modeling of the Piano

Many researchers are currently engaged in computer modeling of various musical instruments. This work has many different goals. Much modeling work is designed for use in electronic instruments, such as electric pianos. Another goal is to use modeling to better understand how different parts of an instrument contribute to the overall tone. For example, in this chapter we have discussed how the hammers, strings, and soundboard all contribute to the composition of a piano tone, that is, the relative strengths of the different partials as in Figs. 20.7 and 20.8. Our discussion to this point has been qualitative – to go further we must estimate the various effect quantitatively, and that requires computer modeling. As examples of such modeling work we will describe two recent projects by the author; however, many other workers are active in this field and we refer the interested reader to several recent publications for descriptions and references to this work (Bader 2005; Bensa et al. 2005; Deveaux et al. 2003; Penttinen et al. 2006).

We saw in Sect. 20.6 that the modes of a soundboard play a very important role. We can use modeling to understand the mode frequencies and their spatial patterns, and to predict how these can be changed by varying the design of the soundboard. One way to model soundboard motion is to treat the board as many small pieces and use Newton's laws of motion to compute the motion of each piece. Each of these pieces experiences a force from adjacent pieces, which can be calculated from the elastic properties of the soundboard wood. Currently work models the soundboard as about 10^4 individual pieces, with the known elastic properties of the wood and the arrangement of soundboard ribs and bridges all included. We have used this approach to calculate the mechanical impedance of the soundboard studied in Fig. 20.11, and the solid curve in that figure shows the results (Giordano 1997; Giordano and Jiang 2004). The model does not give a precise match to the experimental results, but this is not expected because the model used only the average elastic constants for soundboard spruce, whereas there can be significant variations from tree to tree and board to board. Even so, the model reproduces the general behavior of the real soundboard, including the average level of Z .

If the model is not expected to perfectly reproduce the behavior of any real soundboard, what good is it? We suggest that the model would be very useful in exploring new soundboard designs. For example, the model could be used to compute the mechanical response of soundboards made from carbon composites or other new materials. We expect that the model will give accurate results for the changes in soundboard behavior that result from using new materials. This information can be very useful for soundboard designers.

In another application of modeling, we have computed the sound production efficiency of a soundboard. We have already mentioned that a soundboard radiates sound very weakly when the wavelength is larger than the size of the soundboard. To be more quantitative requires a careful calculation that includes the vibrational modes of the soundboard along with the motion of the surrounding air. Such a calculation must combine the soundboard calculation in Fig. 20.11 along with

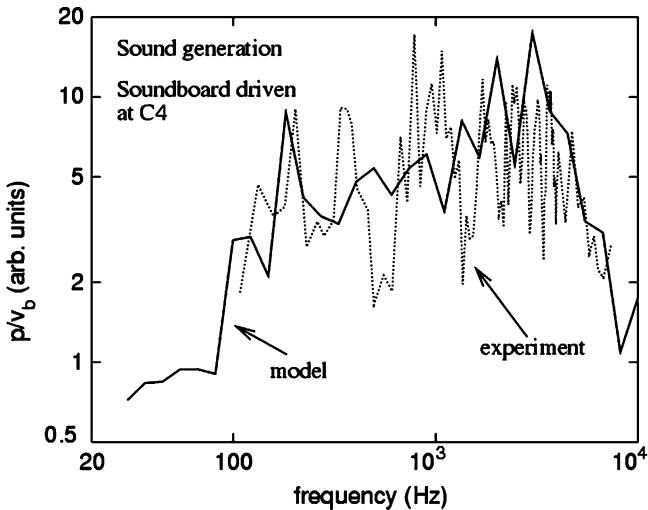


Fig. 20.13 Sound pressure p generated by a vibrating soundboard. The vertical axis shows p/v_b where v_b is the soundboard velocity at the driving point. The driving point was the point where the strings for middle C contact the bridge. The *dotted curve* shows results for a soundboard from an upright piano (after Giordano and Jiang 2004).

the pressure waves in the surrounding air (Giordano and Jiang 2004). The strategy is to again treat this combined system as a collection of vibrating pieces, making up the board and the room air.

To achieve a useful frequency range requires a large number of air “pieces,” 10^7 or more for a typical-size room, but this is feasible with current desktop computers. Some results are given in Fig. 20.13, which shows the sound amplitude (as measured by the pressure) as a function of the frequency of the force applied to the board. The dotted curve shows experimental results while the solid curve is the model. The model gives the expected fall-off at low frequencies. In future work we plan to compare in detail with results like those in Fig. 20.8.

20.9 Lessons

This chapter has reviewed the basic elements of a piano and how they give rise to the characteristic piano tone. The nonlinearity of the hammers, the effect of string stiffness, and the details of how a soundboard produces sound all make important contributions that can be understood from simple physical arguments.

Acknowledgments The author is deeply grateful to many students who have collaborated in work on the physics of the piano and other musical instruments, including A. Korty, J. Winans, J. Jourdan, S. Dietz, J. Roberts, L. Reuff, J. Millis, M. Jiang, K. Lie, J. Skodrack, and C. McKinney. I also thank A. Askenfelt, A. Chaigne, T. Rossing, A. Tubis, and G. Weinreich for patient and very instructive discussions. This work has been supported by NSF.

References

- Bader R (2005) *Computational Mechanics of the Classical Guitar*. Springer, New York.
- Bensa J, Bilbao S, Kronland-Martinet R, Smith JO, and Voinier T (2005) Computational modeling of stiff piano strings using digital waveguides and finite differences. *Acustica/Acta Acustica* **91**, 289.
- Conklin HA, Jr. (1996a) Design and tone in the mechanoacoustic piano. Part I. Piano hammers and tonal effects. *J Acoust Soc Am* **99**, 3286.
- Conklin HA, Jr. (1996b) Design and tone in the mechanoacoustic piano. Part II. Piano structure. *J Acoust Soc Am* **100**, 695.
- Conklin HA, Jr. (1996c) Design and tone in the mechanoacoustic piano. Part III. Piano and scale design. *J Acoust Soc Am* **100**, 1286.
- Deveaux G, Chaigne A, Joly P, and Becache E (2003) Time-domain simulation of a guitar: model and method. *J Acoust Soc Am* **114**, 3368.
- Fletcher N and Rossing T (1991) *Physics of Musical Instruments*. Springer-Verlag, New York.
- Giordano N (1997) Simple model of a piano soundboard. *J Acoust Soc Am* **102**, 1059.
- Giordano N (1998) Sound production by a piano soundboard: experiment. *J Acoust Soc Am* **103**, 1648.
- Giordano NJ (2010) *Physics of the Piano*. Oxford University Press, Oxford.
- Giordano N and Jiang M (2004) Physical modeling of the piano. *Eur J Appl Signal Proc* **2004-7**, 926.
- Giordano N and Nakanishi H (2006) *Computational Physics*, 2nd ed. Prentice-Hall, Englewood Cliffs, NJ.
- Giordano N and Winans JP, III (2000) *J Acoust Soc Am* **107**, 2248.
- Good EM (2001) *Giraffes, Black Dragons, and Other Pianos*, 2nd ed. Stanford University Press, Stanford, CA.
- Helmholtz HLF (1954) *On the Sensations of Tone*. Dover, New York.
- Pentinen H, Pakarinen J, Valimaki V, Laurson M, Li H, and Leman M (2006) Model-based sound synthesis of the guqin. *J Acoust Soc Am* **120**, 4052.
- Peterson D (2010) *The Science of String Instruments*. Springer, New York.
- Pollens S (1995) *The Early Pianoforte*. Cambridge University Press, Cambridge.
- Ripin EM, Schott H, Barnes J, O'Brien GG, Dowd W, Wright D, Ferguson H, and Caldwell J, eds (1989) *Early Keyboard Instruments*. W.W. Norton, New York.
- Rossing T (2010) *The Science of String Instruments*. Springer, New York.
- Suzuki H and Nakamura I (1990) Acoustics of pianos. *Appl Acoust* **30**, 147.
- Weinreich G (1977) Coupled piano strings. *J Acoust Soc Am* **62**, 1474.

Chapter 21

Hammered Dulcimer

David Peterson

21.1 History

Paul Gifford's treatise, *The Hammered Dulcimer: A History*, traces the development of the hammered dulcimer from its eleventh-century forerunners (*psaltery*, *qanun*, *monochord*, and *string drum*) to current forms: *santur* (Turkey, Iran, Iraq, India); *Hackbrett* (Germany, Scandinavia); *cimbalom* (Central Europe); *salterio* (Mexico); *yang qin* (China and other east Asian countries); and *hammered dulcimer* (America, British Isles) (Gifford 2001).

By the fifteenth century, the European hammered dulcimer was physically similar to its modern version. Despite considerable variation in the number of strings per course, the range (number of courses), diatonic or chromatic tuning schemes, the number and styles of bridges, framing, decoration, hammers, cultural expression and even the trapezoidal shape – the basic concept of the instrument varied little over the centuries. Most commonly, there was one bass bridge on the right and a treble bridge on the left that divided the strings into a ratio of 2:3, thereby creating a musical fifth. Soft iron wire was available by 1350 (providing a soft mellow tone) and high-tensile-strength steel music wire became available by 1830 (providing a more metallic sound with prominent and more slowly decaying high overtones) (Birkett and Poletti 2007).

There are physical and cultural reasons for this historical stability. A metal wire sounds best if it is near breaking strength and as thin as possible, and this dictates a limited range of string lengths (middle C is generally about 60 cm long in pianos and dulcimers). Because of scaling, the length of the top strings determines plausible lengths for the lower strings and thus the shape and size of the instrument. Except for occasional and brief popularity in high society, the hammered dulcimer was primarily a folk instrument used for weddings, dances, and small-time entertainment, so there was little incentive to change a functional and traditional design.

D. Peterson (✉)

University of Central Arkansas, 56 Ridge Drive, Greenbrier, AR, USA

e-mail: drpdpr@windstream.net

In North America, immigrants brought various members of the hammered dulcimer family with them. In the nineteenth century, ethnic pockets of dulcimer players and makers were found in rural areas, mostly around the Great Lakes and in a few cities. Despite ready availability (e.g., obtainable from Sears and Roebuck catalogs before 1906) and promotion by Henry Ford in the early twentieth century, the number of players decreased and reached minimal maintenance levels by mid-twentieth century.

But the hammered dulcimer had its place in the 1970s folk revival in America, which encouraged a proliferation of dulcimer clubs, festivals, and small-scale builders. Strangely enough, these groups usually allied themselves with the more numerous mountain (lap) dulcimer players, even though the mountain dulcimer is an unrelated instrument, both physically and in terms of musical styles. Interest in dulcimers, either hammered or lap, has since leveled off, and consolidation among builders has occurred. There are currently two dulcimer factories, Dusty Strings (DS) and Master Works (MW). There are probably fewer than 50 full-time hammered dulcimer makers, and many more part-time builders, together producing perhaps 5,000–10,000 instruments per year.

There have been significant design changes in the last 30 years. Current enthusiasts build lighter instruments (15 vs. 50+ lb) with expanded ranges (three octaves or more) but with fewer strings per course. They get a stronger bass sound with less resonance (faster tone decay). The modern instrument is highly portable and designed for amplified folk performance.

For most of its history, the hammered dulcimer supplied rhythm and chord backup for other lead instruments such as the violin, but it is now commonly played solo or as an equal partner in an ensemble.

21.2 The Basic Instrument

A hammered dulcimer with 15 treble courses and 15 bass courses (known as a 15/15), measures about 21 in. along the top rail, 42 in. along the bottom rail, 15–18 in. from top to bottom, and 2 $\frac{3}{4}$ in. deep (Figs. 21.1 and 21.2). Although some builders still use the more traditional 3–4 strings per course, most modern instruments have two strings per course in order to reduce tension on the instrument and save weight. A common tuning scheme is shown in Fig. 21.3. The hammered dulcimer is cleverly designed such that the bass strings pass through the treble bridge, and vice versa. This allows easy hammering access to the strings. Both strings cross over small side bridges near the pin blocks and terminate in hitch pins or tuning pins. When played, lightweight wooden hammers create a unique percussive sound followed by a pleasant, slowly decaying after-sound, hence the name – hammered *dulcimer* (Greek for “sweet sound”).

Diatonic scales are particularly easy to play on a hammered dulcimer. Each scale starts at a scale marker on a bridge – the solid dots in Fig. 21.3. In order to play an A scale starting at A3 on the right side of the treble bridge (starting with the left hand) the player continues, alternating hands, on the right side with B3, C4#, and D4, and



Fig. 21.1 A basic hammered dulcimer with 15 treble courses and 15 bass courses with birch soundboard and walnut rails, made by author



Fig. 21.2 The treble bridge. Bass strings pass over the bass bridge and through the holes in the treble bridge, and vice versa. Diatonic scale markers on the bridge occur on every third course. The bridges are made of walnut and the soundboard is Baltic birch. Modern dulcimers use plastic bridge caps (Delrin). Cuts on the top of the holes help to decouple string courses

then crosses the left hand over the treble bridge to play E4, F4#, G4#, and A4 on the left side of the bridge. This pattern of hammering is the same for all diatonic scales – D3, G3, C4, and F4 on the bass bridge (crossing to the treble bridge) and A3, D4, G4, and C5 on the treble bridge. Many notes, like E4, can be played in more than one location. This redundancy facilitates rapid and efficient hammering. For instance, if the A3 scale is started with the right hand, then the natural continuation is to play B3, C4#, D4, and E4 on the right side of the bridge and then cross over the bridge with the left hammer to play F4#, G4#, and A4.

Hammered dulcimers are less stable than pianos in response to temperature, humidity, playing repetition, and even playing inactivity. Tuning is such an arduous chore that, within reason, players sometimes practice with out-of-tune instruments. Even an immediate tuning does not protect a public performer from strings slipping out of tune during a performance – so players carry their tuning wrenches with them at all times. Tuning stability is a major problem.

Treble Bridge	Bass Bridge
---D ₆ / G ₅ ---	--- D ₅ # ---
--- C ₆ / F ₅ ---	--- C ₅ ---
--- B ₅ / E ₅ ---	--- A ₄ # ---
--- A ₅ / D ₅ ---	--- A ₄ ---
--- G ₅ • C ₅ ---	--- G ₄ ---
--- F ₅ #/ B ₄ ---	--- F ₄ • ---
--- E ₅ / A ₄ ---	--- E ₄ ---
--- D ₅ • G ₄ ---	--- D ₄ ---
--- C ₅ # / F ₄ #---	--- C ₄ • ---
--- B ₄ / E ₄ ---	--- B ₃ ---
--- A ₄ • D ₄ ---	--- A ₃ ---
--- G ₄ # / C ₄ #---	--- G ₃ • ---
--- F ₄ # / B ₃ ---	--- F ₃ # ---
--- E ₄ • A ₃ ---	--- E ₃ ---
--- D ₄ # / G ₃ #---	--- D ₃ • ---

Fig. 21.3 Typical tuning for a 15/15 hammered dulcimer. The dots indicate the starting notes of the five easily playable major scales – A, C, D, F, and G. The hammering pattern for each major scale is the same: play four notes on one side of a bridge and continue with the next four on another bridge or side. Duplicate notes facilitate fast play. The instrument is chromatic from C4 to G5, but awkward locations make fluid playing of chromatic scales difficult

21.3 Inharmonicity and Scaling

For efficiency of sound production and good sound quality, a dulcimer string should have the highest string tension possible using the smallest string diameter. As can be seen in Fig. 21.4, at the high end, dulcimer string tension is at the breaking limit, and at the low end it is near the lower limit for good tone (less than 30% of breaking strength). Thus the tuning range of a dulcimer cannot be extended without using wound strings.

In an ideal string with no stiffness, modal frequencies f_n are integer multiples of the fundamental frequency f_1 , $f_n = nf_1$. But in real strings, stiffness, which increases with string diameter, leads to stretched partials, $f_n > nf_1$. If this inharmonic effect is small, the result can be an enriched sound, but extreme stretching results in the clanking sound of a rod. A lesser inharmonic effect generates beats and harshness between modes when several strings are played simultaneously. For the tuning range of a dulcimer, the stretched mode frequencies can be approximated by:

$$f_n = nf_1 \left(1 + 0.76(n^2 - 1) \frac{a^4}{L^2 T} \right),$$

where a (mm) is the string radius, L (m) is the string length, and T (N) is the string tension (Fletcher and Rossing 1991). From this formula it is clear that small string diameters and large string tensions reduce the inharmonic effect. The detrimental effect for hammered dulcimers is less than for pianos because of the smaller range

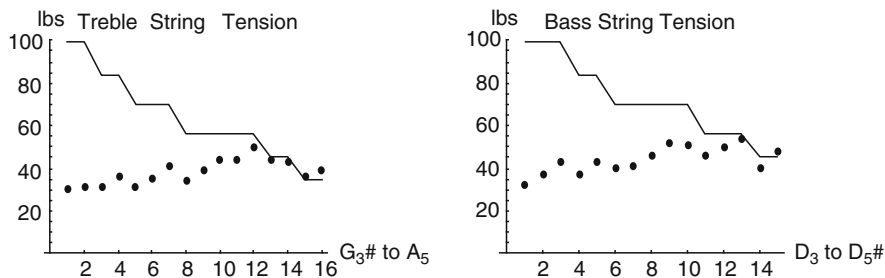


Fig. 21.4 Comparing string tension (dots) with the breaking strength (solid line) of strings for a 16/15 dulcimer (MW) with steel strings, assuming $220,000 \text{ lb in.}^{-2}$ tensile strength for music wire. String numbers are on the x-axis

in the dulcimer. For the “worst” string on a hammered dulcimer, G3#, the fourth harmonic is about 0.2% (5 cents) sharp.

The scaling problem in a dulcimer is that the lower strings are too loose. If string tension T were uniformly near the breaking strength throughout an instrument, then T/μ would be constant for all strings, because T and the linear string density μ are both multiples of the string radius squared. In this case, frequency and string length would be inversely proportional, $L = \frac{\sqrt{T/\mu}}{2f}$. But because frequency doubles with each octave increase, this proportionality forces the string length L to decrease by one-half for each octave increase. Therefore, instead of a dulcimer shaped like a trapezoid with straight sides, an ideal dulcimer would have sides in an exponential curve with base 2. Furthermore, to accommodate a two-octave range on a single bridge, the lowest string would need to be four times the length of the top string, giving unwieldy instrument lengths of 70+ in, at the base. For a real instrument with linear sides, T/μ cannot be constant; so for lower strings, T is reduced and μ is increased by using larger-diameter strings, wound strings, or other metals with higher densities. The challenge with using wound strings is to make the transition from steel strings to wound strings uniform in loudness and tone quality.

21.4 Lateral Stability

The string force on a hammered dulcimer is impressively large. We will consider the effect of string forces parallel to the side rails separately from the perpendicular force of the bridges on the frame. The strings are not parallel to the rails because they must pass over the treble and bass bridges, but because the string angles are small, the component of string tension parallel to the end rails is essentially that of the string (within 1%).

A steel string of length L , diameter d , and frequency f , has string tension given by $T = \pi\rho(Lfd)^2$, where $\rho = 7,700 \text{ kg m}^{-3}$ is the density of steel. For a typical 16/15 dulcimer with two strings per course, the total tension for the treble strings is about

1,230 lb, with tension reaching a peak of 50 lb at the twelfth string from the bottom, Fig. 21.4. For the bass strings the total tension is about 1,330 lb, with a peak tension of 54 lb at the 13th string from the bottom.

While a total string tension of 2,560 lb is large, wood has a high level of resistance to compressive forces. Any wood used for bracing in a hammered dulcimer has a compressive strength in excess of 4,000 psi parallel to the grain (7,580 psi for walnut). Therefore, end rails, with a cross section of $2\frac{1}{4}$ in. $\times \frac{3}{4}$ in. could theoretically support more than 13,500 lb of string tension. Looking at this in another way, if all the string tension T were uniformly applied to end rails with cross sectional area $A = 3.375$ in.² (ignoring other structural elements), the relative change in end rail length due to string tension T would be $\Delta L/L = (T/A)/E = 0.00045$, where E is Young's modulus parallel to the grain (1.68×10^6 psi for walnut). So along the longest rail, the change in length due to string tension is less than 1/64th of an inch. With modern glues and good joinery, a hammered dulcimer should easily withstand compressive forces with minimal distortion.

The real issues of string tension are the warping of the instrument (vertical deflection) due to the perpendicular forces of the bridges on the frame and tuning sensitivity due to changes in temperature and humidity.

21.5 Instrument Warp

All hammered dulcimers bow (deflect) in the middle to some extent even when new. Plastic creep in the joints and deflection continues indefinitely. Depending on construction design, maximum deflection can be several millimeters along the treble bridge, long rail, and even the pin block. Apart from a rare total collapse and unsightly pulled joints, the worst result of deflection is a warped sound board that resembles the shape of a potato chip. However, instruments can remain playable with a pleasant sound even with a warped sound board or a distorted frame.

The net effect of variable string tensions and lengths is the horizontal bridge force shown in Fig. 21.5. The lowest treble strings are loose enough to make their correct string position easily displaced or adjusted. On the other hand, total bridge loads, 124 lb for the treble and 200 lb for the bass, are large enough to make adjustment of bridge position difficult without releasing most string tension.

Although the back plate and sound board can add considerable structural strength, we will estimate the immediate bending deflection of the end rails and parallel interior braces as if they were subject to point loads at bridge locations (some designs distribute the loads differently, but the general conclusions are the same). Because the interior braces end at the pin block, they are best modeled as simply supported (hinged) beams; see Fig. 21.6.

The end rails and pin blocks have an extended glue joint with large surface area, so a clamped beam model might be correct, depending on construction. With a load at the center, simply supported beams deflect four times more than clamped beams.

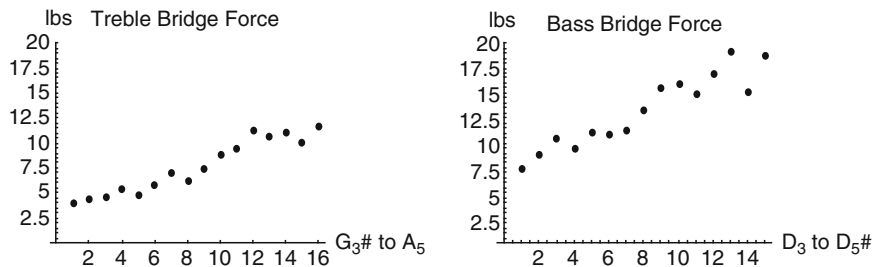


Fig. 21.5 The downward force exerted on the bridge by dulcimer strings (MW). String numbers are on the x -axis



Fig. 21.6 The interior braces of a hammered dulcimer terminate at the pin block and may be modeled as simply supported (hinged at the end) beams. The end rails will be glued to the top and bottom braces. Because they extend across the entire pin block, they can be modeled as clamped beams

In our case, with a hypothetical load of C at $0.4L$ (the location of the treble bridge) and D at $0.8L$ (the approximate location of a bass bridge), for reasonable bridge loads, the maximum deflection is very near the center. For a rectangular beam of length L , height h , and width w , the deflections are given by:

$$d_{ss} = \frac{L^3}{EI}(0.0197C + 0.012D) \text{ and } d_{clamped} = \frac{L^3}{EI}(0.0047C + 0.0018D),$$

where E is Young's modulus and the moment of inertia is $I = wh^3/12$.

We can draw several general conclusions from these formulas:

- Even though the load per string at the high end is double or triple the low end, because of the term L^3 , deflection of the long end rail will be five to six times as large as that of the short end rail.

- In terms of bending resistance, the type of wood used for end rails or bracing makes small difference because there is relatively small variation in E (less than 20%) among commonly used woods. For the end rails, visual appearance is more important than strength concerns. Weight is an issue though. For instance, white oak is 13% stronger than Sitka spruce, but is 80% heavier.
- Interior braces deflect relatively more than end rails because they are simply supported (factor of 4) and h is smaller (I is 40% smaller). Furthermore, depending on design, they support more strings per brace. As a result, most hammered dulcimers deflect significantly in the middle and rock when set on a flat surface.
- Instruments can be made lighter and stronger by manipulating the moment of inertia I – by an increase in h , decrease in w , holes or slots in the braces, or tapers in the braces.

21.6 Tuning Stability

21.6.1 Tuning Stability: Temperature

Temperature changes will cause significant mistuning in a hammered dulcimer no matter how long an instrument is allowed to adjust because the change in string tension is much quicker and larger than any dimension change in the body; see Fig. 21.7. Each string goes up in pitch when the temperature decreases. Even worse, the changes are larger for the lower strings, so the instrument will not be in tune with itself. A good measure of this effect is heat diffusivity, $D = k/c\rho$, where k = conductivity, c = specific heat, and ρ = density. The diffusivity value for steel is almost 20 times that of wood (maple), $D_s = 1.4 \times 10^{-5}$ and $D_w = 7.1 \times 10^{-7} \text{ m}^2 \text{ s}^{-1}$.

Suppose that a flat wooden plate of thickness h is initially $\theta^\circ\text{C}$ above ambient temperature. After a short time, it can be shown that a good approximation for the difference between the core and ambient temperature is given by $T_w(t) = 1.27\theta e^{-\lambda_w t}$, where $\lambda_w = \pi^2 D_w/h^2$. A similar expression holds for a steel string of radius a , $T_s(t) = 1.6\theta e^{-\lambda_s t}$, where $\lambda_s = 2.4^2 D_s/a^2$, noting that $a \ll h$ for all structural elements. The net result is a much larger value of λ for steel than

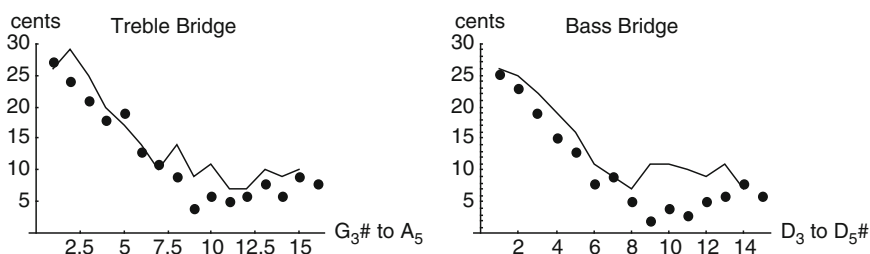


Fig. 21.7 The frequency increase caused by a decrease of 8°C in two instruments, dots (MW), solid line (Peterson, author)

wood. Thus that a sound board may take several minutes to change 8°C , whereas the strings are totally adjusted in a few seconds. In order to model the effects of temperature change, imagine a string of length L contracting due to a decrease in temperature. The string is then stretched back to its original length. The temperature change θ causes a relative change in length $\Delta L/L = \alpha\theta$, where $\alpha = 1.2 \times 10^{-5}/^{\circ}\text{C}$ is the coefficient of thermal expansion for steel. Stretching back to original length causes a change in tension ΔT , so that $\Delta L/L = -\Delta T/AE$, for string cross-sectional area A and steel modulus E . Therefore, $\Delta T = -\alpha AE\theta$. Taking differentials of the string relation $T = 4\mu L^2 f^2$, and setting $\Delta L = 0$ because there is no immediate instrument frame response to temperature change, and therefore no net string length change, we obtain:

$$\frac{\Delta f}{f} = \frac{\Delta T}{2T} = \frac{-\alpha AE\theta}{2T} = \frac{-\alpha E}{2\rho} \cdot \frac{\mu}{T} \cdot \theta, \quad (21.1)$$

where ρ is the volume density of steel and μ is the linear density of the string.

Equation (21.1) tells us, perhaps counter-intuitively, that a decrease in temperature causes an increase in frequency. In an ideally scaled instrument, μ/T would be constant and, from (21.1), the instrument would remain in tune with itself during temperature changes. However, from Fig. 21.4, one can deduce that this ratio can vary by a factor of more than 3, with the bass notes being furthest from unity. For the largest string, which is at lowest tension, from (21.1) we get an upper bound on frequency change on a typical hammered dulcimer, $\Delta f/f = 0.240\%$. The just noticeable difference for pure tone fundamental frequencies in the dulcimer range, 146–1,320 Hz, is about 2–5 Hz, so changes of less than 5°C could go unnoticed by a listener. But an instrument played in sunlight or under stage lights might quickly become miserably out of tune. Table 21.1 compares the predicted [by (21.1)] and actual frequency change for a hammered dulcimer (MW) subject to a temperature decrease of 11°C .

There is one other factor to consider. Even though the frame dimensions do not change appreciably in response to quick temperature changes, the instrument does respond to the resulting changes in string tension. Thus the predicted values in Table 21.1 are too high. This effect will vary, depending on construction, but it is least important for treble strings. Examples are given in Table 21.2. The data was obtained by loosening every fourth course on the instruments.

Table 21.1 Actual and predicted change, from (21.1), in frequency caused by a temperature decrease of 11°C assuming the coefficient of thermal expansion for music wire is $\alpha = 12 \times 10^{-6}/^{\circ}\text{C}$

Note	Bass bridge (Hz)			Treble bridge (Hz)		
	D3	D4	G4	A3	G4	D5
f	146.8	293.7	392.0	220.0	392.0	587.3
Δf , actual	3.0	2.6	3.6	3.8	5.2	5.1
Δf , predicted	3.8	3.7	4.1	5.9	5.5	5.6

The predicted values are too large because there has not been a correction for changes in the frame due to increased tension. The just noticeable difference for pure tones in this range is 2–3 Hz

Table 21.2 Frequency decrease caused by a 25% decrease in instrument tension for typical dulcimers having different bracing design and soundboard construction

Note	Bass bridge (cents)				Treble bridge (cents)			
	E3	B3	F4	C5	A3	E4	B4	F5
Δf (Co)	53	55	55	28	38	35	30	22
Δf (Pet)	46	45	25	15	62	55	44	33

As tension is released, the instrument expands. As a consequence, when temperature changes, the wood parts in the dulcimer body do not immediately change dimensions in response to the temperature change, but the frame will change shape in response to the change in string tension. A related consequence of this effect is that the retuning of some dulcimer strings will affect the tuning of the remaining strings.

21.6.2 Tuning Stability: Humidity

Hammered dulcimers go sharp in high humidity and flat in low humidity, with the largest effect on the four or five lowest strings. Indeed, by adjusting these lower strings occasionally, it is sometimes possible to keep a dulcimer relatively in tune with itself during humidity fluctuations. The time scale is vastly slower for humidity changes than for temperature changes. The tuning changes shown in Fig. 21.8 occurred over 12 h in response to a sudden increase in relative humidity from 57 to 88%.

The equilibrium moisture content of wood depends on temperature and humidity in a complicated way. For instance, at 70°F, wood in equilibrium at 90% humidity has 2.4 times the water content than at 45% humidity; extensive data on wood properties can be found in the *Wood Handbook* (Forest Products Laboratory 1987). Wood expands as it absorbs moisture and shrinks when it dries, but the rates of change are highest in the direction of the annual rings (tangential), about half as much perpendicular to the rings (radially), and very little along the grain (longitudinally). Thus, plain sawn wood shrinks and swells more in width and less in thickness than does quarter-sawn wood. Table 21.3 gives shrinkage rates for woods commonly used for braces, side rails, pin blocks, and sound boards in hammered dulcimers.

In the piano, according to some tuners, the sound board is the culprit for humidity sensitivity. The sound board is stiff, thick, and slightly arched toward the strings. Under high humidity conditions it absorbs moisture and swells, producing an upward bulge. This puts additional tension on the strings and increases pitch. However, this reasoning does not work for hammered dulcimers because sound boards are thin (about 0.25–0.35 in.), weakly braced, and, due to warping, often inadvertently arched away from the strings. But if the braces, bridges, sound board, and back board were to swell, then there would be increased tension on the strings because the bridges are elevated above the main frame. Assuming that most of these parts are plain sawn hardwoods, the estimated change in dimension, going from 55 to 88% humidity (10.3–19.5 moisture content), is 1.3%, or 0.053 in. But changing

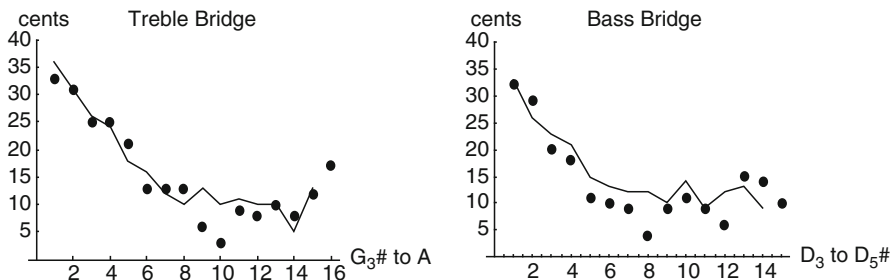


Fig. 21.8 The 12-h increase in frequency for a sudden humidity change from 57 to 88% for two hammered dulcimers (MW, dots; Pet, solid line). For all woods there is a hysteresis effect in absorption and desorption cycles. The instruments returned to the original tuning within 24 h, but not in 12 h

Table 21.3 Average radial and tangential shrinkage rates for common woods used in dulcimer building, green to oven dry. Individual variation within species can be significant – up to 50%. Generally, hardwoods are less stable than softwoods

	Cherry	Maple	White oak	Black walnut	Spruce	Mahagonny	Redwood
Percent radial	3.7	4.8	5.6	5.5	4.3	3.0	2.2
Percent tang.	7.1	9.9	10.5	7.8	7.5	4.1	4.9

the dimensions of the bridges by this amount does not give the instrument response shown in Fig. 21.8. Placing a 1/16-in. shim under the strings of a tuned dulcimer gives frequency changes that are fairly uniform on each bridge with nearly twice the increase on the bass bridge.

A contributing factor in humidity instability in the hammered dulcimer is the expansion and contraction of the longitudinal frame elements. Although the longitudinal contraction from green to oven dry is small, from 0.1 to 0.2% for most woods, the theoretical effect of such a shrinking (or swelling) gives a tuning reaction curve similar to that in Fig. 21.8. We are left to conclude that the uneven tension of the strings and changes in wood dimensions (radial, tangential, and longitudinal) in virtually all wood parts of the instrument, even the plywood, contribute to moisture-related tuning problems.

The effect of heat and moisture is complicated by two factors. When moist wood is heated, it tends to expand because of normal thermal expansion and to shrink because of the decrease in moisture content. For most playing conditions, in the long run, the loss of moisture will exceed the heating effect on the wood and will augment the effect of heating on the strings. Also, for outdoor playing, a higher daytime temperature usually means lower humidity. This has contradictory effects on the wood, but similar effects on instrument tuning.

21.6.3 String–Bridge Friction

Friction between the bridge caps and strings can cause string tensions to vary between the two sides of the treble bridge. This is why the strings on the right side of the treble bridge are tuned first. One assumes that because of bridge friction, the correct pitch on the right will then hold while the left side is tuned. A difference of as much as 0.5% of the string tension can hold under static conditions, but as soon as the string is hammered, tension is nearly equalized on both sides of the bridge. So a hammered dulcimer with a misplaced treble bridge is impossible to hold in tune. Similarly, the string segments between the side bridges and the endpins and the tuning pins can be at different tensions from the playing string. If the angle of the pin block is large, these string fragments may not immediately equalize tension during playing, but rather slip gradually. In a related matter, since the strings clearly slide across the bridge caps during play, bridge friction is a potential source of energy loss.

21.7 The Percussive Sound: Hammer and String Interaction

Although both pianos and hammered dulcimers use hammered strings, there are significant differences that give each its distinctive tone. During play, the dulcimer hammer seldom becomes a projectile as in a piano, but rather, the player accelerates the hammer during the stroke so that the rebound will be enough to allow another stroke without actually lifting the hammer; the player's hands replace the piano action. This allows hammered dulcimer players to play flams, ruffs, and double stoke rolls like drummers.

The net effect of light, hard hammers in hammered dulcimers is a strong percussive sound consisting of short-lived, high-frequency, nonharmonic sounds and low-frequency body modes unrelated to the strings. The strike position in the hammered dulcimer is not only variable but is also near a bridge, rather than the terminal end as in the piano. So the strike ratio α , strike point to bridge distance divided by the string length, is of particular interest.

If a string were infinite, a hammer would not bounce after a strike but would rather slow to a stop. Finite string length gives reactance so that the string will act like a spring. But this implies that the hammer and string remain in contact for at least the time required for a wave to reflect off the bridge and return to the hammer, minimum time $t_\alpha = 2\alpha L/c$ s (L = string length, c = transverse wave velocity). For the striking distances of 3–8 cm typically found among dulcimer players, t_α ranges between 0.16 and 0.68 ms. Because the observed contact time for a hammer and string is $T_c = 1.5\text{--}5.0$ ms, there must be several reflections between the hammer and bridge before the hammer is thrown free; Figs. 21.9 and 21.10. These reflected waves have a fundamental frequency that is $1/\alpha$ of the original string. Figure 21.9 illustrates several common features: there are multiple hammer-to-bridge

reflections (4–5), a wooden hammer produces more high-frequency string noise than does a padded hammer, and a padded hammer stays in contact with the string longer than a wooden hammer.

Figure 21.10 illustrates that a hammer can strike a string, be thrown free by a reflection from the bridge, and then regain contact with the string. In this case, the high-frequency signal created by the short string segment dominates the signal even after the hammer is thrown free. The two sources of high-frequency noise, short string segment and hard hammer chatter, initially dominate the sound, and while rapidly decaying, may persist for up to 100 ms.

String–hammer interactions have been studied extensively in the piano (Askenfeldt and Chaigne 1994). The following conclusions are also valid in a hammered dulcimer:

- Increasing the hammer weight increases the hammer contact time, and hence the number of bridge–hammer reflections. Bridge force, and hence loudness,

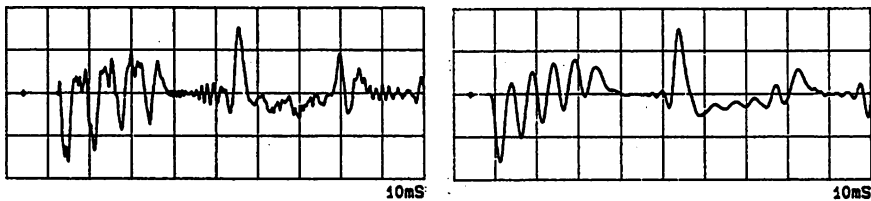


Fig. 21.9 String velocity in the direction of strike for G3#, the lowest treble course on a hammered dulcimer (DS), for a wooden hammer (*left*) and a padded hammer (*right*). The roughness and sharp peaks in the left graph indicate high-frequency noise with the wooden hammer. The magnetic velocity detectors were 4 cm from the bridge; the strike distance is 7 cm from the bridge; and the string length $L = 53.4$ cm, so the strike ratio $\alpha = 7/53.4 = 0.13$. The hammer contact time, $T_c \approx 3$ ms for the wooden hammer, is considerably shorter than the period $T = 4.82$ ms, so the prominent reflection spike from the right-side bridge reaches the detector in about 4.32 ms with no additional hammer interaction. During the time that the hammer is in contact with the string, the string segment of length αL between the hammer and the treble bridge supports approximately $T_c/(\alpha T) = 4.8$ reflections

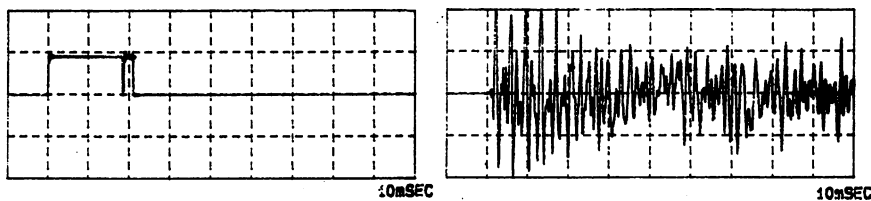


Fig. 21.10 Hammer contact time and vertical bridge acceleration for a wooden hammer on a midrange bass string D4 (MW), $L = 50$ cm, $T = 3.4$ ms, $\alpha = 0.12$, and $T_c = 2.07$ ms. As in this example, it is not uncommon for a hammer to lose and regain string contact one or more times. The number of reflections before the hammer is thrown free is $T_c/(\alpha T) = 5.2$, but there is no apparent reflected pulse from the left bridge or evident fundamental wave of length $T = 3.4$ ms. High-frequency noise dominates the signal

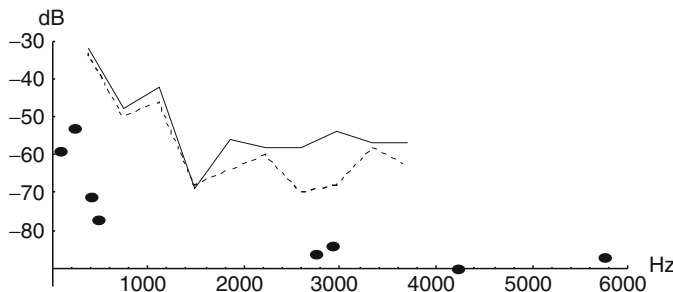


Fig. 21.11 Four low-frequency body modes (dots) and four high-frequency hammer noise frequencies (dots) compared to ten string mode frequencies (solid line, wooden hammer; dashed line, padded hammer) for a strike on F4# (370 Hz), time averaged over the first 100 ms (Lindsey dulcimer). The low-frequency modes occur with either hammer; the high-frequency noise is from a wooden hammer. The relative dB levels only show that while percussion effects dominate initially and are a distinctive feature of the hammered dulcimer sound, these effects decay very quickly because they are not sustained by the strings

increases with heavier hammers, and lighter hammers have a stronger high spectra.

- Increasing the strike ratio α increases hammer contact time, decreases maximum hammer force, and generates a more complex hammer force. Although the player controls α , it is not usually an inadvertent player variable.
- Hammer velocity increases the spectral content, i.e., waveforms sharpen.
- Softer hammers tend to filter out hammer chatter, leading to less high-level spectral content.
- Using softer bridge caps such as Delrin and wood, rather than brass or steel, leads to shorter resonance times and less high-level spectral content.

There is one other percussive effect – low-frequency body modes – which can best be heard by damping the strings and tapping the treble bridge with a padded hammer. During play, the smaller the playing ratio α , the larger the effect. Figure 21.11 gives the frequencies of both wooden hammer noise and inharmonic, short duration body modes compared to string frequencies for a F4# on the treble bridge.

But the hammered dulcimer body has mass and stiffness, so the radiated sound from the instrument only partially resembles the bridge or string motions; see Fig. 21.12.

21.8 Hammers and Course Spacing

Hammers and hammer grips have varied widely among cultures and between individual players. The most common American hammer is a lightweight, wooden hammer about 21-cm long and weighing about 8 g. During play, hammers are held

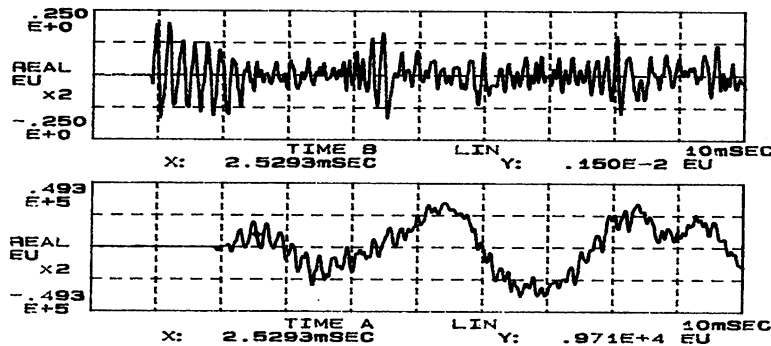


Fig. 21.12 Bridge acceleration (top) and projected sound pressure levels (bottom) for a wooden hammer striking C4 on the treble bridge of a dulcimer (MW). $L = 61.2 \text{ cm}$, $T = 3.8 \text{ ms}$, $\alpha = 0.049$, $T_c \approx 1.5 \text{ ms}$. The projected sound initially consists of the high-frequency components from the bridge superimposed on a short duration wave with a period of about 3 ms. The fundamental period of 3.8 ms becomes visually evident only after many periods. The travel time to the microphone caused the 0.88 ms time delay between the signals

loosely between the thumb and fingers. The head weight of a hammer affects instrument timbre and playing ability. A very light hammer generates more high-frequency sounds and hammer chatter, and it is hard to play forcefully. A heavier hammer penetrates the string too far and can be ponderous to play fast. That being the case, most players get accustomed to a certain length, weight, and style and they then stick with it.

Nothing changes the sound of a hammered dulcimer more than switching from a wooden hammer to a padded hammer. A wooden hammer with leather padding does not generate as much high-frequency noise, Fig. 21.9, so the initial sound is less percussive. Although players would characterize the padded hammer sound as being more mellow, it is mostly on the basis of the attack, because the after-sound from a wooden hammer and a padded hammer are hard to distinguish.

In the drive for lighter and lighter instruments, builders have shrunk the distance between the rails. This means less space between courses, and therefore less error margin for hammer strikes. An experienced player might play more fluidly on a smaller instrument, but for many players, larger distances between courses would be beneficial. It is easier to play an instrument with more strings per course because there is a bigger target, of course. But in addition, the hammer rebounds better and drum rolls are easier to control.

21.9 String Coupling and Resonance Time

The undamped hammered dulcimer resonates for a long time, less than an undamped piano resonates, but long enough so that fast tunes can get muddled. This is enough of a playing problem to inspire builders to use low resonance times

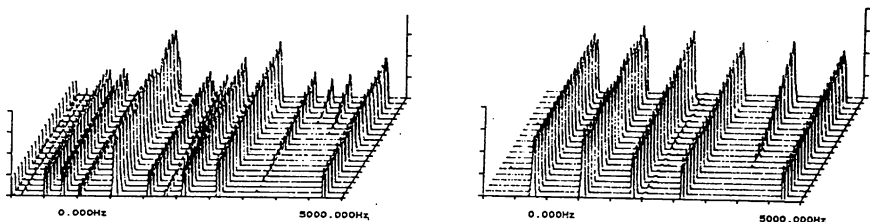


Fig. 21.13 The power spectrum for vertical string velocity at 20-ms intervals for strings coupled by the treble bridge. Decay rates depend on time and mode frequency. The string on the left is C5 (523.3 Hz, range = -116 to -46 dBv) and the right is G5 (785 Hz, range = -110 to -40 dBv). The G5 was struck 6 cm from the bridge and C5 was driven by bridge coupling alone. Because $f_G = 3/2f_C$, mode coupling occurs only for multiples of $2f_G = 3f_C = 1,570$ Hz. String amplitudes are comparable and the coupling occurs within several periods of the strike. For other frequency multiples, $f_C, 2f_C, 4f_C, 5f_C, f_G, 3f_G, \dots$, coupling is inefficient. There are similar results when the situation is reversed and C5 is struck

as a selling point. But dulcimer literature seldom clearly defines resonance time (or sustain), in part because there is a frequency and time dependency. For our purposes, resonance time is the reciprocal of the decay time τ , where τ is rate of sound pressure level decrease per second, dB/s. For pianos, initial decay rates vary from about 4 dB/s at the bass end to 80 dB/s at the treble end (Fletcher and Rossing 1991). The decay rates in dulcimers are somewhat less than the midrange values for a piano. The nature of mode-dependent decay rates is shown in the “waterfall” graphs in Fig. 21.13. Strong string coupling across the treble bridge also complicates the issue.

The strings can be thought of as a reservoir of stored energy. But the mechanical impedance for vertical vibrations of a sound board, which varies with location and frequency, is much larger than string impedance, so the flow of energy from vertical string vibrations to the sound board is slow. Dulcimer soundboards are much stiffer parallel to the instrument plane than vertically. Therefore, the transfer of horizontal string vibrations is even slower. This means that vertical string vibrations will decay faster than horizontal string vibrations, contributing to a dual (time varying) decay rate.

Thinking only in terms of vertical string vibrations, paired strings that are tuned in unison have two fundamental modes of vibration, in-phase and out-of-phase. The out-of-phase mode has strings going in opposite directions with little bridge movement because string forces cancel at the bridge, so its decay time is long. For the in-phase mode, the direction of bridge force is the same for both strings, so bridge movement increases. The resulting decay rate due to sound board coupling is double that of a single string. Therefore, the in-phase mode decays faster than the out-of-phase mode. In the real world, hammered dulcimer strings seldom remain tuned in unison, and hammer strikes are far from perfectly vertical. These “dual” decay effects are less noticeable in a hammered dulcimer than in a piano, perhaps because rocking bridge motions in the dulcimer transfer energy between the various string modes.

In addition to paired string coupling, there is instrument-wide coupling between strings that have modes with common frequencies. If a string is struck, other strings will vibrate sympathetically and continue even if the initial string is damped. In the hammered dulcimer, the treble bridge makes this effect especially strong, as can be seen in Fig. 21.13. Sympathetic vibrations can be annoying as well if they involve string ends that are not in harmony. Piano builders either muffle these segments with felt or actually tune them (duplex scaling). No current dulcimer builder does either.

Ultimately, strings stop vibrating because they lose energy through air friction and internal friction, or because there is a transfer of energy to the sound board. Little can be done with air friction or internal friction, but energy transfer rates are an element of design. The ratio, r , between string impedance and sound board impedance is roughly proportional to a^2/t^2 , for string radius a and sound board thickness t . This causes a dilemma for hammered dulcimer design. Resonance times can be reduced by increasing r , but this means either using larger string diameters, with more string inharmonicity and higher string tension, or using thinner sound boards, which may already be too weak to withstand current tension without warping. There are partial solutions. Sound boards can be tapered so that bass areas are thinner, thus supporting a louder and faster decaying sound. The constant of proportionality defining r includes stiffness and mass terms. Sound boards that are thicker, but lighter and stronger, can have higher values for r .

21.10 Sound Board and Body Modes

In order to effectively radiate sound, a sound board must be free to vibrate at the playing frequencies of the instrument. There are natural frequencies of plate vibration (modes), but unlike those of strings, the frequencies are not harmonic. Both the mode frequencies and vibration patterns depend on the geometry of the sound board and the boundary conditions – clamped, hinged, or free. The only easy mathematical solution is for hinged, isotropic rectangular plates; Fig. 21.14. A mode is more easily excited (has less impedance) if it is driven at an anti-node, a point of maximal vibration. Thus, the driving location on the sound board is important. In the hammered dulcimer one consequence is that the redundant strings, which are tuned the same, have different driving points and so will have different timbre.

If m is the number of vertical nodal lines and n is the number of horizontal nodal lines, then the mode frequencies for a simply supported, isotropic rectangular plate are given by:

$$f_{m,n} = 0.453 c_L h \left[\left(\frac{m+1^2}{L_x} \right) + \left(\frac{n+1^2}{L_y} \right) \right] \quad (21.2)$$

where L_x and L_y are the plate dimensions and $c_L = \sqrt{\frac{E}{\rho(1-\nu^2)}}$, where E = Young's modulus, ρ = density, and ν = Poisson's ratio. In a dulcimer, the trapezoidal shape and the mixed-boundary conditions complicate the story, but the general

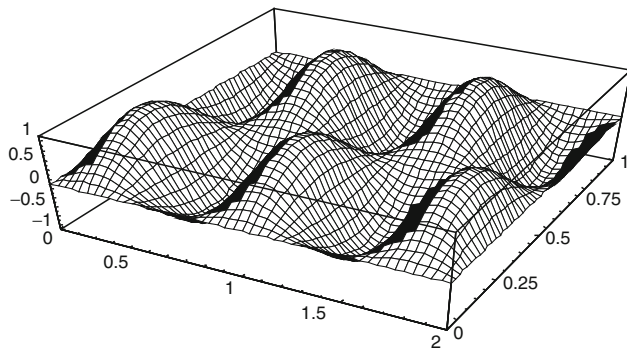


Fig. 21.14 A (4,1) mode (four nodal lines along the x -axis and one along the y -axis) for a simply supported rectangular plate. A plate has similar (m,n) modes for all nonnegative integers m and n

indications of (21.2) remain valid. The high-frequency modes are well represented by various choices of m and n , but it is the low-frequency notes that can be weak in a hammered dulcimer. From (21.2), we see that the bass range can be extended by decreasing h or by increasing L_x and L_y . In addition, mode frequencies are higher for clamped plates and lower for free plates. So ideally, for low-frequency response, we want a large, thin sound board with free-boundary conditions.

There are two different styles of dulcimer sound boards: fixed and floating. A fixed sound board is glued to the pin block and part of the end rails, leaving some of the boundary along the rails free to vibrate. A floating sound board has no glued edges but may slide into pin block slots. In both cases, the sound board is supported at the bridges by small dowels or braces that run nearly perpendicular to, and on top of, the longitudinal braces as seen in Fig. 21.6. The shape, size, and exact location of these braces are a critical element in dulcimer design. If these braces are flat and placed right under the bridges, then the sound board is clamped along the bridges, and the sound board is effectively split into smaller right and left halves. If the sound board is strong enough, it is possible to offset these braces from the bridges with resulting hinged conditions. The mechanics of this brace placement is an art form among builders. Regardless of design, the braces under the sound board couple the sound board with the longitudinal braces and thus to the back plate.

The advantage of a fixed sound board is that it becomes a structural element, greatly increasing the stiffness of the body with no additional weight. It actually allows for weight reduction since the longitudinal braces and back plate can be thinner. This “unibody” construction also encourages whole body modes of vibration. A disadvantage of unibody construction is that mode frequencies are higher because of clamped boundary conditions. The advantage of a floating sound board is that it is freer to vibrate, although there is generally some sort of clamped or hinged condition at the pin blocks. The disadvantage of a floating soundboard is that the instrument must be heavily built in order to resist bending loads.

The (0,0) mode (no nodal lines) has the lowest frequency. The instrument depicted in Fig. 21.15 has a good bass response because the (0,0) mode frequency,

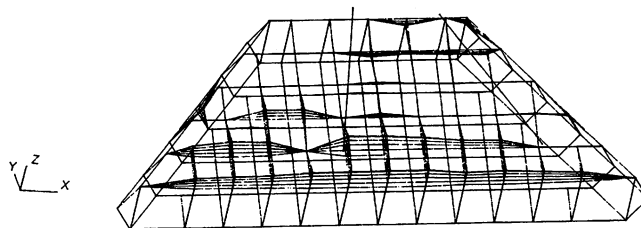


Fig. 21.15 The (0,0) mode, 129 Hz, of a dulcimer with unibody construction (MW). Notice the large amplitude along the bottom rail

129 Hz, is comfortably below the lowest note on a hammered dulcimer, D3 (146.3 Hz). Higher frequency modes include mixed sound board and back plate modes, with some modes being segmented by the bridges and braces.

21.11 Sound Board Materials, Back Plates, and Design

In wood, sound travels faster along the grain than across the grain. For spruce, $v = 5,200 \text{ m/s}$ with the grain and $1,700 \text{ m/s}$ across the grain. So, with the possible exception of using plywood, hammered dulcimer soundboards are not isotropic, but the parameters in (21.2) are still important. Builders select sound board material on the basis of stiffness (E), density (ρ), workability, and appearance. Baltic birch plywood is a common choice because it is strong, stable, readily available, of uniformly good quality, and inexpensive. Other common woods are spruce, mahogany, redwood, and cypress. All things being equal, thin sound boards have a better bass response. However some builders are experimenting with thicker, composite sound boards with a lightweight inner core and durable outside shell. Carbon fiber sound boards and frames may be used in the future. Tapered or arched sound boards can be an alternative to a flat plate.

Back plates made of 3/4-in. boards used to bear a large share of the responsibility for preventing warping, but with unibody construction, thin plywood, 3/8-in. or even 1/4-in. Baltic birch has become the builder's choice. This makes the back plate a more efficient radiator of sound.

21.12 Bridges, Bridge Caps, and Bridge Vibrations

The treble and bass bridges convey string vibrations to the soundboard and elevate the strings to playing position. As vibrating elements by themselves they contribute little because they are stiff and short. But they are an important design consideration. One normally thinks of a bridge as vibrating up and down in response to vertical string forces, but hammered dulcimer bridges also rock in the string direction in response to the changes in string tension as the string goes through



Fig. 21.16 Elaborate carving on the treble bridge of a *yang qin* built in China in the 1950s. The instrument has extensive mother-of-pearl inlays so the carving may have been merely incidental. This 7/7 dulcimer has four strings per course, an arched sound board, and narrow steel bridge caps. Despite the artwork and carving, it has a tinny sound with a weak bass

maximal and minimal deflections. The amplitudes of these two bridge motions are of the same order of magnitude. The driving efficiency of this rocking motion can be improved if the bracing under the soundboard does not clamp the soundboard to the bridge.

A continuous bridge would couple all the strings together. The most extreme way to counteract this is with individual bridges – horsemen. But these are irritatingly unstable. In the *yang qin*, fancy carving works to isolate the strings and possibly damp string vibrations, as seen in Fig. 21.16. The American technique is to isolate each course by cutting slots on the top of the bridge, as in Fig. 21.2.

Walnut, maple, rosewood and cherry are common bridge materials. Because of different modal decay rates, each may make small differences in timbre and resonance times. Rosewood is the expensive choice.

Virtually all bridge caps before 1970 were made of thin brass or steel wire. A hard plastic such as Delrin is now almost universal. A softer bridge cap tends to absorb high frequencies and decrease the metallic sound of brass caps. Sustain is also reduced because string energy is absorbed in the cap itself. The logical extreme is wooden bridge caps or wooden side bridges with holes for the strings. Such instruments are most effective when playing fast music not needing sustain.

21.13 Pin Blocks, Pins, and Hitch Pins

Any hardwood that is strong and does not split can serve as a pin block. If the pin block has an exterior exposure, visual appearance is a consideration. Hard maple is the industry standard, although laminated pin block material for pianos might offer better long-term stability. Pin block material should be of minimal thickness to save weight, except that the pin blocks are also the main structural element of the side, and they will bow in if undersized.

When pin block material swells in response to high moisture conditions, wood is compressed against the steel pins. Over many such cycles, permanent damage occurs and the pins loosen up. Laminated pin blocks shrink less than solid wood and therefore are less likely to have loose pins. Piano pins come in sizes with different diameters so that a loose pin can be replaced with a slightly larger pin. Zither pins used in dulcimers come in only one size. But the 62 zither pins for a 16/15 dulcimer weigh 3 lb less than 62 piano pins, so as long as there are minimal tuning problems, the lightweight choice is obvious to both builders and consumers.

Hitch pins are standard. The issue is whether to use two individual strings with looped ends and two hitch pins per course, or whether to save time, as they do in a piano, and run one piece of wire from a tuning pin across a bridge, make one turn around one hitch pin and return the wire across the bridge to another tuning pin for the second string. The problem with the second method is that the bottom string in a course has more tension than the top string because it is 2 mm or so longer. For a midrange treble string, D4, the difference in tension is $\Delta T \approx 2T(\Delta L/L) = 0.25$ lb. One loop around a hitch pin seems sufficient to maintain this difference, except there is likely to be slippage over many hammer blows. So, single, looped strings should give more stable tuning. Another concern is that with double the tension a hitch pin might bend over or damage the pin block.

21.14 Sound Radiation Patterns

A player mostly hears sound from the sound board, but what does the dulcimer sound like from a different position? This relates to the question of where to place an acoustic microphone. The standard soundman choice is over the sound board, right in the player's way. If the timbre of an instrument is relatively unchanged by position, then placing a microphone out of the way at the back of an instrument might be the right choice. Figure 21.17 shows that for the dulcimer under consideration (L_i), timbre changes significantly with microphone position, with radical changes in the fundamental mode. Contact microphones or built-in adjustable microphones are an alternative.

21.15 Unimportant Characteristics: Sound Holes, Special Finishes, Peglegs, and Perfect Fifths

Sound holes serve no acoustic purpose in a hammer dulcimer, and they do tend to weaken the sound board in a critical area of stress. An instrument would be better without sound holes, except that builders embellish them as a decoration. Sound holes do offer some spatial orientation to a player, but good scale markers on the bridges do the same thing better.

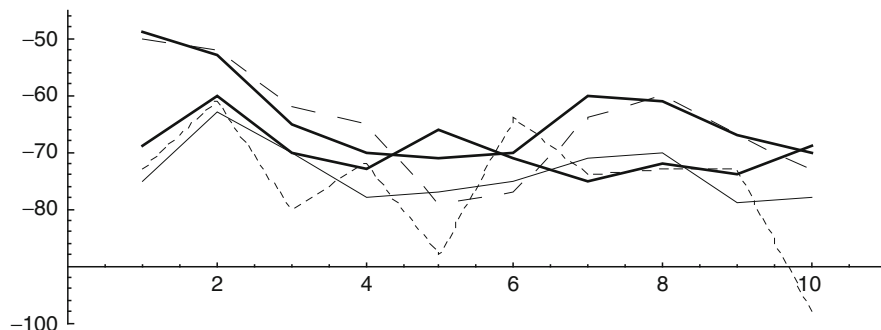


Fig. 21.17 Time-averaged (0–1 s) power spectrum (dB) for the first ten modes of a hammered dulcimer (L_i) in an anechoic chamber for five different angles shows significantly different radiation patterns. The angle measure is a rotation from the position perpendicular to the sound board toward the short rail, $0^\circ = \text{thick solid}$, $30^\circ = \text{medium thick solid}$, $90^\circ = \text{thin solid}$, $180^\circ = \text{close dashed}$, $330^\circ = \text{wide dashed}$. The wooden hammer strike was on a midrange treble string A4, $\alpha \approx 0.1$. The microphone distance was 2 ft. This instrument has a thick back plate, and different results are possible for other types of construction. In general, though, back plate modes are quite different than sound board modes so differences in timbre are expected

Dulcimers need to be protected from the weather. Several layers of lacquer or polyurethane will do this and enhance the wood as well. However, no finish will protect the instrument from humidity changes. Unlike the violin, the type of finish has no significant effect on acoustical properties.

Body mobility is useful for a dulcimer player so playing while standing is easier than while seated. Fancy stands offer no mechanical advantage to playing. Playing a dulcimer with a single leg, that is, a pegleg, in the middle is a trick.

The hammered dulcimer is built to support musical fifths across the treble bridge and between the bass and treble bridge, but these are far from perfect fifths. All players use electronic tuners to tune so while in theory there is a perfect fifth across the treble bridge this is unlikely to be actually true.

References

- Askenfeldt, A., Chaigne, A. (1994). Numerical simulations of piano strings. II. Comparisons with measurements and systematic exploration of some hammer and string parameters. *J. Acoust. Soc. Am.* **95**, 1631–1641.
- Birkett, P., Poletti, P. (2007). Reproduction of Authentic Historical Soft Iron Wire for Musical Instruments. Internet: sbirkett@real.uwaterloo.ca.
- Fletcher, N., Rossing, T.D. (1991). *The Physics of Musical Instruments*. Springer-Verlag, New York, pp. 60–61, 331–337.
- Forest Products Laboratory (1987). “Wood Handbook,” Agricultural Handbook 72, Forest Service, U.S. Department of Agriculture, Washington, DC.
- Gifford, P. (2001). *The Hammered Dulcimer: A History*. The Scarecrow Press, Inc., Lanham, MD.

Chapter 22

Electric Guitar and Violin

Colin Gough

Almost all the instruments described in this book have their origins in historical cultures dating back over many centuries. In contrast, the electric guitar and violin are clearly twentieth-century innovations. They are products of the electronics age following invention of the rectifying thermionic valve (tube) by John Ambrose Fleming in 1904, the amplifying triode valve (tube) by Lee de Forest in 1907, and the vacuum-filled amplifying valve (tube) by Irving Langmuir in 1915. By 1916, such valves were already being used in radio receivers, and important advances were being made in microphone, amplifier, and loudspeaker design. This, and the increasingly wide distribution of mains electricity in the 1920s, provided the technology and infrastructure for the development of the electric guitar and violin and their lower-pitched relations – the bass guitar, viola, cello, and string-bass. Although we focus here on the electric guitar and violin, almost everything discussed in this chapter is also relevant to their lower-pitched relations.

In the first section, we briefly describe the emergence of the electric violin and guitar within the context of early acoustic recordings, and radio and public performances, in which conventional acoustic stringed instruments such as the guitar and violin were placed at a huge disadvantage compared to the much louder wind and brass sections of big band groups and orchestras. We then describe in a little more detail the early innovations, which led to today's familiar shapes and sounds of today's electric violin and guitar. The third section describes the design and influence on the sound of magnetic and piezoelectric pickups, with a brief interlude on some of the special effects that characterize the sounds of many guitarists and pop music groups of the 1960s and onward. We conclude by describing the use of the electric violin in advancing our understanding of the acoustics of the traditional violin and especially those factors in the perceived sound and quality that can be related to the damped, multiresonant, filtering action of the violin shell.

There are a number of publications describing the history and design of the electric guitar and violin (Bacon 2006; Evans 1977; Graesser and Holliman 1998;

C. Gough (✉)
44 School Road, Birmingham B13 9SN, UK
e-mail: profgough@googlemail.com

Ratcliffe 2005; Smith 1987), and a wealth of information available on the web (e.g. www.digitalviolin.com). Most important innovations were made by designers working for commercial companies, mostly in America, with freely downloadable patent applications (www.google.com/patents) providing details of important developments. These will be frequently referenced, for example, in the form [Charles Chew 1885/7 US 358542] – an early patent for a silent, stick-like, practice violin, similar in shape to many modern electric violins, where the application and awarding dates are both indicated.

22.1 Historical Background

In acoustic recordings before 1925, all the energy required to cut the grooves in recorded discs had to be supplied by the sound of the performer's voice or instrument. This placed stringed instruments such as the violin and guitar at a major disadvantage relative to much louder wind and brass instruments; see, for example, Day (2000) for a fascinating account of such problems. This led to several attempts to develop louder stringed instruments, including the use of steel-cored strings and the use of additional acoustic resonators and horns attached to stringed instruments. Several of those active in such innovations were later at the forefront of the development of electric instruments, and many of the early designs retained features of these earlier instruments.

Figure 22.1 shows a typical 1911 recording session in Berlin, with a pair of recording horns driving a single cutting head – one horn for the singer and the other



Fig. 22.1 A 1911 acoustic recording session in Berlin with all the violinists playing Stroh violins

for the orchestra. The violinists are all playing solid-body Stroh violins with acoustic horns attached (Heaney 2007). In early orchestral recordings, saxophones were often used to boost the sound of the violas, while tubas replaced the cello and double-bass (Day 2000).

The electric guitar and violin were developed in the late 1920s and early 1930s, with most of the technology used today already established, at least in rudimentary form, by the early 1940s. The first electric guitars used a magnetic pickup on all-metal, Hawaiian-style, guitars – instruments with steel-cored strings played across the lap. The use of magnetic pickups on Spanish-style, hollow-bodied, guitars initially proved troublesome, with problems from distortions, overtones, and acoustic feedback. To circumvent many of these problems, Les Paul, Paul Bigsby, and Leo Fender in the early 1940s pioneered the use of solid-bodied wooden guitars using compact magnetic pickups very similar to those in use today.

By the late 1930s and early 1940s the electric guitar and violin had become firmly established in jazz- and big-band groups, and were features in bands such as Bert Lynn's All-Electric Orchestra, with the whole string section playing electric instruments (see photographs in Smith 1987, p. 15). By 1940, the outstanding jazz guitarist Charley Christian, playing and recording with the Benny Goodman Band, had established the electric guitar as an instrument with its own unique voice. Christian played on the Gibson ES-150 Spanish guitar, with a state-of-art magnetic pickup that remains popular amongst jazz guitarists today and is still known as the Charley Christian pickup.

There was a slight hiatus in the development of electric instruments in the war years, but by the 1950s and 1960s, several commercial companies were producing a wide range of solid-bodied electric guitars, which were defining the distinctive sounds of popular music – and rock-and-roll in particular. The electric guitar is commercially the most successful of all musical instruments in the Western World – and almost certainly outstrips the sales of all other stringed instruments put together.

It took somewhat longer for the electric violin to be widely adopted into popular musical culture, although today almost every pop group includes an array of electric violins and often cellos and string-basses in the backing group, if not in live performance then on recordings.

We now trace the development of the electric guitar and violin in a little more detail.

22.2 The Electric Guitar

In 1923, Lloyd Loar of the Gibson Mandolin-Guitar Company demonstrated what appears to have been the first electric guitar. The electric signal was generated by a modified carbon-granule microphone, which sensed the vibrations of the bridge induced by the plucked strings. However, the output was rather erratic and particularly susceptible to humidity. Unsurprisingly, attempts to market it in 1929 by the Stromberg-Voisinet Company were unsuccessful.

Arguably the most important figure in the development of both electric guitars and violins was George Beauchamp, a Texan-born violinist and Hawaiian guitar player. In 1926, in collaboration with five Dopyera brothers, he set up the National Guitar Company, with the initial aim of producing acoustic Hawaiian guitars with an array of hollow metallic resonators attached to the bridge (Smith 1987). The Dopyera brothers had previously manufactured banjos, but these were declining in popularity by the early 1920s. The early National instruments were Hawaiian-style guitars with cast aluminum bodies. They were manufactured by the Rickenbacker Company, which by 1925 was producing as many as 50 guitar bodies a day. National ultimately produced two types of guitars – a conventionally shaped guitar with a round neck, mostly used by blues musicians, and a Hawaiian style instrument with a flat neck.

Later, in collaboration with Paul Barth, Beauchamp developed a more compact magnetic pickup [Barth 1941/43, US 2310606], which sensed the vibrations of the strings directly – the forerunner of all magnetic pickups in use today. An earlier version is included in his 1934 patent application [Beauchamp 1934/37, US 2089171] for the banjo-style Hawaiian guitar shown in Fig. 22.2a. The pickup used a pair of horseshoe magnets, with pole-pieces under each string to concentrate the magnetic field into these regions. A single large coil, wound around the six pole-pieces, sensed the changes in magnetic flux as the plucked strings vibrated toward and away from the

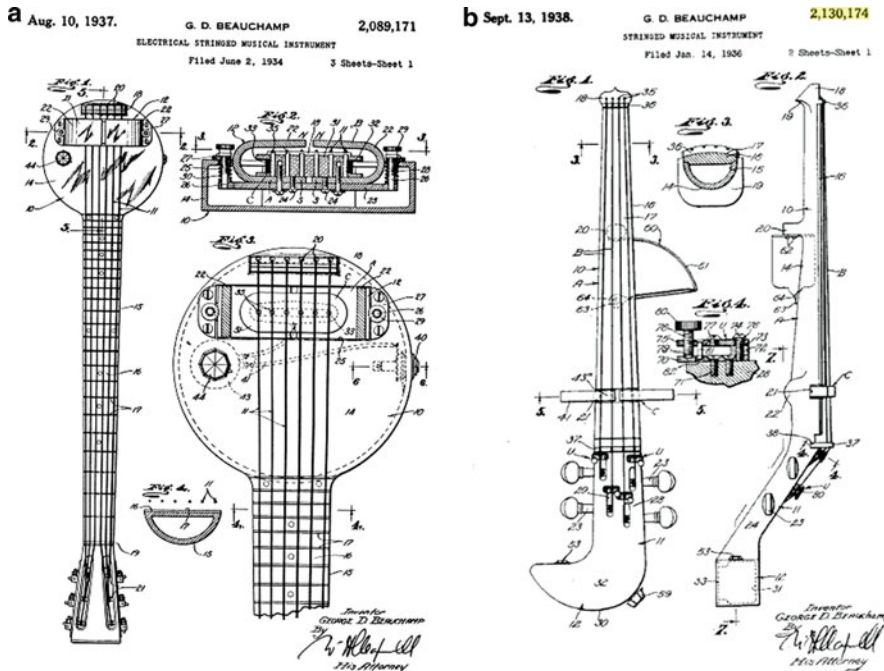


Fig. 22.2 Beauchamp's patent applications for (a) the "Frying Pan" guitar and (b) electric violin

ends of the pole pieces. Magnetic pickups rely on the strings being magnetic, so cannot be used with gut- or nylon-strung acoustic instruments.

Beauchamp and his colleagues subsequently formed the Ro-Pat-In Corporation to manufacture electric guitars and by 1932 were marketing both the “Frying Pan” model illustrated in Fig. 22.2a, and a more conventionally shaped wooden model, the “electro Spanish guitar.” In 1934, the company was renamed the Electro String Instrument Corporation and the guitars referred to as “Rickenbacker Electros.” By 1936, the company was also manufacturing electric mandolins, bass viols, violins, cellos and violas, in addition to guitars.

The next significant development was a very much more compact, single-coil, magnetic pickup designed by Walter Fuller for the Gibson Company [Miller 1938/39, US 2145490]. It was originally developed in 1935 for the EH-150, Hawaiian-style, electric guitar, and was subsequently used on the 1936 ES-150 hollow-bodied wooden guitar, which is still considered one of the best sounding electric jazz guitars (Smith 1987). In 1946, Gibson introduced their first solid-body electric guitar using a newly designed P-90 magnetic pickup, and in 1957 introduced the humbucker pickup – designed to eliminate pickup from mains power supplies – which is widely used on many modern instruments.

By 1937, a number of companies in addition to Gibson and Rickenbacker – National-Dobro, Epiphone, Tutmark and Audiovox – were also manufacturing a wide range of electric instruments, including easily portable, upright, electric string-basses.

Since 1929, the famous guitar player Les Paul had been experimenting with solid-bodied electric guitars at weekends (Smith 1987). In 1941, he produced “the Log,” with the strings and magnetic pickups mounted on a solid length of 4 in. × 4 in. wood. This allowed the plucked string to ring for very long times, because very little energy was transferred to the body at the bridge. However, it was left to two of his friends, Leo Fender and Paul Bigsby, to be credited with the first “modern-style” solid-body guitars (Smith 1987). Fender quickly set up the Fender Electrical Instrument Company, to patent and manufacture such instruments [Fender 1951/51, US Des. 164,227]. Their instruments also incorporated a vibrato- or tremolo-arm attachment originally developed by Bigsby (Smith 1987) and the subject of a later patent by Fender [Fender 1954/56, 2741146]. By 1948, Fender had introduced its Broadcaster guitar, renamed the Telecaster in 1950. In 1952, Gibson introduced their first solid-body guitar, designed in consultation with Les Paul after whom it was named, while Fender introduced its three-pickup Stratocaster guitar in 1953 (Smith 1987).

Modern replicas of some of these famous instruments are shown in Fig. 22.3. Such instruments became the Stradivari and Guarneri instruments of the burgeoning world of leading rock bands and the iconic artists of the 1950s and early 1960s. Original electric guitars have fetched very high prices, such as a Fender Composite Stratocaster of ~1956/1957, played by Eric Clapton, which sold for \$959,500 in 2004 at a charity auction at Christie’s in New York. A Fender Stratocaster played by Jimi Hendrix at the Woodstock Festival in 1969 is believed to have been sold privately for considerably more (*The Sunday Times*, December 12, 2004).



Fig. 22.3 Modern replicas of famous guitars of the late 1950s by three of the most influential American electric guitar manufacturers. Famous players using such instruments are also indicated

The subsequent development of electric guitars included many futuristic designs including instruments with double necks, initially by Semie Moseley in 1954, followed by Gibson in 1958. The use of solid wooden bodies led to guitars with completely differently shaped bodies, like Gibson's Flying V (1957) and Explorer (1958) models. Smith (1987) illustrates the development of electric guitars with many photographs and details of historically important instruments.

The emergence of rock music and rock-and-roll in the 1960s led to an explosive growth in the electric guitar market and the development of ever-louder amplifiers and special effects, which helped create the distinctive sounds of such artists and groups as the Beatles, the Rolling Stones, Jimi Hendrix, Les Paul, Eric Clapton, Cream, the Who, the Yardbirds, Jeff Beck, Led Zeppelin, Traffic, the Doors and many others.

The innovative companies responsible for the initial development of the electric guitar – Gibson, Rickenbacker and Fender – remain amongst the most prominent makers today, though they face increasing competition from many rivals, especially from the Far East. In addition, there are a large number of individual craftsmen creating custom-designed instruments, no longer constrained by traditional designs.

Future developments in consumer electronics and computing will undoubtedly lead to major advances in the ease with which such instruments can be played and the sounds manipulated. Gibson already markets a “Robotic” guitar with a computer-controlled tuning system, alongside other electronic refinements.

Wireless connectivity is removing the need for cables between the instrument, amplifier, and sound system. Inexpensive computer-controlled boxes already exist in the research laboratory, and will undoubtedly be commercialized in the near future, which will enable sounds to be transformed in almost any conceivable way.

22.3 The Electric Violin

The development of the electric violin followed similar lines to that of the electric guitar with many of the same innovators and companies involved. Accounts of the early development of the electric violin are included in many of the earlier references cited for the guitar (Evans and Evans 1977; Smith 1987), and Graesser and Holliman (1998) which also includes many fine photographs and detailed descriptions of modern, hand-crafted instruments.

The first known reference to an electric violin appears in an article written for *Radio News* (1927). It describes the amplification of a conventional violin using a carbon button microphone located close to the treble foot of the bridge, with a battery-driven amplifier and loudspeaker. The editor remarks that, “[I]t has been found possible to make the leading violin louder than an entire orchestra by attaching a small microphone to the violin itself and amplifying it to such a degree that the violin will over-shadow a 50-piece orchestra without difficulty.”

In 1928, Victor Pfeil patented the first, solid-bodied, electric violin [Pfieil 1928/32, US 181717]. The strings were mounted on a stick-like object, with the string vibrations sensed by the rocking motion of the bridge induced by the string vibrations. An iron lever was attached to the underside of the rocking bridge, forcing the lever to move between the poles of a magnet and inducing a voltage in a surrounding coil. A patent in the following year [Eisenberg 1929/33, US 1900489], using a similar rocking-bridge pickup, describes a skeletal-frame body, similar in shape to many modern-day, mass-marketed electric violins. In France, Gabriel Dimitru also patented a rather similarly instrument [France (Seine), Brevet d’Invention (686,683)]. However, the first electric violin to be commercially marketed was almost certainly the Vivi-tone violin designed by Lloyd Loar [1933/35, US 2020842] for the Acousti-Lectric Company of Kalamazoo, Michigan. It also used a rocking bridge magnetic pickup.

At around the same time, the Rickenbacker Guitar Company introduced the “Electro” violin designed by George Beauchamp [1936/38, US 2130174] illustrated in Figs. 22.2b and 22.4a. The violin used steel strings mounted on a solid bakelite body shaped rather like a short hockey stick. It had no peg-box or scroll, but had tuning pegs mounted on the near side of the bridge close to the chin, with additional fine-tuning adjusters on each string. An electromagnetic pickup, with a rather large pair of protruding horseshoe magnets, was used to sense the string vibrations at about one-seventh of the string length from the bridge. Many features of this initial patent predate supposedly “innovative” features of several modern instruments.



Fig. 22.4 An early Rickenbacker (a) “Electro” violin (1936) and (b) string-bass (1943) of the later design, both designed by Beauchamp

A later Electro model replaced the bakelite body with a hollow metal tube [Beauchamp 1940/43, US 2310199], to which a conventional neck and scroll were attached. This made for a very light string-bass; Fig. 22.4b. In this later model, the magnetic pickup was located close to the bridge, which was less in the way of the bow. Smith (1987, p. 15) includes 1939–1940 photos of Bert Lyn’s All Electric Orchestra, all using Beauchamp’s electric violin, cello, and bass instruments (and guitar).

The next major advance was made by Hugo Benioff, a geophysicist, who was already famous for designing seismographs around the world, which he used to map the sliding motion of tectonic plates over each other in the resulting areas of intense

seismic activity now known as *Benioff zones*. He also measured the strain across the St. Andreas fault in California, using a large piezoelectric crystal. Benioff applied his exceptional instrumentation skills to the design and development of piezoelectric transducers for the violin and cello [Benioff 1938/40, US 2222057] and piano [Benioff 1959/62, US 3049958]. In collaboration with the Baldwin Piano Company, he developed a conventionally strung piano without a sound board, using instead piezo-pickups at the end of each string to sense and then electronically amplify the string vibrations. A highly acclaimed recital on such an instrument was given by Rosalyn Tureck in Carnegie Hall. But to his dismay, the collaboration was terminated, when the company accountants claimed the piano would cost over \$100,000 to manufacture.

On June 13, 1938, the *New York Times* reported that “after many years of research, Benioff had invented a “seismographic” electric violin, astonishing musicians by the depth, volume, and clarity of its tones.” Many leading musicians tested the instrument and “without exception pronounced Dr. Benioff’s invention superior in tone to the orthodox counterparts.” Benioff used a pair of piezoelectric crystals mounted on either side of short and relatively thin, vertical cantilevers, supporting each string. The bending of each cantilever induced a voltage in the piezo-crystals proportional to the force acting on them from the vibrating string. This innovation was the forerunner of the wide range of piezoelectric bridge transducers in common use today and of the later multistring piezoelectric pickups, in particular those developed by Max Mathews [1988/89, US 4860625] and Richard Barbera [1987/89, US 4867027].

Unlike the electric guitar, the electric violin never became a major commercial success until well toward the end of the twentieth century, despite its occasional use in dance and jazz bands in the intervening period. But today, there is scarcely a pop singer or group that does not include an array of electric violins in its backing section. Moreover, the electric violin has a modest presence in classical music, with several leading violinists, such as Nigel Kennedy and Vanessa May, and the cellist Yo-Yo Ma, frequently feature electric instruments in their performances and recordings, often with music specially written for such instruments by leading composers.

One of the attractions of electric instruments is the ease with which additional strings can be added to increase the playing range, with five- or six-string violins and cellos commonplace. In addition, electric instruments no longer need to have the large bodies required to radiate sound efficiently. They can therefore be far more robust and compact than their traditional counterparts. Compact electric string-basses are particularly popular in many jazz, rock, and pop-groups.

Many companies worldwide now produce electric violins, cellos and basses in addition to guitars. There are also a large number of excellent makers of hand-crafted, custom-designed, instruments. A small selection of such instruments, illustrating the creativity in design afforded by solid-bodied instruments, is shown in Fig. 22.5.

There is also a rapidly expanding market for colorful and inexpensive “student-quality” electric violins, which are easier to bow than conventional instruments and



Fig. 22.5 Three handcrafted modern electric violins and one bass

can be electronically filtered to give a much more encouraging, less grating, sound than generally produced by a beginner learning to play on a small-sized violin. Moreover the violin can be played silently and listened to through headphones, without distracting the rest of the family or neighbors. A strong argument can be made for beginners to start learning on such instruments until they have gained the necessary skills to make an acceptable sound on a conventional acoustic instrument.

22.4 Acoustic, Magnetic, and Piezoelectric Pickups

There are currently three main types of pickup used to convert the vibrations of the plucked or bowed strings into electrical signals – acoustic, magnetic, and piezo-electric. Each pickup imparts its own characteristics to the amplified sound of the instrument, which also depends on the location of the pickup, amplification, and subsequent electronic processing, as described in this section.

22.4.1 Acoustic Pickups

The easiest way to amplify the sound of a conventional acoustic instrument is to mount a small microphone close to the body, or sometimes even inside the instrument. Alternatively, one can affix an inexpensive thin-film piezo pickup (available as an encapsulated device) to a vibrating surface of the instrument.

In both cases, the sound will be somewhat different from the normal radiated sound, because any microphone or transducer will be sensitive to the air or plate vibrations in the immediate locality of its mounting position, rather than experiencing the sound or vibrations of the instrument as a whole. However, such transducers can easily be attached to an acoustic guitar, violin, cello, or bass, without any significant modification, other than requiring some way to attach a lead or wireless connection to the amplifying electronics. A player can therefore easily switch between playing the instrument normally or with electric amplification. The instrument also feels perfectly natural to play, and the sound quality remains to a large extent determined by the acoustic properties of the instrument itself – unless significantly changed by subsequent audio signal processing.

A potential problem with any such pickup is acoustic feedback, resulting in the familiar howls of many public address systems when the amplifier gain is too high. Contact film pickups are less susceptible to such problems than microphones. However, contact pickups are more susceptible to *microphonics* (spurious signals) from accidental hitting or tapping the body of the instrument.

22.4.2 Magnetic Pickups

From the earliest days of the electric guitar, magnetic pickups have been used to sense the vibrations of the plucked strings directly. Magnetic pickups were also initially used for the electric violin, sensing the bowed-string-induced rocking motion of the bridge. Major advances in design and magnet technology have led the much more compact types of magnetic pickup in wide use on guitars today. In contrast, most electric violins now use piezo pickups attached to or encapsulated in the bridge.

A magnetic pickup works by sensing the vibrations of a plucked steel string vibrating close to one end of a magnetized iron rod or pole. The vibrations change the amount flux passing through the pole piece. This induces a voltage in the surrounding multturn coil, which is then amplified and filtered as appropriate. The geometry is illustrated schematically in Fig. 22.6a. Provided that the string vibrations are not too large, the induced voltage will be proportional to the vertical velocity of the wire, assuming the string is located immediately above the pole piece. Any transverse motion will induce a much weaker pickup at twice the string frequency, since the induced signal will be the same whether the string moves to the left or right.

The stronger is the magnetizing field, the larger will be the induced signal. Modern magnets are usually complex alloys of iron, with small additions of aluminum, cobalt, and nickel to improve their hysteretic magnetic properties. Professor Steven Errede at the University of Illinois at Urbana-Champaign has published detailed measurements on several hundred commercial magnetic pickups (Dünnewald 1991). Typical magnetic field at the ends of the pole pieces are ~600–800 G for a fully magnetized

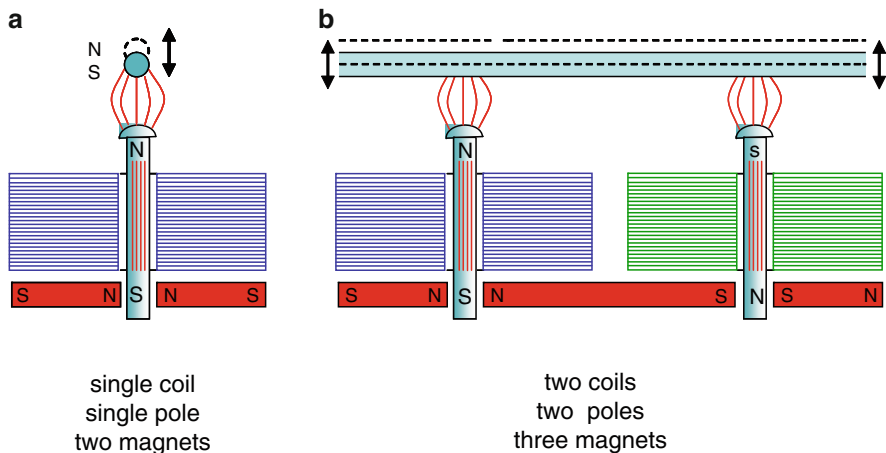


Fig. 22.6 (a) Single-pole pickup illustrated transverse to length of steel string, and (b) the Gibson *super-humbucking* pole configuration, with the coils surrounding the poles to the left and right wound in opposite directions to eliminate mains pickup

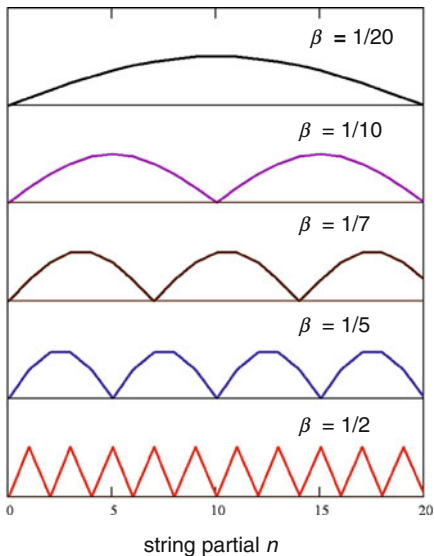
AlNiCo-III alloy, ~900–1,100 G for an AlNiCo-V alloy, and ~800–1,100 G for modern ceramic materials.

Magnetic pickups can clearly only be used with steel strings. The inharmonicity of solid steel strings – resulting from their finite rigidity – immediately introduces a much more “metallic,” longer-ringing sound than that of gut strings on an acoustic instrument.

Magnetic pickups also have a peak in their output at a resonant frequency $f_o = (1/2\pi) \sqrt{1/LC}$ and a significantly reduced response at higher frequencies. This results from the large inductance L (typically several henries) and capacitance C between the very large number of coil windings. Resonances for single-coil pickups are typically in the range 5–10 kHz, with a quality factor $Q \sim 4–8$, the latter limited by the large resistance of the coils $\sim 5–10 \text{ k}\Omega$. All such parameters are strongly design- and, to some extent, frequency-dependent (Dünnewald 1991). Different pickups therefore produce different sounds, so the choice of which magnetic pickup to use can be a highly charged subjective issue. The relatively high impedance (reactive and resistive) of the coil winding requires the use of an amplifier with an input impedance of at least $1 \text{ M}\Omega$, if the output signal is not to be attenuated significantly, especially at high frequencies.

The sound produced by a magnetic pickup also depends on their position along the length of the vibrating string, illustrated schematically in Fig. 22.7. If, for example, the pickup were to be placed at the center of the string, it would only be sensitive to the odd partials of the plucked string, because all the even partials would have a node at that point. Likewise, if the pickup were located at a fractional distance β along the string, there would be no output from the $1/\beta$ -th partial or any of its multiples, but it would have maxima in between, as illustrated.

Fig. 22.7 The dependence of the sensitivity of the n th partial of a plucked note for a magnetic pickup located at a fractional length β of the vibrating string from the bridge



Sets of pickups at different lengths along the string therefore produce different sounds. Transducers close to the bridge will give a relatively low output for the lower partials, but will retain a strong output with no significant *drop-out* across the audio frequency range resulting in a bright sound. Conversely, transducers near the end of the fingerboard will have a much stronger output for the lowest partials, but a marked attenuation of some of the acoustically important higher partials, resulting in a more mellow tone. A set of pickups located in between will give an intermediate sound quality. By varying the combination of signals from pickups at different positions along the length of the string, the player has considerable control over the kinds of sound produced. Typical pickup positions for modern instruments can clearly be seen in Fig. 22.3.

A potential problem with magnetic pickups is *hum* from nearby mains power supplies. Nonlinearity in mains power transformers and other electrical equipment generates magnetic pickup at multiples of the 50–60 Hz supply frequency – well into the audio range. Such pickup can usually be eliminated by the use of what are termed *humbucking* coils patented in 1955 by Seth Lover for Gibson [1955/59, US 2896491]. This involves the use of two closely spaced pickups along the string with their outputs added, but with their sensing coils wound in opposite directions, so that external pick in one is canceled by the other. A schematic diagram illustrating one such coil and polarizing magnet configuration is shown in Fig. 22.6b. This accounts for the familiar double row of poles of humbucking coil pickups on the Gibson and Rickenbacker instruments in Fig. 22.3.

Because humbucking systems use two pickup coils, they have a larger inductance and stray capacity than single-coil pickups. This results in a lower resonant

frequency and high-frequency cut-off than single-coil pickups, resulting in a somewhat mellower tone. They also have a slightly different frequency response because they sense the motions at different points along the string. The use of single- or double-coil pickups and their placement along the string results in marked degree of flexibility in the design of pickups for the electric guitar, which accounts for the different sounds of commercial instruments.

22.4.3 Special Sound Effects

Almost all electric guitars have easily operated volume and tone controls on the instrument itself. The tone controls are often just simple CR-filters attenuating or enhancing the bass and treble responses. However, with the increasing sophistication of audio processing technology, computer-controlled software and audio digital signal processors, the sound can now be transformed in almost any conceivable way.

In the 1960s, it became fashionable to include additional sound *effects*, for example, by introducing a controlled amount of distortion resulting from clipping the tops off of the waveforms, giving the sound an additional buzz, edge, and impact. Other popular effects included the use of:

Phasers where the pickup signal is divided into two paths. In one path the phases of the various partials is changed. When the two signals are recombined, additional *notches*, or zeroes, in the output spectrum occur, when the amplitudes and phases of particular partials cancel. By varying the phase changes with time (e.g., driven by a low-frequency electric oscillator) a number of interesting sounds can be produced.

Flangers are essentially phasers in which the filter characteristics are determined by delaying one signal relative to the other. This produces a distinctive sound quality, that can again be varied electronically. Feedback can also be incorporated to obtain interesting reverberation effects.

Wah-wah used by Leo Fender as early as 1945, involves feeding the guitar sound through a filter with a formant structure similar to that of the human voice. By modifying the strengths and positions of such formants with a foot pedal, the plucked strings can be made to mimic the *wah-wah* sound of the human voice. The intensity of the sound can be used to control the formants to obtain other interesting sounds.

In recent years, sound processing has been transformed by the use of computers and dedicated digital sound processors. In addition, there has been a shift from analog to digital electronics, with Gibson introduced the first fully digital electronics guitar in 2002, and more recently a guitar with computer-controlled tuning screws to tune each string automatically. Despite such advances, many players take great pride in playing instruments that reproduce the iconic sounds of the 1960s.

22.4.4 Piezoelectric Pickups

Although the first electric violins tended to use magnetic pickups actuated by the rocking action of the bridge, guitar-like magnetic pickups sensing the motion of the string directly have never been popular, because they require steel strings, which are less flexible and are more difficult to bow than gut or synthetic strings. The majority of electric violins therefore use piezo (piezoelectric) pickups attached to or encapsulated in the bridge.

A piezoelectric material is an insulator with an asymmetric molecular structure (see, e.g., Gautschi 2002). Introducing strain can result in atoms on one side of a thin slab of piezoelectric material acquiring a positive charge, while atoms on the opposite side acquire an equal but negative charge. The charge is proportional to the amount by which the material is strained (i.e., compressed, stretched, bent, or sheared). Rather like the magnetism of a magnet, the effect can be increased in strength by initially *electrifying* or *polarizing* the piezoelectric material in a very strong electric field.

Changes in surface charge can then be sensed by the voltage $\Delta V = \Delta Q/C$ across metal electrodes attached to the surfaces, where ΔQ is the deformation-induced charge and C is the capacity between the electrodes, typically 100–1,000 pF. The voltages produced by compressing a modern piezoelectric material can be many thousands of volts, generating the spark in a handheld gas lighter. Their high sensitivity to strain makes them ideal detectors of the small strains set up in the bridge by the force acting on it by bowed or plucked strings.

A particularly useful transducer is the bimorph piezo-strip, in which two long strips of piezoelectric material are glued together with a metallic electrode between them. As the strip is bent, the piezo above the central strip is extended while the other is compressed. This results in equal and opposite charges and voltages across the two outer surfaces. Small amounts of bending cause very large changes in the extension and compression along the length giving a large output.

Although the voltages produced by a piezoelectric transducer can be very large, the pickup can also be very rapidly discharged by the input resistance R of any amplifier placed across it. The CR discharging time-constant is 10^{-3} s for a 1,000-pF device connected to a 1-MΩ input impedance amplifier. This would lead to a very rapid attenuation of audio signals at kHz frequencies and below. To achieve a strong output across the whole audio frequency range, amplifiers with input resistances of at least 10^7 to -10^8 Ω must be used. Fortunately, this is not a problem using modern solid-state electronics.

For bowed string instruments there is a virtue in making use of a low-frequency cutoff. This arises because, at the start of every bowed note, or at any time the bow changes direction, there is a sudden change in direction of the force exerted by the bowed string on the bridge. This step in the dc-force is picked up by any piezoelectric crystal mounted on the bridge, and results in a characteristic and annoying *clunk* in the output sound. Most of the associated sound energy is concentrated below ~250 Hz, which will still be strongly radiated by a high-quality sound system.

However, for a real violin, very little of this sound is heard, because the violin is such a poor radiator of sound below the air resonance at ~280 Hz.

Like magnetic pickups on the guitar, piezoelectric pickups are susceptible to mains hum, but this time from electric rather than magnetic fields generated by adjacent mains power supplies. In the absence of any electrical screening, the voltage on the pickup can be as large as a few volts, which appears on both electrodes, in addition to the strain-induced voltage across them. Although an ideal amplifier would only be sensitive to the difference in voltages across its inputs, in practice, amplifiers are also sensitive to their average voltage. To minimize such problems one needs to screen the pickups and connecting leads as well as possible and to use well-designed amplifiers with a high *common-mode* rejection. Most manufacturers of piezoelectric pickups provide helpful information on their websites about minimizing such problems.

Figure 22.8a illustrates typical mounting positions for a number of commercially available piezo pickups mounted on a conventional violin bridge. Transducer A measures the velocity or acceleration at the top of the bridge. The transducers B bridging and C wedged into the side-slot respond to the flexing of the top of the bridge relative to the supporting feet, while the embedded piezo bimorph strip E measures such bending directly. The two transducers D clamped between the feet of the bridge and the top plate respond either to the force exerted by the feet on the top plate or to the induced plate bending, depending on their design. Ideally, at low frequencies, all such transducers should give an output proportional to the force of the bowed strings on the bridge. However, the bridge and sometimes the pickups themselves have a resonant peak in their output at ~1.5–3.0 kHz and a sharp decrease in sensitivity at higher frequencies, as

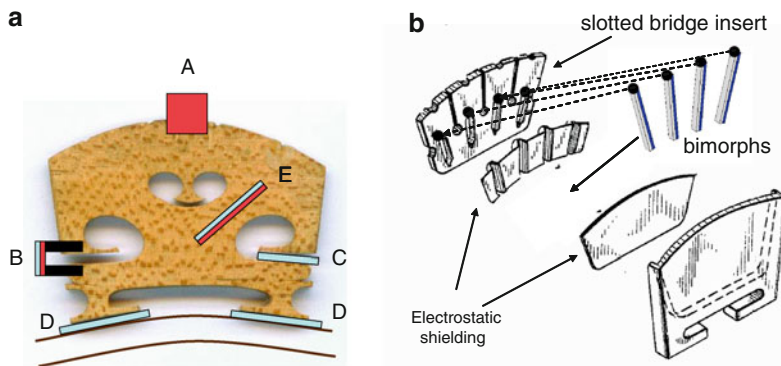


Fig. 22.8 Piezoelectric crystal configurations on (a) a conventional violin bridge and (b) an exploded view of a multidetector array to record signals from individual strings (after Barberi patent)

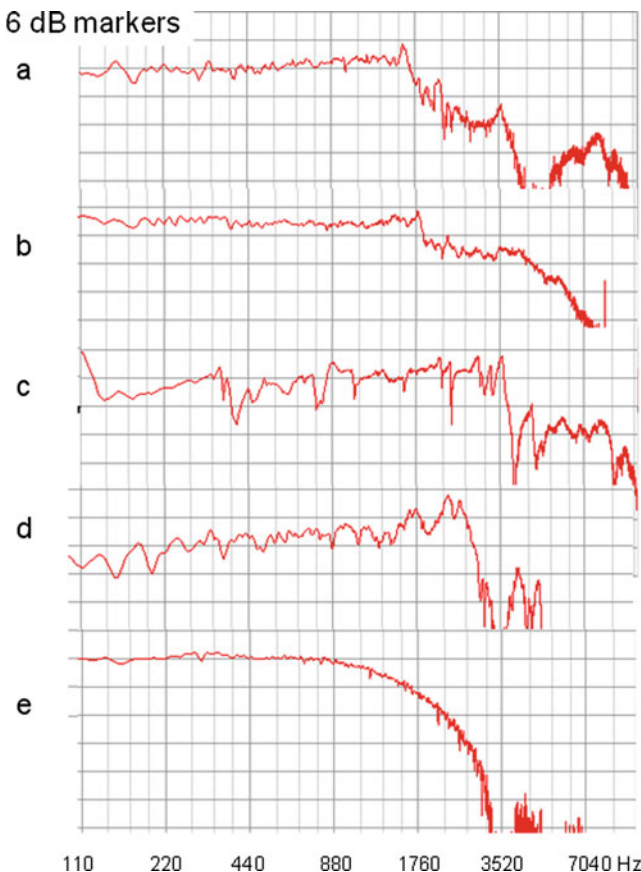


Fig. 22.9 Frequency response of piezo pickups from impact measurements illustrating marked differences between different transducers and mountings. (a) Barcus–Berry side-clip on Vuillaume, (b) Violectra bridge on electric violin, (c) encapsulated piezo in solid bridge on electric violin, (d) Twin-T under-feet Carmen pickup on electric violin, and (e) Shadow-Twin on Vuillaume

illustrated by some representative measurements in Fig. 22.9. Superimposed on the overall trend, there is often additional structure from the resonances of all the strings supported by the bridge.

Many electric violins use a somewhat heavier bridge, often with separate piezo pickups under each string. Such pickups can be used as separate inputs to drive a MIDI or more sophisticated computer-controlled sound systems, or can be connected in series to give a single output. A schematic exploded view of the Barberi multistring transducer [187/89, US 4867027] is illustrated in Fig. 22.8b. An additional objective of such a pickup is to give an output from each pickup that is insensitive to the vibrations of adjacent strings.

For research, one often requires transducers that only respond to the forces exerted by the bowed string, unaffected by any resonances of the bridge or body of the instrument. It can be argued that this should be the aim of any commercial pickup, too, because nowadays it is relatively simple to achieve any desired frequency response by subsequent analog or digital filtering.

Benioff [1938/40, US 2222057] and Matthews [1988/89, US 4860625] pioneered the design of such bridges using piezo crystals to measure the bending of short cantilevers supporting the individual strings. Scherer [1966/69, US 3453920] patented a bridge with orthogonally oriented pairs of pressure sensitive piezo crystals, to record both the vertical and horizontal forces exerted by the bowed string on the bridge – in much the same way as that used in stereo pickups for LP records. A similar design was used by McIntyre and his colleagues in Cambridge to investigate details of the bowed string waveforms (McIntyre et al. 1981).

Like the electric guitar, the use of a solid body and a heavy bridge on an electric violin has a marked effect on the way the strings vibrates after it is plucked or bowed – because of the much reduced transfer of energy from the strings to the body of the instrument. Although considered a virtue for certain guitar styles, this can be a problem for the electric violin or cello, especially for the heavy lower strings, which can continue ringing for several seconds. Moreover, if a relatively light bridge is used, there can be significant coupling between the strings via the bridge. Notes played on higher strings can then excite sympathetic vibrations of the higher partials of the lower strings. These keep ringing for long after the note that excited them has stopped, providing a troublesome drone at the pitch of the lowest open string. The only way to prevent such a problem is to design a bridge that minimizes the coupling between adjacent strings or to introduce some additional damping of the lowest resonating string. One way to achieve this is to mount the lowest string across a thick rubber ring, which increases the damping without changing significantly the pitch of the note.

22.4.5 Other Types of Pickups

Although magnetic and piezoelectric devices are by far the most common transducers in use today, a number of new transducer types are beginning to appear on the market. These include optical pickups (e.g., Lightwave Systems, California], which use infrared photo-detectors to sense the vibrations of the string close to the bridge, and magneto-resistive or Hall-effect pickups to replace conventional magnetic pickups. In addition, a number of guitar manufacturers now incorporate piezo pickups in the saddle, which can be used in combination with magnetic pickups to give an even wider range of tonal characteristics.

22.5 The Electric Violin as a Research Tool

Electric violins with transducers accurately measuring the force of the bowed string on the bridge provide an invaluable tool for investigating the acoustics of real violins. Figure 22.10 illustrates the different ways in which the acoustic and electric violin convert the bowed-string force at the bridge into radiated sound. In the electric violin, the acoustic filtering of the multiresonant shell of the violin is replaced by electronic filtering, which can range from the simple analog tone controls used in many commercial instruments, a bank of resonant filters, to a powerful, computer-controlled, digital signal processing system. Whereas the acoustic violin radiates sound via the vibrational modes excited on its shell – with a highly directional multiresonant response – the electric violin uses a loudspeaker (or a pair of headphones), ideally with a flat-frequency response.

The dotted lines in Fig. 22.10 illustrate how the bowed string input and output sound from a real violin can, in principle, be fed into an electric violin to reproduce the sound of the original instrument. The filter characteristics can then be changed, allowing the player and listener to assess the relative importance of various filter characteristics on the output sound.

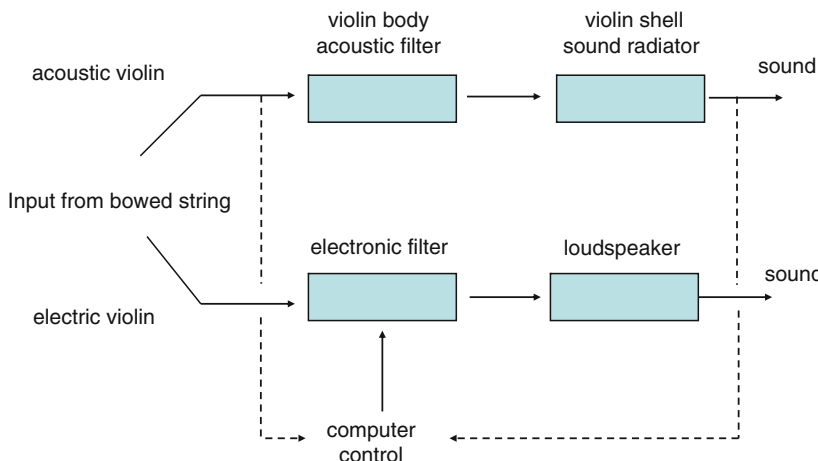


Fig. 22.10 A schematic representation of the signal paths of an acoustic and electronic instrument with *dashed lines* indicating the use of inputs from a real violin controlling the output of an electric violin

22.5.1 Multiresonant Filter Characteristics

Mathews and Kohut (1972) at the Bell Laboratories pioneered the use of the electric violin as a research tool. They used a bank of resonant filters with adjustable resonant frequencies and damping, to mimic the multiresonant response of the violin. To measure the bowed string vibrations they used two horseshoe magnets attached to the face of a relatively heavy bridge, with the four pole-pieces immediately below the four strings. The motion of the strings in the magnetic field induced voltages in the metal-covered strings, which were added together, amplified, passed through the filter bank, and played back to a panel of listeners through a loudspeaker.

A range of experiments were performed, initially with a bank of 20 resonant frequencies chosen to reproduce 17 prominent peaks on a Stradivarius response curve, plus three additional higher frequencies to cover a frequency range extending to 4,500 Hz. The damping of each resonance could be varied to give an essentially flat response across the whole spectrum to a response with peak-to-valley height differences between resonances of order 20–30 dB. Subjective listening tests were made as a function of damping for notes played with and without vibrato. To eliminate the inevitable variability in performance of the player, a tape recording of a given sequence of notes was used as the input for all subjective assessments using different filter bank arrangements.

Members of the listening panel were mostly violinists or those used to listening to violins. The sound was judged best for a peak-to-valley ratio of around 10 dB. The flat response gave an even slightly harsh sound and was unresponsive to the use of vibrato and modulations in bow pressure. When the damping was reduced to give a large peak-to-trough ratio ~20 dB, the sound became hollow with obvious changes in intensity from note to note. This implies that damping must always be a compromise between being too large, resulting in an unresponsive instrument, or too small, resulting in a hollow-sounding uneven instrument.

The authors then doubled the number of resonances keeping the peak-to-valley difference ~12 dB. The resulting sound was judged to be slightly more brilliant, but the difference was small. In a second experiment they used 24 equally spaced resonances, a tone apart, with an unchanged peak-to-valley ratio. This was judged to be slightly better than the 20 Strad-based resonances, and was comparable in quality to the sound of the higher-density filter bank. The one exception to the above results was the sound of low notes on the G string, which for the evenly spaced resonances sounded more like a viola, while the more widely spaced “Strad resonances” sounded more like a violin.

These observations highlight the importance of peaks and valleys in the frequency response of real violins, which give rise to complex time-varying waveforms and fluctuating variations in timbre when vibrato is used. Mathews (1969) had already argued that such complexity was important in any subjective assessment of the richness of tone of an instrument. Later researchers (Meyer 1992; Mellody and Wakefield 2000; Gough 2005) have also used electric violins to demonstrate and assess this hypothesis.

Mathews and Kohut also noted solid-bodied electric violins appear to be somewhat easier to play than conventional violins, with an apparent quickness in response and longer decay times, especially on the lower strings. This is almost certainly associated with the reduced loss of energy transfer from the string to the body of a solid-bodied electric instrument.

22.5.2 Sound Perception and Acoustical Properties

A rather different kind of project, addressing the relationship between the perceived sound of a violin and its acoustical properties, is currently being undertaken by Claudia Fritz in Cambridge, in collaboration with Jim Woodhouse, Brian Moore, and Eric Cross, who are leading experts in acoustics, psychoacoustics, and music, respectively (Fritz et al. 2007). For the first time, rigorous psychoacoustic procedures have been used to relate differences in the perception of sounds to differences in the measured acoustical properties of violins. This is the first step toward a rigorous psychoacoustic exploration of why some violins sound better than others.

To accomplish this task, a normal violin with a conventional bridge with force-sensitive pickups under each string was played by a skilled player. This signal was then used as the input to an artificial electric violin corresponding to the lower half of Fig. 22.10. In an independent set of measurements, the input admittance (induced velocity per unit applied force) of the bowed violin was measured at the point of string support on the bridge. The frequency response of the admittance exhibits all the excited resonances of the body of the instrument and was used as the filter for the electric violin. The measured input from the bowed string could then be “played” through this filter and listened to by members of the assessment panel through high-quality headphones. To give a more realistic impression of the radiated sound of the original instrument, the amplitude of the air resonance at around 280 Hz was increased to reflect its strong radiating properties.

The experiment used the SignalWizard 2 audio signal processor developed by Patrick Gaydecki (2007), which allows the real-time filtering of an input audio signal using any previously measured or computed frequency or impulse response. It is then easy to compare sounds as the filter properties are changed by controlled amounts. This can be done using the real-time input from a violinist playing the electric violin, though more reliable, reproducible, subjective testing requires a previously recorded bowed input signal.

The investigation examined by how much the center frequencies and amplitudes of the three acoustically important low-frequency resonances of the violin (A_0 , B_1^- , and B_1^+) and the four frequency bands considered by Dünnewald (1991) to define the richness, nasality, brilliance, and clarity of a violin’s tone (190–650, 650–1,300, 1,300–4,200, and 4,200–6,400 Hz) needed to be changed before such changes became audible. A large number of musicians and nonmusicians were tested and their individual responses were analyzed.

Typically, musicians were slightly better at discriminating small changes than nonmusicians, though not surprisingly the results varied from note to note, as their partials were affected in different ways by the changes made. In general, it was found that the amplitudes of individual resonances could be changed by $\sim 4\text{--}8$ dB and resonant frequencies by 10–20% before musicians could detect a difference in the sound. Such information is clearly important to makers, as it implies that positions and amplitudes of resonances can be changed by quite significant amounts before changes can be heard in the perceived sound. The authors were also able to demonstrate that their findings were in excellent agreement with current models of auditory perception.

22.5.3 *Real-Time Synthesis of Cremonese Instruments*

Finally, we briefly mention attempts by Gabi Weinreich and the distinguished American violin maker Joe Curtin (2007) and by Gough (2005) to reproduce in real time the sounds of great Italian instruments on the electric violin. In both investigations, the SignalWizard processor was again used, but this time with a filter derived from the radiated sound following a sharp tap at the bridge, rather than the induced motion of the bridge. The SignalWizard digitizes the input signal from the bowed electric violin, essentially producing a sequence of sharp taps at the digitizing rate, with heights that follow the input waveform. Each one of these taps then generates a pulse of sound identical to the measured tap tone response of the original instrument. The sound at any moment is therefore the sum of sounds from all earlier taps, a process known as *convolution*.

In principle, this means that anyone can reproduce the sound of a great Italian instrument on an electric violin, providing the acoustic impulse response of the Stradivari or other chosen instrument has first been measured. However, there are some intrinsic problems. The most important of these arises because the acoustic impulse response is recorded at a particular point in the original performance space. The sound would therefore only be the same, if it was listened to with one ear using a specially designed headphone that mimicked the response of the microphone originally used to record the sound. Instead, the sound would generally be replayed by a loudspeaker in yet another performance space. However, this may not be such a serious problem, firstly because the sound quality of a great violin being played by a great player does not change significantly from position to position in the recording studio or concert hall. Furthermore, a great violin still sounds wonderful when one ear is covered in the concert hall or when only one ear is used on a stereo pair of headphones.

Even if the routine reproduction of the sound of really great instruments may be something of a dream, one can certainly change the sound of the electric violin dramatically in many ways using a computer-controlled signal processor. This must

surely be one of the most important opportunities for the future development of the instrument.

For this to happen, the electric violin has to be made even easier to use. Future developments may well include electric violins with rechargeable batteries driving an integrated, on-board, computer to control the filter characteristics and the sound of an integrated loudspeaker. The instrument would then be truly portable. At the flick of a switch (or voice command) the player could choose to play a Stradivarius, Guarnerius, or two-stringed Chinese violin, use automatic pitch correction to play in tune, play double bass parts on the violin, produce sounds completely different from that of any other known musical instrument, and play with any prerecorded band, orchestral group, or pianist. The possibilities are limitless. It would be fascinating to read the contents of a similar chapter on electric stringed instruments in 50 years time!

References

- Bacon T (2006) *Electric Guitars: The Illustrated Encyclopedia*, Thunder Bay Press, San Diego, CA
- Day T (2000) *A Century of Recorded Music* (Yale University Press, New Haven and London)
- Dünnewald H (1991) Deduction of objective quality parameters on old and new violins. J Catgut Soc (Series II) 1, 1–5
- Errede S (2008) http://online.physics.uiuc.edu/courses/phys199pom/Labs/Electric_Guitar_Pickup_Measurements.pdf
- Evans T, Evans MA (1977) *Guitars: From the Renaissance to Rock* (Paddington Press, New York & London)
- Fritz C, Cross I, Moore BCJ, Woodhouse J (2007) Perceptual thresholds for detecting modifications applied to the acoustical properties of a violin. J Acoust Soc Am 122, 3640–3650
- Gautschi GH (2002) *Piezoelectric SensoNics* (Springer, New York)
- Gaydecki P (2007) A new multi-channel real-time digital signal processing platform for acoustic signal processing and sensor response emulation. J Phys Conf Ser 76, 012048
- Gough CE (2005) Measurement, modeling, and synthesis of violin vibrato sounds. Acta Acustica/Acoustica 91, 229–240
- Graesser H, Holliman A (1998) *Electric Violins* (Verlag Erwin Bochinsky, Frankfurt)
- Heaney BA (2007) *A Short Illustrated History of Stroh Violins, 1899–1949* <http://www.digital-violin.com/StrohViolin1.html>
- Mathews MV (1969) *The Technology of Computer Music* (MIT Press, Cambridge, MA)
- Mathews MV, Kohut J (1972) Electronic simulation of violin resonances. J Acoust Soc Am 53, 1620–1626
- McIntyre ME, Schumacher RT, Woodhouse J (1981) Aperiodicity in bowed-string motion. Acustica 49, 13–32
- Melldoly M, Wakefield GH (2000) The time-frequency characteristics of violin vibrato: modal distribution analysis and synthesis. J Acoust Soc Am 107, 598–611
- Meyer J (1992) Zur klanglichen wirkung des streicher-vibratos. Acustica 76, 283–291
- Radio News (1927) Vol. 8, No. 10, April
- Ratcliffe A (2005) *Electric Guitar Handbook* (New Holland Publishers, UK)
- Smith RR (1987) *The History of Rickenbacker Guitars* (Rickenbacker Int Corp, Fullerton, CA)
- Weinreich G, Curtin J (2007) *Michigan Daily*, March 22. <http://media.www.michigandaily.com/media/storage/paper851/news/2007/03/22/TheBSide/Making.The.Perfect.Violin-2786562.shtml>

Chapter 23

Virtual String Synthesis

Nelson Lee and Julius O. Smith III

23.1 Introduction

In this chapter, we discuss methods for real-time synthesis of stringed instruments. Interest in this topic is wide and varying, as both studio and performance uses for realistic virtual stringed instruments are becoming increasingly possible with gains in computing power.

Having a high-fidelity physics-based virtual stringed instrument model is useful for many applications. Current sample-based synthesizers, which are based on audio recordings, do not allow fine control of the excitation of the strings of the instrument. Synthesizers based on physical models, in contrast, promise unlimited control over the expressive nuances of string excitation. The synthesis parameters are also more intuitive, because they have corresponding meanings in the physical world. Changing intuitive parameters can result in more realistic changes to the sound produced.

Another of many applications includes automatic transcription and re-synthesis of old recordings (Esquef et al. 2002; Välimäki et al. 2006). Given that there is a mechanism for processing old recordings and mapping them to how they were played on the instrument, with a high-fidelity synthesis model and the necessary performance parameters, re-synthesis of old recordings can be made to sound like what they would, had they been made with today's technology. Figure 23.1 shows the block diagram of such a system. The focus of this chapter is on the third circled block, the physical model of the plucked stringed instrument.

The goal of this chapter is to outline procedures for making a virtual stringed musical instrument based on a combination of physical theory and laboratory measurements from a real instrument. Because this topic is too large to be covered

N. Lee (✉)

Center for Computer Research in Music and Acoustics (CCRMA), Stanford University,
The Knoll, 660 Lomita, Stanford, CA 94302-8180, USA
e-mail: nalee@ccrma.stanford.edu

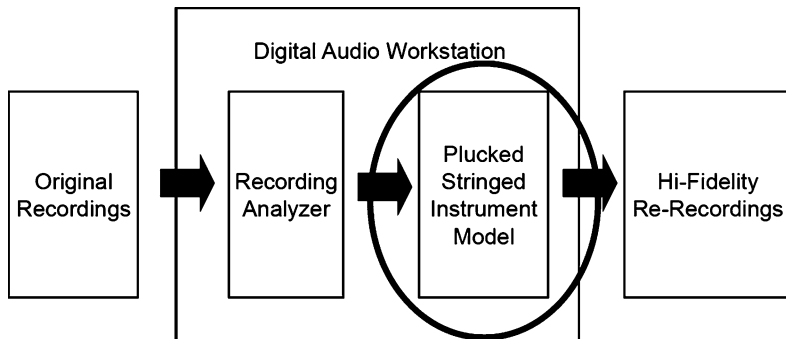


Fig. 23.1 Block diagram of a performance parameter estimation and re-synthesis of old recordings application

in the available space, we will make extensive use of pointers to supporting information. In addition to the traditional bibliographic citations, we will refer the reader to additional online books, related websites, and laboratory exercises covering elementary models and techniques used. Our goal is to make it possible to follow online links in this chapter in order to flesh out the complete details of the theory and practical techniques summarized here. For the advanced reader (such as a seasoned graduate student working in the area of virtual musical instrument design), this chapter will hopefully prove sufficiently self-contained to be used as a laboratory guide.

In the following sections, we provide a summary of common terms used in the digital modeling field, then briefly review elementary components of stringed musical instruments and how they may be modeled efficiently for real-time digital synthesis applications. We then summarize practical measurements and calibration techniques for various instrument modeling components. Finally, we discuss methods specifically for estimating parameters of a plucked stringed instrument.

A useful abstraction that illustrates our modeling approach for virtual stringed instruments is shown in Fig. 23.5. Not only is this decomposition useful for compartmentalizing from a modeling perspective, it is useful in performing measurements on the instrument as well as following the physical flow of how a stringed instrument is played: energy injected into the system to how energy reaches our ears by pressure waves created by the vibration of the instrument's body.

23.2 Nomenclature

To acquaint the reader with the digital domain, where the topic of virtual stringed instruments resides, we provide here a summary of terms and basic principles.

23.2.1 Digital Signals

In the present epoch, signals created or manipulated are typically digital. Through hardware, digital signals are later converted to analog form, but for the purposes of this chapter, all signals discussed are digitally sampled. Figure 23.2 shows the samples one may see, as taken from a sinusoidal signal, and the true analog signal from which the digital samples were sampled.

23.2.1.1 Sampling

Certain issues arise when we discuss sampling. For example, as Fig. 23.3 shows, between the two samples marked as starred points, an infinite number of signals could have been sampled to give the samples shown. We have drawn a DC signal of 0, a triangular signal, and three sinusoids that all pass through the starred points.

Within the digital domain, we are limited by the rate at which samples are taken. This is known as the *sampling rate*, the number of samples that are taken per second. The sampling rate also tells us the maximum discernible frequency component of a signal that can be captured digitally. This frequency, the highest frequency component we can determine, has been proven to be half the sampling rate.

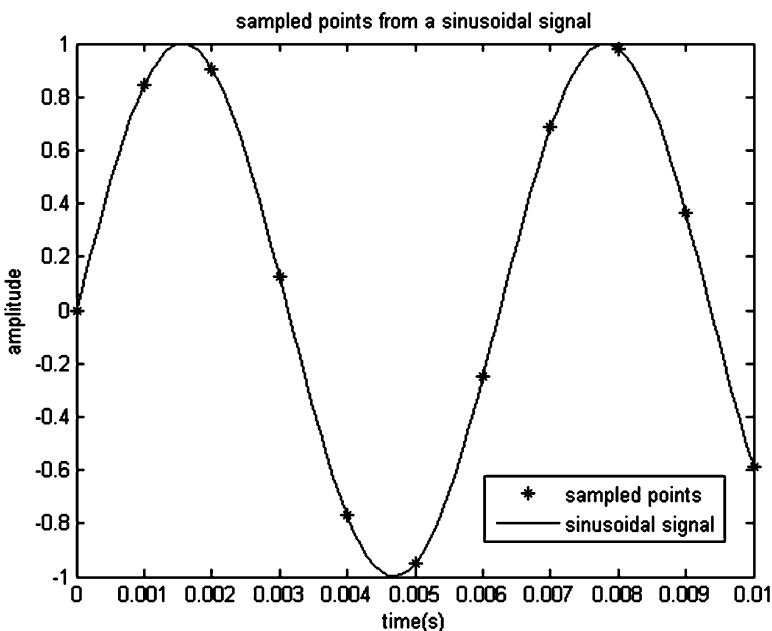


Fig. 23.2 Here we show the analog sinusoidal signal that could have generated the samples as starred points

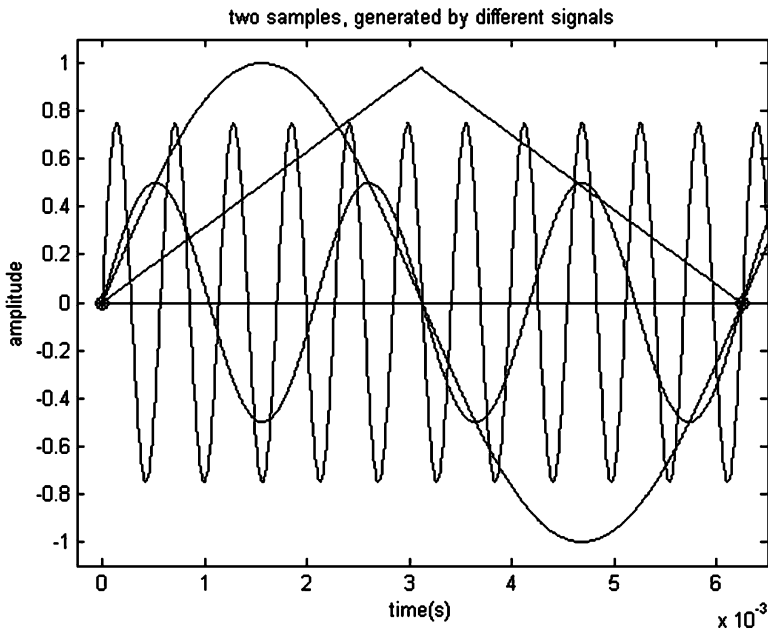


Fig. 23.3 Many analog signals could have been sampled to have generated the points at the *far left* and *right* of the graph with amplitudes 0. The signals plotted include three sinusoids, a DC signal of 0, and a triangular signal

For example, take the standard put in place for music CDs. The sampling rate is 44.1 kHz, which means that the highest frequency component within a music CD is 22.05 kHz. Since the limit of human hearing is 20 kHz, every frequency that can be heard by the human ear can be captured in a music CD. We refer readers interested in sampling theory to Oppenheim and Willsky (1996).

23.2.1.2 Sum of Sinusoids

From Fourier analysis, any signal can be composed of a sum of an infinite number of sinusoids (Oppenheim et al. 1989). Any arbitrary digital signal can be represented, and in general, approximated by a sum of sinusoids (approximated because having an infinite sum is unrealizable on any computing platform). Therefore, in digital signal processing, a digital signal can be viewed as being the sum of certain frequency components, with relative phase differences amongst them.

As an example, Fig. 23.4 shows how a signal is the sum of two sinusoids. Viewing the signal's Fourier transform, we are able to see that the signal is composed of two sinusoidal components at their respective frequencies. In essence, a digital signal, represented as samples taken in time, have a one-to-one mapping to

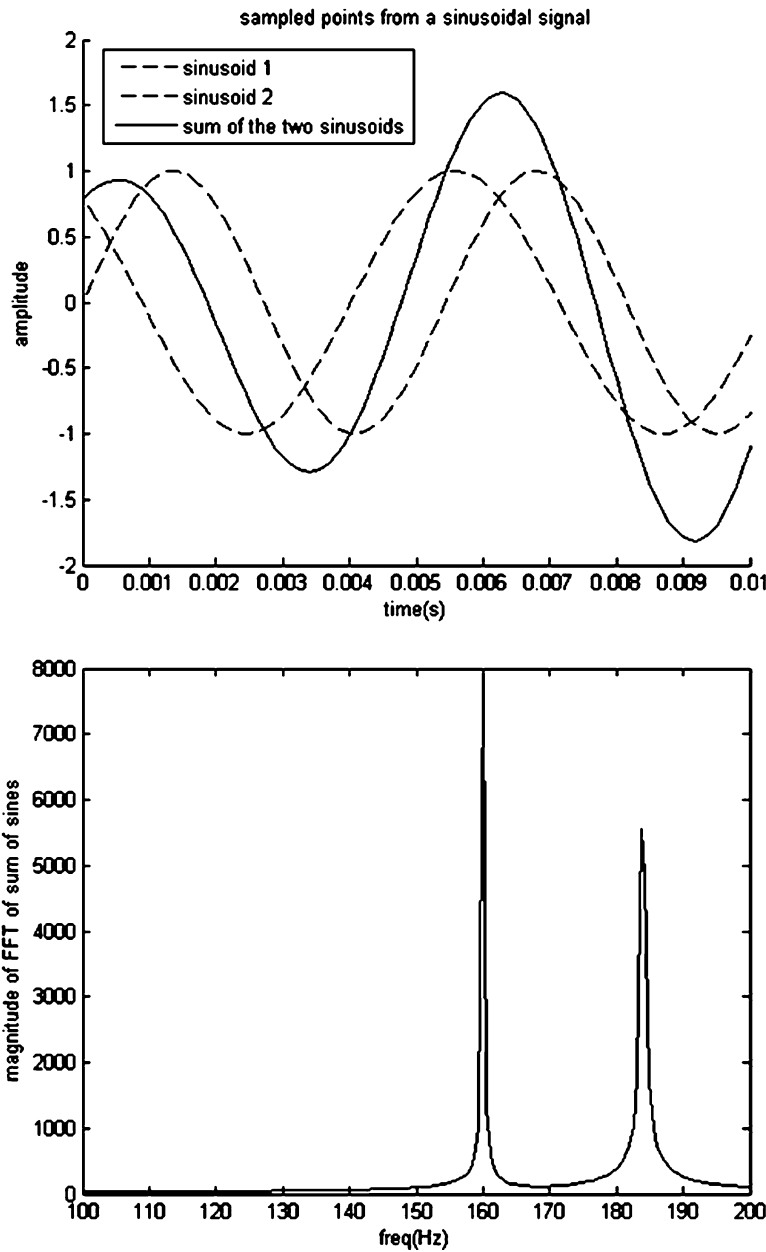


Fig. 23.4 (a) Time-domain signal equal to the sum of two sinusoids: one at 160 Hz and one at 184 Hz. (b) Spectral view of the signal in (a)

a Fourier signal in the frequency domain. Thus, in the case of digital filtering, it is often simpler to understand the function of a filter by its frequency response, both magnitude and phase, where the magnitude response determines how a corresponding time-domain signal with a specific frequency component is scaled, and the phase response determines how a corresponding time-domain signal with a specific frequency component is delayed, respectively.

23.2.2 Digital Filtering

Another frequently used term that takes on many meanings is the *digital filter*. For this chapter, a digital filter takes an arbitrary input digital signal, $x(n)$, and outputs a signal $y(n)$. In this broad sense, we can view the digital filter as a black box that performs any number of possible tasks. However, most filters used for audio are linear and time-invariant (LTI) (Smith 2007b). For example, an *equalizer* in a digital media player on a personal computer is a commonly used LTI audio filter. An LTI filter can be described by its *frequency response*, a complex function of frequency that specifies the gain and delay imposed by the filter on sinusoidal signal components at frequencies up to half the sampling rate. The filter that outputs its input, meaning $y(n) = x(n)$ is also a digital filter; though a trivial one. Cementing these concepts with Sect. 23.2.1, the trivial filter described has a frequency response of magnitude one at all frequencies, and a frequency response with zero-phase at all frequencies. In our equalizer example, the ideal frequency response would have a zero-phase frequency response, with a magnitude response equal to the desired scaling given by the user of the equalizer.

23.3 Elements of Stringed Instruments

In all stringed instruments, the strings are put into motion by an external force typically applied by a finger, plectrum (*pick*), hammer, or bow. The vibrating string transfers energy into the body/resonator of the instrument, which in turn produces pressure waves in the air that propagate to our ears (Fig. 23.5).

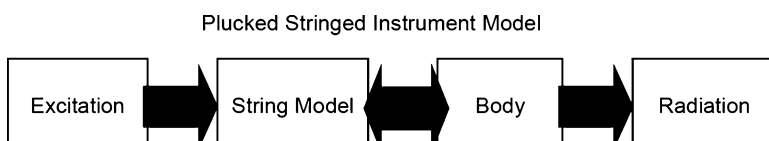


Fig. 23.5 Stringed instrument decomposition abstraction block diagram

23.3.1 Vibrating String

In this section, we briefly describe the physics of the string and its corresponding virtual representation. We describe how this model of the string is analogous to its physical counterpart and describe various initial conditions for the different ways the string can be set into motion. We then discuss more complex modeling techniques for the vibrating string, initial pitch shifts, the coupling of multiple strings and the vibration of the string in two orthogonal planes, and how such modeling techniques can describe natural phenomena such as two-stage decay.

23.3.1.1 D'Alembert's Wave Equation

The formulation of the wave equation and its solution in 1747 by d'Alembert (1973) is the theoretical starting point for vibrating string models. The wave equation, written as

$$K \frac{\partial^2 y}{\partial x^2} = \varepsilon \frac{\partial^2 y}{\partial t^2} \quad (23.1)$$

where K is the string tension, ε is the linear mass density, and $y(t, x)$ is the string displacement as a function of time (t) and position along the string (x). It can be derived directly from Newton's second law applied to a differential string element. In addition to introducing the equivalent of the 1D wave equation, d'Alembert introduced its solution in terms of traveling waves:

$$y(t, x) = y_r \left(t - \frac{x}{c} \right) + y_l \left(t + \frac{x}{c} \right) \quad (23.2)$$

where $c = \sqrt{K/\varepsilon}$ denotes the wave propagation speed. Though each individual traveling wave is normally unobservable in the physical world, they are useful constructs for modeling the physical behavior of the string, the displacement of which is equal to the sum of the two traveling waves.

Figure 23.6 shows an idealized infinite-length physical string's displacement, initially displaced to form a triangular pulse. The initial string shape is equal to the sum of its left and right traveling-wave components at time $t = 0$. By symmetry, the two components are equal. The arrows in Fig. 23.6a show the points of displacement at time $t = 0$. Subsequent frames are shown, as the bottom plot of each frame corresponds to the physical displacement of the string. The top and middle plots correspond to the right and left traveling waves, respectively. Further details are given in (Smith 2010).¹

¹ http://ccrma.stanford.edu/~jos/pasp/Traveling_Wave_Solution_I.html

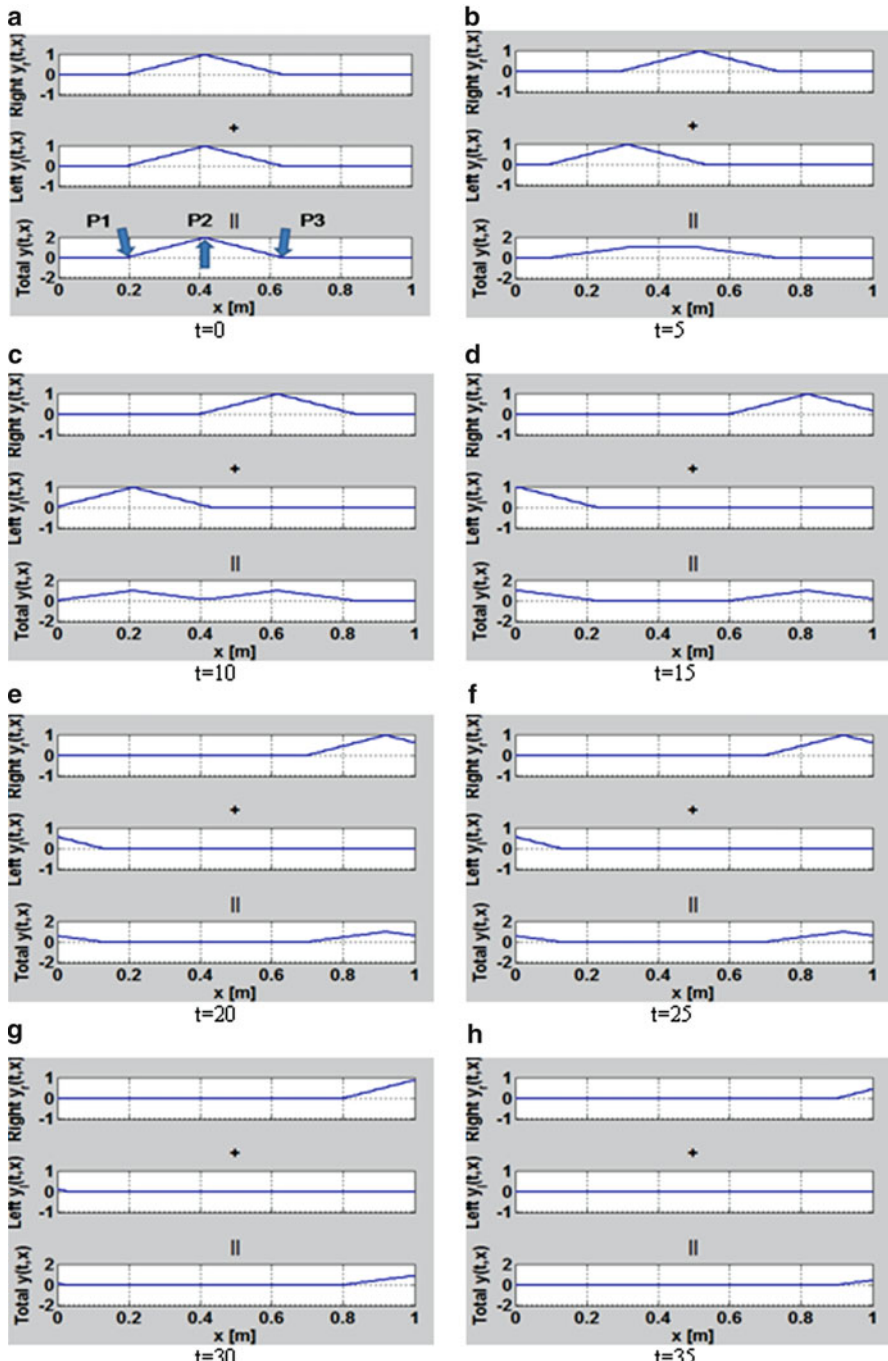


Fig. 23.6 Example of the traveling-wave solution to an infinite-length string that is displaced to an amplitude of 2 at time $t = 0$. We note that the string is held in place at three points, P1, P2, and P3 at $t = 0$. The *top plot* of each figure shows the right traveling wave, the *middle plot* the left traveling wave, and the *bottom plot* the physical displacement, equal to the sum of the top and middle plots. (Plots generated using scripts developed by Ed Berdahl)

D'Alembert's solution to the wave equation provides the theoretical basis for digital waveguide models of stringed instruments.

23.3.1.2 The Delay Line

In this section we present the fundamental computing block used in digital waveguides. We present different views of this data structure and use it for building string models for the remainder of this chapter.

The data structure of the delay line naturally arose from digital computing. From a computer science perspective, the delay line is simply an array of values. In the computer music community, the delay line is the digital implementation of simulating propagation distance. Figure 23.7 shows an example of a length 6 delay line, where at each time slice, values are shifted right. The input signal, into the delay line is $x(n)$, such that the values input into the system are the first five nonzero numbers of the Fibonacci sequence, (1, 1, 2, 3, 5).

As shown in Fig. 23.7, the sequence of values is used to represent space. At each tick, or change in time, the values shift right representing propagation of values. For the remainder of the chapter, we assume that a delay line represents space and

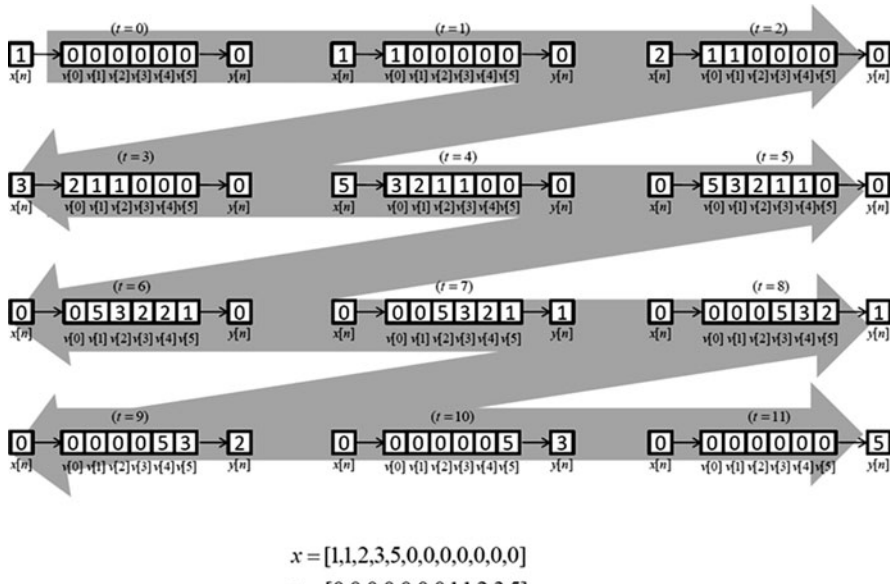


Fig. 23.7 A detailed depiction of a delay line and how it is used. Beginning at the *upper left*, a 1 is supplied as input, and the initial state of the delay line is 0. The next figure to the *right* is one sampling instant later, at which time the input 1 occupies the first delay element, and another 1 is presented at the input. In the next frame, the first two delay cells contain a 1, and a 2 is the next input, and so on. In computer science terminology, the delay line is a first-input, first-output (FIFO) queue for signal samples, clocked at the sampling frequency

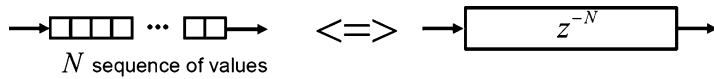


Fig. 23.8 Equivalence between a sequence of values and a delay line block diagram

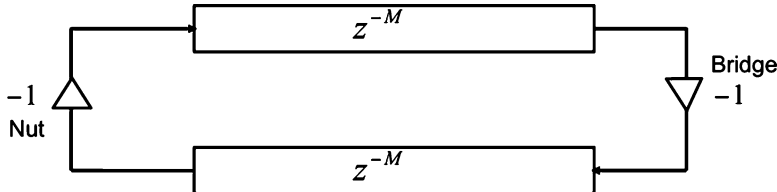


Fig. 23.9 A digital waveguide consisting of two delay lines in series in a loop. Note that the inverters between the delay lines are only present when acceleration, velocity, and displacement of the string is modeled, and it is rigidly terminated

changes occur to its values through time. For simplification, we draw a delay line as a box with the negative exponent of z being the length of the delay. The z corresponds to the variable of the z -transform, where a single unit delay is z^{-1} (Oppenheim and Schafer 1975; Smith 2007b). We denote this equivalence in Fig. 23.8.

For the musical acoustics community, such a data structure is invaluable in modeling propagation. In artificial reverberation, delay lines can be used to simulate the indirect paths of a signal (Schroeder 1961; Moorer 1979; Smith 2010).²

23.3.1.3 Digital Waveguide Models

Observing the solution to the wave equation in (23.2), the displacement of a string is the sum of two traveling waves moving in opposite directions. We model each traveling wave's propagation path with a delay line. As Fig. 23.9 shows, the data structure of two delay lines in series in a loop models the physical behavior of the vibrating string as the virtual implementation of the theoretical solution of the sum of two traveling waves.

To cement these abstractions, we present an example of how a vibrating string is modeled with the digital waveguide with initial conditions of a triangular pulse near the middle of the string. Because the sum of the left and right traveling-wave components always equals the displacement of the physical string, we initialize each delay line with a triangular pulse with half the amplitude of the physical string

² Two lab assignments pertaining to delay lines and how they are used to model propagation distance are available online at http://ccrma.stanford.edu/realsimple/lattice_ladder/ and <http://ccrma.stanford.edu/realsimple/reverb/>

such that the sum of corresponding values from both delay lines equals the amplitude of the pluck for the physical string.

At $t=0$, we allow values to propagate. Depending on what the sampling rate is, the physical length of each sample in the delay lines is set assuming a constant propagation speed c .

As Fig. 23.6 shows, the string is held in place at points P1, P2, and P3, which is necessary because the string is infinite. At $t=0$, we release the string at these points. What we obtain from our virtual model is two traveling waves moving in opposite directions such that the sum of corresponding values always equals the displacement of the physical string (Smith 1992).

We now relate the parameters of the digital waveguide to physical characteristics of the string. Our simple digital waveguide, shown in Fig. 23.9, consists of two delay lines each of length M . The frequency of the digital waveguide is directly related to the sampling rate of our system and the length of the delay lines, M .

Assuming a sampling rate fs , we can determine how long it would take for an impulse to travel to both ends of the string and back. If an impulse is placed in the first sample of the first delay line, we confirm that it takes $2M$ samples of propagation for the impulse to return to its original position, which is equivalent to $T = 2M/fs$ seconds. Therefore, in our lossless string-model, a traveling wave takes T seconds to reflect from one end and back. Inverting T , we now know that the virtual string oscillates at a fundamental of $f_1 = 1/T$ Hz.

Because each delay line corresponds to one direction of a traveling wave of the string, we have an intuitive physical mapping between the digital waveguide and the physical string. In Fig. 23.9, we have inverters between the two delay lines. The inverter on the left of the figure corresponds to the *nut* of the instrument, and the second inverter to the *bridge* of the instrument. Note that the inverters are only present in our digital waveguide when acceleration, velocity, and displacement waves are modeled with the waveguide. For a more detailed discussion on alternative wave variables modeled in digital waveguides, see Smith (2010).³

23.3.1.4 Natural Decay of the String

If an ideal string is rigidly terminated on both ends, energy injected into the string remains within the string (neglecting damping by the surrounding air). However, in real strings, air friction and internal damping cause the string's motion to decay over time (Chaigne 1991). By inserting a low-pass filter into the digital waveguide, as shown in Fig. 23.10, we can model the string's decay properties in our virtual model (Smith 1993). Computing the loop filter's coefficients is discussed in Sect. 23.5.3.1.

Extending our simple digital waveguide, as shown in Fig. 23.10 we add the string's damping into the waveguide's feedback loop. This maps physically to

³ http://ccrma.stanford.edu/~jos/pasp/Alternative_Wave_Variables.html

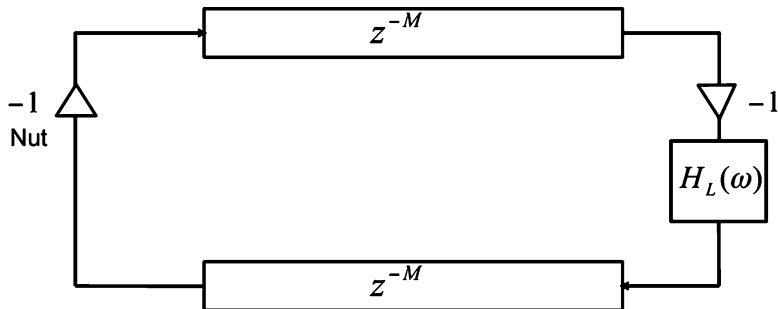


Fig. 23.10 An extension of our simple digital waveguide by including loss through a loop filter. Note that the inverters between the delay lines are only present when acceleration, velocity, and displacement of the string is modeled

energy loss in the string from friction, the string's properties, and other more minute, time-invariant effects.

We use a frequency low-pass filter $H_L(\omega)$ to calibrate our waveguide to match the decay as measured from a real guitar string. In the context of a digital waveguide, $H_L(\omega)$ is called the *loop filter*.

23.3.1.5 Modeling Two Planes of Vibration

In the physical world, the strings of an instrument vibrate in three dimensions. Neglecting longitudinal waves reduces the motion at each point along the string to two dimensions. This two-dimensional (2D) motion can be represented as the vector sum of motion in two orthogonal planes. In previous sections, we discussed modeling vibrations of the string with a single digital waveguide. To a first approximation, the single digital waveguide representing the transverse motion of the string is an adequate model. However, more realistic behavior can be obtained by using two digital waveguides, each representing motion in one orthogonal plane. With two digital waveguides and a general 2×2 coupling matrix, effects such as detuning, two-stage decay, and beating can be correctly modeled (Weinreich 1977).

Figure 23.11 shows the block diagram of two linearly coupled digital waveguides. One digital waveguide corresponds to the “vertical” direction, defined as orthogonal to the instrument body’s top-plate. The second digital waveguide, corresponds to the “horizontal” direction parallel to the instrument’s top-plate. As a simplification, we often ignore the direct effects of the bridge on the horizontal plane of motion by not having $H_{hh}(\omega)$ in Fig. 23.11.

Two-stage decay is clearly present in many stringed instruments. For example, piano tuners tune groups of strings per note to exhibit two-stage decay. The first decay is fast, to emphasize the attack of the note, and the second decay slower to maintain sustain of the note. With two digital waveguides, each having different loop-filters for each digital waveguide, one can be set to decay at a faster rate than the other, such that the two-stage decay phenomenon is modeled.

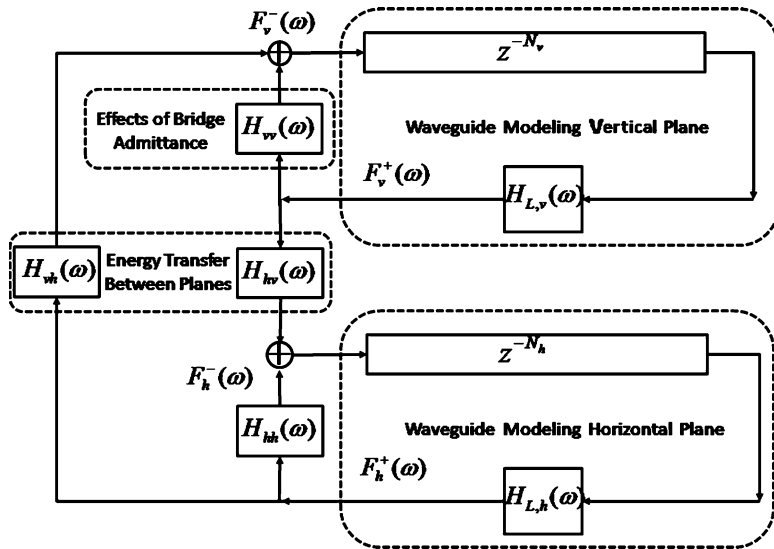


Fig. 23.11 Two linearly coupled digital waveguides. Each waveguide represents one plane of motion of the string. The vertical plane denotes the transverse direction with respect to the body of the instrument. H_{vv} corresponds to the strings interaction with the instrument's body. H_{vh} and H_{hv} correspond to the coupling between the two orthogonal planes of motion

Another phenomenon observed in physical instruments is fundamental frequencies that differ for each plane of vibration (Lee 2007). This phenomenon occurs because the bridge is typically more compliant in the vertical direction than in the horizontal plane, resulting in a different effective string length in the two planes. This effect can be modeled using two digital waveguides having different lengths, as discussed further in Sect. 23.3.1.

Another phenomenon that is sometimes important is a higher fundamental frequency at the start of a plucked tone (Tolonen et al. 2000; Pakarinen et al. 2005). This occurs because of the higher average tension in the string when it is displaced (and stretched) by plucking. This effect can be modeled using time-varying delay-line lengths (via some form of delay-line interpolation, as discussed further below).

23.3.1.6 Varying the Digital Waveguide

In Sect. 23.3.1.3, we discussed how digital waveguides model propagation of traveling waves along a physical string. The single parameter that can change is the total delay in the loop. Because the described system is linear and time-invariant (Smith 2007b), the digital waveguide's delay lines, presented in Sect. 23.3.1.3, can be lumped into one delay line with delay $N = 2M$. Figure 23.12 shows such a simplification. Though this simplifies the block diagram of a digital waveguide, it

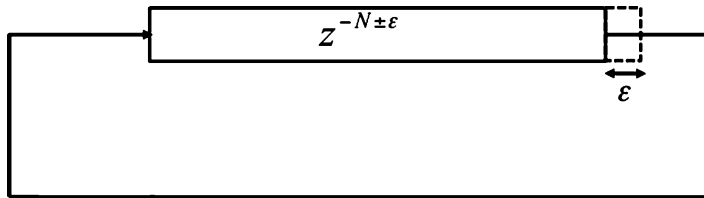


Fig. 23.12 Combining the delay lines in the digital waveguide and showing a fraction sample

loses its direct physical mapping: viewing the delay lines as traveling waves moving in opposite directions. However, the systems are equivalent. For our discussion on time-varying lengths for digital waveguides, we discuss digital waveguide's with a single delay line, and thus with a single delay length.

Once reduced to this form, the digital waveguide has a single parameter – its total delay N . By changing N through time, the digital waveguide effectively models a changing propagation distance. The most notable physical everyday occurrence of such an effect occurs whenever an ambulance or police car with its sirens on passes us. The pitch of the siren is higher on approach and lower after passing. This phenomenon, known as the *Doppler effect* (Laroche 1998), is the basis for many effects and sounds in the musical community, such as the flanger and the Leslie speaker (Smith 1984; Smith et al. 2002). In the digital domain, however, the delay-line length is an integer; therefore, interpolation algorithms are needed to provide a smooth change in delay line lengths (Schafer and Rabiner 1973; Smith and Gossett 1984; Smith and Friedlander 1985; Laakso et al. 1996; Putnam and Smith 1997). For a detailed overview of various interpolation methods, we refer the reader to: http://ccrma.stanford.edu/~jos/pasp/Delay_Line_Interpolation.html.

An online lab that steps the reader through digital implementations of the Doppler effect, flanger, and Leslie speaker can be found at: http://ccrma.stanford.edu/realsimple/doppler_flanger_leslie/.

23.3.2 Plucking the String

Returning to our two-delay-line implementation of the digital waveguide, we describe how to excite the virtual string model with a clear mapping to the physical world. Figure 23.13 shows a digital waveguide where, for each delay line, we have summed into the X th sample. Here we input at each time-slice our excitation signal $e(n)$.

23.3.2.1 Theoretical Plucks

If we want an impulse at the sampling distance of where the pluck position of the guitar would be, we calculate X such that the samples for each delay line summed

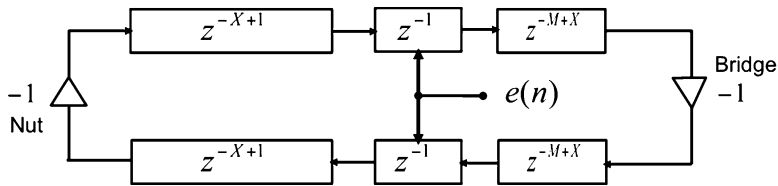


Fig. 23.13 Summing into the X th sample where the excitation signal is fed into the waveguide

into correspond to the same physical location of the instrument (Jaffe and Smith 1983). We then set $e(0) = 1$ and $e(n) = 0$ for all $n > 0$.

As Karplus and Strong (1983) discovered, exciting a delay-line loop with an impulse is psychoacoustically plain, whereas exciting it with random values results in a richer sound.

With delay lines modeling displacement, we can linearly interpolate between the pluck-point to the two ends of the string for both traveling waves for an excitation that displaces the string at a single point, causing the remainder of the string to displace linearly to the ends of the string. Furthermore, if the delay lines represent acceleration or curvature, this ideal-pluck is a single nonzero sample in each delay line. Note that since the digital waveguide is a sampled model of a continuous system, band-limiting conditions need to be accounted for. A detailed description can be found in (Smith 2010).⁴

23.3.2.2 Complexities of Real Plucks

As discovered in the Karplus–Strong algorithm, short noise bursts produce psychoacoustically rich excitations for delay-line loops. However, as explored further in Sect. 23.5.2, the pluck itself is psychoacoustically significant. As any plucked stringed instrument musician can verify, reproducing a pluck exactly by hand is extremely difficult, if not impossible. Studies have been made of guitar plucks (Chaigne 1992). In such research, elaborate devices have been constructed to reproduce the same pluck precisely. As discussed later in Sect. 23.5.2, real plucks are more complicated than short bursts of white noise. Each pluck has characteristics unique to its particular occurrence.

With idealized plucks and digital waveguides, one can easily build a virtual electric guitar using digital waveguides.⁵

⁴ http://ccrma.stanford.edu/~jos/pasp/ideal_plucked_string.html

⁵ An online laboratory outlining the steps for doing so can be found at http://ccrma.stanford.edu/realsimple/subsec_guitar.html. See also http://ccrma.stanford.edu/realsimple/faust_strings/

23.3.3 Body Resonance

This section describes the integration of the instrument body into our digital waveguide model. We extend our digital waveguide string model with the instrument's driving-point admittance. With the inclusion of the instrument body's resonator, we can attach multiple instantiations of our digital waveguide model to account for multiple strings coupled at the bridge of the instrument (Smith and Van Duyne 1995).

23.3.3.1 Driving-Point Admittance

The driving-point admittance of the body of the instrument characterizes linear interactions between the string and the body in both directions: meaning energy transferred from both string to body and body to string. The driving-point admittance is defined as follows:

$$\Gamma(\omega) = \frac{V(\omega)}{F(\omega)} \quad (23.3)$$

where for a given frequency ω , the ratio between the Fourier transform of the velocity and force is known. A physical explanation of the driving-point admittance is to view the admittance as a measure of how readily force exerted at the contact point at a certain frequency results in motion at that same frequency (Fletcher and Rossing 1998). Because the body of the guitar is a rigid structure that exhibits standing waves at particular frequencies, known as the *modes* of the guitar, the body vibrates naturally at these frequencies.

A brief overview of the mechanics of our physical model thus far: the string vibrates upon excitation. Its end is connected to the body of the instrument at the bridge, transferring energy from the initial pluck at the fundamental frequency and its harmonic series. According to the driving-point admittance, the force applied at the bridge by the string results in motion of the bridge and top-plate. The resulting motion is dependent upon the construction of the top-plate of the instrument, which determines its modes of vibration. The acoustic instrument then propagates waves according to its top-plate movement, thereby coloring the resulting sound waves heard by our ears.

23.3.3.2 Filtering with the Driving-Point Admittance

The simplest extension of our current digital waveguide model is to use the driving-point admittance of the instrument to derive a proper reflection filter to replace the -1 associated with the 'bridge' in Fig. 23.13. see (Smith 2010) for details regarding the derivation of transmission and reflection filters from the driving-point admittance. A discussion of what measurements are needed to compute the driving-point admittance can be found in Sect. 23.4.2.

In Fig. 23.14 the output of the digital waveguide is convolved with the driving-point admittance. Because the virtual instrument described up to this point is linear

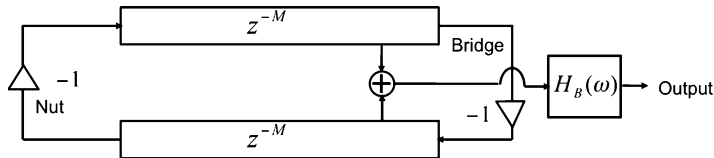


Fig. 23.14 Convolving the physical output of the digital waveguide with the driving-point admittance

and time-invariant, the driving-point admittance of the instrument can be used to excite the digital waveguide by commuting the admittance with the digital waveguide. Though this is unrealizable in the physical world, the two systems are the same. This method of using the driving-point admittance to drive the digital waveguide is known as *commuted synthesis*.^{6,7}

23.3.3.3 Bidirectional Interaction

In the physical world, the motion of the string exerts a force on the bridge resulting in a velocity at the point of contact. In Sect. 23.3.3, from a physical perspective, only energy passing from the string to the body is modeled. However, we can extend our current model to account for not only the influence of the string to the bridge, but also the influence of the bridge to the string. Network theory applied to this junction results in a bidirectional model (Van Valkenburg 1960; Newcomb 1966; Belevitch 1968).

Figure 23.15 is an illustration of six strings attached to a common bridge. The simplifying assumption is that all strings move at the same velocity as the bridge at the bridge.

$$H_B(\omega) = \frac{2}{R_b(s) + R_1 + R_2 + \Gamma + R_6}$$

where $R_b(s) = \frac{1}{\Gamma_b(s)}$, where $\Gamma_b(s)$ is the driving-point admittance of the bridge and R_i is the wave impedance of string i . Furthermore, each string's wave impedance can be computed using its physical characteristics through the following equation:

$$R_i = \sqrt{K_i \varepsilon_i} = \frac{K_i}{c_i} = \varepsilon_i c_i,$$

where K_i is the string tension, ε_i is the string's linear mass density, and c_i is the speed at which waves on the string travel both left and right. For more information

⁶http://ccrma.stanford.edu/~jos/pasp/commuted_synthesis_strings.html

⁷An online laboratory for creating an acoustic guitar physical-model using commuted synthesis is available in the RealSimple collection: http://ccrma.stanford.edu/realsimple/acoustic_guitar/acoustic_guitar.html

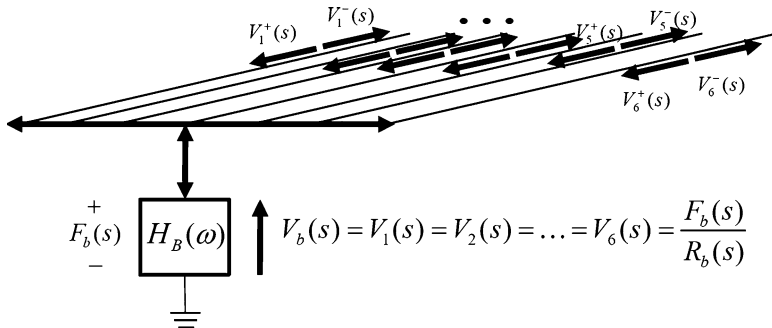


Fig. 23.15 An illustration of six strings attached at the bridge of the instrument. The simplifying assumption is that all strings move at the same velocity as the bridge at the bridge

on network theory and how it applies to musical acoustics, we refer readers to: http://ccrma.stanford.edu/~jos/pasp/introduction_lumped_models.html.

23.3.3.4 String–Body Scattering Junction

Continuing our discussion in Sect. 23.3.3. To model multistringed instruments, we naturally extend our model so that each digital waveguide models a string of the instrument, with all strings attached to a bridge model of some kind.

The simplest bridge model, as described in the previous section, is a common connection point for all strings. That is, all string endpoints move with the same velocity, and this velocity equals the vertical bridge velocity driving the top-plate of the instrument. From the point of view of a wave traveling down the string toward the bridge, the bridge creates a so-called *scattering junction* at the end of the string. An incident traveling wave at the junction “scatters” into all of the strings, as well as contributing to bridge motion.

All that is needed to determine the scattering relations at the bridge is the impedance of each connecting element. The string wave impedances are generally assumed to be equal to some real, positive value. The string wave impedance is given by

$$R = \sqrt{K/\varepsilon}$$

where K is tension and ε is mass density along the string.

The bridge impedance (Sect. 23.3.1) is generally a complex-valued function of frequency, thus yielding reflection and transmission *filters* (as opposed to coefficients). It is often formulated as an external *load* impedance, driven by the strings, representing the driving-point impedance of the instrument’s bridge and top-plate.⁸

⁸ http://ccrma.stanford.edu/~jos/pasp/loaded_waveguide_junctions.html

Figure 23.15 shows a diagram of our virtual model of a multistring instrument with all strings coupled at the bridge.

With such a model, we are able to physically model certain interactions occurring at the bridge between the strings and body of the instrument. In the case of the acoustic guitar, all the strings are coupled at the bridge such that energy transfers from one string to another through the bridge. This effect is very prominent, in that musicians often change their technique to account for *leakage* of energy. Guitar players refer to this phenomenon as *open-string noise*, which typically occurs when a guitar player plays on strings without muting the remaining strings, resulting in sympathetic vibration. This can be especially problematic for musicians playing microphoned acoustic instruments, because the sympathetic vibration can lead to unwanted feedback. For electric guitar players, when the outputs of the pickups are amplified to create distortion, unwanted sympathetic vibration obscures the sounds of the played strings.

Figure 23.16 shows a block diagram modeling an instrument having two strings coupled together at a string–body scattering junction. The digital waveguides representing each string are simplified in that they move only in the transverse plane. As shown, energy from one string can excite the other string (Smith 1993; Karjalainen et al. 1993). Furthermore, the scattering-junction output may contain the effects of body resonances in the filter $H_b(z)$. Each single-plane digital waveguide in Fig. 23.16 can be upgraded to a dual-plane digital waveguide, as shown in Fig. 23.11. In the two-string case, the result is a set of four coupled digital waveguides.

23.3.4 Pressure Radiation

The signal $v_b(n)$ in Fig. 23.16 of the previous section corresponds to the physical bridge velocity in the vertical direction normal to the top-plate of the instrument. Motion in the other two orthogonal directions is typically neglected. This signal can be used as the final guitar output signal when modeling strings terminated by piezoelectric crystals, as in so-called electric-acoustic guitars, and some guitar synthesizer controllers. For a full acoustic guitar simulation, this signal is next filtered by a *body*

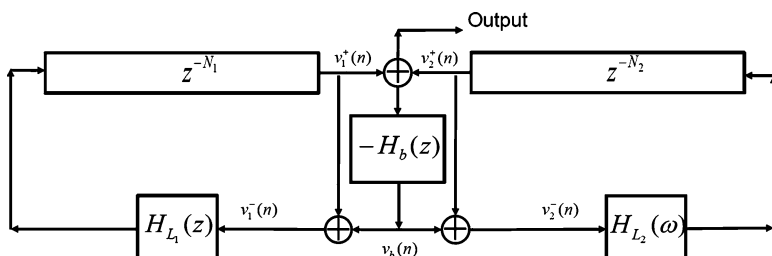


Fig. 23.16 A block diagram of multiple strings of an instrument connected at a single scattering junction with the body of the instrument

resonator and possibly also a *radiation filter*. In other words, the bridge velocity signal must be filtered to correspond to the transfer function from the bridge to the listener's ears. In principle, two such filters are needed, one for each ear, but typically only one is used, because guitars are normally heard at distances that are large compared to top-plate dimensions (the *far field*).

The bridge-to-ear filtering is typically assumed to be linear and time-invariant (LTI), so that the filter's transfer function $H_{be}(z)$ can be estimated using a recording of the bridge velocity $v_b(n)$ and the sound pressure $p_e(n)$ at a point in space (nominally where an "ear" is to be located). If $X(z)$ denotes the z transform of time-domain signal $x(n)$, then we have

$$H_{be}(z) = \frac{P_e(z)}{V_b(z)}.$$

In practice, methods such as described in the next section are used to obtain robust estimates of the bridge-to-ear filtering. Some specific methods are discussed in Smith (1983) and Välimäki and Tolonen (1998).

Measuring the bridge-to-ear transfer function has the disadvantage that the measurements and filter-modeling must be repeated for every geometry. That is, if the ear moves, or if the guitar changes orientation, etc., then the $H_{be}(z)$ changes somewhat. To support a variety of geometries in one model, one can model more physical details. In particular, the sound pressure is synthesized at any number of virtual microphone positions by means of a simplified Kirchhoff–Helmholtz integral over the radiating surfaces determined by the modal state (King 1934), or one can start with the Rayleigh integral. A less expensive refinement is to develop a set of *directional radiation filters* that vary as a function of guitar orientation relative to the listener.

In real-time guitar-sound synthesis, point-to-point transfer functions are typically preferred over computing a delayed surface integral over the entire radiating guitar body, for computational simplicity.

23.4 Measurements

This section reviews techniques for acoustic measurement relevant to building a virtual acoustic guitar.

23.4.1 String Vibration

Various techniques can be used to measure string vibration at a point along its length. For electric guitars, a magnetic pickup is typically used. In the traditional single-coil magnetic pickup (e.g., as used in the Fender Stratocaster electric guitar),

a strong permanent magnet is wound with copper wire. The string magnetizes in the presence of the magnetic field, and when the string moves, the changes in the magnetic flux field cause current to flow in the copper wires. This signal is roughly proportional to the vertical velocity of the string, which is next amplified in an electric guitar.

In guitars such as Gibson's Les Paul model, a double-coil magnetic pickup is used, configured so as to reject *common mode* interference from outside sources of electromagnetic interference. Solid-body electric guitars such as the Stratocaster and Les Paul are close to being purely electric in the sense that energy is maintained within the vibration of the string to drive the pickups that transduce its sound. The guitar body is literally a block of solid wood meant to not resonate or color the timbre of the guitar's sound, thereby minimizing energy transferred into the guitar body, thus creating a longer sustain in the string.

Another method for measuring a string's displacement, often used in musical acoustics laboratories, is based on a light-emitting-diode (LED) and a phototransistor. The phototransistor measures the amount of light received from the LED. The geometry is arranged so that the light received is proportional to string displacement, or at least related to displacement by a known or measurable function. This is an inexpensive method for measuring the string motion at a *point* in two orthogonal planes.

Another method used for measuring the motion of a string is laser vibrometry, which is based on optical interference of a laser beam and its reflection from a point along the string.

23.4.2 Bridge Impedance

From the string's point of view, the guitar body is fully characterized by its *driving-point impedance* at the bridge. In particular, the bridge *reflection filter* ($H_{vv}(\omega)$) in Fig. 23.11) can be based on measurements of this impedance. Input impedance measurements are often used in the field of musical acoustics to characterize the response of a stringed instrument's resonant body, and as a basis of comparison among different instruments (Christensen and Vistisen 1980; Richardson et al. 2002).

As introduced in Sect. 23.3.3 above, the driving-point impedance is given by the force divided by velocity at each frequency. In general, the driving-point impedance of a bridge is a 3×3 matrix, corresponding to three spatial axes. However, the most important spatial dimension is the "vertical" dimension normal to the top-plate of the guitar; the bridge does not move nearly as much in the horizontal direction, and longitudinal modes in the string are typically neglected (even though they can be quite audible) (Askenfelt 1990).

To measure the driving-point impedance of a guitar body at its bridge, we need to measure

1. The force applied (in the vertical direction) by the string to the bridge at the driving point, and
2. The resulting driving-point velocity (in the vertical direction).

Velocity is often measured by integrating acceleration, where acceleration is measured using an *accelerometer*. An accelerometer may be built by placing a mass next to a piezoelectric crystal (which translates acceleration into a force on the crystal which then puts out a proportional voltage.) The accelerometer should be placed as close as possible to the driving point, and it should be as light as possible to minimize *mass loading*, which contributes to error in the impedance measurement. The applied string force is proportional to the slope (in the vertical plane) of the string at the driving point. Therefore, it can be estimated (up to some frequency limit) as a linear function of the displacement of a point close to the driving point. The valid frequencies are those for which the wavelength is long compared with the displacement-measurement distance from the bridge driving point.

In practice, a commonly used method for measuring driving-point impedance is to strike the driving point with a so-called *force hammer*, measuring bridge motion with a lightweight accelerometer. A force hammer has an output signal corresponding to the applied force (e.g., measured using a piezoelectric crystal in the hammer-head base). The velocity is given by the time-integral of acceleration measured by the accelerometer. When simultaneously measuring the acoustic body response with a microphone, care must be taken to minimize the direct signal from the impact. Another difficulty with the force hammer is striking exactly the same point in exactly the same direction so that the results can be averaged together to maximize signal-to-noise ratio.

A generally superior practical method for measuring driving-point impedance is by means of a so-called *shaker*. A shaker will normally have a transducer base containing both a force gauge and accelerometer. It is thus capable of measuring both applied force and driving-point velocity. The driving signal, typically white noise, is supplied externally. As with the force hammer method, both force and accelerometer signals are recorded to compute the driving-point admittance. However, a major advantage of the shaker over the force hammer is that the input/output signals can be recorded over an arbitrary time period. This allows use of low-level driving signals, improving linearity of the system (and minimizing direct-signal propagation to an acoustic microphone), and the measurement noise can be made arbitrarily small by averaging the results over time.

23.4.3 Body Vibration

Understanding the vibrational modes of the resonating surfaces of an instrument, such as acoustic guitar plates, can shed light on the radiation efficiency at various frequencies and in various directions. The body resonances filter the signal from the

vibrating string and contribute to the characteristic timbre of the instrument. Many resonant modes are visible as dips in the bridge impedance (peaks in the admittance versus frequency). Acoustic instruments are often adjusted based on measured mode *mobilities* (admittance magnitude). However, not all modes observed in the bridge impedance correspond to radiated sound. Some, such as in the neck, can absorb and dissipate vibrational energy without emitting a significant amount of radiated sound.

A scanning-point vibrometer, for example, by Polytec, can be used to measure surface vibration and construct three-dimensional views of its structural motion by means of software.

23.4.4 Pressure Radiation

To measure a point-to-point transfer function for pressure radiation, the instrument may be taken into an anechoic chamber and excited by one of the methods outlined in Sect. 23.4.2. The pressure signal generated from the motion of the instrument may be recorded using a microphone some distance away from the instrument (on the order of 1 m is typical). The Fourier transform of the measured pressure signal divided by the known excitation signal at the bridge yields the frequency response from the bridge to the microphone position, and a digital filter can then be fit to approximate this frequency response (Smith 1983; Välimäki and Tolonen 1998; Karjalainen et al. 2000).

23.5 Parameter Estimation

This section reviews methods for calibrating the model elements discussed in Sect. 23.3 to match measurements discussed in Sect. 23.4.

23.5.1 Short-Time Fourier Transform

Some of the methods to be discussed are based on the short-time Fourier transform (STFT), which can be considered a modern digital implementation of a *spectrogram*.⁹ The STFT computes the spectral content of a signal over time. It is carried out by taking a short segment of the signal to be analyzed (e.g., on the order of 100 ms or less), multiplying it by some *window* function (such as a *raised cosine* window; no window is called the *rectangular window*), and performing the fast

⁹ http://ccrma.stanford.edu/~jos/sasp/short_time_fourier_transform.html

Fourier transform (FFT) on the windowed signal segment (Välimäki et al. 1996). Zero-padding is typically used to provide spectral interpolation (Smith 2007a). The spectral content is then stored and the next segment of the signal is processed in the same way. This process is repeated until the end of the signal. A description of the parameters of the STFT and its application can be found in Sect. 23.5.2.

23.5.2 *Excitation*

As discussed in Sect. 23.3.2, the excitation to our virtual instrument is a wavetable signal. In the literature, there are several methods for computing excitation signals from actual recordings. This methodology (as opposed to calculating excitations from first principles) generally yields the best-sounding models (Lee et al. 2007a, b).

In recent years, two main approaches for obtaining excitation signals from recordings have emerged: (1) inverse-filtering, and (2) constant overlap-add (COLA) methods. We briefly describe the problem and give an overview of these methods below.

The goal of excitation-extraction is to remove the tonal components that ring after the initial onset, and to reduce the energy during the onset at those components to match the general energy levels at other frequencies. Figure 23.17a, c show a recorded guitar note on the guitar’s high E string and its STFT, respectively. As shown, at the onset of the note, essentially all frequency bins contain energy. After the initial attack, most of the energy becomes concentrated around the harmonics of the fundamental frequency.

With the problem now graphically represented, we describe how the two different methods approach removal of harmonic peaks in the STFT. The inverse-filtering methods remove the harmonic peaks by effectively multiplying each spectral frame of the STFT by a *comb filter*, which “notches out” the spectral peaks. Conceptually, this comb filter is the inverse of the string, where the string is viewed as a filter applied to the excitation signal. The COLA methods remove the harmonic peaks by applying nonlinear averaging to the spectral magnitudes around the base of each peak in the STFT frame.

The first method we consider is the *matrix-pencil inverse-filtering* (MPIF) method (Hua and Sarkar 1990). It computes the sinusoidal components of a signal using the matrix-pencil method (Laroche 1993), and performs inverse-filtering with the sinusoidal components to remove the tonal components leaving the excitation (Laroche and Meillier 1994).

The second method may be called the *sines-plus-noise inverse-filtering* (SPNIF) method. It is similar to the MPIF method in that sinusoidal components are computed, but instead of using the matrix-pencil method, a generative sinusoidal model is used (Tolonen 1998; Välimäki and Tolonen 1998). A residual signal is computed by subtracting synthesized quasi-sinusoidal components from the original recording. Inverse-filtering is then performed on the recording using a digital

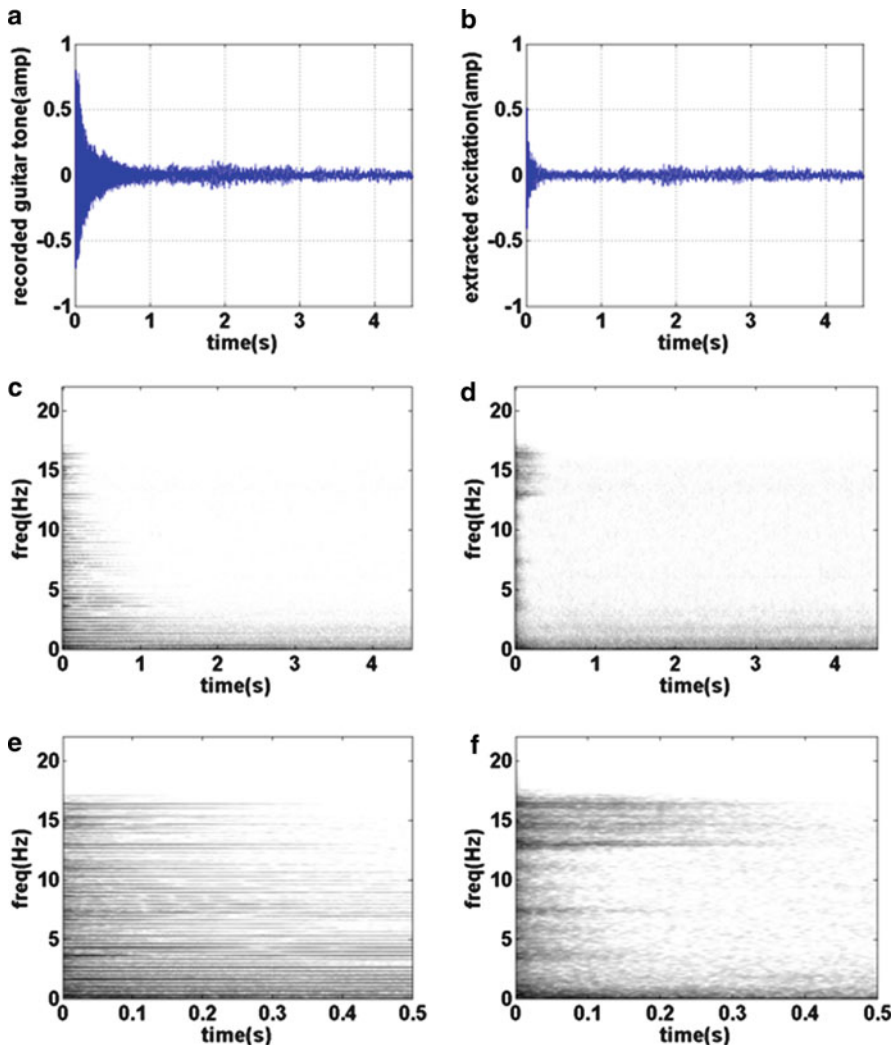


Fig. 23.17 The figures on the left show the time-domain plot of a recorded guitar tone, its spectrogram spanning 4.5 s, and its spectrogram spanning 0.5 s, respectively. The plots on the right show the same recorded guitar tone but with harmonic peaks removed using the SSI method. Note the flatness of the spectrum over time in the excitation extracted signal

waveguide tuned for the recording where scaled versions of the residual and sinusoidal signals are added together to help remedy the notches created from inverse-filtering (Serra 1997).

The third method, the *magnitude spectrum smoothing* (MSS), uses a different kind of STFT processing. Within each STFT spectral frame, a low-pass filter is applied to the magnitude spectrum. The inverse FFT is then taken, and the resulting time-signal is stored in a buffer for overlap-add signal reconstruction (Laurenti and Poli 2000).

The last method, the *statistical spectral interpolation* (SSI) method, is similar to the MSS method, but it removes harmonic peaks prior to smoothing the magnitude spectrum. The spectral magnitudes at the peaks are replaced by magnitudes that are statistically likely based on a fitted normal distribution with mean and covariance matched to those of the magnitudes surrounding the spectral peak (Lee et al. 2007a, b).

In our tests, the SSI method produces the best-sounding excitations. We therefore present that method in detail below.

23.5.2.1 The Statistical Spectral Interpolation Method

From a high-level viewpoint, the SSI method only modifies the magnitudes of the STFT of the guitar tone without affecting phase information. The method collects statistics on the magnitudes of frequencies surrounding harmonic peaks and uses these statistics to generate nondeterministic gain changes for the magnitudes at these peaks, without modifying the phase. With inverse-filtering methods, modifying phase inevitably introduces artifacts. Thus, this method's primary goal is to minimally alter the original tone.

The STFT is used for analyzing and modifying the original recorded tone. The STFT can be seen as a sliding window that takes at each sample-window a FFT of the windowed signal. The transform of that windowed portion is then modified, and the IFFT is then taken and saved in a buffer. The window is then slid according to how much overlap is wanted. The parameters for the STFT are the type of window used, the length of the window, and the number of samples the window slides by. Sample parameters for the method are a Hamming window of length 2^{12} samples with 0.9 overlap (hop size of 410 samples). Though 2^{12} samples with a sampling-rate of 44,100 Hz is long (≈ 100 ms), pre-echo-distortion artifacts are remedied by starting the algorithm during the onset of the recorded tone.

Actual processing occurs at each window of the STFT. Consider each FFT window taken to be a frame for processing. Within each frame, the harmonic peaks of the recorded tone are attenuated. Harmonic peaks can be found using the *quadratically interpolated FFT* (QIFFT) method (Smith and Serra 1987).

Assuming that the fundamental frequency of the recorded tone is at f_1 in Hz. A bandwidth W_p in Hz is specified, indicating the width of the peak. Another bandwidth W_n in Hz is specified indicating the width of the interval used for statistics collecting with respect to the fundamental frequency f_1 . In using the SSI method for the recording in Fig. 23.17a, $W_p = 0.3 \cdot f_1$ and $W_n = 0.75 \cdot f_1$. These values ensure that the points used for statistics collecting do not reach into the next harmonic peak but are large enough to obtain a reasonable mean and standard deviation.

For each harmonic i with frequency f_i , the following is defined and used for processing. Define a set of indices, Γ , with frequency values that satisfy the following:

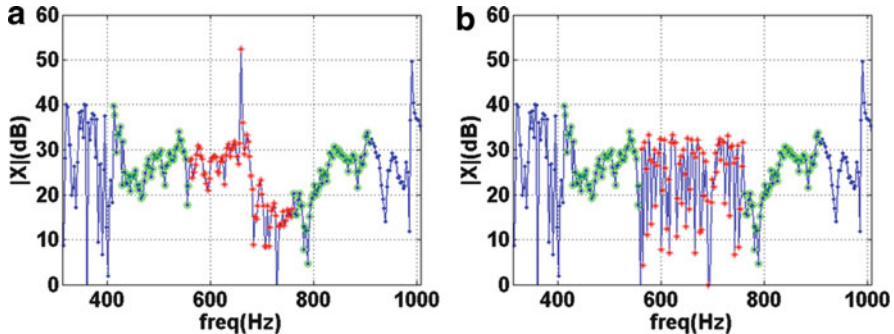


Fig. 23.18 Removing the peak at 660 Hz: *Starred points* are FFT values to be changed. *Circle dots* are FFT values to be used for statistics collecting. *Left plot* shows pre-peak-removal. *Right plot* shows post-peak-removal

$$\forall \gamma \in \Gamma, W_p \leq |v_\gamma - f_i| \leq W_n, \quad (23.4)$$

where v_k corresponds to the frequency in Hz of the k th FFT bin. The values in Γ correspond to indices within the current frame with frequencies that lie within the specified band W_n but outside the band W_p centered around f_i . See the circled points in Fig. 23.18.

The mean and standard deviation of the magnitude of values in FFT bins in Γ are computed as follows:

$$\mu = \frac{1}{|\Gamma|} \sum_{i \in \Gamma} |X_i| \quad (23.5)$$

$$\sigma = \sqrt{\frac{1}{|\Gamma|} \sum_{i \in \Gamma} (|X_i| - \mu)^2} \quad (23.6)$$

Define the set of indices, Δ , with frequency values that satisfy the following:

$$\forall \delta \in \Delta, |v_\delta - f_i| \leq W_p. \quad (23.7)$$

The values in Δ correspond to indices within the current frame with frequencies that lie within the specified band W_p centered around f_i . The magnitudes at these frequencies are changed to remove the peak. See the starred points in Fig. 23.18.

Thus, for all bins with indices in Δ , magnitude values are modified to remove the observed peaks. This occurs as follows:

For each $\delta \in \Delta$, generate a value $\rho \sim \mathcal{N}(\mu, \sigma)$

$$X_\delta := \frac{\rho}{|X_\delta|} X_\delta \quad (23.8)$$

Note that in this section, the noise-floor spectral magnitude squared is approximated with a normal distribution instead of a Rician distribution. We have found that such an

approximation leads to psychoacoustically satisfactory results and as such, we leave the exploration and usage of the more expensive, exact distribution for future work.

Figure 23.18 shows the points the algorithm uses for statistics collecting and the points with gains altered. Figure 23.18a shows the magnitudes of a frame of the STFT of a recorded guitar tone. The starred-points denote points that include the harmonic peak requiring a flattening of its spectral magnitude. The circled-points denote points surrounding the peak from which a normal distribution is fitted. The starred-points' magnitudes are then reduced by a scaling factor that is sampled from the distribution computed from the circled-points. Figure 23.18b shows the same frame but with the starred-points scaled according to the distribution computed from the circled-points. This ensures that the extracted excitation maintains a statistically flat-spectrum. As shown, the peak at 660 Hz is entirely removed.

23.5.3 String

23.5.3.1 Loop Filter Estimation

As discussed in Sect. 23.3.1.4, the loop filter gives the digital waveguide frequency-dependent damping. Similar to what is used in artificial reverberation, the time for frequencies to decay 60 dB, known as t_{60} , is used to determine the gains of the filter. We define t_{60} to be the time in seconds for a signal to decay 60 dB. For obtaining gains for the fundamental and harmonics of our loop filter, we compute t_{60} for each of these frequencies over time using the *energy decay relief* (EDR) (Tolonen 1998; Lee et al. 2006).

For the remainder of this section, we commute the second delay line shown in Fig. 23.10 with the loop filter and combine the delay lines. The resulting system, shown in Fig. 23.19 is equivalent to the one shown in Fig. 23.10 as the delay line and loop filter components are linear and time-invariant.

Similar to the STFT, the EDR shows the spectral components over time of a given signal. The single difference between the STFT and the EDR is that the square magnitudes of the FFT of each frame is used instead of the magnitudes. With the EDR, the amount of energy in each FFT bin is given over time. An advantage of using the EDR over the STFT is that energy decreases monotonically, whereas magnitudes, as used by the STFT, may increase and decrease resulting in noisier data for decay estimation.

The EDR is defined as follows:

$$\text{EDR}(t_n, f_k) = \sum_{m=n}^M |H(m, k)|^2, \quad (23.9)$$

where $H(m, k)$ corresponds to the k th FFT bin at frame m of the EDR. M corresponds to the total number of frames in our EDR. Thus, $\text{EDR}(t_n, f_k)$ represents the total amount of energy remaining in the signal at time $t = t_n$ for frequency f_k . Figure 23.20

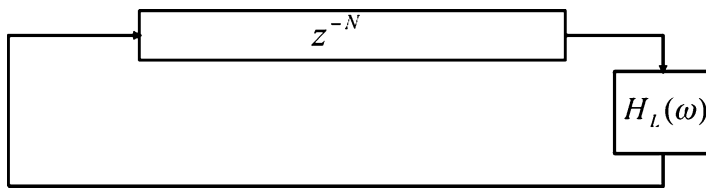
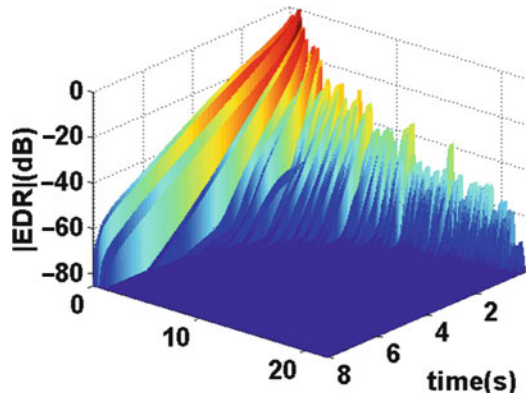


Fig. 23.19 Digital waveguide model with one single delay line and loop filter

Fig. 23.20 Plot of the energy decay relief (EDR) of a plucked guitar note



shows a three-dimensional plot of the EDR over time and frequency of a recorded guitar tone. The x -axis corresponds to frequency in Hz, the y -axis time in seconds, and the z -axis the corresponding EDR magnitude in dB. The figure shows the energy decay of each harmonic peak of the signal. As shown, lower-frequency components decay slower than higher-frequency components. Furthermore, lower-frequency components have more energy at time $t = 0$.

Because the displacement of the string decreases exponentially, viewing its motion and EDR in log space, we expect linear decays, as Fig. 23.20 shows.

For each frequency f_k in the set of frequencies closest to the fundamental and harmonic frequencies, we fit a line to the time-decay of its EDR. The primary parameter for estimation is the slope of the line. Figure 23.21 shows EDR plots for the fundamental frequency and five harmonics. Each plot in Fig. 23.21 corresponds to taking a 2D slice (fixed frequency value) of Fig. 23.20. The EDR for each frequency over time is plotted in blue. The estimated line is shown in red. The estimation used only the segments of the EDR for which the red line overlaps the blue. As shown, the line estimated nearly matches exactly the subset of EDR points used.

Given the estimated slope, m_k , for frequency f_k , $t_{60}(k) = -60/m_k$. With $t_{60}(k)$ computed for the fundamental and harmonic frequencies, we now relate the decay times to the gains of the loop filter.

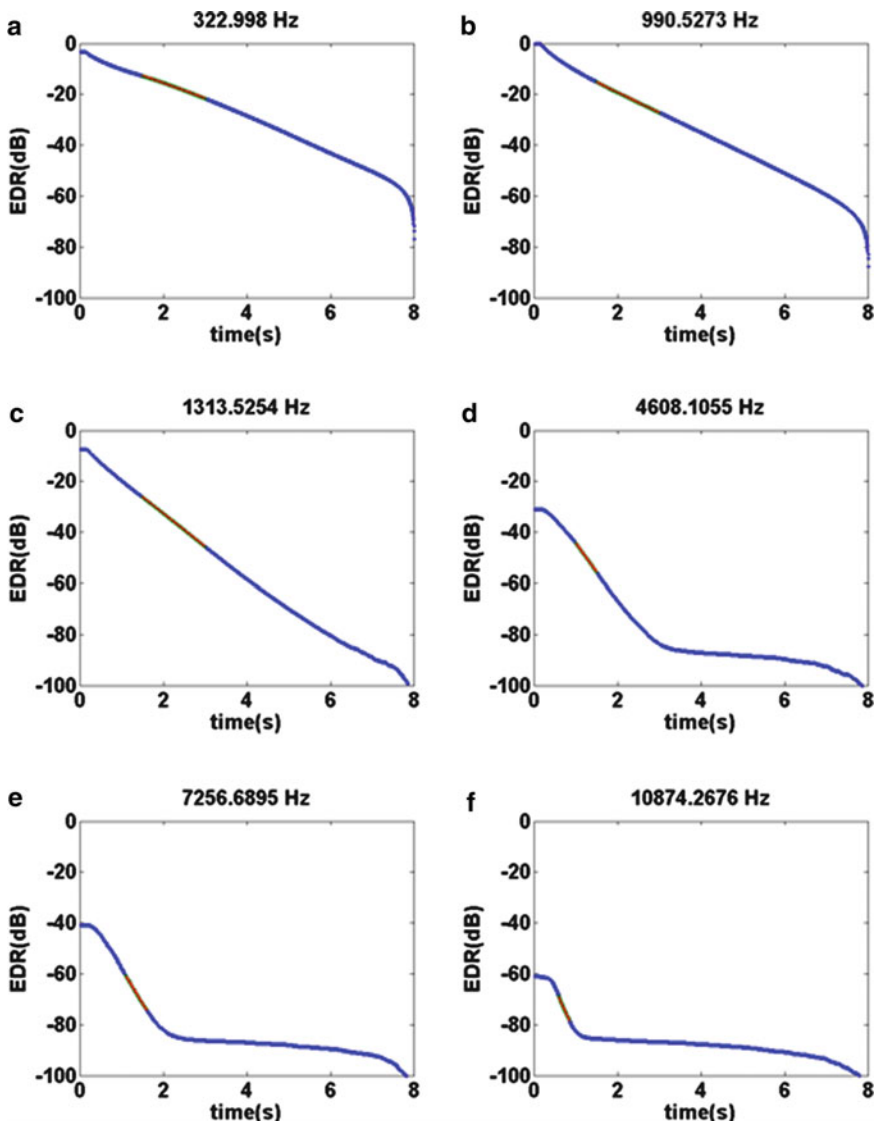


Fig. 23.21 Plots of the fundamental and EDRs of five harmonics are shown in each plot in blue. The overlapping red segments were fitted with the underlying blue points and plotted using the estimated slopes

$$|G(\omega_k)|^{t_{60}(k)/T} = 0.001 \quad (23.10)$$

where $|G(\omega_k)|$ corresponds to the per-sample desired gain of our filter. We also have the relation that

$$|H(\omega_k)_L| = |G(\omega_k)|^M \quad (23.11)$$

$$|H(\omega_k)|^{1/M} = |G(\omega_k)| \quad (23.12)$$

where $|H(\omega_k)_L|$ is the desired loop filter gain. This relates our per sample gain with the desired loop filter gain in series with a length M delay line. Substituting $|H(\omega_k)_L|$ for $|G(\omega_k)|$ in (23.10), we obtain

$$|H(\omega_k)|^{t_{60}(k)/MT} = 0.001 \quad (23.13)$$

Taking $20 \log_{10}$ of both sides yields

$$20\log_{10}|H(\omega_k)| = -60 \frac{MT}{t_{60}(k)} \quad (23.14)$$

To specify gains at frequencies between the fundamental and harmonics, we linearly interpolate between points for which we have gains. In special cases, the gains at DC up until the fundamental frequency are set to the value of the gain computed at the fundamental. For frequencies between the last harmonic and half the sampling rate, the gains decrease at an arbitrary slope.

With the gains specified for the loop filter, a complex spectrum with minimum-phase is computed (Smith 1983). A least-squares fit or the Steiglitz–McBride iteration is used to compute the coefficients for an arbitrary order filter (Smith 1983; Bank and Välimäki 2003).

Figure 23.22 shows the desired gains and t_{60} s computed for a recorded guitar note. The fundamental is 330 Hz. Gains for the fundamental and harmonic frequencies are circled in red. All other points are linearly interpolated between these gains and the constants we set for DC and half the sampling rate. Gains below the fundamental to DC are set to the value of the gain at the fundamental frequency. The gain at half the sampling rate was arbitrarily set to –4.08 dB. Figure 23.22a shows gains from DC up to 5 kHz. Note that the same recorded note was used to generate Figs. 23.17, 23.18, 23.20–23.22.

23.5.4 Body Resonator

In our synthesis model, the body resonator has a driving-point admittance that filters the output of the string model to transform force waves along the string into velocity waves at the bridge (Lambourg and Chaigne 1993). Taking the inverse-FFT of the measured driving-point admittance, we obtain the impulse response of the body of the instrument. This time-domain signal can be stored as a wavetable for convolution with the output of the synthesis string-model. Figures 23.23 and

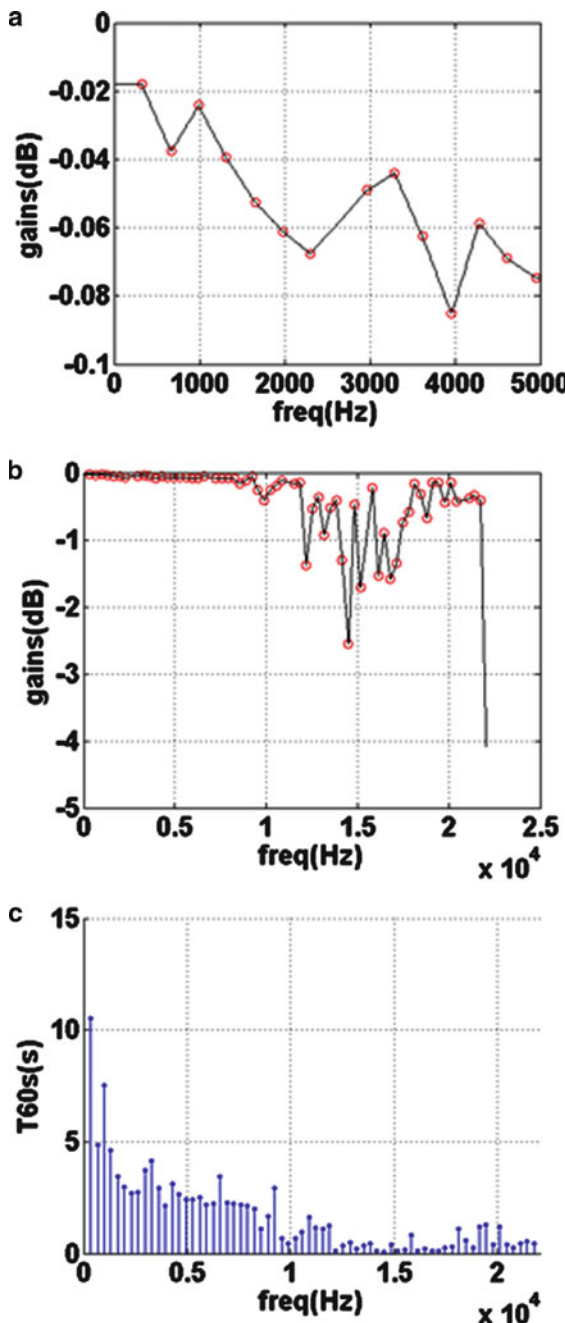


Fig. 23.22 Plots of estimated gains and t_{60s} from a recorded guitar tone for a loop filter. The fundamental frequency is 330 Hz. Circled points correspond to gain values for the fundamental and harmonic frequencies. All other points were linearly interpolated. The gain at DC was set to be the same as that of the fundamental. The gain at half the sampling rate was set arbitrarily to -4.08 dB. The lowest plot shows the time for each harmonic to decay 60 dB

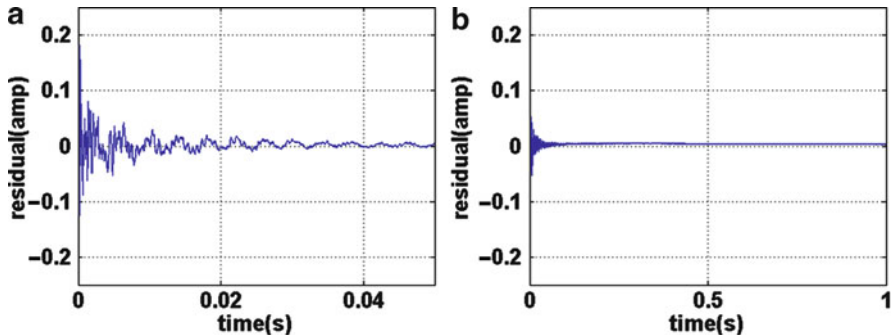


Fig. 23.23 Plots of the measured body response from a gypsy guitar. (a) Shows the first 50 ms of the response. (b) Shows the first second of the response

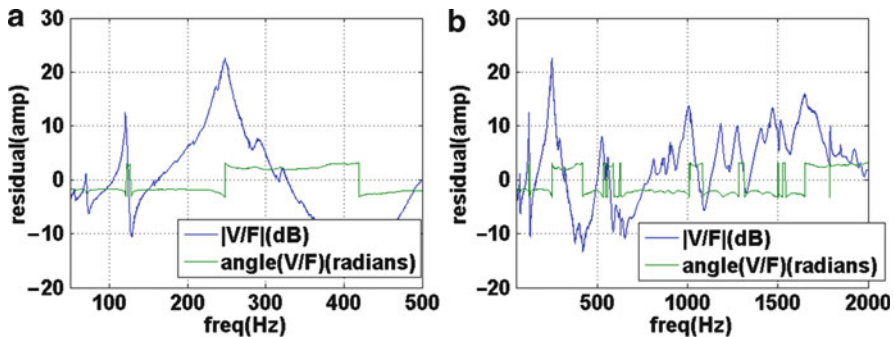


Fig. 23.24 Plots of the measured body admittance from a gypsy guitar

23.24 show the time-domain signal and spectrum (both magnitude and phase, respectively) of a measured guitar's body impulse response. As shown, the impulse response lasts well over 50 ms. Viewing its spectrum in Fig. 23.24, we note peaks that occur near 120 and 250 Hz.

23.5.4.1 Low-Order Filter Implementations

When latency and time-efficiency are of concern, the length of the body's impulse response can become an issue. To address this, the impulse response of the body can be approximated using lower-order filters (each representing a body mode with low damping) together with a shortened body impulse-response. These techniques were introduced in the context of commuted synthesis of strings (Smith 1993; Karjalainen et al. 1993; Smith 2010).

To shorten the body impulse response, methods for removing the narrowest peaks in the frequency response are applied, leaving a residual signal and a low-cost representation for the removed resonating peaks. This reduces the length of the

original impulse response while representing the primary modes parametrically. The two general approaches for dealing with spectral peak removal include subtraction and inverse-filtering methods.

The two basic methods are as follows:

1. Complex Spectral Subtraction

$$H_r(z) = H(z) - \frac{b_0 + b_1 z^{-1}}{1 + a_1 z^{-1} + a_2 z^{-2}}, \quad (23.15)$$

where $H_r(z)$ corresponds to the shortened body impulse response while $H(z)$ corresponds to the measured body impulse response. The parameters to be estimated are the second-order filter coefficients b_0 , b_1 , a_1 , and a_2 .

Complex spectral subtraction requires careful estimation of the phase, amplitude, frequency, and bandwidth for peak removal. Furthermore, the resonators must run in parallel with the residual. Therefore, advantages obtained from commuted synthesis are lost as the approximated body impulse response model is not readily commutable with the string component of our physical model (Bradley et al. 1995).

2. Inverse-Filtering

$$H_r(z) = H(z)(1 + a_1 z^{-1} + a_2 z^{-2}), \quad (23.16)$$

where $H_r(z)$ again corresponds to the shortened body impulse response with $H(z)$ equal to the measured body impulse response. In this form, the residual signal is readily commutable with the string component of our physical model as resonators are factored instead of subtracted. Furthermore, estimating the coefficients of the filter for peak removal requires only the frequency and bandwidth of the peak and not the amplitude and phase as is required for complex spectral subtraction (Smith 2010).

Applying inverse-filtering as described above, we take the original body response shown in Fig. 23.23, and remove the peak centered around 120 Hz using a second-order notch-filter having a bandwidth of 10 Hz. The residual, shown in Fig. 23.25, is significantly shorter than the original response. Whereas in Fig. 23.23a, the response lasts for well over 50 ms, in the residual signal, its amplitude oscillates near the noise floor at around 30 ms. Figure 23.25b shows the spectrum, both magnitude and phase, of the response after inverse-filtering. Compared with Fig. 23.24a, the peak at 120 Hz is completely removed.

23.5.5 Radiated Sound Pressure

Similar to how the driving-point admittance is used to model the transfer of energy from the string to the bridge, and vice versa, the transfer function from the top-plate acceleration to sound pressure at a point in space produces the final sound output from our model.

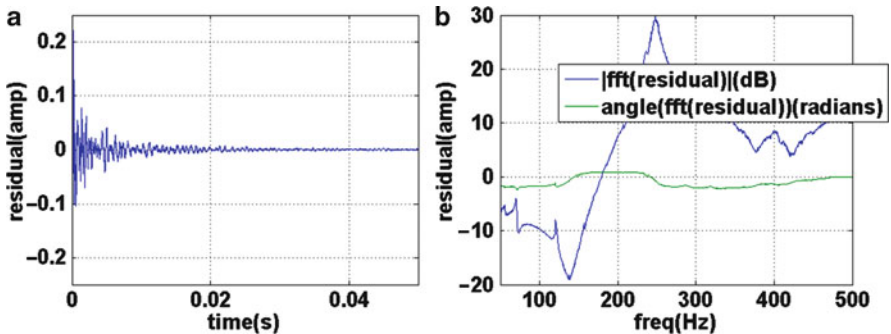


Fig. 23.25 Plots of the measured body admittance with the peak at 120 Hz removed. Note that the response is now shorter compared with the original body response in Fig. 23.23a.

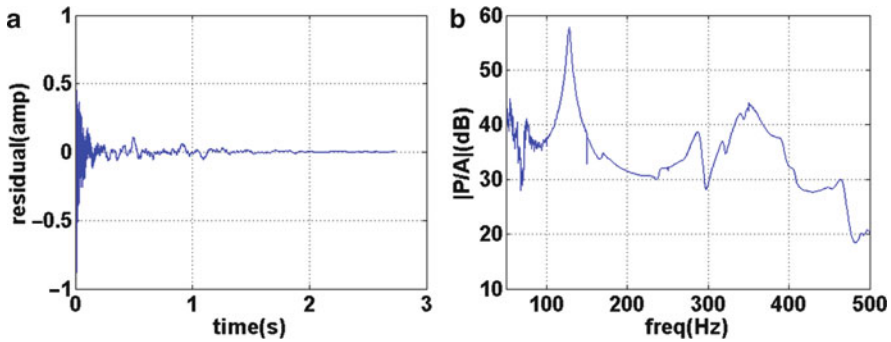


Fig. 23.26 Plot of the measured radiation response from a gypsy guitar. The recordings were made in an anechoic chamber as described in [Section 23.4.4](#). (a) Shows the time-domain signal of the measured response. (b) Shows the magnitude response of the measured radiation response

Using the measurements described in [Sect. 23.4.4](#), we compute the point-to-point transfer function from the bridge to a single point in space. The resulting response is shown in [Fig. 23.26a](#). The spectrum of the response is shown in [Fig. 23.26b](#). Observing [Fig. 23.26a](#), the length of the impulse response is close to 2 s long. Similar to the issues addressed with the body response, having to store the entire radiation impulse response in a wavetable is costly in terms of memory. Therefore, the methods discussed for removing spectral peaks for the body response can be directly applied to the radiation response.

23.5.5.1 Low-Order Filter Implementations

Using the same techniques described in [Sect. 23.5.4.1](#), a reduction in the length of the resulting impulse response can be made by factoring out frequency components of the signal having the most energy, and replacing them with low-order resonators

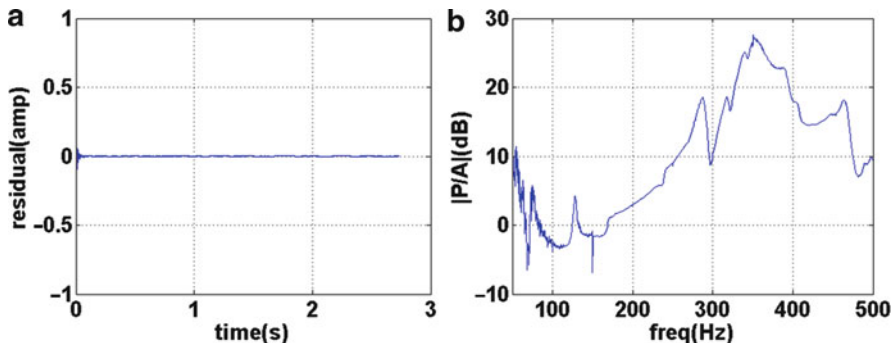


Fig. 23.27 Plot of the measured radiation response from a gypsy guitar with the peak at 127 Hz removed. Compared with Fig. 23.26, both the time-domain signal in the filtered response is shorter and the peak at 127 Hz in the spectral domain is removed. (a) Removing the peak of the measured radiation response at 127 Hz. The plot shows the signal from time 0 to 3 s. (b) FFT of the measured radiation response with the peak at 127 Hz removed. The plot shows the magnitude at frequencies between 50 and 500 Hz

(Karjalainen et al. 2003). Either complex spectral subtraction or inverse-filtering methods can be used. However, as done for the body response, we opt to use inverse-filtering.

Figure 23.27 shows the results of removing the peak centered around 127 Hz with a bandwidth of 10 Hz. Similar to the results obtained in Sect. 23.5.4.1, the radiation-filter impulse response is significantly shortened. As Fig. 23.27a shows, the residual signal approaches 0 within 0.1 s. Whereas, as shown in Fig. 23.26a, the radiation response lasts for well over a second. Furthermore, the peak in the spectral domain is entirely removed. As shown in Fig. 23.27b, the peak is close to 60 dB lower than the peak at 127 Hz in the original radiation response shown in Fig. 23.26b.

23.5.5.2 Combining and Interpolating Between Measurements

Because multiple plucks and excitations of a guitar can be made in one lab session, every note on the guitar can be recorded, thereby obtaining measurements of the top-plate acceleration and corresponding pressure waves for each note. Since each individual note is quasi-harmonic, it only provides significant information at the fundamental and harmonic frequencies. In other words, each note provides *samples* of the estimated frequency response at the string-mode frequencies. The results for all recorded notes can be combined in various ways. For example, the frequency-response samples based on all recorded notes can be superimposed to obtain a more densely sampled frequency response, and these points may be interpolated to provide a continuous frequency-response estimate.

23.6 Summary and Conclusion

This chapter has reviewed building blocks for virtual stringed musical instruments, with the emphasis on the acoustic guitar. The acoustic elements of a guitar were reviewed, as well as methods for measuring their characteristics, and methods for constructing virtual counterparts for purposes of real-time sound synthesis.

References

- Askenfelt, A., (1990). *Five Lectures on the Acoustics of the Piano*, Royal Swedish Academy of Music, Stockholm. Lectures by H.A. Conklin, A. Askenfelt, E. Jansson, D.E. Hall, G. Weinreich, and K. Wogram. Sound example CD included. Publication No. 64. http://www.speech.kth.se/music/5_lectures/
- Bank, B., and Välimäki, V. (2003). Robust loss filter design for digital waveguide synthesis of string tones, *IEEE Sig. Proc. Lett.* **10**, 18–20, January.
- Belevitch, V. (1968). *Classical Network Theory*, Holden-Day, San Francisco.
- Bradley, K., Cheng, M.H., and Stonick, V.L. (1995). Automated analysis and computationally efficient synthesis of acoustic guitar strings and body, *Proceedings of the IEEE Workshop on Applications of Signal Processing to Audio and Acoustics*, New Paltz, NY, October, IEEE Press, New York, pp. 238–241.
- Chaigne, A. (1991). Viscoelastic properties of nylon guitar strings, *Catgut Acoust. Soc. J.* **1**(Series I), 21–27.
- Chaigne, A. (1992). On the use of finite differences for musical synthesis: application to plucked stringed instruments, *J. d'Acoust.* **5**(2), 181–211.
- Christensen, O., and Vistisen, R.B. (1980). A simple model for low-frequency guitar function, *J. Acoust. Soc. Am.* **68**, 758–766.
- d'Alembert, J.I.R. (1973). Investigation of the curve formed by a vibrating string, 1747, *Acoustics: Historical and Philosophical Development*, R.B. Lindsay, ed., pp. 119–123, Dowden, Hutchinson, and Ross, Stroudsburg, PA.
- Dalmont, J.P., and Bruneau, A.M. (1992). Acoustic impedance measurements: plane-wave mode and first helical mode contributions, *J. Acoust. Soc. Am.* **91**, 3026–3033.
- Esquef, P.A.A., Välimäki, V., and Karjalainen, M. (2002). Restoration and enhancement of solo guitar recordings based on sound source modeling, *J. Audio Eng. Soc.* **50**(4), 227–236.
- Fletcher, N.H., and Rossing, T.D. (1998). *The Physics of Musical Instruments*, 2nd ed., Springer-Verlag, New York.
- Hua, Y., and Sarkar, T. (1990). Matrix pencil method for estimating parameters of exponentially damped/undamped sinusoids in noise, *IEEE Trans. Acoust. Speech Signal Process.*, **ASSP-38** (5), 814–824.
- Jaffe, D.A., and Smith, J.O. (1983). Extensions of the Karplus–Strong plucked string algorithm, *Comp. Music J.* **7**(2), 56–69, 198.
- Karjalainen, M., Esquef, P.A.A., and Välimäki, V. (2003). Making of a computer carillon, *Proceedings of the Stockholm Music Acoustics Conference (SMAC03)*, **1**, 339–342, Stockholm, Sweden, August 6–9.
- Karjalainen, M., Välimäki, V., and J’anosy, Z. (1993). Towards high-quality sound synthesis of the guitar and string instruments, *Proceedings of the 1993 International Computer Music Conference*, Tokyo, pp. 56–63, Computer Music Association, September 10–15, <http://www.acoustics.hut.fi/vpv/publications/icmc93-guitar.htm>
- Karjalainen, M., Välimäki, V., Penttilä, H., and Saastamoinen, H. (2000). DSP equalization of electret film pickup for the acoustic guitar, *J. Audio Eng. Soc.* **48**(12), 1183–1193.

- Karplus, K., and Strong, A. (1983). Digital synthesis of plucked string and drum timbres, *Comp. Music J.* **7**(2), 43–55.
- King, L.V. (1934). On the acoustic radiation pressure on spheres, *Proc. Roy. Soc. London, Ser. A Math. Phys. Sci.* **147**(861), 212–240 (November 15).
- Laakso, T.I., Välimäki, V., Karjalainen, M., and Laine U.K. (1996). Splitting the unit delay: tools for fractional delay filter design, *IEEE Signal Process. Mag.*, **13**, 30–60.
- Lambour C., and Chaigne, A. (1993). Measurements and modeling of the admittance matrix at the bridge in guitars, *Proceedings of the Stockholm Musical Acoustics Conference (SMAC-93)*, 448–453.
- Laroche, J. (1993). The use of the matrix pencil method for the spectrum analysis of musical signals, *J. Acoust. Soc. Am.* **94**, 1958–1965.
- Laroche J. (1998). Time and pitch scale modification of audio signals, *Applications of DSP to Audio & Acoustics*, M. Kahrs and K. Brandenburg, eds., Kluwer, London, pp. 279–309.
- Laroche, J., and Meillier, J.L. (1994). Multichannel excitation filter modeling of percussive sounds with application to the piano, *IEEE Trans. Speech Audio Process.*, **2**(2), 329–344.
- Laurenti, N., and Poli, G.D. (2000). A method for spectrum separation and envelope estimation of the residual in spectrum modeling of musical sound, *Proceedings of the International Conference on Digital Audio Effects (DAFx-00)*, Verona, Italy, <http://www.dafx.de/>
- Lee N., Cassidy, R., and Smith, J.O. (2006). Use of energy decay relief (EDR) to estimate partial-overtone decay-times in a freely vibrating string. Invited paper at *The Musical Acoustics Sessions at the Joint ASA-ASJ meeting*, Honolulu.
- Lee, N., Chaigne, A., Smith, J.O., and Arcas K. (2007). Measuring and understanding the gypsy guitar, *Interantional Symposium on Musical Acoustics*, Barcelona, Spain, September 9–12.
- Lee, N., Duan, Z., and Smith, J.O. (2007). Excitation extraction for guitar tones, *Proceedings of the International Computer Music Conference (ICMC07)*, Copenhagen, Denmark, August 27–31.
- Moorer, J.A. (1979). About this reverberation business, *Comp. Music J.* **3**(2), 13–18.
- Newcomb, R.W. (1966). *Linear Multiport Synthesis*, McGraw-Hill, New York.
- Oppenheim, A.V., and Willsky, A.S. (1996). *Signals and Systems*, 2nd ed., Prentice-Hall, Englewood Cliffs, NJ.
- Oppenheim, A.V., and Schafer, R.W. (1975). *Digital Signal Processing*, Prentice-Hall, Englewood Cliffs, NJ.
- Oppenheim, A.V., Schafer, R.W., and Buck, J.R., (1989). *Discrete-Time Signal Processing*, 2nd ed., Prentice-Hall, Englewood Cliffs, NJ .
- Pakarinen, J., Välimäki, V., and Karjalainen, M. (2005). Physics-based methods for modeling nonlinear vibrating strings, *Acta Acust. Acust.* **91**(2), 312–325.
- Putnam, W., and Smith, J.O. (1997). Design of fractional delay filters using convex optimization, *Proceedings of the IEEE Workshop on Applications of Signal Processing to Audio and Acoustics*, New Paltz, NY, October, IEEE Press, New York, <http://ccrma.stanford.edu/~jos/resample/optfir.pdf>
- Richardson, B.E., Hill, T.J.W., and Richardson, S.J. (2002). Input admittance and sound field measurements of ten classical guitars, *Proceedings of the Institute of Acoustics 2002*, **24**(2), 1–10, Institute of Acoustics.
- Schafer R.W., and Rabiner, L.R. (1973). A digital signal processing approach to interpolation, *Proc. IEEE* **61**, 692–702.
- Schroeder, M.R. (1961). Improved quasi-stereophony and colorless artificial reverberation, *J. Audio Eng. Soc.* **33**, 1061.
- Serra, X. (1997). Musical sound modeling with sinusoids plus noise, *Musical Signal Processing*, C. Roads, S. Pope, A. Piccialli, and G. De Poli, eds., pp. 91–122. Swets & Zeitlinger Publishers, Netherlands.
- Smith, J.O. (1983). *Techniques for digital filter design and system identification with application to the violin*, PhD thesis, Electrical Engineering Department, Stanford University (CCRMA);

- CCRMA Technical Report STAN-M-14, <http://ccrma.stanford.edu/STANM/STANM/stanm14/>
- Smith, J.O. (1984). An allpass approach to digital phasing and flanging, *Proc. of the 1984 International Computer Music Conference*, Paris, Computer Music Association; CCRMA Technical Report STAN-M-21, <http://ccrma.stanford.edu/STANM/STANM/stanm14/>
- Smith, J.O. (1992). Physical modeling using digital waveguides, *Comp. Music J.* **16**, 74–91, Winter. Special issue: *Physical Modeling of Musical Instruments, Part I*. <http://ccrma.stanford.edu/~jos/pmudw/>
- Smith, J.O. (1993). Efficient synthesis of stringed musical instruments, *Proceedings of the 1993 International Computer Music Conference*, Tokyo, 64–71, Computer Music Association.
- Smith, J.O. (2007a). *Mathematics of the Discrete Fourier Transform (DFT) with Audio Applications*, 2nd ed., online book, <http://ccrma.stanford.edu/~jos/mdft/>
- Smith, J.O. (2007b). *Introduction to Digital Filters with Audio Applications*, online book, <http://ccrma.stanford.edu/~jos/filters/>
- Smith, J.O. (2010). *Physical Audio Signal Processing*, online book, August edition, <http://ccrma.stanford.edu/~jos/pasp/>
- Smith, J.O., and Friedlander, B. (1985). Adaptive interpolated time-delay estimation, *IEEE Trans. Aerospace Electron. Sys.* **21**, 180–199.
- Smith, J.O., and Gossett, P. (1984). A flexible sampling-rate conversion method, *Proceedings of the International Conference on Acoustics, Speech, and Signal Processing*, San Diego, vol. 2, pp. 19.4.1–19.4.2, IEEE Press, New York, March; expanded tutorial and associated free software available at the Digital Audio Resampling home page: <http://ccrma.stanford.edu/~jos/resample/>
- Smith, J.O., and Serra, X. (1987). PARSHL: A program for the analysis/synthesis of inharmonic sounds based on a sinusoidal representation. In: *Proceedings of the 1987 International Computer Music Conference*, Champaign-Urbana, Computer Music Association. Expanded version available online at <http://ccrma.stanford.edu/~jos/parshl/>
- Smith, J.O., and Van Duyne, S.A. (1995). Commuted piano synthesis, *Proceedings of the 1995 International Computer Music Conference*, Banff, pp. 319–326, Computer Music Association, <http://ccrma.stanford.edu/~jos/pdf/svd95.pdf>
- Smith, J.O., Serafin, S., Abel, J., and Berners, D. (2002). Doppler simulation and the leslie, *Proceedings of the COST-G6 Conference on Digital Audio Effects (DAFx-02)*, Hamburg, Germany, September 26, pp. 13–20, <http://www.dafx.de/>
- Tolonen, T. (1998). *Model-based analysis and re-synthesis of acoustic guitar tones*, MS Thesis, Helsinki University of Technology, Espoo, Finland; Report 46, Laboratory of Acoustics and Audio Signal Processing.
- Tolonen, T., Välimäki, V., and Karjalainen, M. (2000). Modeling of tension modulation nonlinearity in plucked strings, *IEEE Trans. Speech Audio Process.*, **8**(3), 300–311.
- Välimäki, V., and Tolonen, T. (1998). Development and calibration of a guitar synthesizer, *J. Audio Eng. Soc.* **46**(9); *Proceedings of the 103rd Convention of the Audio Engineering Society*, New York, September 1997.
- Välimäki, V., Huopaniemi, J., Karjalainen, M., and J’anosy, Z. (1996). Physical modeling of plucked string instruments with application to real-time sound synthesis, *J. Audio Eng. Soc.*, **44**(5), 331–353.
- Välimäki, V., Pakarinen, J., Erkut, C., and Karjalainen, M. (2006). Discrete-time modelling of musical instruments, *Rep. Progress Phys.* **69**(1), 1–78.
- Van Valkenburg, M.E. (1960). *Introduction to Modern Network Synthesis*, John Wiley, New York.
- Weinreich, G. (1977). Coupled piano strings, *J. Acoust. Soc. Am.* **62**, 1474–1484.

Index

A

A0–A1 cavity mode model, 330–331

Accelerance

banjo, 71

cellos, 247

guitars, 49–52

violin, 222

Acoustic guitars

force exerted, 20–21

frequency response, 21–22

schematics, 20

Agraffe, 356

Agren, C.H., 312

Aizawa, H., 174

Amati, Andrea, 245

Amati, Hieronymus, 265, 267

Anderson, P., 225

Ando, T., 191

Ando, Y., 185, 190

Andreas, 6

Anomalous low frequencies (ALF), 287

Antinodes, 13

Antonio, 265, 267

Appalachian dulcimers, 99

Archtop mandolins

f-holes, 81

oval soundhole, 81

Asian musical instruments, 173–176. *See also*

Plucked string instruments

Askenfelt, A., 6, 218, 253, 259, 282, 296, 347, 350, 351

B

Bach, J.S., 6, 141, 142, 301, 354

Backhaus, Hermann, 210

Baltic psaltries

carved

body resonances, 105–108

drilling-enlarging technique, 113

electronic TV holography, 105

Estonia, kannel, 103

Finland, kantele, 103

history, 103–104

Latvia, kokle, 103

light construction, 112

Lithuania, kankles, 103

Northwestern Russia, gusli, 103

playing techniques, 104–105, 114

radical design, 114–115

sound boxes, 102

sound hole distribution, 111–112

sound quality, 103

string coupling, 103, 109–111

traditional-style designs, 113–114

without frets, 102

modernized

chromatic baltic psalteries, 118–121

diatonically tuned versions, 117–118

Banerji, B., 347

Banjo

bridges

acoustic anisotropy, 71

resonances, 71, 72

string vibrations, 72

total sound pressure *vs.* frequency, 72–73

classifications, 59

features, 59–60

harmonics analysis, 67–68

head modes

Fourier analysis, 66

head tension, 65–66

holographic interferometry, 65, 66

low-frequency response, 66–67

impedance matching, 74–75

- Banjo (*cont.*)
 neck, 73–74
 parts, 60–61
 Raejusters, 60, 69
 resonator
 adjustments, 69
 cavity tuning, 69
 Helmholtz resonator, 68–69
 maximum sound volume, 70
 resonance measurement, 69
 total sound fraction *vs.* frequency, 70
 rims, 73–74
 sound radiation
 vs. frequency response, 62–64
 power spectrum, 62
 vibrations, 63–64
 structural dynamics model, 59
 tone rings, 73–74
- Barbera, Richard, 401
- Barlow, C.Y., 229
- Baroque violins, 310
 acoustics
 bass viol, 313–314
 tenor viol, 313
 treble viol, 312–313
 development, 311–312
- Barth, Paul, 396
- Bassbar, 234–235
- Ba Than, U., 168
- Beauchamp, George, 396, 399
 Beauchamp violin design, 399–400
- Beck, Jeff, 398
- Beebe, C., 123, 125
- Beethoven, 78
- Bell, A.J., 158, 164
- Benioff, Hugo, 400, 401, 410
 Benioff violin design, 400–401
- Bernoulli, Daniel, 2
- Besnainou, C., 37, 242
- Bigsby, Paul, 395, 397
- Bissinger, G., 213–216, 221, 225, 231, 233, 235, 240, 241, 306, 317, 336
- Biwa. *See* Satsuma biwa
- Boccherini, 4
- Body resonance
 bi-directional interaction, 433–434
 driving-point admittance, 432
 filtering, 432–433
 string-body scattering junction, 434–435
- Body resonator
 low-order filter, 449–450
 response and admittance, 447, 449
- Bork, I., 6
- Borman, T.M., 230
- Boullosa, R.R., 53
- Bouncing rate, 296–297
- Boutillon, X., 203
- Boutin, H., 242
- Bow
 camber effect, 279–281
 François Tourte, 281
 hair elasticity effect, 282
 pernambuco, 281
 rosin/friction, 282–283
 snakewood, 281
 tonal quality, 281–282
- Bowed string instruments, 2–3
 cellos, 245
 medieval (*see* Medieval bowed string instruments)
 structural acoustics, 324–325
 traditional and octet, 329
 violin (*see* Violin)
 viols (*see* Viols)
- Bowed strings
 anomalous low frequencies (ALF)
 flattening effect, 203
 musical terms, 204
 reflected torsional waves, 205
 sound spectra, 204
 synchronizing mechanism, 205
 timing mechanism, 203
 violin G string, 205
 waveforms, 206–207
- dynamics, 202–203
- kinematics
 bowing condition limits, 199
 bowing force range, 199, 200
 bridge force waveform, 201, 202
 displacement and velocity, 197, 198
 friction force, 198
 ingenious vibration microscope, 200
 multiple-flyback motion, 201
 Raman model, 201
 string motion, 197, 198
 velocity and displacement curves, 201
 vibration cycle, 198, 199
- Bowing techniques
 B5 harmonics, 290, 291
 bouncing rate, 296–297
 bow acceleration, 292
 bow-hair ribbon, 293
 bowing parameters
 corner rounding, 288
 Helmholtz mode, 287
 pitch flattening, 289

- Schelleng diagram, 288, 289
 sul ponticello, 290
 détaché, 294–295
 double stops, 292
 flautando, 290
 friction force, 293–294
 harmonics and intonation, 291–292
 light bowing, 295
 martelé, 295
 spiccato/sautillé/ricochet, 295–296
 string spectrum, 297–298
 thumb rule, 290
 tone onsets, attacks, 292–294
- Bowlback mandolin. *See* Neapolitan mandolin
- Bracing
 asymmetrical and radial, guitars, 34–35
 hammered dulcimer, 376, 380
 ladder, 88
 mandolin, 87
 patterns, 79
 X-bracing, 81
- Brant, Henry, 320
- Brauchli, B., 123, 136
- Bretos, J., 225
- Bridge hill, 264
- Bridges
 banjo, 71–73
 guitars and lutes, 33
 hammered dulcimer, 389–390
 impedance, 437–438
 violin
 force transfer function, 232
 in-plane modes, 231–232
 mode frequency, 233
 resonance, 231–232
 schematics, 231
 tuning, 232
- Broadwood, 6
- Bucur, V., 131
- Burmese arched harp
 construction, 168–169
 history, 167–168
 intonations, 170
 playing techniques, 168–169
 plucked tone measurements, 170–171
 scales and tunings, 169–170
- Bynum, E., 245, 253
- C**
 Cabral, P.C., 54
 Caldersmith, G.W., 5, 19, 26, 32, 35, 36
 Campbell, M., 301
- Campbell, P., 301
 Campbell, R., 77
 Castanet, Burmese, 167
 Caussé, R., 241
 Cavity modes, 320
 C-bout rhomboid mode (CBR), 324
 CBR. *See* C-bout rhomboid mode
- Cello
 body modes
 A₀, 251, 252
 A₁, 251–252
 B₁, 252
 C, 252, 253
 frequencies, 253
 holographic interferograms, 251–252
 resonance (mode) frequencies, 254
 vs. double bass, 259
 exploded view, 245, 246
 family, 256
 history, 245
 mobility, 255
 modal analysis
 frequency response, 247–248
 labeling resonances, 249
 mode observation, 249
 vibration modes, 248–249
 sound spectra, 254–255
 vibration mode, component part
 air cavity modes, 250–251
 plate modes, 250
 vs. violin dimensions, 246
 vs. violin resonances, 254
- Chaigne, A., 347
- Christensen, O., 5, 26
- Christian, Charley, 395
- Cimbalom, 99, 117, 118. *See also* Hammered dulcimer
- Cittern, 47
- Clapton, Eric, 397, 398
- Classical guitar
 bracing, 34–35
 frequencies, principal modes, 25
 holographic interferograms, 28, 29
 sound quality, 32
 sound spectrum, 22
 top plate resonance, 28
 vibration modes, 23–24
- Clavichord, 5–6
- design
 brass strings, 137
 double-fretted, 136
 fretting, 137–138
 Helmholtz resonance, 137

- Hubert clavichord, 137
 string lengths and diameters, 138
- Keyboard tuning**
 cycle of fifths, 141
 harmonics, 140
 inharmonicity, 142
 Pythagorean comma, 141
 quarter-comma meantone, 141
 syntonic comma, 141
 temperament, 141
 string excitation, 139–140
- Cocchi, A., 255
- Cohen, D.J., 77, 87, 88
- Coincidence frequency, 239–240
- Colichon, Michel, 313
- Complex spectral subtraction, 450
- Conklin, H.A., 6
- Conklin, H.A. Jr., 347, 365
- Consorts, 4
- Convolution, 414
- Costa, Lorenzo, 307
- Courtney, P.E., 255
- Cousineau, Jacques-Georges, 151
- Cremer, L., 3, 201, 210, 221, 225, 233, 240
- Cremona, 265, 267
- Cremonese instruments, 414–415
- Cristofori, Bartolomeo, 6, 353, 354, 360
- Cross, Eric, 413
- Curtin, J., 209, 229, 241, 342, 414
- Cylinderback mandolin, 81
- Cymbals, Burmese hand, 167
- D**
- d'Alembert, J.I.R., 2, 11, 15, 423
- D'Alembert's wave equation, 423–425
- Dalinger double bass, 265–266
- Dalinger, Sebastian, 263, 266
- David, Gerard, 304
- Davis, T., 90
- Day, T., 394
- Dedilho, 47
- de Forest, Lee, 393
- del Gesu, Giuseppe Guarneri, 2
- del Gesu, Guarneri, 217, 326
- de Torres Jurado, Antonia, 4, 19
- Dickey, J., 59
- Digital waveguide model, 426–427
- Dimitru, Gabriel, 399
- Directional tone color (DTC), 215–216
- Dolmetsch, Arnold, 5
- Double bass
 body size and sound radiator, 271–273
 bridge hill, 264
 vs. cello, 259
 vs. Dalinger bass, 8–10
 directional radiation, 275–276
 player's support, 269–270
 scaling, 270–271
 schematics, 260
 stage risers, 273–275
 tone quality, 264–265
 vibration modes
 bowed instruments, 259
 mobility curves, 261–263
 mode shapes, 260
 in playing, 260–261
 vs. violin and cello, 263–264
 violin octet, 268
- Dowland, John, 4
- Driving-point admittance, 432
- DTC. *See* Directional tone color
- Ducornet, Marc, 138
- Duhamel, Jean-Marie, 2
- Dulcimer
 hammered, 117, 352 (*see also* Hammered dulcimer)
 history, 5–6
- Dünnewald, H., 214–217, 242, 306, 307, 413
- Dünnwald-type bridge driver, 214
- E**
- Eban, G., 35
- Edge, Anthony, 310, 311, 313
- EDR. *See* Energy decay relief
- Eggers, F., 253
- Eldredge, N., 104
- Electric guitar
 body vibrations and dead spots, 39
 development, 395–396
 electric bass, 39
 electromagnetic pickups, 38
 features, 37–38
 frying pan, 396–397
 future developments, 398–399
 history, 394–395
 magnetic pickups, 38–39, 396–397
 modern replicas, 397–398
 optical pickups, 39
 piezoelectric pickups, 39
- Electric violin, 240–241
 Beauchamp design, 399–400
 Benioff design, 400–401
 Cremonese instruments, 414–415
 development, 399

- hand-crafted design, 401–402
history, 394–395
multiresonant filter characteristics, 412–413
pickups
 acoustic, 402–403
 magnetic, 403–406
 optical pickups, 410
 piezoelectric, 407–410
 special sound effects, 406
signal path schematics, 411
sound perception and acoustical properties, 413–414
Elejabarrieta, M.J., 54, 55
Ellis, Bernard, 303, 305, 306
Energy decay relief (EDR)
 definition, 444
 gain *vs.* frequency, 447, 448
 loop filter, 445
 plucked guitar note plot, 444–445
 vs. time, 445–446
English guitar, 48
Erard, Sébastien, 6, 151
Errede, Steven, 403
Escapement, 356
Estonia, kannel, 103, 119, 120
Experimental modal analysis, 7–8, 319
- F**
Fado, 47
Farina, A., 241
Fast Fourier transform (FFT), 212
Fender, Clarence Leonidas, 5
Fender, Leo, 395, 397, 406
Finger picking/strumming, 17
Finger-string interaction, 17
Finite element analysis (FEA), 319
Finland, kantele, 103, 120
Firth, I.M., 41, 157, 158, 164, 253
Fixed soundboard, 388
Flangers, 406
Flatback mandolins, 80–81
Fleming, John Ambrose, 393
Fletcher, H.A., 215
Fletcher, N.H., 5, 100, 123, 136, 201, 203
Floating soundboard, 388
Folk guitar
 air cavity modes, 24, 25
 frequencies, principal modes, 25
 low-frequency response curve, 26
 plate motion, 28
 sound radiation patterns, 31
 sound spectrum, 30–31
 vibrational motion, 27
Force hammer, 438
Ford, Henry, 372
Fourier analysis, 14
Fourier, Jean Baptiste, 212
Frequency response function (FRF), 8, 213
Friedlander, F.G., 220
Fritz, C., 242, 413
Frying pan guitar, 396–397
Fryxell, Robert, 210
Fuller, Walter, 397
- G**
Galilei, Vincenzo, 151
Galileo, 2
Galluzzo, P.M., 217, 218
Gayageum, 190–193
Gaydecki, P., 413
Geissler, P., 225
Geomungo, 192
Gerle, Hans, 304
Gervaise, Benoit, 308
Ghosh, R.N., 347
Gibson mandola, 96
Gibson, Orville, 78
Gifford, Paul, 371
Gill, D., 77
Giordano, N., 17, 353
Gore, Trevor, 35
Gorrill, S., 241
Gough, C.E., 393, 414
Graesser, H., 399
Grand piano, 355
Gregorian, A., 221
Guarneri, Andrea, 263
Guarneri del Gesu, Giuseppe, 230
Guarneri, Joseph, 2
Guettler, K., 205, 279, 296
Guitars. *See also* Portuguese guitar
 acoustic guitars
 classical guitar (*see* Classical guitar)
 folk guitar (*see* Folk guitar)
 force exerted, 20–21
 frequency response, 21–22
 schematics, 20
 electric guitars (*see also* Electric guitar)
 body vibrations and dead spots, 39
 electric bass, 39
 electromagnetic pickups, 38
 features, 37–38
 magnetic pickups, 38–39

- optical pickups, 39
- piezoelectric pickups, 39
- gypsy guitar**, 37
- vs. harp, 165
- quality**
 - asymmetrical and radial bracing, 34–35
 - bridge, 33
 - design and construction, 33
 - top plate and braces thickness, 33–34
- scaled guitars**, 35–36
- sound radiation**, 30–32
- string forces**, 29–30
- synthetic materials**, 37
- telecaster**, 5
- types**, 4
- vibrations**
 - low-frequency resonances, 27–28
 - modal shapes, 28–29
 - normal modes, 22
 - three-oscillator model, 27
 - two-oscillator model, 26
 - vibration modes, component parts, 23–25
- Güttler, K., 218
- Gypsy guitar**, 37

- H**
- Haas, A., 103, 113
- Haines, D.W., 37, 174, 175, 229
- Hair scales, 282
- Hall, D.E., 6, 347, 350
- Hammered dulcimer**, 117
 - basic instrument
 - diatonic scales, 372–373
 - 15 treble/bass courses, 372–373
 - treble bridge, 372–373
 - tuning scheme, 373–374
- bridge caps and vibrations, 389–390
- course spacing, 384–385
- history, 371–372
- hitch pins, 391
- inharmonicity and scaling, 374–375
- instrument warp
 - deflections, 377–378
 - horizontal bridge force, 376–377
 - simply supported beams, 376–377
- lateral stability, 375–376
- pegleg, 392
- percussive sound
 - hammer-to-bridge reflection, 382–383
 - string-hammer interaction, 383–384
 - string velocity, 382–383
- perfect fifth, 392
- pin blocks, 390–391
- soundboard**
 - advantages, 388
 - back plates, 389
 - body modes, 387–388
 - fixed and floating, 388
 - materials, 389
- sound holes, 391–392
- sound radiation pattern**, 391
- string coupling and resonance time**
 - power spectrum, 385–386
 - vibrations, 386–387
- tuning stability**
 - humidity, 380–381
 - string-bridge friction, 382
 - temperature, 378–380
- Hammered strings**
 - dulcimer, hammered, 352
 - dynamics**
 - displacement and velocity, 348–349
 - spectrum, 348–349
 - striking string, 347–348
 - piano hammers** (*See Piano hammers*)
 - striking position, 351
- Hammers**
 - compression characteristics, 360
 - schematics, 360
 - spectral analysis, 361–362
 - string, 361
 - tones, 362–363
- Hanson, R.J., 203–205
- Harmonic series**, 358
- Harp**. *See also Burmese arched harp*
 - decay times, 163, 164
 - vs. guitar, 165
 - origins and development, 145–146
- soundboard**
 - celtic seaboard, 156
 - cracking prevention, 157
 - damping, 164
 - resonance, 163
 - soundholes, 158
 - sound output, 157
 - vibrational behavior, 158, 159
- soundbox**
 - acoustic velocities, 160, 162
 - antinodes, 162
 - bending modes, 160
 - Helmholtz and pipe resonances, 158, 160
 - low-frequency behavior, 160
 - low modes of vibration, 160, 161

- sound radiation, 164–165
strings
 diatonic vs. chromatic stringing, 151
 empirical dependencies, 153
 history, 150–151
 inharmonicity, 152
 pitch dependencies, 153
 sharpening mechanisms, 151–152
 sound spectrum influence, 153, 155–156
 and sound temporal development, 156,
 157
 spacing, 152
 47-string Salvi Aurora, 153, 154
string-soundboard interaction, 164
structure
 configuration, 148
 erard double-action sharpening
 mechanism, 149, 150
 geometry and coordinate system, 146,
 147
 mechanical connection, 149
 Salvi Aurora, 146, 148, 149
 soundboard, 146, 147
 soundbox, 148
Harpsichord, 16–17
 acoustic balance
 Baroque pitch, 134
 components, 132
 decay time, 133
 Ruckers instrument, 133
 sound level, 134
 buff stop, 134
design
 construction, 125, 126
 extensions, 134–136
 hitchpins, 126
 jack, 126, 127
 operation basis, 124
 pedal mechanism, 127
 string tension, 124
Flemish instruments, 135
keyboard tuning
 cycle of fifths, 141
 harmonics, 140
 inharmonicity, 142
 Pythagorean comma, 141
 quarter-comma meantone, 141
 syntonic comma, 141
 temperament, 141
lute stop, 135
plucked strings
 fundamental vibration frequency, 127
 harmonics, 129
 lute stop, 130
 metal strings, 127–128
 scaling parameters, 128
 string composition and diameter
 variation, 128, 129
 tone quality, 129
pull-down mechanism, 135
soundboard and radiation
 acoustic and vibrational properties, 131
 exploded view, 131
 internal damping, 132
 sound quality, 130
 vibrational mode shapes, 131
 string scaling, 123
Harpsichords, 5–6
Harris, N., 229
Heat diffusivity, 378
Hebenstreit, Pantaleon, 354
Helmholtz motion, 218–219
Hendrix, Jimi, 397, 398
Henrique, L., 54, 55
Hill, T.J.W., 53
Hitch pins, 391
Hochbrucker, Jacob, 151
Holliman, A., 399
Holographic interferometry
 banjo, 66, 68
 cello, 251–252
 cellos, 250–253
 guitar, 27–29, 35
 mandolin, 83–84
 modal analysis, 9
 psalteries and zithers, 107, 108
 violin, 224–225
Horiuchi, R., 189
Horton, N.G., 38
Hubbard, F., 123, 136
Hubert, Christian Gottlob, 136, 138
Humbucking coil systems, 405–406
Hutchins, C.M., 1–3, 36, 210, 222, 227–229,
 256, 268, 317–323, 326–330, 332,
 337–339, 341–343
Hutchins-Schelleng violin octet
 A1 radiation in B1 region, 326–327
 development
 evolution, 321–323
 signature modes, 323–324
 direct radiation mechanisms, 321
 history, 319–320
 material properties, 325
 modal and acoustical analyses
 A0 and A1 coupling, 336–337
 A1 mode status, 338–340

A1 radiation, 340
 averaged corpus vibration, 333–335
 force hammer impact excitation,
 333–334
 lower/upper bout pressure ratio,
 340–341
 relative strength, 341
 rib height and pressure ratio, 338
 tests, 332–333
 wall compliance and cavity mode
 frequencies, 337–338
 mode, 317
 nomenclature, 319
 radiation mechanisms, 324–325
 resonance, 320–321
 scaling
 A0 equation, 330–331
 assumptions, 327–328
 flat plate equations, 329–330
 practicality, 328–329
 shape similarity, 331–332
 shape/size, 318
 signature modes, 318

I

Impulsive waves, 12
 Inácio, O., 53
 Inverse filtering, 450

J

Jahnel, F., 4, 19
 Jansson, E.V., 5, 6, 21, 32, 33, 53, 223,
 225, 228, 231, 305, 321, 322,
 339, 347, 351
 Japanese instruments
 koto, 190–192
 Satsuma biwa (*see* Satsuma biwa)
 shamisen, 187–190
 Johnson, Ieva Sijats, 112
 Johnson, J.R., 78
 Jones, Richard, 308–310

K

Karplus, K., 431
 Kasha, M., 35
 Kasil, King, 192
 Keller, J.B., 220
 Kennedy, Nigel, 401
 Khin May, Daw, 168, 170
 Kimura, M., 204, 205

Kirnberger III, 141
 Kishi, K., 185
 Knott, G.A., 225, 322
 Kohut, J., 7, 215, 241, 412, 413
 Kondo, M., 201
 Koto
 harmonic structure, 191
 pentatonic scale, 190
 sound holes, 190
 transfer function, 192
 tuning, 192
 vibrato effects, 192
 Kottick, E.L., 123, 136
 Koussevitzky, Serge, 265, 267
 Krigar-Menzel, O., 201
 Kubata, H., 201
 Kuus, Alfred, 117, 118
 Ky, Lovikka, 118

L

Lang, 266
 Langhoff, A., 214, 235, 253
 Langmuir, Irving, 393
 Latvia, kokle, 103, 119
 Lauterborn, W., 241
 Lawergren, B., 201
 Le Carrou, J.-L., 17
 Lee, N., 417
 Leoncavallo, 78
 Linarol, Francesco, 308–310
 Linear superposition principle, 12
 Linear system, 319
 Lithuania, kankles, 103
 Loar, Lloyd, 78, 395, 399
 Loos, U., 217
 Lover, Seth, 405
 Lundberg, R., 40
 Lutes
 European short lute, 41, 42
 long-necked lute, 41–44
 mechanical admittance, 41
 plectrum, 4
 Renaissance, 40
 Turkish tanbur, 41–44
 uses, 4
 Lynn, Bert, 395, 400

M

Maala, Väino, 120
 Magnitude spectrum smoothing method
 (MSS), 441–442

- Mandocello, 82–83, 96
Mandola, 82–83
Mandolin
 archtop mandolins
 f-holes, 81
 oval soundhole, 81
 cylinderback mandolins, 81
 family, 77–78
 flatback mandolins, 80–81
 F5 mandolin, 78
 general similarity law, 95
 Gibson mandola, 96
 Helmholtz air resonance frequency, 95
 mandocello, 82–83, 96
 mandola, 82–83
 Neapolitan mandolin, 79–80
 normal mode frequencies
 asymmetric radial bracing pattern, 79, 91–92
 firmer bass response, 91
 modal analysis, 87
 (0,0) mode, 91
 (1,0) mode, 92
 plate/air phase relationships, 88, 90
 normal mode shapes
 Helmholtz air resonance, 86–87
 ODS, 84–85
 two-oscillator and three oscillator model, 86
 normal vibration modes and holographic interferometry, 83–84
octave mandolin, 82–83
operating deflection shape (ODS), 83
popularity, 78
sustainability, 89, 92–94
Mandoline. *See* Neapolitan mandolin
Marie Antoinette, Queen, 151
Marshall, K.D., 225, 322
Marty, Simon, 35
Mascagni, 78
Masino, T.R., 233
Mathematical modal analysis, 8
Mathews, M.V., 7, 215, 241, 401, 410, 412, 413
Matrix-pencil inverse-filtering (MPIF)
 method, 440
Maung Maung Gyi, U., 168
Ma, Yo-Yo, 401
May, Vanessa, 401
McIntyre, M.E., 201, 214, 216–218, 410
Mechanical admittance, 222
Medieval bowed string instruments
 fiddles
 acoustical properties, 305–306
 C holes, 303
 construction, 302, 303
 rebecs (*see* Rebecs)
Meinel, H.F., 210, 214
Melody, M., 215
Memling, Hans, 302
Mersenne, M., 2, 210, 314
Meyer, Erwin, 210
Meyer, J., 5, 6, 21, 53, 92
Mobility curves
 cello and violin, 248
double bass
 Dalinger bass, 266
 definition, 261–262
 double bass bridge, 265
 double bass vs. violin and cello, 263–264
 measurement, 262, 265
 mode shapes, 261, 262
 player's support, 269–270
 quality, 264, 266
 small and large bass, 269
Möckel, O., 229
Modal analysis
 and acoustical analysis, Hutchins-Schelleng violin octet
 A0 and A1 coupling, 336–337
 A1 mode status, 338–340
 A1 radiation, 340
 averaged corpus vibration, 333–335
 force hammer impact excitation, 333–334
 lower/upper bout pressure ratio, 340–341
 relative strength, 341
 rib height and pressure ratio, 338
 tests, 332–333
 wall compliance and cavity mode frequencies, 337–338
 cellos, 247–249
 experimental modal testing, 7–8, 319
 holographic modal analysis, 9
 mathematical modal analysis, 8
 sound field analysis, 9
 violin, 225
Molin, N-E., 225, 260
Monochord, 357
Monroe, Bill, 78
Moore, Brian, 413
Moore, T.R., 38, 59
Moral, J.A., 228, 229
Moseley, Semie, 398
Mozart, Leopold, 6, 78, 284–285

- Mühlung, Kristi, 120
 Müller, G., 241
 Müller, H.A., 225, 232
 Multiresonant filter characteristics, 412–413
 Musical acoustics, 1
 Myall, Norman, 309, 311–313
 Myint Maung, U., 168, 170, 171
- N**
 Nakamura, I., 6
 Neapolitan mandolin, 79–80
 Neupert, H., 123, 136
 Nodes, 13
 Northwestern Russia, gusli, 103
- O**
 Octave mandolins, 82–83
 Octave stretching, 359–360
 ODS. *See* Operating deflection shape
 Operating deflection shape (ODS)
 baltic psaltries, 105–108
 cello, 248
 guitars, 22
 Hutchins-Schelleng violin octet, 325
 mandolin, 83
 violin, 222
 Oppenheim, A.V., 420
 Ordu\$\$\$a-Bustamante, F., 53, 55
- P**
 Parameter estimation, virtual string instruments
 body resonator (*see* Body resonator)
 excitation
 MPIF, 440
 MSS, 441–442
 SPNIF, 440–441
 SSI, 442–444
 radiated sound pressure
 low-order filter, 451–452
 measurement, 452
 radiation response measure, 450–451
 STFT, 439–440
 string loop filter estimation
 digital waveguide model, 445
 EDR (*see* Energy decay relief)
 Partials, 358
 Patch near-field acoustical holography (pNAH), 323
 Paul, Les, 5, 395, 397, 398
- Peekna, A., 99, 115
 Pegleg, 392
 Percussive sound, 382–384
 Peterson, D., 371
 Pfeil, Victor, 399
 Phaser effect, 406
 Philp, Eugene, 36
 Piano, 6
 Piano acoustics
 design, 355–356
 hammers (*see* Piano hammers)
 history, 353–355
 modeling, 368–369
 soundboard
 mechanical response, 366
 patterns, 365–366
 second partial behavior, 363–364
 sound production, 363
 speaker, 363
 vibrational modes, 364–365
 tones, 367
 vibrating strings
 arrangement, 356–357
 harmonic frequencies, 358–359
 monochord, 357
 octave stretching, 359–360
 schematics, 355
 standing waves, 357–358
 Young's modulus, 359
- Pianoforte, 354
 Piano hammers
 acoustics
 compression characteristics, 360
 schematics, 360
 spectral analysis, 361–362
 string, 361
 tones, 362–363
 hardness, 349–350
 string excitation, 350–351
- Pickering, N.C., 218
 Pickups, electric violin
 acoustic, 402–403
 magnetic
 humbucking systems, 405–406
 resonant frequency, 404
 sensitivity dependence, 404–405
 steel string vibrations, 403–404
 optical pickups, 410
 piezoelectric
 bowed string instruments, 407–408
 frequency response, 408–409
 heavy bridge, 409–410
 material, 407

- mounting position, 408
special sound effects, 406
- Pin block, 390–391
- Pipa, 186
- Pitteroff, R., 201
- Plectrum, 354
- Plucked string instruments
- classification
 - abscissa, 175
 - acoustical properties, 176
 - hachion, 173
 - soundboard, 174
 - sound board wood, 176
 - sound-hole structure, 174
 - transmission characteristics, 175
 - wood properties, 174
 - force, transverse and longitudinal, 15–16
 - frequency analysis, 14
 - Japanese koto and Korean gayageum
 - geomungo, 192
 - harmonic structure, 191
 - pentatonic scale, 190
 - sound holes, 190
 - transfer function, 192
 - tuning, 192
 - vibrato effects, 192
 - Japanese Satsuma biwa
 - vs Chinese pipa, 186
 - fundamental structure, 176, 177
 - sawari mechanisms, 180–184
 - sound characteristics, 185–186
 - string tension, 176
 - structural response, 178–180
 - Japanese shamisen
 - sawari mechanism, 189–190
 - string-bridge-membrane system, 187–189
 - plucking
 - finger picking/strumming, 17
 - plectrum, harpsichord, 16–17
 - rest and free strokes, 17
 - spectrum, 14–15
 - time analysis, 14, 16
 - transverse waves
 - impulsive waves, reflection and interference, 12
 - standing waves, 12–13
- pNAH. *See* Patch near-field acoustical holography
- Pölkki, J., 114
- Portuguese guitar
 - Coimbra guitar, 48–49
 - frequency response *vs.* resonance, 56–57
- Lisbon guitar, 48–49
- origin, 47–48
- Porto guitar, 48
- subjective acoustical quality evaluation
 - listening tests, 54
 - objective parameters, 53–54
 - test procedure, 55–56
 - tests conditions, 54–55
- timbre, 56
- vibroacoustic behavior
 - accelerance FRF, 50–51
 - Helmholtz resonance, 50–52
 - modal characteristics, 49
 - monopole and dipole modes, 52–53
 - vibroacoustic transfer functions, 49
- Powell, R.L., 225
- Praetorius, M., 311
- Psalteries
 - baltic (*see* Baltic psalteries)
 - plucking stiffness and strength, 100–101
 - string
 - materials, 101–102
 - stress, 100
 - zither family, 99
- Puccini, 78
- Pythagoras, 1, 357
- ## Q
- Quiescent camber (QC), 280
- ## R
- Radiation efficiency, 240
 - Radiation ratio, 229
 - Radiativity, 319
 - Rae, J., 59
 - Raejusters, 60, 69
 - Raman, C.V., 3, 201, 210, 220, 347
 - Raphael, 308
 - Raps, A., 201
 - Rayleigh, L., 3
 - Rebecs
 - acoustical properties, 306–307
 - sound characteristics, 303, 304
 - structural features, 304
 - Reinecke, W., 225, 265
 - Reinel, 266
 - Reinhardt, Django, 37
 - Renaissance viols
 - acoustics, 309–310
 - development, 307–309
 - Richardson, B.E., 5, 21, 23, 26, 33, 34, 92

- Rickenbacher, Adolph, 5
 Roberts, G.W., 24, 26, 33
 Roberts, M., 224
 Rodgers, O.E., 214, 225, 228, 233
 Rossing, T.D., 1, 11, 19, 21, 26, 59, 60, 77,
 83, 86–88, 92, 99, 100, 123,
 197, 201, 203, 209, 221, 224,
 245, 260, 347
 Rossini, 19
 Ross, R.E., 21, 26
 Rubio, David, 305, 313
 Ruckers, Andreas, 125
 Ruckers, Hans, 5
 Ruggieri, Francesco, 263
 Russell, R., 123, 136
- S**
 Sachs, C., 145
 Saldner, H.O., 235
 Sampling rate, 419
 Sanders, L.C., 215
 Satsuma biwa
 vs. Chinese pipa, 186
 fundamental structure, 176, 177
 sawari mechanisms
 collision process, 184
 degree of reverberation, 181
 Kyushu type, 181, 182
 numerical simulations, 184
 plucked string vibration (Doubt), 183
 Runge-Kutta method, 182
 tori-kuchi or shohgen, 180
 sound characteristics, 185–186
 string tension, 176
 structural response, 178–180
 Saunders, F., 3, 210, 216, 319–322
 Saung gauk. *See* Burmese arched harp
 Savage, W.R., 131, 132
 Savart, Felix, 2, 3, 210, 228
 Scattering junction, 434
 Schelleng, J.C., 36, 175, 197, 201, 203, 210,
 218, 219, 229, 289, 298, 317, 318,
 320, 321, 324, 326, 328–330, 332,
 337, 339, 340
 Schelleng's ratio, 340–341
 Scherer, 410
 Schleske, M., 212, 229, 234, 235, 322, 328,
 330, 342
 Schmitz, H.-E., 178, 185
 Schneider, Richard, 35
 Schubert, 19
 Schumacher, R.T., 203, 218
- Second harmonics. *See* Standing waves
 Senda, T., 184
 Sethares, W.A., 142
 Shaker, 438
 Shamisen
 sawari mechanism, 189–190
 string-bridge-membrane system,
 187–189
 Shaw, E.A.G., 322
 Short-time-Fourier-transform (STFT),
 439–440
 Silbermann, Gottfried, 6, 354
 Sines-plus-noise inverse-filtering method
 (SPNIF), 440–441
 Sizzle, 215
 Smallman, Greg, 34, 36
 Smith, J.O., 417, 427, 436
 Smith, R.R., 398, 400
 Sor, Fernando, 4, 19
 Sound field analysis, 9
 Sound holes, 391–392
 Sound radiation
 banjo, 62–64
 guitars, 30–32
 hammered dulcimer, 391
 harp, 164–165
 harpsichord, 130–132
 violin, 235–238
 Spanish-style harp, 157
 Sparks, P., 77
 Spear, R., 342, 343
 Standing waves
 piano, 357–358
 plucked strings, 12–13
 Statistical spectral interpolation method (SSI),
 442–444
 Stein, Nannette, 6
 Steinway, Henry, 6
 Stephey, L.A., 59
 Stetson, K.A., 225
 STFT. *See* Short-time-Fourier-transform
 Stradivari, Antonio, 2
 Strings
 damping, 285
 tension, 284–286
 torsion, 287
 wave resistance/impedance, 283–284
 Strong, A., 431
 Structural acoustics, 324–325
 Strutt, J.W., 3
 Sulis, Dorian, 185
 Sundin, H., 322
 Suzuki, H., 6

T

Taguti, T., 88, 180, 184, 185

Takasawa, Y., 187

Tangent, 354

Tap tones

Chladni patterns, 227

Italian violins, 228

plate tuning, 228–229

radiation ratio, 229

Tarrega, Francisco, 4, 19

Taskin, Paul, 5

Taylor, Brook, 2

Témkin, I., 104

Thwaites, S., 123, 136

Tiideberg, Ilmar, 118, 119

Tohnai, K., 178, 180, 184, 185

Tolonen, T., 436

Toshikawa, 184

Tourte, Francois, 2, 210, 279, 281, 282

Transverse waves

plucked strings, 12–13

Tronchin, L., 255

Tsuruta, Kinshi, 182

Tuning stability, hammered dulcimer

humidity, 380–381

string-bridge friction, 382

temperature

vs. frequency, 378–379

tension, 379–380

thermal expansion, 379

Tureck, Rosalyn, 401

Turkish tanbur, 41

Turnbull, H., 4, 19

Tyler, J., 77

V

Valette, C., 285

Välimäki, V., 436

Ventapane, Lorenzo, 263

Verdi, 19

Vermeij, K., 123, 136

Vihuela, 19

VIOCadeas analysis, 319

Viola, 47

Violin

vs. cello, 254

component parts

bassbar and soundpost, 234–235

bridge (*see* Bridge)

enclosed air, 230

fingerboard, 234

mass, 229–230

ribs, 233

tap tones (*see* Tap tones)

top and back plates, 227

vs. double bass, 263–264

electric (*see* Electric violin)

electric and virtual, 241–242

evaluation, 211–212

frequency response, 213

high-frequency radiation, 239–240

history, 209–210

low-frequency radiation

monopole radiation, 237, 239

total radiation, 239

volume fluctuation, 237, 239

naming modes, 221

playability

bow force limits, 219–220

damping, 220

Helmholtz motion, 218–219

mobility, 218

radiation damping, 240–241

research, 210–211

sound analysis, 212–213

sound radiation measurement

experimental setup, 236

microphone position, 235–238

radiativity, 235

single microphone measurement,

237

single response curves, 237–238

spikiness, 237

tone quality

acoustical measurement, 213–214

DTC, 215–216

Dünnwald-type bridge driver, 214

echoes, 214–215

projection/carrying power, 216–217

sizzle, 215

timbre, 214

vibrations

modal analysis, 225

modal overlap, 226

normal modes, 222–223

statistical overlap, 226

three-dimensional model, 224–225

two-dimensional model, 223–224

Violin octet, 268

Viols

baroque viols (*see* Baroque viols)

family, 301

medieval bowed string instruments

(*see* Medieval bowed string instruments)

- Viols (*cont.*)
 renaissance viols
 acoustics, 309–310
 development, 307–309
- Virtual string instruments, 7
 applications, 417
 body resonance
 bi-directional interaction, 433–434
 driving-point admittance, 432
 filtering, 432–433
 string-body scattering junction, 434–435
 decomposition abstraction block diagram, 422
 digital nomenclature
 filtering, 422
 sampling, 419–420
 sum of sinusoids, 420–422
 measurements
 body vibration, 438–439
 bridge impedance, 437–438
 pressure signal, 439
 string vibration, 436–437
 old recordings, 417–418
 parameter estimation
 body resonator, 447–450
 excitation, 440–444
 radiated sound pressure, 450–452
 short-time-Fourier-transform, 439–440
 string, 444–447
 plucking string
 complexities, 431
 theoretical, 430–431
 pressure radiation, 435–436
 vibration string
 D'Alembert's wave equation, 423–425
 delay line, 425–426
 digital waveguide model, 426–427
 natural decay, 427–428
 plane vibration, 428–429
 varying digital waveguides, 429–430
- Virtual violin
 digital bow, 241
 reciprocal bow, 241–242
- Vistasen, R.B., 26
- Vivaldi, 78
- von Helmholtz, H.L.F., 3, 197, 200, 201, 210, 218, 347, 367
- von Hornbostel, E.M., 145
- von Weber, 19
- Vuillaume, Jean Baptiste, 2, 210
- W**
- Wah-wah effect, 406
- Wakefield, G., 215
- Waltham, C., 145
- Way, D.J., 138
- Weinreich, G., 6, 215, 216, 235, 239, 241, 414
- Werckmeister III, 141
- Wien, 263
- Wilfer, 266
- Wilkins, R.A., 250
- Williams, J., 34
- Williamson, M.C., 168, 170
- Williamson, R.M., 167, 170
- Willsky, A.S., 420
- Winans, J.P., 17
- Wogram, K., 6
- Wolf note, 220
- Wolf tones, 284
- Woodfield, I., 307
- Woodhouse, J., 214, 216–219, 226, 231, 255, 305, 413
- Wungyi, Myawadi, 168
- Y**
- Yako, M., 190
- Yamanaka, K., 88
- Yoshikawa, S., 173, 174, 176
- Young's modulus, 359
- Z**
- Zithers
 fretted (alpine), 116
 without fretboard, 115
- Zuckermann, W.J., 123
- Zwicker, T., 5